„Ungewöhnliche Phosphaoligocyclen aus $1\lambda^3$-Phosphaalkinen und verschiedenen Halogeniden der Gruppen 13 und 15“

“Unusual Phosphorus Oligocycles from $1\lambda^3$-Phosphaalkynes and Various Halides of Group 13 and 15 Elements”

Von der Fakultät Chemie der Universität Stuttgart
zur Erlangung der Würde eines Doktors
der Naturwissenschaften (Dr. rer. nat.)
genehmigte Abhandlung

vorgelegt von
M. Sc. **Bani Fwaz Mutasem Z.**
Aus Anjara/Ajlun/Jordanien

Hauptberichter:	Prof. Dr. G. Becker
Mitberichter:	Priv.-Doz. Dr. M. Niemeyer
Weiterer Prüfer:	Prof. Dr. S. Hashmi
Prüfungsvorsitzender:	Prof. Dr. T. Schleid
Tag der mündlichen Prüfung:	21.12.2007

Institut für Anorganische Chemie der Universität Stuttgart
2007

VERLAG GRAUER · Beuren · Stuttgart · 2007

„Ungewöhnliche Phosphaoligocyclen aus 1λ^3-Phosphaalkinen und verschiedenen Halogeniden der Gruppen 13 und 15“

“Unusual Phosphorus Oligocycles from 1λ^3-Phosphaalkynes and Various Halides of Group 13 and 15 Elements”

Von der Fakultät Chemie der Universität Stuttgart
zur Erlangung der Würde eines Doktors
der Naturwissenschaften (Dr. rer. nat.)
genehmigte Abhandlung

vorgelegt von
M. Sc. **Bani Fwaz Mutasem Z.**
Aus Anjara/Ajlun/Jordanien

Hauptberichter:	Prof. Dr. G. Becker
Mitberichter:	Priv.-Doz. Dr. M. Niemeyer
Weiterer Prüfer:	Prof. Dr. S. Hashmi
Prüfungsvorsitzender:	Prof. Dr. T. Schleid
Tag der mündlichen Prüfung:	21.12.2007

Institut für Anorganische Chemie der Universität Stuttgart
2007

Bani Fwaz, Mutasem Z.:
Unusual Phosphorus Oligocycles from 1λ^3-Phosphaalkynes and Various Halides of Group 13 and 15 Elements.
VERLAG GRAUER, Beuren und Stuttgart, 2007.

ISBN 978-3-86186-549-0

D 93
Dissertation Universität Stuttgart, Institut für Anorganische Chemie, 2007.

Von der Fakultät Chemie der Universität Stuttgart zur Erlangung der Würde eines Doktors der Naturwissenschaften (Dr. rer. nat.) genehmigte Abhandlung
vorgelegt von Bani Fwaz Mutasem Z. aus Anjara, Ajlun/Jordanien.

Hauptberichter:	Prof. Dr. G. Becker
Mitberichter:	Priv.-Doz. Dr. M. Niemeyer
Weiterer Prüfer:	Prof. Dr. S. Hashmi
Prüfungsvorsitzender:	Prof. Dr. T. Schleid
Tag der mündlichen Prüfung:	21.12.2007

E-Mail: banifawaz@yahoo.com

Printed in Germany.
Druck: F. u. T. Müllerbader GmbH
Forststr. 18, 70794 Filderstadt, Germany

VERLAG ULRICH E. GRAUER
Linsenhofer Str. 44, 72660 Beuren, Germany
Tel. +49 (0)7025 842140, Fax +49 (0)7025 842499
Internet: http://www.grauer.de/, E-Mail: grauer@grauer.de

Selbständigkeitserklärung

Hiermit erkläre ich, daß ich die vorliegende Arbeit selbständig und nur unter Verwendung der angegebenen Literatur und Hilfsmittel angefertigt habe.

Stuttgart, den 30.10.2007 M. Sc. Mutasem Bani Fwaz

Die vorliegende Arbeit wurde am
Institut für Anorganische Chemie
der Universität Stuttgart
unter der Leitung von Herrn Professor
Dr. Gerd Becker angefertigt.

Meinem Doktorvater,
Herrn Prof. Dr. Gerd Becker,
danke ich herzlich für die Themenstellung,
die Bereitstellung ausgezeichneter
Arbeitsbedingungen, wertvolle
Anregungen und Diskussionen sowie sein stetes
Interesse an dieser Arbeit.

Meinen Eltern,
meiner Schwester und meinen Brüdern,
meiner Frau,
meinen Söhnen und meinen Töchtern
gewidmet

Exposé for the Dissertation
“Unusual Phosphorus Oligocycles from $1\lambda^3$-Phosphaalkynes and Various Halides of Group 13 and 15 Elements”

This work has involved the reaction of kinetically stable $1\lambda^3$-phosphaalkynes, R–C≡P, with dialkylaluminium chlorides, halodiorganylphosphines and dichloro(dialkylamino)arsines in order to study the influence of alkyl and aryl groups in various mixed organyl halides of group 13 and 15 elements on reaction routes and unusual phosphorus oligocyclic molecular structures that could be isolated and characterized by spectroscopic methods, X-ray structure analysis as well as theoretical investigations. When mixtures of 2-*tert*-butyl- or 2-(1-adamantyl)-$1\lambda^3$-phosphaalkyne and slightly more than three equivalents of dialkylaluminium chloride are allowed to warm up to room temperature, the 1:2 insertion products, bridged by a third chloroalane molecule, precipitate in high yields. In these compounds **1**, dative bonding between phosphorus or chlorine as a donor and aluminium as an acceptor atom is reponsible for the formation of the bicyclic dialkyl[bis(alkylchloroalanyl)organylmethyl]phosphine•di-alkylchloroalane (1/1) complexes. From reactions of various halodiorganylphosphines, ionic compounds with a 2,4-di-*tert*-butyl-3,3-diorganyl-$1\lambda^3,5\lambda^3$-diphospha-3-phosphoniatricyclo-[2.1.0.0^{2,5}]pentane cation (**2**) could be isolated and characterized by spectroscopic methods and X-ray structure analysis; remarkably the P–P bond (213 pm) was found to be rather short with respect to the standard value (221 pm).

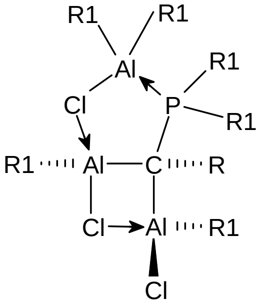

1

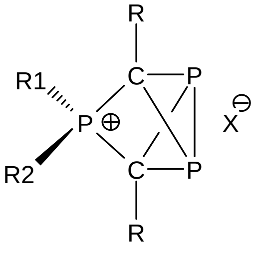

2

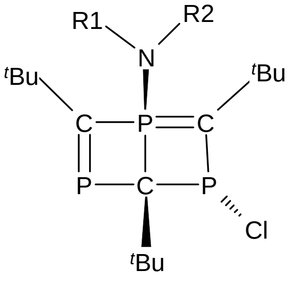

3

The reactions of various dichloro(dialkylamino)arsines take quite a different route in that the rather unusual oligocycle 2,4,6-tri-*tert*-butyl-3-chloro-1-dialkylamino-$1\lambda^5\sigma^4,3\lambda^3\sigma^3,5\lambda^3\sigma^2$-triphosphabicyclo[2.2.0]hexa-1,5-diene (**3**) – an ylide with an unusually long P–Cl bond (245.5 pm) – could be isolated. Furthermore, while investigating the suitability of various starting compounds, dichloro[4-(dimethylamino)phenyl]arsine (**4**) and tris[4-(dimethyl-amino)phenyl]arsine (**5**) were obtained by the action of *N*,*N*-dimethylaniline on arsenic(III) chloride, both of which had been made directly by a one-step reaction to give the first product (**4**) in high yield and free from hydrochloride and the second product (**5**) in a moderate yield; both crystal structures were solved for the first time and are presented here.

Contents

List of symbols and abbreviations

J	coupling constant
δ	chemical shift
$\tilde{\nu}$	wave number
Ad, 1-Ad	1-adamantyl
b.p	boiling point
n-Bu	*n*-butyl
^{t}Bu	*tert*-butyl
°C	degree celcius
Cp*	pentamethylcyclopentadienyl
conc.	concentrated
CDNB	1-cyno-3,5-dinitrobenzene
DME, dme	1,2-dimethoxyethane
DMSO	dimethylsulfoxide
DMT	*N*,*N*-dimethyl-*p*-toluidine
DFT	density functional theory
DABCO	1,4-diazabicyclo[2.2.2]octane
DBU	1,8-diazabicyclo[5.4.0]undec-7-ene
d	doublet
dd	doublet of doublet
ddd	doublet of doublets of doublets
eq.	equivalent
Et	ethyl
FA	fluoranil (2,3,5,6-tetrafluoro-*p*-chinone)
GED	gas electron diffraction
h	hour
HFB	hexafluorobenzene
IR	Infrared spectroscopy
^{i}Pr	*iso*-propyl
K	Kelvin temperature
MHz	Mega Herz
m.p	melting point

mmol	millimol
Me	methyl
Mes	2,4,6-trimethylphenyl
Mes*	2,4,6-tri-*tert*-butylphenyl
m	multiplet
NBO	natural bond orbital
NMR	nuclear magnetic resonance
Ph	phenyl
p-Tolyl	*para*-tolyl; 4-methylphenyl
pm	picometer
q	quartet
r.t	room temperature
R	Raman spectroscopy
R_f	2,4,6-tris(trifluoromethyl)phenyl
s	singlet
t	triplet
TCB	1,2,4,5-tetracyanobenzene
THF	tetrahydrofuran
XRD	X-ray diffraction

1. Introduction

1.1. Preparation of 1λ³-Phosphaalkynes

Methylidynephosphine, H–C≡P, the parent compound of 1λ^3-phosphaalkynes containing a triple bond between phosphorus and carbon, was first proposed by *Albers* in 1950 [1]. More than ten years later *Gier*, an industrial chemist at *Du Pont*, reported the formation of minor amounts from phosphine in an electric discharge between graphite electrodes and an isolation by trapping the volatile products under reduced pressure at low temperature [2]. This discovery which clearly established that systems with a carbon-phosphorus $2p_\pi(C)$-$3p_\pi(P)$-triple bond could indeed exist, signaled the start of the chemistry of low coordinated phosphorus compounds.

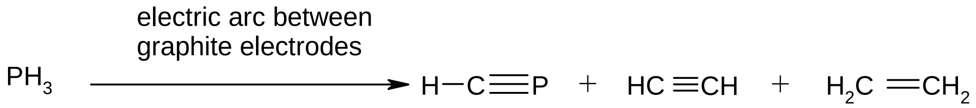

I

As to the formation of the parent compound H–C≡P, it is noteworthy that in 1992 *Mathey* and co-workers found a new access. This research group had started with the flash vacuum thermolysis (FVT) of 1-vinylphosphirane at 700 °C which produced ethylidyne-phosphine (1λ^3-phosphapropyne), presumably via rearrangement of vinylphosphinidene formed first [3].

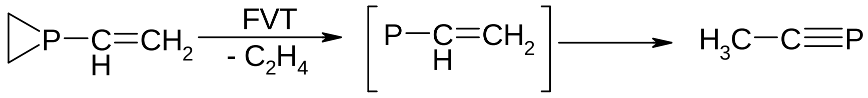

Only one year later, *Mathey* and *Le Floch* reported on an analogous preparation of H–C≡P but now via a flash vacuum thermolysis of triallylphosphine at 700 °C and a pressure of 10^{-3} Torr. Surprisingly, methylidynephosphine was formed as the major product which could be purified by trap-to-trap distillation [4, 5]. Several compounds, however, were observed as by-products, the two major ones are the parent λ^3-phosphinine C_5H_5P and its 3-methyl derivative. The analogous thermolysis of diallylvinylphosphine resulted in the almost exclusive formation of the unsubstituted λ^3-phosphinine C_5H_5P.

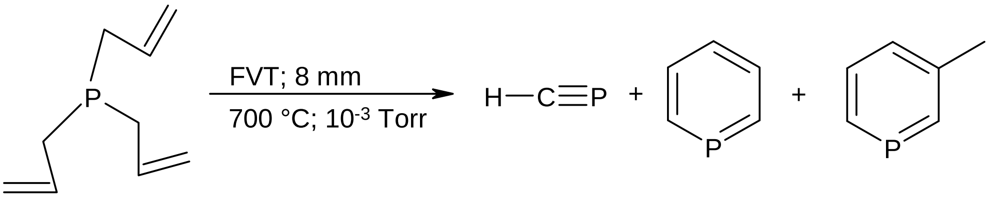

$1\lambda^3$-Phosphaalkyne H–C≡P is a colourless gas, stable only under vacuum and at low temperature. Whereas *Gier's* product has been reported to polymerize at temperatures above –124 °C, *Mathey's* $1\lambda^3$-phosphaethyne can be stored for long periods of time in solution, preferably in toluene or benzene at –80 °C, without apparent decomposition. A reason for this increased stability might be the absence of traces of impurities.

Several kinetically unstable $1\lambda^3$-phosphaalkynes R–C≡P were obtained by stripping two equivalents of hydrogen chloride from substituted organyl dichlorophosphines $R{-}CH_2{-}PCl_2$ (R = H, 25-30% yield [6-9]; Me 8-30% yield [9-12]) or from substituted 1,1-dichloroorganylphosphines $R{-}CCl_2{-}PH_2$ (R = H, Me, Et, ^{n}Bu, Me_3Si, Cl) [13]. All yields with 1,1-dichloroorganylphosphines as starting compounds were in the 60 to 80% range, and the method is undoubtly an advance in the synthesis of short-lived $1\lambda^3$-phosphaalkynes.

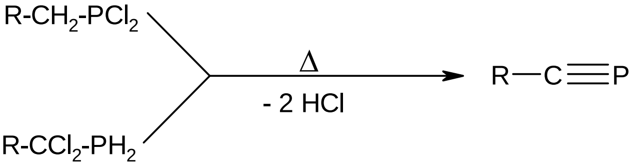

Another method to prepare methylidynephosphine has been detected in the pyrolysis of 2-*tert*-butyl-$1\lambda^3$-phosphaalkyne at 950 °C and a pressure of $5 \cdot 10^{-4}$ mbar [8] or of cyclopropylphosphirane at 700 °C and $1.7 \cdot 10^{-3}$ mbar [14].

Furthermore, $1\lambda^3$-phosphaalkynes $R{-}CH_2{-}C{\equiv}P$ (R = H, Me, Ph) with substituents bearing primary carbon atoms adjacent to the P≡C unit were prepared in good yields by low-temperature Lewis base induced rearrangement of primary ethyn-1-ylphosphines; the mechanism involves a *P*-unsubstituted $1\lambda^3$-phosphaallene intermediate [15]. Remarkably, the starting compounds are accessible via a reduction of the corresponding phosphonates with $AlHCl_2$ [16].

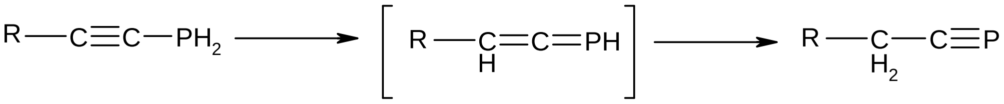

Another elimination route to generate the P≡C group represents the stripping of one or two equivalents of chlorotrimethylsilane from either a suitable 1λ^3-phosphaalkene [17, 18] or dichloro[tris(trimethylsilyl)methyl]phosphine [19]. A detailed description for the synthesis of the latter compound and its thermal conversion to chloro[bis(trimethylsilyl)methylidene]-phosphine can be found in Science of Synthesis [20].

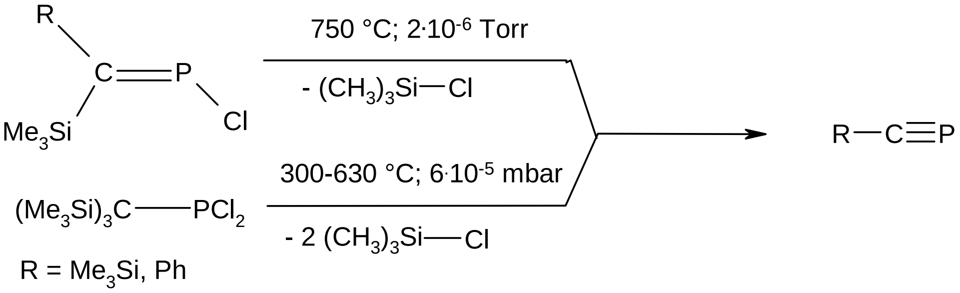

A combined method involving hydrogen chloride abstraction with 1,4-diazabicyclo[2.2.2]octane (DABCO) first and subsequent thermal elimination of chlorotrimethylsilane to give 2-trimethylsilyl-1λ^3-phosphaalkyne from bis(trimethylsilyl)-methyldichlorophosphine has been reported by *Appel* and *Westerhaus* [18].

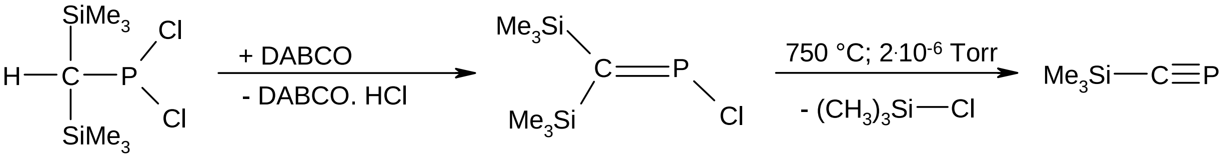

Pyrolysis of di-*tert*-butyl[diazo(trimethylsilyl)methyl]phosphine [19] or 1-[diazo-(trimethylsilyl)methyl]phosphirane [21] led to the formation of trimethylsilyl-1λ^3-phosphaalkyne, too.

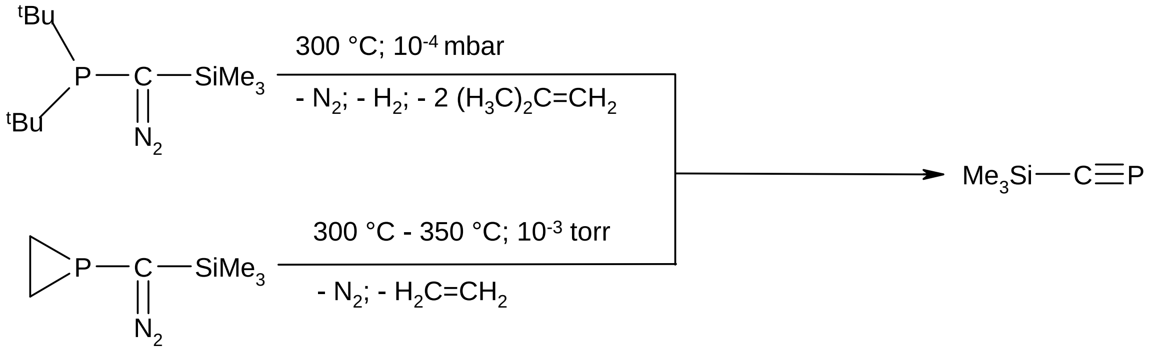

As can be taken from a short publication by *Niecke* and others [22] this 1λ^3-phosphaalkyne is also formed from triphenylphosphine stablized bis(trimethylsilyl)methylidenephosphenium trifluoromethylsulfonate. Unfortunately yields have not been given for the synthesis of such an important compound.

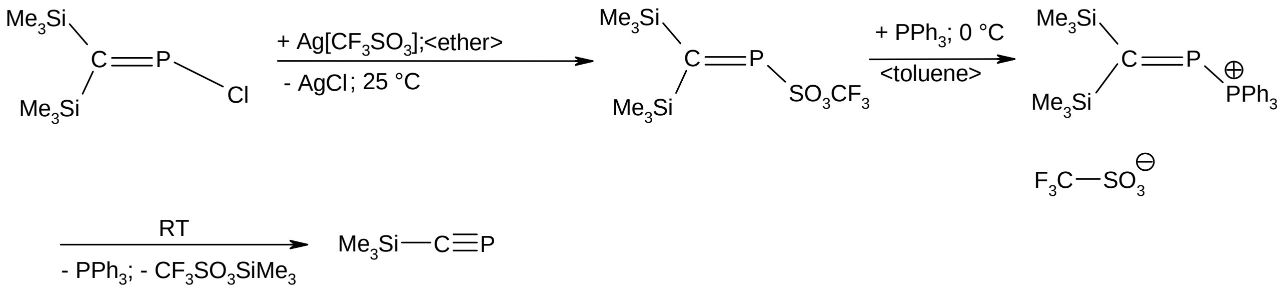

Available information about the synthesis of trifluoromethyl-1λ^3-phosphaalkyne is extremely scanty. The compound has been obtained by the pyrolysis of pentafluoroethylphosphine [10].

$$CF_3\text{-}CF_2\text{-}PH_2 \xrightarrow[-\ 2\ HF]{\Delta} CF_3\text{—}C\equiv P$$

A simple route to kinetically unstablized 1λ^3-phosphaalkynes in 20 to 81% yield is made feasible by a hydrogen chloride elimination of 1,1-dichloroorganylphosphines with the strong lewis base 1,8-diazabicyclo[5.4.0]undec-7-ene (DBU) at low temperature [23].

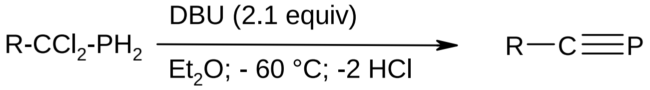

$$R\text{-}CCl_2\text{-}PH_2 \xrightarrow[Et_2O;\ -60\ °C;\ -2\ HCl]{DBU\ (2.1\ equiv)} R{-}C{\equiv}P$$

R = H, Me, Et, ^{n}Bu, $(CH_2)_2Ph$,
$CH_2CH{=}CH_2$, $(CH_2)_2CH{=}CH_2$, C_6H_{11}

In general the aforementioned procedures are not appropriate to obtain 1λ^3-phosphaalkynes in preparative amounts. Therefore, the decisive breakthrough in the chemistry of these compounds was the synthesis of the thermally high stable 2-*tert*-butyl derivative (**II**) by *Becker*, *Gresser* and *Uhl* [24]. Thereafter a rapid development in this as yet scarcely studied field began. The results of these investigations on compounds typically provided with bulky substituents at carbon are summarized in several reviews and articles [24-41]. Among those 2-alkyl- and 2-aryl-1λ^3-phosphaalkynes which are kinetically highly stablized, the adamantly (**III**) [28], the 2,4,6-tri-*tert*-butylphenyl (Mes*) [30] and the 2,4,6-trimethylphenyl (Mes) derivative (**IV**) [38] also deserve special attention.

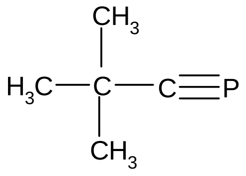

II

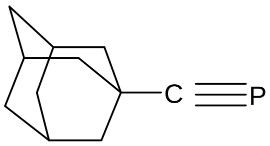

III

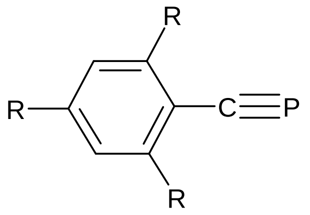

IV [R = H_3C, $(H_3C)_3C$]

The synthesis of 2-organyl-1λ^3-phosphaalkynes starts from tris(trimethylsilyl)phosphine which is isolated in high yield from the reaction of sodium/potassium alloy with white [33] or red [42] phosphorus in 1,2-dimethoxyethane followed by addition of a slight excess of chlorotrimethylsilane. In an alternative preparation, the more reactive complex bis(tetrahydrofuran)lithium bis(trimethylsilyl)phosphanide might be applied; it is obtained quantatively from the reaction of tris(trimethyl)phosphine with various organolithium reagents [33]. Treatment of either compound with acyl halides results in the formation of acylbis(trimethylsilyl)phosphines. These phosphines are thermally unstable and rearrange at room temperature via 1,3-migration of one trimethylsilyl group from phosphorus to oxygen to give the corresponding *E/Z*-1λ^3-phosphaalkenes. The final elimination of hexamethyldisiloxane is catalyzed by small pieces of solid sodium hydroxide and furnishes the corresponding 1λ^3-phosphaalkynes in very high yields (Scheme 1.1).

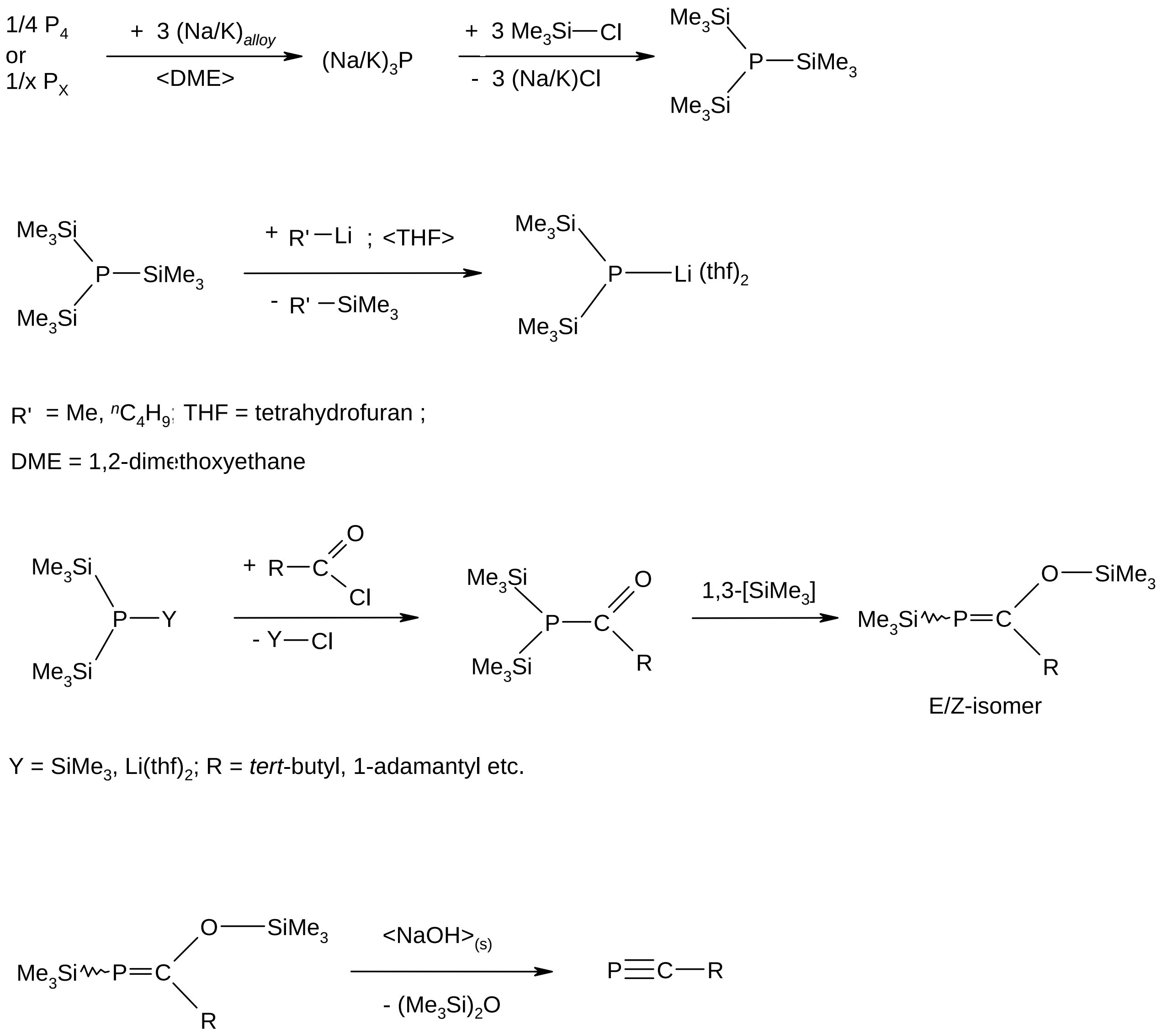

R' = Me, $^{n}C_4H_9$; THF = tetrahydrofuran ;

DME = 1,2-dimethoxyethane

Y = $SiMe_3$, $Li(thf)_2$; R = *tert*-butyl, 1-adamantyl etc.

Scheme 1.1

A new and completely unexpected access to 2-*tert*-butyl- and 2-(1-admantyl)-1λ^3-phosphaalkyne stems from research in transition metal chemistry. *Figueroa* and *Cummins* [43] treated the anion of phosphinidene tris[(3,5-dimethylphenyl)neopentylamino]niobium with the corresponding acyl chloride and succeeded in the isolation and characterization of complexces featuring a four-membered Nb–P=C–O heterocycle. Thereafter, these compounds were shown to cleave thermally when the temperature was elevated slowly and to furnish the 1λ^3-phosphaalkyne within several hours.

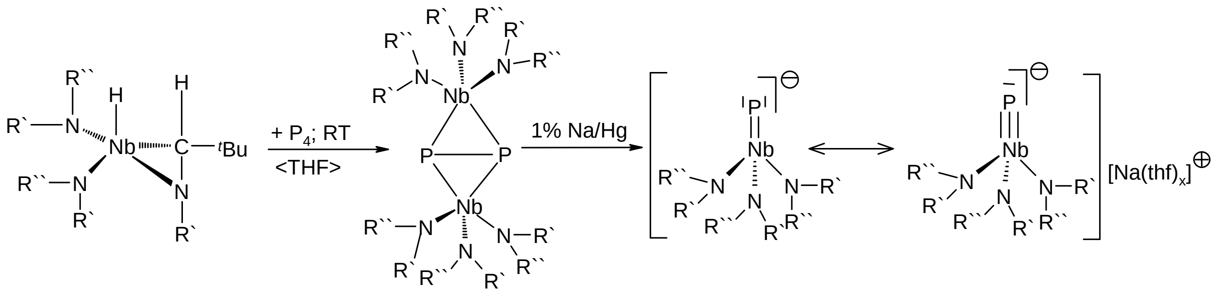

R` = 3,5-dimethylphenyl; R`` = neopentyl ; THF = tetrahydrofuran

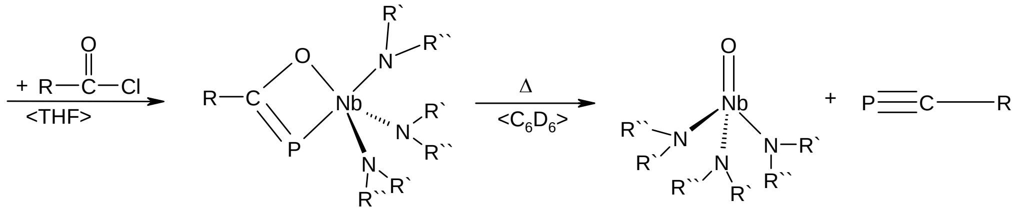

R = *tert*-butyl, 1-adamantyl

Among heteroatom-substituted 1λ^3-phosphaalkynes the majority of compounds has been obtained and characterized only in recent years. They were prepared according either to the following or to similar equations (see below), but some of these compounds such as the fluorine derivative reported already in 1978 [44-46] or the triisopropylsiloxy derivative [47, 48] are thermally unstable.

$$CF_3-PH_2 \xrightarrow[-\,2\ HF]{<KOH>_S;\ RT} F-C\equiv P$$

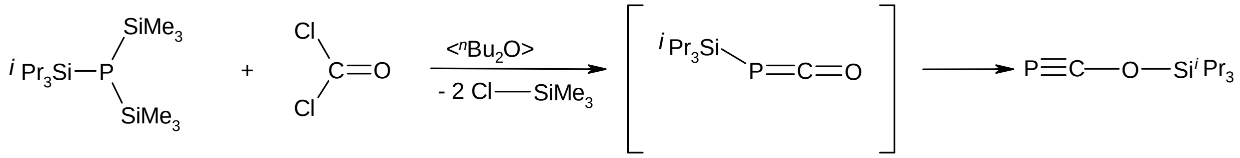

Very surprisingly, the reaction of dimethyl or diethyl carbonate with lithium bis(trimethylsilyl)phosphanide furnishes the corresponding alkoxytrimethylsilane and the air and moisture sensitive 1λ^3-phosphaalkyne (dme)$_2$Li–O–C≡P [49, 50].

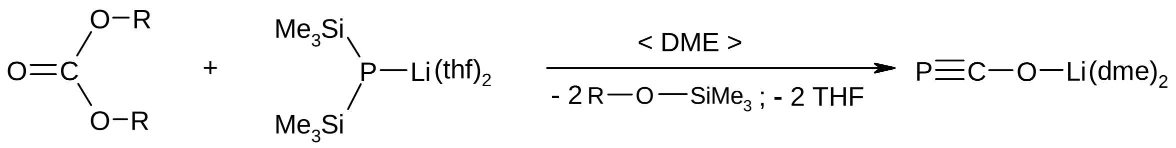

R = CH_3, C_2H_5;
DME = 1,2-dimethoxyethane;
THF = tetrahydrofuran

The sulfur derivative $[(dme)_3Li]^{\oplus}[S{-}C{\equiv}P]^{\ominus}$ was prepared similarly from *O,O'*-diethyl thiocarbonate [51].

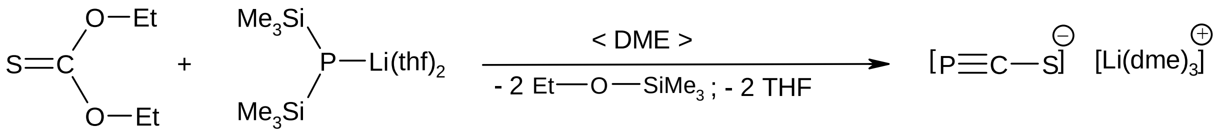

DME = 1,2-dimethoxyethane;
THF = tetrahydrofuran

Unfortunately, the high reactivity of these $1\lambda^3$-phosphaalkynes restricts the scope of investigations into their chemistry. Very recently the compounds $[Ph_4P]^{\oplus}[(F_3C)_3B{-}C{\equiv}P]^{\ominus}$ and $[Ph_4P]^{\oplus}[(F_3C)_3B{-}C{\equiv}As]^{\ominus}$ [52] have been reported; their unusually high thermal stability will probably open a new chapter in $1\lambda^3$-phosphaalkyne and $1\lambda^3$-arsaalkyne chemistry.

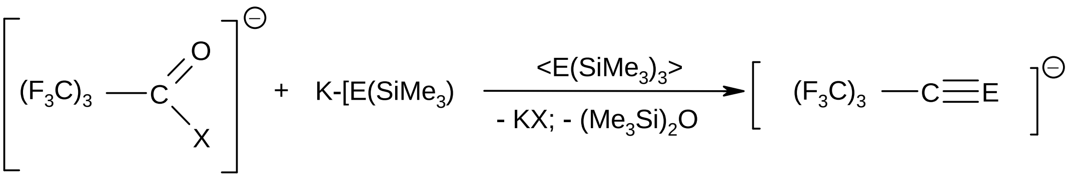

X = Cl, Br ; E = P, As

Heteroatom-substituted $1\lambda^3$-phosphaalkynes with an amino group at carbon are known to have quite a different reactivity when compared to the alkyl and aryl substituted derivatives. This property may be attributed to the influence of the nitrogen lone pair on the charge distribution in the multiple bond [53, 54]. Up to now only a small number of those $1\lambda^3$-phosphaalkynes have been reported, namely the 2-(2,2,6,6-tetramethylpiperidino) (scheme 1.2) [55, 56],

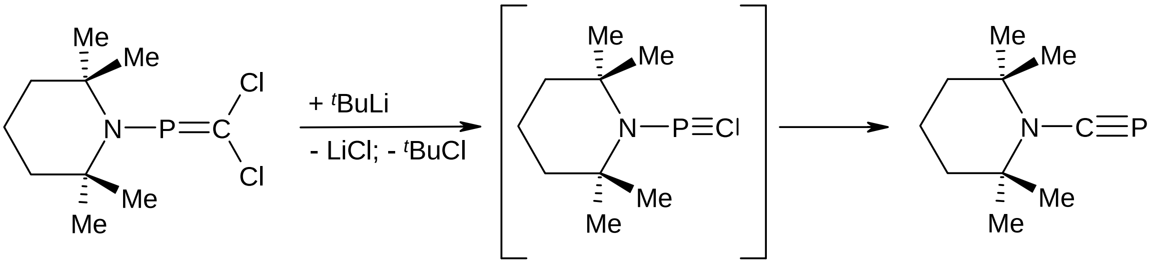

Scheme 1.2

the thermally unstable 2-(diisopropylamino) (scheme 1.3) [57, 58] and the 2-(isopropyl-trimethylsilyl)amino derivative (scheme 1.4) [59].

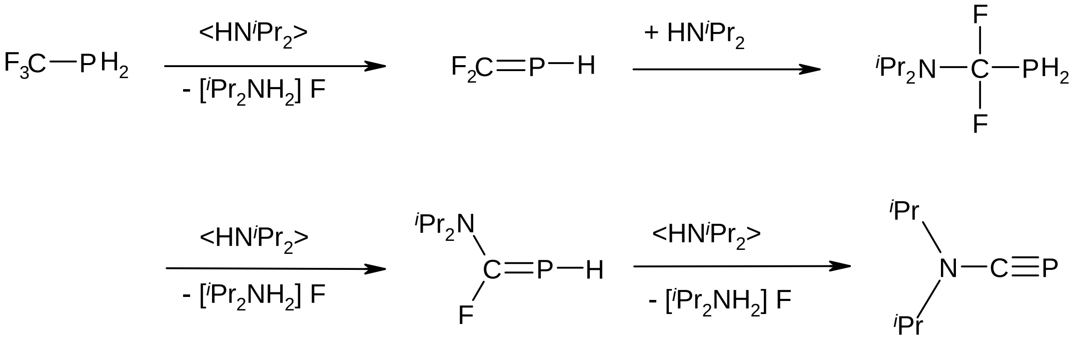

Scheme 1.3

The high thermal stability of 2-(isopropyltrimethylsilyl)amino-1λ^3-phosphaalkyne ^{i}Pr(Me$_3$Si)N–C≡P, prepared from tris(trimethylsilyl)phosphine and isopropyl isocyanate via addition and ZnCl$_2$-catalyzed elimination of hexamethyldisiloxane and characterized by low-temperature X-ray structurel analysis, allows a reaction with potassium *tert*-butoxide to form potassium 1-isopropyl-1-aza-3λ^3-phosphaallen-3-ide K[^{i}Pr–N=C=P]. The compound formed was isolated and characterized as the [18]crown-6 ether complex and exhibits high, but different reactivity toward for example chlorotriorganylsilanes R$_3$SiCl and triorganylstannanes R$_3$SnCl [59].

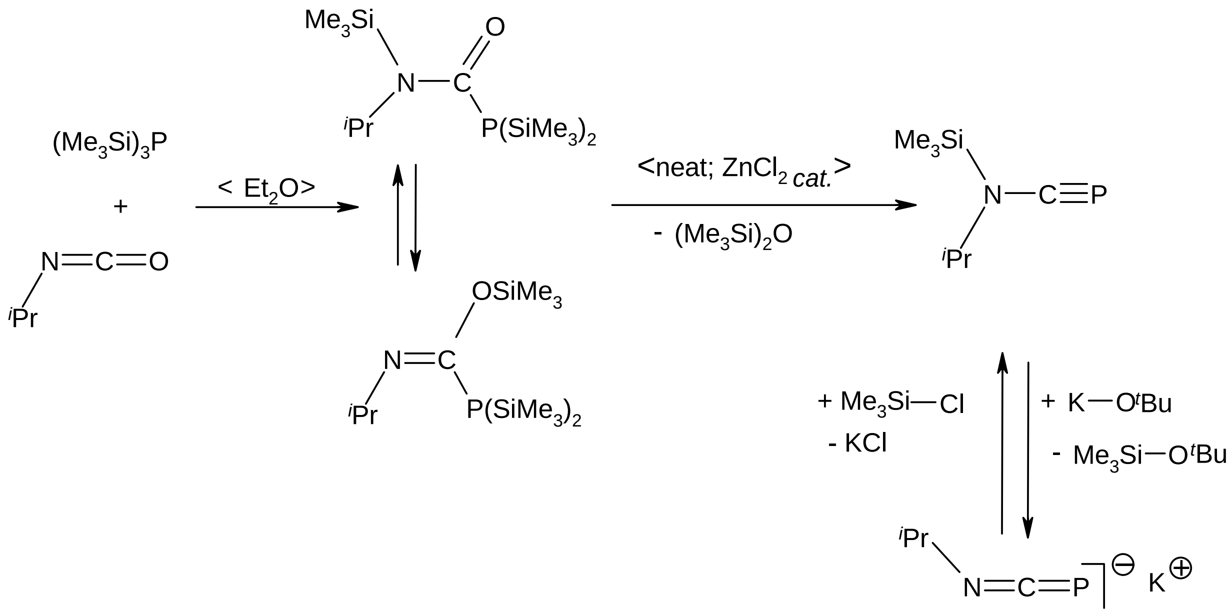

Scheme 1.4

The results of an X-ray structure determination show the bond length to be intermediate between those expected for an 1-aza-3λ^3-phosphaallen-3-id and an 3λ^3-phosphaalkynylamide.

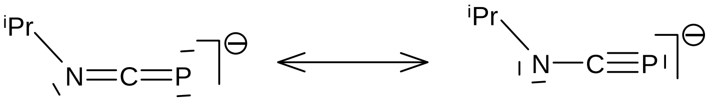

1.2. Some Aspects of $1\lambda^3$-Phosphaalkyne Reactivity

Since the electronegativity values of phosphorus (2.06) and carbon (2.50) [60] differ only slightly, $1\lambda^3$-phosphaalkynes exhibit a relatively unpolar P≡C triple bond. Therefore, their chemical reactivity is in many aspects similar to that of alkynes and differs considerably from that of the homologous nitriles.

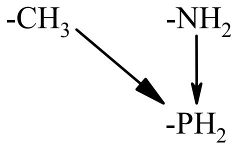

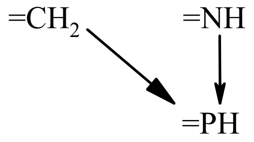

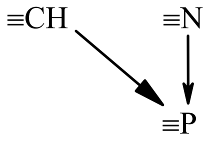

Furthermore, *R. Hoffmann's* isolobal relationship [61] shows also in principle the interchangeability of the fragments ≡CH and ≡P. Thus it is not too surprising that for example the oligomers of $1\lambda^3$-phosphaalkynes often resemble very strongly their totally organic root compounds.

From a very elementary point of view, $1\lambda^3$-phosphaalkynes are expected to dimerize to different types of heterocycles, namely $1\lambda^3,2\lambda^3$-diphosphatetrahedranes **V** [62, 63] as well as $1\lambda^3,2\lambda^3$-diphospha- (**VI** [64]) and $1\lambda^3,3\lambda^3$-diphosphacyclobutadienes **VII** [62-66]. These compounds are not known in the free stable; they are, however, often assumed to be intermediates leading to higher aggregates in oligomerization reactions [64-69]. Remarkably, the diphosphacyclobutadienes (diphosphetes) show a relatively high stability as ligands in transition metal complexes [70-72].

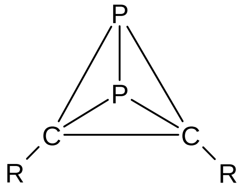

V

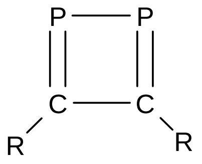

VI

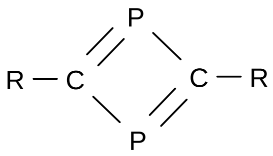

VII

Binger and co-workers were the first to obtain thermally stable 2,4,6-tri-*tert*-butyl-$1\lambda^3,3\lambda^3,5\lambda^3$-triphospha-dewar benzene **VIII** and 2,4,6-tri-*tert*-butyl-$1\lambda^3,3\lambda^3,5\lambda^3$-triphosphabenzene **IX** as the first stable examples of $1\lambda^3$-phosphaalkyne trimers in the free state [68].

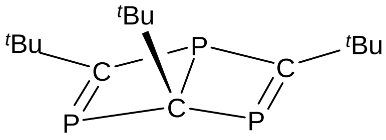

VIII

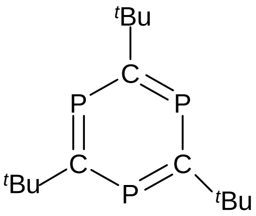

IX

Tetramerization of 2-*tert*-butyl-$1\lambda^3$-phosphaalkyne leads to different P–C cage compounds, one of which is the highly symetrical 2,4,6,8-tetra-*tert*-butyl-$1\lambda^3$,$3\lambda^3$,$5\lambda^3$,$7\lambda^3$-tetraphosphacubane **X**. This compound exhibits fascinating spectroscopic and structural features resulting from a unique bonding situation, in which the strong interaction of the lone pair electrons at phosphorus with the σ*(P–C) antibonding orbitals of the cube reduces the nucleophilicity of the phosphorus atoms considerably [62, 63, 65, 66]. This heterocycle was also isolated by *Merz* in more than 80% yield as a solid state adduct with the solvent benzene, after a solution of ten equivalents of 2-*tert*-butyl-$1\lambda^3$-phosphaalkyne had been treated with one equivalent of bis(dichloroarsanyl)methane at room temperature [73]. Further tetramers are the bishomoprismane **XI** [66, 74], the cuneane **XII** [66, 75], if the loss of an *iso*-butene unit is disregarded, the $1\lambda^3$,$2\lambda^3$,$4\lambda^3$,$7\lambda^3$-tetraphospha- (**XIII** [64]) and the $1\lambda^3$,$2\lambda^3$,$5\lambda^3$,$6\lambda^3$-tetraphosphatricyclo[4.2.0.0^{2,5}]octadiene (**XIV**) as well as the $1\lambda^3$,$3\lambda^3$,$5\lambda^3$,$7\lambda^3$-tetraphosphabarrelene **XV** [64]. In addition the pentamer **XVI** [76-78] and the hexamer **XVII** [79] are also known; they represent the largest oligomers reported so far. Definitely, these investigations show $1\lambda^3$-phosphaalkynes R–C≡P to be ideal starting materials for the formation of organophosphorus cage compounds as a result of their enormous potential for cycloaddition and cyclooligomerization reactions.

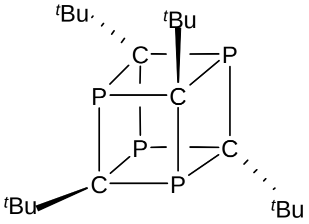

X

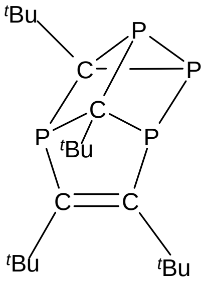

XI

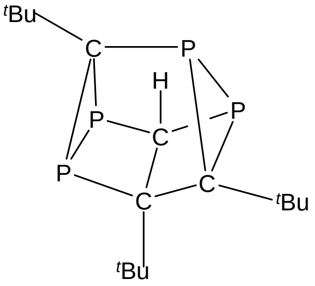

(loss of $H_2C{=}CMe_2$)

XII

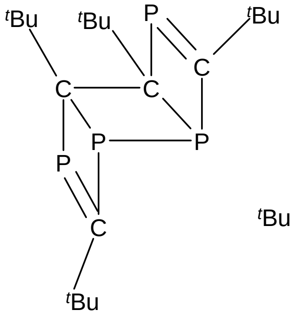

XIII

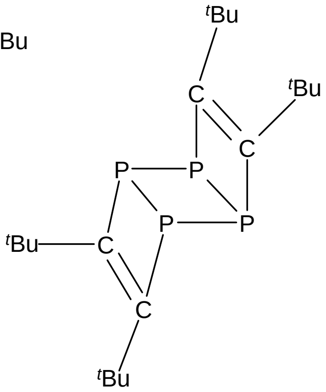

XIV

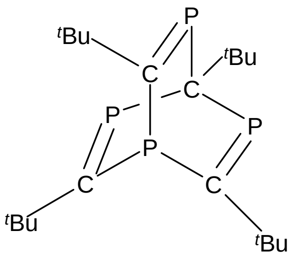

XV

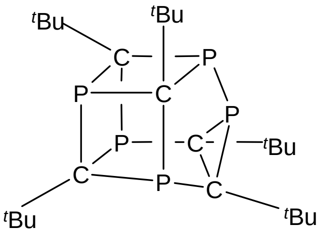

XVI

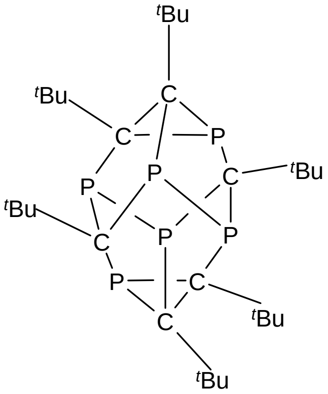

XVII

Becker and co-workers [37, 80-82] were the first who examined the insertion reactions of 1λ^3-phosphaalkynes with halides of different main group elements. Very often, the λ^3-phosphaalkene formed first cannot be isolated since subsequent cycloaddition reactions, rearrangements and the formation of phosphorus oligocyclic cage compounds take place. In this introduction we give only a short survey, refer to some unusual phosphorus heterocycles obtained from 1λ^3-phosphaalkynes and various halides of group 13 to 15 elements and postpone a detailed discussion to the following chapters. Many of the compounds mentioned here could be isolated and characterized by spectroscopic methods, X-ray structure analyses and theoretical investigations. Fortunately, based on detailed investigations by several co-workers of our group, a general reaction scheme may now be outlined explaining even the formation of rather complicated cages (Scheme 1.5).

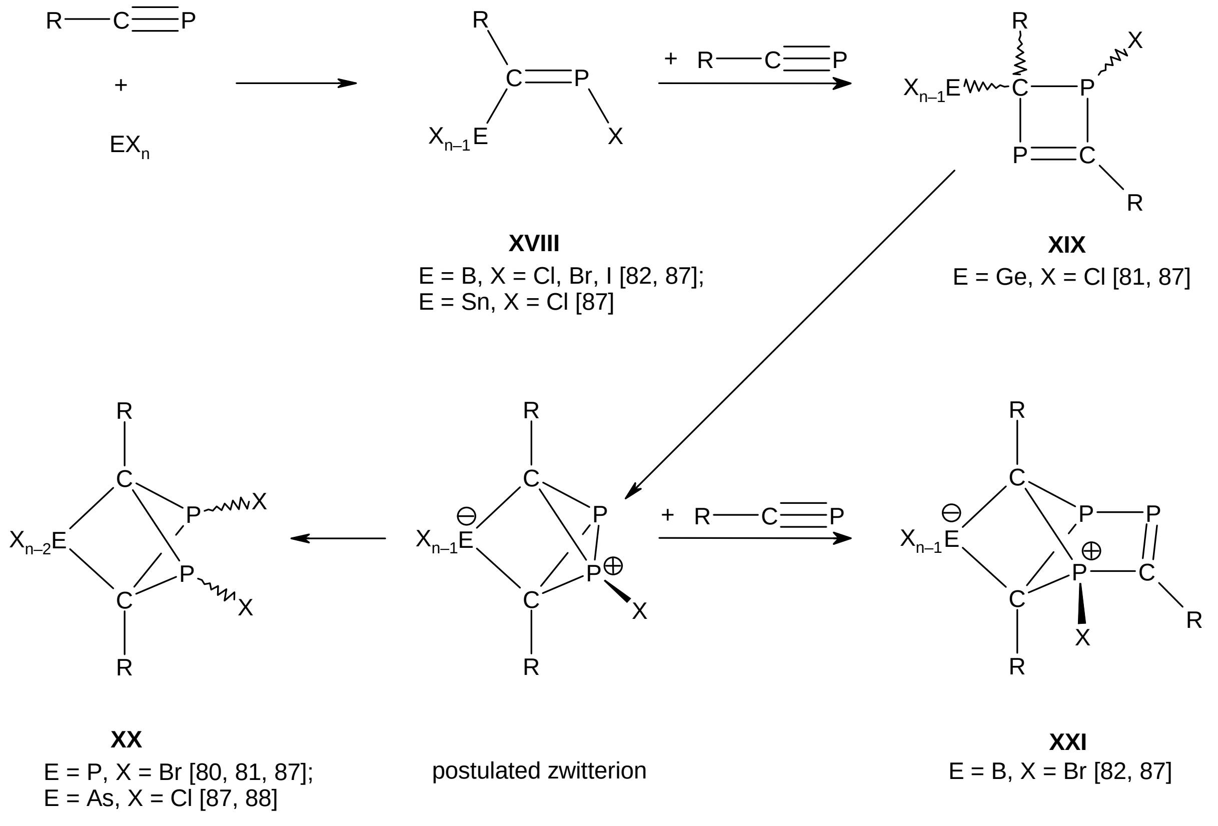

XVIII
E = B, X = Cl, Br, I [82, 87];
E = Sn, X = Cl [87]

XIX
E = Ge, X = Cl [81, 87]

XX
E = P, X = Br [80, 81, 87];
E = As, X = Cl [87, 88]

postulated zwitterion

XXI
E = B, X = Br [82, 87]

Scheme 1.5

As can be taken from scheme 1.5, variations depending upon the nature of the main-group element E itself and the substituents attached to it are possible. In a first step the P≡C unit of the 1λ^3-phosphaalkyne inserts into the element–halogen bond to furnish the λ^3-phosphaalkene **XVIII**. Up to now it is unknown whether the initial attack occurs at phosphorus, the π system of the triple bond or even at carbon, and whether or not a Lewis acid-base complex is formed as an intermediate. In any case, the organic substituent R and the halogen atom X are usually found in a *trans* position at the C=P bond. Subsequent [2+2]cycloaddition of a second 1λ^3-phosphaalkyne molecule affords the 1,2-dihydro-1λ^3,3λ^3-diphosphete **XIX**; a compound of this type is the final product in the reaction of 2-*tert*-butyl-1λ^3-phosphaalkyne and germanium(IV) chloride [81, 87]. If in the 1,2-dihydro-1λ^3,3λ^3-diphosphete the Lewis acidity of the exocyclic EX_{n-1} group is sufficiently high, a transannular electrophilic attack at the *sp*^{2}-hybridized carbon follows to leave a halogen-substituted, positively charged phosphorus atom as part of a postulated zwitterion. Further stabilization is achieved either by a 1,3-migration of a halide anion from element E to phosphorus or by the addition of a third 1λ^3-phosphaalkyne molecule to furnish the 2-elementa-4λ^3,5λ^3-diphosphabicyclo[1.1.1]pentane **XX** [80, 81, 87, 88] or the 7-elementa-2λ^3,3λ^3,5λ^5-triphosphatricyclo[3.2.0.0^{2,6}]hept-3-ene-5-ium-7-uide **XXI** [82, 87], respectively. In both reactions the P–P bond of the still undetected intermediate is cleaved.

In the present dissertation further reactions of 2-*tert*-butyl- and 2-(1-adamantyl)-1λ^3-phosphaalkyne with several chloroorganylalanes, -phosphines and dichlorodialkylamino-arsines were performed. We start with a description of our investigations on aluminium compounds.

2. Reactions of 1λ^3-Phosphaalkynes with Dialkylaluminium Chlorides

2.1. Introduction

As already discussed at some length in Chapter one, 1λ^3-phosphaalkynes feature a chemical reactivity which resembles much more that of organic alkynes than that of the homologous nitriles. Since organic alkynes are known to undergo insertion reactions readily with a variety of boranes [89-92] furnishing carborane clusters, the formation of analogous phosphacarborane clusters has to expected using 1λ^3-phosphaalkynes as starting materials. Indeed, *Paetzold* and co-workers [93] have shown that the reaction of 2-*tert*-butyl-1λ^3-phosphaalkyne with the bis(dimethylsulfane) adduct of decaborane [$B_{10}H_{12}(SMe_2)_2$] gives the remarkable product [$B_{10}H_{11}(SMe_2)$][^{t}BuCPH][$B_{10}H_{12}$] in which a partially hydroborated phosphaalkyne bridges two decaborane units.

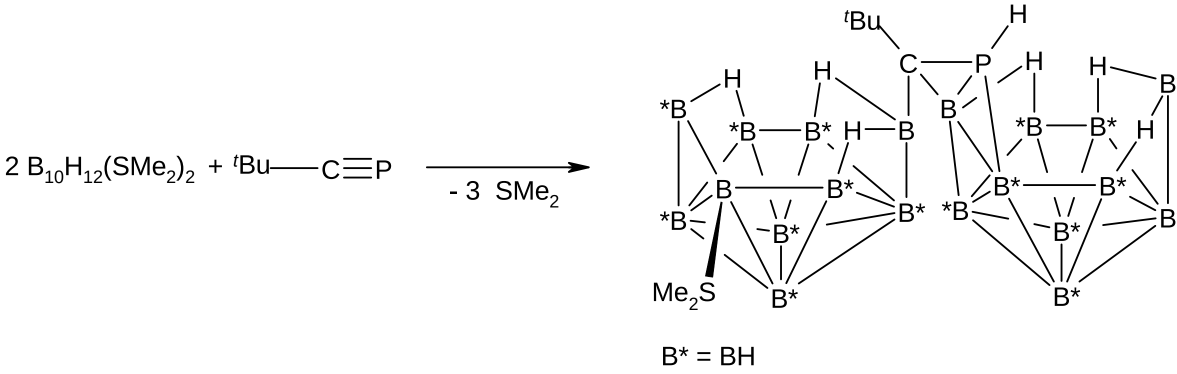

Unbridged clusters of the type *nido*-R–CHP$B_{10}H_{13}$ were isolated from the reaction of 2-*tert*-butyl- or 2-(1-adamantyl)-1λ^3-phosphaalkyne with the bis(acetonitrile) adduct of decaborane [$B_{10}H_{12}(CH_3CN)_2$] [94]. When, however, tetraborane(10) is used as starting material in a gas-phase reaction, 2-*tert*-butyl-1λ^3-phosphaalkyne forms the *nido* five-vertex phospha-carbaborane cluster 2-^{t}Bu-1,2-PCB_3H_5 [95].

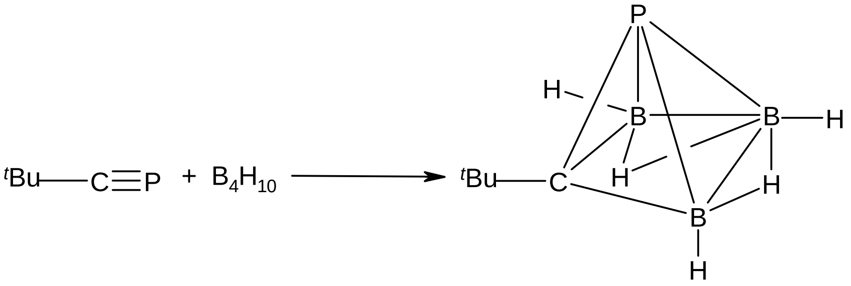

Finally, *Ionkin* et al. [96] studied the insertion of the P≡C fragment into the B–H bond of the following monoborane derivative which resulted in the synthesis of a substituted 1,1-alkyldiboranylphosphine.

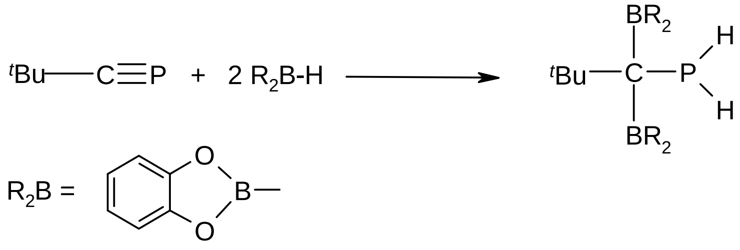

In contrast to investigations on B–H compounds just described, the reactivity of 1λ^3-phosphaalkynes towards halides of group 13 elements is much better known. For a deeper understanding, however, the well-known reactions of alkynes with halides of the main group elements boron [97] and aluminium [98, 99] have to be considered first. Here, only simple insertion and [2 + 2] addition reactions have been observed.

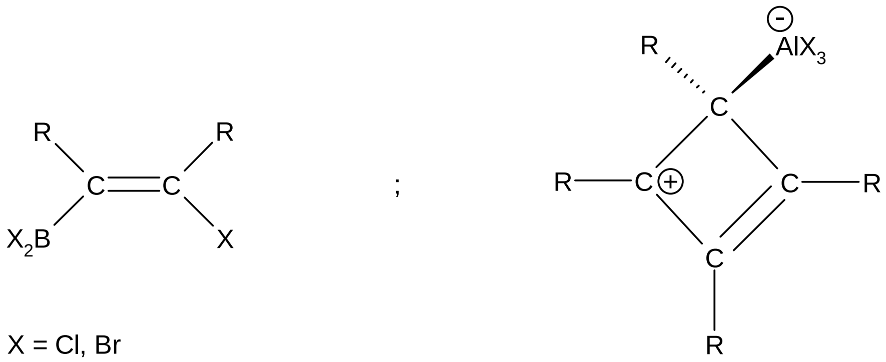

The reactions of 1λ^3-phosphaalkynes have been found to start in an analogous way but further insertion and addition reactions lead to much more complicated compounds. To begin with boron(III) chloride, bromide and iodide, solutions of these compounds react smoothly at ambient temperature with 2-*tert*-butyl-1λ^3-phosphaalkyne in hydrocarbon solvents to give the corresponding 1-halogen-2-dihalogenoboranyl-1λ^3-phosphaalkenes as the *E*-isomers first. These compounds are the result of an intermolecular insertion of the P≡C unit into only *one* of several element halogen bonds. The direction of addition follows the electronegativity values of phosphorus and carbon in that an element–carbon bond is formed as a consequence of the higher value for carbon (2.50 *vs.* 2.06) [60].

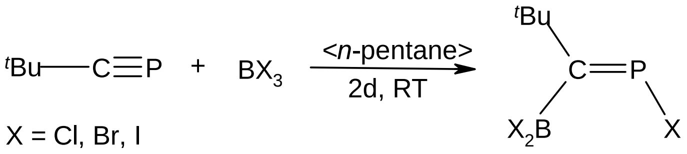

For example such an insertion compound was obtained for the first time from the reaction of boron(III) bromide and isolated as colourless needles from a liquid. It exhibits an $^{11}B\{H\}$ resonance at 55.9 ppm and feature low-field shifts of both the phosphorus (262.0 ppm) and the *sp*^{2}-hybridized carbon atoms (218.0 ppm) which indicate the presence of a P=C double bond. Furthermore, δ $^{31}P\{H\}$ values of 270.2 and 237.0 ppm and δ $^{13}C\{H\}$ values of 215.0 and 220.6 ppm have been recorded in the spectra of the corresponding dichloroboranyl and diiodoboranyl derivatives. An X-ray structure determination of the bromine derivative shows the planes of the trigonal-planar dibromoboranyl group and the π(C=P) system to be orthogonal [82]. As the Lewis acidity of the boron atom is still maintained, the liquid chloro compound forms a pyridine complex, the structure of which has also been determined with large colourless cuboid-shaped single crystals [100].

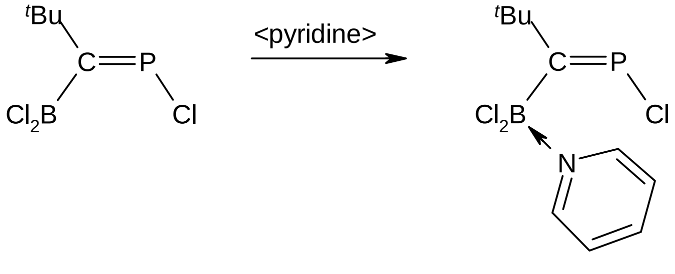

Subsequent [2+2]cycloaddition of a second equivalent of 1λ^3-phosphaalkyne should afford a 1,2-dihydro-1λ^3,3λ^3-diphosphete. This type of intermediate has as yet not been detected in the reactions with boron(III) or phosphorus(III) halides. It has, however, already been mentioned in the introduction that this heterocycle is the final product of the reaction of 1λ^3-phosphaalkynes with germanium(IV) chloride in a molar ratio of 2:1, from which it could be obtained in high yield after three weeks at 80 ºC in toluene as solvent [81, 87]. According to Scheme 1.5 on page 26 and Scheme 2.1 on page 31, the next intermediate is supposed to be the postulated zwitterion resulting from a transannular electrophilic attack of the dibromoboranyl group at the *sp*^{2}-hybridized carbon atom at position 4 of the heterocycle. This zwitterion might be formulated with two resonance structures, one featuring a phosphonium and the other featuring a phosphenium cation (Scheme 2.1).

In the case of extremely Lewis acidic halides of main group elements such as boron(III) bromide the 1,3-migration of a halide anion from e.g. boron to phosphorus cannot take place.

As an alternative the addition of a third 1λ^3-phosphaalkyne molecule to the P–P$^{\oplus}$ unit of the postulated zwitterion and the formation of a now spirocyclic intermediate might occur as a next step. The formulation of such an reaction mechanism is based on results published by the research groups of *Hogeveen* [83], *Breslow* [84] and others [85, 86] who studied the addition of alkynes to phosphenium ions. In the reaction mechanism discussed here a further rearrangement of the analogously formed spirocycle has to be assumed. After all, the reaction of the 1-halogen-2-dihalogenoboranyl-1λ^3-phosphaalkene and 2-*tert*-butyl-1λ^3-phosphaalkyne in a molar ratio of 1:2 furnishes the rather complicated oligocycle 5,7,7-tribromo-1,4,6-tri-*tert*-butyl-2,3,5-triphospha-7-bora-tricyclo[3.2.0.0^{2,6}]hept-3-ene-5-ium-7-uide **XXI**; the compound could be isolated as orange rods in 40% yield after two weeks at 5 °C in cyclopentane**.** Its structure features a relatively short transannular contact between the three- and the four-coordinate phosphorus atoms of only 244 pm. Quantum chemical calculations showed that only a very week bond can be expected between these two atoms [82].

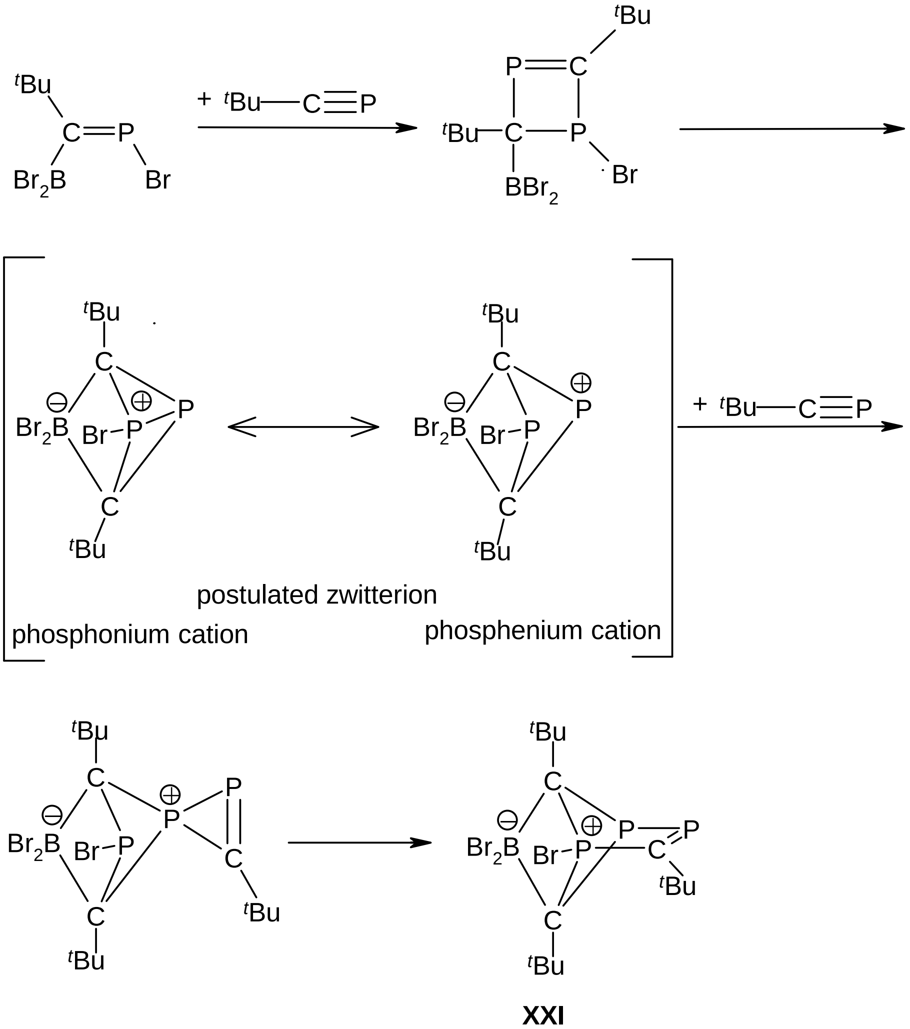

Scheme 2.1

When 2-*tert*-butyl-1λ^3-phosphaalkyne is used in excess and has not been freed completely from hexamethyldisiloxane, its subsequent reaction with 1-bromo-2-dibromoboranyl-1λ^3-phosphaalkene leads to a five-membered heterocycle. A trimethylsiloxy group is introduced at boron and the obviously very reactive P=C fragment of this intermediate which, however, remains undetected, inserts into the P–Br bond of a further unreacted 1λ^3-phosphaalkene molecule. Finally, a Lewis acid-base interaction between the phosphorus atom of the PBr_2 group and the boron atom of the BBr_2 substituent results in cyclization and formation of the final product [82].

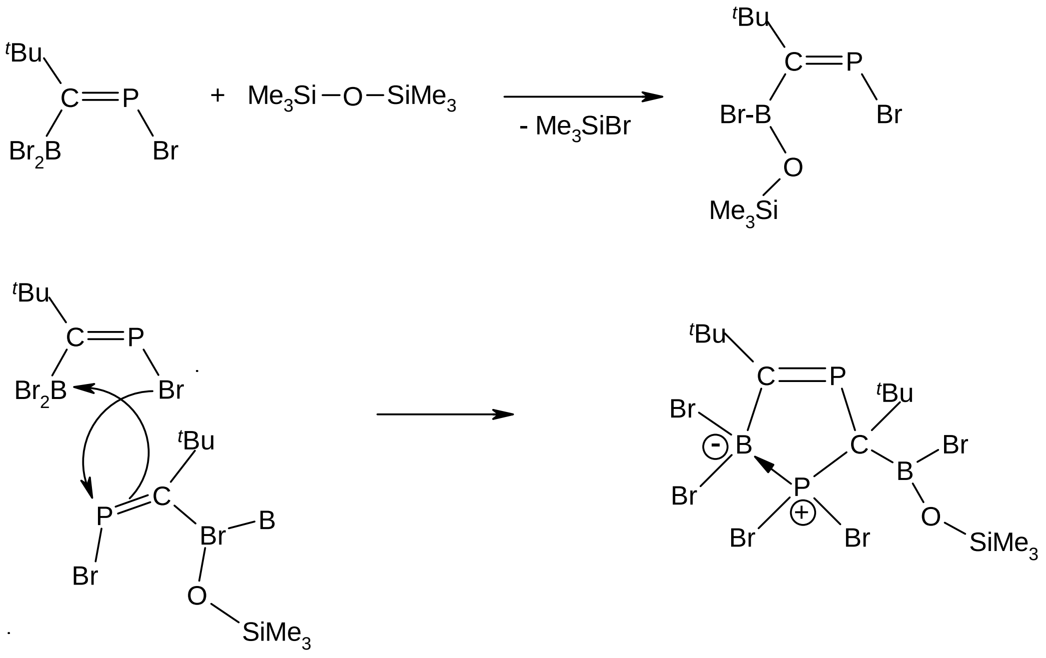

In contrast to the aforementioned studies on boron halides, the reactions of 1λ^3-phosphaalkynes with aluminium and gallium compounds take quite a different route. With aluminium(III) chloride [75, 101], bromide [75, 88, 101], and iodide [75, 102] or gallium(III) chloride [102, 88] and bromide [82, 88] in a molar ratio of 3:1 the spirocyclic complex **XXII** is formed (Scheme 2.2). This spirocyclic product has also been prepared by the reaction of 2-(1-adamantyl)-1λ^3-phosphaalkyne and boron tris(triflate) [103].

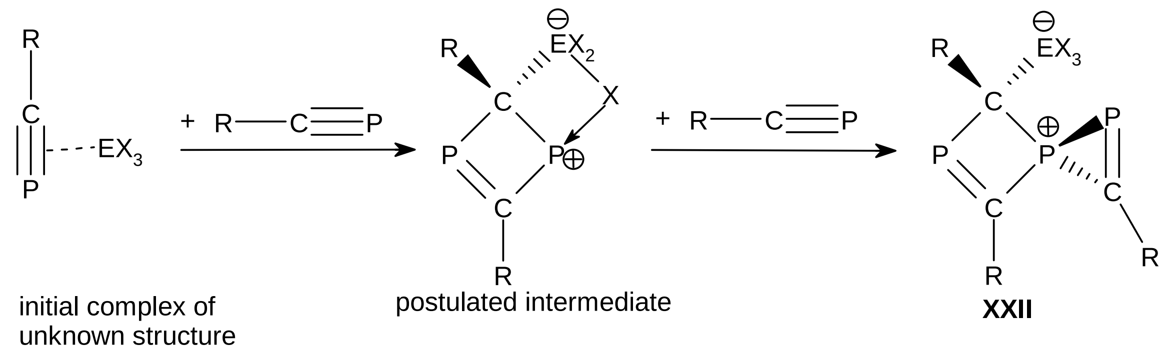

XXII

R = *tert*-butyl;
E = Al, X = Cl, Br, I;
R = 1-adamantyl, 1,1-dimethylpropyl;
E = Al, X = Cl;

R = *tert*-butyl;
E = Ga, X = Cl, Br;
R = 1-adamantyl;
E = B, X = OSO_2CF_3

Scheme 2.2

One should be aware that, in contrast to the reactions of boron(III) halides, the halogen-aluminium and halogen–gallium bonds remain uncleaved. From reactions of trialkylalanes and -gallanes, however, various cages with rather complicated structures (**XXIII** – **XXVI**) could be isolated [75, 104-106]. It may be concluded from the constitution of the products alone that the reaction starts with the insertion of a P≡C fragment into only one of three Al–C bonds and that the very reactive 1λ^3-phosphaalkene R′–P=C(R)–AlR′$_2$ which was detected $^{31}P\{^1H\}$ NMR spectroscopically at low temperature [105] is the key intermediate. Remarkably, the molecular framework observed in the oligocycles **XXI** (page 31), **XXV** and **XXVI** seems to be quite common and has, for example, been reported for a similar tantalum [80, 107] and recently for a magnesium compound [108].

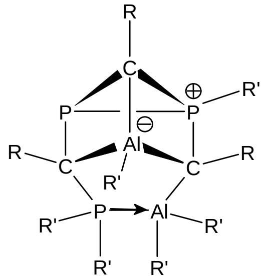

XXIII

R = *tert*-butyl, 1-adamantyl, 1,1-dimethylpropyl;
R`= methyl, ethyl, propyl
[75, 104, 105]

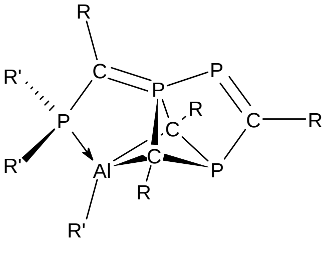

XXIV

R = *tert*-butyl; R` = ethyl
[75, 104]

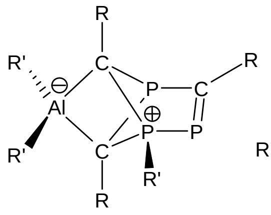

XXV

R = *tert*-butyl, 1-adamantyl, 1,1-dimethylpropyl;
R` = isobutyl, 2-phenylpropyl
[75, 106]

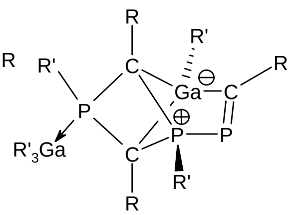

XXVI

R = *tert*-butyl, 1-adamantyl;
R` = ethyl [106]

The addition of Grignard reagents to 2-*tert*-butyl-1λ^3-phosphaalkyne very probably starts at the carbon atom of the C≡P unit and produces thermally stable 2λ^3-phosphavinyl magnesium halides, [R–P=C^{t}Bu(XMg←OEt$_2$)]$_2$, all of which are substituted at the phosphorus centre by an alkyl group [109] and two of which have been structurally characterised. X-ray structure analyses reveal that dimeric through symmetrical Mg–Cl–Mg bridges and crystallize as thier (*Z*)-isomers. Owing to a reverse polarity of the $^{\delta-}C\equiv P^{\delta+}$ and $^{\delta+}C\equiv N^{\delta-}$ triple bond the direction of this addition is opposite to that of Grignard reagents to nitriles.

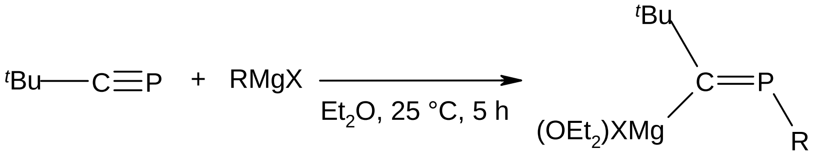

R = *cyclo*-C_6H_{11}, *cyclo*-C_5H_9,
C_2H_5, 2,4,6-$(CH_3)_3H_2C_6$; X = Cl, Br

In our work the reactions of the Lewis acidic dialkylaluminium chlorides have been found to start with an analogous attack at carbon atom of the $1\lambda^3$-phosphaalkynes accompanied by a similar 1,3-shift of the alkyl group. Further insertion and addition reactions, however, lead to much more complicated compounds of two fused four- and five-membered rings. The reaction of the $1\lambda^3$-phosphaalkynes with organolithium reagents is more complex and will not be discussed here [110].

The different reactivities of boron (III) (Scheme 1.5 and Scheme 2.1) and aluminium(III) or gallium(III) halides (Scheme 2.2) are very well understood when bond dissociation energies [111] are taken into account. Remarkably, the major influence arises from the formation of a very strong B–C (448(29) kJ mol^{-1}) in contrast to a rather weak Al–C linkage (255 kJ mol^{-1}). The B–Cl (536(29) kJ mol^{-1}) and the Al–Cl bonds (494(13) kJ mol^{-1}) which are to be cleaved, are of similar strength and obviously the formation of a P–Cl bond (289(42) kJ mol^{-1}) cannot compensate for an insertion into the Al–Cl moiety. Analogous arguments hold for the gallium(III) compounds.

In his thesis *Löw* [112] studied the addition of dimethylaluminium chloride to 2-*tert*-butyl-$1\lambda^3$-phosphaalkyne. He realized that only one of the two Al–C bonds of the starting molecule is involved in the insertion reaction and that each P≡C unit is converted into a $Me_2P–CAl_2$ fragment. The product isolated first, however, is an molecular complex of the underlying insertion compound and a third equivalent of dimethylaluminium chloride; it consists of two fused four- and five-membered heterocycles each of which contains two chlorine bridged aluminium atoms. Concentrating such a solution is acompanied by a thermal decomposition of the complex and the third equivalent of dimethylaluminium chloride is removed with the solvent. As a consequence the insertion compound dimerizes to form a six-membered heterocycle, both P–C–Al$_2$ fragments of which are furthermore bridged on both ends by P→Al and Al←Cl linkages, respectively.

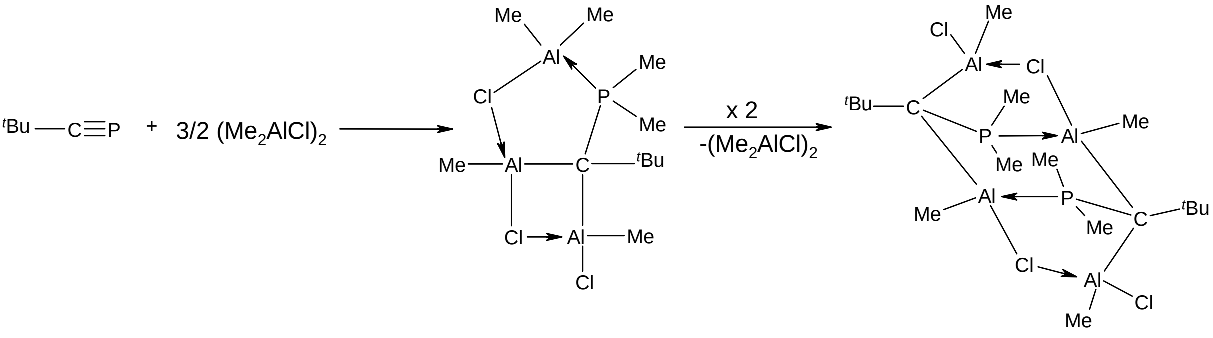

XXVII

In extension of our research on 1λ^3-phosphaalkynes. Additional studies in this field deal with reactions of 2-(1-adamantyl)-1λ^3-phosphaalkyne instead of the *tert*-butyl derivative and of diethylaluminium chloride instead of dimethylaluminium chloride.

2.2. Dialkyl[bis(alkylchloroalanyl)organylmethyl]phosphine•Dialkylchloroalane(1/1) (1a, 1b, 1c, and 1d)

2.2.1. Preparation and Reaction Mechanism

When mixtures of 2-*tert*-butyl- or 2-(1-adamantyl)-$1\lambda^3$-phosphaalkyne and slightly more than three equivalents of the corresponding dialkylaluminium chloride in *n*-hexane are allowed to warm up from –78 °C to room temperature, the 1:2 insertion compound, bridged by a third chloroalane molecule, precipitates as a colourless solid. In these complexes (**1**, Scheme 2.3), dative bonding between phosphorus or chlorine as a donor atom and aluminium as an acceptor atom results in the formation of a bicyclic system.

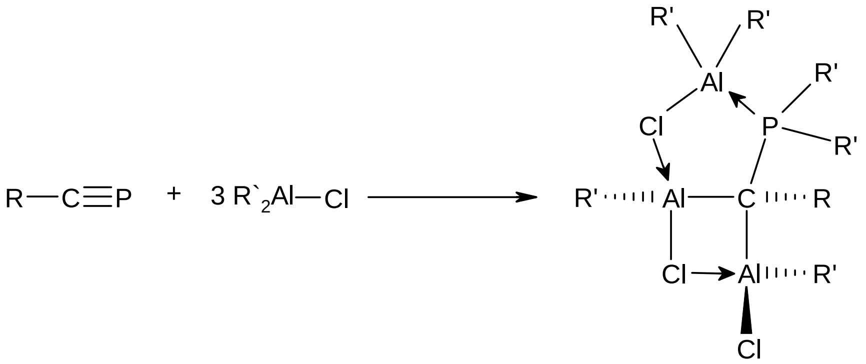

1a : R = *tert*-butyl, R\` = methyl;
1b : R = *tert*-butyl, R\` = ethyl;
1c : R = 1-adamantyl, R\` = methyl;
1d : R = 1-adamantyl, R\` = ethyl

Scheme 2.3

Without further filtration, solvent and excess dialkylaluminium chloride were removed very slowly over several days under reduced pressure. After washing the residue with cold *n*-hexane the dialkyl[bis(alkylchloroalanyl)organylmethyl]phosphine•dialkylchloroalane(1/1) complexes (**1a**, **1b**, **1c**, **1d**) were isolated in high yields. Recrystallization of **1a** and **1b** from toluene and of **1c** and **1d** from a mixture of cyclopentane and *n*-hexane afforded colourless crystals suitable for X-ray structure analyses.

The structures of the finally isolated complexes are in accordance with previous results in that, here again, the Al–Cl bond of the starting compound remains intact [82, 75, 88, 101, 102] and only one of the two Al–C bonds is cleaved. In all reactions the addition of the C–Al moiety to the P≡C group is in accordance with the polarity of the bonds involved; subsequent steps are mostly a consequence of the Lewis acidity of the aluminium centres. Taking into account bond energy data already discussed for a P≡C–insertion into either the Al–Cl or Al–C bond and repeating arguments given by *Löw* for the reaction of dimethylaluminium chloride with 2-*tert*-butyl-$1\lambda^3$-phosphaalkyne [112], additional studies made possible to work out a modified reaction scheme (Scheme 2.4). This scheme is still based on the results of X-ray structure analyses, which show that the solid compounds **1a-1d** are built up of two fused four- and five-membered rings, but it accounts much better for the observed NMR data which will be discussed at some length in the next section.

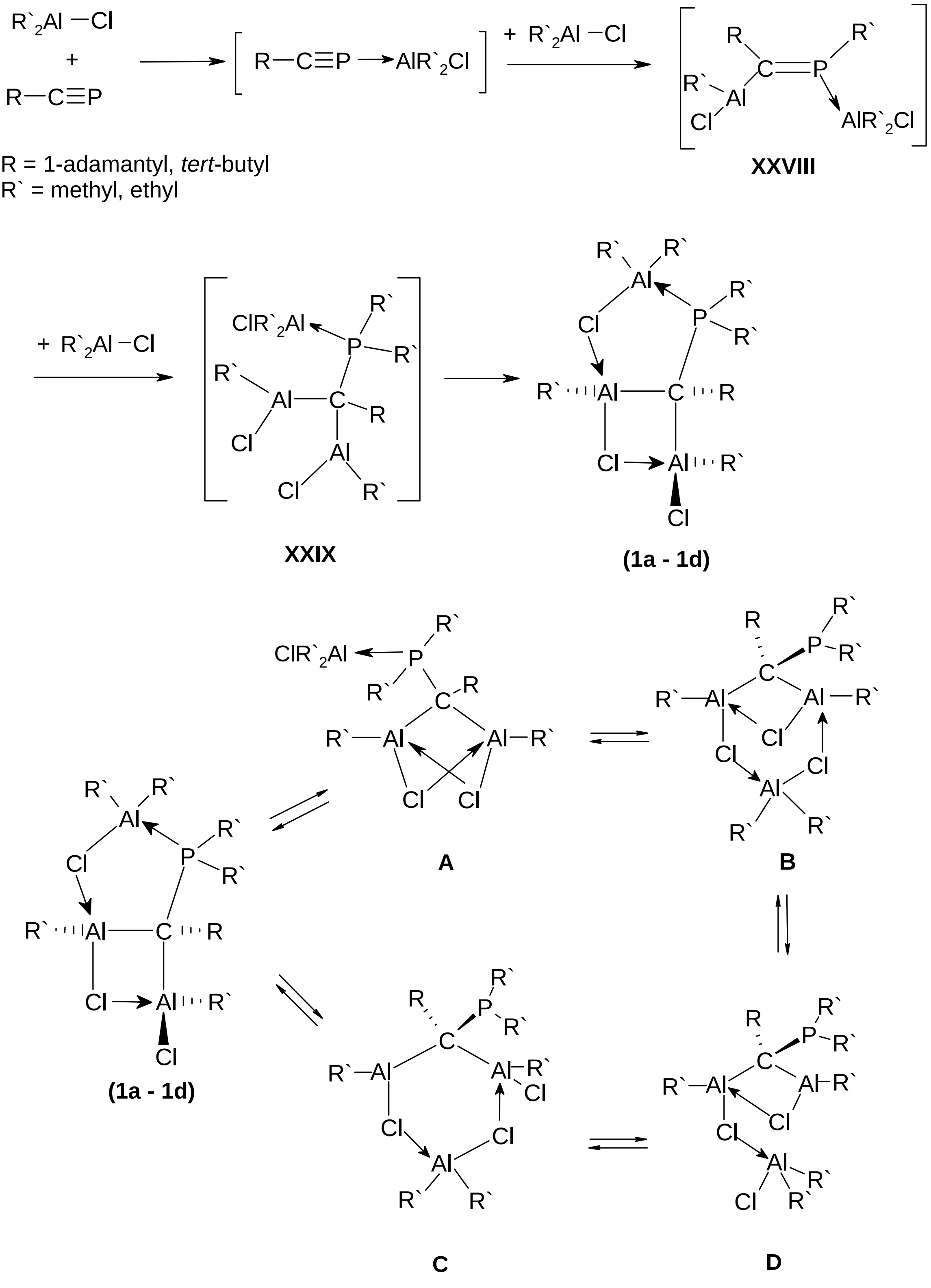

R = 1-adamantyl, *tert*-butyl
R\` = methyl, ethyl

XXVIII

XXIX

(1a - 1d)

A

B

C

D

Scheme 2.4

2.2.2. NMR Spectroscopic Characterization

Already the $^{31}\mathrm{P}\{^{1}\mathrm{H}\}$ NMR spectra of compounds **1a**-**1d** dissolved in d_6-benzene indicate that several isomers must exist in solution. Signals at high and also at low field are observed with different intensity ratios at ambient temperature as well as at 80 °C in d_8-toluene [112] (see Figure 2.2.1 and also the Experimental Part). The presence of two well separated shift regions is caused by either complexed or uncomplexed phosphorus atoms; this phenomenon can be explained by a competition of both the Lewis-basic centres phosphorus and chlorine for the Lewis acidic centre aluminium. From the broadening of the high field signals one can deduce that they originate from phosphorus atoms coordinated to aluminium. The broadening is at least partly a consequence of the quadrupole interaction between the phosphorus and aluminium nucleus (^{27}Al: $s = 5/2$, electric quadrupole moment $Q_b = 0.1402(10) \bullet 10^{-28}$ m^2, 100% natural abundance [113a]).

Provided that two aluminium atoms (Al*) and one carbon (C*) of isomer **1** are centres of atomic chirality one can predict four $^{31}\mathrm{P}\{^{1}\mathrm{H}\}$ NMR signals. With further regard to one broad line of isomer **A** (Scheme 2.5) the total number of high field signals will sum up to five. Indeed, in the spectra of compounds **1b** and **1c** five lines of that kind can be observed. Narrow signals in the low field region can be attributed to uncomplexed phosphorus atoms. Those atoms are present in the isomers **B** to **D** (Scheme 2.6) which are predicted to give rise to two, two and two $^{31}\mathrm{P}\{^{1}\mathrm{H}\}$ NMR-signals. A maximum number of six relatively intense lines is observed in the spectrum of compound **1b** (Fig. 2.2.1.b).

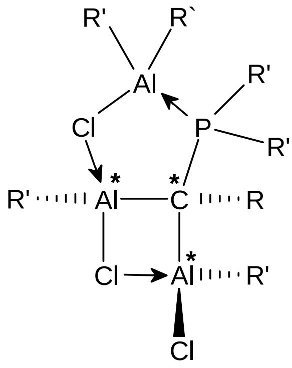

1

four $^{31}\mathrm{P}\{^{1}\mathrm{H}\}$ NMR signals

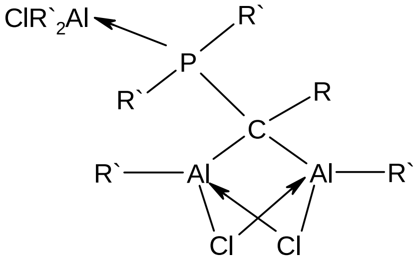

A

one $^{31}\mathrm{P}\{^{1}\mathrm{H}\}$ NMR signal

Scheme 2.5. For the dialkyl[bis(alkylchloroalanyl)organylmethyl]phosphine•dialkylchloroalane(1/1) complexes two different types of isomers should be observed in the high field region of the $^{31}\mathrm{P}\{^{1}\mathrm{H}\}$ NMR spectra. Centres of atomic chirality have been marked with an asterisk (*).

a) Compound **1a** (^{t}Bu/Me$_2$)

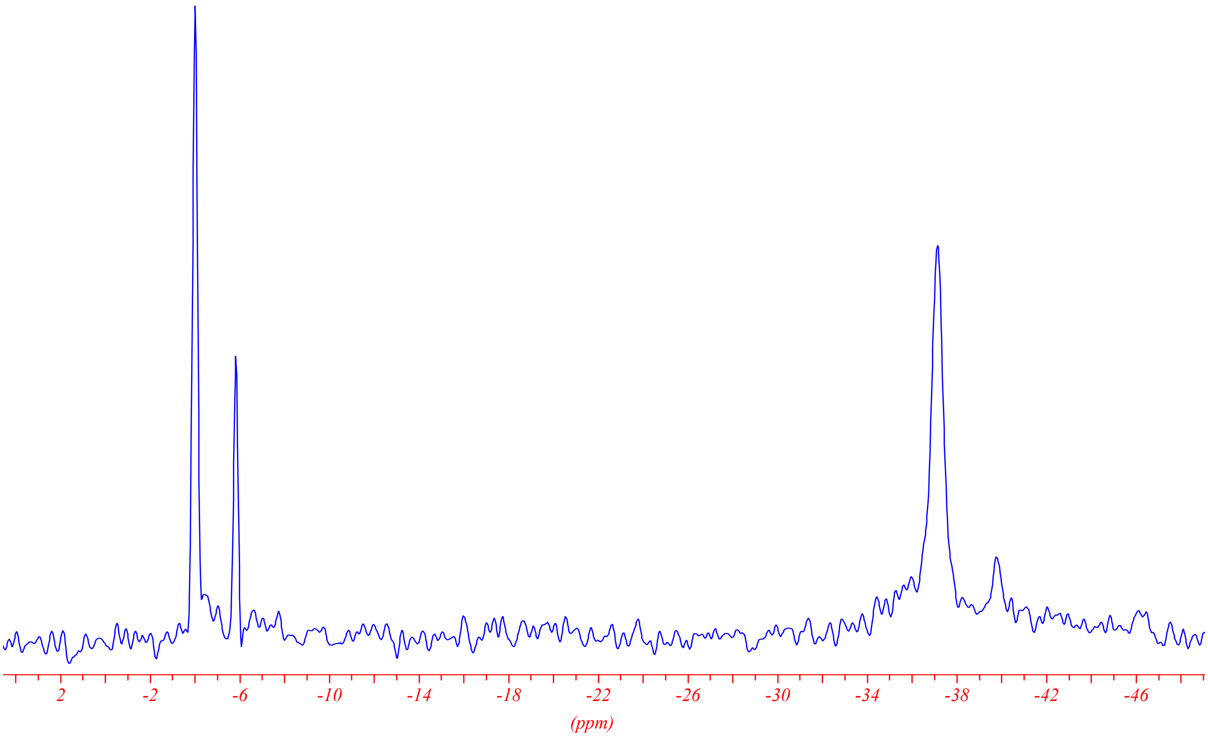

b) Compound **1b** (^{t}Bu/Et$_2$)

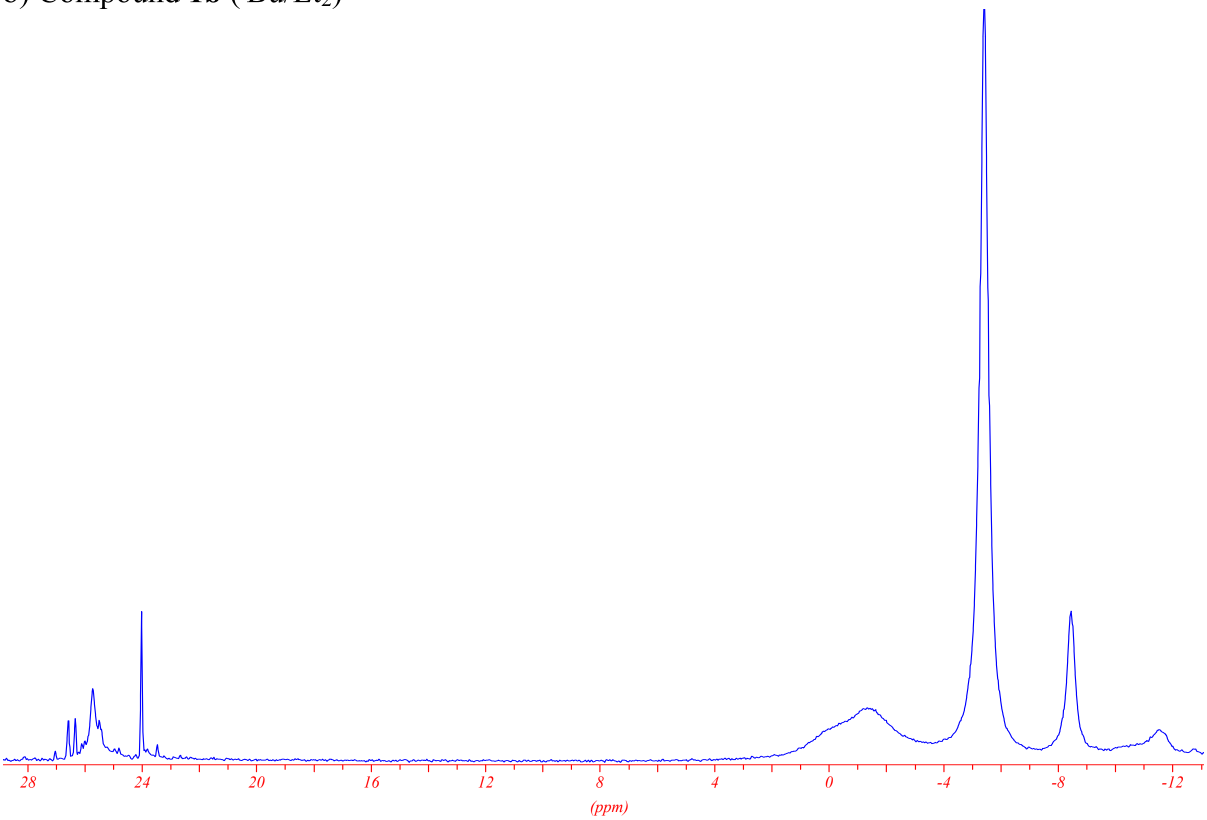

c) Compound **1c** (Ad/Me$_2$)

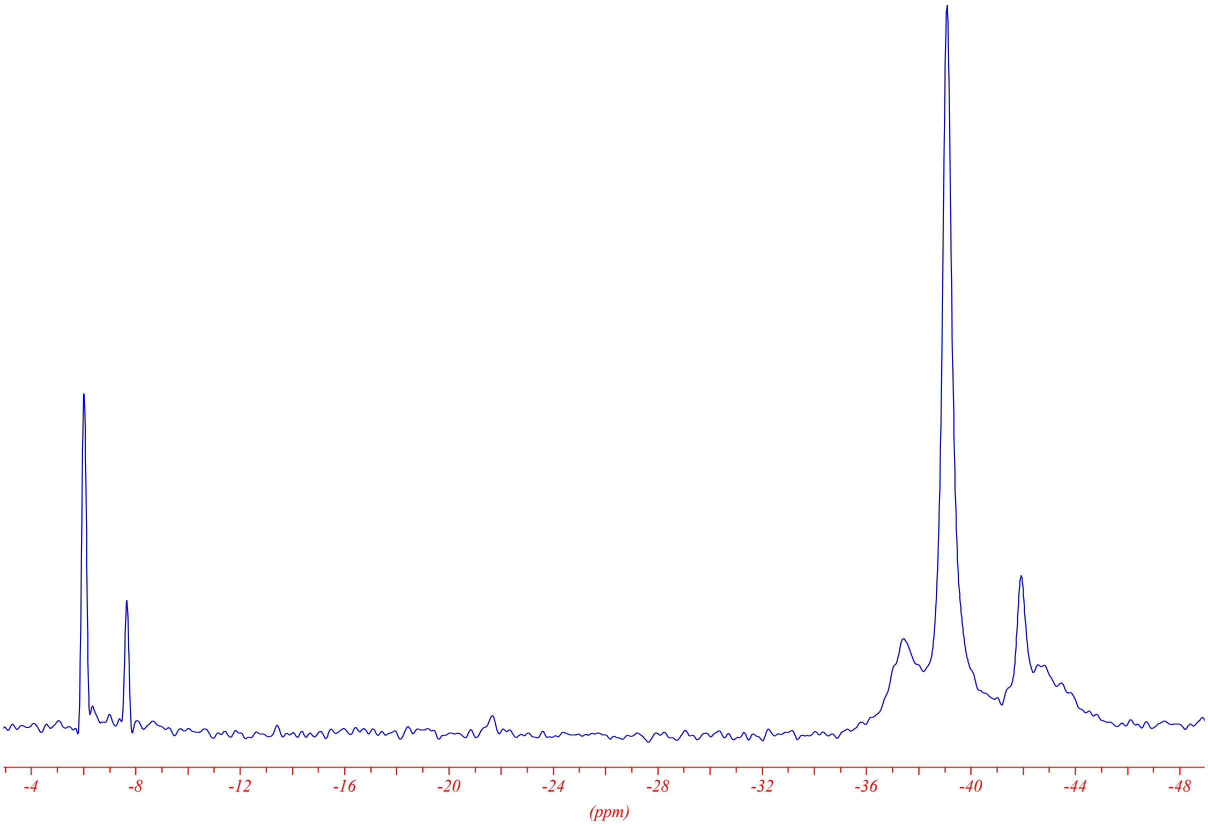

d) Compound **1d** (Ad/Et$_2$)

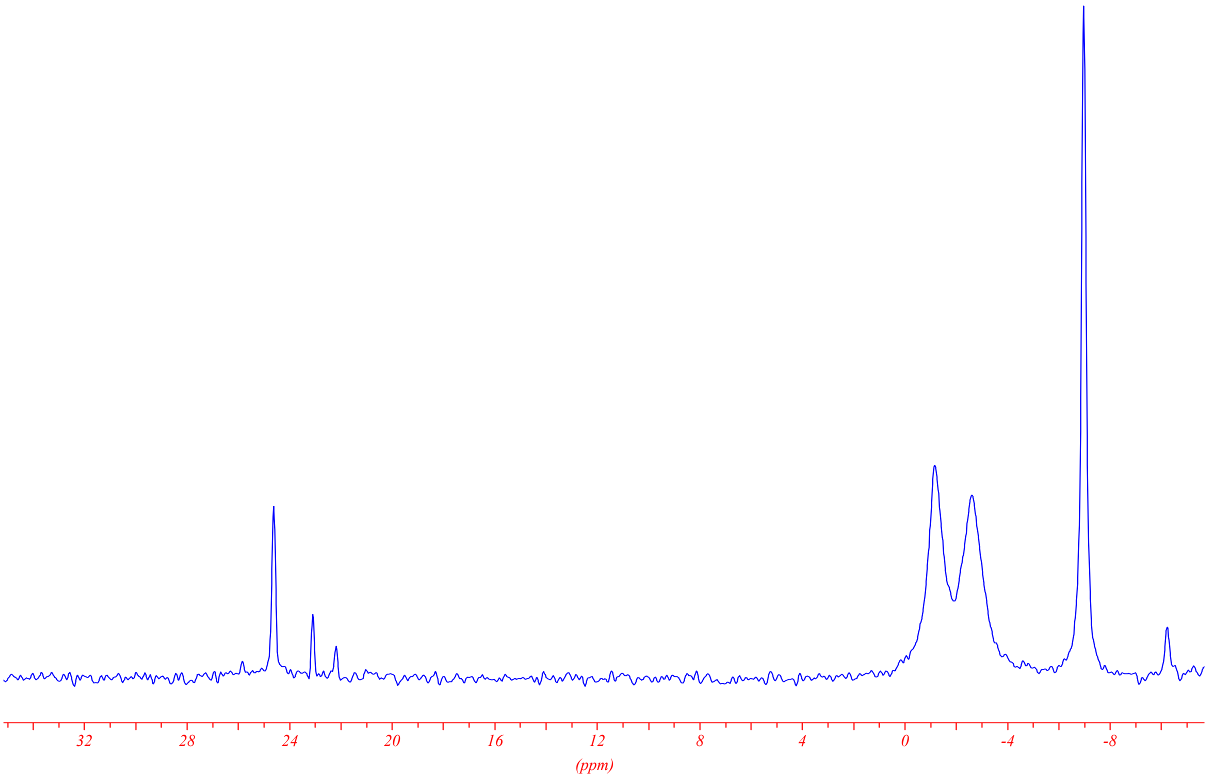

Figure 2.2.1. ^{31}P{^{1}H} NMR spectra of the compounds **1a** (^{t}Bu/Me$_2$), **1b** (^{t}Bu/Et$_2$), **1c** (Ad/Me$_2$), and **1d** (Ad/Et$_2$) dissolved in d_6-benzene at room temperature

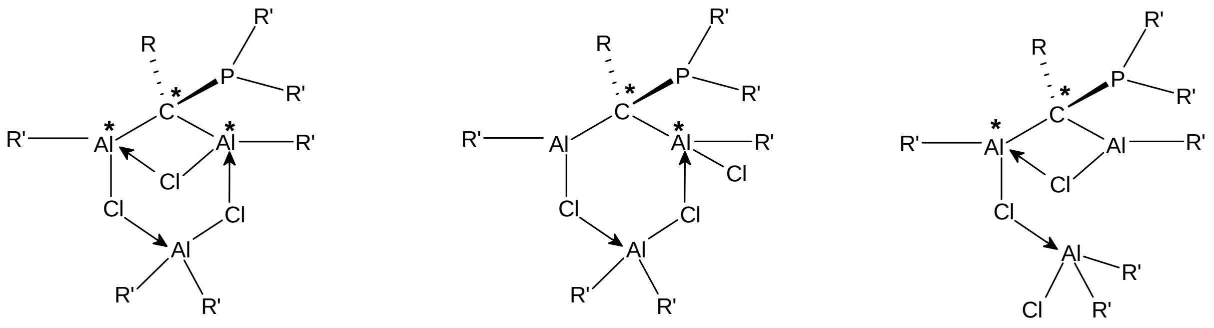

B **C** **D**

two $^{31}P\{^1H\}$ NMR signals two $^{31}P\{^1H\}$ NMR signals two $^{31}P\{^1H\}$ NMR signals

Scheme 2.6. For the dialkyl[bis(alkylchloroalanyl)organylmethyl]phosphine•dialkylchloroalane(1/1) complexes three different kinds of isomers should be observed in the low field region of the $^{31}P\{^1H\}$ NMR spectra. Centres of atomic chirality have been marked with an asterisk (*).

The $^{31}P\{^1H\}$ NMR spectrum of compound **1b** exhibits a beginning broadening of one of its low field signals. A possible interpretation of this phenomenon might be an increasing intramolecular interaction of the uncomplexed phosphorus as a donor and aluminium as an acceptor atom thus forming a three-membered heterocycle *via* a dative P→Al bond. Two possibilities are depicted in Scheme 2.7 representing different coordination numbers of 5 and 4 at aluminium.

Scheme 2.7. Possible formations of three-membered heterocycles *via* a dative P→Al bond

The $^{27}Al\{^1H\}$ NMR spectra of the complexes **1a**-**1d** dissolved in d_6-benzene as well, show very broad singlets between 177 and 140 ppm. As can be taken from the literature [113b] this region is attributed to four coordinated aluminium. With related organoaluminium compounds the chemical shift values $\delta(^{27}Al)$ have been taken as an indicator for the coordination number of aluminium atoms. For monomeric compounds R_3Al with three-coordinated aluminium, $\delta(^{27}Al)$ values between 280 and 210 ppm were reported, whereas for $(R_nAlX_{3-n})_m$ oligomers (n = 1, 2, 3; m = 2, 3) with four-coordinated aluminium a chemical shift region between 180 and 125 ppm seems to be typical. Compounds with five-coordinated aluminium atoms show δ(^{27}Al) values between 125 and 100 ppm [113b].

Remarkably, an inspection of the ^{31}P{^{1}H} NMR spectrum of compound **1b** reveals a very strong high field signal at –5.4 ppm and additionally only weak or very weak signals in the high and low field regions. With this observation in mind, the corresponding ^{13}C{^{1}H}- and ^{1}H NMR spectra are supposed to be rather uncomplicated and are discussed first. Indeed, the ^{13}C{^{1}H} signals of complex **1b** (Fig. 2.2.2.b) are easy to interpret; two broad singlets at 3.7 and 7.5 ppm, the former of which is slightly split, arise from the methylene carbon atoms, and two narrow singlets centered at 8.6 and 11.5 ppm come from the methyl carbon atoms of the Al–CH_2–CH_3 groups. This observation indicates two types of aluminium-bound alkyl groups; one is attributed to the complexing diethylchloroalane molecule and the other one to both the ethylchloroalanyl substituents. The spectrum also exhibits a doublet (only visible on expansion) for P–CH_2–$\mathbf{C}H_3$ at 9.4 ppm with a coupling constant $^{2}J_{(C,P)}$ of 2.1 Hz and a doublet for P–$\mathbf{C}H_2$–CH_3 at 24.1 ppm with $^{1}J_{(C,P)}$ = 21.6 Hz. Furthermore, two doublets of different intensities, one at 36.1 ppm with a coupling constant $^{3}J_{(C,P)}$ of 6.3 Hz and the other one at 38.3 ppm with $^{2}J_{(C,P)}$ = 10.0 Hz can be assigned to the carbon atoms of the *tert*-butyl group, namely $(H_3\mathbf{C})_3C$ and $(H_3C)_3\mathbf{C}$. The ^{13}C{^{1}H} NMR signal of the P**C**Al_2 group could be not detected due to two neighbouring aluminium atoms; the quadruple moments reduce the signal resolution completely. Some very weak signals with an intensity ratio of the 1:5 in relation to the previous signals are observed at 8.5 ppm (only detectable on expansion) and 11.3 ppm as well as at 36.3 ppm ($^{3}J_{(C,P)}$ = 6.8 Hz) and 38.50 ppm ($^{2}J_{(C,P)}$ = 10.5Hz); they are attributed to the Al–CH_2–$\mathbf{C}H_3$, $(H_3\mathbf{C})_3C$ and $(H_3C)_3\mathbf{C}$ carbon atoms of less abundant isomers. A very weak and unidentified singlet is apparent at 27.3 ppm.

The ^{1}H NMR spectrum of compound **1b** shows two overlapping quartets for Al–$C\mathbf{H}_2$–CH_3 at 0.43 and 0.46 ppm with an intensity ratio of 1:4:6:4:1 (highest resonance at 0.45 ppm) and a coupling constant $^{3}J_{(H,H)}$ of 8.03 Hz along with a slightly broadened triplet for Al–CH_2–$C\mathbf{H}_3$ at 1.27 ppm and an identical $^{3}J_{(H,H)}$ value. In the related Lewis acid-base adduct triethylaluminium•tris(trimethylsilyl)phosphine $Et_3Al \leftarrow P(SiMe_3)_3$ [114], the multiplicity of the ^{1}H-NMR signals, the coupling constant and the chemical shift values of the ethyl groups at aluminium agree well with the parameters of **1b**. The resonances of the ethyl groups at phosphorus are split into a doublet of triplets at 0.89 ppm for P–CH_2–$C\mathbf{H}_3$ with coupling constants $^{3}J_{(P,H)}$ of 18.4 Hz and $^{3}J_{(H,H)}$ of 7.6 Hz as well as into an only partially resolved multiplet for P–$C\mathbf{H}_2$–CH_3 in the range of 1.55 to 1.77 ppm. As can be taken from the literature

[115, 116], for the methylene groups of triethylphosphine Et_3P a very small coupling constant $^2J_{(H,P)}$ of 0.5 Hz is observed compared to the $^3J_{(H,P)}$ value of 13.7 Hz for the methyl group; this is also true for compound **1b**. Furthermore, one intense singlet at 1.11 ppm is assigned to the *tert*-butyl group of the main-isomer; a weaker signal at 1.18 ppm with only a fifth of the previous intensity comes from a different isomer. The origin of a weak singlet at 1.4 ppm cannot be ascertained; a very weak signal at 2.1 ppm arises from toluene, which was used as solvent in the crystallization process. All chemical shift values of the ethyl groups at aluminium and phosphorus as well as the relevant parameters of the *tert*-butyl group are in agreement with data reported for compounds **XXIII** and **XXIV** [104, 105] (see page 33).

a) Compound **1a** (^{t}Bu/Me_2)

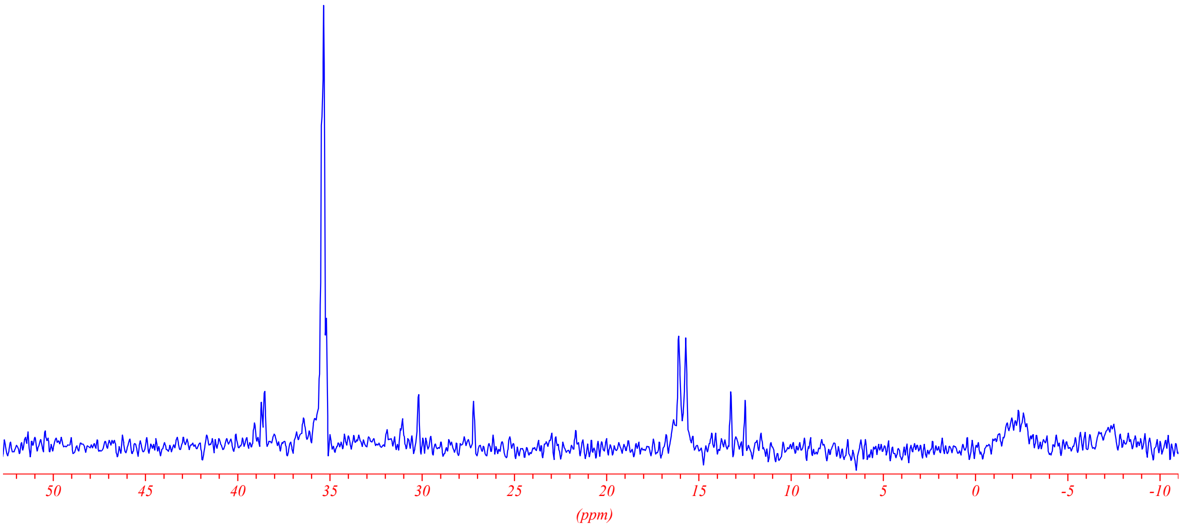

b) Compound **1b** (^{t}Bu/Et_2)

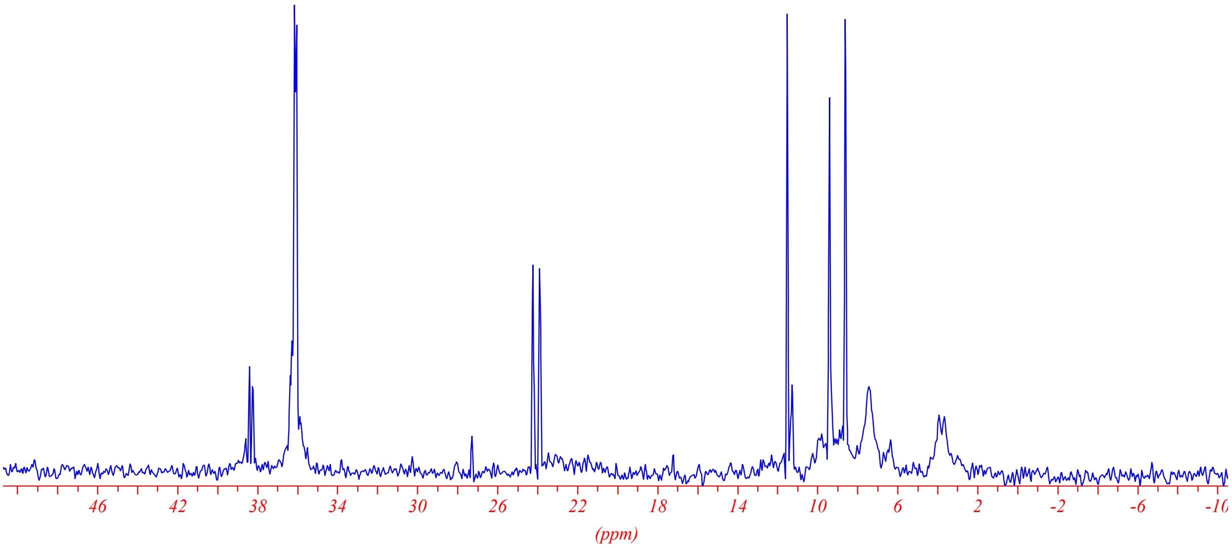

c) Compound **1c** (Ad/Me$_2$)

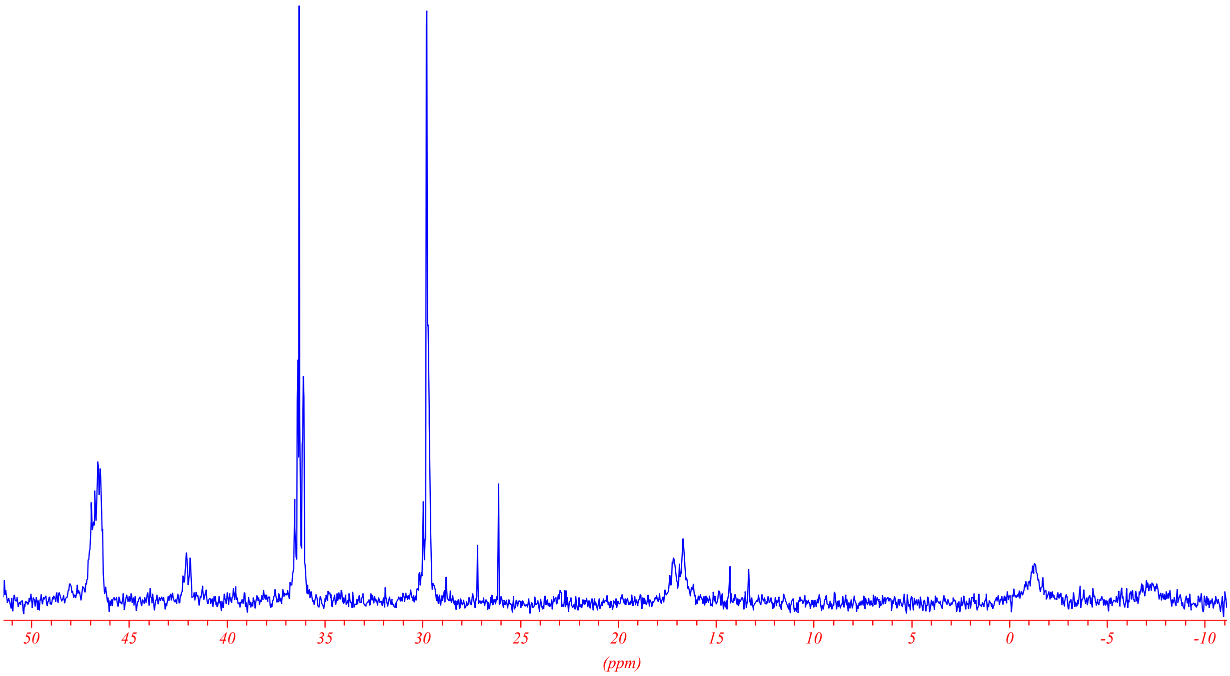

d) Compound **1d** (Ad/Et$_2$)

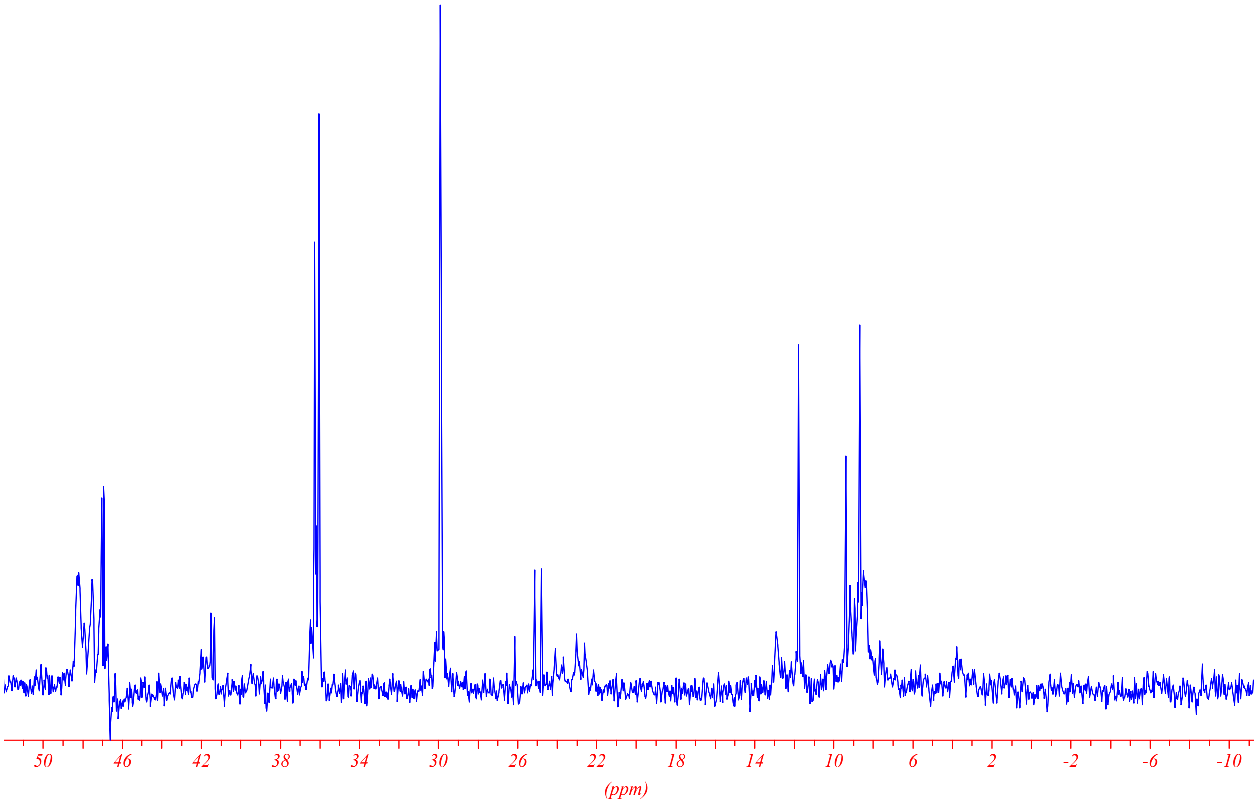

Figure 2.2.2. $^{13}C\{^1H\}$ NMR spectra of the compounds **1a** (^{t}Bu/Me$_2$), **1b** (^{t}Bu/Et$_2$), **1c** (Ad/Me$_2$), and **1d** (Ad/Et$_2$) dissolved in *d*$_6$-benzene at room temperature

a) Compound **1a** (^{t}Bu/Me$_2$)

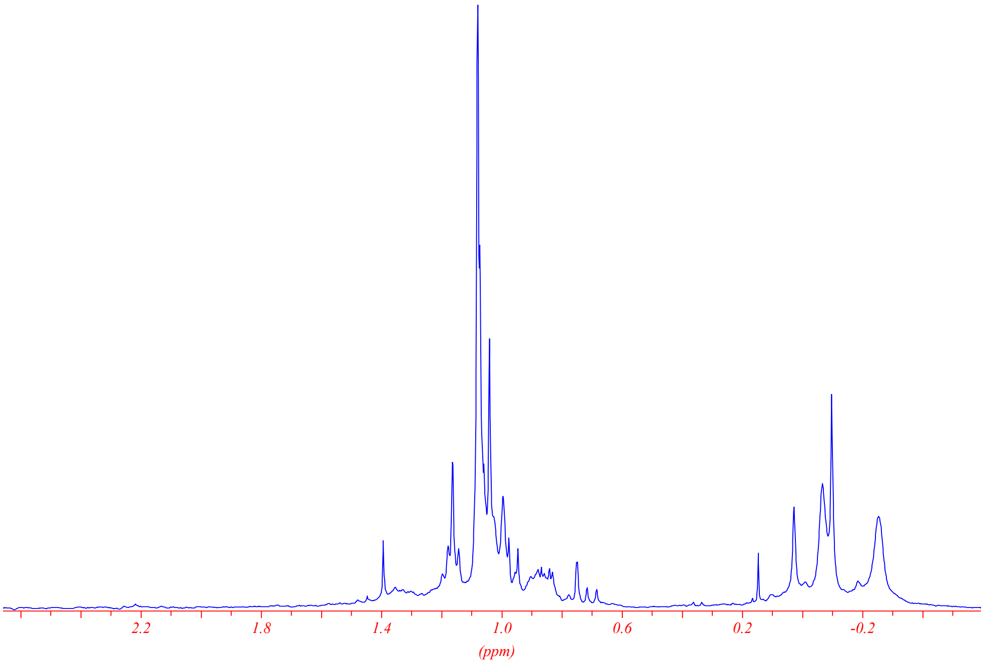

b) Compound **1b** (^{t}Bu/Et$_2$)

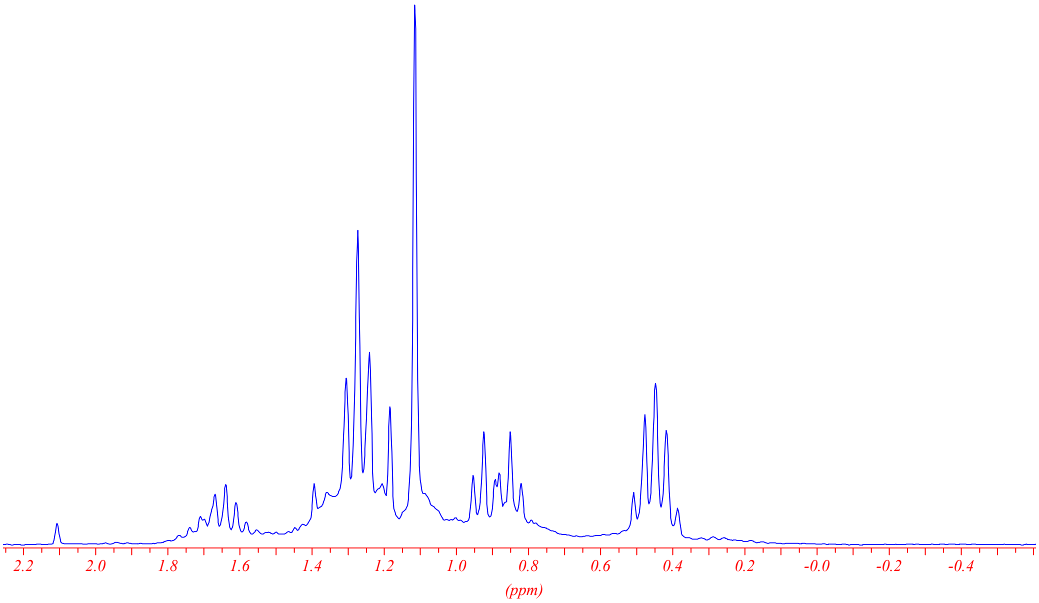

c) Compound **1c** (Ad/Me$_2$)

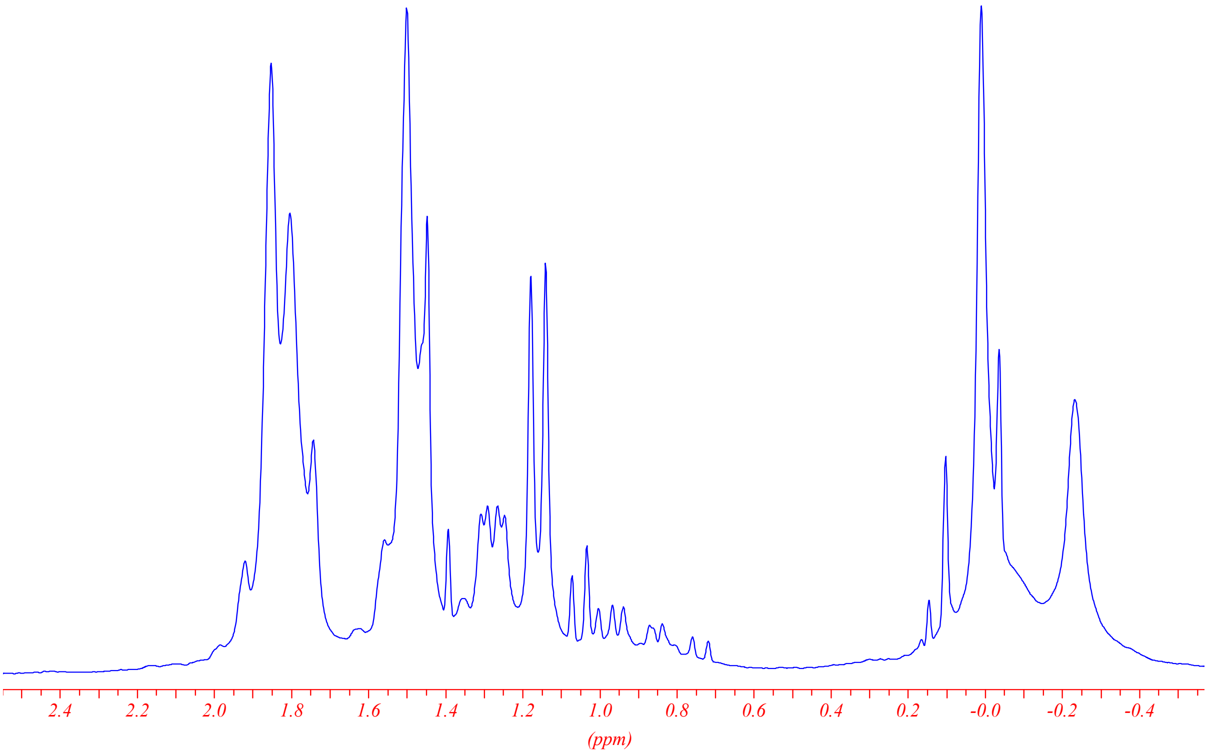

d) Compound **1d** (Ad/Et$_2$)

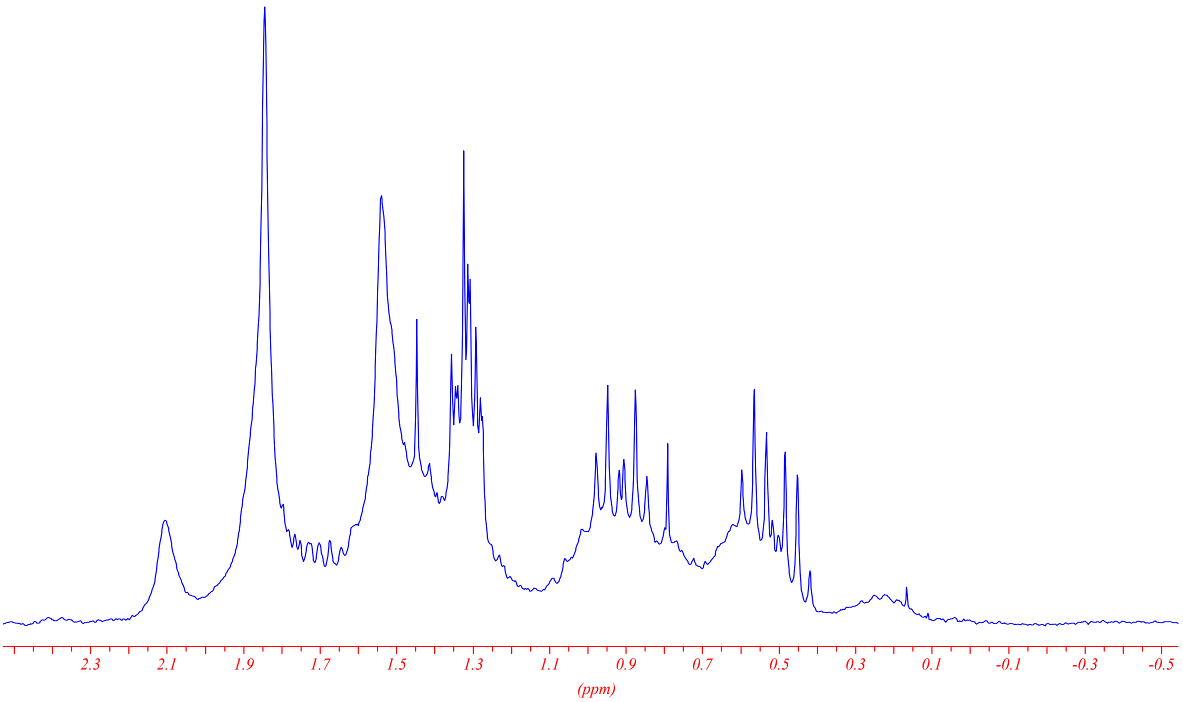

Figure 2.2.3 ^{1}H NMR spectra of the compounds **1a** (^{t}Bu/Me$_2$), **1b** (^{t}Bu/Et$_2$), **1c** (Ad/Me$_2$), and **1d** (Ad/Et$_2$) dissolved in d_6-benzene at room temperature

On the basis of the assignment given for compound **1b** the $^{13}C\{^{1}H\}$- and ^{1}H NMR spectra of complex **1d** can be interpreted in a similar way. Two broad singlets at 3.6 and 8.4 ppm arise from the methylene carbon atoms and two narrow singlets centered at 8.7 and 11.8 ppm originate from the methyl carbon atoms of different Al–CH$_2$–CH$_3$ groups. The spectrum also exhibits a doublet at 9.40 ppm with a small coupling constant $^{2}J_{(C,P)}$ of 2.04 Hz and a doublet at 25.0 ppm with a larger $^{1}J_{(C,P)}$ value of 21.4 Hz, arising from the methyl and methylene carbon atoms of the two P–CH$_2$–CH$_3$ groups, respectively. Furthermore, three doublets of different intensities and a singlet can be assigned to the adamantyl group. In this context, however, one should be aware that the numbering scheme used here follows Fig. 2.2.4 and does not tally with the systematic nomenclature or the molecular structures described in the next section. The first doublet at 29.90 ppm characterized by a coupling constant $^{4}J_{(C,P)}$ of 2.5 Hz arises from the carbon atoms (C3, C5, C7), the second less intense one at 41.4 ppm with $^{2}J_{(C,P)}$ = 10.4 Hz from (C1) and the third one at 47.0 ppm with a coupling constant $^{3}J_{(C,P)}$ of 6.4 Hz from (C2, C8, C9). The singlet at 36.02 ppm can be attributed to the carbon atoms (C4, C6, C10). The assignment of signals to various adamantyl carbon atoms is in agreement with data reported for both the compounds 2-(1-admantyl)-1λ^{3}-phosphaalkyne and its corresponding phosphaalkene [28].

Again, the $^{13}C\{^{1}H\}$ NMR signal of the P**C**Al$_2$ group could be not detected. Weak singlets at 8.90 and 12.8 ppm as well as two sets of resonances at 22.8 ($^{1}J_{(C,P)}$ = 24.4 Hz) and 23.9 ppm ($^{1}J_{(C,P)}$ = 25.4 Hz) may be attributed to the Al–CH$_2$–**C**H$_3$ and P–**C**H$_2$–CH$_3$ carbon atoms of different isomers, respectively. Two weaker sets of resonances each at 30.1 ($^{4}J_{(C,P)}$ = 2.04) and 30.2 ($^{4}J_{(C,P)}$ = 1.74 Hz), at 36.2 (s) and 36.3 (s), at 41.8 ($^{2}J_{(C,P)}$ = 13.0 Hz) and 41.9 ($^{2}J_{(C,P)}$ = 13.7 Hz) as well as at 47.5 ($^{3}J_{(C,P)}$ = 5.1 Hz) and 48.2 ($^{3}J_{(C,P)}$ = 6.1 Hz) are supposed to orginate from the adamantyl carbon atoms (C3, C5, C7), (C4, C6, C10), (C1), and (C2, C8, C9) of two further isomers. A very weak, unidentified singlet is apparent at 26.1 ppm.

The ^{1}H-NMR spectrum exhibits two quartets at 0.46 ppm and 0.55 ppm with the same coupling constant $^{3}J_{(H,H)}$ of 8.03 Hz originating from the Al–C**H**$_2$–CH$_3$ methylene groups. A doublet of triplets at 1.31 ppm with coupling constants $^{4}J_{(H,P)}$ = 1.37 Hz and $^{3}J_{(H,H)}$ = 8.03 Hz along with a triplet at 1.32 ppm and an $^{3}J_{(H,H)}$ value of 8.03 Hz are supposed to come from different Al–CH$_2$–C**H**$_3$ groups. As for the ethyl substituents at phosphorus the ^{1}H-resonances of the methyl group are split into a doublet of triplets (0.91 ppm; $^{3}J_{(P,H)}$ = 18.1 Hz, $^{3}J_{(H,H)}$ = 7.50 Hz), whereas the methylene groups give rise to a multiplet in the range of 1.61 to 1.80 ppm. Multiplets in the range of 1.45 to 2.2 ppm are assigned to the adamantyl group. The origin of a weak singlet at 0.79 ppm cannot be ascertained; the same is true for several very broad signals to be observed in the range from 1.1 to 0.1 ppm.

The $^{13}C\{^1H\}$ spectrum of complex **1c** shows two broad singlets at –7.1 and –1.3 ppm arising from the Al–CH_3 groups. The spectrum also exhibits a doublet at 16.94 ppm with a coupling constant $^1J_{(C,P)}$ of 24.6 Hz coming from the P–CH_3 substituents, and reveals five different sets of resonances with an intensity ratio of (1:1:4:2:1) observed for each of the four carbon positions of the adamantyl group. One set is attributed to the main isomer (Table 2.2.1) and four other sets to different isomers (see Experimental Part). A weak doublet (only detectable on expansion) with an intensity ratio of 1:4 in relative to the doublet mentioned above is observed in the P–**C**H_3 region at 17.1 ppm with a coupling constant $^1J_{(C,P)}$ of 24.2 Hz. Some weak signals at 13.3, 14.3, 26.1, 27.2, and 28.8 ppm cannot be identified. The characteristic $^{13}C\{^1H\}$ NMR parameters of the major isomer are summarized in Table 2.2.1.

The ^1H NMR spectrum of compound **1c** reveals three relatively narrow singlets at –0.04, 0.1, and 0.15 ppm as well as two broad signals at –0.23 and 0.01 ppm orginating from methyl groups at aluminium. The two intense signals are attributed to the main isomer and three other resonances to different isomers. The signal of the methyl groups bound to phosphorus appears at 1.16 ppm and is split into a doublet with a coupling constant $^2J_{(P,H)}$ of 7.7 Hz. Some weaker doublets characterized by similar coupling constants of 8.1, 6.4, 6.4, 5.6, 6.2, 7.5, 8.9, and 8.7 Hz, are observed at 0.74, 0.84, 0.85, 0.95, 1.02, 1.05, 1.27, and 1.29 ppm with an intensity ratio of 1:1:1:2:2:3:5:5, respectively; they are attributed to P–CH_3 groups of different isomers. Multiplets ranging from 1.39 to 2.0 ppm are assigned to the adamantyl group.

The $^{13}C\{^1H\}$ spectrum of complex **1a** exhibits two broad singlets at –7.4 and –2.3 ppm arising from the Al–CH_3 groups and a doublet at 15.9 ppm with a coupling constant $^1J_{(C,P)}$ of 25.0 Hz coming from the methyl groups at phosphorus. A second but weak doublet (only visible after expansion) with an intensity ratio of 1:3 in relative to the previous one appears at 16.2 ppm with a coupling constant $^1J_{(C,P)}$ of 26.2 Hz. As for the *tert*-butyl substituent, two doublets of different intensities can be observed, one at 35.40 ppm with a coupling constant $^3J_{(C,P)}$ of 6.1 Hz and the second one at 38.60 ppm with $^2J_{(C,P)}$ = 10.7 Hz. In the same region some weaker signals are detected at 35.50 and 39.0 ppm with an intensity ratio of 1:3 in relative to the previous signals, they are split into doublets with coupling constants $^3J_{(C;P)}$ = 7.1 Hz and $^2J_{(C,P)}$ = 11.2 Hz, respectively; the splitting, however, can be discerned only after expansion.

In the Al–CH_3 region the ^1H NMR spectrum of compound **1a** reveals three relatively narrow singlets at –0.1, 0.03 and 0.15 ppm as well as two broad signals at –0.07 and –0.25 ppm. Two more intense signals are attributed to the main isomer and three less intense ones to different isomers. The methyl groups at phosphorus give rise to a doublet at 1.05 ppm split with a coupling constant $^2J_{(H,P)}$ of 7.80 Hz; furthermore, a doublet of lower intensity (1:3) is observed

Table 2.2.1. Characteristic $^{13}C\{^{1}H\}$ NMR parameters of the major isomer of the dialkyl[bis(alkylchloroalanyl)organylmethyl]phosphine•dialkylchloroalane(1/1) complexes **1a** – **1d** along with some data of the $^{27}Al\{^{1}H\}$ NMR spectra. Chemical shift δ (ppm); coupling constant J (Hz); peak width at half height $w_{1/2}$ (Hz), d_6-benzene solutions

	δ(R–Al)b)	δ(R–P)c)	δ((**C**(CH$_3$)$_3$) or (C3, C5, C7)d)	δ((C(**C**H$_3$)$_3$) or (C4, C6, C10)d)	δ(C1)d)	δ(C2, C8, C9)d)	δ(^{27}Al{^{1}H}) ($w_{1/2}$)
1aa)	−7.4 (s, br, **C**H$_3$) −2.3 (s, br, **C**H$_3$)	15.9 (d, **C**H$_3$) $^{1}J_{(C,P)} = 25$	38.60 (d) $^{2}J_{(C,P)} = 10.7$	35.40 (d) $^{3}J_{(C,P)} = 6.1$			168 (4432)
1ba)	3.7 (s, br, **C**H$_2$) 7.5 (s, br, **C**H$_2$) 8.6 (s, **C**H$_3$) 11.5 (s, **C**H$_3$)	9.40 (d, **C**H$_3$) $^{2}J_{(C,P)} = 2.10$ 24.1 (d, **C**H$_2$) $^{1}J_{(C,P)} = 21.6$	38.3 (d) $^{2}J_{(C,P)} = 10.0$	36.1 (d) $^{3}J_{(C,P)} = 6.1$			177 (4380)
1ca)	−7.1 (s, br, **C**H$_3$) −1.3 (s, br, **C**H$_3$)	16.94 (d, **C**H$_3$) $^{1}J_{(C,P)} = 24.6$	29.80 (d) $^{4}J_{(C,P)} = 0.93$	36.30 (s)	42.0 (d) $^{2}J_{(C,P)} = 10.4$	46.5 (d) $^{3}J_{(C,P)} = 5.0$	140 (4400)
1da)	3.6 (s, br, **C**H$_2$) 8.4 (s, br, **C**H$_2$) 8.70 (s, **C**H$_3$) 11.8 (s, **C**H$_3$)	9.40 (d, **C**H$_3$) $^{2}J_{(C,P)} = 2.04$ 25.0 (d, **C**H$_2$) $^{1}J_{(C,P)} = 21.4$	29.90 (d) $^{4}J_{(C,P)} = 2.5$	36.02 (s)	41.40 (d) $^{2}J_{(C,P)} = 10.4$	47.0 (d) $^{3}J_{(C,P)} = 6.4$	149 (4526)
Corresponding phosphaalkene [28]			29.1(d) $^{4}J_{(C,P)} = 2.0$	36.9(s)	47.5(d) $^{2}J_{(C,P)} = 22.3$	41.9(d) $^{3}J_{(C,P)} = 12.9$	
		[This work]	28.8(d) $^{4}J_{(C,P)} = 2.5$	36.6(s)	47.2(d) $^{2}J_{(C,P)} = 22.4$	41.6(d) $^{3}J_{(C,P)} = 13.7$	
2-(1-admantyl)-1λ^{3}-phosphaalkyne [28]			27.8(s)	35.7(s)	38.5(d) $^{2}J_{(C,P)} = 18.0$	42.9(d) $^{3}J_{(C,P)} = 6.0$	
		[This work]	27.9(s)	35.9(s)	38.5(d) $^{2}J_{(C,P)} = 18.3$	43.1(d) $^{3}J_{(C,P)} = 5.6$	

a) The $^{13}C\{^{1}H\}$ NMR signal of the P**C**Al$_2$ group cannot be detected. b) Alkyl group bound to aluminium; c) alkyl group bound to phosphorus; d) adamantly group (see Fig. 2.2.4).

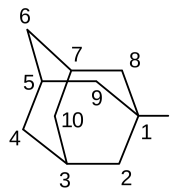

Figure 2.2.4. Numbering scheme for the carbon atoms of the adamantyl groups used in the discussion of the NMR spectra of compounds **1c** and **1d**

at 0.96 ppm with a coupling constant $^2J_{(H,P)} = 7.60$ Hz. As for the *tert*-butyl group one intense signal at 1.08 ppm is assigned to the main isomer, and a signal of less intensity (1:3) at 1.16 ppm to a second isomer. The origin of a weak singlet at 1.4 ppm cannot be ascertained. Some additional but weak doublets in the range from 0.70 to 0.86 ppm also come from CH_3–P groups and indicate that more than two isomers are present.

In the aforementioned discussion only the strongest and best resolved $^{13}C\{^1H\}$- and ^1H NMR signals could be assigned to at least one isomer. But in cases where broadening of the signals reduces their resolution, it was impossible to determine their origin. Further NMR parameters are listed in the Experimental Part.

2.2.3. Discussion of the Molecular Structures of 1a, 1b, 1c, and 1d

2.2.3.1. Crystal Data, Measuring Technique and Structure Analyses

Relatively large colourless cuboids suitable for X-ray structure analyses can be obtained when solutions of the compounds **1a** and **1b** in toluene are kept for three weeks at –60 °C. Similarly shaped crystals of compounds **1c** and **1d** precipitated from a 1:1 mixture of *n*-hexane and cyclopentane within two weeks at the same temperature. Data essential for structure determinations of **1a**, **1b** and **1c** were collected on a four-circle diffractometer P21 (Syntex, Cupertino, USA) whereas for **1d** a P4 diffractometer (Siemens Analytical X-ray Instruments Inc., Madison/Wisconsin, USA) was applied and as before graphite monochromatized Mo-K_α radiation (λ = 71.073 pm) was used. Lattice parameters were calculated from the exact positions of a selected number of reflections (Table 2.1) and refined thereafter. The determination of the monoclinic space group $P2_1/c$ (**1a** and **1d**) or $P2_1/n$ (**1b**) is based on unit cell dimensions and systematic absences (Table 2.1), whereas for **1c** space group $P\overline{1}$ was chosen over $P1$ mainly on grounds of E-value statistics and successful structure refinement. Since the asymmetric unit of **1c** contains two crystallographically independent molecules and one molecule of co-crystallizing cyclopentane the designation **1c•C_5H_{10}(2/1)** will be used for further discussion.

The crystal structures were solved by statistical methods employing the software package SHELXTL Version 5.10 [118-120] which also includes the program XP used for the analyses of molecular geometry and the preparation of drawings. Due to relatively low calculated absorption coefficients (Table 2.1) and the cuboid shape of the crystals absorption corrections were considered to be unnecessary. After all aluminium, chlorine, phosphorus and carbon atoms had been located step by step and their positions as well as their isotropic replacement parameters had been refined by full-matrix least-squares calculations, the structure determinations were continued with individual anisotropic U_{ij}-values. At the end the atomic coordinates of hydrogen atoms could either be taken from a different Fourier map and refined with their isotropic replacement parameters or were calculated on the basis of an idealized geometry which means a C–H distances of 98 pm and 99 pm of methyl and methylene groups, respectively, tetrahedral angles and a staggered arrangement of bonds at carbon. Furthermore the riding model applied ensures that a change in the carbon position is automatically transferred to the adjacent hydrogen atoms. The individual isotropic U-values of these hydrogen atoms were adopted from the pertinent carbon atom and increased by a factor of 1.5 for the methyl groups and 1.2 for the methylene units of the ethyl group, cyclopentane and adamantyl group as well as the methine units of the adamantyl moiety. Finally the parameters of all heavier atoms were subjected to a last least-squares refinement to take into account the incorporation of hydrogen atoms.

As for the structures discussed here the solution of the hydrogen problem developed as follows: all hydrogen atoms of compound **1b** could be located and their individual parameters were refined. In the course of the structure determinations of compounds **1a** and **1d**, only the hydrogen atoms of two methyl groups (C11 and C31) and two hydrogen atoms of the methylene group C31, respectively, could not be taken from the difference Fourier map; they had to be calculated as described above. All the hydrogen atoms of co-crystallisate **1c•C_5H_{10}(2/1)** were calculated as described above; the position of hydrogen atoms of the cyclopentane solvent molecule and the adamantyl moiety were treated as idealized contributions with a C–H distances of 99 pm and 100 pm for the methylene and methine units, respectively.

Crystallographic parameters and details of data collection have been summarized in Table (2.1). Bond lengths and angles as well as characteristic torsion angles can be found in Table (2.2). Final atomic coordinates and equivalent isotropic as well as anisotropic displacement parameters are given in Table 9.2.1 of the appendix.

Table 2.1. Crystal Data and Details of Structure Refinement for the Compounds **1a**, **1b**, **1c•C_5H_{10}(2/1)**, and **1d**.

Substituents at C/P; Compound	^{t}Bu/Me$_2$ **1a**	^{t}Bu/Et$_2$ **1b**	Ad/Me$_2$ **1c•C_5H_{10}(2/1)**	Ad/Et$_2$ **1d**
Empirical formula	$C_{11}H_{27}Al_3Cl_3P$	$C_{17}H_{39}Al_3Cl_3P$	$C_{17}H_{33}Al_3Cl_3P^{a)}$	$C_{23}H_{45}Al_3Cl_3P$
Molecular weight	377.61	461.74	455.85$^{a)}$	539.85
Melting point (°C)	118	129	133$^{b)}$	149
Diffractometer	P2$_1$	P2$_1$	P2$_1$	P4
Wavelength (pm)	71.073	71.073	71.073	71.073
Temperature (°C) of measurement	–100 ± 3	–100 ± 3	–100 ± 3	–100 ± 3
Shape and crystal size (mm)	colourless cubes; 0.4 x 0.4 x 0.4	colourless cuboids; 0.5 x 0.55 x 0.5	colourless cuboids; 0.8 x 0.7 x 0.4	colourless cuboids; 0.8 x 0.55 x 0.5
Crystal system	Monoclinic	Monoclinic	Triclinic	Monoclinic

Space group [117]; Systematic Absences	$P2_1/c$ (No.14); h0ℓ: ℓ = 2n +1, 0k0: k = 2n +1	$P2_1/n$ (No.14); h0ℓ: h + ℓ = 2n +1, 0k0: k = 2n +1	$P\bar{1}$ (No.2); none	$P2_1/c$ (No.14); h0ℓ: ℓ = 2n +1, 0k0: k = 2n +1
Number of reflections for cell dimensions; 2θ range (min. < 2θ < max.)	30 15.80°, 25.80°	35 15.12°, 27.02°	37 10.84°, 23.31°	67 10.27°, 24.94°
Unit cell dimensions a/pm	872.2(2)	834.71(17)	1215.2(2)	1146.80(17)
b/pm	2720.6(5)	1712.3(3)	1530.8(3)	1770.6(3)
c/pm	861.0(2)	1765.0(4)	1570.2(3)	1519.4(2)
α/°			68.52(3)	
β/°	103.33(3)	94.86(3)	81.57(3)	111.837(10)
γ/°			78.80(3)	
Volume (m^3)	$1987.9(7) \cdot 10^{-30}$	$2513.7(9) \cdot 10^{-30}$	$2657.2(9) \cdot 10^{-30}$	$2863.7(8) \cdot 10^{-30}$
Z)[c]	4	4	4 + 2[d]	4
Calculated density (kg/m^3)	$1.262 \cdot 10^3$	$1.220 \cdot 10^3$	$1.227 \cdot 10^3$	$1.252 \cdot 10^3$
Calculated absorption coefficient (μ/m^{-1})[e]	$0.659 \cdot 10^3$	$0.533 \cdot 10^3$	$0.509 \cdot 10^3$	$0.478 \cdot 10^3$
Absorption correction	None	None	None	None
F(000)	792	984	1040	1152
θ-Range for data collection (°)	2.50 to 30.00	1.66 to 30.00	1.40 to 27.00	1.85 to 27.00
Limiting indices	$-12 \le h \le 12$; $-38 \le k \le 34$; $-9 \le l \le 12$	$-1 \le h \le 11$; $-1 \le k \le 24$; $-24 \le l \le 24$	$-2 \le h \le 15$; $-19 \le k \le 19$; $-19 \le l \le 20$	$-8 \le h \le 14$; $-22 \le k \le 22$; $-19 \le l \le 18$
Scan modes [f]	Wyckoff-scan	Wyckoff-scan	Wyckoff-scan	ω-scans
Scan width (°) and velocity ((°) Min^{-1})	1.6; 4.0 to 29.3	1.4; 3.0 to 29.3	1.4; 4.0 to 29.3	1.4; 0.0 to 54.0
Reflections collected	7084	9256	12174	6527
Unique reflections (m)	5784	7342	11614	6222
Reflections observed with [I > 2 σ (I)] [g]	4230	5425	7883	4606
Parameters refined (n)	249	373	490	443
Restraints	0	0	0	0
Space filling (packing or Kitaigorodskii coefficient)[h]	72%	73%	69%[i]	73%
Goodness-of-fit (GOF)[j]	1.030	1.067	1.026	1.140
Isotropic R-indices[j]: R1/wR2 using all data R1/wR2 with [I>2σ(I)]	 0.1388/0.3114 0.1090/0.2911	 0.1422/0.3174 0.1117/0.2967	 0.1978/0.4020 0.1524/0.3766	 0.1350/0.2935 0.1059/0.2796
Anisotropic R-indices[j]: R1/wR2 using all data R1/wR2 with [I>2σ(I)]	 0.0822/0.1938 0.0586/0.1642	 0.0924/0.2066 0.0659/0.1847	 0.1513/0.3275 0.1092/0.3023	 0.1083/0.2414 0.0810/0.2281
Final R-indices[j]: R1/wR2 using all data R1/wR2 with [I>2σ(I)]	 0.0696/0.1244 0.0451/0.1124	 0.0733/0.1212 0.0471/0.1069	 0.1204/0.2301 0.0791/0.1962	 0.0894/0.1678 0.0626/0.1530
Indices f and g of weighting scheme w^{-1} [K]	f = 0.0548; g = 1.0981	f = 0.0534; g = 0.9365	f = 0.0965; g = 9.9786	f = 0.0940; g = 0.6464
Largest diff. peak; deepest hole ($10^{-30} e.m^{-3}$)	0.659; –0.728	0.402; –0.316	1.859; –0.529	1.027; –0.643

a) For only one molecule of **1c** (without cyclopentane); b) compound **1c** without cyclopentane (removed by evacuation); c) number of molecules in the unit cell; d) four molecules of compound **1c** and two molecules of cyclopentane; e) linear absorption coefficient $\mu = \Sigma\sigma_i / V_c$ [121]; f) Registration of the background at the beginning and at the end of the measurement with an overall duration equal to the time of measurement; g) Reflections with strongly negative intensity were not considered for refinement; h) calculated from the Kitaigorodskii formula [122]; bond lengths taken from **Table 2.2**; C–H; 108, van der Waals radii Al 205, P 190, C 180, Cl 180, H 117 pm [122-124]; i) including cyclopentane; j) for a definition of different quality factors R see Appendix, page 282; k) weighting scheme $w^{-1} = [\sigma^2(F_o)^2 + (f P)^2 + (g P)]$ with $P = 1/3(F_o^2 + 2F_c^2)$.

Table 2.2. Characteristic Bond Lengths (pm) and Bond Angles (deg.) as well as Torsion Angles for the Structures of **1a**, **1b**, **1c•C$_5$H$_{10}$(2/1)**, and **1d.**
The co-crystallizate **1c•C$_5$H$_{10}$(2/1)** contains the molecules **1.1c** and **1.2c**.

a) Bond lengths	^{t}Bu/Me$_2$ **1a**	^{t}Bu/Et$_2$ **1b**	Ad/Me$_2$ **1.1c**	Ad/Me$_2$[h] **1.2c**	Ad/Et$_2$ **1d**	Average
P4-C5	180.3(2)	181.1(2)	180.7(5)	182.0(6)	182.3(3)	181.3
P4-C41[a]	183.0(3)	184.3(2)	182.3(5)	181.8(6)	185.6(4)	183.4
P4-C42	182.7(3)	185.7(2)	183.1(6)	183.7(6)	186.7(4)	184.4
C5-C51/C50[b]	158.6(3)	158.8(3)	158.1(6)	158.4(7)	157.7(4)	158.3
C5-Al1	199.3(2)	198.9(2)	199.6(5)	198.3(5)	200.2(3)	199.3
C5-Al6	204.2(2)	204.2(2)	203.2(5)	204.3(5)	205.9(3)	204.4
Al1-C11	193.4(3)	195.3(3)	194.8(6)	193.8(7)	196.4(4)	194.7
Al6-C61	194.1(3)	196.2(3)	194.6(6)	193.5(6)	196.4(4)	195.0
Al1-Cl2	227.4(1)	227.2(1)	225.4(2)	229.2(3)	227.8(1)	227.4
Al1-Cl7	229.6(1)	229.8(1)	230.0(2)	230.5(2)	232.0(1)	230.4
Al6-Cl61	214.1(1)	216.2(1)	215.3(2)	216.0(2)	217.5(1)	215.8
Al6-Cl7	237.9(1)	235.6(1)	235.8(2)	236.7(2)	234.1(1)	236.0
P4-Al3	243.3(1)	245.2(1)	243.2(2)	242.8(2)	244.4(1)	243.8
Al3-C31[c]	199.2(2)	197.9(3)	203.3(4)	197.0(6)	200.1(3)	199.5
Al3-C32	193.8(3)	196.4(2)	193.4(7)	195.9(7)	196.0(4)	195.1
Al3-Cl2	233.0(1)	233.2(1)	232.2(2)	232.5(3)	233.4(1)	232.8

b) Bond angles	^{t}Bu/Me$_2$ **1a**	^{t}Bu/Et$_2$ **1b**	Ad/Me$_2$ **1.1c**	Ad/Me$_2$[i] **1.2c**	Ad/Et$_2$ **1d**	Average
C5-P4-Al3	113.5(8)	110.9(7)	112.0(2)	114.0(2)	109.5(1)	112.0
C5-P4-C41[d]	114.7(1)	114.5(1)	115.2(2)	115.5(3)	115.6(2)	115.1
C5-P4-C42	113.3(1)	110.4(1)	112.5(2)	113.0(3)	111.0(2)	112.0
Al3-P4-C41	102.5(1)	101.7(1)	103.5(2)	101.9(2)	99.8(1)	101.9
Al3-P4-C42	111.5(1)	117.2(8)	112.0(2)	111.0(2)	119.8(1)	114.3
C41–P4–C42	100.1(2)	101.7(1)	100.9(3)	100.2(3)	100.8(2)	100.7
P4-C5-Al1	112.0(1)	114.4(1)	112.9(2)	111.7(3)	115.7(2)	113.3
P4-C5-Al6	108.5(1)	107.5(1)	107.0(2)	107.4(3)	106.5(2)	107.4
P4-C5-C51[e]	118.8(2)	118.0(1)	119.9(3)	119.5(3)	118.0(2)	118.8
Al1-C5-Al6	91.6(1)	91.4(1)	91.9(2)	91.4(2)	91.1(1)	91.5
Al1-C5-C51/C50	110.7(2)	110.9(1)	110.1(3)	112.5(4)	110.6(2)	111.0
Al6-C5-C51/C50	111.9(2)	111.5(1)	111.5(3)	110.5(3)	111.5(2)	111.4
C5-Al1-Cl2	108.1(7)	107.6(6)	109.4(2)	108.2(2)	107.5(1)	108.1
C5-Al1-Cl7	95.5(7)	95.0(7)	95.0(2)	95.4(2)	95.0(1)	95.2
C5-Al1-C11[f]	133.3(1)	134.4(1)	133.6(2)	132.8(3)	135.2(2)	133.9
Cl2-Al1-Cl7	97.92(4)	97.98(4)	99.1(1)	97.8(1)	97.6(5)	98.1
Cl2-Al1-C11	106.1(1)	105.7(1)	105.1(2)	106.2(3)	107.2(1)	106.1
Cl7-Al1-C11	110.4(1)	110.2(1)	109.3(2)	111.0(3)	107.6(2)	109.7
C5-Al6-Cl7	91.7(7)	91.8(7)	92.3(2)	91.9(2)	92.9(1)	92.1
C5-Al6-Cl61	112.6(7)	112.5(7)	112.0(2)	112.8(2)	113.2(1)	112.6
C5-Al6-C61[f]	127.4(2)	127.3(1)	127.3(2)	127.1(2)	128.2(2)	127.5
Cl7-Al6-Cl61	101.2(4)	100.1(4)	98.4(8)	98.9(1)	99.3(5)	99.6
Cl7-Al6-C61	108.2(1)	109.4(1)	114.1(2)	111.8(2)	107.8(1)	110.3
Cl61-Al6-C61	110.4(1)	110.3(1)	108.2(2)	109.2(2)	109.6(1)	109.6
Al1-Cl7-Al6	76.5(3)	76.6(3)	76.9(7)	76.2(8)	77.0(4)	76.6
P4-Al3-Cl2	95.8(4)	97.0(3)	97.2(8)	95.8(1)	98.3(5)	96.8
P4-Al3-C31[f]	106.4(8)	107.5(1)	106.8(1)	108.1(2)	105.7(1)	106.9
P4-Al3-C32[f]	117.7(1)	120.4(2)	120.4(2)	117.1(2)	121.0(1)	119.3
Cl2-Al3-C31	101.4(8)	100.9(1)	102.0(1)	104.1(2)	102.4(1)	102.1
Cl2-Al3-C32	110.3(1)	107.0(1)	110.1(2)	110.8(2)	104.3(1)	108.5
C31-Al3-C32	121.2(1)	119.7(1)	117.1(2)	117.9(3)	121.1(2)	119.4
Al3-Cl2-Al1	103.7(4)	102.0(3)	103.7(8)	103.6(1)	100.8(5)	102.7

c) Torsion Angles [j)]	^{t}Bu/Me$_2$ **1a**	^{t}Bu/Et$_2$ **1b**	Ad/Me$_2$ **1.1c**	Ad/Me$_2$ **1.2c**	Ad/Et$_2$ **1d**
P4-C5-Al1-Cl2	28.5(1)	28.4(1)	24.1(3)	27.7(3)	25.6(2)
C5-Al1-Cl2-Al3	−23.1(8)	−28.3(7)	−15.8(2)	−23.8(2)	−29.2(1)
Al1-Cl2-Al3-P4	10.5(4)	18.1(4)	4.2(1)	11.6(1)	21.8(6)
Cl2-Al3-P4-C5	5.0(1)	−4.2(7)	9.3(2)	3.2(2)	−10.1(1)
Al3-P4-C5-Al1	−21.2(1)	−14.9(1)	−21.1(3)	−19.6(3)	−9.2(2)
C5-Al6-Cl7-Al1	15.3(7)	16.0(6)	14.0(1)	15.8(2)	14.1(1)
Al6-Cl7-Al1-C5	−15.8(7)	−16.5(6)	−14.3(1)	−16.3(2)	−14.6(1)
Cl7-Al1-C5-Al6	17.9(8)	18.5(7)	16.2(2)	18.4(2)	16.2(1)
Al1-C5-Al6-Cl7	−17.2(7)	−18.0(7)	−15.7(2)	−17.9(2)	−16.0(1)
C31-Al3-P4-C41	−15.6(1)	−22.6(2)	−10.6(3)	−15.0(3)	−26.4(2)
C51/C50-C5-P4-C41	−34.9(2)	−33.7(2)	−35.4(4)	−36.7(5)	−31.8(3)
C51/C50-C5-Al6-C61	−18.7(3)	−21.1(2)	−26.2(4)	−22.4(5)	−18.7(3)
C11-Al1-C5-C51/C50	28.5(2)	29.7(2)	25.2(5)	30.7(6)	23.9(3)
P4-C5-Al6-Cl61/Cl62	−28.2(1)	−32.4(1)	−30.3(2)	−30.7(3)	−31.9(2)

a) Mean C–C distance of the ethyl groups at phosphorus 153.2, individual values between 152.5(3) and 154.5(5); b) mean C–C distance of *tert*-butyl and 1-adamantyl groups at carbon 153.8, individual values between 152.0(8) and 156.3(5); c) mean C–C distance of the ethyl groups at aluminum 152.4, individual values between 149.7(5) and 154.0(6); d) mean P–C–C angle of the ethyl groups at phosphorus 113.4, individual values between 111.4(3) and 115.3(3); e) mean C–C–C angle of *tert*-butyl and 1-adamantyl groups at carbon 109.7, individual values between 105.2(3) and 113.3(4); f) mean Al–C–C angle of the ethyl groups at aluminum 114.8, individual values between 112.1(4) and 118.1(3). j) The torsion angle A–B–C–D is defined as positive if, when viewed along the B–C bond, atom A must be rotated clockwise to eclipse atom D [125, 126]. h) Mean C–C distance of the cyclopentane molecule 142.7, individual values between 134(2) and 160(3); i) mean C–C–C angle of the cyclopentane molecule 107.6, individual values between 104.6(12) and 114.6(15).

2.2.3.2. Discussion of Bond Lengths and Bond Angles

Although several isomers can NMR spectroscopically be detected for each of the dialkyl[1,1-bis(alkylchloroalanyl)organylmethyl]phosphine•dialkylchloroalane(1/1) complexes **1a** – **1d** in solution, X-ray structure analyses reveal that always the same isomer composed of a four- and a five-membered heterocycle is least soluble and precipitates. The respective molecular structures are depicted in stereoscopic view in Figs. 2.1 – 2.4. Additionally a molecule of co-crystallizing cyclopentane is shown in Fig. 2.3.

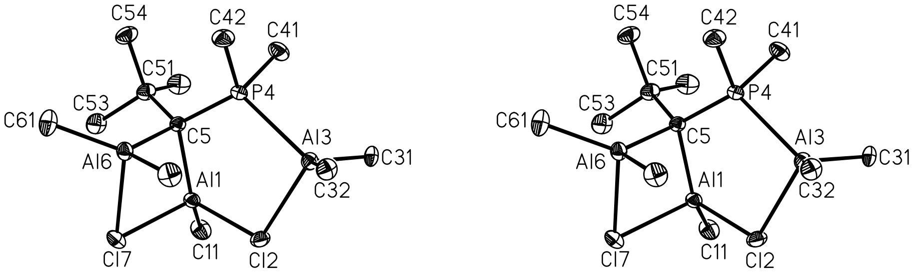

Figure 2.1. Stereoscopic view of **1a**. Thermal ellipsoids are at 30% probability; hydrogen atoms are omitted for clarity. The atoms Cl61 and C52 have not been labeled.

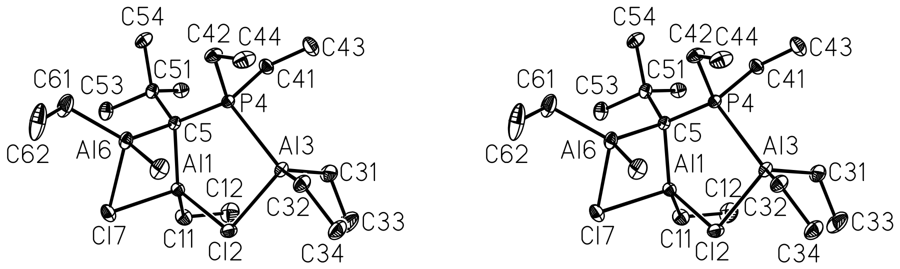

Figure 2.2. Stereoscopic view of **1b**. Thermal ellipsoids are at 30% probability; hydrogen atoms are omitted for clarity. The atoms Cl61 and C52 have not been labeled.

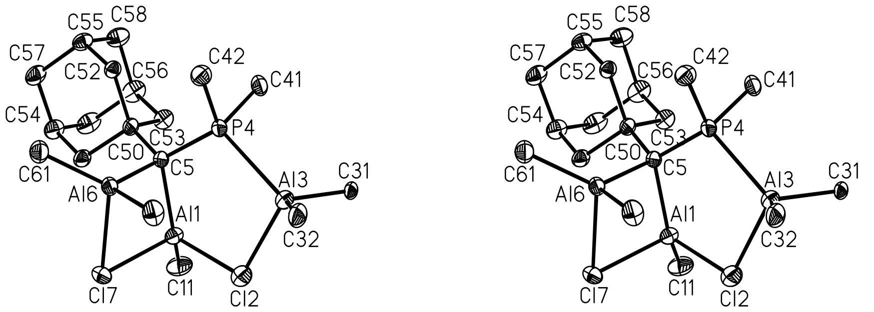

Molecule **1c.1**

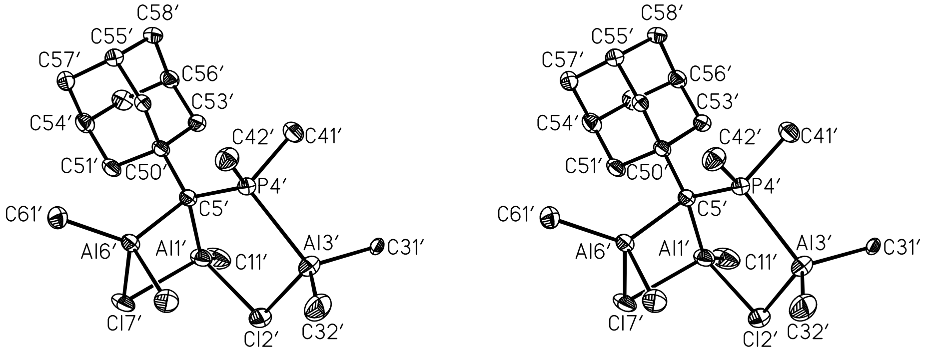

Molecule **1c.2**

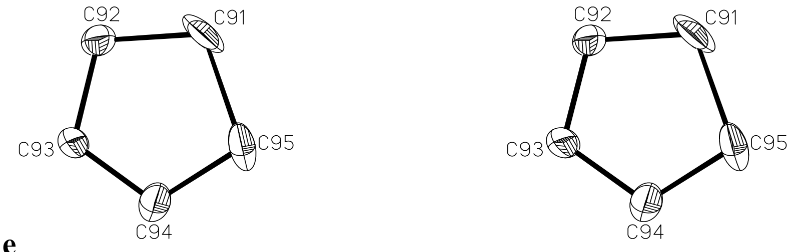

Cyclopentane molecule

Figure 2.3. Stereoscopic view of both the independent molecules **1c.1** and **1c.2** of compound **1c**•C_5H_{10}**(2/1)** as well as the solvent molecule C_5H_{10}.

Thermal ellipsoids are at 30% probability for **1c.1** and **1c.2** and at 5% for co-crystallizing cyclopentane; hydrogen atoms are omitted for clarity. The atoms C51, C59 and Cl61 of **1c.1** as well as C52′, C59′ and Cl62 of **1c.2** have not been labeled. Cl62 stands for the systematically correct label Cl61′.

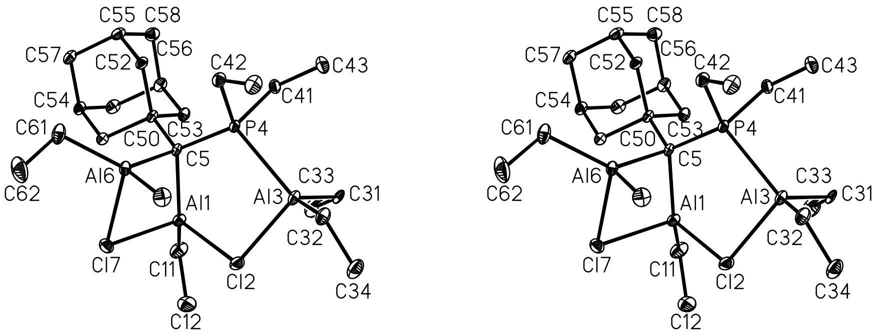

Figure 2.4. Stereoscopic view of **1d**. Thermal ellipsoids are at 30% probability; hydrogen atoms are omitted for clarity. The atoms C51, C59, C44, and Cl61 have not been labeled.

Since the $P\equiv C$ unit of the $1\lambda^3$-phosphaalkyne inserts into only one Al–C bond of the dialkylchloroalane molecules involved, a compound with two geminal alkylchloroalanyl substituents at the same carbon atom C5 is obtained. Whereas in one of these substituents the chlorine atom Cl61 remains unbridged the other one (Cl7) connects the two aluminium atoms Al1 and Al6 thus forming a four-membered heterocycle. With regard to mean Al–Cl values of 230.4 pm and 236.0 pm the bridge Al1–Cl7–Al6 can be considered to be nearly symmetrical, but as expected a slightly weaker bond to aluminium atom Al6 which is already linked to the terminal chlorine atom Cl61 is quite obvious.

Dative bonds between phosphorus (P4) and aluminium (Al3) on one end and between chlorine (Cl2) and aluminium (Al1) on the other are responsible for the complexation of a third dialkylchloroalane molecule to the insertion compound and the formation of a five-membered heterocycle. With regard to average values of 232.8 and 227.4 pm the bridge Al3–Cl2–Al1 is quite similar in symmetry, but surprisingly chlorine atom Cl2 has much more approached aluminium atom Al1 so that the longer Al–Cl distance is now observed to aluminium Al3 of the original molecule. Obviously a flat potential minimum exists where the chlorine atom can easily move to the opposite side. Remarkably, at distances of 238.16 and 233.95 pm on the one hand and of 237.2 and 233.8 pm on the other an analogous situation has been observed for the Al–Cl→Al-bridges of the polymorphous (space group $P2_1/n$ and $P\bar{1}$, respectively) dimer **XXVII** (see Table 2.3) by *Löw* in his thesis [112]. Apart from these details, however, for the complexes **1a** – **1d** slightly shorter Al–Cl bond lengths are met in the Al–Cl–Al bridges of the five-membered heterocycles; with regard to differences of only 3.0 and 3.2 pm, however, the deviations from values of the four-membered rings are rather small.

In Table 2.3 further compounds with Al–Cl–Al bridges as essential parts of five- and four-membered heterocycles have been compiled; characteristic bond lengths and angles are compared with those of the complexes **1a** – **1d.** Since in all of these adducts a neutral chlorodiorganylaluminium molecule is bound to an Al–C–P or an Al–C unit, the carbon atom of which is to some extend negatively charged, the parameters of the Al–Cl–Al bridges are found to be rather similar but again the Al–Cl distances vary considerably between 226.0 and 241.0 pm (**XXXI**). Furthermore, in the five-membered heterocycles the angles at the bridging chlorine atom Cl2 show values between 102.7° (average for **1a** – **1d**) and 106.9° (**XXVII**) [112], whereas in the four-membered heterocycles narrower angles between 76.6° and 78.8° are observed (Table 2.3). For the structures of dimeric dichloromethylalane [130] and dichloro[bis(trimethylsilyl)methyl]alane [131] which are discussed in some detail in the next paragraph, values of 91.1° and 91.01°, respectively, have been reported.

Table 2.3. Characteristic Bond Lengths (pm) and Angles (°) of Some Typical Compounds (**XXVII**, **XXX** – **XXXII**)[a)] with Al–Cl–Al Bridges in Comparison with Average Values of the Adducts **1a** – **1d.** The numbering scheme follows that already applied for the adducts **1a** – **1d** in Fig. 2.1 to 2.4.

	Average **1a-1d**	**XXVII** ($P2_1/n$) [112]	**XXVII** ($P\bar{1}$) [112]	**XXX** [127]	**XXXI** [128]	**XXXII** [129]
Five-membered heterocycle P4–C5–Al1←Cl2–Al3						
Al1←Cl2	227.4	234.0	233.8	239.2		
Cl2–Al3	232.8	238.2	237.2	227.3		
Al3←P4	243.8	243.4	243.3	243.1		
P4–C5	181.3	180.3	180.3	181.1		
C5–Al1	199.3	201.9	201.9	204.7		
Al1←Cl2–Al3	102.7	106.9	106.9	106.8		
Cl2–Al3←P4	96.8	85.8	85.7	91.3		
Al3←P4–C5	112.0	109.0	108.9	105.5		
P4–C5–Al1	113.3	105.6	105.4	114.4		
C5–Al1←Cl2	108.1	102.1	102.2	99.2		
Four-membered heterocycle C5–Al1–Cl7→Al6						
C5–Al1	199.3				211.6	198.4
Al1–Cl7/ Al1←Cl7	230.4				226.0	237.1
Cl7→Al6/ Cl7–Al6	236.0				241.0	238.1
Al6–C5/ Al6←C5	204.4				202.5	204.3
Al1-Cl7→Al6/ Al1←Cl7–Al6	76.6				78.4	78.8
Cl7→Al6–C5/ Cl7–Al6←C5	92.1				94.3	90.9
Al6–C5–Al1/ Al6←C5–Al1	91.5				91.0	97.1
C5–Al1–Cl7/ C5–Al1←Cl7	95.2				96.3	92.7

a) For structural formula of the compounds see next page.

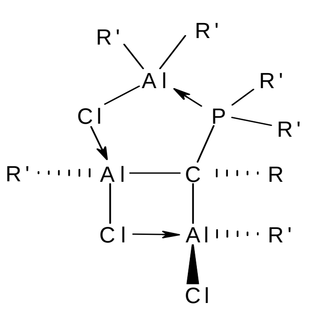

1a-1d

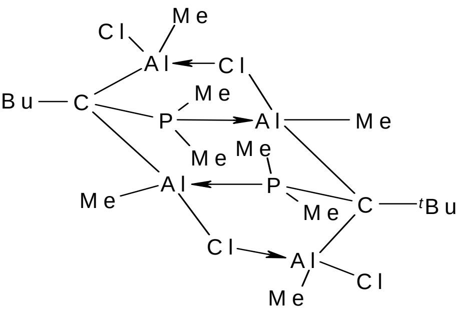

XXVII

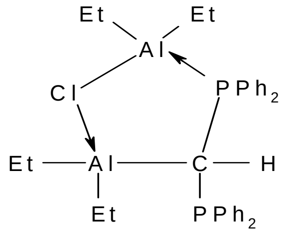

XXX

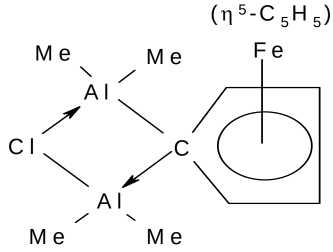

XXXI

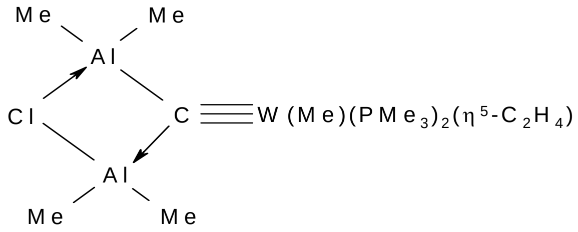

XXXII

In comparison to the average bond length of all bridging Al–Cl entities of 231.7 pm in the adducts **1a** – **1d**, the terminal bond Al6–Cl61 exhibits a much shorter distance of 215.8 pm only. The observed difference of 15.9 pm is found to be rather large but the length corresponds very well with the standard value of 213.5 pm published by *Haaland* and *Blom* [132-134] some years ago. For the terminal Al–Cl bonds in the gaseous dimer Al_2Cl_6 a rather short distance of 207 pm has been reported [135] but with respect to the value of the bridging Al–Cl entities of 225 pm the difference (18 pm) is fairly similar. X-ray structure analyses of dimeric dichloromethyl- [130] and dichloro[bis(trimethylsilyl)-methyl]alane [131] also reveal short terminal Al–Cl bonds of 205.0 and 206.8 pm, respectively, whereas the bridging Al–Cl distances cover a range between 225.4 and 237.9 pm. Longer terminal Al–Cl bonds are observed in the tetrahydrofuran complexes of dichloro(2,4,6-tri-*tert*-butylphenyl)aluminium (213.1 and 217.3 pm) and chloro(2,4,6-tri-*tert*-butylphenyl)-hydridoaluminium (217.4 pm) [136] with sterically crowded aluminium atoms of coordination number four.

Surprisingly, already in the complexing dialkylchloroalane molecules of **1a** – **1d** the distances Al3–C31 and Al3–C32 between aluminium and both the adjacent carbon atoms of the alkyl substituents vary considerably between 197.0 and 203.3 pm on the one side and between 193.4 and 196.4 pm on the other. Since neither these differences of 6.3 and 3.0 pm, respectively, in the lengths of chemically equivalent bonds nor the difference of 4.4 pm between their average values of 199.5 and 195.1 pm are difficult to understand, only a specification but not an interpretation of these Al–C values can be given. Mean Al–C bond lengths of 194.7 and 195.0 pm for Al1–C11 and Al6–C61, respectively, as short as the average of Al3–C32, are also observed between the geminal aluminium atoms of the Al_2C-group arising from the insertion reactions, and their alkyl substituents. Likewise carbon atom C5 of the former P≡C unit forms two Al–C bonds of different lengths. Whereas one distance (C5–Al1, 199.3 pm) equals Al3–C31, the other one (C5–Al6) comes up to a much higher value of 204.4 pm. A similar length of 204.7 pm has been reported by *Schmidbaur* et al. [127] for the endocyclic Al–C bond of the complex [1,1-bis(diphenylphosphanyl)methyl]diethylalane•chlorodiethylalane (**XXX**, Fig. 2.5).

Gas electron diffraction reveals an Al–C bond length of 195.7 pm for monomeric trimethylalane [137]. Whereas similar values between 194.9 and 195.6 pm have been determined by X-ray structure analyses for the terminal Al–C distances of the dimer $Al_2(CH_3)_6$ [138], the bonds in the Al–C–Al bridges were found to be considerably longer (212.3 to 212.5 pm). A length of 197.3 pm has been published for the adduct $(H_3C)_3Al \leftarrow P(CH_3)_3$ in the gas phase [139].

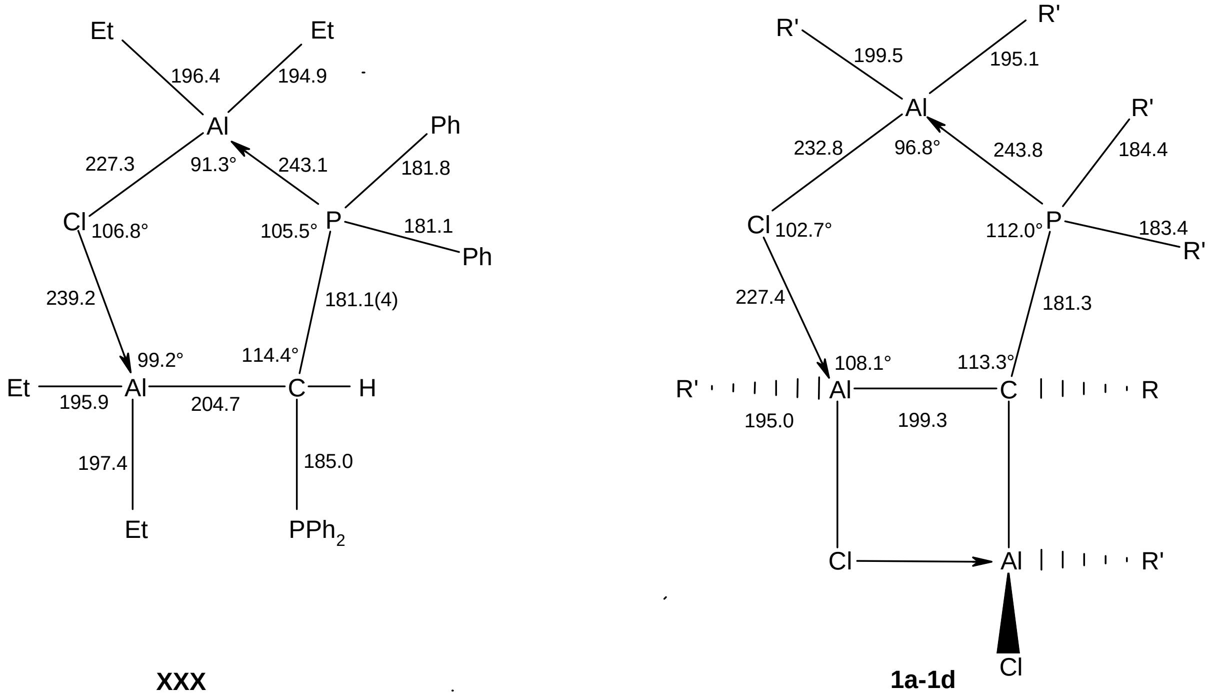

XXX **1a-1d**

Figure 2.5. Characteristic bond lengths and angles in the five-membered heterocycle of the complex [1,1-bis(diphenylphosphanyl)methyl)]diethylalane•chlorodiethylalane [127] in comparison with average values of compounds **1a** – **1d.**

Finally, one should mention that in the four-membered heterocycles of compounds **1a** – **1d** the intramolecular distances Al1····Al6 vary only slightly between values of 288.1 and 290.0 pm. With respect to an average of 289.1 pm both atoms approach each other to such an extent that the element-element distance of metallic aluminium (286.3 pm) [140] is almost achieved. As for the endocyclic angles in the four- and five-membered heterocycles, most average values do not differ by more than 6° from the right or the tetrahedral angle, respectively; stronger deviations to values of 76.6° and 96.8° are observed merely for the angles Al1–Cl7–Al6 and P4–Al3–Cl2. A main reason for this conformity might be the same coordination number four for the ring atoms phosphorus, carbon, aluminium and two for chlorine (Cl7 and Cl2).

The length of the dative bond between the phosphorus atom of the initially formed insertion product and the aluminium atom of the complexing chlorodiorganylalane exhibits only slightly differing values between 242.8 and 245.2 pm (average 243.8 pm). A similar distance of 243.1 pm has been reported by *Schmidbaur* et al. for compound **XXX** (Fig. 2.5); in his thesis [112] *Löw* ascertained analogous Al←P bond lengths of 243.4 and 243.3 pm in both the polymorphous (space group $P2_1/n$ and $P\overline{1}$, respectively) forms of bis[[1,1-bis(chloromethylalanyl)-2,2-dimethylpropyl]dimethylphosphane-*Al*,*P*] **XXVII** (see footnote a) of Table 2.3) – a compound obtained from complex **1a** by liberation of chlorodimethylalane.

In their publication on the gas phase structure of the adduct $Me_3Al{\leftarrow}PMe_3$ *Haaland*, *Weidlein* and coworkers [139] have compiled a series of very different Al–N compounds and emphasized that the Al–N distance depends strongly on the portion of dative bond involved. The highest values have been determined for pure dative bonds in Lewis acid-base complexes of composition $R'_3Al{\leftarrow}NR_3$, whereas the shortest bond is observed in aluminium nitride (CN = 4; wurtzite structure) with a portion of only 25% dative bond.

Already a short inspection of bond lengths compiled in Table 2.5 for various types of Al–P compounds, however, reveals that *Haaland's* approach to Al–N distances [139] can only partially be transferred to phosphinoalanes and Lewis acid-base adducts between alanes and phosphines. Indeed, the lowest values of 234.2 and 236.7 pm have been reported for the length of the completely covalent or nearly covalent Al–P bond of the monomeric phosphinoalane $(2,4,6\text{-}{}^{i}Pr_3H_2C_6)_2Al{-}P(1\text{-ad})(SiPh_3){\bullet}0.5$hexane [141] and aluminium phosphide AlP (CN = 4; sphalerite structure) [142]. Both lengths approach the corrected sum (236.0 pm [164]) of covalent radii for aluminium (130 pm [164]) and phosphorus (110 pm [164]). Much longer distances of 251 to 256 pm, however, are known for the completely dative Al←P bonds in Lewis acid-base adducts such as $Ph_3Al{\leftarrow}P(SiMe_3)_3$ [154], $Me_3Al{\leftarrow}PPh_3$ [161], and $Et_3Al{\leftarrow}P(SiMe_3)_3$ [114], respectively, or for $Me_3Al{\leftarrow}PMe_3$ in the gas phase [139]. Quite obviously, the bond lengths increase to even higher values of 265 to 276 pm, when very bulky substituents are bound to both or only one of the central atoms.

The majority of compounds, however, exhibit bond lengths which fall into the intermediate range of 239 to 252 pm. As for the Lewis acid-base adducts relatively short Al←P distances are observed when the phosphine is coordinate to an aluminium(III) halide. The shortness of the distances can be attributed in part to the inductive effect of the more electronegative substituent X at the aluminium atom, which substantially increases the Lewis acidity. Without doubt this argument holds also for mixed compounds R_nAlCl_{3-n}, the Lewis acidity of which is, however, reduced to some extend by the organyl substituents. The length of the Al←P bond in these adducts with organylaluminium halides varies considerably e.g. from 249.8 pm in $Br(Me_3SiCH_2)_2Al \leftarrow P(SiMe_3)_3$ to 242.5 pm in the six-membered heterocycle **B** (footnote of Table 2.5).

With regard to an average value of 243.8 pm the compounds **1a** – **1d** of this thesis featuring dialkylchloroalane as a Lewis acid and a completely dative bond between phosphorus and aluminium are met nearly in the middle of that range. Very remarkably, they are accompanied by three four-membered heterocycles $[Br(Me_3SiCH_2)Al–P(SiMe_3)_2]_2$ (243.5; 243.6 pm), $[Me_2Al–P(SiMe_3)_2]_2$ (245.3; 246.0 pm), and $[Et_2Al–P(SiMe_3)_2]_2$ **I** (245.4; 246.0 pm), the Al–P bonds of which have to be considered as half-way dative and half-way covalent (see footnote b) of Table 2.4). Whereas one can easily understand that these values coincide with the mean of the bond lengths determined for the above mentioned monomeric phosphinoalane (234.2 pm [141]) and the adduct $Me_3Al \leftarrow PMe_3$ (253 pm [139]), reasons for the shortening of the pure dative bond in compounds **1a** – **1d** and in the analogous five- and six-membered heterocycles of *Schmidbaur*, *Karsch* and co-workers [127, 148] are not known for sure. Most probably inductive effects of the chlorine atom at aluminium could be responsible.

An inquiring of *Cambridge Structural Database* [165] revealed that for a series of relevant compounds the P–C bond lengths shorten strongly when the oxidation state of the central phosphorus atom changes from + III to + V. In review articles published some years ago *Gilhany* [166-168] explained this phenomenon with an alteration of the valence state from almost p^3 in e.g. phosphines to sp^3 in e.g. oxophosphoranes. Parallel to an increase in coordination number, this effect is additionally intensified by a stronger Coulomb attraction between the positively charged phosphorus atom and the more electronegative carbon. For example, the average P–C distance of 183.0 pm in triphenylphosphine [169] changes to 176.0 pm in triphenylphosphinoxide [170]. Independently, *Ochs* [171] and *Binder* [172] determined a similar P–C distance of 176.9 pm for solid hexakis-(phenyldioxophosphorane).

Remarkably, such a strong bond shortening as discussed before is not observed in the adducts **1a** – **1d**. Even though the exocyclic distances P4–C41 and P4–C42 between phosphorus and the alkyl substituents vary considerably between 181.8 and 185.6 pm on the one side and between 183.1 and 186.7 pm on the other, both the average bond lengths of 183.4 and 184.4 do not deviate significantly from the standard value of 185.0 pm reported for uncomplexed trialkylphosphines [167]. Analogous results have been obtained for the compounds trimethylphosphine (184.6 pm [173]) and its trimethylaluminium complex $Me_3Al{\leftarrow}PMe_3$ (182.2 pm [139]) by gas electron diffraction; the P–C distance shortens by only 2.4 pm. In his thesis *Ochs* [171] specifies a P–C bond length of 183.6 pm for the borane adduct of phenylbis(trimethylsilyl)phosphine.

Table 2.4. Characteristic Al–P Distances (pm) in Comparison with the Average (av.) Value of the Adducts **1a-1d.**

	Al–P distances	literature
1a – 1d	243.8 (av.)$^{a)}$	[this work]
$(2,4,6\text{-}{}^{i}\mathrm{Pr_3H_2C_6})_2\mathrm{Al{-}P(1\text{-}ad)(SiPh_3)\cdot 0.5hexane}$	234.2	[141]
$\mathrm{(AlP)_x}$	236.7	[142]
$\mathrm{Br_3Al{\leftarrow}P(SiMe_3)_3\cdot toluene}$	239.1	[143]
$\mathrm{Cl_3Al{\leftarrow}P(SiMe_3)_3\cdot toluene}$	239.2	[143]
A$^{b)}$	240.3, 241.2	[144]
$\mathrm{Me_3N{\rightarrow}H_2Al{-}P(2,4,6\text{-}Me_3H_2C_6)_2}$	240.9	[145]
$[{}^{i}\mathrm{BuAl{-}P(SiPh_3)]_4}$	241.4 (av.)	[146]
$\mathrm{Et_2O{\rightarrow}{}^{t}Bu_2Al{-}P(2,4,6\text{-}{}^{i}Pr_3H_2C_6)(SiPh_3)}$	241.6	[147]
B$^{b)}$	242.5	[148]
C$^{b)}$	243.1	[127]
D$^{b)}$ ($P\bar{1}$)	243.3	[112]
D$^{b)}$ ($P2_1/n$)	243.4	[112]
$\mathrm{[Me_2Al{-}PMe_2]_3}$	243.4$^{c)}$	[149]
$\mathrm{Cl_2EtAl{\leftarrow}P(SiMe_3)_3}$	243.5	[150a]
$\mathrm{[Br(Me_3SiCH_2)Al{-}P(SiMe_3)_2]_2}$	243.5, 243.6	[151]
E$^{b)}$	244.1	[104]
$\mathrm{[(Me_3Si)_2Al{-}P(}c\mathrm{\text{-}C_6H_{11})(H)]_3}$	244.4 (av.)	[152]
$\mathrm{[(Me_3Si)_2Al{-}PPh_2]_2}$	244.6 (av.)	[152]
$\mathrm{[Me_2Al{-}CH_2{-}PMe_2]_2}$	245.1	[148]
F$^{b)}$	245.1	[153]
G$^{b)}$	245.3	[144]
H$^{b)}$	245.38	[104]
$\mathrm{[Me_2Al{-}P(SiMe_3)_2]_2}$	245.3, 246.0	[150b]
$\mathrm{[Et_2Al{-}P(SiMe_3)_2]_2}$ (**I**)$^{b)}$	245.4, 246.0	[150a]
$\mathrm{[(Me_3Si)_2Al{-}P(SiMe_3)(Ph)]_2}$	246.6 (av.)	[152]
$\mathrm{ClPh_2Al{\leftarrow}P(SiMe_3)_3}$	246.7	[154]
$\mathrm{H_3Al{\leftarrow}P(}c\mathrm{\text{-}C_6H_{11})_3}$	246.7	[155]
$\mathrm{H_3Al{\leftarrow}P{}^{t}Bu_3}$	247.1	[156]
$[{}^{i}\mathrm{Bu_2Al{-}PPh_2]_2}$	247.5, 247.6	[157]
$\mathrm{Cl_2MeAl{\leftarrow}PPh_2{-}CH_2{-}PPh_2{\rightarrow}AlCl_3}$	245.1, 249.7	[158]
$\mathrm{Br(Me_3SiCH_2)_2Al{\leftarrow}P(SiMe_3)_3}$	249.8	[151]
$\mathrm{Me_2(4\text{-}Me\text{-}2,6\text{-}{}^{t}Bu_2\text{-}C_6H_2O)Al{\leftarrow}PMe_3}$	249.9	[159]
${}^{i}\mathrm{Bu_2ClAl{\leftarrow}P(SiMe_3)_3}$	250.4	[150a]
J$^{b)}$	250.9, 254.2	[144]
$\mathrm{Ph_3Al{\leftarrow}P(SiMe_3)_3}$	251.4, 252.1$^{d)}$	[154]
$\mathrm{Me_3Al{\leftarrow}PMe_3}$	253$^{c)}$	[139]
$\mathrm{(Me_3Al)_3{\leftarrow}[(Ph_2P{-}CH_2{-}CH_2)_2PPh]\cdot 0.5C_6H_6}$ (**K**)$^{b)}$	250.4, 253.1, 253.5	[160]
$\mathrm{Me_3Al{\leftarrow}PPh_3}$	253.5	[161]
$\mathrm{Me_3Al{\leftarrow}PPh_2{-}CH_2{-}CH_2{-}PPh_2{\rightarrow}AlMe_3}$	254.4	[160]
$\mathrm{Et_3Al{\leftarrow}P(SiMe_3)_3}$	255.5	[114]
$\mathrm{Me_3Al{\leftarrow}P(}o\mathrm{\text{-}tolyl)_3}$	258.4	[161]
$\mathrm{Me_3Al{\leftarrow}PPh_2{-}CH_2{-}PPh_2{\rightarrow}AlMe_3}$	252.1, 258.5	[162]
${}^{t}\mathrm{Bu_3Al{\leftarrow}P(C_3H_7)_3}$	259.5	[163]
${}^{t}\mathrm{Bu_3Al{\leftarrow}P{}^{i}Pr_3}$	266.7	[114]
$\mathrm{(Me_3C\text{-}CH_2)_3Al{\leftarrow}P(SiMe_3)_3}$	267.0 (av.)$^{e)}$	[151]
oligomeric $\mathrm{[H_3Al{\leftarrow}P({}^{i}Pr_2)CH_2CH_2({}^{i}Pr_2)P){\rightarrow}AlH_3]_n}$	270.8, 275.5	[155]

a) Individual values between 242.8(2) and 245.2(1); b) for formulas see footnote on next page; c) results of a gas electron diffraction; d) two crystallographically independent molecules in the asymmetric unit; e) average Al–P distance of three crystallographically independent molecules in the asymmetric unit.

b) Structural formulas of compounds **1a** – **1d** and **a** – **k**.

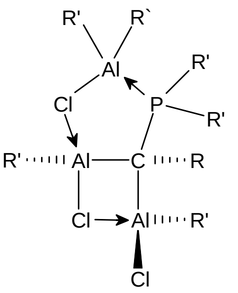

1a - 1d

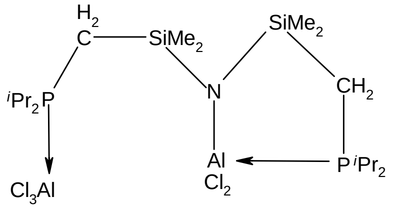

A

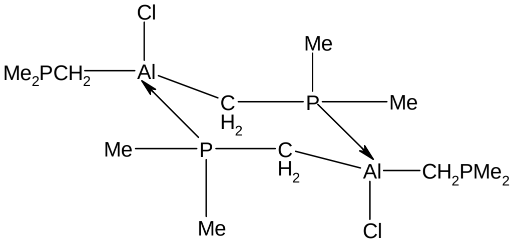

B

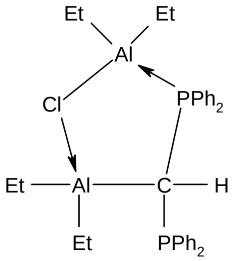

C

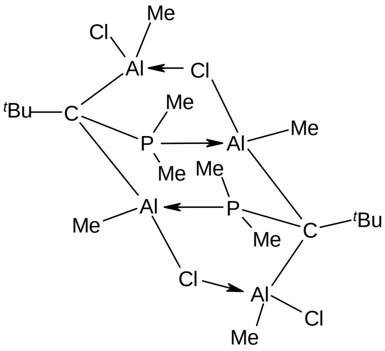

D

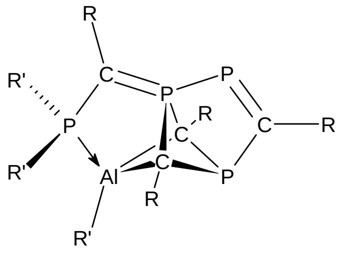

R = *tert*-butyl; R` = ethyl

E

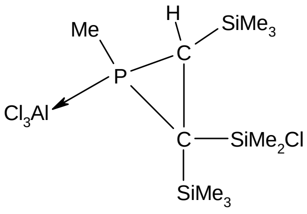

F

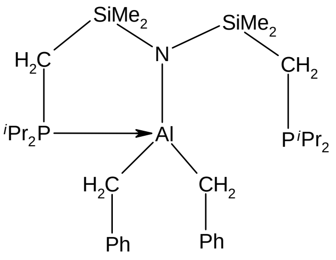

G

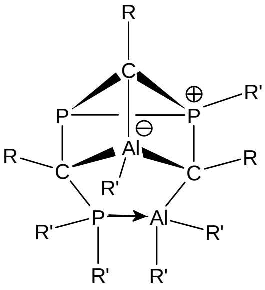

R = *tert*-butyl; R`= ethyl

H

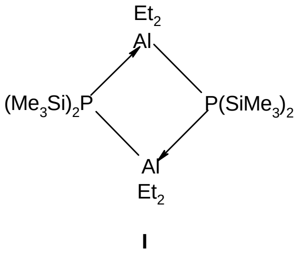

I

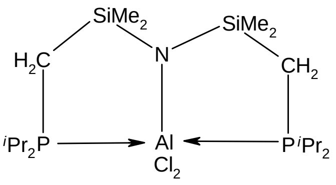

J

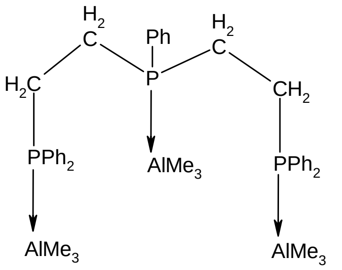

K

At the moment an interpretation of the only slight shortening of P–C bonds upon complexation and the rather large variations of the P4–C4*n* values (*n* = 1 or 2) in the adducts **1a** – **1d** can hardly be given. We assume that the slight shortening might essentially be attributed to an only weak increase of the positive charge at phosphorus when the atom acts as center of a Lewis base and that the influence of an altered valence state might be negligible.

With regard to an average of 181.3 pm the bond P4–C5 exhibits slightly lower values of 180.3 to 182.3 pm. A similar distance of 181.1 pm has been reported by *Schmidbaur* et al. [127] for the analogous compound **XXX** (Fig. 2.5). With the assumption given above in mind, an increased Coulomb attraction between carbon atom C5, here more negatively charged by two neighbouring aluminium atoms (Al1 and Al6), and the a priori positively charged phosphorus atom seems to be responsible for the additional bond shortening.

In this context one should mention *Karsch's* interpretation of bond lengths in the centrosymmetric dimer ($Me_2Al–CH_2–PMe_2)_2$. He noted [148] that the endocyclic P–C bond is shortened by 3.0 pm with respect to the average of the exocyclic P–C distances, and that in contrast to this result the length of the endocyclic Al–C bond exceeds the average of the exocyclic ones by 3.0 pm. Since dimer **L** may be considered as to be composed of two dimethyl(dimethylalanylmethyl)phosphine (**L1**) or of two dimethyl-(dimethylalanyl)methylenephosphorane molecules (**L2**), the mesomeric form **L2** with its polar ylidic double bond gains importance and its contribution explains the shortening of the endocyclic $P^{\oplus}–C^{\ominus}$ distance. Coincidentally the endocyclic Al–C single bond is converted into a weaker and hence longer dative bond. Such a suggestion seems reasonable as the adduct $Me_3PCH_2AlMe_3$ can be synthesized by direct combination of the compounds Me_3PCH_2 and $AlMe_3$ [174]. It is monomeric in benzene and may be sublimed without decomposition. The structure has been established by spectroscopic techniques but has not yet been corroborated by diffraction methods.

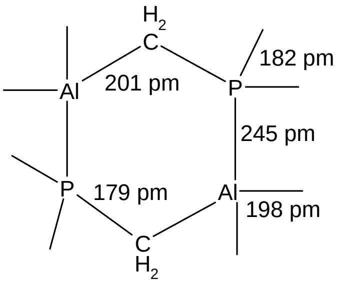

L

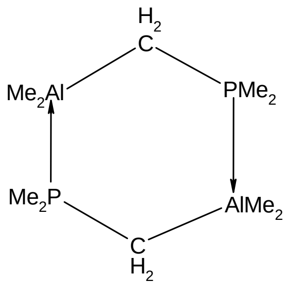

L1

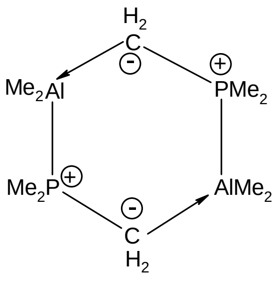

L2

According to an article published by *Allman* [175] in 1977 the conformation of five-membered heterocycles can easily be recognised by their torsion angles. Whereas the sequence $(+\alpha, -\beta, 0, +\beta, -\alpha)$ characterizes the *envelope* conformation (mirror symmetry), the presence of a *twisted* conformation (C_2-symmetry) is indicated by $(+\alpha, -\beta, \gamma, +\beta, -\alpha)$. Since the observed values (Table 2.2) are more or less in accordance with the first possibility, in all four complexes **1a** – **1d** the *envelope* conformation is realized. One, however, should not fail to mention that for **1a** and **1d** the deviations from the predicted sequence are rather large. An analogous *envelope* conformation has also been observed by *Schmidbaur* et al. for compound **XXX** [127] (Fig. 2.5).

Table 2.5. a) Deviations (pm) from planarity of the four- and five-membered heterocycles of compounds **1a** – **1d**.

	C5	Al6	Cl7	Al1		P4	C5	Al1	Cl2	Al3
1a	17.5	–14.9	13.2	–15.9	**1a**	–7.8	19.7	–21.3	14.7	–5.3
1b	–18.2	15.6	–13.8	16.5	**1b**	–0.47	16.7	–24.9	21.6	–12.9
1c.1	–15.9	13.6	–12.1	14.3	**1c.1**	10.7	–18.0	15.3	–7.9	–0.22
1c.2	–18.1	15.3	–13.6	16.4	**1c.2**	–6.3	18.8	–21.6	15.6	–6.5
1d	–16.1	13.9	–12.4	14.5	**1d**	–4.5	–13.2	25.0	–24.6	17.2

b) Dihedral angle (°) between the planes of the four- and five-membered heterocycles of compounds **1a** – **1d**.

1a	**1b**	**1c.1**	**1c.2**	**1d**
77.0	74.8	78.0	77.2	73.2

Further information on the deviations from planarity of the four- and five-membered heterocycles are given in Table 2.5. The dihedral angle between the two planes varies only slightly between 73.2° and 78.0°; the average is 76.8°. Figures 2.6 – 2.9 give stereoscopic views of the molecular packing; no intermolecular contacts significantly shorter than *van der Waals* distances were found.

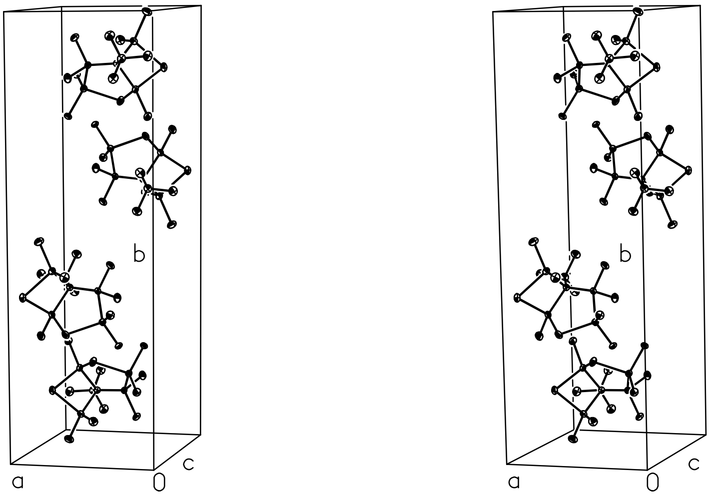

Figure 2.6. Unit cell contents of compound **1a** in stereoscopic view. Thermal ellipsoids are at 30% probability; hydrogen atoms are omitted for clarity.

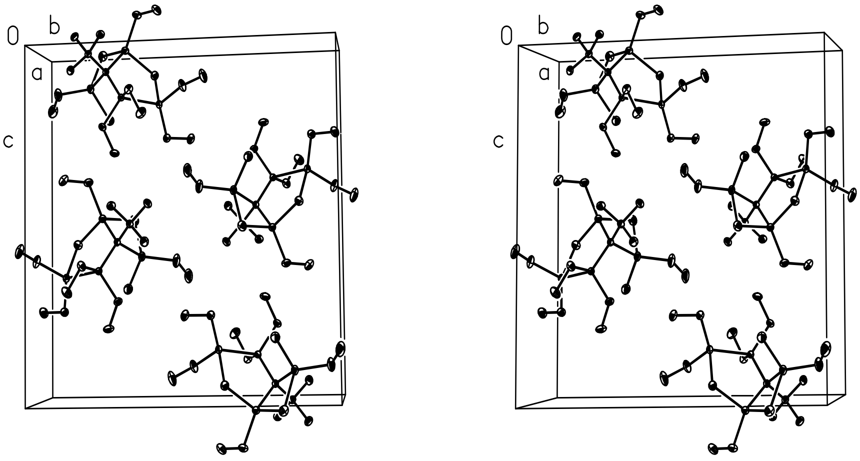

Figure 2.7. Unit cell contents of compound **1b** in stereoscopic view. Thermal ellipsoids are at 30% probability; hydrogen atoms are omitted for clarity.

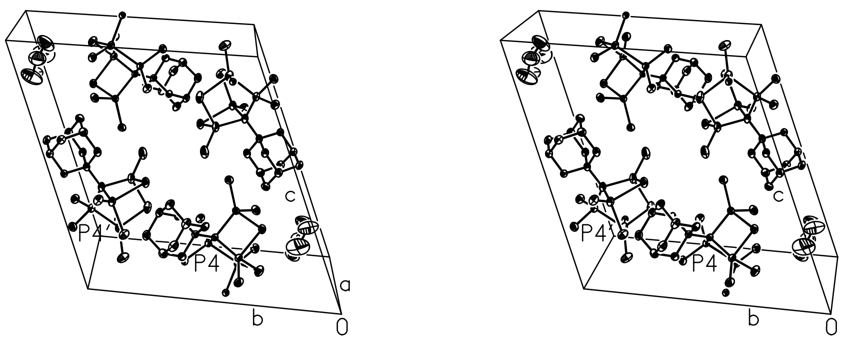

Figure 2.8. Unit cell contents of the co-crystallizate **1c•C$_5$H$_{10}$(2/1)** in stereoscopic view. In order to differentiate between the two crystallographically independent molecules the atoms P4 and P4′ have been labeled. Thermal ellipsoids are at 30% probability; hydrogen atoms are omitted for clarity.

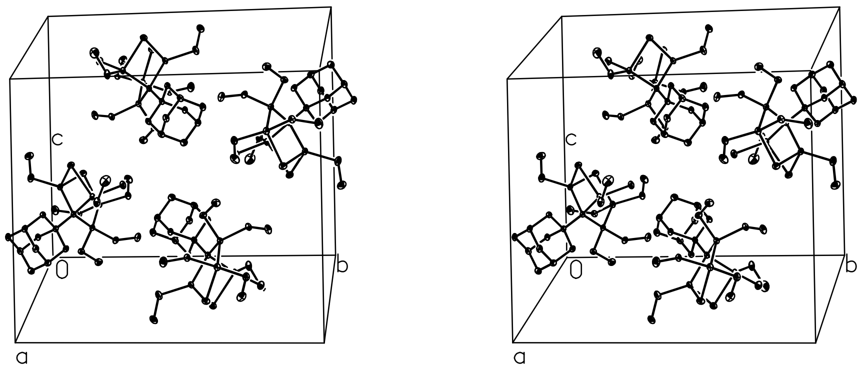

Figure 2.9. Unit cell contents of compound **1d** in stereoscopic view. Thermal ellipsoids are at 30% probability; hydrogen atoms are omitted for clarity.

3. Reactions of 2-*tert*-Butyl-$1\lambda^3$-phosphaalkyne with Halodiorganylphosphines

3.1. Introduction

Solutions of phosphorus(III) chloride, bromide and iodide in benzene react with two equivalents of 2-*tert*-butyl-$1\lambda^3$-phosphaalkyne to form the corresponding 2,4,5-trihalo-$2\lambda^3,4\lambda^3,5\lambda^3$-triphosphabicyclo[1.1.1]pentane heterocycles as final products. According to Scheme 1.5 on page 26 these compounds are the result of an intermolecular insertion of the P≡C unit into only *one* of the phosphorus halogen bonds to furnish a $1\lambda^3$-phosphaalkene first as well as of a subsequent [2+2]cycloaddition with a second equivalent of $1\lambda^3$-phosphaalkyne which should afford a 1,2-dihydro-$1\lambda^3,3\lambda^3$-diphosphete. However, none of these intermediates could be observed when the reaction was monitored by $^{31}P\{^1H\}$ NMR spectroscopy.

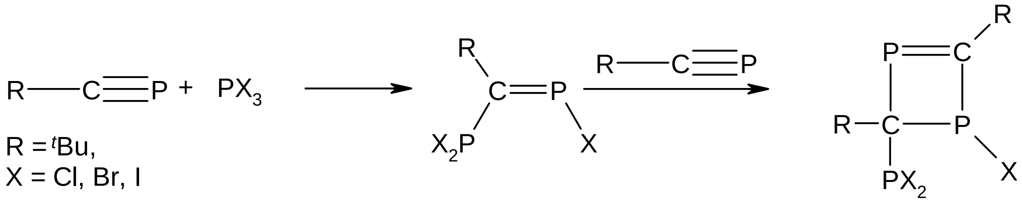

In the 1,2-dihydro-$1\lambda^3,3\lambda^3$-diphosphete the Lewis acidity of the exocyclic PX_2 group is supposed to be sufficiently high so that a transannular electrophilic attack at the *sp*^{2}-hybridised carbon of the P=C bond can follow. The resulting highly reactive zwitterion comprises a dihalogen-substituted negatively charged as well as a halogen-free positively charged phosphorus atom and stabilizes by 1,3-migration of a halide anion.

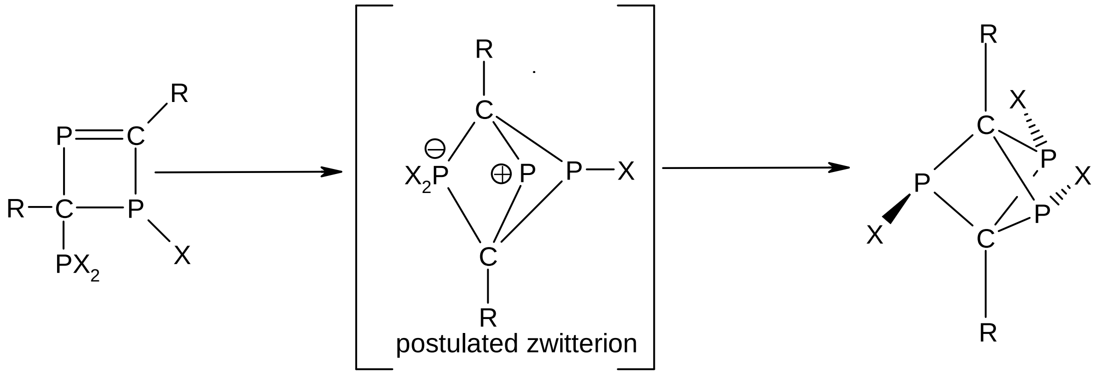

In detail the synthesis of 2,4,5-tribromo-1,3-di-*tert*-butyl-$2\lambda^3,4\lambda^3,5\lambda^3$-triphosphabicyclo-[1.1.1]pentane starts with phosphorus(III) bromide and 2-*tert*-butyl-$1\lambda^3$-phosphaalkyne. The oligocycle is isolated after three days at 60 ºC in benzene as solvent and obtained as colourless rods in 73 to 79% yield after repeated recrystallisation from *n*-pentane. An X-ray structure determination reveals molecular C_3 symmetry; bond lengths and angles do not deviate substantially from expected values [80, 81, 87]. Subsequent treatment of this compound with three equivalents of lithium trimethylsilanide at –70 °C in *n*-hexane resulted in a substitution of all bromine atoms for trimethylsilyl groups. Here too, the substituents at phosphorus are arranged in an all-*trans* configuration; as to be expected for reactions at a polycyclic framework, however, the yield is rather low [88].

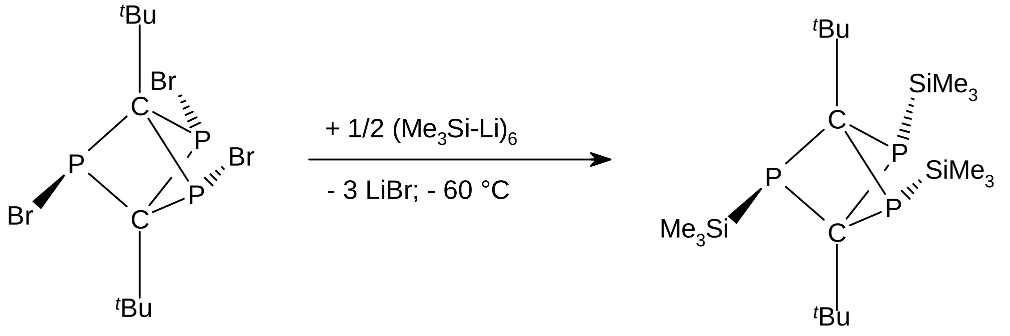

In the presence of electron-rich transition metal fragments such as [M(η^5-C_5R_5)] (M = Co, Rh, Ir; R = H or Me) and $Fe(CO)_3$ [70-72] 1λ^3-phosphaalkynes are known to undergo cyclization reactions which preferentially afford 1λ^3,3λ^3-diphosphacyclobutadienes. The 14 valence electron species Cp_2Zr which is generated *in situ* from the corresponding dichloride and two equivalents of *n*-butyl lithium at –78 °C, however, furnishes the tricyclic 5,5-bis(η^5-cyclopentadienyl)-2,4-diorganyl-1λ^3,3λ^3-diphospha-5-zirconia-tricyclo[2.1.0.0^{1,3}]pentane compounds **XXXIII** [63, 176-179].

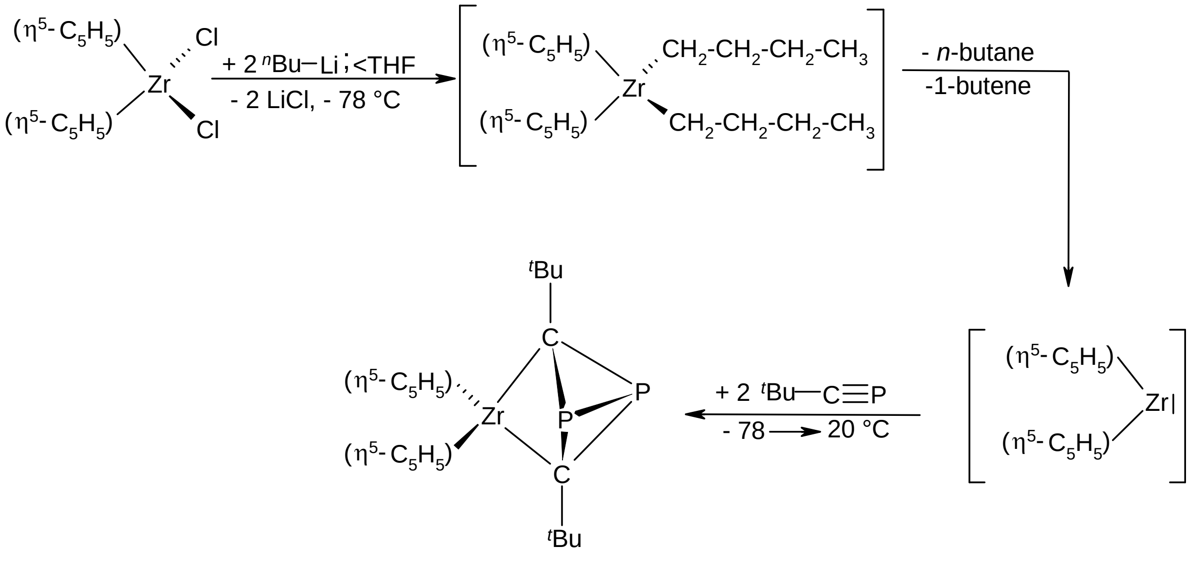

XXXIII

Treating these complexes with phosphorus(V) pentachloride in *n*-hexane at 90 ºC yielded the same heterocycle which had been isolated from the reaction of phosphorus(III) chloride and 2-*tert*-butyl-1λ^3-phosphaalkyne. With phosphorus(III) chloride at 110 ºC in *n*-hexane, however, the P–P bond is preserved and the P–Cl bridged compound 2,4-di-*tert*-butyl-3-chloro-1λ^3,3λ^3,5λ^3-triphospha-tricyclo[2.1.0.0^{2,5}]pentane **XXXIV** can be obtained [180]. The authors of this publication also reported that analogous reactions with phosphorus(III) bromide in tetrahydrofuran at 25 °C or phosphorus(III) iodide in diethylether at 90 °C furnished the same heterocycles which had already been isolated from 2-*tert*-butyl-1λ^3-phosphaalkyne and phosphorus(III) bromide or iodide, respectively.

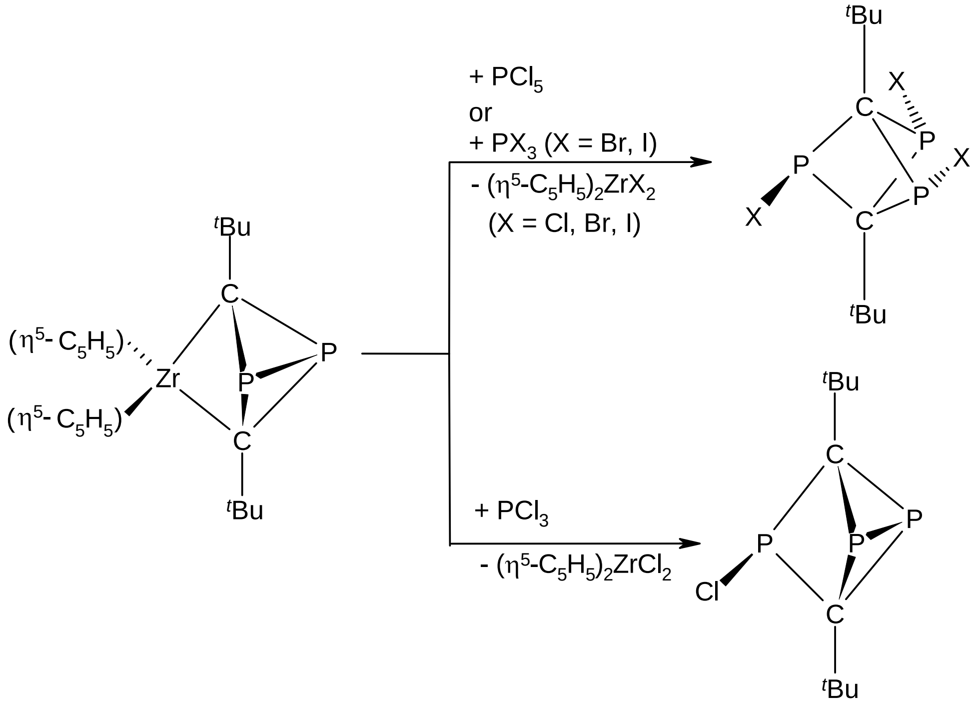

Reaction of 2,4-di-*tert*-butyl-3-chloro-1λ^3,3λ^3,5λ^3-triphospha-tricyclo[2.1.0.0^{2,5}]pentane (**XXXIV**) with antimony(V) chloride failed in that chlorination of the P–P bond occurred to give antimony(III) chloride and the already known 2,4,5-trichloro-2λ^3,4λ^3,5λ^3-triphospha-bicyclo[1.1.1]pentane (see Scheme below). With stoichiometric amounts of aluminium(III) chloride, however, a colourless solution was obtained from which small amounts of a white precipitate separated. Redissolving this solid by gentle warming and storage of the resulting solution for 24 h at 20 °C furnished colourless crystalline blocks. A single-crystal X-ray structure analysis showed this compound to consist of *nido*-[3,5-^{t}Bu$_2$-1,2,4-C$_2$P$_3$]$^{\oplus}$ cations and separated [AlCl$_4$]$^{\ominus}$ anions which are weakly linked together by rather long Cl...P interactions in a range of 337 to 358 pm.

In the cation three phosphorus and two carbon atoms each of which is connected to a *tert*-butyl substituent form a square-pyramidal framework. The diamond-shaped basis of this polyhedron consists of two carbon and only two of the three phosphorus atoms in an alternating arrangement, whereas the third one is four-coordinate and occupies the apical position. Application of Wade’s rules leads to a *nido*-species the framework of which is held together by seven electron pairs. With respect to the overall composition $[R_2C_2P_3]^{\oplus}$ the polyhedron has to be considered an octahedron with one vertex removed; here the carbon atoms occupy the sites of lowest connectivity [181]. Remarkably, the analogous but neutral compound *nido*-2-^{t}Bu-1,2-PCB_3H_5 has been obtained from the reaction of 2-*tert*-butyl-1λ^3-phosphaalkyne and B_4H_{10} (see Page 28, Chapter 2). In the valence shell both species are isoelectronic to the $[Me_5C_5]^{\oplus}$ cation.

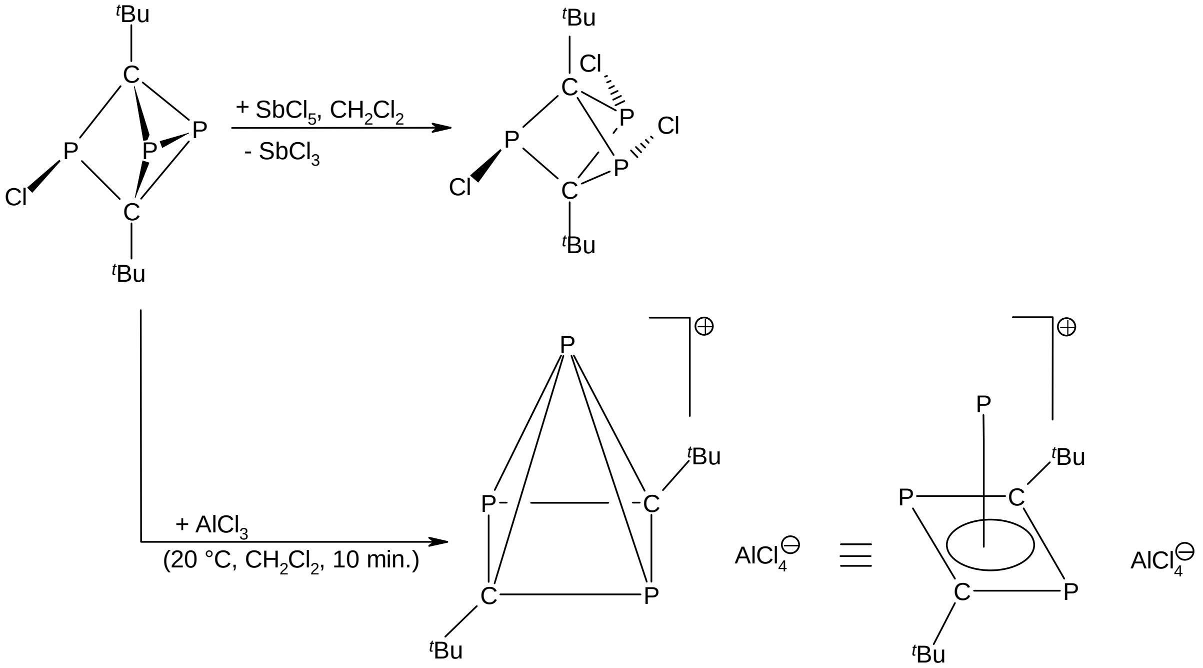

Furthermore, in a lecture given at the University of Stuttgart in January 2006 and published later [182] *Russell* disclosed that two different structures can be observed when 5,5-bis(η^5-cyclopentadienyl)-2,4-diorganyl-1λ^3,3λ^3-diphospha-5-zirconia-tricyclo[2.1.0.0^{1,3}]pentane is treated with arsenic(III) or antimony(III) chloride. In case of the antimony compound the formation of the so-called housene structure is favoured due to a transannular electronic interactions between the σ* (Sb–Cl) orbital and the π-system of the P=C unit and additionally between the empty π*-system of the P=C unit and the σ (Sb–P) orbital.

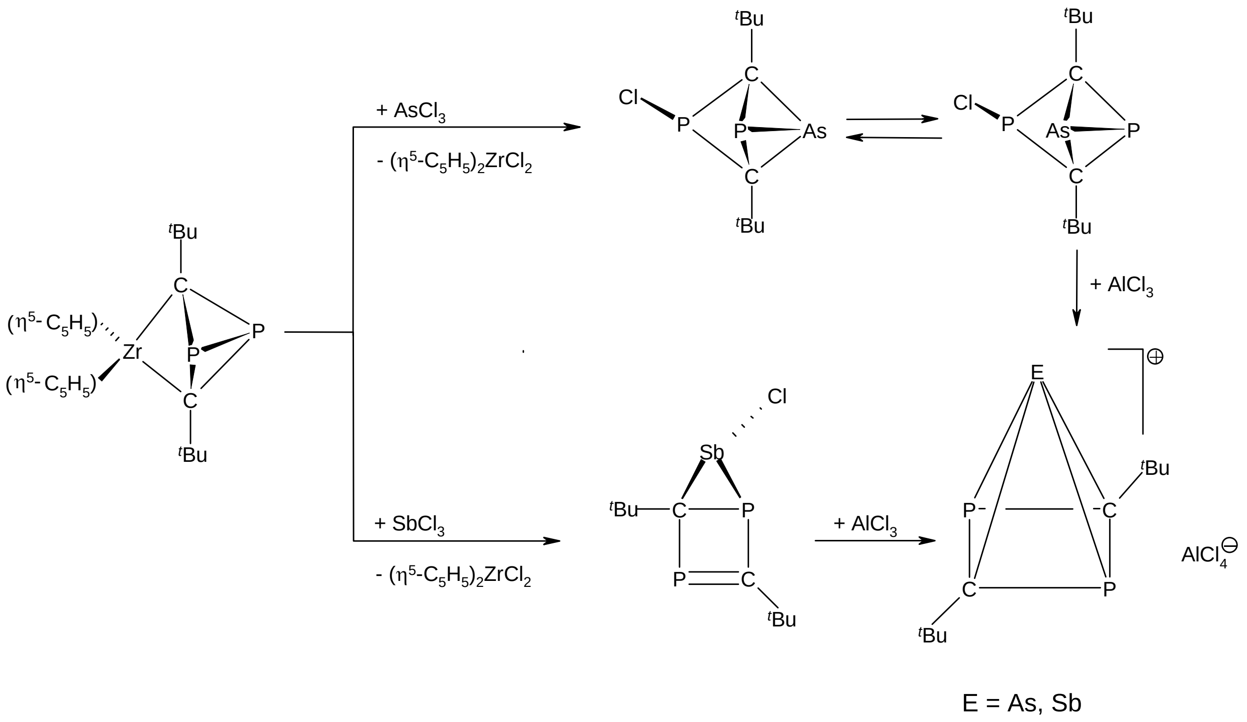

Reduction of 2,4-di-*tert*-butyl-3-chloro-1λ^3,3λ^3,5λ^3-triphospha-tricyclo[2.1.0.0^{2,5}]pentane with magnesium or potassium in tetrahydrofuran [183] furnished almost quantitatively the compounds [$Mg_2(\mu\text{-}Cl)_3(thf)_6$][2,5-^{t}Bu$_2-1\lambda^3$,3$\lambda^3$,4$\lambda^3$-$P_3C_2$] and K[2,5-^{t}Bu$_2-1\lambda^3$,3$\lambda^3$,4$\lambda^3$-$P_3C_2$]. The mechanistic insight gained from these studies opened a new and "*economic*" synthesis of the already known anion [2,5-^{t}Bu$_2$-1λ^3,3λ^3,4λ^3-P_3C_2]$^\ominus$, the preparation of which was first reported by *Becker* et al. [80] and improved by *Nixon* and co-workers later on [184].

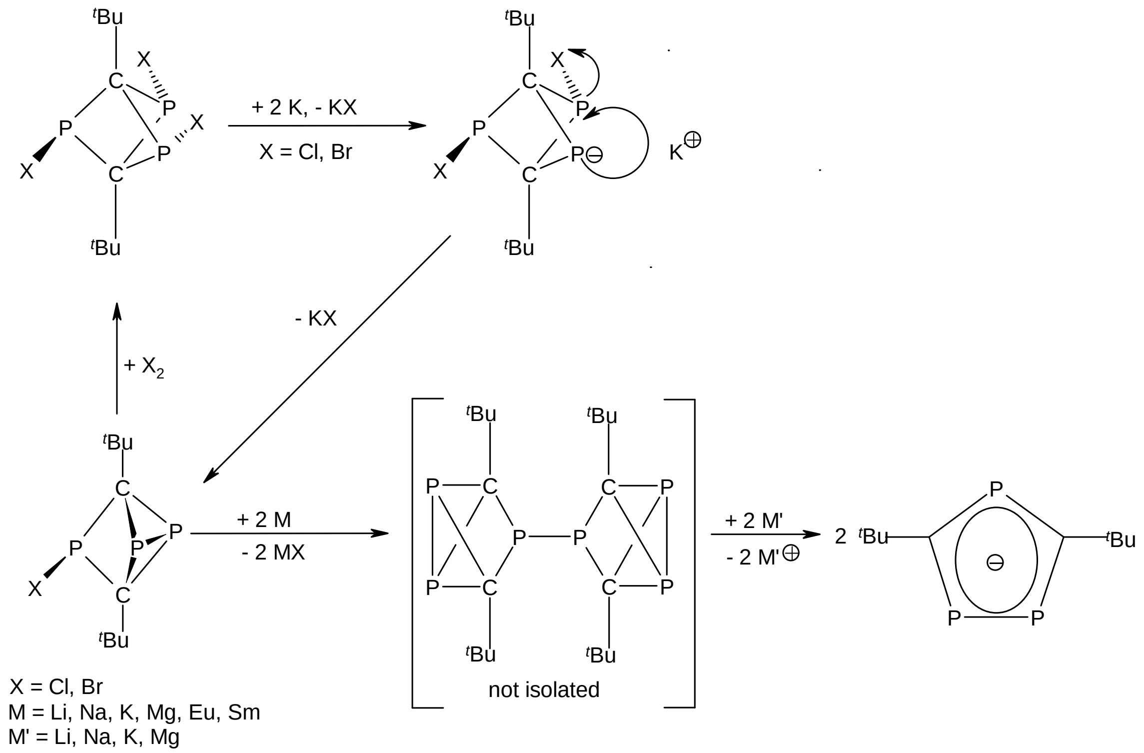

Surprisingly, reactions of organophosphorus dihalides turned out to be rather complex and, in particular, the formation of by-products is scarcely understood. For example, with dichlorophenylphosphine *Dautel* obtained minor amounts of the heterocycle 2,4,5-tri-*tert*-butyl-1-phenyl-1λ^3,3λ^3-diphosphole **XXXV** along with the expected 1,3-di-*tert*-butyl-2,4-dichloro-5-phenyl-2λ^3,4λ^3,5λ^3-triphosphabicyclo[1.1.1]pentane **XXXVI** [88].

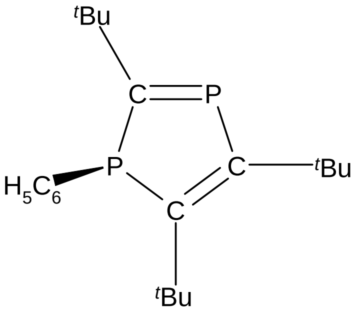

XXXV

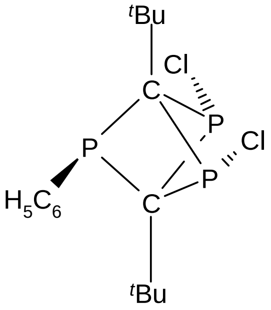

XXXVI

In his thesis he also studied the addition of bromo- and chlorodiphenylphosphine to 2-*tert*-butyl-1λ^3-phosphaalkyne and determined the crystal structure of the oligocycle prepared from bromodiphenylphosphine [88a]. In extension of our investigations on the reactivity of 2-*tert*-butyl-1λ^3-phosphaalkyne, we have confirmed these results, additionally employed several chlorodiorganylphosphines with different alkyl and aryl substituents as starting materials and repeated the above mentioned structures determination of the oligocycles prepared from bromo- [88a] and chlorodiphenylphosphine [88b] in order to improve the parameters.

3.2. 2,4-Di-tert-butyl-3,3-diorganyl-1λ^3,5λ^3-diphospha-3-phosphonia-tricyclo[2.1.0.0^{2,5}]-pentane Halides

3.2.1. Preparation and Reaction Mechanism

Solutions of the halodiorganylphosphine and of slightly more than two equivalents of 2-*tert*-butyl-1λ^3-phosphaalkyne in cyclopentane are combined dropwise at –70 °C and the mixture is allowed to warm up slowly to room temperature. Within about four days it changes its colour to brown-yellow and a white solid precipitates. Without further separation the solvent is removed to leave a brown-yellow solid. This crude product is extracted with hot toluene until the suspension changes its colour to yellow-orange. Whereas the solution removed at + 4 °C with a pipet is rejected, the remaining solid is dissolved in dichloromethane. On cooling the ionic compound containing the 1λ^3,5λ^3-diphospha-3λ^5-phosphonia-tricyclo[2.1.0.0^{2,5}]pentane cation precipitates as a colourless solid; relatively high yields of 73 to 79% were obtained.

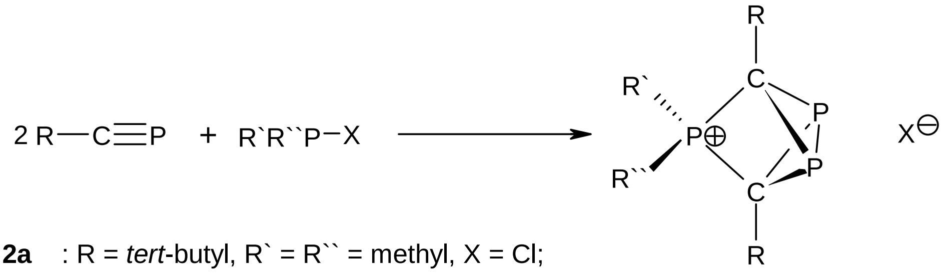

2a : R = *tert*-butyl, R` = R`` = methyl, X = Cl;
2b : R = *tert*-butyl, R` = R`` = ethyl, X = Cl;
2c : R = *tert*-butyl, R` = isopropyl, R`` = phenyl, X = Cl;
2d.1 : R = *tert*-butyl, R` = R`` = phenyl, X = Cl;
2d.2 : R = *tert*-butyl, R` = R`` = phenyl, X = Br
2e : R = *tert*-butyl, R` = R`` = isopropyl, X = Cl

Scheme 3.1

Renewed recrystallization of the compounds **2a**, **2b**, **2c**, **2d.1**, and **2d.2** (Scheme 3.1) from dichloromethane gave colourless crystals suitable for X-ray structure analyses. Since all attempts to crystallise the oily compound **2e** which had been prepared from chlorodiisopropylphosphine, failed, its structure had to be deduced from NMR data only. Unfortunately chloro-di-*tert*-butylphosphine did not react.

The reaction mechanism given below is based on the results of the X-ray structure analyses. One has to realise, however, that with halodiorganylphosphines only one phosphorus–halogen bond is available for an initial insertion of the $1\lambda^3$-phosphaalkyne. Therefore a slight variation of the original mechanism outlined in Scheme 1.5 (Chapter 1, Page 26) has to be taken into consideration. Again, a transannular attack of the R`R``P group at the *sp*^{2}-hybridized carbon atom of the still undetectable 1,2-dihydro-$1\lambda^3,3\lambda^3$-diphosphete is expected to occur, but in contrast to Scheme 1.5 this attack has to be nucleophilic and an *umpolung* has to be assumed. The postulated intermediate specified in Scheme 3.2, stabilises by formation of a P–P bond and an accompanying elimination of a halide anion to give the corresponding $1\lambda^3,5\lambda^3$-diphospha-$3\lambda^5$-phosphoniatricyclo[2.1.0.0^{2,5}]pentane cation.

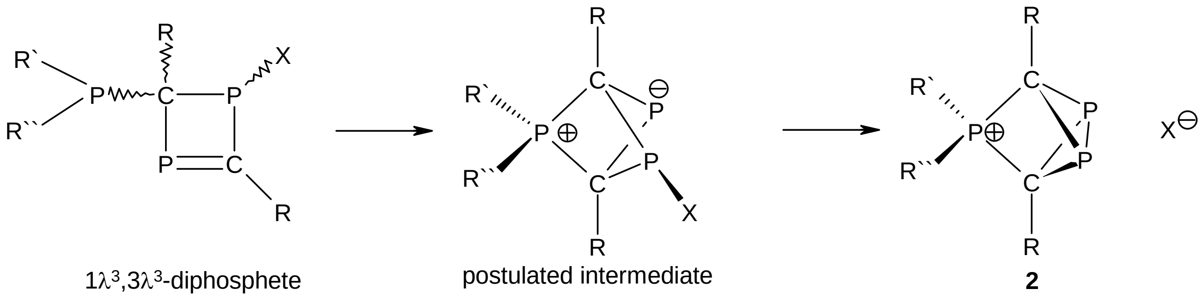

$1\lambda^3,3\lambda^3$-diphosphete

postulated intermediate

2

Scheme 3.2

3.2.2. NMR and IR Spectroscopic Characterization

The $^{31}P\{^{1}H\}$ NMR spectra of the compounds **2a**, **2b**, **2d.1**, **2d.2**, and **2e** dissolved in chloroform-d_1 reveal the signals of an A_2X spin system. With an intensity ratio of 2:1 the doublets of the two chemically equivalent phosphorus atoms P1 and P5 and the triplets of the positively charged phosphorus atoms P3 appear at rather high and at relatively low field, respectively (Fig.3.2.1a). The appertaining $^{2}J_{(P3,P1/P5)}$ coupling constants (Table 3.1) are very small and vary between 10.8 Hz and 1.3 Hz. The spectrum of compound **2c**, prepared from chloro(isopropyl)phenylphosphine, however, is found to be more complicated. Since the cation no longer exhibits a mirror plane through the atoms C2, C4 and P3 (Fig.3.3), the two phosphorus atoms P1 and P5 become chemically inequivalent. With an intensity ratio of 1:1:1 the $^{31}P\{^{1}H\}$ NMR spectrum reveals the signals of an AMX spin system; it is characterised by a singlet of the positively charged phosphorus atom ($^{2}J_{(P3,P1/P5)} < 0.5$ Hz) and two doublets of the atoms P1 and P5, coupled with a rather large constant $^{1}J_{(P1,P5)}$ of 172.2 Hz (Fig.3.2.1b).

Table 3.1. Characteristic NMR Parameters for the Atoms of the Central Oligocycle in Several Co-crystallisates Containing the 2,4-Di-*tert*-butyl-3,3-diorganyl-$1\lambda^3,5\lambda^3$-diphospha-3-phosphonia-tricyclo[$2.1.0.0^{2,5}$]pentane Cation.
Chemical shift values δ (ppm); coupling constants J (Hz); $CDCl_3$ solution

Compound	δ($\underline{C}$–P)	$^{1}J_{(C,P3)}$	$^{1}J_{(C,P1/P5)}$	δ (P1/P5)	δ (P3)	$^{2}J_{(P3,P1/P5)}$
2a (Me, Me, Cl)	48.1(dt)	59.5	42.1	–264.1(d)	104.0(t)	10.8
2b (Et, Et, Cl)	40.8(dt)	52.5	41.8	–286.5(d)	119.5(t)	1.5
2c (^{i}Pr, Ph, Cl)	42.9(dt)	51.5	41.7	–289.6(d) –278.3(d) $^{1}J_{(P1,P5)}$ =172.2	110.6(s)	< 0.5
2d.1 (Ph, Ph, Cl)	47.6(dt)	58.2	43.3	–281.9(d)	85.1(t)	4.1
2d.2 (Ph, Ph, Br)	47.9(dt)	57.8	43.4	–280.8(d)	85.0(t)	4.5
2e (^{i}Pr, ^{i}Pr, Cl)	38.0(dt)	45.8	41.5	–285.8(d)	130.5(t)	1.3

In the $^{13}C\{^{1}H\}$ NMR spectra of compound **2c**, however, several C,P couplings to the a priori chemically non-equivalent phosphorus atoms P1 and P5 become so similar that the P–P group can be treated as a *pseudo*-A2 system. As a consequence, for all compounds the bridging quaternary carbon atoms of the central oligocycles reveal doublets of triplets (Table 3.1 and Fig.3.2.2e). Whereas in all cations the methyl carbon atoms of the *tert*-butyl substituents give rise to pseudo-quintets with an intensity ratio of approximately 1:2:2:2:1 (Fig.3.2.2b) – or in an alternative description to doublets of triplets –, due to an unobservable

a) Compound **2a** (Me, Me, Cl)

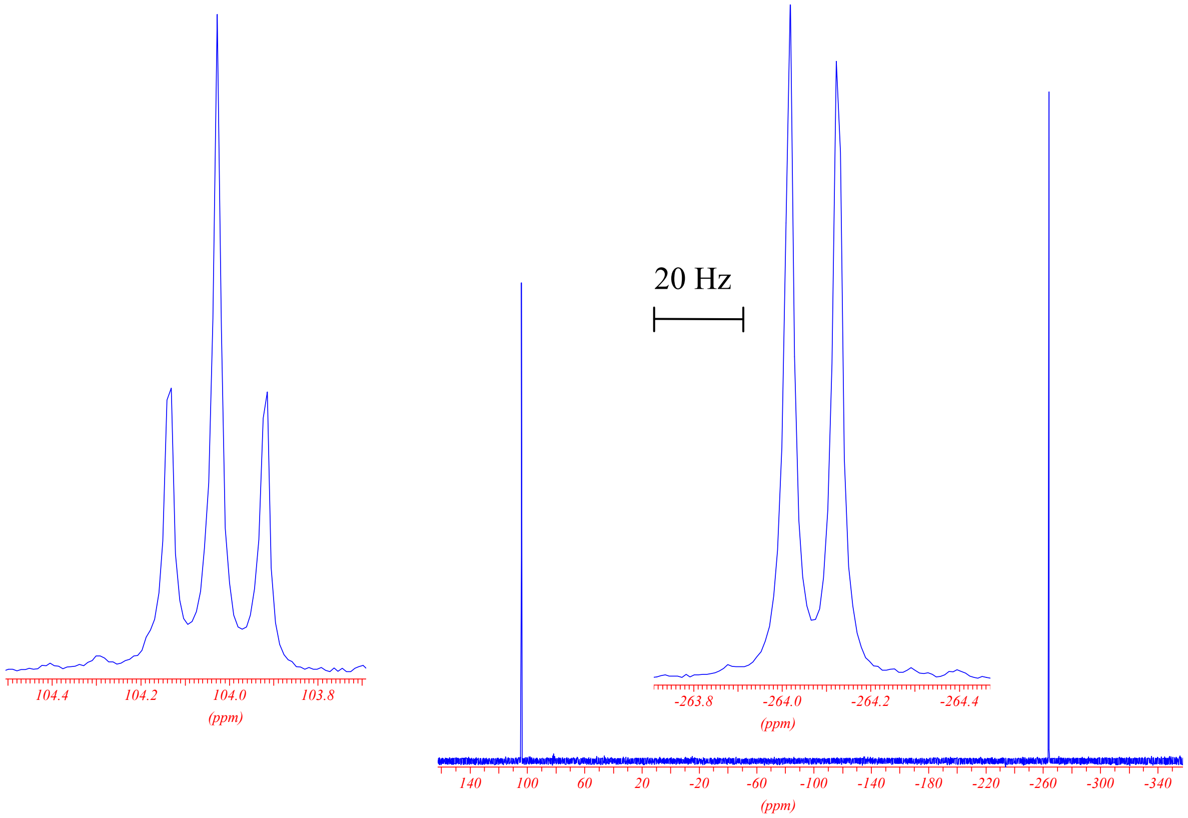

b) Compound **2c** (^{i}Pr, Ph, Cl)

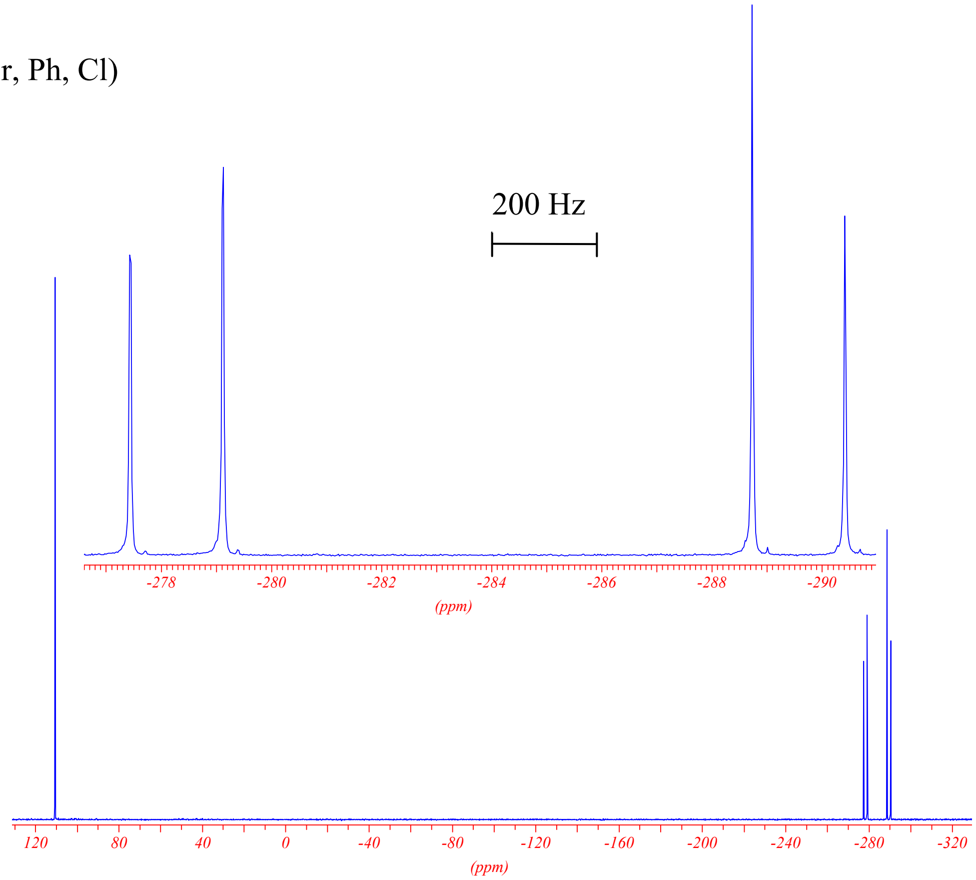

Figure 3.2.1. ^{13}P{^{1}H} NMR spectra of the compounds **2a** (Me, Me, Cl) (a) and **2c** (^{i}Pr, Ph, Cl) (b) dissolved in $CDCl_3$ at room temperature, whereas the resolved signals are additionally shown on the upper left of signals.

$^{2}J_{(C,P3)}$ coupling the adjacent quaternary carbon atoms show only triplets in the spectra of the compounds **2a**, **2b**, **2c** (Fig. 3.2.2c), **2d.1**, and **2e**. The spectrum of compound **2d.2**, however, exhibits a doublet of triplets with a very small $^{2}J_{(C,P3)}$ value of 0.96 Hz (Table 3.2).

Singlets at about 5.2 ppm in the ^{1}H NMR and at about 53.3 ppm in the $^{13}C\{^{1}H\}$ NMR spectra, respectively, spring from the co-crystallizing solvent dichloromethane. Due to a different treatment of the compounds in vacuo the contents may vary from 0.0 to 0.8 mole per formula unit. Furthermore, a strong ^{1}H NMR singlet in a range of 0.74 to 1.03 ppm is assigned to the *tert*-butyl groups (see Experimental Part).

Table 3.2. Characteristic NMR Parameters for the Carbon Atoms of the *tert*-Butyl-Substituents in Several Co-crystallisates Containing the 2,4-Di-*tert*-butyl-3,3-diorganyl-1λ^3,5λ^3-diphospha-3-phosphonia-tricyclo[2.1.0.0^{2,5}]pentane Cation.
Chemical shift values δ (ppm); coupling constants J (Hz); $CDCl_3$ solution

Compound	$\delta(\underline{C}(CH_3)_3)$	$^{2}J_{(C,P3)}$	$^{2}J_{(C,P1/P5)}$	$\delta(C(\underline{C}H_3)_3)$	$^{3}J_{(C,P3)}$	$^{3}J_{(C,P1/P5)}$
2a (Me, Me, Cl)	31.7(t)	< 0.5	4.8	30.1(dt)	5.1	2.4
2b (Et, Et, Cl)	31.5(t)	< 0.5	4.9	30.3(dt)	5.1	2.7
2c (^{i}Pr, Ph, Cl)	31.5(t)	< 0.5	4.6	30.5(dt)	5.6	3.1
2d.1 (Ph, Ph, Cl)	32.1(t)	< 0.5	4.7	30.4(dt)	5.3	2.6
2d.2 (Ph, Ph, Br)	32.4(dt)	0.96	5.1	30.7(dt)	5.5	2.7
2e (^{i}Pr, ^{i}Pr, Cl)	30.4(t)	< 0.5	5.4	30.0(dt)	4.6	3.1

In the ^{1}H NMR spectrum of compound **2a** the signal of the two methyl groups connected directly to the positively charged phosphorus atom appears at 3.1 ppm and is split into a doublet with a coupling constant $^{2}J_{(H,P3)}$ = 12.9 Hz. The pertinent $^{13}C\{^{1}H\}$ NMR spectrum reveals a doublet of triplets at 18.7 ppm arising from a coupling with two different types of the phosphorus atoms and exhibits $^{1}J_{(C,P3)}$ and $^{3}J_{(C,P1\text{ and }P5)}$ constants of 32.9 Hz and 4.9 Hz, respectively.

The methyl and methylene ^{1}H NMR-signals of the ethyl groups of compound **2b** are observed at 1.63 and 3.43 ppm, respectively. They are split into a doublet of triplets with two different coupling constants of 7.4 Hz for $^{3}J_{(H,H)}$ and of 17.6 Hz for $^{3}J_{(H,P3)}$, and into a doublet of quartets with a $^{2}J_{(H,P3)}$ value of 11.8 Hz. In the $^{13}C\{^{1}H\}$ NMR spectrum the methyl and methylene carbon atoms give rise to two doublets of triplets at 8.8 ppm and 26.6 ppm, exhibiting $^{2}J_{(C,P3)}$ and $^{4}J_{(C,P1\text{ and }P5)}$ constants of 5.7 Hz and 2.9 Hz in the high field and $^{1}J_{(C,P3)}$ and $^{3}J_{(C,P1\text{ and }P5)}$ constants of 26.9 Hz and 3.8 Hz in the low field region, respectively.

In the ^{1}H NMR-spectrum of compound **2c** the two methyl groups of the isopropyl substituent are observed at 1.6 ppm as a doublet of doublets with $^{3}J_{(H,H)}$ and $^{3}J_{(H,P3)}$ coupling constants of 6.9 Hz and 17.9 Hz, respectively. Furthermore, the neighboring CH-group appears as a multiplet in a range of 4.9 to 5.05 ppm. Two multiplets between 7.54 and 7.72 ppm and between 8.56 and 8.65 ppm come from the hydrogen atoms of the phenyl group. In the pertinent $^{13}C\{^{1}H\}$ NMR spectrum the two methyl carbon atoms reveal a doublet of doublets at 17.8 ppm with $^{2}J_{(C,P3)}$ and $^{4}J_{(C,P1\ \text{or}\ P5)}$ coupling constants of 4.6 Hz and of 2.03 Hz, respectively. The neighboring methylidyne carbon atom gives rise to a doublet of doublets of doublets at 31.0 ppm with a $^{1}J_{(C,P3)}$ coupling constant of 23.9 Hz and of two different $^{3}J_{(C,P1\ \text{or}\ P5)}$ values of 5.1 Hz and of 1.5 Hz.

Furthermore, four different low field $^{13}C\{^{1}H\}$ NMR signals (Table 3.2) can be ascribed to the phenyl group at phosphorus atom P3. Here, the assignment is based on data reported for the carbon atoms in the phenyl substituents of the two different (8-dimethylamino-naphth-1-yl)(dialkyl)phenylphosphonium iodides **A1** and **A2** [185]: The doublet of doublets of doublets at 124.8 ppm springs from the *ipso*-carbon atom and is characterized by a $^{1}J_{(C,P3)}$ coupling constant of 53.3 Hz and by two different $^{3}J_{(C,P1\ \text{or}\ P5)}$ values of 6.2 Hz and 2.1 Hz. A doublet at 135.3 ppm with a $^{4}J_{(C,P3)}$ coupling constant of 3.1 Hz is attributed to the *para*-carbon atom, whereas a doublet of doublets at 132.6 ppm with $^{2}J_{(C,P3)}$ and $^{4}J_{(C,P1\ \text{or}\ P5)}$ coupling constants of 8.9 Hz and of 4.3 Hz, respectively, springs from the carbon atoms in *ortho*-position. Finally, the doublet at 130.2 ppm with a $^{3}J_{(C,P3)}$ coupling constant of 10.7 Hz has to be assigned to the the *meta*-carbon atoms. As in the two reference compounds the $^{3}J_{(C,P)}$ couplings to the *meta*-carbon atoms are found to be slightly larger than the $^{2}J_{(C,P)}$ values involving the *ortho*-carbon atoms [185].

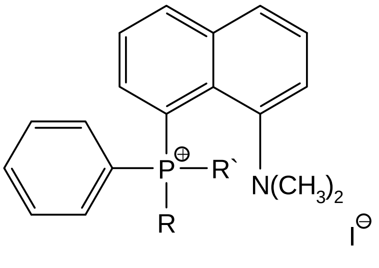

A1 = R = R` = Me
A2 = R = Me; R` = Et

The ^{1}H NMR spectra of the two nearly identical compounds **2d.1** and **2d.2** show very similar data for the phenyl region; two multiplets between 7.7 and 7.80 ppm and between 7.8 and 8.2 ppm are observed for compound **2d.1**, whereas the corresponding signals of compound **2d.2** appear in ranges of 7.7 to 7.9 ppm and 8.2 to 8.3 ppm. As in compound **2c**, the pertinent $^{13}C\{^{1}H\}$ NMR spectra reveal four different signals for the phenyl carbon atoms (Table 3.2).

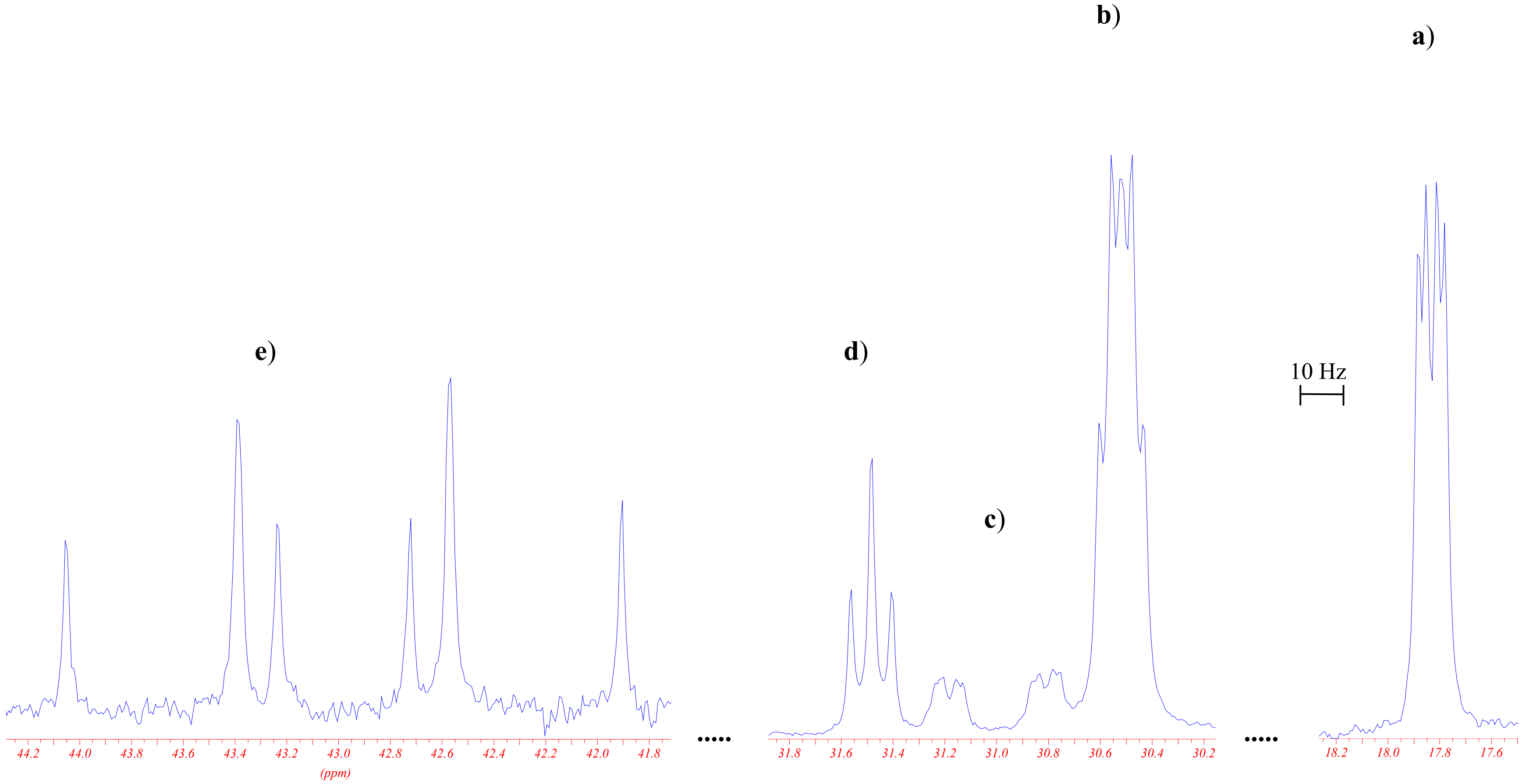

Figure 3.2.2. Characteristic sections of the $^{13}C\{^1H\}$ NMR spectrum of compound **2c** dissolved in $CDCl_3$ at room temperature. **a)** Doublet of doublets for $(H_3\mathbf{C})_2CH\text{–}P3$ (isopropyl); **b)** pseudoquintett (equal to doublet of triplets) for $(H_3\mathbf{C})_3C$ (*tert*-butyl); **c)** doublet of doublets of doublets for $(H_3C)_2\mathbf{C}H\text{–}P3$ (isopropyl); **d)** triplett for $(H_3C)_3\mathbf{C}$ (*tert*-butyl); **e)** doublet of triplets for the carbon atoms **C**(–P3/P1 and P5) of the central oligocycle.

The *ipso*-position gives rise to a doublet of triplets at 124.2 ppm in compound **2d.1** and at 124.6 ppm in compound **2d.2**; for the appertaining coupling constants $^{1}J_{(C,P3)}$ values of 58.6 and 58.2 Hz and $^{3}J_{(C,P1\text{ and }P5)}$ values of 4.7 and 4.5 Hz, respectively, have been ascertained. The doublet of the *para*-carbon atom is similarly observed at 136.2 (**2d.1**) and 136.3 ppm (**2d.2**) with $^{4}J_{(C,P3)}$ coupling constants of 3.2 and 3.1 Hz, respectively. Doublets at 133.0 and 133.4 ppm come from the *ortho*-carbon atoms of **2d.1** and **2d.2**; they are characterized by $^{2}J_{(C,P3)}$ coupling constants of 10.0 and 10.1 Hz, respectively. Finally, the doublets at 130.4 (**2d.1**) and 130.6 ppm (**2d.2**) with $^{3}J_{(C,P3)}$ coupling constants of 11.1 and 11.3 Hz, respectively, have been ascribed to the *meta*-position.

Table 3.2. Characteristic NMR Parameters for the Carbon Atoms of the Phenyl Substituents in Several Co-crystallisates Containing the 2,4-Di-*tert*-butyl-3,3-diorganyl-$1\lambda^{3},5\lambda^{3}$-diphospha-3-phosphonia-tricyclo[2.1.0.0^{2,5}]pentane Cation in Comparsion with Corresponding Data of the Compounds **A1** and **A2**.

Chemical shift values δ (ppm); coupling constants J (Hz); $CDCl_3$ solution

Compound	δ(*ipso*-C)	δ(*meta*-C)	δ(*ortho*-C)	δ(*para*-C)
2c	124.8 (ddd) $^{1}J_{(C,P3)} = 53.3$ $^{3}J_{(C,P1\text{ or }P5)} = 6.2; 2.1$	130.2 (d) $^{3}J_{(C,P3)} = 10.7$	132.6 (dd) $^{2}J_{(C,P3)} = 8.9$ $^{4}J_{(C,P1\text{ or }P5)} = 4.3$	135.3 (d) $^{4}J_{(C,P3)} = 3.1$
2d.1	124.2 (dt) $^{1}J_{(C,P3)} = 58.6$ $^{3}J_{(C,P1\text{ and }P5)} = 4.7$	130.4 (d) $^{3}J_{(C,P3)} = 11.1$	133.0 (d) $^{2}J_{(C,P3)} = 10.0$ $^{4}J_{(C,P1\text{ and }P5)} < 0.5$ Hz	136.2 (d) $^{4}J_{(C,P3)} = 3.2$
2d.2	124.6 (dt) $^{1}J_{(C,P3)} = 58.2$ $^{3}J_{(C,P1\text{ and }P5)} = 4.5$	130.6 (d) $^{3}J_{(C,P3)} = 11.3$	133.4 (d) $^{2}J_{(C,P3)} = 10.1$ $^{4}J_{(C,P1\text{ and }P5)} < 0.5$ Hz	136.3 (d) $^{4}J_{(C,P3)} = 3.1$
A1	113.5 (d) $^{1}J_{(C,P)} = 95.2$	130.1 (d) $^{3}J_{(C,P)} = 13.5$	129.3 (d) $^{2}J_{(C,P)} = 11.1$	136.6 (d) $^{4}J_{(C,P)} = 3.6$
A2	111.4 (d) $^{1}J_{(C,P)} = 91.7$	129.9 (d) $^{3}J_{(C,P)} = 13.2$	129.5 (d) $^{2}J_{(C,P)} = 10.4$	136.5 (d) $^{4}J_{(C,P)} = 3.6$

In the ^{1}H NMR spectrum of compound **2e** the methyl groups of the isopropyl substituents at phosphorus atom P3 appear at 1.4 ppm and are found to be split into a doublet of doublets with $^{3}J_{(H,H)}$ and $^{3}J_{(H,P3)}$ coupling constants of 7.1 Hz and 16.3 Hz, respectively. A multiplet between 2.9 and 3.2 ppm is assigned to the neighboring CH-groups. The pertinent $^{13}C\{^{1}H\}$ NMR spectrum reveals a doublet of triplets at 17.6 ppm for the methyl carbon atoms and a second doublet of triplets at 31.65 ppm for the methylidyne carbon atoms. The high field doublet of triplets is characterized by $^{2}J_{(C,P3)}$ and $^{4}J_{(C,P1\text{ and }P5)}$ coupling constants of 5.2 and 2.5 Hz, whereas the low field doublet of triplets shows $^{1}J_{(C,P3)}$ and $^{3}J_{(C,P1\text{ and }P5)}$ values of 20.2 and 3.7 Hz, respectively.

Since Infrared and Raman spectra of different crystalline solids containing the 2,4-di-*tert*-butyl-3,3-diorganyl-1λ^3,5λ^3-diphospha-3-phosphonia-tricyclo[2.1.0.0^{2,5}]pentane cation could be measured as nujol mull between CsBr disks and in glass capillaries, respectively, by comparison a tentative assignment is possible for the majority of vibrations in the low wave number region (Table 3.4):

Bands near 1000 cm^{-1} in both the Infrared and Raman spectra may be attributed to the C–C pulsation of the phenyl substituents. In accordance with a publication of *Randle* and *Whiffen* on halo-benzenes [186] it refers to the phenyl breathing mode **p** (Fig. 3.2.3). Bands in the 940 – 825 cm^{-1} region spring from the C–C vibrations of the ethyl and isopropyl groups at phosphorus as well as the *tert*-butyl substituents in 2,4-position and from the methyl rocking vibration ρCH_3 of the methyl entities. Bands near 815 cm^{-1} and at 674 cm^{-1} have to be assigned to the symmetric CC_3-vibration of the *tert*-butyl substituents and the P–C stretching vibration of the P–^{i}Pr unit, respectively. In the 726 – 694 cm^{-1} region bands can be ascribed to the stretching vibrations of P–C units which most probably are antisymmetricly combined with the ring deformation γ of the skeleton. Moreover, vibrations between 637 and 612 cm^{-1} can be assigned to the in-plane ring deformation δCCC of the phenyl substituents (**s)** and the deformation γ of the trigonal bipyramidal skeleton. Bands between 588 and 565 cm^{-1} may be attributed to the pulsation of the skeleton and comprise the P–C and P–P stretching vibrations. Since bands in the 560 – 587 cm^{-1} region are observed in phenyl derivatives only, they are assigned to "X"-sensitive puckering mode **y** of the P–Ph unit. Bands near 530 cm^{-1} may ascribed to a combination of stretching vibration and deformation (ν, δ) of the skeleton, whereas bands between 513 and 481 cm^{-1} can be assigned to the "X"-sensitive vibration mode **t** of the phenyl ring. Finally, two partially overlapping bands between 422 and 384 cm^{-1} probably spring from a combination of P–C and P–P stretching vibrations within the skeleton.

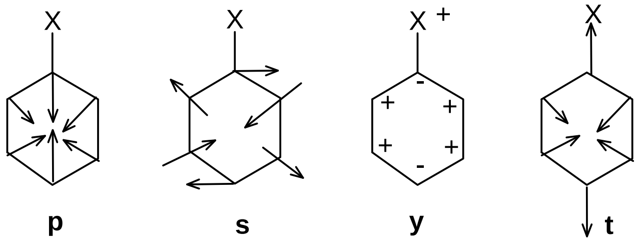

Figure 3.2.3. Mode diagrams for the vibrations of the phenyl group in the region between 1000 and 480 cm^{-1} together with the code letter designation as published by *Randle* and *Whiffen* [186]

Table 3.4. Characteristic IR Absorptions and Raman Lines for the Co-crystallisates Containing the 2,4-Di-*tert*-butyl-3,3-diorganyl-$1\lambda^3,5\lambda^3$-diphospha-3-phosphonia-tricyclo[2.1.0.$0^{2,5}$]pentane Cation
IR: crystalline solids as nujol mull between CsBr disks; Raman: crystalline solids in glass capillaries; $\tilde{\nu}$ (cm^{-1}); vvs, very very strong; vs, very strong; s, strong; ms, moderate strong; m, medium; mw, medium weak; w, weak; vw, very weak; vvw, very very weak; br, broad; sh, shoulder

2a		**2b**		**2c**		**2d.1**		**2d.2**		Tentative Assignment
IR	RE	IR	RE	IR	RE	IR	RE	IR	RE	
				994 m	993 s	997 sh	999 ms	996 sh	999 ms	ν CC(Ph) pulsation
						992 m	993 m	994 m	993 m	
	940 vw	933 w	934 mw,b		931 mw	938 w,b	939 w	940 w,b	940 w	ν CC (Et,^{i}Pr,^{t}Bu) + ρ CH_3
	932 w(m)		929 mw,b	880 ms	883 vw	893 vvw		894 vvw		
870 m	871 mw	871 s	872 mw	857 s-vs	859 mw	859 s,b	857 w-vw	859 s,b	858 w-vw	
			831 mw		825 (m)w					
814 w,b	815 m(w)	814 vw	814 m(w)	814 mw	813 mw	815 (m)w	815 w	815 (m)w	815 w	ν_S CC_3(^{t}Bu)
722a) vs		721 m(w)		714 vs	713 mw	726 vs	726 w,b	724 vs	726 w,b	ν PC_{as} (+ γ ring skeleton) antisymmetric
698 m	699 mw	714 ms			708 w	709 s		709 s		
	697 mw	706 ms	702 mw	698 s	703 w	694 s(-vs)	698 mw	694 s(-vs)	698 mw	
				674 s	674 ms,b					ν P–^{i}Pr
637 mw	637 mw	633 mw	633 mw	630 ms	629 mw	631 ms	631 w,b	629 ms	631 w,b	δ CCC (Ph) + γ skeleton
	611 w				612 m	615 w	614 mw	615 w	614 mw	
565 w	568 vs	568 vw	569 vs	576 m	576 vs	588 s	587b) vvs	588 s	587b) vvs	ν skeleton (pulsation) (ν PC + ν PP)
				560 m	561 ms	570 m	587b) ?	570 m	587b) ?	X-sensitive (PPh)
534 w	534 m(w)	~528 w,b	534 mw	532 mw	532 mw	529 w	530 mw	529 w	530 mw	ν,δ skeleton (?)
				510 s	510 s	513 ms	512 m	513 ms	511 m	ν Ph-ring (X-sensitive)
				487 m	487 w	507 s-vs	505 mw	507 s-vs	505 mw	
c)						481 ms		481 ms		
412 m(w)	412 m(s)	409 mw		422 mw	422 ms	407 m,b	408 mw	405 m,b	408 mw	ν (PP) + ν (PC) skeleton (?)
	396 m(w)		384 s				405 sh		405 sh	

a) Nujol band additionally; b) superposition of two bands; c) unassigned band at 457 w,b.

3.2.3. Structures of the Co-crystallisates 2a – 2d • x CH_2Cl_2

3.2.3.1. Crystal Data, Measuring Technique and Structure Analyses

By recrystallization from dichloromethane the co-crystallisates **2a•CH_2Cl_2(1/1)** and **2b•CH_2Cl_2(2/4)** could be obtained as colourless thick needles (columns) within a period of three to four weeks at –60 °C. From the same solvent similarly shaped crystals of **2c•CH_2Cl_2(1/2)**, **2d.1•CH_2Cl_2(1/1)**, and **2d.2•CH_2Cl_2(1/1)** precipitated already within one week at –13 °C. Repeatedly too large crystals had to be cut into small block-shaped fragments suitable for X-ray structural analyses. For a better understanding of the following discussion one has to realize that all structures were found to be ionic with separated cations and halide anions and to contain one or two solvent molecules per formula unit depending on the substituents methyl, ethyl, isopropyl, and phenyl at the positively charged phosphorus atoms. Moreover, from the notations of the co-crystallisates the ratio of cations and anions to solvent molecules may easily be deduced. For example, the asymmetric unit of the adduct **2b•CH_2Cl_2(2/4)** comprises two crystallographically independent cations, two anions and four solvent molecules. Compound **2d.1•CH_2Cl_2(1/1)** and **2d.2•CH_2Cl_2(1/1)** differ only in the halide anions chloride and bromide.

Data essential for structure determinations of the adducts **2b•CH_2Cl_2(2/4)**, **2c•CH_2Cl_2(1/2)**, and **2d.1•CH_2Cl_2(1/1)** were collected on a four-circle diffractometer P2$_1$ (Syntex, Cupertino, USA), whereas for **2a•CH_2Cl_2(1/1)** and **2d.2•CH_2Cl_2(1/1)** a P4 diffractometer (Siemens Analytical X-ray Instruments Inc., Madison/Wisconsin, USA) was applied and, as before, graphite monochromatized Mo-K$_\alpha$-radiation (λ = 71.073 pm) was used. Lattice parameters were calculated from the exact positions of a selected number of reflections (Table 3.1) and refined thereafter. The determination of the monoclinic space group $P2_1/c$ for **2c•CH_2Cl_2(1/2)** or $P2_1/n$ for **2d.1•CH_2Cl_2(1/1)** and **2d.2•CH_2Cl_2(1/1)** is based on unit cell dimensions and systematic absences (Table 3.1), whereas for **2a•CH_2Cl_2(1/1)** and **2b•CH_2Cl_2(2/4)** space group $P\bar{1}$ was chosen over $P1$ mainly on grounds of E-value statistics and successful structure refinements.

The crystal structures were solved by statistical methods employing the software package SHELXTL Version 5.10 [118-120] which also includes the program XP used for the analyses of molecular geometry and the preparation of drawings. Due to relatively low calculated absorption coefficients for nearly all structures (Table 3.1) and despite column shaped crystals absorption corrections were considered to be not necessary. Only the data set of co-crystallisate **2d.2•CH_2Cl_2(1/1)** prepared from bromodiphenylphosphine was corrected by application of the computer program *DIFABS* (T_{min} = 0.416, T_{max} = 1.000) [187]. After the halogen, phosphorus and carbon atoms had been located step by step and their positions as well as their isotropic replacement parameters had been refined by full-matrix least-squares calculations, the structure determinations were continued applying individual anisotropic U_{ij}-values. At the end the atomic coordinates of hydrogen atoms could either be taken from a different Fourier map and refined with their isotropic replacement parameters or were calculated on the basis of an idealized geometry which means a C–H distances of 96 pm and 97 pm of methyl and methylene groups, repectively, tetrahedral angles and a staggered arrangement of bonds at carbon. Furthermore the riding model applied ensures that a change in the carbon position is automatically transferred to the adjacent hydrogen atoms. The individual isotropic U-values of these hydrogen atoms were adopted from the pertinent carbon atoms and increased by a factor of 1.5 for the methyl groups and of 1.2 for the phenyl substituents, the methylene units of the cations and all of dichloromethane molecules. Finally the parameters of all heavier atoms were subjected to a last least squares refinement to take into account the incorporation of hydrogen atoms.

As for the structures discussed here the solution of the hydrogen problem developed as follows: in the co-crystallisates **2c•CH_2Cl_2(1/2)** and **2d.1•CH_2Cl_2(1/1)** all hydrogen atoms of the cations could be located and their individual parameters were refined, but in the dichloromethane molecules the positions had to be calculated as described above. For the co-crystallisates **2a•CH_2Cl_2**(1/1)**,** **2b•CH_2Cl_2(2/4)** and **2d.2•CH_2Cl_2(1/1)**, all hydrogen atoms in the cations as well in the dichloromethane molecules were calculated as described above; only in the phenyl substituents for the co-crystallisate **2d.2•CH_2Cl_2(1/1)** the position of hydrogen atoms were treated as idealized contributions with a C–H distance of 93 pm. Furthermore, the X-ray structure analysis of the adduct **2a•CH_2Cl_2(1/1)** shows disorder with respect to the positions of the two chlorine atoms in the dichloromethane molecule.

Crystallographic parameters and details of data collection have been summarized in Table 3.1. Final atomic coordinates and equivalent isotropic as well as anisotropic displacement parameters are given in Table 9.3.1 of the Appendix. Bond lengths and angles as well as characteristic torsion angles can be found in Table 3.2.

Table 3.1. Crystal Data and Details of Structure Refinement for the Co-crystallisates **2a•CH_2Cl_2(1/1)**, **2b•CH_2Cl_2(2/4)**, **2c•CH_2Cl_2(1/2)**, **2d.1•CH_2Cl_2(1/1)**, and **2d.2•CH_2Cl_2(1/1)** (**2a** – **2d**: 2,4-Di-*tert*-butyl-3,3-diorganyl-1λ^3,5λ^3-diphospha-3-phosphonia-tricyclo[2.1.0.0^{2,5}]pentane Halide).

Substituents at P and halide; co-crystallisates	Me/Me/Cl; **2a•CH_2Cl_2(1/1)**	Et/Et/Cl; **2b•CH_2Cl_2(2/4)**	Ph/^{i}Pr/Cl; **2c•CH_2Cl_2(1/2)**	Ph/Ph/Cl; **2d.1•CH_2Cl_2(1/1)**	Ph/Ph/Br; **2d.2•CH_2Cl_2(1/1)**
Empirical formula[a)]	$C_{13}H_{26}Cl_3P_3$	$C_{16}H_{32}Cl_5P_3$	$C_{21}H_{34}Cl_5P_3$	$C_{23}H_{30}Cl_3P_3$	$C_{23}H_{30}BrCl_2P_3$
Formular weight[a)]	381.60	494.58	556.64	505.73	550.19
Decomposition point (°C)	157	168	184	196	243
Diffractometer	P4	$P2_1$	$P2_1$	$P2_1$	P4
Wavelength (pm)	71.073	71.073	71.073	71.073	71.073
Temperature (°C) of measurement	–100 ± 3	–100 ± 3	–100 ± 3	–100 ± 3	–100 ± 3
Shape and crystal size (mm)	Colourless thick needles 0.5 x 0.4 x 0.4	Colourless thick needles 0.6 x 0.5 x 0.3	Colourless thick needles 0.6 x 0.5 x 0.3	Colourless thick needles 0.6 x 0.5 x 0.4	Colourless thick needles 0.4 x 0.3 x 0.3
Crystal system	Triclinic	Triclinic	Monoclinic	Monoclinic	Monoclinic
Space Group [117]; Systematic Absences	$P\bar{1}$ (No.2)	$P\bar{1}$ (No.2)	$P2_1/c$ (No.14); (h0ℓ: ℓ = 2n +1; 0k0: k = 2n +1)	$P2_1/n$ (No.14); (h0ℓ: h + ℓ = 2n +1; 0k0: k = 2n +1)	$P2_1/n$ (No.14); (h0l: h + ℓ = 2n +1; 0k0: k = 2n +1)
Number of selected refl.[b)]; 2θ range (°)[c)]	50; 10.00→24.79	36; 20.31→28.01	30; 15.57→28.46	33; 15.34→25.66	59; 9.38→25.01
Unit cell Dimensions: a/pm	842.9(4)	1089.5(2)	1856.3(4)	986.4(2)	999.1(3)
b/pm	1058.8(3)	1321.5(3)	863.7(2)	1658.8(3)	1648.5(4)
c/pm	1133.5(3)	1782.3(4)	1761.1(4)	1629.6(3)	1623.2(4)
α/°	94.85(2)	94.30(3)			
β/°	91.22(3)	94.53(3)	99.37(3)	99.78(3)	99.388(17)
γ/°	108.62(3)	103.06(3)			
Volume (10^{-30} m^3)	954.0(6)	2480.4(9)	2785.8(10)	2627.7(9)	2637.6(12)
Z[d)]	2 + 2	4 + 8	4 + 8	4 + 4	4 + 4
Calculated density (10^3 kgm^{-3})	1.328	1.324	1.327	1.278	1.386
Calculated absorption coefficient μ (10^3 m^{-1})[e)]	0.719	0.7781	0.701	0.540	1.952
Absorption correction	None	None	None	None	Calc.[f)]
F(000)	400	1032	1160	1056	1128
θ-Range for data collection (°)	1.81 to 30.00	1.59 to 26.09	2.22 to 30.00	1.76 to 30.01	1.77 to 30.00
Limiting indices	–11 ≤ h ≤ 11; –14 ≤ k ≤ 14; –15 ≤ l ≤ 15	–10 ≤ h ≤ 13; –16 ≤ k ≤ 15; –22 ≤ l ≤ 21	–26 ≤ h ≤ 24; –12 ≤ k ≤ 3; –5 ≤ l ≤ 24	–13 ≤ h ≤ 13; –9 ≤ k ≤ 23; –22 ≤ l ≤ 22	0 ≤ h ≤ 14; 0 ≤ k ≤ 23; –22 ≤ l ≤ 22
Scan mode[g)]	ω-scan	Wyckoff-scan	Wyckoff-scan	Wyckoff-scan	ω-scan
Scan width (°); Velocity (deg min^{-1})	2.4; 3.0 to 60.0	1.6; 4.0 to 29.0	1.6; 4.0 to 29.3	1.4; 4.0 to 29.3	1.8; 3.0 to 60.0
Reflections collected	5763	10322	8376	8063	7934
Unique reflections (m)	5426	9784	8124	7660	7539
Observed Reflections [I > 2σ (I)] [h)]	2430	7080	5456	5313	2688
Parameters refined (n)	198	449	394	373	268
Restraints	0	0	0	0	0
Space filling[i,j)]	70%	71%	75%	71%	72%
Goodness-of-fit (GOF)[k)]	1.031	0.982	1.042	1.033	0.981

Isotropic R-indices$^{k)}$					
R1/wR2 using all data	0.3025/0.4654	0.1927/0.4301	0.1796/0.3349	0.1688/0.3453	0.3066/0.3514
R1/wR2 with [I>2σ(I)]	0.1846/0.4191	0.1533/0.4047	0.1333/0.3135	0.1264/0.3181	0.1416/0.2979
Anisotropic R-indices$^{k)}$					
R1/wR2 using all data	0.2445/0.3554	0.1183/0.2873	0.1215/0.2363	0.1232/0.2482	0.2724/0.2854
R1/wR2 with [I>2σ(I)]	0.1293/0.3080	0.0869/0.2648	0.0801/0.2119	0.0847/0.2225	0.1023/0.2213
Final R-indices$^{k)}$					
R1/wR2 using all data	0.2189/0.3476	0.0991/0.1892	0.1043/0.1756	0.1080/0.1987	0.2610/0.2597
R1/wR2 with [I>2σ(I)]	0.1053/0.2830	0.0683/0.1655	0.0627/0.1472	0.0698/0.1689	0.0889/0.1869
Indices f and g of weighting scheme w^{-1} $^{l)}$	f = 0.1698; g = 1.6298	f = 0.0538; g = 14.2046	f = 0.0788; g = 3.1234	f = 0.0893; g = 4.4029	f = 0.1000; g = 0.0000
Largest diff. peak; deepest hole (10^{-30}e.m^{-3})	1.227; –0.538	0.555; –0.593	0.905; –0.517	1.881; –1.126	1.636; –0.910

a) Co-crystallisates with one or two molecules of dichloromethane per formula unit; b) selected reflections used for the determination of cell dimensions; c) min.< 2θ <max.; d) number of ionic species and dichloromethane molecules in the unit cell; e) linear absorption coefficient $\mu = \Sigma\sigma_i / V_c$ [121]; f) computer program DIFABS to model the absorption surface of the crystal [187]; g) registration of the background at the beginning and at the end of the measurement with an overall duration equal to the time of measurement; h) reflections with strongly negative intensity were not considered for refinement; i) calculated from the Kitaigorodskii formula [122]; bond lengths taken from Table 3.2; C–$H_{aliph.}$ 108, C–$H_{arom.}$ 104; van der Waals radii: Br 195, P 190, C 180, Cl 180, H 117 pm [122,124]; j) including the different number of dichloromethane molecules; k) for a definition of the different quality factors R see Appendix, page 282; l) weighting scheme $w^{-1}=[\sigma^2(F_o)^2+(f\,P)^2+(g\,P)]$ with $P=1/3(F_o^2+2F_c^2)$.

Table 3.2. Characteristic Bond Lengths (pm) and Angles (°) as well as Torsion Angles for the Co-crystallisates **2a•CH$_2$Cl$_2$(1/1)** (= Me/Me/Cl), **2b•CH$_2$Cl$_2$(2/4)** (= Et/Et/Cl), **2c•CH$_2$Cl$_2$(1/2)** (= Ph/^{i}Pr/Cl), **2d.1•CH$_2$Cl$_2$(1/1)** (= Ph/Ph/Cl), and **2d.2•CH$_2$Cl$_2$(1/1)** (= Ph/Ph/Br)

2a – **2d**: 2,4-Di-*tert*-butyl-3,3-diorganyl-$1\lambda^3$,$5\lambda^3$-diphospha-3-phosphonia-tricyclo[2.1.0.0^{2,5}]pentane Halide

a) Bond lengths	Me/Me/Cl	Et/Et/Cl Molecule 1	Et/Et/Cl Molecule 2	Ph/^{i}Pr/Cl	Ph/Ph/Cl	Ph/Ph/Br	Average
P1–P5	211.9(3)	212.0(2)	212.0(2)	213.7(1)	214.9(2)	213.7(4)	213.0
P1–C2	187.5(7)	189.8(5)	190.2(5)	192.0(3)	188.7(4)	187.0(9)	189.2
P1–C4	187.9(8)	190.8(5)	190.1(5)	190.9(3)	191.2(3)	190.2(9)	190.2
P5–C2	188.8(7)	190.1(5)	189.6(5)	188.5(3)	193.2(3)	191.4(8)	190.3
P5–C4	189.2(7)	190.4(5)	190.4(5)	191.7(3)	188.8(3)	187.0(9)	189.6
C2–C21	154.1(10)	153.0(6)	152.2(6)	152.2(4)	152.2(5)	150.0(12)	152.3
C4–C41	149.0(10)	151.9(7)	151.7(6)	152.6(5)	153.2(4)	150.8(12)	151.5
P3–C2	176.5(7)	179.2(5)	179.5(5)	179.1(3)	179.0(3)	177.7(8)	178.5
P3–C4	179.8(6)	179.6(5)	179.9(5)	179.9(3)	179.8(3)	179.0(8)	179.7
P3–C311[a), b)]	177.6(8)	179.0(5)	178.9(5)	180.6(3)	180.0(3)	177.9(8)	179.0
P3–C321[c)]	178.0(8)	179.4(5)	179.1(5)	181.8(3)	179.5(3)	178.3(9)	179.4
C21–CH$_3$[d)]	152.0	152.9	152.7	153.2	153.1	152.3	152.7
C41–CH$_3$[d)]	153.1	152.4	152.4	153.0	153.3	152.8	152.8
C–Cl[e)]	175.2	172.9	173.2	175.8	175.5	171.9	174.1

b) Bond angles	Me/Me/Cl	Et/Et/Cl Molecule 1	Et/Et/Cl Molecule 2	Ph/^{i}Pr/Cl	Ph/Ph/Cl	Ph/Ph/Br	Average
P5–P1–C2	56.0(2)	56.1(2)	55.9(2)	55.1(1)	56.8(1)	56.6(3)	56.1
P5–P1–C4	56.1(2)	56.1(2)	56.1(2)	56.2(1)	55.0(1)	54.8(3)	55.7
P1–P5–C2	55.3(2)	56.0(2)	56.1(2)	56.6(1)	54.8(1)	54.6(3)	55.6
P1–P5–C4	55.5(3)	56.3(2)	56.1(2)	55.9(1)	56.1(1)	56.2(3)	56.0
C2–P1–C4	74.8(3)	74.3(2)	74.3(2)	74.0(1)	74.6(1)	74.5(4)	74.4
C2–P5–C4	74.2(3)	74.4(2)	74.4(2)	74.6(1)	74.1(1)	74.2(3)	74.3
P1–C2–P5	68.7(3)	67.9(2)	67.9(2)	68.3(1)	68.5(1)	68.8(3)	68.3
P1–C4–P5	68.4(3)	67.6(2)	67.8(2)	67.9(1)	68.9(1)	69.0(3)	68.3
P1–C2–P3	93.5(3)	93.3(2)	93.4(2)	92.4 (1)	93.3(2)	93.3(4)	93.2
P1–C4–P3	92.2(3)	92.8(2)	93.2(2)	92.5(2)	92.2(1)	91.8(4)	92.5
P5–C2–P3	93.2(3)	92.7(2)	92.8(2)	93.7(2)	91.8(1)	92.0(4)	92.7
P5–C4–P3	92.1(3)	92.5(2)	92.5(2)	92.3(2)	93.0(2)	93.1(4)	92.6
P1–C2–C21	124.7(6)	126.0(4)	125.2(3)	124.3(2)	126.7(2)	126.7(7)	125.6
P1–C4–C41	126.8(5)	125.8(4)	125.3(4)	126.2(2)	122.5(2)	122.2(7)	124.8
P5–C2–C21	126.1(5)	125.8(4)	126.1(3)	126.8(2)	123.7(2)	123.2(6)	125.3
P5–C4–C41	127.6(6)	125.8(4)	125.4(4)	123.2(2)	128.4(2)	128.7(6)	126.5
P3–C2–C21	131.4(6)	131.4(4)	131.6(3)	131.6(2)	132.7(3)	132.7(6)	131.9
P3–C4–C41	130.4(6)	132.0(4)	132.4(3)	133.7(2)	131.9(2)	132.0(6)	132.1
C2–P3–C4	79.2(3)	79.8(2)	79.4(2)	79.9(1)	79.8(2)	79.6(4)	79.6
C2–P3–C311[f), g)]	115.9(4)	117.6(2)	118.4(2)	113.7(1)	119.4(1)	119.6(4)	117.4
C4–P3–C311[h), i)]	118.9(4)	118.2(3)	118.4(2)	117.4(2)	114.8(1)	115.4(4)	117.2
C2–P3–C321[f), g)]	118.5(4)	118.1(2)	117.8(2)	117.2(2)	115.9(2)	116.0(4)	117.3
C4–P3–C321[h), i)]	116.0(4)	117.9(2)	118.0(2)	120.2(2)	118.1(1)	118.2(4)	118.1
C311–P3–C321	106.9(4)	104.6(2)	104.3(2)	106.8(2)	107.4(1)	106.7(4)	106.1
C2–C21–CH$_3$[j)]	109.0	109.5	109.5	109.4	109.7	110.4	109.6
H$_3$C–C21–CH$_3$[k)]	110.0	109.4	109.5	109.5	109.2	108.5	109.4
C4–C41–CH$_3$[j)]	109.9	109.3	109.1	109.8	109.2	110.0	109.6
H$_3$C–C41–CH$_3$[k)]	109.0	109.6	109.9	109.2	109.7	108.9	109.4
Cl–C–Cl[l)]	114.0	112.2	111.1	111.6	110.8(3)	113.3(1)	112.2

c) Torsion Angles[m)]	Me/Me/Cl	Et/Et/Cl Molecule 1	Et/Et/Cl Molecule 2	Ph/^{i}Pr/Cl	Ph/Ph/Cl	Ph/Ph/Br
P1–C2–C21–C23	−161.8(5)	−165.6(4)	−168.1(4)	−170.7(3)	−149.5(3)	−149.2(7)
P5–C2–C21–C24	165.5(6)	161.6(4)	159.9(4)	155.5(3)	177.6(3)	177.0(6)
P1–C4–C41–C43	170.3(6)	164.9(4)	166.1(4)	150.4(3)	176.7(2)	179.6(6)
P5–C4–C41–C44	−160.9(6)	−161.7(4)	−160.2(4)	−174.2(3)	−149.8(3)	−149.3(7)
P3–C2–C21–C22	−177.9(6)	177.4(4)	177.0(4)	176.0(3)	−169.1(4)	−170.7(7)
P3–C4–C41–C42	−174.0(7)	−178.4(5)	−176.8(5)	171.3(3)	−173.3(3)	−173.7(7)
C2–P3–C311–C312		48.6(5)	45.1(5)	−98.2(3)	−170.2(2)	−173.0(6)
C2–P3–C321–C322		−44.2(5)	−46.7(5)	−49.0(3)	−82.3(3)	−79.6(8)
C4–P3–C311–C312		−44.4(5)	−48.1(5)	171.2(2)	97.8(3)	95.0(7)
C4–P3–C321–C322		49.0(5)	46.1(5)	45.0(3)	9.8(3)	12.1(8)
C2–P3–C311–C316				78.7(3)	17.3(3)	17.4(8)
C4–P3–C311–C316				−11.9(3)	−74.7(3)	−74.6(7)

a) Mean C–C distance of the ethyl groups 152.2, individual values 151.5(7) and 152.8(7); b) mean C–C distance of the isopropyl group 153.4, individual values 153.2(5) and 153.6(5); c) mean C–C distance of all phenyl substituents 138.7, individual values vary between 135.5(14) and 140.7(12); d) mean C–CH_3 distances of the *tert*-butyl groups, individual values vary between 148.8(11) and 154.4(14); e) mean C–Cl distances of the solvent molecules, individual values vary between 166.0(2) and 178.0(2); f) mean P3–CH_2–CH_3 angle of the ethyl groups 117.2, individual values 116.9(4) and 117.4(4); g) mean P3–CH–CH_3 angle of the isopropyl group 113.1, individual values 111.9(3) and 114.2(3); H_3C–CH–CH_3 angle 110.6(3); h) mean P3–C–C angle of all phenyl substituents 120.1, individual values vary between 119.4(2) and 121.0(2); i) mean C–C–C angle of all phenyl substituents 120.0, individual values vary between 118.5(8) and 121.8(9); j) mean C–C–CH_3 angles of the *tert*-butyl groups, individual values vary between 108.4(6) and 111.0(8); k) mean H_3C–C–CH_3 angles of the *tert*-butyl groups, individual values vary between 107.3(7) and 111.1(4); l) mean Cl–C–Cl angles of the solvent molecules, individual values vary between 110.8(4) and 117.1(8). m) The torsion angle A–B–C–D is defined as positive if, when viewed along the B–C bond, atom A must be rotated clockwise to eclipse atom D [125, 126].

3.2.3.2. Bond Lengths and Bond Angles

Figs. 3.1 to 3.5 show plots of the five analogous 2,4-di-*tert*-butyl-3,3-diorganyl-1λ^3,5λ^3-diphospha-3-phosphonia-tricyclo[2.1.0.0^{2,5}]pentane cations as determined by X-ray structure analyses of the co-crystallizates **2a – 2d • x CH_2Cl_2** together with the pertinent halides in stereoscopic view. The central tricyclic framework consists of the unit P1–P5 on one side and the phosphonium cation with the atom P3 on the other. They are bridged by two quarternary carbon atoms C2 and C4 each of which is connected further to a *tert*-butyl group. The remaining substituents at phosphorus atom P3 might be either alkyl or aryl groups or both.

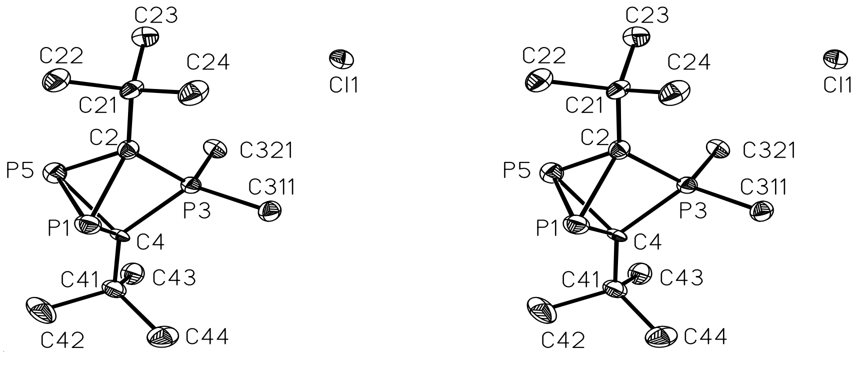

Figure 3.1. Stereoscopic view of cation and anion (at upper right) in the co-crystallizate **2a•CH_2Cl_2(1/1)**. Thermal ellipsoids are at 30% probability; hydrogen atoms and the co-crystallizing dichloromethane molecule have been omitted for clarity.

Molecule **2b.1**

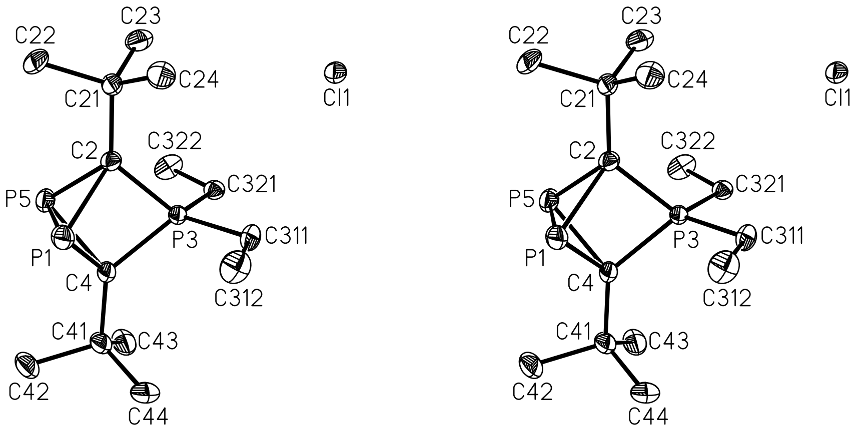

Molecule **2b.2**

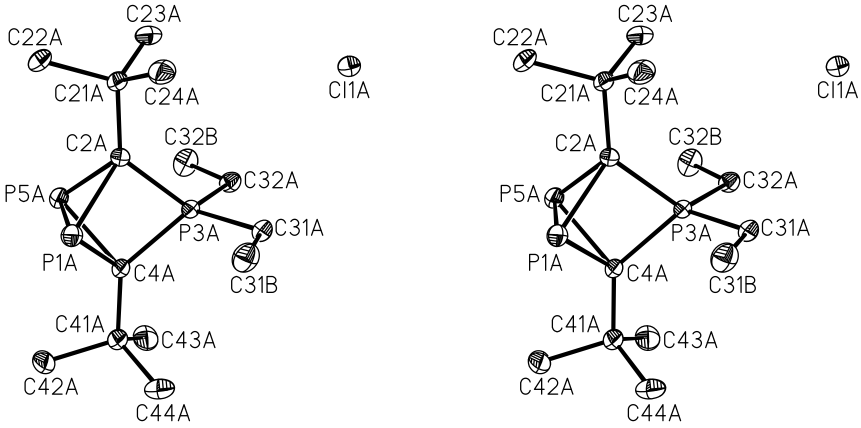

Figure 3.2. Stereoscopic view of cation and anion (at upper right) in the crystallographically independent species **2b.1** and **2b.2** of the co-crystallizate **2b•CH$_2$Cl$_2$(2/4)**. Thermal ellipsoids are at 30% probability; hydrogen atoms and co-crystallizing dichloromethane molecules have been omitted for clarity.

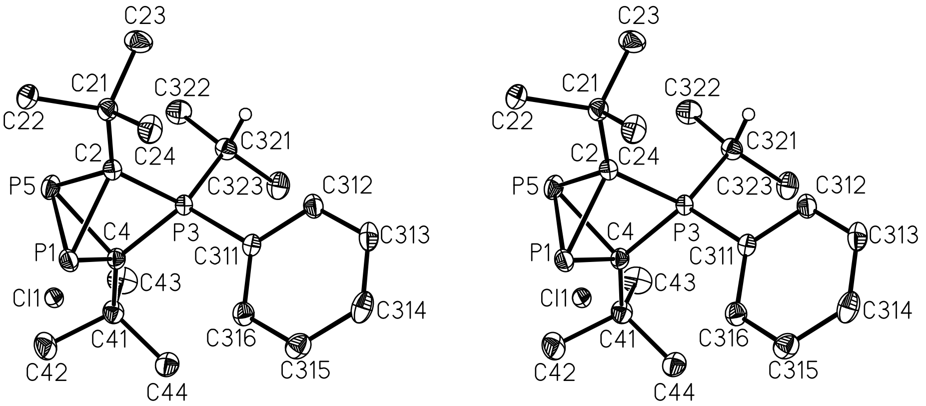

Figure 3.3. Stereoscopic view of cation and anion (at lower left) in the co-crystallizate **2c•CH$_2$Cl$_2$(1/2)**. Thermal ellipsoids are at 30% probability; hydrogen atoms and co-crystallizing dichloromethane molecules have been omitted for clarity; only the CH–hydrogen atom of the isopropyl group is shown.

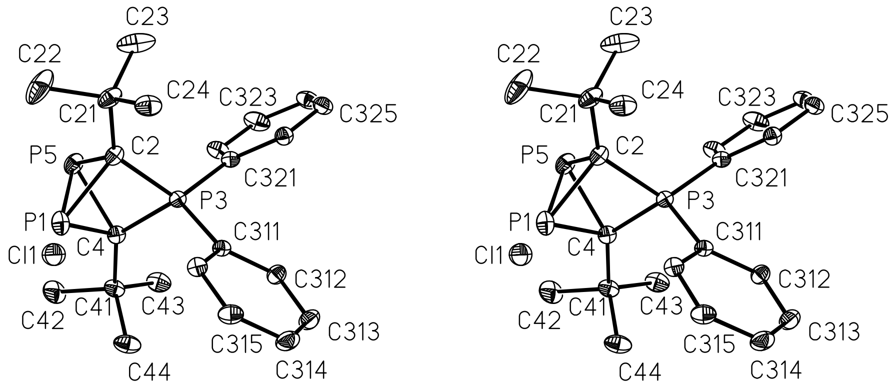

Figure 3.4. Stereoscopic view of cation and anion (at lower left) in the co-crystallizate **2d.1•CH_2Cl_2(1/1)**. Thermal ellipsoids are at 30% probability; hydrogen atoms and the co-crystallizing dichloromethane molecule have been omitted for clarity. Absent numbering follows logically from that given.

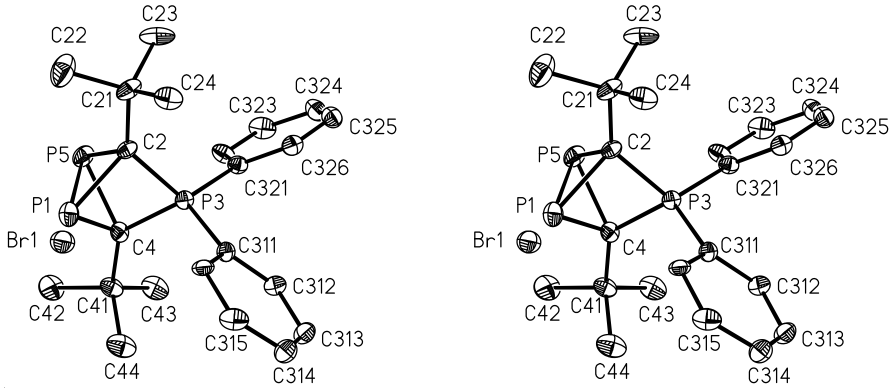

Figure 3.5. Stereoscopic view of cation and anion (at lower left) in the co-crystallizate **2d.2•CH_2Cl_2(1/1)**. Thermal ellipsoids are at 30% probability; hydrogen atoms and the co-crystallizing dichloromethane molecule have been omitted for clarity. Absent numbering follows logically from that given.

For a detailed discussion of bond lengths and angles one has to realize the high structural conformity of all cationic frameworks and the existence of a *pseudo*-mirror plane comprising the atoms P1, P5 and P3; they allow the use of mean values as classified in Table 3.3. Consequently, each framework consists of two nearly identical face-sharing tetrahedra and may therefore be considered a trigonal bipyramide. Since, however, the number of bonds along the equatorial edges has been reduced from three to only one (P1–P5), the polyhedron is surrounded by two triangles (P1, P5, C2 and P1, P5, C4) and two quadrangles (C2, P3, C4, P1 and C2, P3, C4, P5).

Table 3.3. Average Bond Lengths (pm) and Angles (°) in the Cations of the Co-crystallizates **2a•CH$_2$Cl$_2$(1/1)**, **2b•CH$_2$Cl$_2$(2/4)**, **2c•CH$_2$Cl$_2$(1/2)**, **2d.1•CH$_2$Cl$_2$(1/1)**, and **2d.2•CH$_2$Cl$_2$(1/1)**

Compound	**2a** Me/Me/Cl	**2b** Et/Et/Cl	**2c** Ph/^{i}Pr/Cl	**2d.1** Ph/Ph/Cl	**2d.2** Ph/Ph/Br	Mean value
P1–P5	211.9	212.0	213.7	214.9	213.7	213.0
P1–C2/C4$^{a)}$ P5–C2/C4	188.0	190.2	190.8	190.5	188.9	189.7
P3–C2/C4$^{b)c)}$	178.6	179.5	179.5	179.4	178.4	179.1
C2–P1/P5–C4$^{c)}$	74.5	74.4	74.3	74.4	74.4	74.4
P5–P1–C2/C4$^{c)}$ P1–P5–C2/C4	55.7	56.1	56.0	55.7	55.6	55.8
P1–C2/C4–P5$^{c)}$	68.6	67.8	68.1	68.7	68.9	68.4
P1–C2/C4–P3$^{c)}$ P5–C2/C4–P3	92.8	92.9	92.7	92.6	92.6	92.7
C2–P3–C4	79.2	79.6	79.9	79.8	79.6	79.6

a) Average value of P1–C2, P1–C4, P5–C2, and P5–C4; b) average value of P3–C2 and P3–C4. c) All following expressions have to be applied analogously.

Already a first inspection of Table 3.2.a) reveals a completely unexpected shortening of the bond P1–P5 with respect to the standard value of 221 pm [188]. At an average of 213.0 pm the distances in all these cations vary only slightly between 211.9 pm (**2a**: Me/Me/Cl) and 214.9 pm (**2d.1**: Ph/Ph/Cl). Surprisingly, similar P–P bond lengths have been observed with analogous compounds (Table 3.4) in which the $R_2P^{\oplus}$ unit is replaced by a (η^5-C_5H_5)$_2$Zr (**XXXIII**; 214.7 pm [179]), O=C (**XXXVII**; 211.8 pm [189]), I$_2$Ge (**XXXVIIIa**; 214.4 pm [190a]), and I–P group (**XXXVIIIb**; 215.4 pm [190b]. Even the 1λ^3,2λ^3,3λ^3-triphosphabicyclo[1.1.0]butane derivates Mes*P$_3$C(SiMe$_3$)$_2$ (**XXXIX** [191]) and [(Me$_3$Si)$_2$N–(Me$_3$Si)N]P$_3$C(SiMe$_3$)$_2$ (**XL** [192]) with an *unbridged* butterfly structure exhibit short P–P bonds of 213.6 and 215.8 pm, respectively, and fit therefore very well in this type of diphosphanes. Remarkably, the shortening of the central P–P distance is accompanied by elongations of the neighbouring P–C bonds. In the cations discussed here average values for P1–C2, P1–C4, P5–C2, and P5–C4 (Table 3.2.a, Fig.3.6) are found in a narrow range of 189.2 pm to 190.3 pm; the individual distances vary only slightly between 187.0 pm and 191.7 pm and exceed significantly the standard value of 185 pm [167] for an ordinary P–C$_{\text{alkyl}}$ bond. Similar mean bond lengths of 188.2 pm to 189.7 pm have been published for the compounds **XXXII** and **XXXVII** to **XL** with bridged and unbridged butterfly structures. Unfortunately, no interpretation of the bonding situation is available up to know; therefore, theoretical calculations are required very urgently.

In contrast to the elongated mean distance of 189.7 pm to the phosphorus atoms P1 and P5 of the P–P group (Table 3.3), the average bond length between the quarternary carbon atoms C2 and C4 in apical position of the trigonal bipyramidal framework and phosphorus atom P3 of the phosphonium group is found in all cations to be rather short. At an average of 179.1 pm it tallies the mean value of 179.0 pm as determined by X-ray structure analyses for the P–C bond in tetramethylphosphonium cations [193]. An explanation of the P–C bond shortening in phosphonium salts and compounds with pentavalent phosphorus atoms is given in *Gilheany's* review articles [166-168].

Table 3.4. Comparison of Characteristic Average Bond Lengths (pm) and Angles (°) in Diphosphanes with a Brigded or an Unbridged Butterfly Structure and a Central P–P Bond

Compound[a)] X Y, Z	**2a – 2d • x CH_2Cl_2** $P^{\oplus}$(mean values) diorganyl	**XXXII** [179] Zr (η^5-C_5H_5)$_2$	**XXXVII** [189] C O	**XXXVIIIa** [190a] Ge I_2	**XXXVIIIb** [190b] P I	**XXXIX** [191] --- ---	**XL** [192] --- ---
P–P	213.0	214.7	211.8	214.4	215.4	213.6	215.8
C–P	189.7	189.7	189.6	189.0	188.8	188.2	188.2
C–X	179.1	221.2	151.3	195.3	182.9	---	---
P–C–P	68.4	68.9[b)]	68.0[b)]	69.1	69.5	69.2[b)]	70.0
C–P–P	55.8	55.5[b)]	56.0[b)]	55.5[b)]	56.3	55.4[b)]	55.0[b)]
C–X–C	79.6	70.8[b)]	93.1[b)]	74.7[b)]	76.2	---	---
Y–X–Z	106.1	---	---	106.6	---	---	---
Dihedral angle	92.5[c)]	110.0[c)]	91.5[b), c)]	99.2[c)]	93.3[b), c)]	105[d), e)]	103.2[b), d) f), g]
Conjugate dihedral angle[h)]	87.5	70.0	88.5	80.8	86.7	75	76.8

a) The numbering scheme of the ionic species **2a – 2d** (Table 3.2. and 3.3.) has been renounced in order to allow a better comparison with compounds **XXXII** and **XXXVII** to **XL:**

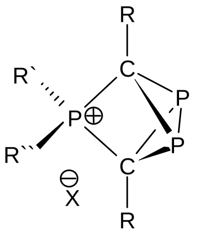

2a - 2d

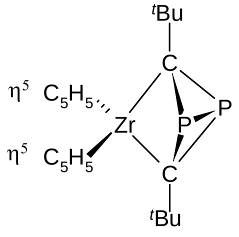

XXXI

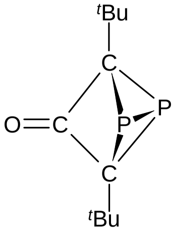

XXXVII

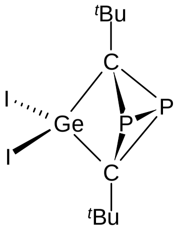

XXXVIIIa

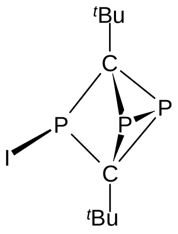

XXXVIIIb

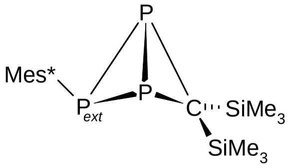

Mes* = 2,4,6-tri-*tert*-butylphenyl

XXXIX

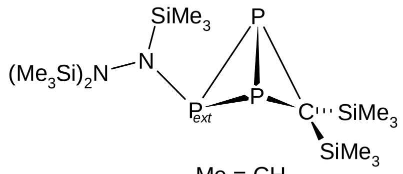

Me = CH_3

XL

b) data from Cambridge Structural Database (CSD) Version 5.28; Cambridge [165]; c) dihedral angle between the two triangular C, P, P planes (see also Table 3.5); d) dihedral angle between the planes C, P, P and P, P, P_{ext}; e) bond lengths P–P_{ext} 223.1 and 222.3 pm; f) bond lengths P–P_{ext} 221.5 and 222.6 pm; g) torsion angle P_{ext}–P–P–C 103.3°; h) conjugate dihedral angle = 180° – dihedral angle.

The angles in the peripheric faces of the tricyclic framework are found almost as expected. In both the largely isosceles triangles P1, C2, P5 and P1, C4, P5 (see below) values near 60° are encountered, but they differ slightly in that the wider angles at carbon exhibit a mean of 68.4°, whereas at the two phosphorus atoms an average of 55.8° has been determined (Table 3.3). Due to the presence of three- (P1 and P5) and four-coordinate phosphorus atoms (P3) the angles in both the peripheric P,C,P,C-quadrangles differ somewhat stronger. Moreover, a total sum of 339.4° only indicates these two planes to be folded; mean values of 129.1° and 128.6° have been determined for the dihedral angles between the two triangles P1, C2, P3// P1, C4, P3 and P5, C2, P3// P5, C4, P3, respectively (Table 3.5). Whereas an average of 92.7° for P1–C2/ C4–P3 and P5–C2/ C4–P3 (Table 3.3) exceeds the mean C–P–C angle of 74.4° at the trivalent phosphorus atoms considerably, an intermediate value of 79.6° is found at the phosphonium center. This strong deviation from a tetrahedral geometry as e.g. reported for undistorted tetramethylphosphonium cations [193] is compensated solely by an increase of the C–P3–$C_{organyl}$ angles to an average of 117.5°, whereas the angle between the two carbon atoms of the organyl groups is found to be 106.1° (Table 3.2.b). Most probably, the expansion of the C–C–P angles at the two apical carbon atoms to an average of 127.7° is caused by steric requirements of the bulky *tert*-butyl substituents. Furthermore, the quadrangle P5, C2, P1, C4 is folded along the bond P5–P1 by a mean value of 92.5° (Table 3.5). Since the sides of both the appertaining largely isosceles triangles P5, C2, P1/ P5, P1, C4 differ somewhat in length, two slightly longer (P1–C4 190.2, P5–C2 190.2) and two slightly shorter distances (P1–C2 189.1, P5–C4 189.5 pm) are observed on apposite sides of the quadrangle.

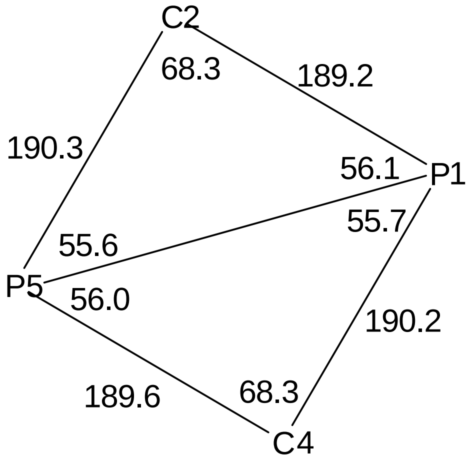

Figure 3.6. Average bond lengths (pm) and angles (°) in the two peripheric C, P, P triangles.

3.2.3.3. Crystal Packing

Intramolecular distances involving phosphorus atoms are given in Table 3.5. The atoms P1 and P5 of the P–P unit approach the central atom (P3) of the phosphonium cation at an average distance of 267.0 pm. This value differs from the standard P–P bond length of (221 pm [188]) by only 46 pm. At 402.5 to 519.7 pm the shortest interionic distance between the phosphorus atom P3 and the halide ($Cl^{\ominus}$, $Br^{\ominus}$), however, is about twice as long as the uncorrected sum of the corresponding covalent radii of the two elements involved: P...Cl 209, P...Br 224 pm [124].

Table 3.5. Selected Distances (pm) Involving Phosphorus Atoms and Selected Dihedral Angles (°) in the Cations of the 2,4-Di-*tert*-butyl-3,3-diorganyl-1λ^3,5λ^3-diphospha-3-phosphonia-tricyclo-[2.1.0.0^{2,5}]pentane Halides.

Distance	Me/Me/Cl	Et/Et/Cl Molecule 1	Et/Et/Cl Molecule 2	Ph/^{i}Pr/Cl	Ph/Ph/Cl	Ph/Ph/Br	Average
P1…P3	265.2	268.4	268.9	267.9	267.4	265.1	267.1
P5…P3	265.8	267.3	267.4	268.2	267.4	265.6	266.9
P3…X	402.5	416.9	412.1	456.3	519.7	518.7	
Dihedral angle							
C2, P5, P1/ C4, P1, P5	86.1	93.4	93.5	93.6	94.0	94.3	92.5
P1, C2, P3/ P1, C4, P3	129.2	129.8	129.8	128.0	129.4	128.6	129.1
P5, C2, P3/ P5, C4, P3	128.1	128.8	128.5	130.1	128.0	128.3	128.6
P1, C2, P3/ P5, C2, P3	111.3	112.1	112.0	111.6	111.5	111.2	111.6
P1, C4, P3/ P5, C4, P3	111.6	112.3	112.2	112.0	111.1	110.9	111.7

Figures **3.7** to **3.11** depict stereoscopic views of the crystal packing; no intermolecular contacts significantly shorter than the *van der Waals* distances were found.

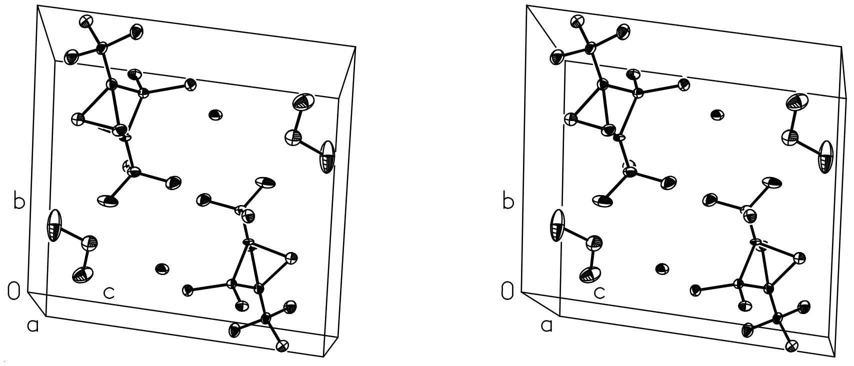

Figure 3.7. Crystal packing of the co-crystallizate **2a•CH_2Cl_2(1/1)** in stereoscopic view. Thermal ellipsoids are at 30% probability; hydrogen atoms have been omitted for clarity.

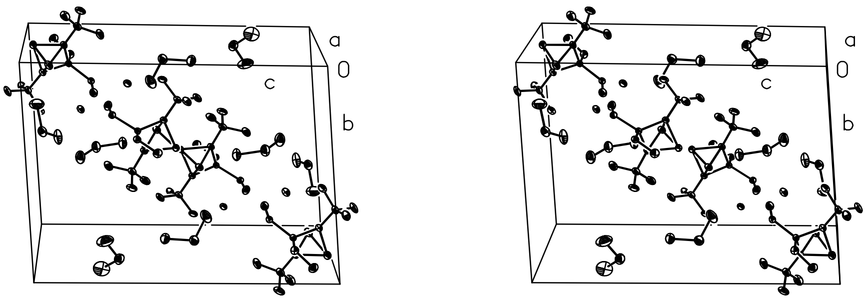

Figure 3.8. Crystal packing of the co-crystallizate **2b•CH$_2$Cl$_2$(2/4)** in stereoscopic view. The unit cell contains four crystallographically independent cations and anions as well as eight solvent molecules. Thermal ellipsoids are at 30% probability; hydrogen atoms have been omitted for clarity.

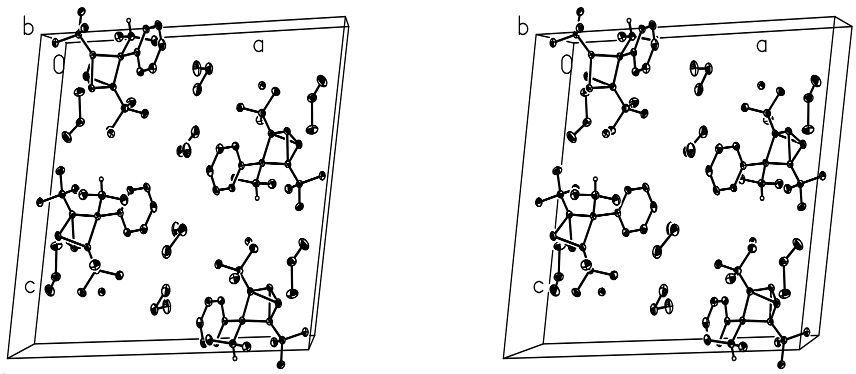

Figure 3.9. Crystal Packing of the co-crystallizate **2c•CH$_2$Cl$_2$(1/2)** in stereoscopic view. Thermal ellipsoids are at 30% probability; except for the CH-group of the isopropyl substituent all hydrogen atoms have been omitted for clarity.

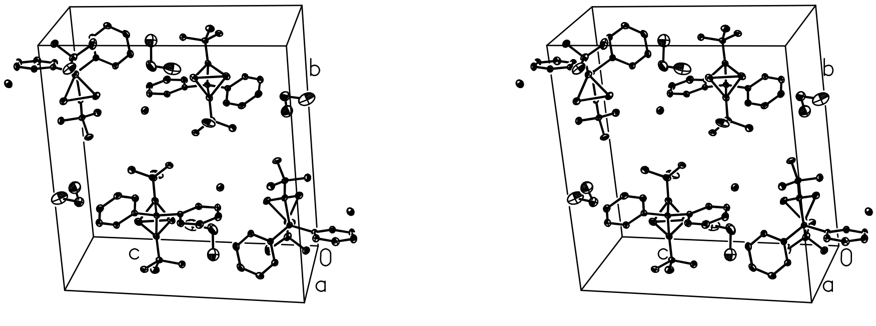

Figure 3.9. Crystal packing of the co-crystallizate **2d.1•CH$_2$Cl$_2$(1/1)** in stereoscopic view. Thermal ellipsoids are at 30% probability; hydrogen atoms have been omitted for clarity.

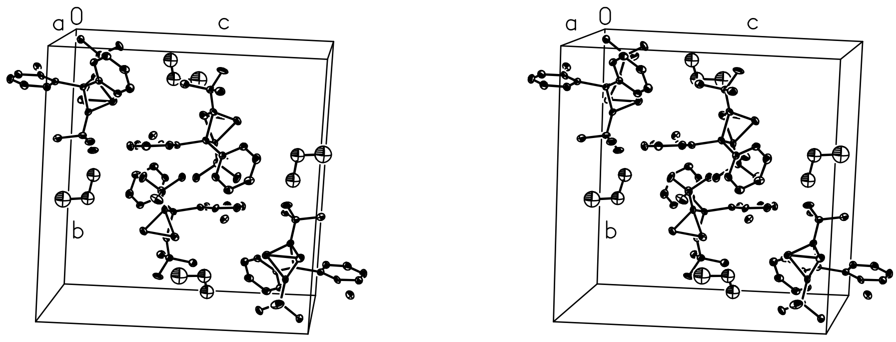

Figure 3.10. Crystal packing of the co-crystallizate **2d.2•CH$_2$Cl$_2$(1/1)** in stereoscopic view. Thermal ellipsoids are at 30% probability; hydrogen atoms have been omitted for clarity.

3.2.3.4. Quantum Chemical Calculations

In the introduction of this chapter the preparation of the ionic compound [3,5-(Me$_3$C)$_2$-1,2,4-C$_2$P$_3$]$^{\oplus}$[AlCl$_4$]$^{\ominus}$ from 2,4-di-*tert*-butyl-3-chloro-1λ^3,3λ^3,5λ^3-triphospha-tricyclo[2.1.0.0^{2,5}]-pentane and aluminium(III) chloride in dichloromethane by *M. Green*, *Ch. A. Russell* and others [181] has been discussed. Very surprisingly, the cation of this species exhibits a pseudo square-based pyramidal framework consisting of a diamond-shaped P$_2$C$_2$ base with alternating phosphorus and carbon atoms and a capping four-coordinate phosphorus. Due to this unusual geometry it has to be considered a 14-electron Wadian *nido*-cluster. Since the phosphonium cations of compounds **2a** to **2d** prepared in this thesis directly from 2-*tert*-butyl-1λ^3-phosphalkyne and halodiorganylphosphines in a molar ratio of 2:1 differ from *Russell's* phosphenium cation not only in two additional organyl substituents but also in the structure of the oligocyclic framework which here can best be described quite conventually as a trigonal bipyramide, quantum chemical calculations were performed on the hydrogen substituted cations first and on compound **2c** subsequently in order to ascertain optimized structural data and relative energies for different isomers.

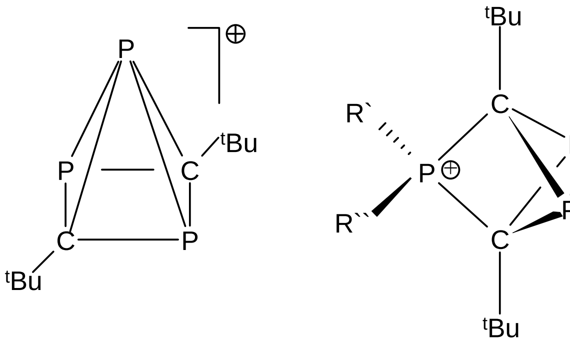

Scheme 3.3.4. Structures of the cationic 14-electron Wadian *nido*-cluster and the trigonal bipyramidal skeleton in the cations of compounds **2a** to **2d**

The results of quantum chemical calculations at B3LYP/6–311+G** (Gaussian 03) level [194] are depicted in Figures 3.11 and 3.12 for the $[H_2P(CH)_2P_2]^{\oplus}$ and the $[P(CH)_2P_2]^{\oplus}$ cation. As for the phosphonium-cation (Fig.3.11) the conventional trigonal bipyramidal framework of point-group C_{2v} represents the absolute minimum on the potential energy surface. Remarkably, the P–P bond is found to be shortened to 216.8 pm, whereas the adjacent P–C distances are elongated to 191.5 pm. Both values are only slightly larger than the average bond lengths of 213.0 and 189.7 pm, respectively, determined from the data of compounds **2a** to **2d** (Table 3.**7**). The P–C distances 178.5 and 179.1 pm of the phosphonium group do not differ in the calculated structure and the experimentally determined one. To our surprise the absolute minimum in energy of the trigonal bipyramidal framework is followed by a second one which has to be attributed to the so-called housene structure [182] of point group C_1 showing a difference of + 77.9 kJ mol^{-1} only.

Table 3.7. Selected Bond Lengths (pm) and Angles (°) of Several 2,4-Di-*tert*-butyl-3,3-diorganyl-1λ^3,5λ^3-diphospha-3-phosphonia-tricyclo[2.1.0.0^{2,5}]pentane Cations in Comparison with Calculated Structural Data and Energies (E) of the $[H_2P(CH)_2P_2]^{\oplus}$ Cation and the Cation of Compound **2c**

Compound	Mean value of **2a – 2d.2**, exp.	$[H_2P(CH)_2P_2]^{\oplus}$, calc.$^{a)}$	**2c**, exp.	**2c**, calc.$^{b)}$
P1–P5	213.0	216.8	213.7	215.3
P1–C2/C4 P5–C2/C4	189.7	191.5	190.8	192.3
P3–C2/C4	179.1	178.5	179.5	182.8
C2–P1/P5–C4	74.4	72.7	74.3	74.2
P5–P1–C2/C4 P1–P5–C2/C4	55.8	55.5	56.0	56.0
P1–C2/C4–P5	68.4	69.0	68.1	68.1
P1–C2/C4–P3 P5–C2/C4–P3	92.7	93.8	92.7	93.3
C2–P3–C4	79.6	79.0	79.9	78.7

a) E(C_{2v}) = 0.0, E(Housene) = 77.9, E(C_2) = 246.6 kJ mol^{-1}; b) E($\mathbf{2\underline{C}}_{calc.}$) = 0.0, E(housene) = 81.5 kJ mol^{-1}

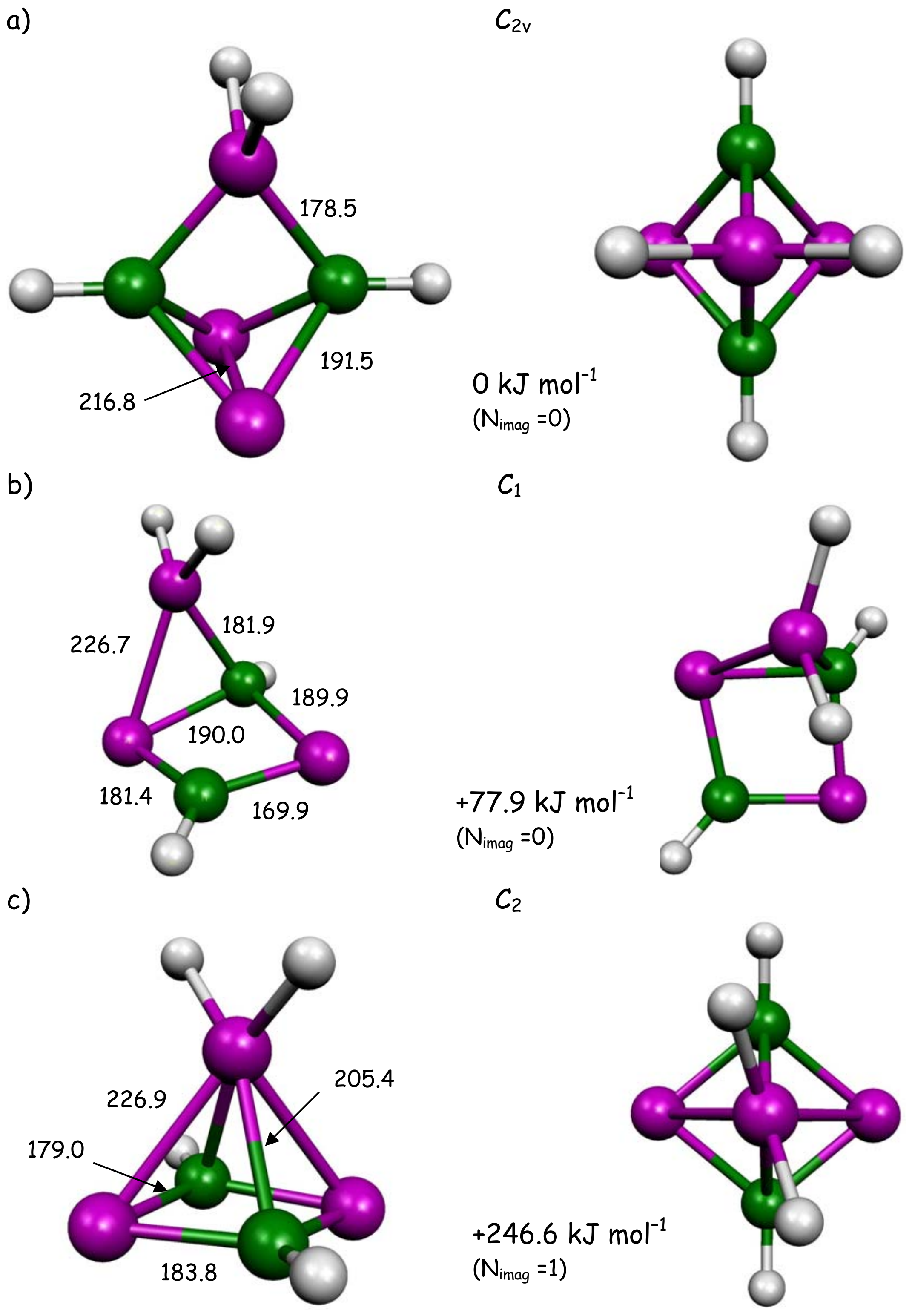

Figure 3.11. Optimized geometries and relative energies (B3LYP/6-311+G**, Gaussian 03) of the $[H_2P(CH)_2P_2]^{\oplus}$ cation
a) conventional trigonal bipyramidal structure; b) opened housene structure; c) pseudo square-based-pyramidal structure.

In view of such a small value the realisation of this opened structure should be possible with appropriate substituents at phosphorus. In order to obtain a better insight on the influence of substituents at the bipyramidal skeleton analogous quantum chemical calculations have been performed for the cation of compound **2c** characterized by a *tert*-butyl group on each apical carbon atom and an isopropyl as well as phenyl substituent at the phosphonium center P3. As a result the energy of the housene structure is found to be increased only slightly to 81.5 kJ mol^{-1}. Finally, the $[H_2P(CH)_2P_2]^{\oplus}$ cation with a pseudo square-based pyramidal framework of point-group C_2 is found to be very high in energy; it exceeds the first minimum by 246.6 kJ mol^{-1} and due to one imaginary frequency is considered to be a transition state only.

Quite a reverse situation is encountered for the $[P(CH)_2P_2]^{\oplus}$-cation (Fig. 3.12). Here the pseudo square-based pyramidal *nido* structure of point-group C_{2v} well known from *Russell's* tetrachloroaluminate(III) [181] is found to be the only minimum on the potential energy surface. Calculated P–P and P–C bond lengths compare very well with the average of experimentally determined data. A phosphenium cation with a trigonal-bipyramidal framework of point-group C_{2v} is higher in energy by 35.7 kJ mol^{-1} only but due to one imaginary frequency it is the structure of a transition state. The opened housene structure corresponds neither to a minimum nor a saddle point on the potential energy surface.

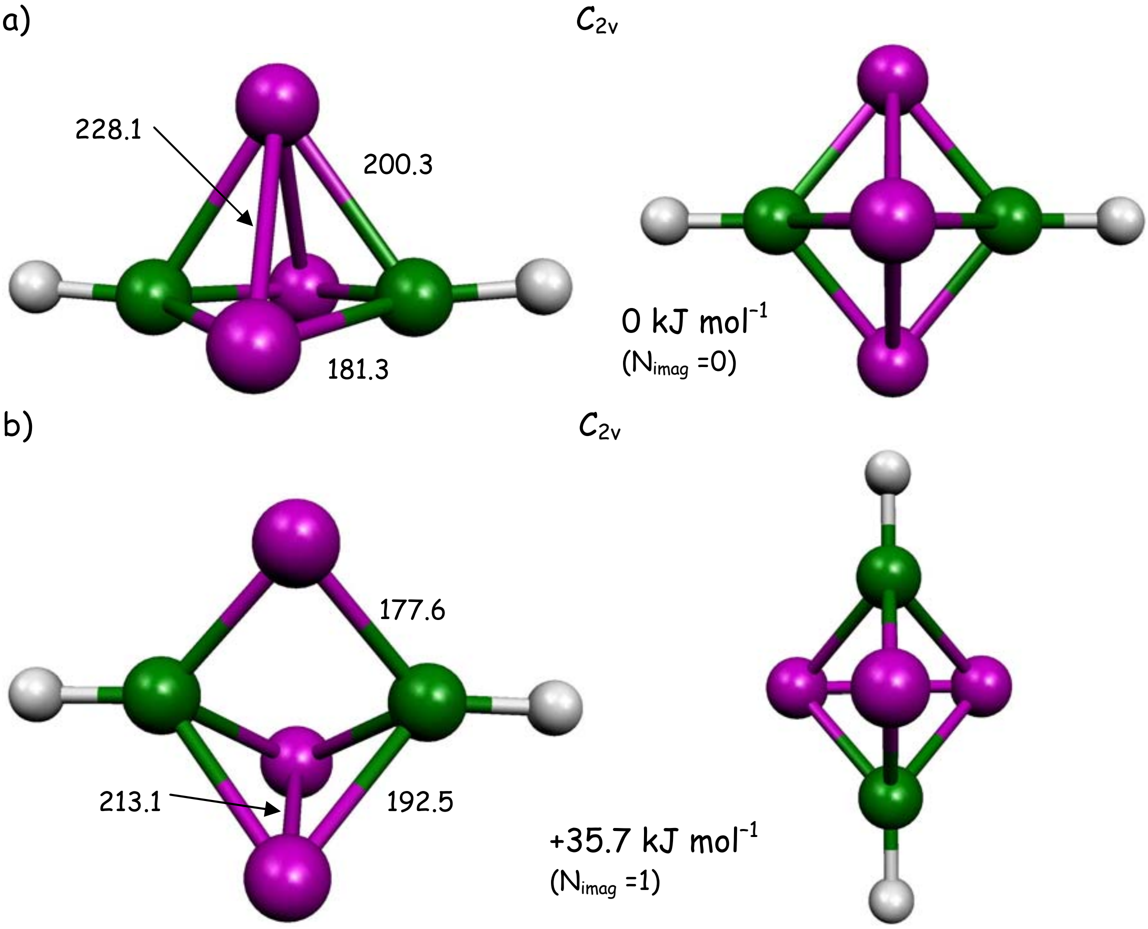

Figure 3.12. Optimized geometries and relative energies (B3LYP/6-311+G**, Gaussian 03) of the $[P(CH)_2P_2]^{\oplus}$cation
a) pseudo square-based-pyramidal *nido*-structure (average bond lengths of *Russell's* tetrachloroaluminate(III) [181]: P–C 180.4, $P^{\oplus}$–C 199.9, $P^{\oplus}$–P 224.5 pm); b) trigonal bipyramidal structure.

As illustrated by the representations of molecular orbitals (Fig.3.13), in the pseudo square-based pyramidal *nido* structure of the $[P(CH)_2P_2]^{\oplus}$ cation featuring point group C_{2v} all *p*-orbitals of the apical four-coordinate phosphorus atom are used to form two P–C and two P–P bonds. When, however, two hydrogen atoms are added to the apical phosphorus atom of this *nido* structure, the symmetry of the resulting $[H_2P(CH)_2P_2]^{\oplus}$ cation is lowered to point group C_2 (Fig. 3.11) and less *p*-orbitals are available to form two P–C and two P–P bonds. Quite evidently, a substantial part of these *p*-orbitals at the apical but now six-coordinate phosphorus atom are applied for the P–H bonds of PH_2 unit; as a consequence, the energy of such a $[H_2P(CH)_2P_2]^{\oplus}$ cation increases and the *nido* structure becomes less stable.

Since a straightforward interpretation of the bonding situation can be achieved on the theoretical basis of the Wadian rules [195] the difference in the ground state structures of the phosphenium cation $[P(CH)_2P_2]^{\oplus}$ and the phosphonium cation $[H_2P(CH)_2P_2]^{\oplus}$ is only at first sight surprising. In clusters which obey these rules the skeleton atoms are supposed to be *sp*-hybridized with one of the two *sp*-hybrid orbitals pointing inwards to the center and the second one being aligned outwards in the opposite direction. The two remaining *p*-orbitals overlap with analogous orbitals of adjacent skeleton atoms and form the so-called surface orbitals. With a pseudo square-based pyramidal structure and one vertex removed the $[P(CH)_2P_2]^{\oplus}$ cation belongs to the group of 14-electron *nido*-clusters. This arrangement of atoms enables the apical phosphorus atom of the phosphenium cation to increase its coordination number from two to four and to form two P–C and two P–P bonds which, however, are supposed to be somewhat weaker than conventional bonds. On the left side of Fig. 3.13 the five highest occupied molecular orbitals (HOMOs) and the lowest unoccupied molecular orbital (LUMO) are shown; the contributions of different surface orbitals as well as of the *sp*-hybrid orbital which is aligned outwards, are clearly discernible.

For comparison the five highest occupied molecular orbitals and the lowest unoccupied molecular orbital of the phosphonium cation $[H_2P(CH)_2P_2]^{\oplus}$ which shows an analogous pseudo square-based pyramidal *nido*-structure, are also presented on the left side of Fig. 3.13. Since this isomer refers to a transition state only, any further discussion may be renounced. As for the conventional trigonal bipyramidal ground state structure one the right side of Fig. 3.13 the phosphorus atom of the phosphonium cation is now located in the center of a strongly distorted tetrahedron. Consequently, the *sp*-hybridisation of *all* skeleton atoms characterizing the phosphenium cation showing the pseudo square-based pyramidal *nido* structure, has to be abandoned and changes towards sp^3 for all four-coordinate atoms. Since now the two remaining *p*-orbitals of an *sp*-hybridisation are no longer available, the construction of surface-orbitals becomes impossible and conventional two-electron two-center bonds are formed. Remarkably, an analogous structural change is observed, when the $1\lambda^3,3\lambda^3$-diphosphacyclobutadienyl germanium compound $Ge(\eta^4-P_2C_2{}^tBu_2)$ with a divalent germanium atom is oxidized with iodine to give an oligocycle which contains a GeI_2-group [181, 196].

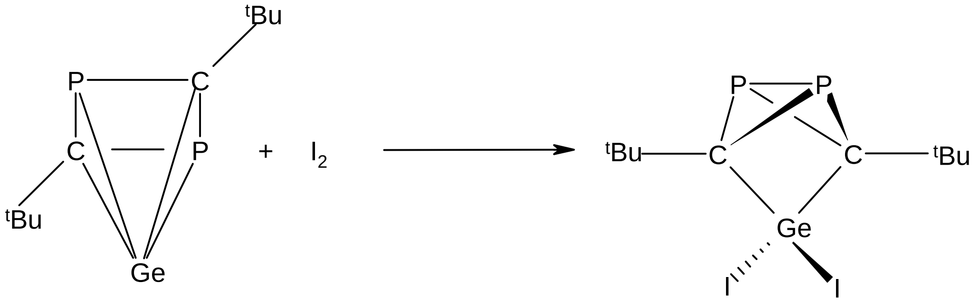

As before, the five highest occupied molecular orbitals (HOMOs) and the lowest unoccupied molecular orbital (LUMO) of the phosphenium cation $[P(CH)_2P_2]^{\oplus}$ featuring an analogous trigonal bipyramidal structure are presented on the right side of Fig. 3.13. Again this isomer refers to a transition state; therefore, a further discussion is considered to be unnecessary.

MO	Square-based pyramidal *nido*-$[\mathrm{P(CH)_2P_2}]^{\oplus}$ (C_{2v})	square-based pyramidal *nido*-$[\mathrm{H_2P(CH)_2P_2}]^{\oplus}$ (C_2)	trigonal bipyramidal $[\mathrm{P(CH)_2P_2}]^{\oplus}$ (C_{2v})	trigonal bipyramidal $[\mathrm{H_2P(CH)_2P_2}]^{\oplus}$ (C_{2v})
LUMO	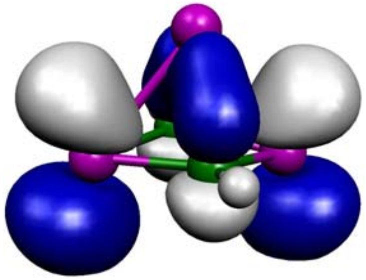	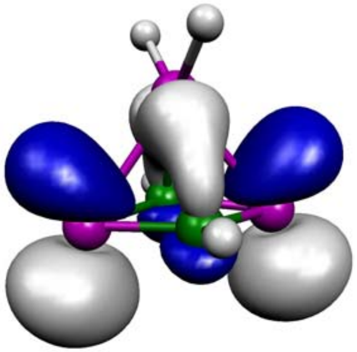	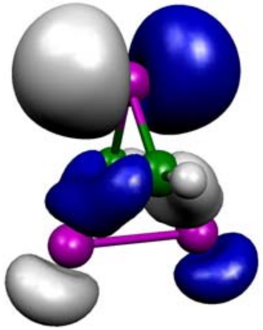	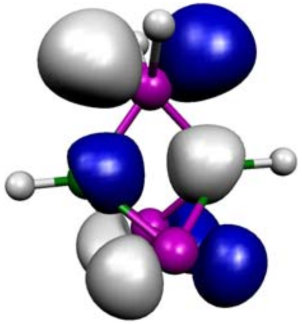
HOMO	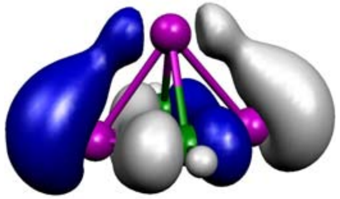	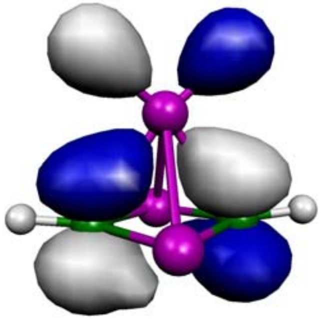	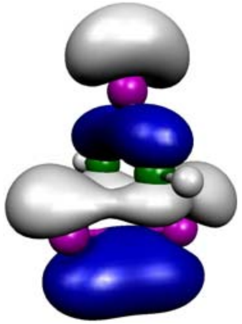	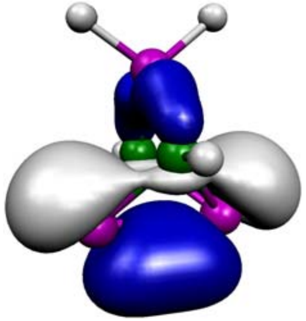
HOMO-1	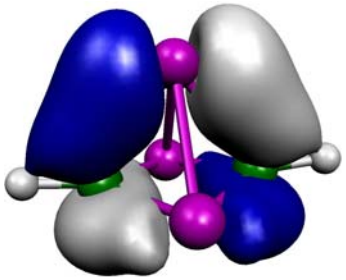	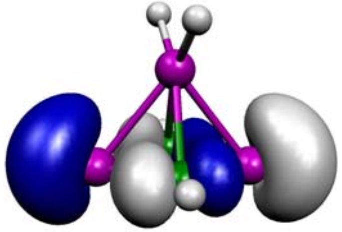	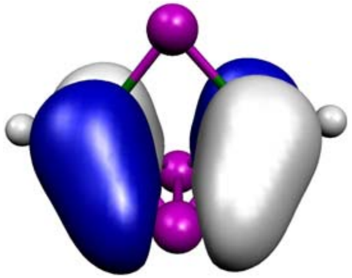	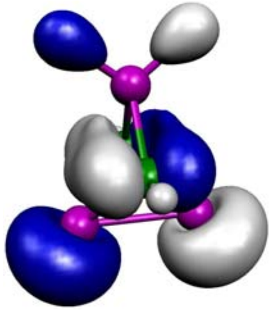

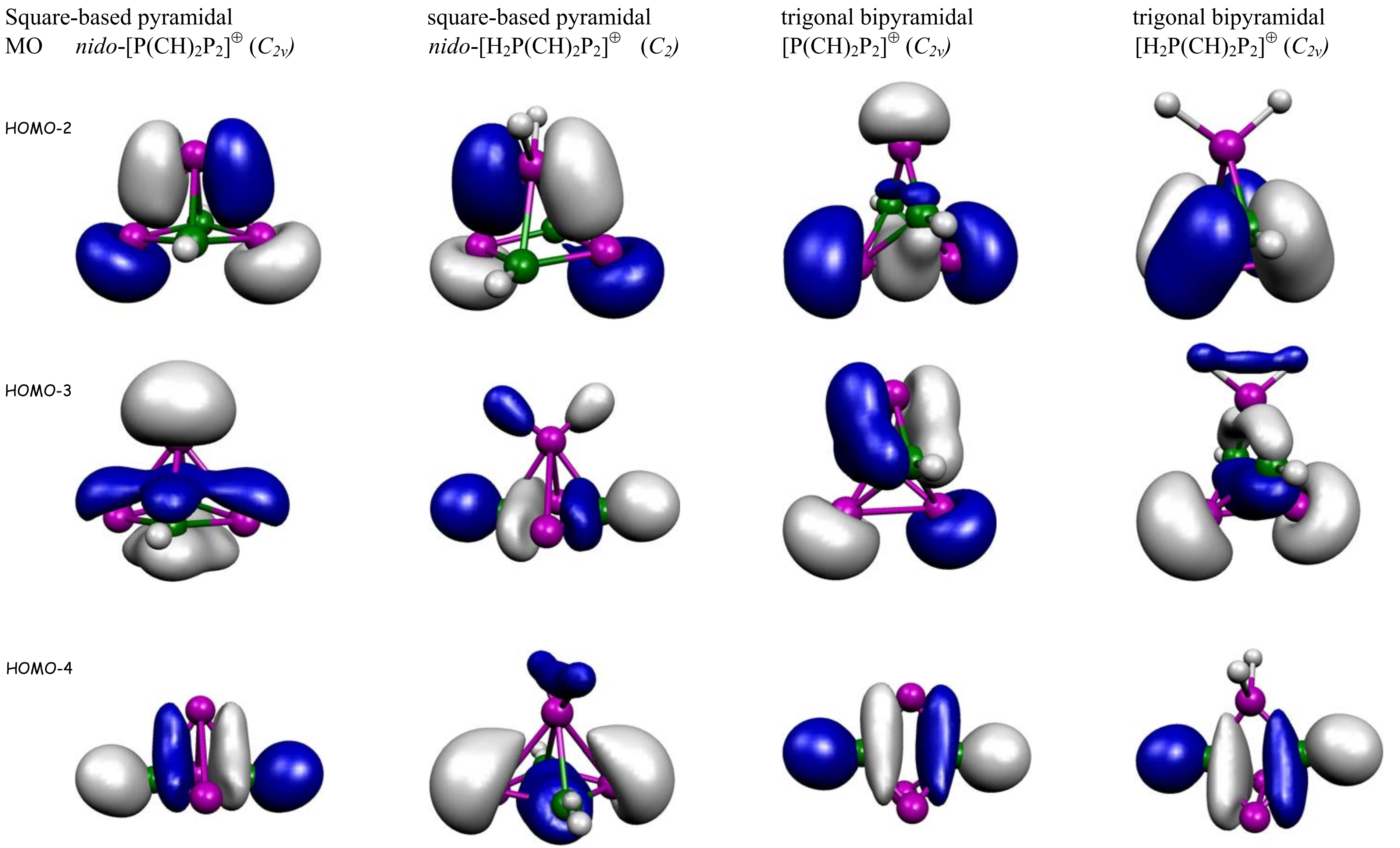

Figure 3.13. Molecular orbitals of the square-based pyramidal *nido* structures of the $[P(CH)_2P_2]^{\oplus}$ and $[H_2P(CH)_2P_2]^{\oplus}$ cations (left) and the trigonal bipyramidal structures of the $[P(CH)_2P_2]^{\oplus}$ and $[H_2P(CH)_2P_2]^{\oplus}$cations (right)

4. Reactions of 1λ^3-Phosphaalkynes with Dichloro(dialkylamino)arsines

4.1. Introduction

The reactivity of covalent halides towards 1λ^3-phosphaalkynes is increased when the central main group element is exchanged for its heavier congener. With this observation in mind it is quite understandable that in many cases the less reactive chlorides can be successfully applied instead of the more reactive bromides. Thus, from a cyclopentane solution of arsenic(III) chloride and 2-*tert*-buty-lλ^3-phosphaalkyne colourless crystals of the corresponding 2λ^3-arsa-4λ^3,5λ^3-diphosphabicyclo[1.1.1]pentane were obtained in 63% yield after several hours at a temperature increasing from 0 to about 20 °C. The $^{31}P\{^1H\}$ NMR spectrum reveals two doublets with a small $^2J_{(P,P)}$ coupling constant of 24.0 Hz only and confirms the expected structure with two chemically non-equivalent phosphorus atoms. Unfortunately, an X-ray analyses shows disorder with respect to the positions of the pnicogen atoms and to the orientation of the molecular core in relation to the peripheral chlorine and *tert*-butyl substituents [87, 88].

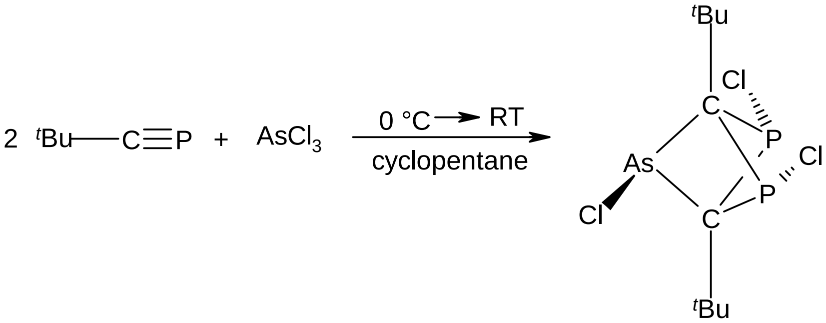

In his thesis *Merz* [73] treated a benzene solution of 2-*tert*-butyl-1λ^3-phosphaalkyne with a tenth of an equivalent of bis(dichloroarsinyl)methane at room temperature. In spite of the fact that the arsenic compound is consumed during the reaction, its function seems to be more catalytic and to initiate a tetramerization of the 1λ^3-phosphaalkyne. After a reaction time of 24 hours the already known [63, 65] 2,4,6,8-tetra-*tert*-butyl-1λ^3,3λ^3,5λ^3,7λ^3-tetraphosphacubane was isolated in more than 80% yield. An X-ray structure analyses showed the pale yellow crystals to be a co-crystallisate and to include one molecule of benzene per formula unit; bond lengths and angles agree very well with reported data [63, 65].

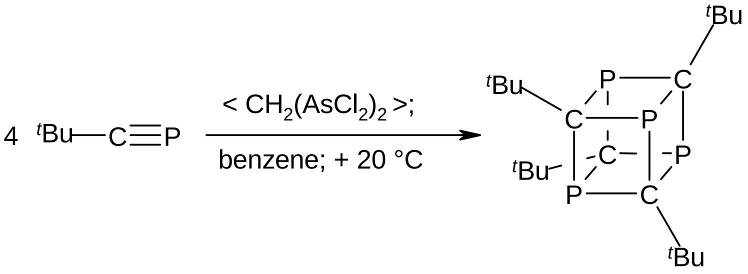

To increase our knowledge on the reactivity of 1λ^3-phosphaalkynes towards arsenic(III) halides, *Ruf* of our research group [100] treated the *tert*-butyl derivative with bis(diethylamino)chloroarsine in a molar ratios of 3:2. Whereas the origin of the deep blue to violet color of the *n*-pentane solution already observed in the beginning of the reaction remains obscure, after several weeks colourless crystals could be isolated in an up to 70% yield. An X-ray structure determination showed the presence of ion pairs in the solid state; the compound is built up of bis(dimethylamino)phosphonio-bridged 1λ^3-arsa-3λ^3,5λ^3-diphospha-2,6-homoprismane cations and dichlorobis(dimethylamino)arsenate(III) anions. In this previously unknown species chloro- and diethylamino substituents occupy axial and equatorial positions of a ψ-trigonal bipyramidal coordination polyhedron, respectively. At 366 pm the interionic As...Cl contact between cation and anion is found to be only slightly shorter than the sum of the corresponding van der Waals radii (380 pm) [124].

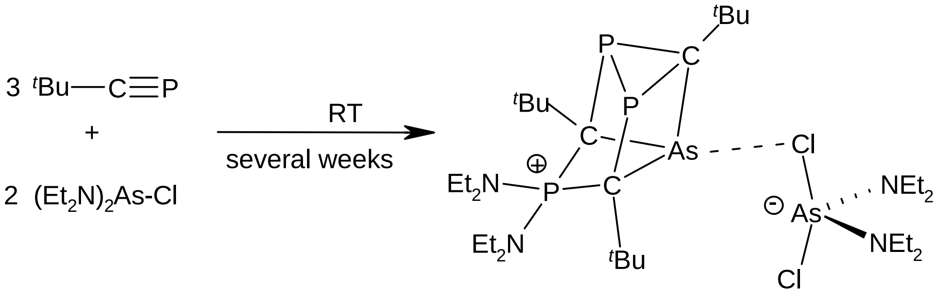

Additionally, *Ruf* began to study the reaction between dichloro(diethylamino)arsine and 2-*tert*-butyl-1λ^3-phosphaalkyne [100]. When after five days at room temperature the *n*-pentane solution of the two starting compounds reacted in a molar ratio of 1:3 had been filtered and freed from the solvent, a deep red oil was obtained which crystallised within several months at –13 °C. An X-ray structure analysis revealed the formation of a derivative of 1,3,5-triphospha-dewarbenzene. Unfortunately, one of the two crystallographically independent molecules of the asymmetric unit was found to be disordered. As will be discussed in detail later on, however, the isolated compound is free of arsenic; probably it precipitated as polymeric arsenic(I) chloride.

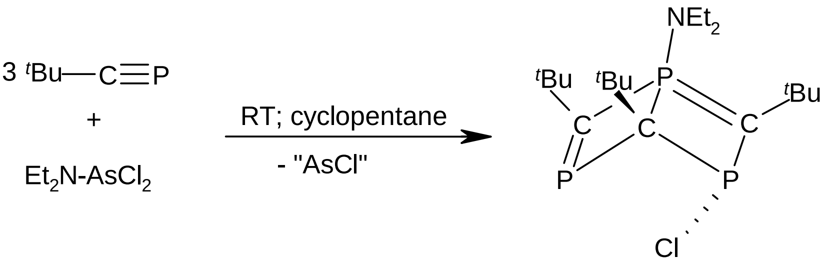

As for trialkyl-substituted 1λ^3,3λ^3,5λ^3-triphospha-dewarbenzenes with three trivalent phosphorus atoms *Binger* and co-workers worked out a highly efficient synthesis of the 2,4,6-tri-*tert*-butyl derivative from 2-*tert*-butyl-1λ^3-phosphaalkyne and [η^4-butadiene-η^8-1,4-bis-(trimethylsilyl)cyclooctatetraen] hafnium [68].

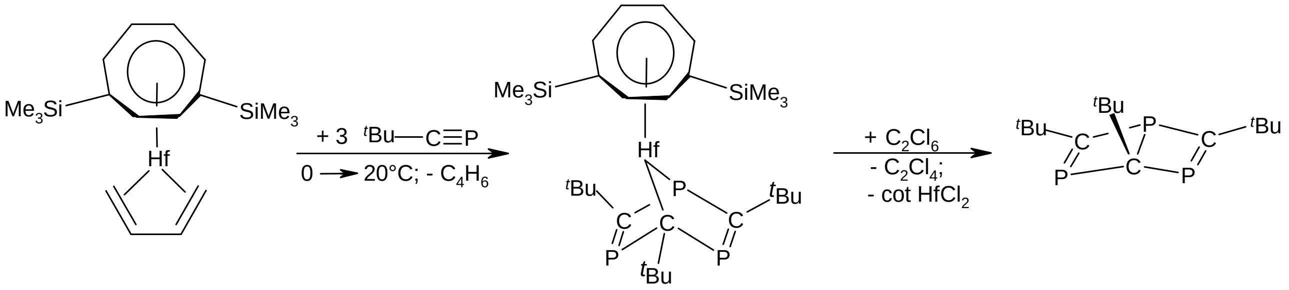

The heterocycle turned out to be stable up to about 100 °C as a solid, whereas in solution it undergoes very slow oligomerization and valence isomerization processes so that after several weeks the corresponding 1λ^3,3λ^3,5λ^3-triphosphabenzene could be obtained in about 20% yield [68, 198]. Initially, the structure of this important compound was based merely on its mass and NMR spectra. In 1998, however, *Binger*, *Krüger* and others [199] published the results of an X-ray structure analysis of 2,4,6-tri-*tert*-butyl-1λ^3,3λ^3,5λ^3-triphosphabenzene. At last, cyclization of 2-*tert*-butyl-1λ^3-phosphaalkyne to furnish the uncomplexed trimer directly in 68% yield could be accomplished in the presence of vanadium(V) *tert*-butylimido trichloride by *Regitz* and his group [200-202].

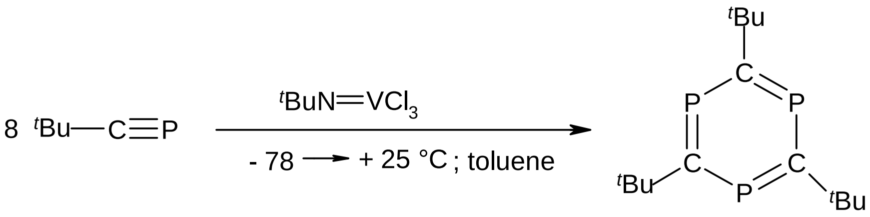

Diels-Alder reactions take place under very mild conditions when 2,4,6-tri-*tert*-butyl-1λ^3,3λ^3,5λ^3-triphospha-dewarbenzene is allowed to react with electron-deficient alkynes such as dimethyl acetylenedicarboxylate and methyl propyonate, or with 2-*tert*-butyl-1λ^3-phosphaalkyne itself. The resultant [2+2+2]cycloadducts such as 2,4,5-tri-*tert*-butyl-1λ^3,3λ^3,6λ^3-triphosphatricyclo[4.2.0.0^{2,6}.0^{3,5}]oct-7-ene-7,8-bis(methylcarboxylate) and 2,4,5,8-

tetra-*tert*-butyl-1λ^3,3λ^3,6λ^3,7λ^3-tetraphosphatetracyclo[4.2.0.$0^{2,6}$.$0^{3,5}$]oct-7-ene are formed regioselectively and could therefore be isolated in excellent yields. They were characterized by X-ray structure analyses as well as their NMR spectra [198].

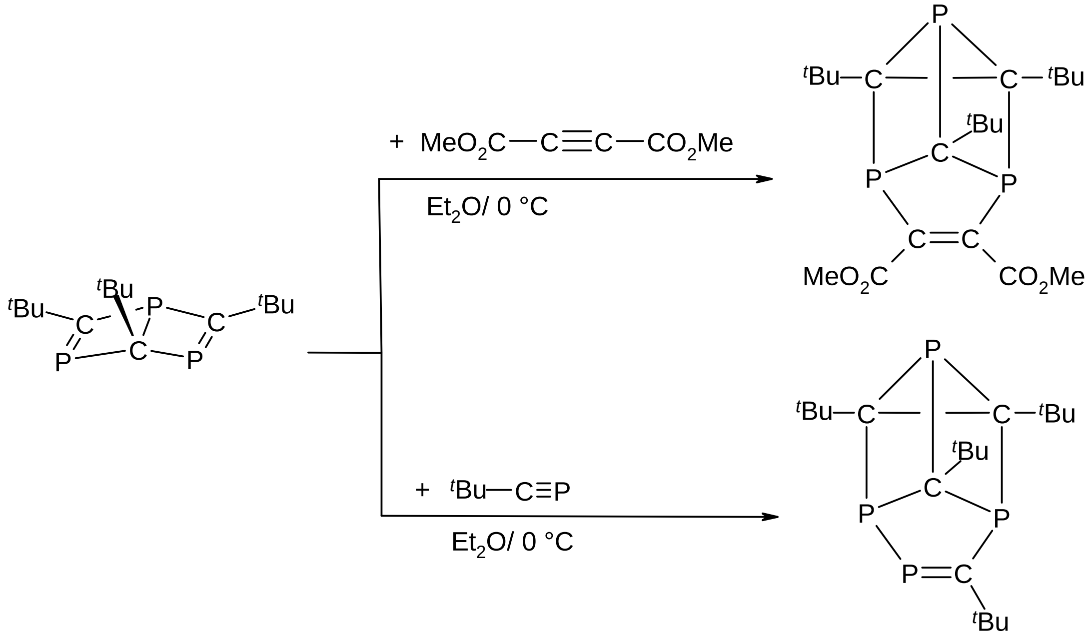

The formation of 2,4,6-tri-*tert*-butyl-1λ^3,3λ^3,5λ^3-triphospha-dewarbenzene as an intermediate has also been postulated in several reactions shown below. The heterocyclic compound, however, could not be isolated, since from a subsequent Diels-Alder reaction with one or two additional equivalents of 2-*tert*-butyl-1λ^3-phosphaalkyne 2,4,5,8-tetra-*tert*-butyl-1λ^3,3λ^3,-6λ^3,7λ^3-tetraphosphatetracyclo[4.2.0.$0^{2,6}$.$0^{3,5}$]oct-7-ene could be obtained [62, 101, 102, 178, 198].

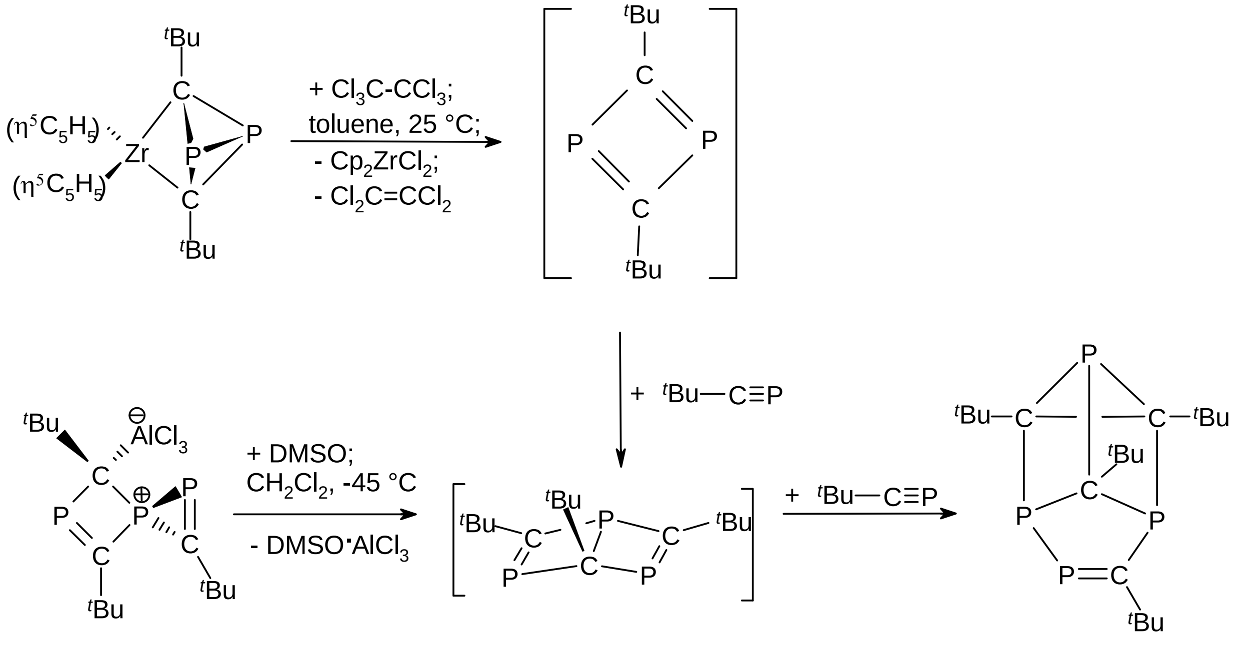

Moreover, 2,4,6-tri-*tert*-butyl-1λ^3,3λ^3,5λ^3-triphospha-dewarbenzene forms a 16-e vanadium complex of remarkably high kinetic stability [203]. In a first step, a tetrahydrofurane solution of [V(η^5-C_5Me_5)(η^6-naphthalene)] reacts at room temperature with three equivalents of 2-*tert*-butyl-1λ^3-phosphaalkyne. A single crystal X-ray diffraction study of the isolated compound showed it to be 14-e vanadium complex of a partially opened 1λ^3,3λ^3,5λ^3-triphosphaprismane; in solution this ligand exhibits a remarkable fluxional behaviour indicative of a valence isomerization taking place. The complex reacts at room temperature easily with one equivalent of carbon monoxide to give a new compound which has also been fully characterized by an X-ray structure analysis as well as its NMR spectra. The results of these studies indicate that in the coordination sphere of the metal atom the $P_3C_3{}^tBu_3$ ligand has rearranged from a 1λ^3,3λ^3,5λ^3-triphosphaprismane to a still complexed 1λ^3,3λ^3,5λ^3-triphospha-dewarbenzene.

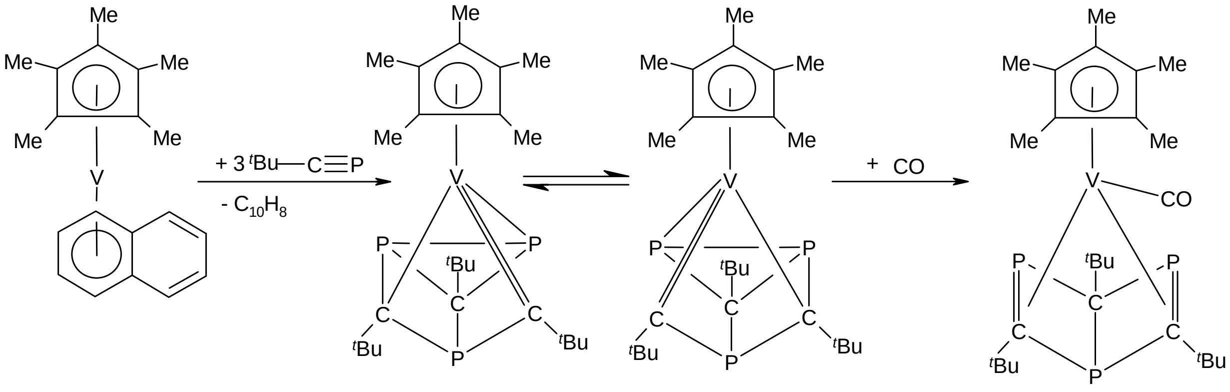

According to ab initio calculations, the parent skeleton of a 1λ^3,3λ^3,5λ^3-triphosphabenzene is by 25 kcal mol^{-1} more stable than that of a 1λ^3,3λ^3,5λ^3-triphospha-dewarbenzene [68, 198]. In continuation of the studies of our research group on the chemical behaviour of 2-*tert*-butyl-1λ^3-phosphaalkyne towards arsenic(III) halides, present investigations deal with reactions of dichloro(dialkylamino)arsines as well as quantum chemical calculations on the structure of the isolated products.

4.2.3-Chloro-1-dialkylamino-1$\lambda^5\sigma^4$,3$\lambda^3\sigma^3$,5$\lambda^3\sigma^2$-triphosphabicyclo[2.2.0]hexa-1,5-dienes

4.2.1. *Preparation and Reaction Mechanism*

Solutions of different dichloro(dialkylamino)arsines in cyclopentane were combined at –78 °C with slightly more than three equivalents of 2-*tert*-butyl-1λ^3-phosphaalkyne dissolved in the same solvent. When the mixtures had been allowed to warm up slowly to room temperature, the reactions required about five days to be complete. Thereafter, insoluble products were filtered off and the solvent was removed to leave a viscous red oil. Crystallization of the main product, a 3-chloro-1-dialkylamino-1$\lambda^5\sigma^4$,3$\lambda^3\sigma^3$,5$\lambda^3\sigma^2$-triphosphabicyclo[2.2.0]-hexa-1,5-diene **(3a – d)**, took place very slowly within several months to give deep red cuboids in yields of 44 to 66%. Surprisingly, the final products are free of arsenic; it has to be assumed that the dark-brown, insoluble precipitate which was cast aside comprises polymeric arsenic(I) chloride.

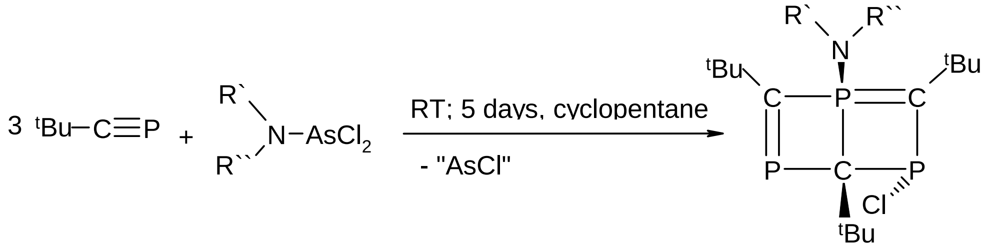

3a : R` = methyl, R`` = methyl; **3b** : R` = ethyl, R`` = ethyl;
3c : R` = *iso*-propyl, R`` = methyl; **3d** : R` = methyl, R`` = ethyl

3

X-ray structure analyses reveal that the 1λ^5,3λ^3,5λ^3-triphospha-dewarbenzenes (**3**) formed are characterized by one pentavalent and two trivalent phosphorus atoms and that the compounds have to be regarded as phosphoranes with an ylenic P^V=C or ylidic $P^{V\oplus}$–$C^\ominus$ and an additional P^{III}=C double bond. For the subsequent discussion the numbering scheme of the 1$\lambda^5\sigma^4$,3$\lambda^3\sigma^3$,5$\lambda^3\sigma^2$-triphosphabicyclo[2.2.0]hexa-1,5-diene (**3**) has been adopted from the analogous organic homocycle bicyclo[2.2.0]hexa-2,5-diene [204, 205] (Scheme 4.2.1).

Scheme 4.2.1. Numbering Scheme of 1$\lambda^5\sigma^4$,3$\lambda^3\sigma^3$,5$\lambda^3\sigma^2$-Triphosphabicyclo[2.2.0]hexa-1,5-diene (**3**) (left) and Bicyclo[2.2.0]hexa-2,5-diene (right).

One major result of the reaction mentioned above is the transfer of the dialkylamino group from arsenic to phosphorus. It may be easily understood in terms of bond dissociation energies of 582(126) and 617(21) kJ mol^{-1} [111] for the presumably weaker As–N and the stronger P–N bond, respectively. With this difference in mind a plausible mechanism can be postulated for the reaction of 1λ^3-phosphaalkynes with dichloro(dialkylamino)arsines. The formation of 1$\lambda^5\sigma^4$,3$\lambda^3\sigma^3$,5$\lambda^3\sigma^2$-triphospha-dewarbenzenes, the constitution of which has been proven without doubt by X-ray structure analyses, starts with an intermolecular insertion of the P≡C unit into the weak As–N bond to furnish the corresponding 1λ^3-phosphaalkene. This step is followed by a subsequent [2+2]cycloaddition of a second equivalent of 2-*tert*-butyl-1λ^3-phosphaalkyne to afford a 1-di-alkylamino-2-dichlorarsanyl-1,2-dihydro-1$\lambda^3\sigma^3$,3$\lambda^3\sigma^2$-diphosphete. Due to their very high reactivity, none of these intermediates could, however, be observed when the reaction was monitored by ^{31}P{^{1}H} NMR spectroscopy.

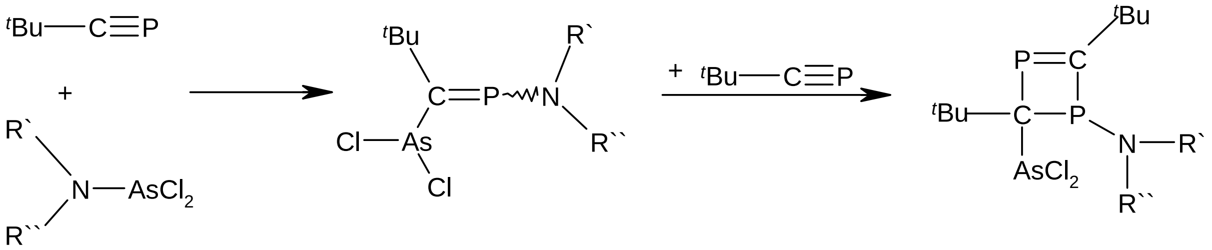

If one realizes that with dichloro(dialkylamino)arsines as starting compounds the arseno group is completely lost, very likely as insoluble "(AsCl)$_x$", a nucleophilic attack of the R`R``N group at the *sp*^{3}-hybridised carbon atom of the 1,2-dihydro-1$\lambda^3\sigma^3$,3$\lambda^3\sigma^2$-diphosphete and an accompanying elimination of a dichloroarsenate(I) anion seem to be obvious. Two different structures may be attributed to the postulated cationic intermediate, one featuring a 2,4-di-*tert*-butyl-5,5-dialkyl-5-azonia-1λ^3,3$\lambda^3\sigma^2$-diphospha-bicyclo[2.1.0]pent-2-ene cation and the other featuring a 2,4-di-*tert*-butyl-1-dialkylamino-1$\lambda^3\sigma^4$,3$\lambda^3\sigma^2$-diphosphet-1-ium cation (Scheme below). In a next step the [2+2]cycloaddition of a third equivalent of 1λ^3-phosphaalkyne results in the formation of a 1$\lambda^5\sigma^4$,3$\lambda^3\sigma^3$,5$\lambda^3\sigma^2$-triphosphabicyclo[2.2.0]hexa-1,5-diene cation the structure of which might be represented by three resonance structures. Finally this cation is stabilizes by addition of a chloride anion at one of the two phosphorus atoms in position 3 or 5 to give the 1$\lambda^5\sigma^4$,3$\lambda^3\sigma^3$,5$\lambda^3\sigma^2$-triphosphabicyclo[2.2.0]hexa-1,5-diene derivatives (**3**).

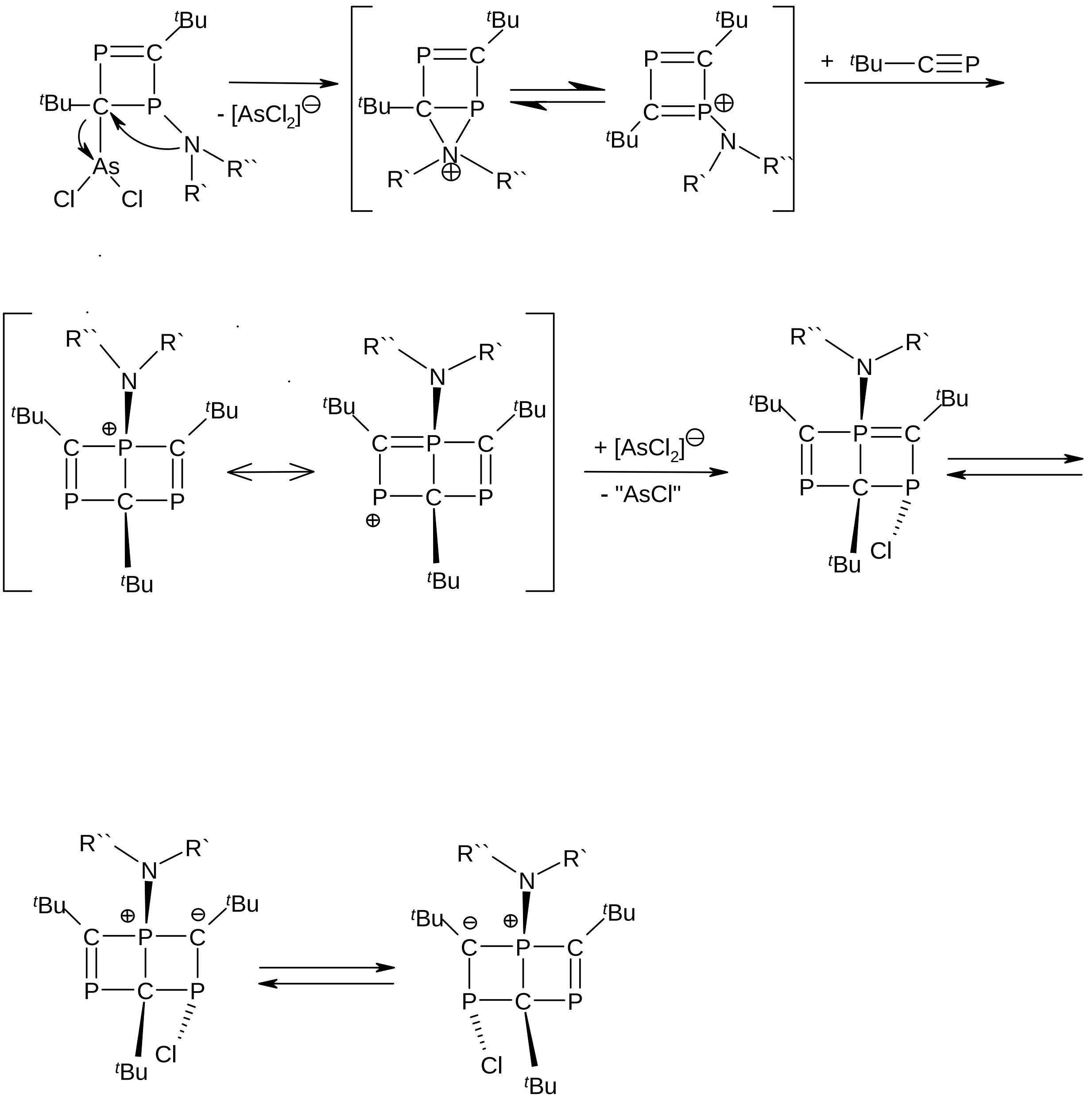
- [AsCl2]⊖
+ tBu—C≡P
+ [AsCl2]⊖
- "AsCl"

4.2.2. NMR Spectroscopic Characterization

The $^{31}P\{^1H\}$ NMR spectra of the compounds **3a** and **3b** taken at room temperature from d_6-benzene solutions, reveal the signals of an AX_2 spin system. With an intensity ratio of 2:1 the doublet of the two chemically equivalent trivalent phosphorus atoms P3 and P5 and the triplet of the pentavalent but four coordinate phosphorus atom P1 appear at rather low (**3a**, 278.9; **3b**, 280.9 ppm) and at relatively high field (**3a**, 51.1; **3b**, 52.0 ppm), respectively (Fig.4.2.1a and Table 4.2.1). A rapid exchange of the halogen atom between the two trivalent phosphorus atoms P3 and P5 will account for their chemical equivalence also in d_8-toluene solutions observed at ambient temperature as well as after cooling to –80 °C. The appertaining $^2J_{(P,P)}$ coupling constants vary only slightly between 11.4 Hz and 13.36 Hz and thereby differ considerably from the characteristic $^2J_{(P,P)}$ value of 23.5 Hz reported by *Binger* et al. for 2,4,6-tri-*tert*-butyl-1λ^5,3λ^3,5λ^3-triphospha-dewar benzene [68]. As can be taken from the literature [74, 198, 206], for oligocyclic phosphorus compounds $^2J_{(P,P)}$ coupling constants between 6.6 and 34.9 Hz have been observed.

The room temperature spectra of compounds **3c** and **3d** which are now characterized by two different substituents at nitrogen exhibit, however, a very broad singlet instead of a doublet but the high field signal is a sharp triplet as before (Fig.4.2.1b and Table 4.2.1). Very surprisingly, only the very broad low field singlets alter considerably with decreasing temperature and exhibit complicated splitting patterns (Figures 4.2.2 and 4.2.3, Table 4.2.2).

Already at 280 K the broad singlet has disappeared and in the spectra of both compounds two new broad lines start to evolve. On further cooling to *e.g* 240 K (Figure 4.2.2) a sharpening of the signals and subsequently a fine structure can be observed. Probably as a result of the two very different nitrogen substituents *iso*-propyl and methyl the two low field signals of compound **3c** are found to be well separated by about 20 ppm. They have to be attributed to two different phosphorus atoms (P3 or P5); their fine structure which starts to disappear again at 190 K is that of a pseudo triplett and arises probably from an ABX spin system. One, however, has to point out that the chlorine exchange between the phosphorus atoms P3 and P5 leads to a very complex situation and that the interpretation of the phenomena observed is not yet conclusive.

As the nitrogen substituents methyl and ethyl are rather similar, the two pseudo triplets of compound **3d** are found to be separated by less than 1 ppm. On further cooling they approach each other, combine and become two lines which finally coalesce at 190 K (Figure 4.2.3).

a) Compound **3a** (Me, Me)

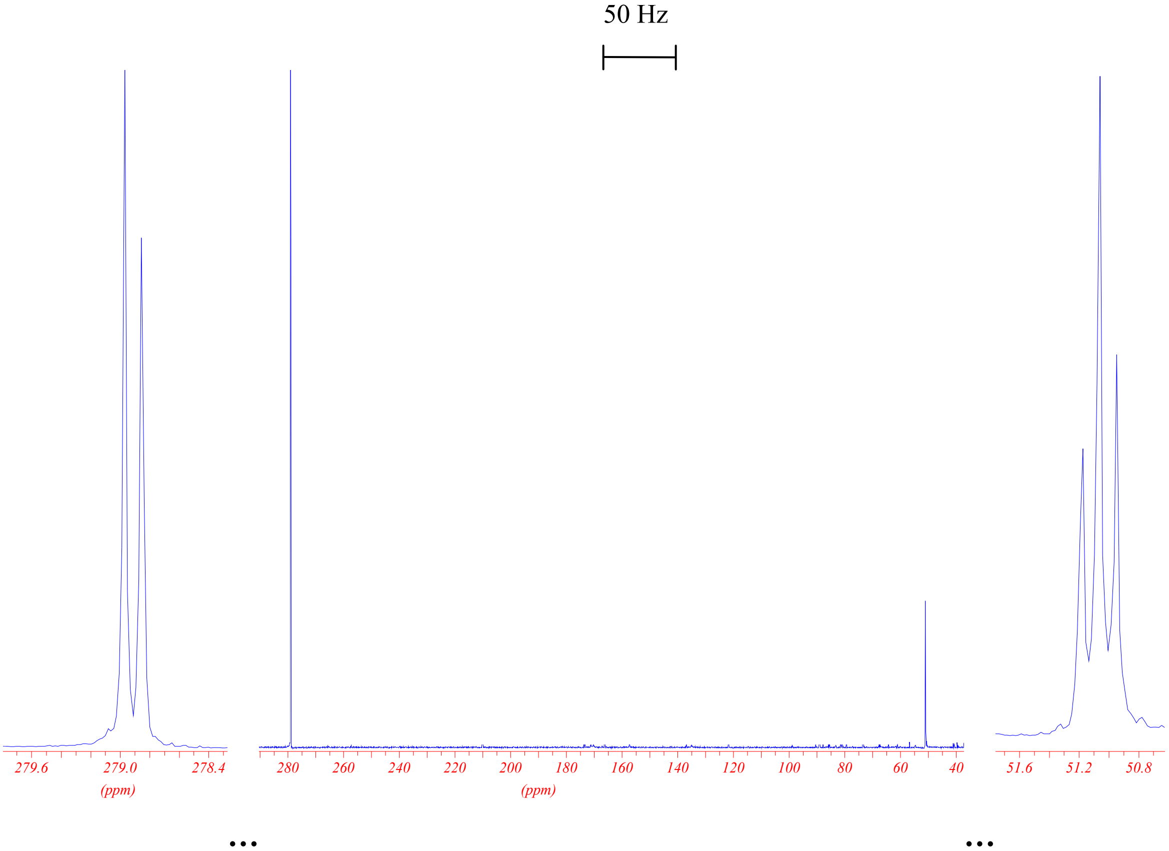

b) Compound **3d** (Et, Me)

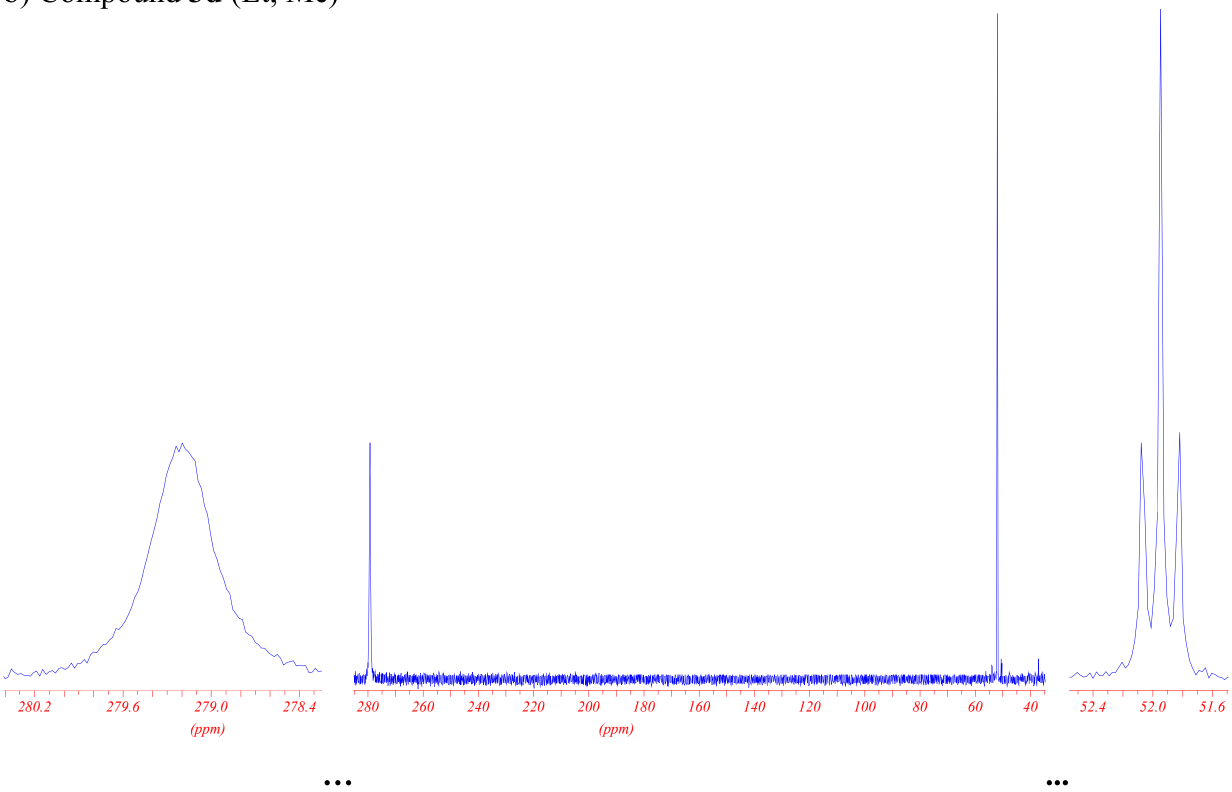

Figure 4.2.1. $^{31}P\{^1H\}$ NMR spectra of the compounds **3a** (Me, Me) (a) and **3d** (Et, Me) (b) taken at room temperature from d_6-benzene solutions.

The complete spectra of both compounds are depicted in the middle, whereas the resolved signals at low field (phosphorus atoms P3 and P5) and high field (P1) are additionally shown on the left and right, respectively.

Table 4.2.1. Characteristic NMR Parameters of the Central Bicyclic Unit in Several Dialkylamino-$1\lambda^5\sigma^4,3\lambda^3\sigma^3,5\lambda^3\sigma^2$-triphosphabicyclo[2.2.0]hexa-1,5-dienes at Room Temperature.
Chemical shift δ (ppm); coupling constants J (Hz); d_6-benzene solution.

Compound	P3/P5	P1	δ(C4)	δ(C2 or C6)
3a (Me, Me)	278.9 (d) $^2J_{(P1,P3/P5)} = 11.4$	51.1(t) $^2J_{(P1,P3/P5)} = 11.4$	64.3 (dt) $^1J_{(C4,P1)} = 57.9$ $^1J_{(C4,P3/P5)} = 32.6$	139.1 (m) $^1J_{(C2/C6, P3/P5)} = 32.1$
3b (Et, Et)	280.9 (d) $^2J_{(P1,P3/P5)} = 12.7$	52.0 (t) $^2J_{(P1,P3/P5)} = 12.7$	64.5 (dt) $^1J_{(C4,P1)} = 57.2$ $^1J_{(C4,P3/P5)} = 32.0$	138.5 (m) $^1J_{(C2/C6, P3/P5)} = 30.9$
3c (^{i}Pr, Me)	281.8 (s,br)	51.0 (t) $^2J_{(P1,P3/P5)} = 13.4$	64.9 (dt) $^1J_{(C4,P1)} = 57.9$ $^1J_{(C4,P3/P5)} = 32.1$	138.80 (m) $^1J_{(C2/C6, P3/P5)} = 31.6$
3d (Et, Me)	279.2 (s,br)	52.0 (t) $^2J_{(P1,P3/P5)} = 13.1$	64.1 (dt) $^1J_{(C4,P1)} = 56.7$ $^1J_{(C4,P3/P5)} = 32.3$	138.5 (m) $^1J_{(C2/C6, P3/P5)} = 33.7$

As will be discussed at full length in the following section 4.2.3., X-ray structure analyses reveal a molecule, which is characterized by an ylidic and a regular P–C double bond of almost equal length ($P1^{\oplus}$–$C2^{\ominus}_{av.}$ 172.2 pm, P5–$C6_{av.}$ 169.6 pm). In addition to these two characteristic features the average bond length P3–C2 is found to be considerably shortened to a value of 172.7 pm, whereas the adjacent phosphorus chlorine bond P3–Cl1 is strongly elongated to 245.5 pm. The bonding situation encountered here makes the already mentioned rapid 1,3-migration of the chlorine atom between the two phosphorus atoms P3 and P5 – as derived from the $^{31}P\{H\}$ NMR spectra – quite understandable (Scheme 4.2.2.).

The formation of an ylidic $P^{\oplus}$—$C^{\ominus}$ bond in compounds **3a** to **3d** gives a straightforward explanation why the adjacent P–Cl bond is found to be strongly elongated. As can already be taken from the word "ylidic", the *sp*^{2}-hybridized carbon atom C2 has to be considered a carbanion, whereas the positive charge is located at the four coordinate phosphorus atom P1. An electronic interaction between the free electron pair at carbon and the empty σ*(P–Cl) orbital not only shortens the bond C2–P3 but also elongates the bond P3–Cl1 by about 60 pm with respect to the standard value of 204 pm (see section 4.2.3).

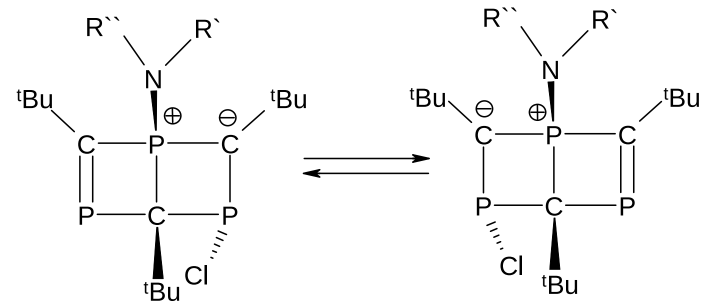

Scheme 4.2.2. 1,3-Migration of the chlorine atom between the two phosphorus atoms P3 and P5 in $1\lambda^5\sigma^4,3\lambda^3\sigma^3,5\lambda^3\sigma^2$-triphosphabicyclo[2.2.0]hexa-1,5-diene compounds

Table 4.2.2 Characteristic ${}^{31}P\{{}^{1}H\}$ NMR Parameters in Several Dialkylamino-$1\lambda^5\sigma^4,3\lambda^3\sigma^3,5\lambda^3\sigma^2$-triphosphabicyclo[2.2.0]hexa-1,5-dienes (**3**) at Various Temperatures (K).
Chemical Shift δ (ppm); coupling constants J (Hz); d_8- toluene solution.

		3a[a]	**3b**[b]	**3c**[c]	**3d**[d]
300 K	δ(P1) =	55.68 (t)	56.68 (t)	55.60 (t)	56.74 (t)
	δ(P3/P5) =	281.04 (d)	282.40 (d)	284.6	282.5
	${}^{2}J_{(P1,P3/P5)}$ =	11.4	12.7	13.4	13.1
280 K	δ(P1) =	55.73 (t)	56.63 (t)	55.59 (t)	56.77 (t)
	δ(P3/P5) =	281.3 (d)	282.8 (d)	280.2, 288.4	282.0, 282.9
	${}^{2}J_{(P1,P3/P5)}$ =	11.4	12.7	13.4	13.1
260 K	δ(P1) =	55.79 (t)	56.69 (t)	55.60 (t)	56.83 (t)
	δ(P3/P5) =	281.58 (d)	282.77 (d)	277.7, 291.8	282.3, 283.3
	${}^{2}J_{(P1,P3/P5)}$ =	11.4	12.7	13.4	13.1
240 K	δ(P1) =	55.79 (t)	55.79 (t)	55.63 (t)	56.90 (t)
	δ(P3/P5) =	281.58 (d)	282.80 (d)	276.9, 293.8	282.7, 283.5
	${}^{2}J_{(P1,P3/P5)}$ =	11.4	12.7	13.4	13.1
220 K	δ(P1) =	55.91 (t)	56.96 (t)	55.66 (t)	56.99(t)
	δ(P3/P5) =	282.15 (d)	283.45 (d)	275.8, 296.0	283.3, 283.8
	${}^{2}J_{(P1,P3/P5)}$ =	11.4	12.7	13.4	13.1
210 K	δ(P1) =	56.03 (t)	56.93 (t)	55.73 (t)	57.04 (t)
	δ(P3/P5) =	282.66 (d)	283.56 (d)	275.8, 296.0	283.7
	${}^{2}J_{(P1,P3/P5)}$ =	11.4	12.7	13.4	13.1
200 K	δ(P1) =	56.10 (t)	57.00 (t)	55.75 (t)	57.10 (t)
	δ(P3/P5) =	283.00 (d)	284.00 (d)	274.4, 298.6	284.0
	${}^{2}J_{(P1,P3/P5)}$ =	11.4	12.7	13.4	13.1
190 K	δ(P1) =	56.15 (t)	57.20 (t)	55.76(t)	57.17(t)
	δ(P3/P5) =	283.27 (d)	284.58 (d)	273.5, 300.1	284.5
	${}^{2}J_{(P1,P3/P5)}$ =	11.4	12.7	13.4	13.1

a, b) ${}^{2}J_{(P1,P3/P5)}$ were calculated from both signals triplet and a doublet. c, d) ${}^{2}J_{(P1,P3/P5)}$ were calculated only from the triplet signal.

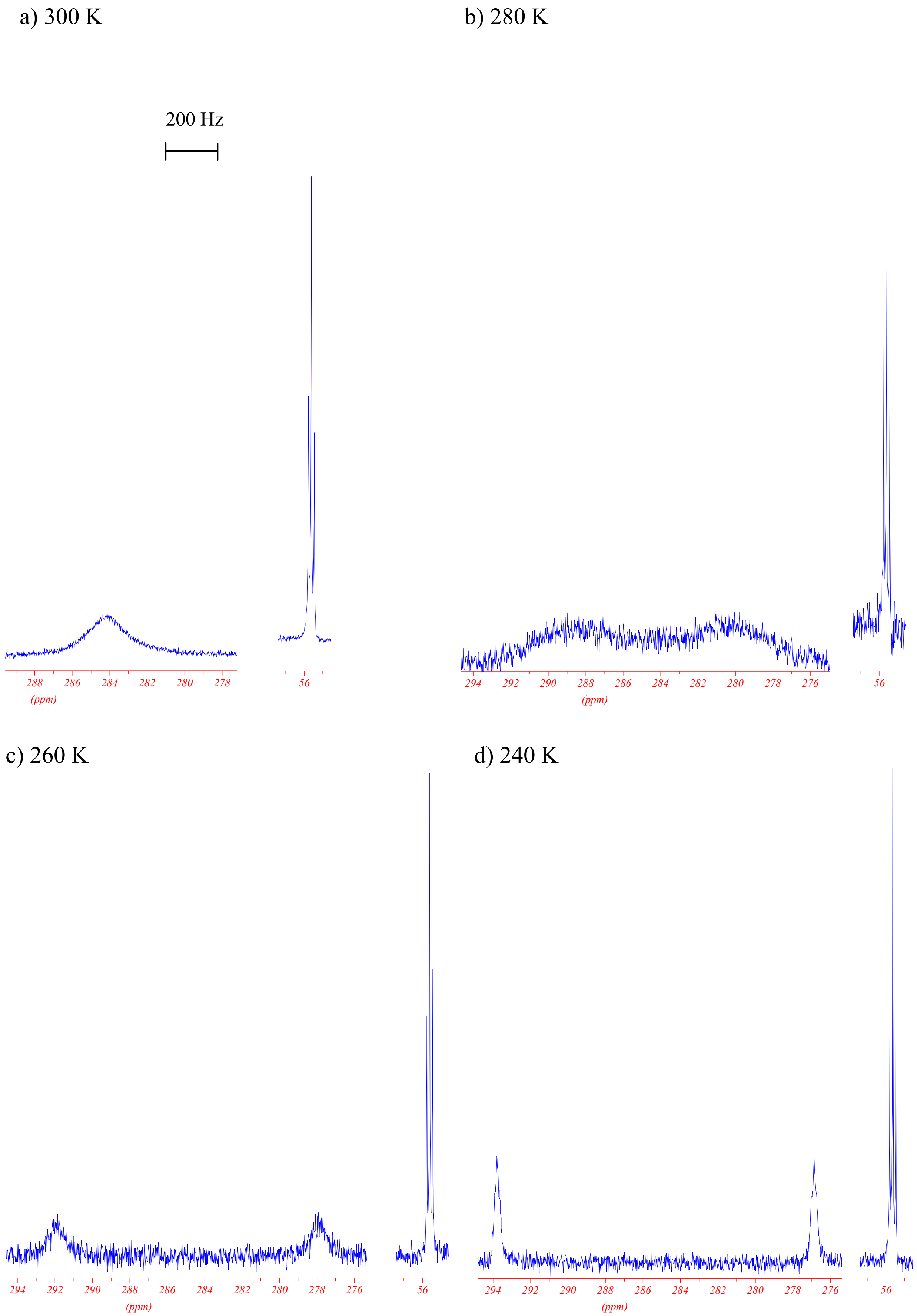
a) 300 K
200 Hz
288
286
284
282
280
278
(ppm)
56
b) 280 K
294
292
290
288
286
284
282
280
278
276
(ppm)
56
c) 260 K
294
292
290
288
286
284
282
280
278
276
(ppm)
56
d) 240 K
294
292
290
288
286
284
282
280
278
276
(ppm)
56

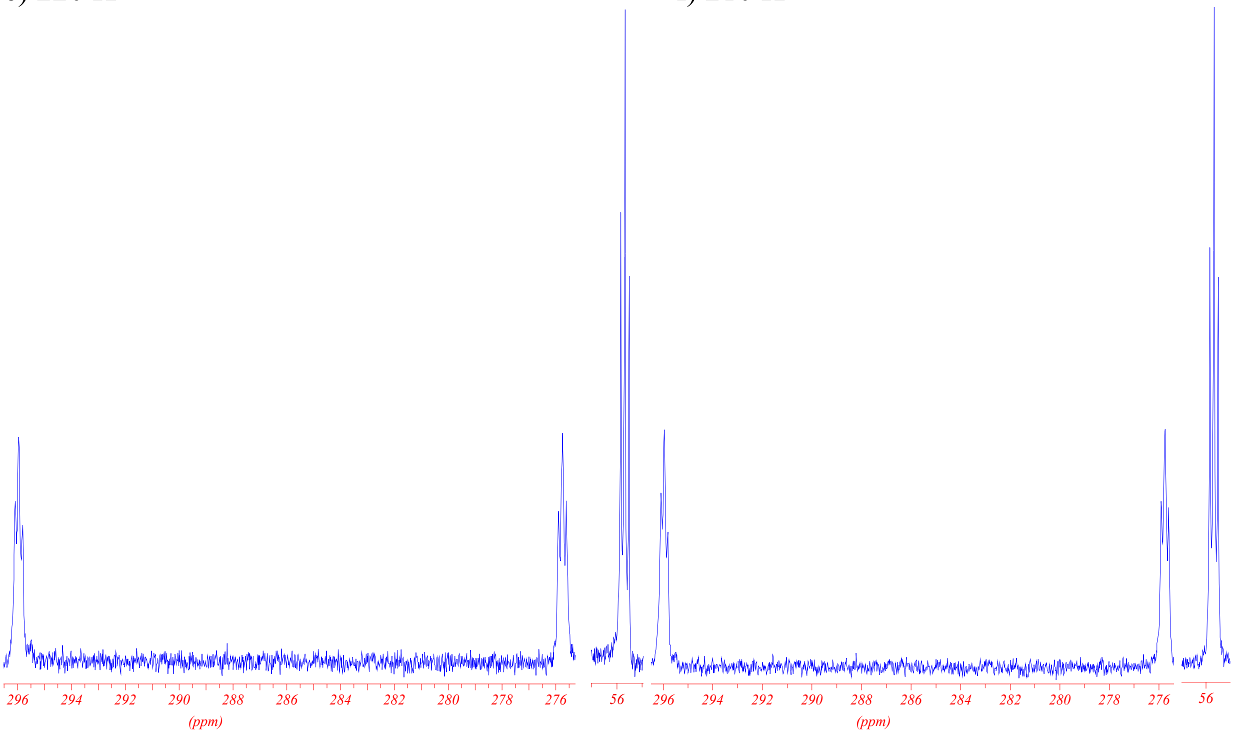

e) 220 K

f) 210 K

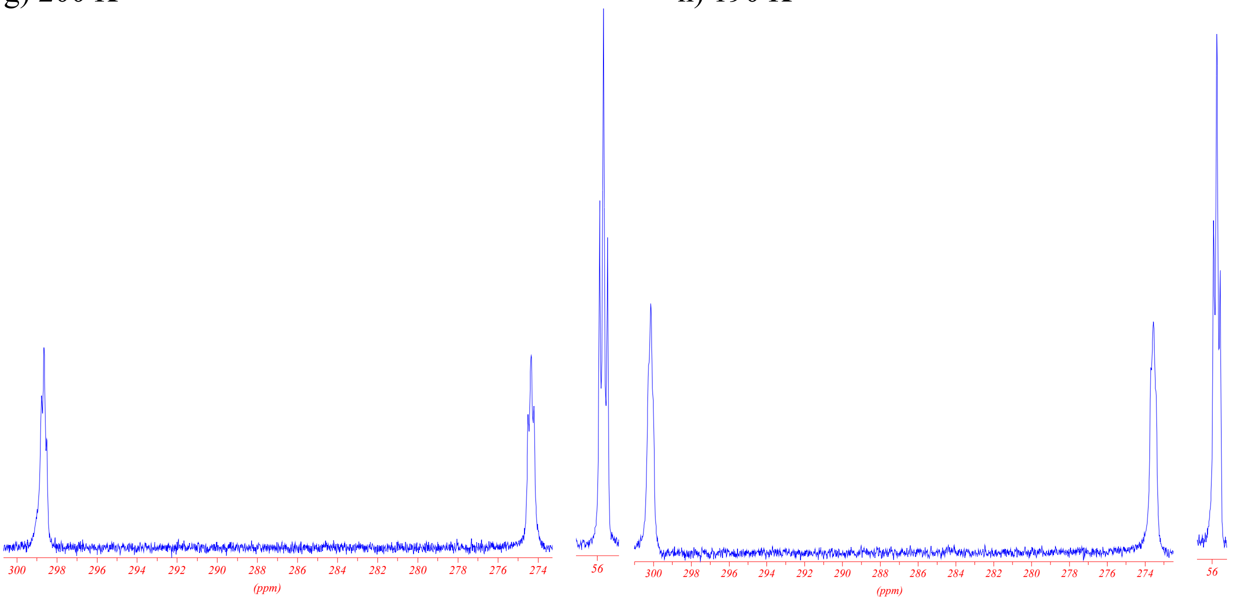

g) 200 K

h) 190 K

Figure 4.2.2. $^{31}P\{^1H\}$ NMR spectra of compound **3c** (^{i}Pr/Me) taken from a d_8-toluene solution at various temperatures between 300 K and 190 K.

Each spectrum shows the strongly temperature dependent low field signals of the phosphorus atoms P3 and P5 on the left and the high field signal of phosphorus atom P1 on the right.

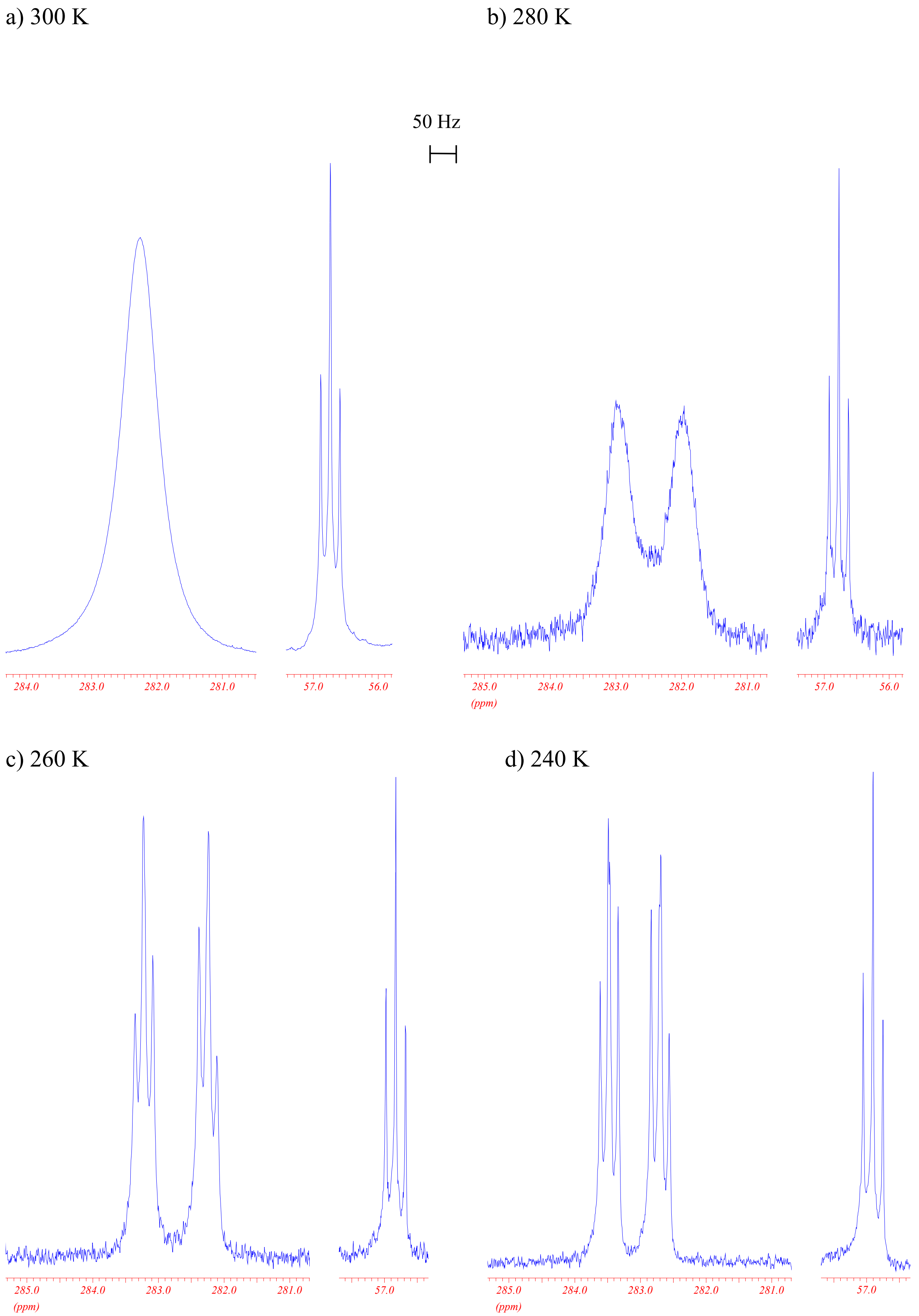
a) 300 K
b) 280 K
50 Hz
284.0
283.0
282.0
281.0
57.0
56.0
285.0
284.0
283.0
282.0
281.0
(ppm)
57.0
56.0
c) 260 K
d) 240 K
285.0
284.0
283.0
282.0
281.0
(ppm)
57.0
285.0
284.0
283.0
282.0
281.0
(ppm)
57.0

e) 220 K f) 210 K

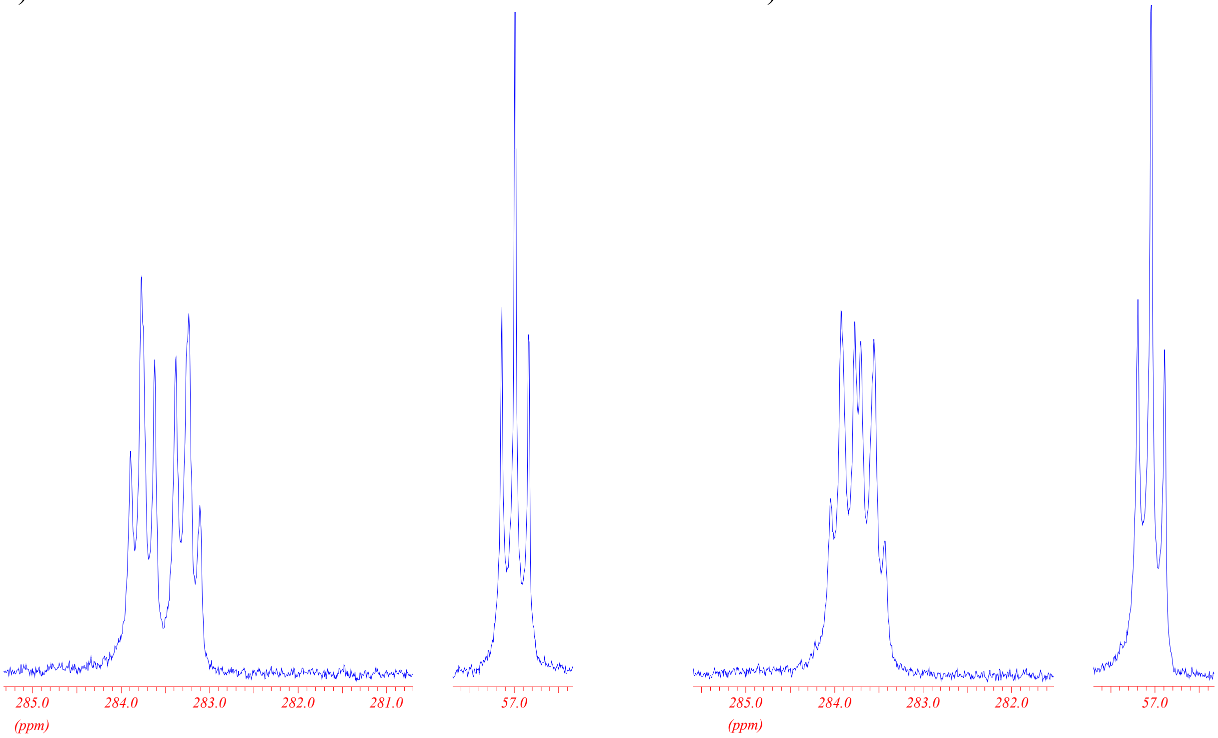

g) 200 K h) 190 K

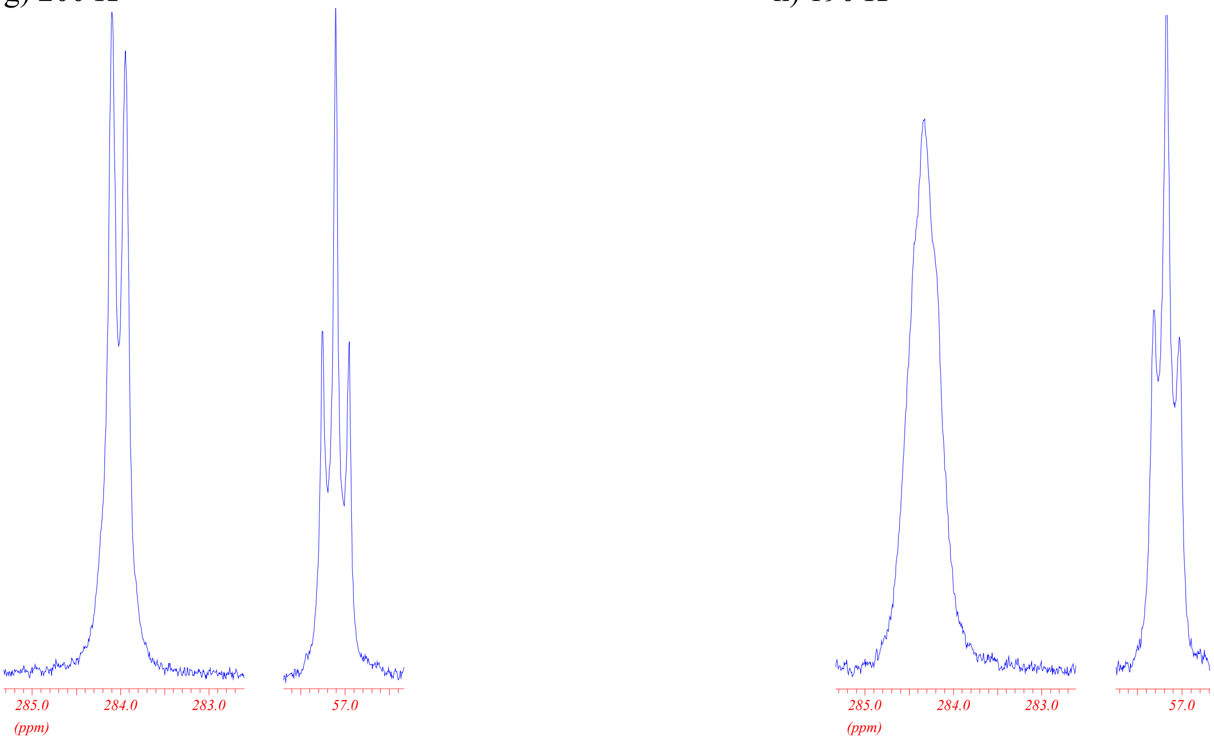

Figure 4.2.3. $^{31}P\{^1H\}$ NMR spectra of compound **3d** (Et/Me) taken from a d_8-toluene solution at various temperatures between 300 K and 190 K.

Each spectrum shows the strongly temperature dependent low field signals of the phosphorus atoms P3 and P5 on the left and the high field signal of phosphorus atom P1 on the right.

Owing to the rapid 1,3-migration of the chlorine atom, in the ambient temperature *$^{13}C\{^1H\}$ NMR spectra* of the compounds **3a** to **3d** several couplings of carbon atoms to the *a priori* chemically nonequivalent phosphorus atoms P3 and P5 become identical; hence, these two phosphorus atoms can be treated as a *pseudo*-A_2 system. As a consequence, for all compounds the bridging quaternary carbon atom C4 of the bicyclic framework and the quaternary carbon atom as well as the methyl carbon atoms of the adjacent *tert*-butyl substituent all reveal doublets of triplets (Tables 4.2.1. and 4.2.2.).

Table 4.2.2. Characteristic Ambient Temperature $^{13}C\{^1H\}$ NMR Parameters of the *tert*-Butyl Carbon Atoms in Several Dialkylamino-$1\lambda^5\sigma^4,3\lambda^3\sigma^3,5\lambda^3\sigma^2$-triphosphabicyclo[2.2.0]hexa-1,5-dienes.

Chemical shift δ (ppm); coupling constants J (Hz); *d_6*-benzene solution.

Compound	$\delta(\underline{C}(CH_3)_3)$ at C4	$\delta(C(\underline{C}H_3)_3)$ at C4	$\delta(\underline{C}(CH_3)_3)$ at C2 or C6	$\delta(C(\underline{C}H_3)_3)$ at C2 or C6
3a (Me, Me)	29.5 (dt) $^2J_{(C,P1)} = 9.7$ $^2J_{(C,P3/P5)} = 5.4$	33.2 (dt) $^3J_{(C,P1)} = 7.80$ $^3J_{(C,P3/P5)} = 4.75$	32.8 (dd) $^2J_{(C2,P1)} = 11.1$ $^2J_{(C,P3/P5)} = 6.3$	35.8 (dd) $^3J_{(C,P1)} = 5.5$ $^3J_{(C,P3/P5)} = 2.7$
3b (Et, Et)	29.4 (dt) $^2J_{(C,P1)} = 9.7$ $^2J_{(C,P3/P5)} = 5.7$	33.4 (dt) $^3J_{(C,P1)} = 7.7$ $^3J_{(C,P3/P5)} = 4.9$	33.1 (dd) $^2J_{(C,P1)} = 11.2$ $^2J_{(C,P3/P5)} = 6.3$	36.0 (dd) $^3J_{(C,P1)} = 5.7$ $^3J_{(C,P3/P5)} = 2.6$
3c (^{i}Pr, Me)	29.6 (dt) $^2J_{(C,P1)} = 9.7$ $^2J_{(C,P3/P5)} = 6.1$	33.4 (dt) $^3J_{(C,P1)} = 9.2$ $^3J_{(C,P3/P5)} = 7.6$	32.4 (dd) $^2J_{(C,P1)} = 11.1$ $^2J_{(C,P3/P5)} = 6.2$	36.1 (dd) $^3J_{(C,P1)} = 6.9$ $^3J_{(C,P3/P5)} = 2.8$
3d (Et, Me)	29.5 (dt) $^2J_{(C,P1)} = 9.7$ $^2J_{(C,P3/P5)} = 5.6$	33.2 (dt) $^3J_{(C,P1)} = 9.5$ $^3J_{(C,P3/P5)} = 7.9$	32.8 (dd) $^2J_{(C,P1)} = 11.1$ $^2J_{(C,P3/P5)} = 6.3$	36.0 (dd) $^3J_{(C,P1)} = 6.2$ $^3J_{(C,P3/P5)} = 2.5$

The two *sp^2*-hybridized carbon atoms in position 2 and 6 of the bicyclic framework chemically also equivalent give, however, rise to a complicated multiplet (Table 4.2.1.), whereas the quaternary carbon atoms as well as the methyl carbon atoms of both the adjacent *tert*-butyl substituents show doublets of doublets (Table 4.2.2.).

As required by theory [207-209] for the two carbon atoms C2 and C6, their ^{13}C nucleus present only once in the same molecule, and the nuclei of the phosphorus atoms P1, P3 and P5 form an AA`MX- or, alternatively, an ABMX spin system. Only on first sight, however, the X-part of such a spin system can reveal the relatively simple pattern of a doublet of doublets of doublets as observed at 138.5 ppm for the diethylamino compound and shown in Figure 4.2.4 [100]. This observation is in accordance with a report of *Binger et al.* [68] on the ^{13}C{^{1}H} NMR spectrum of 2,4,6-tri-*tert*-butyl-1,3,5-triphospha-dewar benzene. Analysis of the multiplets arising from the carbon atoms of the bicyclic framework resulted in a roughly first order pattern of a doublet of doublets of doublets (ddd) for the two outer *sp*^{2}-hybridized carbon atoms.

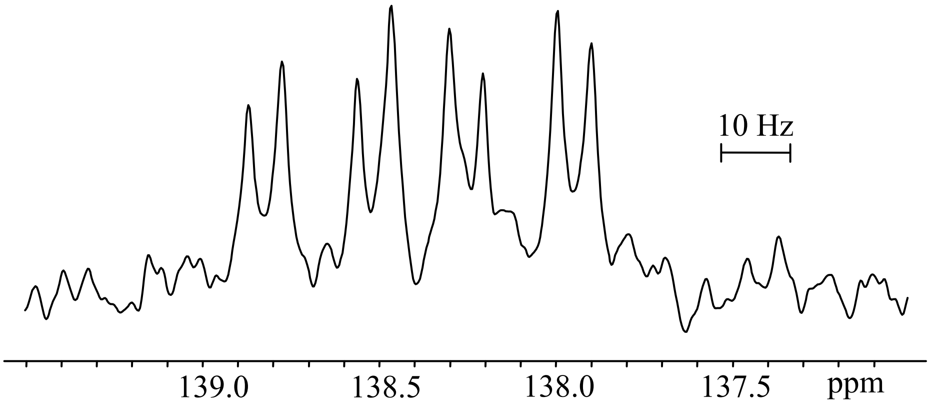

Figure 4.2.4. Ambient Temperature ^{13}C{^{1}H} NMR spectrum of the two *sp*^{2}-hybridized carbon atoms C2 and C6 in the bicyclic framework of the diethylamino compound.

The availability of two terms for the arrangement of four nuclei to be discussed here can be explained as follows: If the fact is neglected that only one of the two trivalent phosphorus atoms P3 and P5 is directly attached to a ^{13}C carbon atom, both ^{31}P nuclei have to be considered chemically equivalent but they are still magnetically non equivalent. With this restriction in mind the AA`MX spin system is realized, otherwise the term ABMX spin system would be more appropriate. Decoupling of the two phosphorus atoms P3 and P5 in a triple resonance experiment with a frequency equivalent to a chemical shift of about 280 ppm reveals the ^{13}C{^{1}H} NMR doublet of an MX spin system (Figure 4.2.5.) [100]; the coupling constant $J_{(C2,P1)}$ or $J_{(C6,P1)}$ of 30.9 Hz can be directly taken from the spectrum. These studies have been performed at ambient temperature first by *Ruf* [100] on the diethylamino compound.

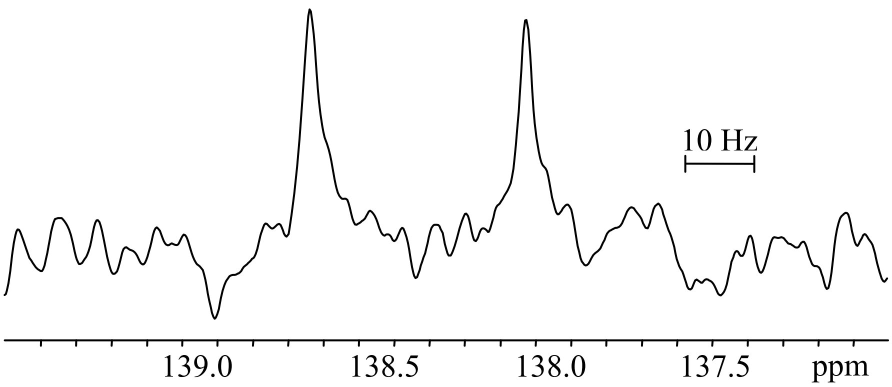

Figure 4.2.5. Triple resonance experiment at ambient temperature with decoupling the phosphorus atoms P3 and P5. The coupling observed is due only to phosphorus atom P1.

A subsequent irradiation of the sample with a frequency equivalent to a chemical shift of about 55 ppm to decouple phosphorus atom P1 (Figure 4.2.6) reveals the four lines multiplet of an AA`X or ABX spin system. Although the carbon atoms C2 and C6 couple differently to, for example, the phosphorus atom P3 the coupling constants $^1J_{(P,C)}$ with the adjacent carbon atom C2 and $^3J_{(P,C)}$ to the more distant atom C6 can be obtained separately neither by experiment nor by computer simulation; only the absolute value of the sum of the coupling constants $^1J_{(C2,P3)}$ and $^3J_{(C6,P3)}$) can be directly determined from the $^{13}C\{^1H\}$ NMR spectrum.

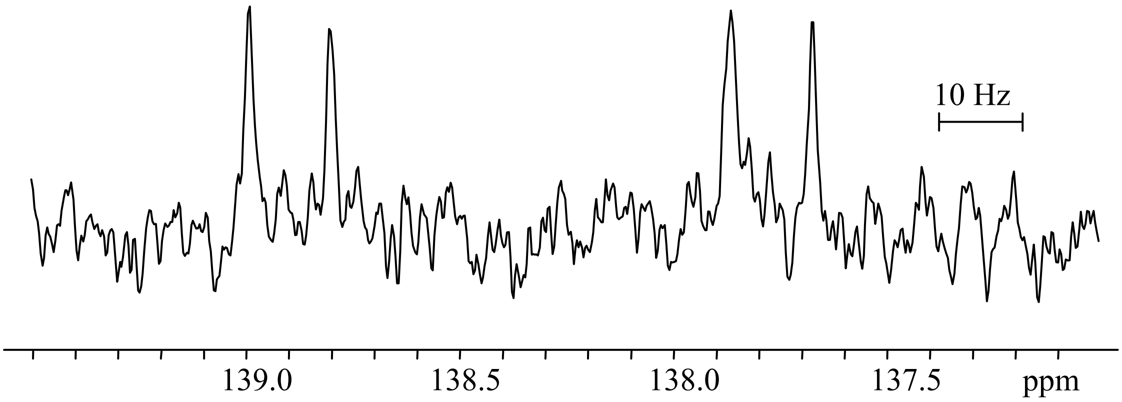

Figure 4.2.6. Triple resonance experiments at ambient temperature with decoupling the phosphorus atom P1. The four observable ^{13}C NMR resonances of the carbon atoms C2 and C6 represent the X-part of an AA`X spin or, alternatively, an ABX spin system.

The ABX or AA`X spin system discussed at some length in different NMR textbooks [207-209] exhibits six lines. As a function of the individual NMR parameters, however, frequently only four lines can be observed; the remaining lines are too weak and do not stand out against the background. Figure 4.2.7 shows the X-part of a computer-simulated spectrum consisting of the four most intense lines of an AA`X spin system [209, 210]. The absolute value of the sum of the corresponding coupling constants $|^1J_{(C2,P3)} + {}^3J_{(C2,P5)}|$ (or $|^1J_{(C6,P5)} + {}^3J_{(C6,P3)})|$) between the internal pair of lines can be directly taken from the spectrum.

The two lines outside are separated by the quantity $2(D_+ + D_-)$, the two parameters D_+ and D_- of which are defined as follows:

$$D_+ = 0.5\ \{0.25\ (J_{(AX)} - J_{(A`X)})^2 + (J_{(AA`)})^2\}^{0.5}$$

$$D_- = 0.5\ \{0.25\ (J_{(AX)} - J_{(A`X)})^2 + (J_{(AA`)})^2\}^{0.5}$$

Quite evidently, these equations cannot be solved owing to too large a number of variables in an AA`X spin system. For a complete analysis and the determination of the coupling constants $J_{(A,X)}$, $J_{(A`,X)}$ and $J_{(A,A`)}$ which here correspond to $J_{(C2,P3)}$ and $J_{(C2,P5)}$ or $J_{(C6,P5)}$ and $J_{(C6,P3)}$ as well as here $J_{(P3,P5)}$) the ^{13}C-NMR satellites of the ^{31}P{H} NMR spectrum are required in addition.

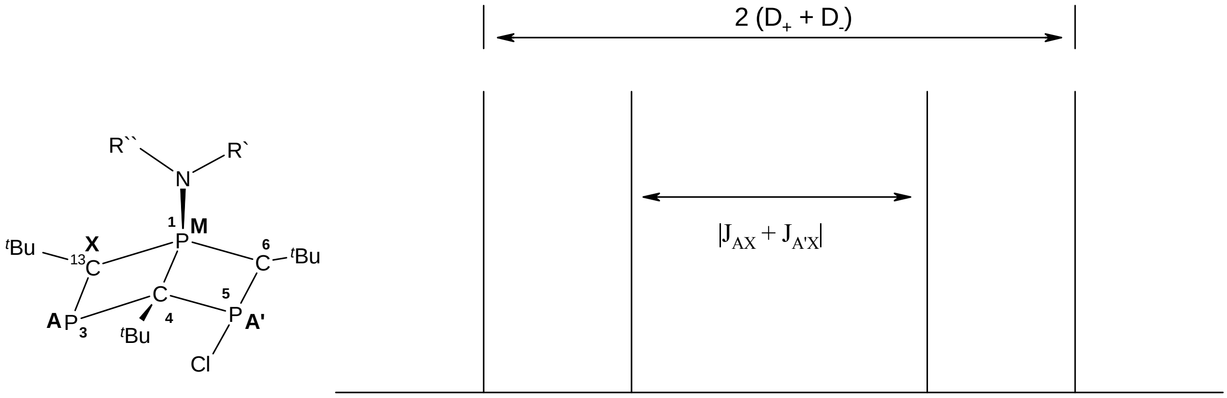

Figure 4.2.7. Analysis of the X-part of an AA`X spin system. The assigment of nuclei follows the formula shown on the left. The P–C multiple bonds are not shown for clarity; the chlorine atom fluctuates between the two phosphorus atoms PA and PA`.

The signal of the carbon atom C4 originates from a separate A_2MX spin system and A_2MX reveals a doublet of triplets at about 64.5 ppm. On irradiating the sample at, or close to, the resonance frequency of the phosphorus atoms P3 and P5 a doublet is observed with a coupling constant $J_{(P1,C4)}$ of about 57.2 Hz. Applying the resonance frequency of phosphorus atom P1, however, results in a triplet with a coupling constant $J_{(C4,P3)}$ or $J_{(C4,P5)}$ of about 32.0 Hz.

In contrast to the low temperature ^{31}P{^{1}H} NMR experiments, up to now the registration of analogous ^{13}C{^{1}H} NMR spectra was unfortunately not yet possible for reasons of a moderate solubility of the compounds and a limited sensitivity of the CH-free carbon atoms involved. Hence, not even the effect of the two phosphorus atoms P3 and P5 becoming chemically non equivalent at low temperature in the methylisopropylamino (**3c**) and the ethylmethylamino derivative (**3d**) (Figures 4.2.2 and 4.2.3, respectively), on the ^{13}C{^{1}H} NMR spectra of these compounds could be elucidated. Furthermore, fastidions but rewarding triple resonance experiments with subsequent decoupling of the different phosphorus atoms which are expected to give a deeper insight into the 1,3-migration of the chlorine atom (Scheme 4.2.2) have also to be performed.

The ^{1}*H NMR spectra* of all compounds reveal two strong signals for the *tert*-butyl substituents in an intensity ratio of 1:2 and a range between 1.04 ppm and 1.37 ppm (see Experimental Part). The dimethylamino substituent of compound **3a** gives rise to a signal at 2.35 ppm which is split into a doublet with a coupling constant $^{2}J_{(H,P1)}$ of 9.4 Hz. The pertinent $^{13}C\{^{1}H\}$ NMR spectrum shows also a doublet with a coupling constant $^{2}J_{(C,P1)}$ of 3.2 Hz at 39.2 ppm.

The methyl and methylene ^{1}H NMR signals of the diethyl amino group of compound **3b** are observed as a first order triplet with a coupling constant $^{3}J_{(H,H)}$ of 7.2 Hz and a broad unresolved multiplet at 0.73 and 2.96 ppm, respectively. In the $^{13}C\{^{1}H\}$ NMR spectrum the methyl and methylene carbon atoms give rise to two doublets at 13.1 ppm and 40.60 ppm, exhibiting a $^{3}J_{(C,P1)}$ constant of 3.1 Hz in the high field and a $^{2}J_{(C,P1)}$ constant of 3.4 Hz in the low field region, respectively.

In the ^{1}H NMR spectrum of compound **3c** the two chemically equivalent methyl groups of the isopropyl substituents at nitrogen are observed at 0.81 ppm as a doublet with a $^{3}J_{(H,H)}$ coupling constant of 6.66 Hz. Furthermore, the neighbouring CH group at 3.93 ppm appears as a doublet of septets with a coupling constant $^{3}J_{(H,P1)}$ of 9.87 Hz and a $^{3}J_{(H,H)}$ value of 6.65 Hz. The methyl hydrogen atoms of the amino group give rise to a signal at 2.28 ppm which is split into a doublet with a coupling constant $^{3}J_{(H,P1)}$ of 9.86 Hz. In the pertinent $^{13}C\{^{1}H\}$ NMR spectrum the two methyl carbon atoms of the isopropyl substituent reveal a doublet at 20.0 ppm with a $^{3}J_{(C,P1)}$ coupling constant of 2.0 Hz. The adjacent methylidyne carbon atom gives rise to a doublet at 48.7 ppm with a $^{2}J_{(C,P1)}$ coupling constant of 2.0 Hz. The methyl carbon atom of amino group reveals a doublet at 28.8 ppm arising from a coupling with phosphorus atom P1 ($^{2}J_{(C,P1)} = 4.6$ Hz).

In the ^{1}H NMR spectrum of compound **3d** the signal of the methyl group at nitrogen at 2.27 ppm is split into a doublet with a coupling constant $^{3}J_{(H,P1)}$ of 10.32 Hz; the methyl and methylene signals of the ethyl at nitrogen group are observed at 0.71 and 3.22 ppm, respectively. They methyl signal is split into a triplet with a $^{3}J_{(H,H)}$ coupling constant of 7.11 Hz, whereas the methylene signal remains broad and unresolved. In the $^{13}C\{^{1}H\}$ NMR spectrum the methyl carbon atom at nitrogen reveals a doublet at 35.6 ppm arising from a coupling with phosphorus atom P1 ($^{2}J_{(C,P1)} = 3.1$ Hz). The methyl and methylene carbon atoms of the ethyl group give rise to two doublets at 13.1 ppm and 45.4 ppm, respectively, exhibiting a $^{3}J_{(C,P1)}$ value of 5.2 Hz in the high field and a $^{2}J_{(C,P1)}$ value of 2.5 Hz in the low field region.

4.2.3. Discussion of the Molecular Structures of 3a, 3b, 3c, and 3d

4.2.3.1. Crystal Data, Measuring Technique and Structure Analyses

Relatively large colorless cuboids suitable for X-ray structure analyses could be obtained when for both the compounds **3a** and **3b** the initially isolated viscous red oil was kept for two to three months at –13 °C. Similarly shaped crystals of compounds **3c** and **3d** precipitated within four weeks at 7 °C from a benzene and within five weeks at –60 °C from a toluene solution, respectively. Data for structure determinations of **3a**, **3b** and **3d** were collected on a four-circle diffractometer P21 (Syntex, Cupertino, USA), whereas for **3c** a P4 diffractometer (Siemens Analytical X-ray Instruments Inc., Madison/Wisconsin, USA) was available; graphite monochromatized MoK$_\alpha$ radiation (λ = 71.073 pm) was used in all experiments.

Lattice parameters were calculated from the exact positions of a selected number of reflections (Table 4.1) and refined thereafter. The determination of the monoclinic space group $P2_1/c$ (**3a**) or $P2_1/n$ (**3c** and **3d**) is based on unit cell dimensions and systematic absences (Table 4.3), for **3b** space group $P\bar{1}$ was chosen over $P1$ mainly on grounds of E-value statistics and successful structure refinement. The asymmetric unit of compound **3b** contains the two crystallographically independent molecules **3b-I** and **3b-II**. Whereas molecule **3b-I** exhibits split positions in a ratio of 0.59 : 0.41 merely for the methyl groups of the *tert*-butyl substituent bound to carbon atom C6 (Fig. 4.10), the second molecule **3b-II** is completely disordered and two models **A** and **B** in a ratio as already given above (Fig. 4.11) have to be introduced to describe the rather complex situation. Furthermore these letters are also applied to distinguish between equivalent atoms. In the course of the structure determination of molecule **3b-II**, however, an adoption of bond lengths and angles from molecule **3b-I** turned out to be necessary and the subsequent refinement had to be performed with restraints. As a consequence the discussion of bond parameters should mostly be confined on molecule **3b-I**.

The crystal structures were solved with statistical methods employing the software package SHELXTL Version 5.10 [118-120]. This package also includes the program XP used for the analyses of the molecular geometry and the preparation of drawings. Due to relatively low calculated absorption coefficients (Table 4.3) and the cuboid shape of the crystals, absorption corrections were considered to be not necessary. After all chlorine, phosphorus, carbon and nitrogen atoms had been located step by step and their positions as well as their isotropic replacement parameters had been refined by full-matrix least-squares calculations, the structure determinations were continued with individual anisotropic U_{ij}-values. At the end the atomic coordinates of hydrogen atoms could either be taken from a different Fourier map and refined with their isotropic replacement parameters (**3a** and **3c**) or were calculated on the basis of an idealized geometry (**3b** and **3d**) which means a C–H distances of 96 pm and 97 pm for methyl and methylene groups, respectively, tetrahedral angles and a staggered arrangement of the bonds at carbon. Furthermore the riding model applied ensures that a change in the carbon position is automatically transferred to the adjacent hydrogen atoms. The individual isotropic U-values of these hydrogen atoms were adopted from the pertinent carbon atom and increased by factors of 1.5 and 1.2 for the methyl and methylene groups, respectively. Finally, the parameters of all heavier atoms were subjected to a last least-squares refinement to take into account the incorporation of hydrogen atoms.

Crystallographic parameters and details of data collection have been summarized in Table 4.3, bond lengths and angles as well as characteristic torsion angles in Table 4.4, final atomic coordinates and equivalent isotropic as well as anisotropic displacement parameters in Table 9.4.1 of the Appendix.

Table 4.3. Crystal Data and Details of Structure Refinement for the 1-Dialkylamino-1$\lambda^5\sigma^4$,3$\lambda^3\sigma^3$,5$\lambda^3\sigma^2$-triphosphabicyclo[2.2.0]hexa-1,5-dienes **3a** to **3d**

Substituents at P1; Compound	Me_2N **3a**	Et_2N **3b**	Me^{i}PrN **3c**	MeEtN **3d**
Empirical formula	$C_{17}H_{33}ClNP_3$	$C_{19}H_{37}ClNP_3$	$C_{19}H_{37}ClNP_3$	$C_{18}H_{35}ClNP_3$
Formular weight	379.80	407.86	407.86	393.83
Decomposition point (°C)	133.0	143.7	151.5	137.8
Diffractometer	$P2_1$	$P2_1$	P4	$P2_1$
Wavelength (pm)	71.073	71.073	71.073	71.073
Temperature (°C) of measurement	–100 ± 3	–100 ± 3	–100 ± 3	–100 ± 3
Shape and crystal size (mm)	deep red cuboids; 0.3 x 0.6 x 0.3	deep red cuboids; 0.3 x 0.5 x 0.3	deep red cuboids; 0.4 x 0.6 x 0.4	deep red cuboids; 0.3 x 0.55 x 0.3
Crystal system	monoclinic	triclinic	monoclinic	monoclinic
Space Group [117]; Systematic Absences	$P2_1/c$ (No.14); h0ℓ: ℓ = 2n + 1; 0k0: k = 2n + 1	$P\bar{1}$ (No.2)	$P2_1/n$ (No.14); h0ℓ: h + ℓ = 2n +1; 0k0: k = 2n + 1	$P2_1/n$ (No.14); h0ℓ: h + ℓ = 2n +1; 0k0: k = 2n + 1
Det. of cell dim.: [a)] sel. refl.; 2θ range (°)	25; 20.17→29.97	35; 15.24→24.95	45; 10.40→24.96	37; 10.38→25.21
Unit cell dim.: a(pm)	1140.2(2)	968.9(8)	990.3(2)	977.6(2)
b(pm)	890.7(2)	1527.0(1)	1636.2(2)	1604.2(3)
c(pm)	2104.3(4)	1688.0(1)	1410.8(2)	1429.2(3)
α(°)		104.28(5)		
β(°)	97.75(3)	100.17(6)	91.36(2)	90.02(3)
γ(°)		94.94(6)		
Volume (m^3)	2117.6(7) • 10^{-30}	2360.0(3) • 10^{-30}	2285.3(6) • 10^{-30}	2241.3(8) • 10^{-30}
Z [b)]	4	4	4	4
Calculated density (kg m^{-3})	1.191 • 10^3	1.176 • 10^3	1.185 • 10^3	1.167 • 10^3
Calculated absorption coefficient μ (m^{-1})[c)]	0.405 • 10^3	0.369 • 10^3	0.380 • 10^3	0.385 • 10^3
Absorption correction	none	none	none	none
F(000)	816	880	880	848
θ-Range for data collection (°)	1.80 to 26.02	1.61 to 27.03	1.91 to 27.50	1.91 to 26.00

Limiting indices	$0 \le h \le 14$; $0 \le k \le 10$; $-25 \le l \le 25$	$-1 \le h \le 10$; $-19 \le k \le 19$; $-21 \le l \le 21$	$-9 \le h \le 12$; $-7 \le k \le 21$; $-18 \le l \le 18$	$-12 \le h \le 0$; $-19 \le k \le 0$; $-17 \le l \le 17$
Scan mode$^{d)}$	Wyckoff-scan	Wyckoff-scan	ω- scan	Wyckoff-scan
Scan width (°); velocity (deg min^{-1})	1.6 ; 4.0 to 29.3	1.4; 4.0 to 29.3	1.6; 3.0 to 55.0	2.4; 4.0 to 29.3
Reflections collected	4350	10760	5511	4630
Unique reflections (m)	4138	9488	5217	4370
Reflections observed with [$I > 2\sigma(I)$] $^{e)}$	2759	6251	3757	2691
Parameters refined (n)	319	712	365	219
Restraints	0	76$^{f)}$	0	0
Space filling $^{g)}$	72%	71%	73%	72%
Goodness-of-fit (GOF)$^{h)}$	1.061	0.990	1.017	1.275
Isotropic R-indices $^{h)}$:				
R1/wR2 using all data	0.2005/0.3871	0.302/0.486	0.1542/0.3323	0.2604/0.4608
R1/wR2 with [$I>2\sigma(I)$]	0.1531/0.3645	0.183/0.405	0.1180 /0.3142	0.1909/0.4262
Anisotropic R-indices $^{h)}$:				
R1/wR2 using all data	0.1419/0.2755	0.137/0.221	0.0993/0.2172	0.1627/0.2751
R1/wR2 with [$I>2\sigma(I)$]	0.0995/0.2536	0.0755/0.184	0.0687/0.2018	0.1008/0.2410
Final R-indices $^{h)}$:				
R1/wR2 using all data	0.1235/0.2351	0.0989/0.1591	0.0752/0.1162	0.1482/0.2343
R1/wR2 with [$I>2\sigma(I)$]	0.0816/0.1986	0.0598/0.1331	0.0445/0.1021	0.0859/0.1960
Indices f and g of weighting scheme w^{-1} $^{i)}$	f = 0.128; g = 2.2982	f = 0.055; g = 1.8707	f = 0.051; g = 0.9339	f = 0.100; g = 0.0000
Largest diff. peak; deepest hole (10^{-30} em^{-3})	0.820; –0.825	0.268; –0.330	0.332; –0.411	0.769; –0.552

a) Determination of cell dimensions: number and 2θ range of selected reflections used; b) number of molecules in the unit cell; c) linear absorption coefficient $\mu = \Sigma\sigma_i / V_c$ [121]; d) registration of the background at the beginning and at the end of the measurement with an overall duration equal to the time of measurement; e) reflections with strongly negative intensity were not considered for refinement; f) see discussion; g) calculated from the Kitaigorodskii formula [122]; bond lengths taken from Table 4.5; C–H 108, van der Waals radii: P 190, C 180, Cl 180, N 157, H 117 pm [122, 124]; h) for a definition of different quality factors R see Appendix, page 282;
i) weighting scheme $w^{-1} = [\sigma^2(F_o)^2 + (f\,P)^2 + (g\,P)]$ with $P = 1/3(F_o^2 + 2F_c^2)$.

Table 4.4. Characteristic Bond Lengths (pm) and Angles (°) as well as Torsion Angles for the Structures of 1-Dialkylamino-$1\lambda^5\sigma^4,3\lambda^3\sigma^3,5\lambda^3\sigma^2$-triphosphabicyclo[2.2.0]hexa-1,5-dienes **3a** to **3d**.

a) Bond lengths	Me$_2$N **3a**	Et$_2$N **3b**a)			Me^{i}PrN **3c**	MeEtN **3d**	Average
		I	**IIA**	**IIB**			
P1–C2	172.9(5)	172.8(4)	171.8(7)	171.2(7)	172.2(2)	175.6(5)	173.0
P1–C4	181.6(5)	181.1(4)	182.1(7)	182.8(7)	180.5(2)	181.6(5)	181.6
P1–C6	179.9(5)	178.2(4)	179.2(6)	178.4(6)	180.3(2)	176.3(5)	178.7
P3–C2	172.6(6)	172.7(4)	172.9(7)	172.9(8)	172.8(2)	172.2(5)	172.7
P3–C4	189.8(5)	188.9(4)	189.4(7)	189.8(8)	188.9(2)	186.9(6)	188.8
P5–C4	187.9(5)	186.6(4)	186.9(7)	187.0(8)	186.9(2)	188.9(5)	187.5
P5–C6	169.7(5)	170.0(4)	169.4(5)	169.1(6)	169.6(2)	171.2(5)	170.0
P3–Cl1	237.6(2)	245.0(3)	241.7(5)	239.7(5)	237.7(1)	266.6(3)	245.5
P5...Cl1	301.6(2)	287.7(3)	296.4(5)	296.5(6)	298.8(1)	265.0(3)	289.9
P1–N1	164.0(4)	162.7(3)	163.0(5)	164.3(5)	163.1(2)	164.8(4)	163.7
N1–C1*n*b)	147.1	148.0	147.3	148.1	147.5	145.9	147.3
C1*n*–Cc)		152.5	152.4	151.8	151.6	157.0(9)	153.3
C2–C21	153.4(7)	152.2(5)	151.8(8)	152.1(9)	152.3(3)	152.4(7)	152.4
C4–C41	153.4(6)	154.9(5)	154.8(8)	155.1(9)	154.2(3)	152.1(7)	154.1
C6–C61	152.5(7)	152.6(5)	151.6(7)	152.1(8)	152.4(3)	153.6(7)	152.5
C–CH$_3$d)	152.2	152.2	152.0	152.2	152.1	152.5	152.2

b) Bond angles	Me$_2$N **3a**	Et$_2$N **3b**a)			Me^{i}PrN **3c**	MeEtN **3d**	Average
		I	**IIA**	**IIB**			
N1–P1–C2	115.2(2)	115.7(2)	116.0(4)	116.8(5)	115.2(1)	115.4(2)	115.7
N1–P1–C4	126.2(2)	126.4(2)	125.0(5)	123.1(6)	125.7(1)	126.7(2)	125.5
N1–P1–C6	113.1(2)	113.1(2)	113.1(3)	113.2(4)	113.6(1)	112.3(3)	113.1
C2–P1–C4	89.5(2)	89.4(2)	89.9(3)	89.4(3)	89.3(1)	88.0(2)	89.3
C2–P1–C6	121.7(2)	120.5(2)	122.1(4)	122.3(5)	121.4(1)	122.0(3)	121.7
C4–P1–C6	87.1(2)	87.8(2)	85.9(3)	86.4(3)	87.6(1)	88.8(2)	87.3
P1–C2–P3e)	95.8(2)	95.7(2)	95.7(3)	96.4(4)	96.0(1)	95.6(2)	95.9
P1–C2–C21f)	135.2(4)	135.7(3)	135.6(6)	134.6(7)	136.5(2)	135.3(4)	135.5
P3–C2–C21	128.1(4)	127.0(3)	126.4(5)	127.8(6)	126.9(2)	126.5(4)	127.1
C2–P3–C4	87.0(2)	86.9(2)	87.2(3)	86.6(3)	86.5(1)	87.4(2)	86.9
C2–P3–Cl1	110.1(2)	109.8(2)	108.0(4)	112.2(5)	110.5(1)	107.0(2)	109.6
C4–P3–Cl1	95.5(2)	91.8(2)	93.6(3)	93.6(3)	95.2(8)	85.5(2)	92.3
P3–Cl1…P5	70.6(6)	71.7(8)	71.3(2)	71.2(2)	70.6(3)	72.5(6)	71.3
C4–P5…Cl1	77.2(2)	79.8(1)	78.1(3)	77.7(3)	77.6(7)	85.6(2)	79.6
C6–P5…Cl1	104.1(2)	104.5(2)	102.7(2)	104.7(3)	104.9(1)	107.1(2)	104.7
P1–C4–P3	87.3(2)	87.6(2)	87.0(3)	87.0(3)	87.9(1)	88.6(2)	87.6
P1–C4–P5	88.9(2)	88.6(2)	89.9(3)	89.0(3)	88.8(1)	87.7(2)	88.8
P1–C4–C41f)	128.8(4)	130.0(3)	128.1(5)	129.1(6)	130.5(2)	129.1(4)	129.3
P3–C4–P5	113.6(2)	113.4(2)	114.6(4)	113.8(4)	113.5(1)	113.6(3)	113.7
P3–C4–C41f)	116.0(3)	115.3(3)	116.1(5)	116.5(5)	114.9(2)	115.9(4)	115.8
P5–C4–C41f)	117.0(3)	117.1(2)	116.2(5)	116.3(5)	116.7(2)	116.9(4)	116.7
C4–P5–C6	88.2(2)	88.5(2)	87.2(3)	87.8(3)	88.8(1)	88.0(2)	88.1
P1–C6–P5e)	95.5(2)	95.0(2)	96.8(3)	96.5(3)	94.6(1)	95.3(3)	95.6
P1–C6–C61f)	134.0(4)	136.4(3)	136.7(5)	135.4(6)	137.5(2)	134.5(4)	135.8
P5–C6–C61f)	127.8(4)	127.0(3)	125.0(4)	125.5(5)	125.2(2)	129.0(4)	126.6
P1–N1–C11e)	122.1(4)	121.9(2)	119.8(5)	120.6(6)	120.1(2)	120.5(4)	120.8
P1–N1–C12	123.9(4)	121.2(3)	123.2(5)	124.0(6)	124.0(2)	122.2(4)	123.1
C11–N1–C12g)	112.3(5)	116.0(3)	116.7(5)	115.0(5)	115.9(2)	114.1(5)	115.0

c) Torsion angles[h)	Me_2N	Et_2N			Me^iPrN	MeEtN
	3a	**3b**[a)			**3c**	**3d**
		I	**IIA**	**IIB**		
P1–C2–P3–Cll	90.2(2)	86.2(2)	88.8(4)	87.0(5)	89.6(1)	79.6(2)
P1–C4–P3–Cl1	–105.6(2)	–105.3(1)	–104.2(3)	–106.8(3)	–105.9(7)	–102.6(2)
P1–C6–P5…Cl1	–72.3(2)	–76.2(2)	–73.1(3)	–73.2(3)	–73.1(1)	–80.6(2)
P1–C4–P5…Cl1	100.9(2)	102.2(1)	99.6(3)	102.1(3)	101.8(8)	103.4(2)
P1–C2–C21–C213	–109.6(6)	–100.1(7)	–90.9(7)	–120.7(9)	–109.4(4)	–76.1(7)
P1–C4–C41–C413	–177.7(4)	176.3(3)	176.5(6)	177.3(7)	179.5(2)	178.9(4)
P1–C6–C61–C612	–66.2(9)	–116.1(7)	–135.6(9)	–164.8(10)	–92.9(3)	–129.0(7)
P3–C4–P5–C6	–90.6(3)	–89.6(2)	–90.6(4)	–89.8(4)	–90.9(1)	–91.5(3)
P3–C2–P1–C6	–81.5(3)	–82.2(3)	–80.9(5)	–79.6(6)	–81.9(1)	–82.3(3)
P3–C4–P1–C6	117.4(2)	116.1(2)	118.5(3)	117.2(4)	117.1(1)	117.5(2)
P3–C2–P1–N1	135.3(2)	135.7(2)	133.8(5)	133.1(7)	134.5(1)	135.2(2)
P5–C4–P3–C2	92.0(3)	91.8(2)	92.2(5)	92.9(5)	92.2(1)	91.5(3)
P5–C6–P1–C2	83.5(3)	85.0(2)	83.0(5)	83.4(5)	83.8(2)	82.6(3)
P5–C4–P1–C2	–118.0(2)	–117.9(2)	–118.4(4)	–119.2(5)	–117.9(1)	–118.2(2)
C4–P1–N1–C11	82.7(5)	82.0(4)	86.3(9)	88.8(10)	77.0(2)	81.4(5)

a) Two symmetry-independent molecules in the unit cell, values are specified for the largely ordered molecule **I** as well as the completely disordered species **II** described by its molecular models **A** and **B** ; b) n =1 or 2, depending on the numbering scheme used; mean values for each diorganylamino group, individual values vary between 145.3(7) and 148.6(3); c) n= 1 or 2, depending on the numbering scheme used; mean C–C distances of the diorganylamino groups, individual values vary between 151.2(4) and 157(1); d) mean $C–CH_3$ distances of the *tert*-butyl groups, individual values vary between 147.5(11) and 156.3(8); e) mean values for the sums of bond angles at C2 (358.5), C6 (358.0), N1 (358.8); individual values vary between 357.4 and 359.4 for C2, between 357.3 and 358.8 for C6 and between 356.8 and 360.0 for N1; f) mean C–C–C angle of the *tert*-butyl groups 109.5, individual values vary between 106.1(7) and 113.0(5); g) mean N–C–C angle of the diorganylamino groups 112.5, individual values vary between 108.1(1) and 115(1), C–C–C angle of the *iso*-propyl substituent 111.0(2). h) The torsion angle A–B–C–D is defined as positive if, when viewed along the B–C bond, atom A must be rotated clockwise to eclipse atom D [125, 126].

4.3.2.3. Discussion of Bond Lengths and Angles

Preliminary survey of the structures 3a – 3d. Figs. 4.9 – 4.13 show stereoscopic views of molecular models determined for four analogous 1-diorganylamino-$1\lambda^5\sigma^4,3\lambda^3\sigma^3,5\lambda^3\sigma^2$-triphosphabicyclo[2.2.0]hexa-1,5-dienes **3a** – **3d** by X-ray structure analyses. Additionally, in Figs. 4.10 and 4.11 the different conformations of the partially disordered molecule **3b-I** and the totally disordered species **3b-II** are depicted.

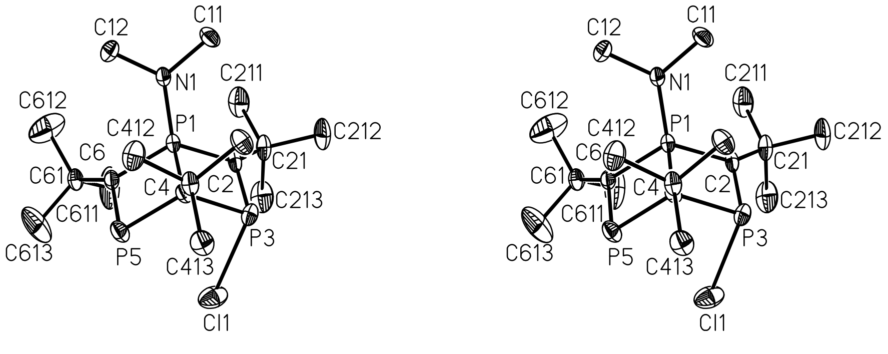

Figure 4.9. Molecule of compound **3a** in stereoscopic view. Thermal ellipsoids are at 30% probability; hydrogen atoms have been omitted for clarity. Absent numbering follows logically from that given.

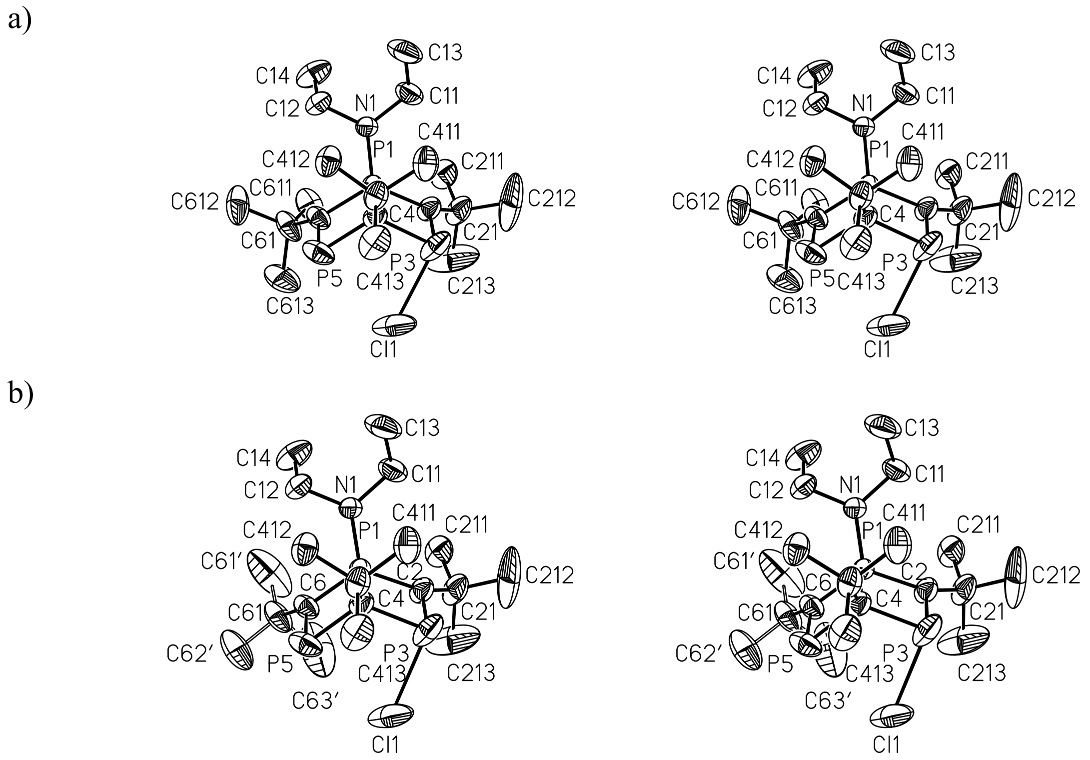

Figure 4.10. Stereoscopic view of molecule **3b-I** in two conformations a) and b) of the *tert*-butyl substituent at carbon atom C6 in a ratio of 0.41 : 0.59. Thermal ellipsoids are at 30% probability; hydrogen atoms have been omitted for clarity. Absent numbering follows logically from that given.

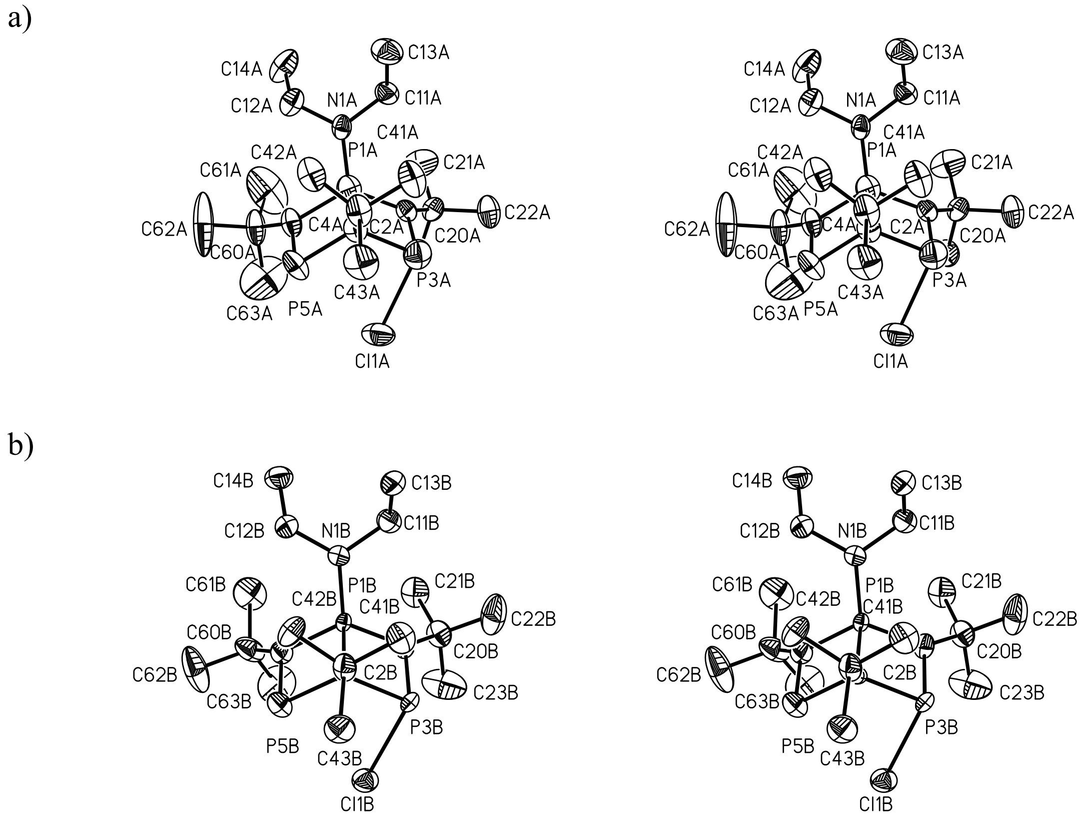

Figure 4.11. Stereoscopic view of the completely disordered species **3b-II** described by its molecular models **A** (a) and **B** (b). Thermal ellipsoids are at 30% probability; hydrogen atoms have been omitted for clarity. Absent numbering follows logically from that given.

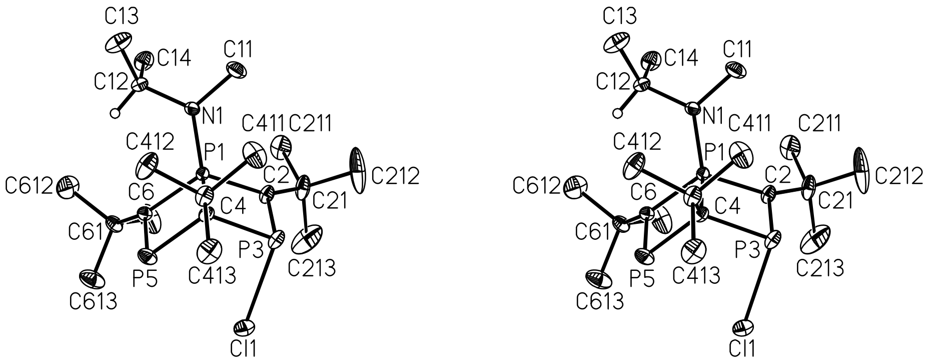

Figure 4.12. Molecule of compound **3c** in stereoscopic view. Thermal ellipsoids are at 30% probability; only the CH-hydrogen atom of the isopropyl group is shown. Absent numbering follows logically from that given.

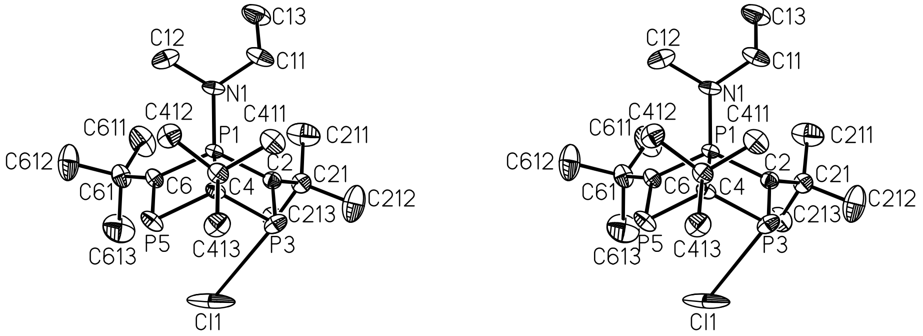

Figure 4.13. Molecule of compound **3d** in stereoscopic view. Thermal ellipsoids are at 30% probability; all hydrogen atoms have been omitted for clarity. Absent numbering follows logically from that given.

As to be concluded already from the systematic name, the bicyclic framework of these triphospha-dewarbenzenes comprises three different types of phosphorus atoms. The pentavalent, but four coordinate atom P1 is essential part of the characteristic P–C unit of an alkylidenetriorganylphosphorane. For the sake of simplification the notation P=C is used very often in the formulas of those compounds; this possibility will also be applied now and then in the following chapters of the thesis. Since, however, the bonding situation is much better described with the mesomeric form of an ylide than an ylene, atom P1 has to be considered the centre of a phosphonium cation, the positive charge of which *might* perhaps to some extent be transferred to the neighbouring dialkylamino group (Scheme 4.1). The trivalent atom P3 is linked on one side to the carbanion C2 of the $P^{\oplus}$–$C^{\ominus}$ ylide and on the other to a chlorine atom. This special sequence of atoms gives rise to an abnormal bonding situation which has to be discussed in detail later on. In solution, however, it facilitates the NMR spectroscopically observed migration of the halogen atom to the other trivalent phosphorus atom P5. As part of an ordinary P=C double bond it is characterized by a coordination number of only 2.

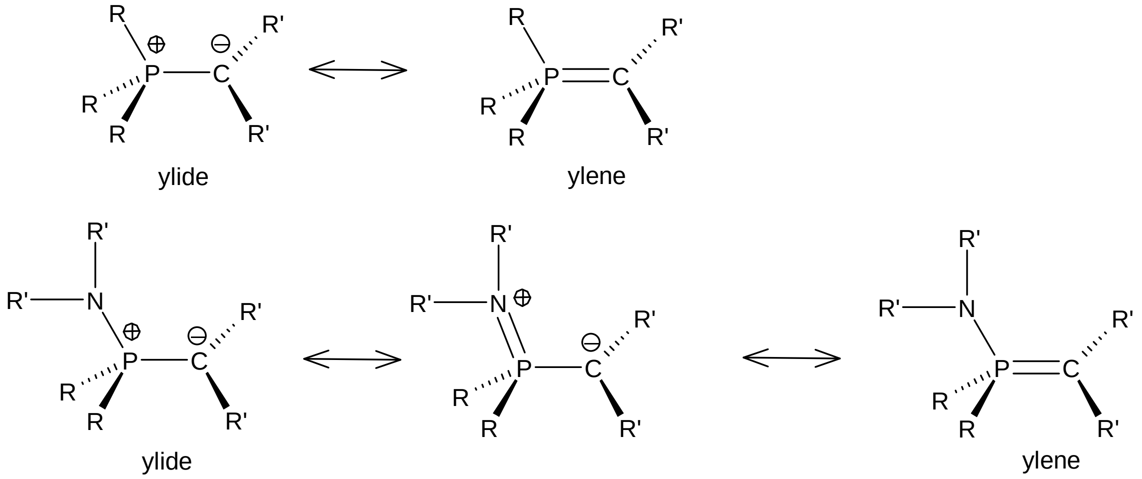

Scheme 4.1. Mesomerism of alkylidenetriorganyl– and alkylidene(diorganylamino)–diorganylphosphoranes.

Comments on the ylidic $P^{\oplus}$–$C^{\ominus}$ bond. Since the ylidic $P^{\oplus}$–$C^{\ominus}$ system forms the predominant feature of the 1,3,5-triphospha-dewarbenzenes **3a** – **3d**, the discussion of bond lengths and angles will start with this part of the molecules. Due to the great importance of alkylidenetriorganylphosphoranes in preparative organic chemistry [168], this class of compounds has been thoroughly studied by X-ray structure analyses and the molecular parameters of numerous derivatives are known at present. As can be taken from the selection of data in Table 4.5 the $P^{\oplus}$–$C^{\ominus}$ distances accumulate at an average of 168.5 pm when non-bulky alkyl or aryl substituents are bound to phosphorus and carbon. Steric strain clearly evident in a compound like triisopropyl(1-methylethylidene)phosphorane might be responsible for an abnormal elongation of the $P^{\oplus}$–$C^{\ominus}$ bond up to a value of 173.1 pm.

The situation, however, becomes more difficult to survey when elementorganic groups are linked to the negatively charged carbon atom. Without going into detail, the afore derived standard value is approximately attained with two phenylsilyl or two diphenylstibanyl substituents, but only *one* diorganylphosphanyl group at carbon. On the contrary, two diorganylphosphanyl or two diphenylarsanyl substituents give rise to an elongation of the $P^{\oplus}$–$C^{\ominus}$ distances up to values near 173.0 pm. Further examples demonstrating the influence of other hetero atoms such as sulphur and selenium or even titanium and zirconium have also been compiled in Table 4.5. An analogous deviation from the standard value is observed when the carbon atom of the P=C unit is linked to an acyl group or a similar electron withdrawing substituent; in this case the lengthening can be attributed to the reduced negative charge at the carbanion and a weaker Coulomb attraction between phosphorus and carbon. Unexpectedly, an adjacent phosphorus–halogen unit P–X causes a similar elongation; as already mentioned this phenomenon will be discussed in detail later on.

Table 4.5. P=C Distances (pm) in Several Characteristic Alkylidenephosphoranes.
Tilt Angles α (°) and Torsion Angles θ (°) of compounds marked with an asterix (*) were calculated from published data and are given in Table 4.10, page 160.

Compound	Method of Determination[a] XRD	GED	QCC	Lit.
$Me_3P=CH_2$	167.8	165.6	167.7	[211]
$(Me_2N)_3P=CH_2$	165.5	162.0	164.7, 165.7, 166.3[b]	[212]
$(H_2N)_3P=CH_2$	–	–	165.4	[212]

Compound	XRD	Lit.	Compound	XRD	Lit.
$Ph_3P=CH_2$	169.7, 168.8[c]	[213]	$Ph_3P=C(COMe)(CO_2{}^tBu)$	174.0	[229]
$Ph_3P=C(CH_2)_2$*	169.6	[214]	$Ph_3P=C(CN)_2$*	175.3	[230]
$Ph_3P=C(CH_2)_3$*	166.8	[215]	$Ph_3P=C(SO_2C_6H_4Me)H$	170.9	[231]
$^iPr_3P=C(CH_3)_2$*	173.1	[216]	$Ph_3P=C(SO_2Ph)Et$	170.7	[232]
$Me_3P=C(SiH_2Ph)_2$	168.5	[217]	$Ph_3P=C(SO_2CH_2Ph)Ph$	172.4	[232]
$Ph_3P=C(SbPh_2)_2$	168.9	[218]	$Ph_3P=C(SPh)(SePh)$	170.8	[233]
$Ph_3P=C(PMe_2)H$	168.1	[213]	$Ph_3P=C[Ti(\eta^5\text{-}Cp)_2Ph]H$	170.9	[234]
$Me_3P=C(PPh_2)H$	168.5	[213]	$Ph_3P=C[(Zr(\eta^5\text{-}Cp)_2Ph]H$	168.9	[235]
$Me_3P=C(PPh_2)_2$*	172.6	[219]	$Ph_3P=C[Hf(\eta^5\text{-}Cp)_2Et]H$	168.1	[236]
$Ph_3P=C(PPh_2)_2$	172.0	[220]	$Ph_3P=C(PCl_2)Me$	171.7	[237-239]
$Ph_3P=C(AsPh_2)_2$*	169.7	[221]	$Ph_3P=C(PMeCl)Ph$	173.0	[240]
$Ph_3P=C(COMe)H$	171.0	[222]	$Ph_3P=C(PCl_2)(2,6\text{-}Cl_2C_6H_3)$	174.1	[237-239]
$Ph_3P=C(CO_2Me)H$	170.4	[223]	$Ph_3P=C(PBr_2)Me$	172.2, 172.7[c]	[237-239]
$Ph_3P=C(CO\text{–}NH\text{–}COPh)H$	171.1	[224]	$Ph_3P=C(SiMe_3)(PBr_2)$	173.7	[237-239]
$Ph_3P=C(CO_2Et)H$	170.6	[225]	$Ph_3P=C(PCl_2)_2$*	173.9	[237-239]
$Ph_3P=C(SePh)(COPh)$	174.6	[226]	$Ph_3P=C(AsCl_2)Me$	172.1	[241]
$Ph_3P=C(COPh)Cl$	173.6	[227]	$Ph_3P=C(AsCl_2)_2$*	173.1	[241]
$Ph_3P=C(COPh)I$	171.3	[227]	$Ph_3P=C(CF_2)_3$	171.3	[242]
$Ph_3P=C(COMe)_2$	175.2	[228]	$Ph_3P=C=PPh_3$	163.2, 163.7[c]	[243]
$Ph_3P=C(COMe)(CO_2Et)$	175.7	[229]	$ClMe_2P=C(SiMe_2\text{-}CH_2)_2SiMe_2$[d]	168.7, 168.5, 168.5[c]	[244]
$Ph_3P=C(CO_2Et)_2$	174.8	[228]	$BrMe_2P=C(SiMe_2CH_2)_2SiMe_2$[d]	164.6	[244]
$Ph_3P=C(COMe)(COPh)$	175.1, 177.0[c]	[225]	$^tBu_2(Cl)P=CPh_2$*	166.7, 167.3, 166.8[c]	[245]
$Ph_3P=C(COMe)(CO_2{}^iPr)$	175.3	[229]	$^tBu_2(Cl)P=CPh(SiMe_3)$*	167.4	[246]

a) Results of X-ray diffraction analysis (XRD), gas electron diffraction (GED) or quantum chemical calculations (QCC); b) for different methods of calculation see the original publication; c) crystallographically independent molecules in the asymmetric unit. d) Structures of the *P*-halogen substituted alkylidenephosphoranes are shown in Scheme 4.2, pages 137-138.

Specification of standards for different types of P–N bonds. In order to appraise the influence of the diorganylamino group at phosphorus atom P1 on the $P^{\oplus}$–$C^{\ominus}$ distances of the triphospha-dewarbenzenes **3a** – **3d** a detailed discussion of P–N bond lengths seems to be necessary. Comprehensive explanations of the theoretical background, however, will be avoided; in this context we refer to review articles such as the excellent contributions of *Gilheany* [247]. For the length of a P–N single bond the method of *Schomaker* and *Stevenson* [134] taking into account different electronegativities of both the elements involved and being modified 19 years later by *Pauling* [124]

$$d_{(P\text{–}N)} = r_N + r_P - c\,|x_N - x_P|$$

1) covalent radii [124]: r_N (74 pm), r_P (110 pm);
2) Pauling electronegativities [197]: x_N (3.0), x_P (2.1);
3) adjustment factor: c (8.0 pm).

leads to a value of 177 pm, whereas with the now generally accepted correction introduced by *Blom* and *Haaland* [133] a shorter distance of 173 pm is obtained.

$$d_{(P\text{–}N)} = r_N + r_P - c\,|x_N - x_P|^{n}$$

1) covalent radii [133]: r_N (73 pm), r_P (109 pm);
2) Allred and Rochow electronegativities [60]: x_N (3.07), x_P (2.06);
3) adjustment factors: c (8.5 pm), n (1.4).

In contrast to these predictions, the majority of aminophosphines [248] show P–N bond lengths which are shortened further. As reported by *Norman* et al. [249], *e.g.*, in the co-crystallizate bis[bis(phenylamino)phosphinyl]aniline–diethylether (1/1) distances vary between 166 and 171 pm, whereas for tris(phenylamino)phosphine only one P–N value of 169.7 pm could be determined due to a crystallographically imposed C_3 symmetry. A combined GED and X-ray structure determination on gaseous and crystalline tris(dimethylamino)phosphine, respectively, published some years ago by *Mitzel*, *Rankin* and others [212] resulted not only in an unexpected correction of the molecular symmetry from C_3 [250] or C_{3v} [251] as assumed in earlier experiments, to C_s [252], but also in the detection of different P–N distances. Whereas XRD-values obtained in a range between 168.1 and 169.9 pm (average 168.7 pm) correlate with an sp^2-hybridisation of four nitrogen atoms in two crystallographically independent molecules of the unit cell, two longer distances of 173.2 and 172.9 pm are shown by nitrogen atoms with a pyramidal geometry. In order to confirm the unexpectedly strong influence of nitrogen hybridisation on the P–N bond lengths the authors verified their experimental results with quantum chemical calculations and obtained similar values of 169.4 and 174.0 pm.

Since only the tris(dimethylamino) derivative has been structurally studied so far and the dependence of the P–N distance on the number of nitrogen atoms at phosphorus has still to be ascertained, [253] analogous quantum chemical calculations were performed on the still unexplored heteroleptic (dimethylamino)methylphosphines $(Me_2N)_{3-x}Me_xP$ (x = 1, 2). As for the results which are discussed in detail in one of the following chapters, the P–N bond length is found again to be strongly dependent on the hybridization of the nitrogen atom. Furthermore, the individual values are scarcely influenced by the number of nitrogen atoms at phosphorus increasing from 171.9 pm for the sp^2-hybridized nitrogen atoms in C_s-symmetric tris(dimethylamino)phosphine to 173.0 pm in C_1-(dimethylamino)dimethylphosphine (Table 4.8). Since quantum chemically obtained bond lengths even calculated at a fairly high level are know to be somewhat elongated with respect to experimental results, the XRD-values of the tris(dimethylamino) derivative may serve as a basis for correction. With a difference of 3.2 pm between the calculated value (171.9 pm) and an average of the experimentally determined bond lengths (168.7 pm) in mind, a $P–N_{sp2}$ distance of 169.8 pm can be predicted for the compounds C_s-$(Me_2N)_2MeP$ and C_1-$(Me_2N)Me_2P$; therefore an almost negligible lengthening of about 1.2 pm will be observed.

Despite careful studies, the attempt to specify a correct standard value for P–N bond lengths in alkylidene(diorganylamino)phosphoranes turned out to be rather complicated. Even on such a simple compound like tris(dimethylamino)methylidenephosphorane C_s-symmetric in the gaseous as well as the solid state, *Mitzel*, *Rankin* and others [212] determined two different P–N distances with the methods of gas electron and X-ray diffraction, respectively. The higher XRD value of 169.8 pm refers to the P–N bond which is found in an almost ecliptical position with respect to the vector of the free electron pair at the methylene group. Furthermore, the pertinent $H_2C–P–N$ angle has increased to a value of 122.4° and due to a sum of angles of 337.3° the nitrogen atom shows a trigonal pyramidal environment. In contrast to these structural parameters the other two dimethylamino substituents are characterized by sp^2-hybridized nitrogen atoms, shorter P–N distances of 166.6° and 166.9° pm and narrower $H_2C–P–N$ angles of 110.6 and 109.4°. Similar results had already been obtained some years before by *Schmidbaur* and coworkers [256, 257] from X-ray structure determinations of the *C*-silylated alkylidene phosphoranes **XLV** and **XLVI** shown in Scheme 4.2, pages 137-138.

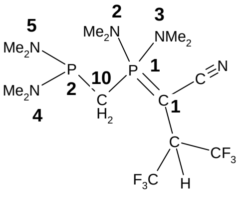

XLI [254]

P1-C1 172.6

P1-N2 166.7
P1-N3 164.9
P1-C10 180.2

C1-P1-N2 117.23
C1-P1-N3 108.37
C1-P1-C10 109.06
N2-P1-N3 103.41
N2-P1-C10 106.62
N3-P1-C10 112.12

P2-N4 167.9
P2-N5 168.9
P2-C10 187.7

$\Sigma\angle$N2 343.62
$\Sigma\angle$N3 357.29
$\Sigma\angle$N4 356.05
$\Sigma\angle$N5 350.30

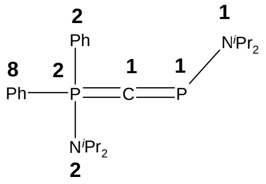

XLII [255]

P2-C1 168.4

P2-C2 183.2
P2-C8 181.1
P2-N2 167.5

C1-P2-C8 116.33
C1-P2-C2 110.68
C1-P2-N2 112.12
C2-P2-C8 105.43
N2-P2-C8 103.97
C2-P2-N2 110.68

P1-C1 164.1
P1-N1 166.8

P2-C1-P1 115.05
C1-P1-N1 108.12

$\Sigma\angle$N1 359.95
$\Sigma\angle$N2 356.22

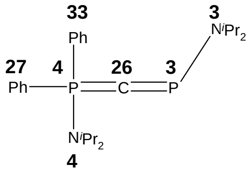

XLIII [255]

P4-C26 167.3

P4-C27 182.0
P4-C33 181.1
P4-N4 167.3

C26-P4-C33 115.37
C26-P4-C27 110.78
C26-P4-N4 111.81
C27-P4-C33 105.97
C33-P4-N4 104.54
C27-P4-N4 107.87

P3-C26 164.1
P3-N3 167.5

P4-C26-P3 116.56
C26-P3-N3 108.22

$\Sigma\angle$N3 359.94
$\Sigma\angle$N4 356.30

Two crystallographically independent molecules in the asymmetric unit

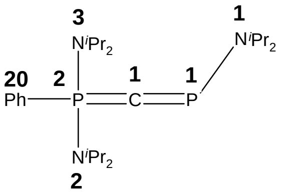

XLIV [255]

P2-C1 166.9

P2-N2 166.1
P2-N3 169.0
P2-C20 184.3

C1-P2-C20 118.02
C1-P2-N2 111.64
C1-P2-N3 113.05
C20-P2-N2 103.66
C20-P2-N3 104.07
N3-P2-N2 105.17

P1-C1 162.9
P1-N1 168.5

P2-C1-P1 125.28
C1-P1-N1 107.48

$\Sigma\angle$N1 359.44
$\Sigma\angle$N2 358.56
$\Sigma\angle$N3 352.17

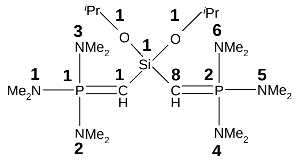

XLV [256]

P1-C1 165.8

P1-N1 167.1
P1-N2 166.4
P1-N3 166.0

C1-P1-N3 118.09
C1-P1-N1 114.88
C1-P1-N2 109.22
N3-P1-N1 100.25
N3-P1-N2 106.68
N1-P1-N2 106.79

$\Sigma\angle$N1 358.76
$\Sigma\angle$N2 356.26
$\Sigma\angle$N3 351.10

P2-C8 165.6

P2-N6 170.3
P2-N5 166.8
P2-N4 166.6

C8-P2-N6 120.68
C8-P2-N4 110.24
C8-P2-N5 112.31
N6-P2-N5 99.81
N6-P2-N4 99.88
N4-P2-N5 113.31

$\Sigma\angle$N4 356.57
$\Sigma\angle$N5 348.60
$\Sigma\angle$N6 336.35

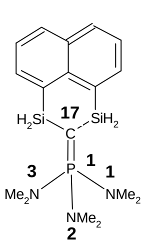

XLVI [257]

P1-C17 166.9

P1-N1 168.9
P1-N2 165.7
P1-N3 165.2

C17-P1-N1 117.90
C17-P1-N2 111.07
C17-P1-N3 110.52
N1-P1-N2 100.61
N1-P1-N3 102.07
N2-P1-N3 114.27

$\Sigma\angle$N1 337.82
$\Sigma\angle$N2 352.58
$\Sigma\angle$N3 352.97

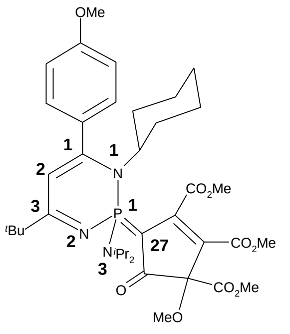

XLVII [258]

P1-C27 173.2

P1-N2 165.5
P1-N1 166.7
P1-N3 164.2

C27-P1-N2 112.54
C27-P1-N1 106.60
C27-P1-N3 114.63
N2-P1-N1 105.24
N2-P1-N3 105.81
N3-P1-N1 111.69

$\Sigma\angle$N1 357.82
$\Sigma\angle$N2 360.00
$\Sigma\angle$N3 359.27

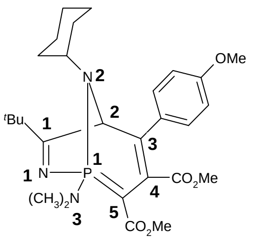

XLVIII [259]

P1-C5 172.4

P1-N1 168.3
P1-N2 167.0
P1-N3 161.3

C5-P1-N1 106.75
C5-P1-N2 106.12
C5-P1-N3 118.42
N1-P1-N2 94.72
N1-P1-N3 112.85
N3-P1-N2 115.14

$\Sigma\angle$N1 360.00
$\Sigma\angle$N2 349.30
$\Sigma\angle$N3 359.55

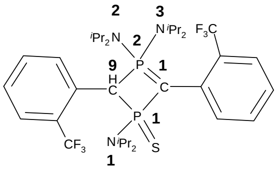

XLIX [260]

P2-C1	172.9
P2-N3	168.1
P2-N2	166.5
P2-C9	186.1
C1-P2-N3	121.31
C1-P2-N2	116.67
C1-P2-C9	88.39
N3-P2-N2	104.32
N3-P2-C9	109.78
N2-P2-C9	116.20
P1-N1	168.0
P1-C1	176.2
P1-C9	187.7
$\Sigma\angle$N1	352.66
$\Sigma\angle$N2	359.97
$\Sigma\angle$N3	359.86

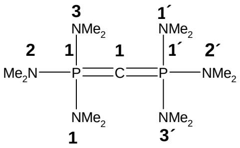

L [261]

P1-C1	158.4
P1-N1	169.7
P1-N2	165.7
P1-N3	166.0
C1-P1-N1	120.52
C1-P1-N2	113.49
C1-P1-N3	113.39
N1-P1-N2	98.62
N1-P1-N3	99.63
N2-P1-N3	109.45
$\Sigma\angle$N1	342.81
$\Sigma\angle$N2	358.24
$\Sigma\angle$N3	358.50

Molecule with a center of inversion

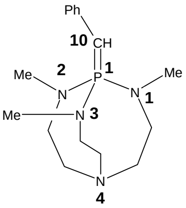

LI [262]

P1-C10	169.1
P1-N1	165.9
P1-N2	165.7
P1-N3	164.7
C10-P1-N1	116.64
C10-P1-N2	109.78
C10-P1-N3	109.28
N1-P1-N2	103.81
N1-P1-N3	106.93
N2-P1-N3	110.28
$\Sigma\angle$N1	359.78
$\Sigma\angle$N2	359.12
$\Sigma\angle$N3	359.22
$\Sigma\angle$N4	359.24

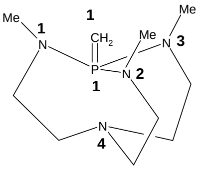

LII [263]

P1-C1	165.8
P1-N3	166.6
P1-N1	166.5
P1-N2	165.6
C1-P1-N3	114.95
C1-P1-N1	114.83
C1-P1-N2	110.02
N3-P1-N1	102.86
N3-P1-N2	106.50
N1-P1-N2	106.99
$\Sigma\angle$N1	349.80
$\Sigma\angle$N2	359.34
$\Sigma\angle$N3	358.69
$\Sigma\angle$N4	357.07

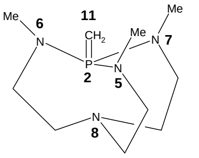

LIII [263]

P2-C11	165.4
P2-N5	166.7
P2-N6	166.2
P2-N3	165.8
C11-P2-N5	115.67
C11-P2-N6	110.99
C11-P2-N7	112.25
N5-P2-N6	104.95
N5-P2-N7	105.24
N6-P2-N7	107.09
$\Sigma\angle$N5	359.43
$\Sigma\angle$N6	359.40
$\Sigma\angle$N7	359.79
$\Sigma\angle$N8	359.05

Two crystallographically independent molecules in the asymmetric unit

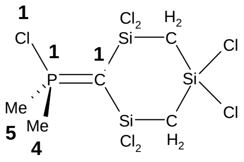

LIV [244]

P1-C1	168.7
P1-Cl1	204.7
P1-C4	178.5
P1-C5	178.1
C1-P1-Cl1	113.65
C1-P1-C4	115.67
C1-P1-C5	115.30
Cl1-P1-C4	101.61
Cl1-P1-C5	101.75
C4-P1-C5	107.12

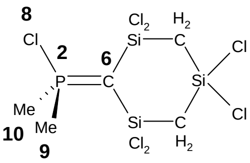

LV [244]

P2-C6	168.5
P2-Cl8	205.0
P2-C9	178.3
P2-C10	178.4
C6-P2-Cl8	113.39
C6-P2-C9	116.12
C6-P2-C10	115.48
Cl8-P2-C9	101.20
Cl8-P2-C10	102.22
C9-P2-C10	106.63

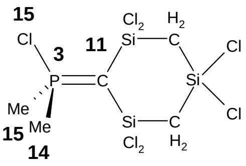

LVI [244]

P3-C11	168.5
P3-Cl15	205.4
P3-C14	178.1
P3-C15	178.3
C11-P3-Cl15	113.31
C11-P3-C14	116.15
C11-P3-C15	115.86
Cl15-P3-C14	101.06
Cl15-P3-C15	102.09
C14-P3-C15	106.49

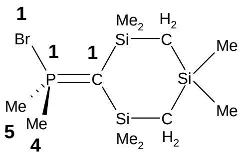

LVII [244]

P1-C1	164.6
P1-Br1	236.6
P1-C4	179.1
P1-C5	179.3
C1-P1-Br1	116.38
C1-P1-C4	117.55
C1-P1-C5	119.31
Br1-P1-C4	97.96
Br1-P1-C5	96.38
C4-P1-C5	105.37

Three crystallographically independent molecules in the asymmetric unit

Scheme 4.2. Characteristic bond lengths and angles of *P*-diorganylamino or *P*-halogen substituted alkylidene phosphoranes. Compound **LVII** attracts attention by its rather long P–Br bond. P=C bond lengths of molecules **LIV** to **LVII** are given in Table 4.5.

Here, however, the situation is not as evident as before, since the longer P–N distances fall into a wider range from 167.1 to 170.3 pm and the shorter ones vary between 165.2 and 166.8 pm. Additionally, one has to notice that in one half of molecule **XLV** [256] all three P–N bonds are of nearly equal length (166.0 to 167.1 pm) and that the wider C–P–N angle does not correlate with the longest bond P1–N1 (167.1 pm; cf. C1–P1–N1 114.88°), but with the shortest one P1–N3 (166.0 pm; cf. C1–P1–N3 118.09°). Among a series of similar alkylidenephosphoranes with one, two or three diorganylamino groups at phosphorus which have been compiled in Scheme 4.2, pages 137 and 138, several molecules can be detected showing analogous irregularities with respect to the P–N and P–C_{phenyl} bonds, respectively.

In order to elaborate common structural features which are characteristic for groups of similar methylenephosphoranes and to shed some light on the influence of different substituents such as methyl, amino, hydrogen, halogen, or silyl on the P–C bond lengths, quantum chemical calculations were performed [253]. Fortunately, analogous calculations at the MP2/6-31G* and MP2/6-311G** level of theory had already been published by *Mitzel*, *Rankin* and others [212] for tris(dimethylamino)methylidenephosphorane and the parent compound $(H_2N)_3P{=}CH_2$, respectively. A comparison of these values with our data obtained at the MP2/6-31G* level and compiled in Table 4.9 of the next chapter, now allows a detailed discussion of the structure of alkylideneaminophosphoranes. Among a diversity of different results assorted on page 157 the following items are of special importance for the heteroleptic aminomethyl-methylenephosphoranes $(H_2N)_{3-x}Me_xP{=}CH_2$ (x = 1, 2) discussed here.

At first, similar to the P–Cl and P–C distances of chloromethylphosphines (Cl_3P, P–Cl 204.3 [264]; $Cl_2P{-}Me$, P–Cl 206.1, P–C 183.1 [265]; $Cl{-}PMe_2$, P–Cl 206.3, P–C 183.6 [266]; PMe_3, P–C 184.6 pm [173]) the P–C and P–N bond lengths turned out to be only slightly dependent on the number of amino or methyl groups at phosphorus. A strong correlation, however, could be observed between the conformation of the molecules and the P–N bond lengths along with a different hybridisation of the appertaining nitrogen atoms. When the P–N bond eclipses the vector of the free electron pair at the ylidic carbon atom, the nitrogen atom N3 is found to be sp^3-hybridized. Furthermore, negative hyperconjugation mainly between the free electron pair and the antibonding σ^*-orbital of the bond P1–N3 results in a strong elongation of its length up to values from 173.0 to 175.9 pm. Inspection of the non-ecliptical positions, however, proved the P–N bonds to be significantly shorter (168.5 to 170.3 pm) and the nitrogen atoms to be sp^2-hybridized. Since *Mitzel*, *Rankin* and others [212] obtained almost identical P–N_{sp2} bond lengths of 166.8 and 167.5 pm from X-ray diffraction studies on tris(dimethylamino)methylenephosphorane and quantum chemical calculations at the MP2/6-

311** level of theory on the compound $(H_2N)_3P{=}CH_2$, respectively, we feel that a length of 167 to 168 pm might be an acceptable standard value for the distance between an *sp*^{2}-hybridized nitrogen atom and the phosphonium center. Quantum chemical calculations calculation [253] at the MP2/6-31G* results in a slightly higher value of 169 pm.

Very surprisingly, the P–N lengths obtained from X-ray structure determinations on miscellaneous 1-dialkylamino-1$\lambda^5\sigma^4$,3$\lambda^3\sigma^3$,5$\lambda^3\sigma^2$-triphosphabicyclo[2.2.0]hexa-1,5-dienes **3a** to **3d** of this thesis were found to be much shorter than the standard value of 168 pm derived above. The nitrogen atoms in question are *sp*^{2}-hybridized as well, but the individual distances fall into a lower range varying only slightly between 162.7 and 164.8 pm. Additionally, from Table 4.4 average values of 163.7 pm and 358.8° can be taken for the P–N bond length and the sum of angles at nitrogen N1, respectively. An inspection of data compiled in Table 4.6 for numerous aminophosphonium cations of the next page, however, reveals similar P–N distances of about 163 pm. We therefore feel that in compounds **3a** to **3d** the $R_2N{-}P^{\oplus}$ part of the heterocycle has to be considered an isolated entity, and that the interactions with the free electron pair at the ylidic carbon atom are almost negligible. With a high degree of probability the free electron pair seems to be much more involved in a negative hyperconjugation with the σ*-orbital of the adjacent P–Cl bond.

Table 4.6. $P^{\oplus}$–N Distances (pm) in Some Characteristic Aminophosphonium Cations

Compund	$P^{\oplus}$–N Distance	Literature
$[Me_3P–NH_2]Cl$	163.2	[267]
$[Et_3P–NH_2]Cl$	162.6	[267]
$[Et_3P–NH_2]I$	165.0	[267]
$[Et_3P–NH_2]_2[B_{10}H_{10}]$	163.0, 163.0	[267]
$[Ph_3P–NH_2]Cl$	161.6	[268]
$[Ph_3P–NH_2]Br$	161.5	[269]
$[Ph_3P–NH_2][SCN]$	160.1	[270]
$[Ph_3P–NH_2]ICl_2$	163.1	[267]
$[Ph_3P–NH_2][PhC(CN)_2]$	162.2	[271]
$[Me_3P–N(H)SiMe_3][O_3S–CF_3]$	162.2, 162.4[a]	[267]
$[Et_3P–N(H)SiMe_3]I$	163.1	[267]
$[Ph_3P–N(H)^iPr]Br$	162.8	[272]
$[(Ph_3P–N(H)^tBu]Br$	162.1	[272]
$[Me_3P–N(SiMe_3)_2]I$	164.3, 164.5[a]	[267]
$[Et_3P–N(SiMe_3)_2]I$	166.0	[267]
$[Ph_3P–N(SiMe_3)_2]I_3$	163.7	[267]
$[Ph_3P–NMe_2]Br_3$	162.9	[273]
$[(PhCH_2)Ph_2P–NEt_2]Cl$	163.0	[274]
$[Ph_3P–N(Me)^tBu]I$	164.6	[272]
$[(PhCH_2)P(–NMe_2)_3]Br$	161.4, 163.4, 163.6	[275]
$[(PhCH_2)P(–NMe_2)_3]Br_3$	162.8, 163.4, 163.6	[275]
$[(PhCH_2)P(–N^nPr_2)_3]Br$	163.0, 163.0, 163.6, 163.9, 164.1, 165.2[a]	[275]
$[(PhCH_2)P(–N^nPr_2)_3]Br_3$	162.5, 164.4, 164.9	[275]
$[(PhCH_2)P(–N^nBu_2)_3]Br_3$	161.3, 162.8, 163.1	[275]
$[(\textit{p}\text{-}Br\text{-}C_6H_4\text{-}CH_2)P(–N^nPr_2)_3]Br$	161.4, 163.0, 163.1	[276]
$[(\textit{p}\text{-}Br\text{-}C_6H_4\text{-}CH_2)P(–N^nPr_2)_3]Br_3$	162.7, 163.7, 164.2	[276]
$[(C_6H_5\text{-}CH_2)P(–N(C_2H_5)_2)_3]Br{\bullet}CH_3CN$	163.2, 163.3, 164.0	[277]
$[(C_6H_5\text{-}CH_2)P(–N(C_2H_5)_2)_3]Br_3$	162.9, 163.1, 163.5	[277]
$[ClP(–N(H)^iPr)_3]Cl$	159.6, 160.1, 160.1	[278]
$[P(–N(H)Ph)_4]Cl$	161.4, 161.7, 161.5, 161.7	[279]
$[P(–N(Me)^iPr)_4]BF_4$	162.8, 163.4, 163.7, 163.7	[280]
$[P(–N(Me)\textit{cy}\text{-hex})_4]BF_4$	163.6	[280]
$[P(–N(Me)\textit{cy}\text{-hex})_4]PF_6$	163.6	[280]

a) Two crystallographicly independent molecules in the asymmetric unit

Negative hyperconjugation of the free electron pair at carbon with the σ^*-orbital of the P–Cl bond. A short inspection of Table 4.4 immediately reveals a totally unexpected elongation of the phosphorus-chlorine bond P3–Cl1. The distance turned out to be so large that it was initially supposed, *i.e.* after the structure determination of compound **3b**, the first example in this series of $1\lambda^5\sigma^4,3\lambda^3\sigma^3,5\lambda^3\sigma^2$-triphosphabicyclo[2.2.0]hexa-1,5-dienes, a complete dissociation of the P–Cl bond and the formation of a phosphonium cation along with a chloride anion. A closer look at the molecular framework (Fig. 4.14), however, proved the chlorine atom Cl1 to be part of a bridge P3–Cl1....P5, asymmetric in compounds **3a** – **3c**, but symmetric in compound **3d**. The effect of a fast chlorine exchange on the NMR spectra of the asymmetric species has already been discussed in this chapter, page 113.

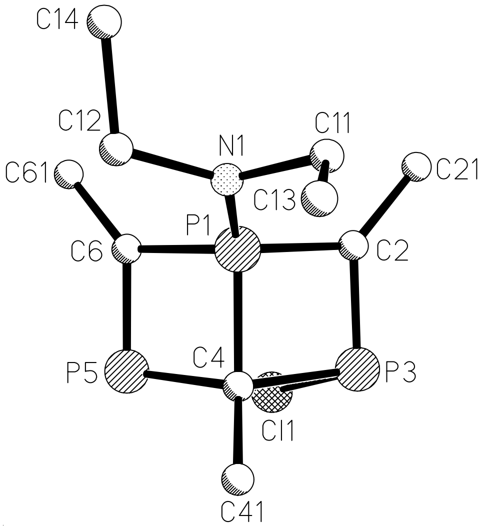

Figure 4.14. Molecular framework of compound **3b** projected onto the plane C2, P3, P5, C6. The methyl groups of the *tert*-butyl substituents have been omitted for clarity.

Whereas the values determined for compounds **3a** to **3c** fall into a rather narrow range between 237.6 and 245.0 pm, an even longer distance of 266.6 pm has been observed for the symmetric species **3d**. The average of all compounds (245.5 pm) exceeds the length of a typical covalent P–Cl bond published *e.g.* for phosphorus(III) chloride (204.3 pm) [264]) by more than 41 pm, but remains shorter than the sum of the appertaining van der Waals radii (370 pm) [124]. Remarkably the lengthening of the P–Cl bond in close vicinity to an ylidic $P^{\oplus}$–$C^{\ominus}$ group is accompanied by a strong shortening of the corresponding carbon-phosphorus bond P3–C2. The individual values differ only insignificantly from the average (172.2 pm) but the shortening of this bond, however, is found to be so strong that it can no longer be considered a single bond. On the contrary, it is about as short as the mean ylidic $P^{\oplus}$–$C^{\ominus}$ distance (P1–C2 173.0 pm) and approaches the average length of the P–C double bond (P5–C6 170.0 pm). Only with compound **3d** a slight deviation has to be noticed as to its rather elongated $P^{\oplus}$–$C^{\ominus}$ bond (175.6 pm).

The peculiarity of significantly elongated phosphorus-halogen bonds in *C*-substituted alkylidenephosphoranes was noticed for the first time in our research group in the thermally rather instable compound 3-*tert*-butyl-1,2,4,4-tetrabromo-2,3-dihydro-1*H*-1λ^3,2λ^3,4λ^5-triphosphole **J** [87] (Table 4.7). This heterocycle forms smoothly when 2-*tert*-butyl-1λ^3-phosphaalkyne is treated with an equimolar amount of bis(dibromophosphanyl)methane at low temperature in cyclopentane solution.

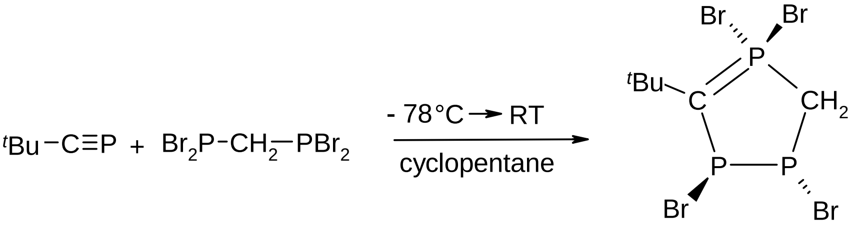

J

Without going into details of the mechanism involved, the reaction may *formally* be described with an oxidative addition of the phosphorus atom of the P≡C unit by one of the four P–Br groups of the halogen compound and a simultaneous attack of the second still intact dibromophosphanyl substituent at the formerly *sp*-hybridized carbon atom. No studies on the reactivity have been carried out so far; an X-ray structure determination, however, shows the phosphorus-bromine bond adjacent to the negatively charged carbon atom of the ylidic P=C unit to be elongated to a distance of 239.0 pm. In contrast, the length of the second P–Br bond (224.9 pm) is found to be only slightly shorter than that of 2,4,5-tribromo-1,3-di-*tert*-butyl-2λ^3,4λ^3,5λ^3-triphosphabicyclo-[1.1.1]pentane (231 pm [87]), but to be nearly as long as in phosphorus tribromide (223.0 pm) [264].

In this context it is worth to note that in the nineties of the last century *Schmidpeter* and his group started systematic investigations on several series of alkylidenephosphoranes, all of which were characterized by P–X units (X = Cl, Br) adjacent to the ylidic carbon atom [237-239]. For a preparation of these compounds, different synthetic routes could be worked out. To obtain [1-(dihalophosphanyl)benzylidene]triphenylphosphoranes, the authours treated benzyltriphenyl-phosphonium bromide or its benzyl-substituted derivatives with phosphorus trihalide PX_3 in the presence of twice the equimolar amount of triethylamine as an HX-acceptor. When, however, phosphorus tribromide was used, the reaction did not stop with the formation of the (dibromophosphanyl)-substituted compound but continued further so that 1,2-dibromo-3-triphenylphoranediyl-1,2-diphosphaindane **K** could be isolated as a by-product in up to 34% yield.

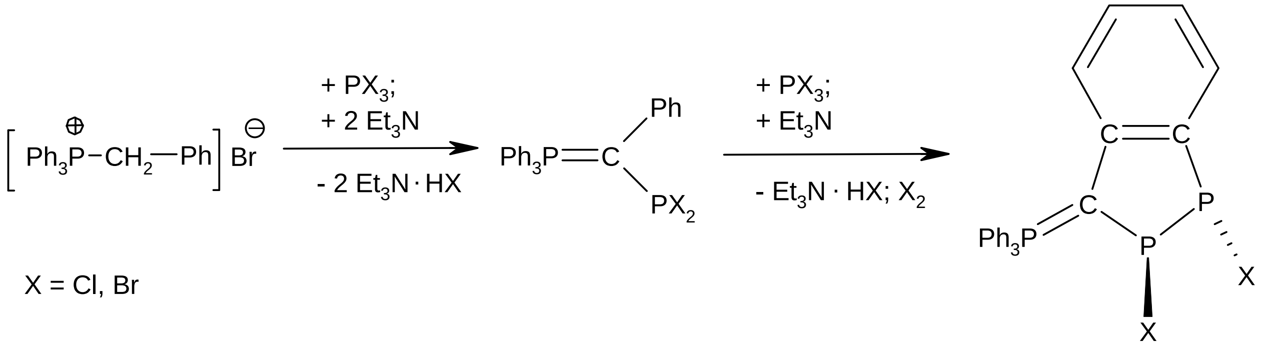

In analogy to compound **J** this cyclic diphosphane is characterized by a (Br)P–P(Br) unit and a negatively charged carbon atom of an ylidic P=C group as components of the five-membered ring. It exhibits two P–Br distances of different lengths – an elongated one (242.4 pm) adjacent to the ylidic carbon atom and a shorter one (230.0 pm) in position 1 of the 4,5-dehydro-1,2-diphospholane heterocycle. Similarly elongated P–Br bonds have also been ascertained in [1-(dibromophosphanyl)ethylidene]- (**H**) and [1-(dibromophosphanyl)-1-(trimethylsilyl)-methylidene]triphenylphosphorane (**I**, Table 4.7).

Table 4.7. Some Characteristic Bond Lengths (pm) and Angles (°) of Various Alkylidenephosphoranes with a P–X Group (X = Cl, Br) at the Carbon Atom of the Ylidic P=C Unit [a]

Compound[a]	**3a – 3c**	**3d**	**A**	**B**	**C**	**D**	**E**[b]	**F**[b]	**G**	**H**[c]	**I**	**J**[e]	**K**[e]
Literature			[237-239]	[237-239]	[237-239]	[240]	[237-239]	[281]	[281]	[237-239]	[237-239]	[87]	[282]
X31	Cl	Cl	Cl	Cl	Cl	Cl	Cl Cl	Cl Cl	Cl	Br Br	Br	Br	Br
X32	C	C	Cl	Cl	Cl	C	Cl Cl	C C	C	Br Br	Br	P	P
P1=C2	172.2	175.6	171.7	174.1	173.9	173.0	173.9	168.3; 170.9	174.0	172.2; 172.8	173.7	168.0	172.6
P3–C2	172.7	172.2	170.0	172.1	174.3	172.5	176.3; 176.0	178.1; 175.9	171.0	167.8; 168.8	171.8	173.0	173.3
P3–X31	240.3	266.6	218.8	212.5	216.3	226.2	210.0; 211.6	225.1; 220.4	235.3	243.6; 248.9	240.1	239.0	242.4
P3–X32			209.9	210.3	208.5		209.3; 208.6			226.2; 223.8	228.2		
P1–C2-P3	95.9	95.6	116.7	114.5	111.8	118.7	111.7	131.0; 131.3	117.8	116.9; 114.5	112.7	115.0	118.8
C2–P3–X31	109.6	107.0	104.2	107.0	104.6	107.2	104.3; 104.3	105.4; 107.3	109.7	101.8; 109.4	106.0	108.1	103.6
C2–P3–X32	86.9	87.4	103.0	104.6	102.8	101.3	102.9; 105.0	83.7; 84.3	101.3	102.5; 101.6	104.7	102.0	93.9
X31–P3–X32	93.9	85.5	92.2	93.3	97.4	92.2	96.0; 97.4	106.1; 105.8	93.97	93.5; 94.8	95.2	85.8	85.8
tilt angle α[f]	55.4(av.)	59.5/53.7	20.8	31.7	25.1	17.2	22.8	-[j]	24.6	20.0; 28.8	33.7	44.8/35.2	44.4
twist angle *θ*[f]	43.4(av.)	41.5/41.9	14.8	2.3	13.7	14.3	9.6	-[j]	19.9	13.9; 22.3	21.8	31.7/29.4	39.2
tilt angle α`[f]	14.8(av.)	14.5/15.7	29.2	38.7	32.7	21.5	41.8	22.7(av.)	19.1	18.0; 23.6	27.9	21.2	22.0
twist angle *θ*`[f]	1.6(av.)	6.2/ 6.5	27.8	34.6	29.2	17.1	33.1; 37.0	14.9(av.)	1.5	4.3; 8.3	23.7	13.8	17.8
ΔP–X (%)	17.6(av.)	30.5/29.7	7.1	4.0	5.9	10.7	2.1; 2.4	9.1(av.)	15.2	11.6; 9.2	7.6	7.1	8.7

a) Formulas and numbering of atoms for the compounds taken into consideration are given in Scheme 4.3. b) Values placed in the second column refer to the dashed part of the molecule (Scheme 4.3). c) Two crystallographicly independent molecules in the asymmetric unit; d) for a definition of the tilt angle *α* and twist angle *θ* see Fig. 4.21 and discussion; e) additional P–Br distances in compound **J**: P1–Br11 220.8, P1–Br12 221.0, P5–Br51 224.9; in compound **K**: P5–Br51 230.3 pm. f) 1-Dialkylamino-1$\lambda^5\sigma^4$,3$\lambda^3\sigma^3$,5$\lambda^3\sigma^2$-triphosphabicyclo[2.2.0]hexa-1,5-dienes:

Substituents (NR$_2$)	Me, Me (**3a**)	Et, Et (**I-3b**)	Et, Et (**IIA-3b**)	Et, Et (**IIB-3b**)	Me, ^{i}Pr (**3c**)	Me, Et (**3d**)
P–X	237.6	245.0	241.7	239.7	237.7	266.6/ 265.0
tilt angle α	55.3	57.7	54.7	55.3	53.9	59.5/ 53.7
twist angle *θ*	43.6	43.1	46.2	41.1	43.1	41.5/ 41.9
tilt angle α`	18.0	17.0	14.2	19.4	18.6	14.5/ 15.7
twist angle *θ*`	2.8	0.8	2.4	0.1	1.8	6.2/ 6.5
ΔP–X (%)	16.3	19.9	18.3	17.3	16.3	30.5/ 29.7

j) No α, *θ* for **F**, no atomic coordinates are available in the literature.

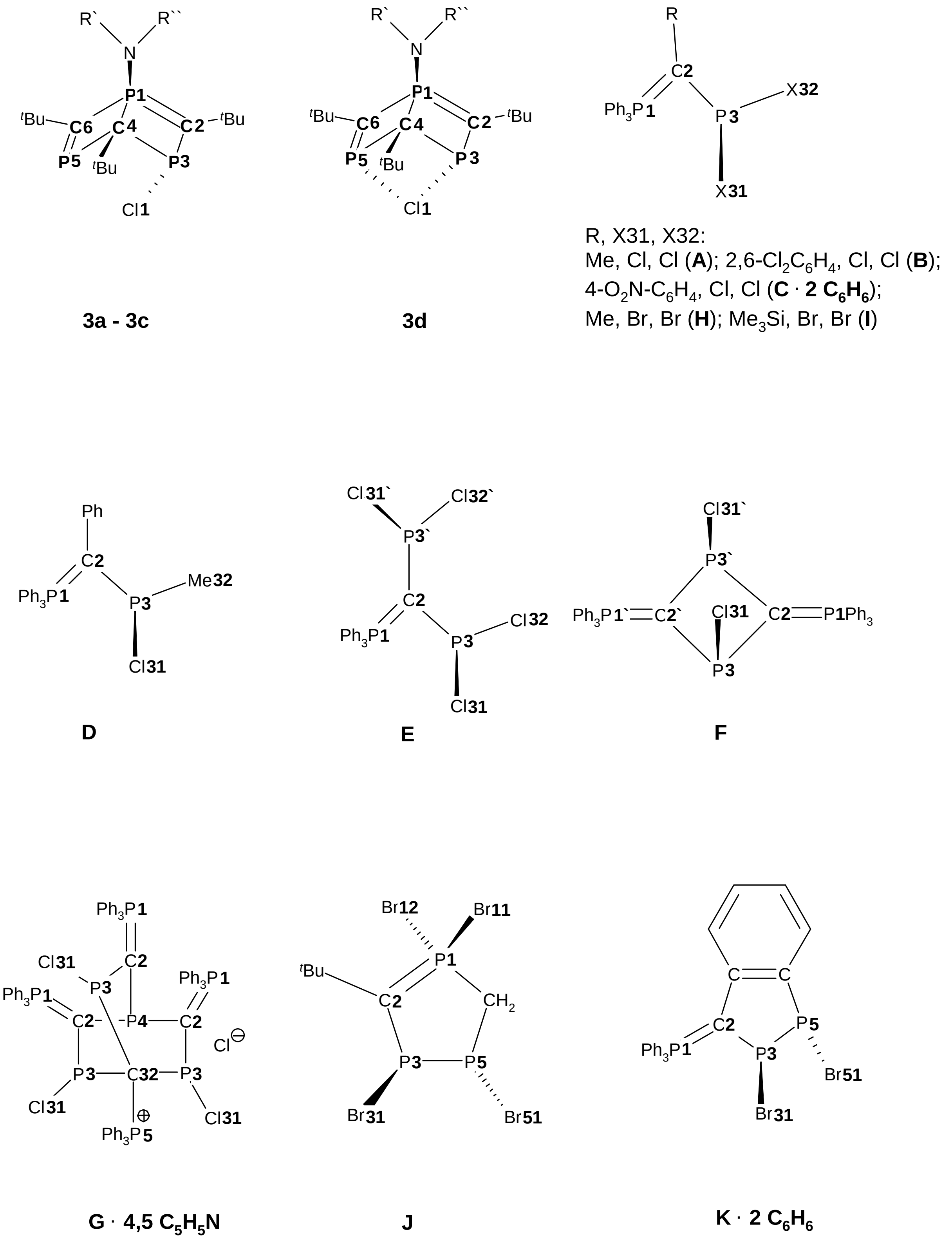

3a - 3c

3d

R, X31, X32:
Me, Cl, Cl (**A**); 2,6-$Cl_2C_6H_4$, Cl, Cl (**B**);
4-O_2N-C_6H_4, Cl, Cl (**C** · **2** $\mathbf{C_6H_6}$);
Me, Br, Br (**H**); Me_3Si, Br, Br (**I**)

D

E

F

G · **4,5** $\mathbf{C_5H_5N}$

J

K · **2** $\mathbf{C_6H_6}$

Scheme 4.3. Various alkylidenephosphoranes characterized by a P–X group (X = Cl, Br) at the carbon atom of the ylidic P=C unit.

An alternative route was found in the reaction of phosphorus trichloride with alkylidenetriphenylphosphoranes [237-239]. Ionic [1-(dichlorophosphanyl)alkyl]triphenylphosphonium chlorides were initially formed as isolable intermediates via addition of the trihalide to the ylidic P=C bond. Thereafter, these compounds could be converted to the aspired [1-(dichlorophosphosphanyl)alkyl]triphenylphosphoranes by a triethylamine-induced elimination of hydrogen chloride. Unfortunately, even at low temperature the addition of phosphorus trichloride to two equivalents of alkylidenetriphenylphosphorane may occur to a considerable extent. A subsequent twofold hydrogen chloride elimination with triethylamine furnishes bis[1-(triphenylphosphorandiyl)alkyl]phosphenium chlorides.

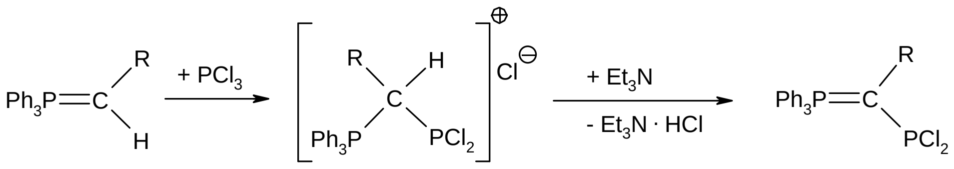

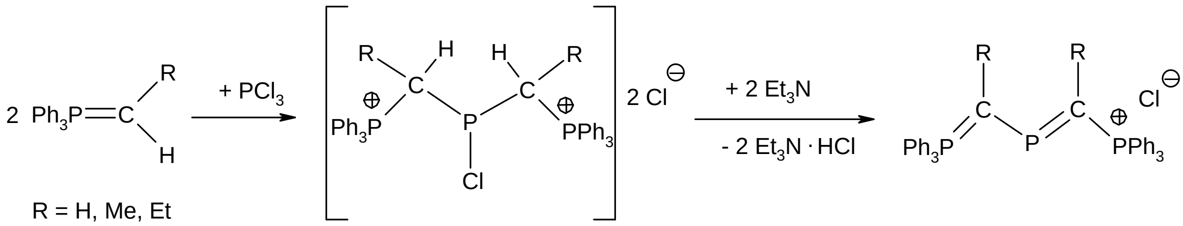

The exchange of trimethylsilyl groups bound to the ylidic carbon atom in *C*-substituted alkylidenetriphenylphosphoranes by PX_2 – units (X = Cl, Br) turned out to be the best access to the corresponding (1-dihalophosphanyl)alkylidene derivatives. This method is applied especially when alkyltriphenylphosphonium bromides fail to react with phosphorus trihalides and triethylamine. The substitution proceeds rather smoothly so that even mixed compounds with both a trimethylsilyl group and a PX_2 unit bound to the ylidic carbon atom have been isolated. They tend to eliminate halotrimethylsilane but the monomer $Ph_3P{=}C{=}P{\sim}X$ formed first is thermally unstable and oligomerises to give a dimer (**F**), a trimer and an ionic tetramer (**G**, Scheme 4.3).

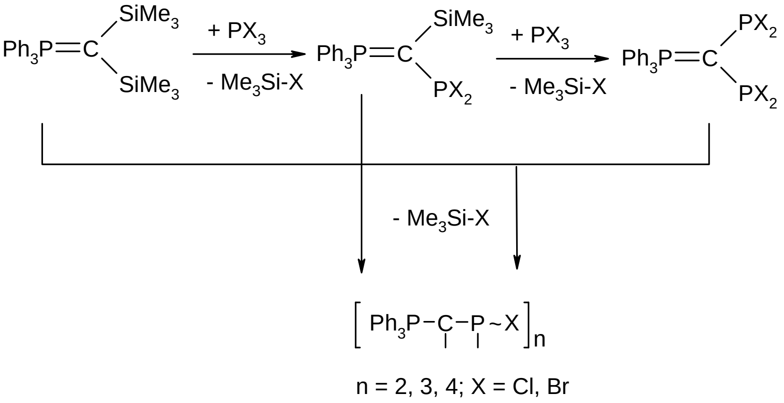

Schmidpeter discovered that the P–Br distance of the bromine compounds correlates with the dihedral angle X–P–C–P. The more this angle tends towards 90°, the longer the P–Br bond becomes. The correlation is not as obvious for the chlorine compounds [237-239].

In order to describe the negative hyperconjugation effect of the P–Cl- and P–Br bonds mentioned, a further pair of angles, α′ and θ′, must be included. α′ is defined as the tilt angle between the *p* orbital of the carbanionic centre and the antibonding orbital of the P–X bond, and θ′ is the dihedral angle between both orbitals. Both angles describe the ability of the orbitals to overlap and thus at the same time their contribution to the negative hyperconjugation, which in turn is associated with a lengthening of the P–X distance.

The last row in Table 4.7 relates the percentage lengthening of the P–X bond compared to the relevant bond lengths of the simple phosphorus halides, PCl_3 and PBr_3. Low values for α′ and θ′ here are associated with a significant lengthening of the P–X distance. Particular attention should be paid to the P–Cl bond in the triphosphadewarbenzene derivatives **3a** – **3d**, which are up to 30% longer than the standard value for phosphorus(III) chloride. The α′ and θ′ angles as mentioned in Table 4.7 for the triphosphadewarbenzene derivatives **3a** – **3d** and the other literature compounds of the longer P–X bond are very well correlated with the dihedral and tilt angle.

X-ray structure analyses (Table 4.4.) reveal a molecule, which is characterized by an ylidic and a regular P–C double bond of almost equal length [$P1^{\oplus}–C2^{\ominus}_{av.}$ 172.2 pm, $P5–C6_{av.}$ 169.6 pm]. In addition to these two characteristic features the average bond length P3–C2 is found to be considerably shortened to a value of 172.7 pm, whereas the adjacent phosphorus chlorine bond P3–Cl1 is strongly elongated to 245.5 pm. The bonding situation encountered here makes the rapid 1,3-migration of the chlorine atom between (Figure 4.15.a) the two phosphorus atoms P3 and P5 – as derived from the $^{31}P\{H\}$ NMR spectra – quite understandable.

We could not yet establish the, however, existence of isolated halide anions in solution or isolate derivatives with separate cations.

The formation of an ylidic $P^{\oplus}—C^{\ominus}$ bond in compounds **3a** to **3b** gives a straightforward explanation why the adjacent P–Cl bond is found to be strongly elongated. As can already be taken from the expresion “ylidic”, the sp^2-hybridized carbon atom C2 has to be considered a carbanion, whereas the positive charge is located at the four coordinate phosphorus atom P1. An electronic interaction between the free electron pair at carbon and the empty σ*(P–Cl) orbital not only shortens the bond C2–P3 but also elongates the bond P3–Cl1 by about 60 pm with respect to the standard value of 204.3 pm (Figure 4.15.b).

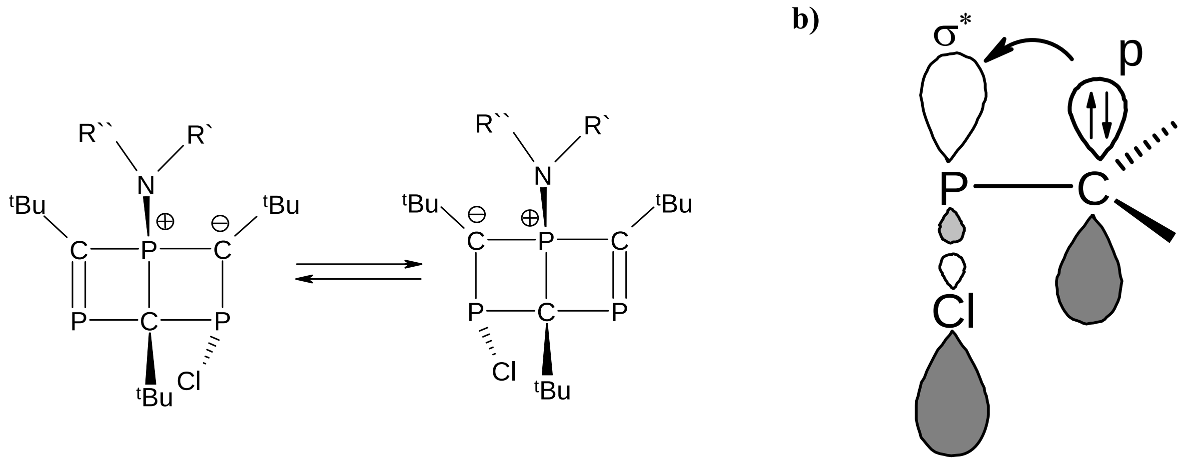

electronic interaction between the free electron pair at carbon and the σ*(P–Cl) orbital

Figure 4.15. Rapid 1,3-chlorine exchange in compounds **3a** to **3b** (a) as a consequence of the strong elongation of the P–Cl bond (b)

The conclusion for these particularly large distances is based on the "*negative hyperconjugation*", introduced by *Schleyer and Kos* [283], and on the "*anomeric effect*" first described by *Kriby* [284].

The arrangement of bonds around nitrogen is planar coordinated (sum of the bond angles around nitrogen lie in the range between ($\sum N$ = 358.3° for **3a** and $\sum N$ = 360.0° for **3c**), as with the sum of bond angles around C2 or C6 within the inaccuracy of the respective standard deviation; sp^2-hybridization of a carbon atom lie in the range $\sum C2(sp^2)$ = 357.7° for **IIB** and $\sum C2(sp^2)$ = 359.4° for **3c** and also lie in the range $\sum C6(sp^2)$ = 357.3° for **3c** and $\sum C2(sp^2)$ = 358.5° for **IIA**. In contrast to these observations, the carbon atom C4 contains a strong central distorted tetrahedral geometry.

The two four-membered heteocyclic rings P1,C2,P3,C4 and P1,C4,P5,C6 of bicyclic triphosphabicyclo[2.2.0]hexa-1,5-dienes are as far as possible planar; only individual atoms protrude slightly from the associated planes C and D (Table 4.6 C and D). The respective folding at the two vectors P1…P3 and/or P1…P5 show the bond angles in the range 4.1° and 6.8°. The calculation of both planes (C and D) of four-membered heterocyclic rings include the average dihedral angles of 62.7°; their associated average angles of the bridgehead atoms C2–P1–C6 and P3–C4–P5 show average values of 121.7° and 113.7°. The means of both average values is 117.7°; the same average dihedral angles of the conjugate angles to 180° of the average dihedral angle between both planes C and D (180°–62.7° = 117.3°).

Table 4.6. Least-Squares Planes and Deviations (pm) of Atoms from Planes for Dialkylamino-$1\lambda^5\sigma^4,3\lambda^3\sigma^3,5\lambda^3\sigma^2$-triphosphabicyclo[2.2.0]hexa-1,5-dienes **3a** to **3d**.

a) Project Plane A

	C2*[a]	P3*	P5*	C6*	Cl1	P1	C4	C21	C41	C61	N1
3a	–1.4	1.4	–1.4	1.4	198.3	–84.8	–103.3	71.7	–232.0	88.6	–206.4
3b	–2.1	2.0	–2.0	2.1	197.4	–86.0	–103.0	76.7	–230.6	87.7	–207.0
3c	–1.7	1.7	–1.7	1.8	197.2	–85.3	–103.0	69.9	–229.4	91.8	–207.7
3d	0.3	–0.3	0.3	–0.3	–198.5	84.2	102.8	–86.1	230.2	–77.2	205.4

b) Plane B

	P3*[a]	C4*	P5*	Cl1	P1	C2	C6	C21	C41	C61	N1
3a	0	0	0	–72.9	181.3	172.3	169.9	273.4	–88.7	267.1	286.1
3b	0	0	0	75.0	–180.8	–172.2	–169.9	–271.0	92.0	–264.9	–285.0
3c	0	0	0	73.6	–180.3	–172.3	–169.5	–271.3	93.9	–260.3	–282.3
3d	0	0	0	72.1	–181.3	–171.9	–171.0	–268.5	88.8	–272.2	–287.4

c) Plane of Four-membered Heteocyclic Ring (C) of Bicyclic

	P1*[a]	C4*	P3*	C2*	C6	P5	Cl1	C21	C41	C61	N1
3a	3.6	–3.3	3.4	–3.8	159.8	166.2	229.5	6.2	–110.6	273.4	–102.5
3b	3.7	–3.4	3.5	–3.7	159.9	165.0	237.8	13.0	–110.7	275.2	–100.3
3c	–3.6	3.3	–3.4	3.8	–160.7	–165.5	–229.2	–3.7	109.1	–279.5	103.3
3d	–3.7	3.5	–3.7	3.9	–156.6	–166.7	–259.6	–20.8	108.6	–263.7	102.9

d) Plane of Four-membered Heteocyclic Ring (D) of Bicyclic

	P1*[a]	P5*	C6*	C4*	P3	C2	Cl1	C21	C41	C61	N1
3a	3.1	3.1	–3.3	–2.9	168.4	152.9	287.6	256.8	–106.5	22.6	–109.8
3b	2.2	2.3	–2.4	–2.1	169.4	153.0	275.9	260.1	–103.0	19.2	–110.2
3c	2.9	3.0	–3.1	–2.8	168.1	152.4	284.6	256.8	–103.9	23.8	–109.5
3d	–3.2	–3.2	3.4	3.0	–165.9	–154.9	–257.3	–267.8	106.8	–11.1	108.5

e) Selected Dihedral Angles (°) between Planes

	A/B	A/C	A/D	B/C	B/D	C/D	P1, C6, P5/P1, P5, C4	P1, C2, P3/P1, C4, P3
3a	87.6	31.6	31.3	90.3	91.5	62.5	5.7	6.5
3b	91.9	31.9	31.7	89.5	88.1	63.2	4.1	6.6
3c	92.6	31.8	31.3	90.1	88.9	62.8	5.4	6.5
3d	87.4	31.5	31.2	90.9	90.6	62.4	5.9	6.8
Average	89.9	31.7	31.4	90.2	89.8	62.7	5.3	6.3

a) Atoms marked with an asterisk define the plane and were used to calculate the plane

Intramolecular distances involving phosphorus atoms are given in Table 4.7. The atoms P3 and P5 of the λ^3-phosphorus approach the bridging atom of four coordinate a positively charged phosphorus atom (P1) at an average distance of 257 pm. This value differs from the standard P–P bond length of (221 pm [188]) by only 36 pm. At 390.4 pm the shortest interionic distance between the phosphorus atom P1 and Cl1, however, is about twice as long as the uncorrected sum of the corresponding covalent radii of the two elements P...Cl 209 [124].

Table 4.7. Atomic Distances (pm) for Dialkylamino-1$\lambda^5\sigma^4$,3$\lambda^3\sigma^3$,5$\lambda^3\sigma^2$-triphosphabicyclo[2.2.0]hexa-1,5-dienes **3a** to **3d**.

Atomic distances	3a	3b	3c	3d	Average
P1…P3	256.4	256.2	256.3	257.5	256.6
P1…P5	258.9	256.8	257.2	256.7	257.4
P1…Cl	391.8	389.7	391.7	388.3	390.4

The packing of the molecules in the unit cell is shown in the stereoscopic drawing in Figures 4.15-4.18. There are no intermolecular contacts less than the *van der Waals* distances.

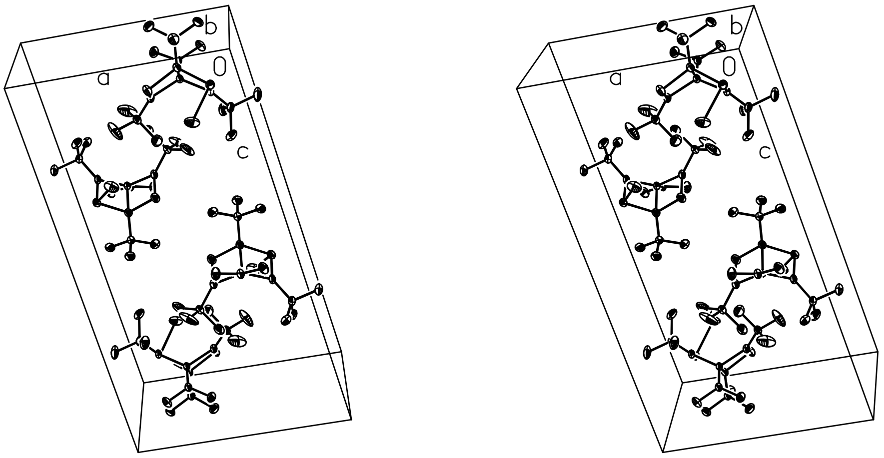

Figure 4.15. Unit cell contents of compound **3a** in stereoscopic view. Thermal ellipsoids are at 30% probability; hydrogen atoms have been omitted for clarity.

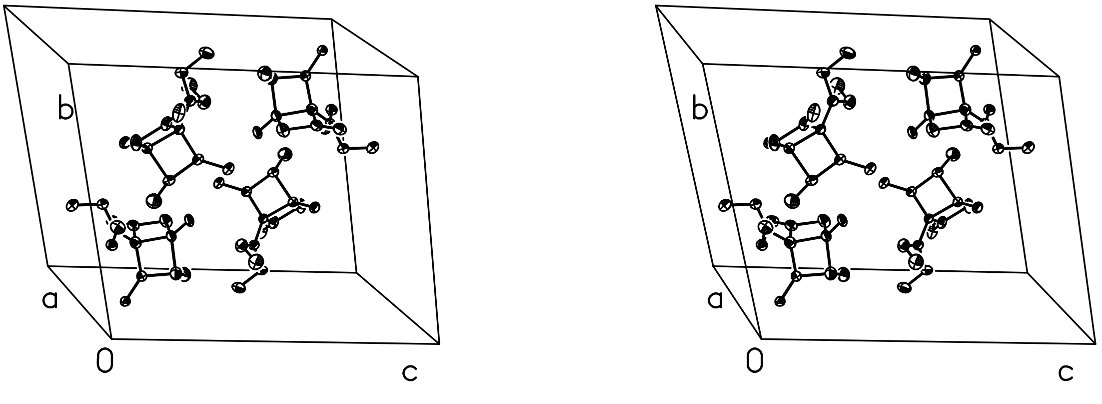

Figure 4.16. Unit cell contents of compound **3b** in stereoscopic view. The unit cell contains two crystallographically independent molecules (**I** and **IIA**) without **IIB**. Thermal ellipsoids are at 20% probability; methyl groups and hydrogen atoms have been omitted for clarity [100].

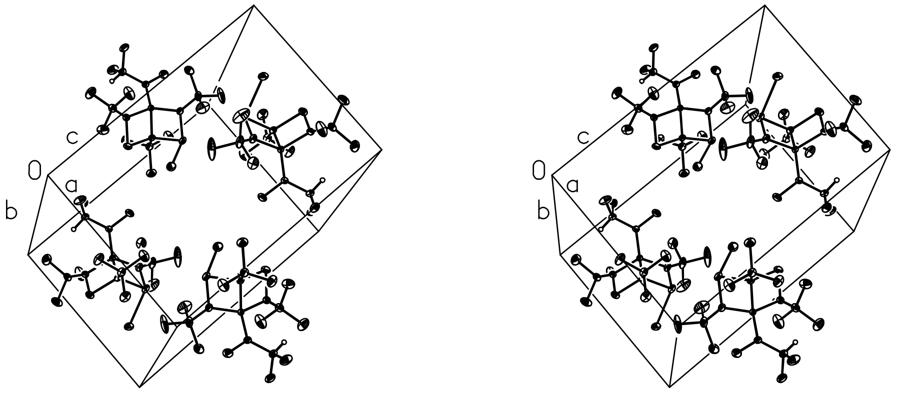

Figure 4.17. Unit cell contents of compound **3c** in stereoscopic view. Thermal ellipsoids are at 30% probability; hydrogen atoms are omitted for clarity; except for the CH–group of the isopropyl substituent is shown.

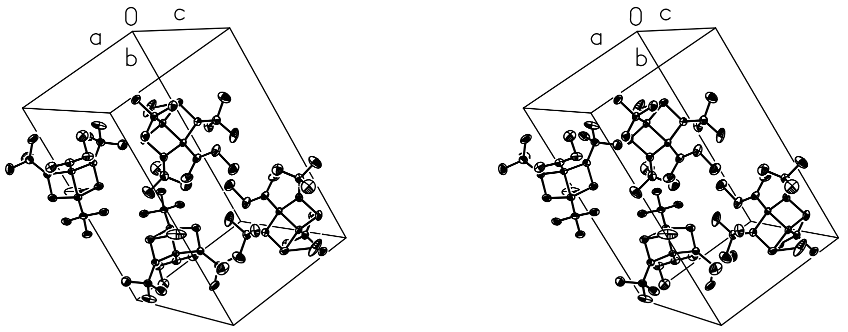

Figure 4.18. Unit cell contents of compound **3d** in stereoscopic view. Thermal ellipsoids are at 30% probability; hydrogen atoms have been omitted for clarity.

4.2.3.3. Quantum Chemical Calculations on (Dimethylamino)phosphines, P-Amino Substituted Methylenephosphoranes and Analogous Derivatives as well as on Triphosphabicyclo[2.2.0] hexa-1,5-dienes

4.2.3.3. Calculations on (Dimethylamino)phosphines. In the course of thorough efforts to trace out correct standards for different types of P–N bond lengths, quantum chemical calculations were performed [253] at the MP2/6-31G* level at first on the still unexplored heteroleptic (dimethylamino)methylphosphines $(Me_2N)_{3-x}Me_xP$ (x = 1, 2). In order to allow a better comparison with already published data the tris(dimethylamino) derivative and trimethylphosphine were included. Calculations on compound $(Me_2N)_3P$ gave exactly the same results as already obtained by *Mitzel*, *Rankin* et al. [212]. The C_s-conformation of the molecule (Fig. 4.19 **a**) was found to be lowest in energy; showing values of 171.9 and 175.5 pm (Table 4.8) the bond lengths between phosphorus and nitrogen in an almost planar and a pyramidal environment, respectively, differ considerably.

For the heteroleptic phosphine $(Me_2N)_2MeP$, C_s-conformation turned out to be the minimum in energy as well (Fig. 4.19 **b**). The P–C bond length of 184.0 pm is by about 1 pm shorter than the calculated and experimentally determined [173] distances of trimethylphosphine. Since the sum of angles (351.3°) indicate an almost planar environment of both the symmetry related nitrogen atoms, the P–N bond length of 173.0 pm does not differ significantly from the $P–N_{sp2}$ value of the tris(dimethylamino) derivative (171.9 pm). In this context one, however, should bear in mind that such a calculated distance of 173.0 pm does correspond to the standard bond length recommended by *Blom* and *Haaland* [133], but in compound C_s-$(Me_2N)_2MeP$ it refers to an sp^2-hybridised and not an sp^3-hybridised nitrogen atom.

Calculations on the second heteroleptic compound $(Me_2N)Me_2P$ revealed that both conformations ascribable to the two point groups C_s (Fig. 4.19 **c**) and C_1 (Fig. 4.19 **d**) are local minima on the potential energy surface; but in this case the C_1-conformer is by 20 kJ mol^{-1} lower in energy than the C_s -conformer. Whereas the P–C bond lengths of 184.5 and 185.7 pm for C_1 and 184.8 pm for C_s (Table 4.8) correspond to the standard value [173], the strongly elongated P–N distance of 177.5 pm in the C_s-conformer is attended by a sum of angles of 331.8° at nitrogen and a pronounced trigonal pyramidal environment. Since, however, a medium value of 347.7° for the nitrogen atom in the C_1-conformer indicates only the onset of planarisation, the P–N distance of 173.9 pm is found to be still relatively long. The results obtained by quantum chemically calculation for trimethylphosphine (Fig. 4.19 **e**) are as expected: the point group of the molecule is C_{3v}; the P–C distance of 185.2 pm corresponds to the standard value [173].

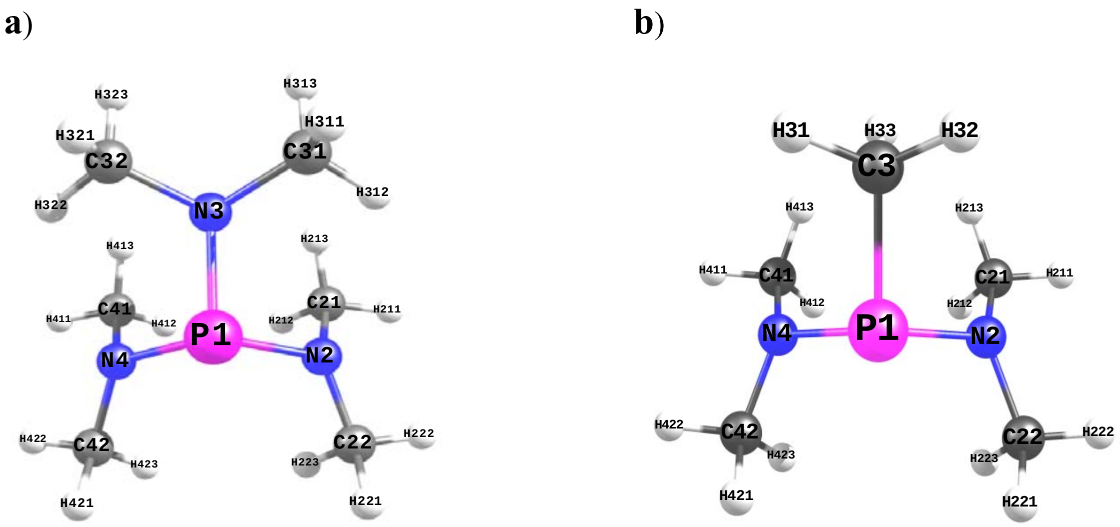

(Me$_2$N)$_3$P; C_s-symmetry

(Me$_2$N)$_2$MeP; C_s-symmetry

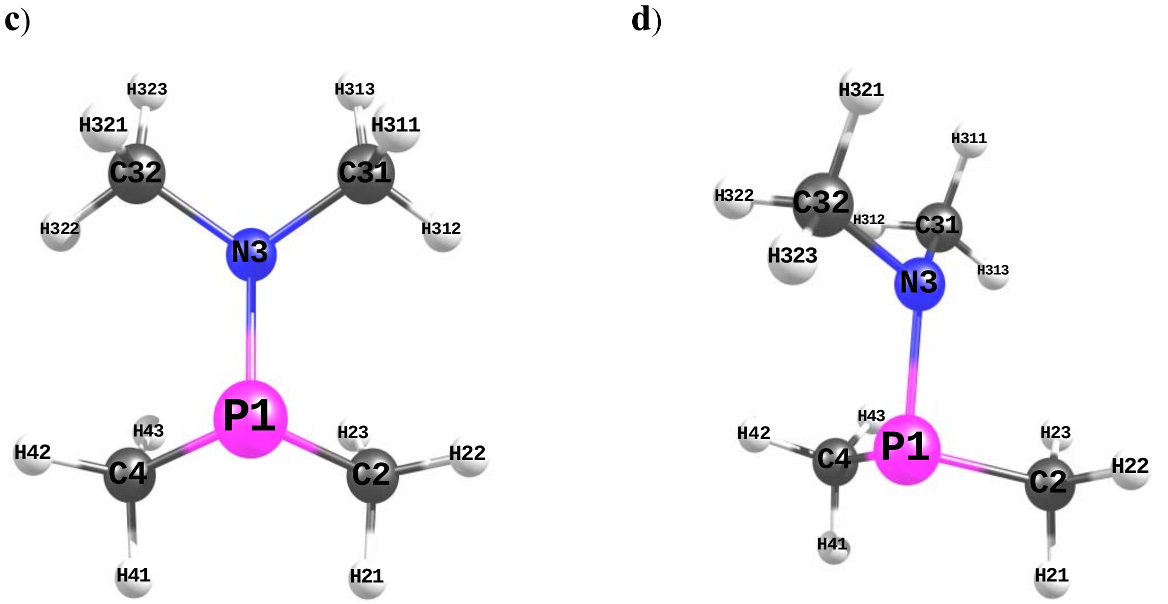

(Me$_2$N)Me$_2$P; C_s-symmetry

(Me$_2$N)Me$_2$P; C_1-symmetry

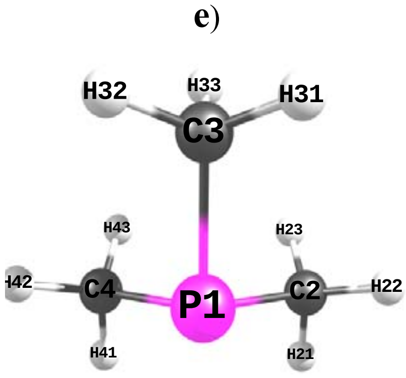

Me$_3$P; C_{3v}-symmetry

Figure 4.19. Molecular models of the compounds (Me$_2$N)$_3$P (**a**), (Me$_2$N)$_2$MeP (**b**), (Me$_2$N)-Me$_2$P (**c** and **d**), and Me$_3$P (**e**) obtained by quantum chemically calculation at the MP2/6-31G* level

Table 4.8. Results of Quantum Chemical Calculations at the MP2/6-31G* Level of Theory on (Dimethylamino)phosphines and Related Compounds.

Compound	$(Me_2N)_3P$	$(Me_2N)_2MeP$	$(Me_2N)Me_2P$		Me_3P
Molecular Symmetry	C_s	C_s	C_s	C_1	C_{3v}
P1–N2	171.9	173.0			
P1–N3	175.5		177.5	173.0	
P1–C2			184.8	184.5; 185.7a)	185.2
P1–C3		184.0			
N2–C21	145.7	145.7			
N2–C22	145.6	145.9			
N3–C31	146.7		146.6	145.7; 146.0b)	
N2–P1–N3	96.5				
N2–P1–N4	112.0	112.5			
P1–N2–C21	116.5	124.4			
P1–N2–C22	123.8	115.4			
C21–N2–C22	113.1	111.5			
P1–N3–C31	112.9		111.3	121.0	
P1–N3–C32	c)		c)	115.1	
C31–N3–C32	109.4		109.2	111.6	
N2–P1–C3		99.7			99.2d)
N3–P1–C2			98.4	105.2; 100.9e)	
N3–P1–C4			c)	98.6	
∑∠N2	353.4	351.3			
∑∠N3	335.2		331.8	347.7	

a) P–C4; b) N3–C32; c) related by symmetry, d) C2–P1–C3, e) N3–P1–C4

Retrospectively, one has to point out that the symmetry degradation from point group C_{3v} to C_s in the tris(dimethylamino) derivative $(Me_2N)_3P$ [212] and from C_s to C_1 in $(Me_2N)Me_2P$ remains difficult to understand. An explanation taking into consideration the steric demand of the dimethylamino groups seems to be plausible but in view of only small differences in energy between the different conformers the problem has to be treated with a high degree of caution.

4.2.3.4. Calculations on Methylenephosphoranes. After successful studies on several (dimethylamino)phosphines quantum chemical calculations [253] switched over on different types of methylenephosphoranes. As discussed in the preceding chapter a comparison of structural data obtained from a greater number of alkylidenephosphoranes with one, two or three diorganylamino groups at phosphorus (Scheme 4.2, pages 137-138) indicate an unexpected correlation between the conformation of the molecules and their bond lengths and angles. Particularly, a strong elongation of the P–N distance, a widening of the C=P–N angle and an sp^3-hybridisation of the nitrogen atom occur when the P–N bond concerned and the vector of the free electron pair at the ylidic carbon atom are found in an ecliptic position.

In order to shed some light on the electronic interactions in those molecules and to elaborate common features for this class of compounds, calculations at the MP2/6–31G* level again were performed on the homoleptic species $Me_3P{=}CH_2$ (Fig. 4.20, **P1**) and $(H_2N)_3P{=}CH_2$ (**P6**) as well as the heteroleptic derivatives $(H_2N)Me_2P{=}CH_2$ (**P2** and **P3**, Table 4.9) and

$(H_2N)_2MeP{=}CH_2$ (**P4** and **P5**). In this series of methylenephosphoranes, however, the dimethylamino substituent of the previously studied phosphines has now been exchanged for the parent NH_2 group in order to save computing time. Moreover, the compounds $H_3P{=}CH_2$ (**P7**), $Cl_3P{=}CH_2$ (**P8**) and $(H_3Si)_3P{=}CH_2$ (**P9**) were included into the calculations.

For a better comparison of results obtained from quantum chemical calculations and compiled in Table 4.9 a uniform numbering scheme has been applied for all methylenephosphorane molecules. Number 1 is assigned to the atoms of the central P=C unit, number 3 to that atom E, the P–E bond of which eclipses the vector of the free electron pair at the ylidic carbon. The two remaining atoms at the four coordinate phosphorus are given the numbers 2 and 4. With a careful inspection of Table 4.9 the following characteristic features can be discerned:

α) The P=C distances vary only slightly between 165.5 and 167.9 pm; the bond length of the trichloro derivative, however, is found to be notably shorter (163.8) and that of the trisilyl compound to be elongated to 172.6 pm.

β) The methylene group adopts a staggered position relative to the other P–E bonds at phosphorus; as a consequence the particular bond P1–E3 roughly dissects its H–C–H angle (Fig. 4.20).

γ) The hydrogen atoms of the methylene group tend very slightly towards atom E3 or its substituents.

δ) In all molecules including even those of the compounds $H_3P{=}CH_2$, $Cl_3P{=}CH_2$ and $(H_3Si)_3P{=}CH_2$, the bond P1–E3 (E = C, N, H, Cl, Si) exceeds the other P–E bonds to the same element E appreciably in length. This phenomenon is best explained with a negative hyperconjugation mainly between the free electron pair at the ylidic carbon atom C1 and the σ^*–orbital of the P1–E3 bond (see further discussion). Typical ranges or values are as follow:

P1–C3 (183.9 to 187.6 pm) *vs.* P1–C2/C4 (181.8 to 182.2 pm)
P1–N3 (173.0 to 175.9 pm) *vs.* P1–N2 (168.5 to 170.3 pm)
P1–H3 (144.0 pm) *vs.* P1–H2 (140.4 pm)
P1–Cl3 (209.3 pm) *vs.* P1-Cl2 (201.4 pm)
P1-Si3 (234.2 pm) *vs.* P1–Si2 (225.0 pm)

ε) The angle C1–P1–E3 varies between 125.4° and 133.1°; it is the largest within the group of C1–P1–E angles. C1–P1–E2 and C1–P1–E4 are substantially smaller (103.8° to 112.6°).

For different P1–E3 bonds the following data were calculated:

C1–P1–C3 (125.4° to 129.5°) *vs.* C1–P1–C2/C4 (109.3 to 110.7°)
C1–P1–N3 (128.3° to 133.1°) *vs.* C1–P1–N2 (106.8° to 112.6°)
C1–P1–H3 (130.7°) *vs.* C1–P1–H2 (111.4°)
C1–P1–Cl3 (126.9°) *vs.* C1–P1–Cl2 (110.7°)
C1–P1–Si3 (129.1°) *vs.* C1–P1–Si3 (103.8°)

ζ) In nearly all molecules under consideration the angle E2–P1–E4 is larger than the angle E3–P1–E2 or E3–P1–E4 irrespective of the element. Here, however, the trisilyl derivative forms an exception.

C2–P1–C4 (106.4° to 109.5°) *vs.* C3–P1–C2/C4 (101.4° to 101.5°)
N2–P1–C4 (108.7° to 115.8°) *vs.* C3–P1–N2 (97.6° to 97.7°)
N2–P1–N4 (119.8° to 121.5°) *vs.* N3–P1–N2 (93.6° to 94.4°)
H2–P1–H4 (105.5°) *vs.* H3–P1–H2 (97.3°)
Cl2–P1–Cl4 (109.7°) *vs.* Cl3–P1–Cl2 (98.6°)
Si2-P1-Si4 (106.0°) *vs.* Si3–P1–Si2 (106.1°)

η) Whereas the sum of angles about atom N3 (326.5° to 330.6°) deviates only very slightly from the value expected for *sp*^{3}-hybridisation, the sum about atom N2 (342.3 to 346.8) already indicates the onset of planarisation.

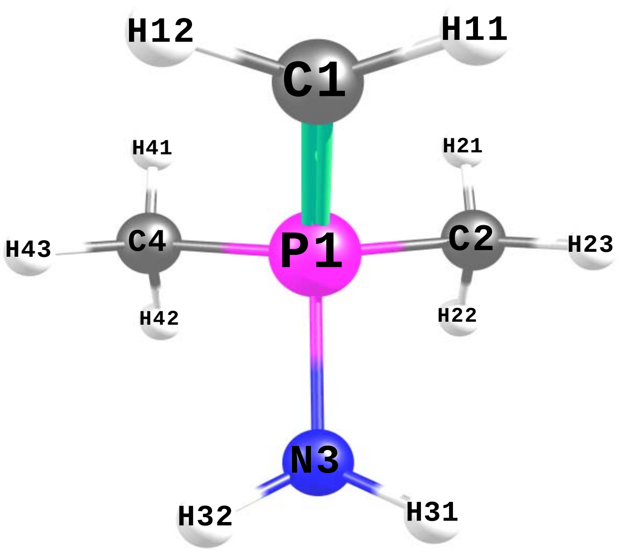

$(H_2N)Me_2P=CH_2$ (**P2**)
C_s-Symmetry

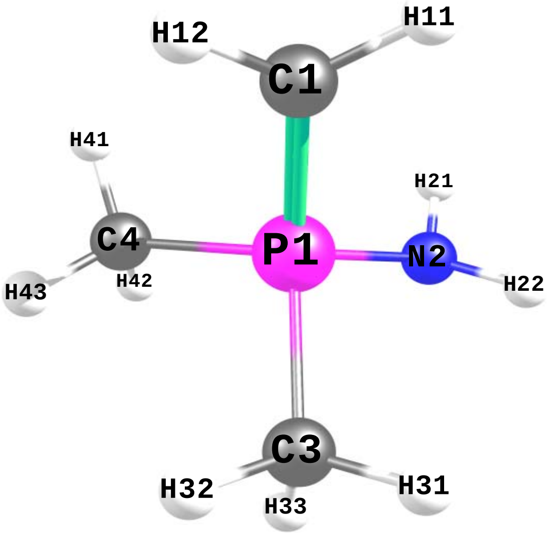

$(H_2N)Me_2P=CH_2$ (**P3**)
C_1-Symmetry

< to Figure 4.20 >

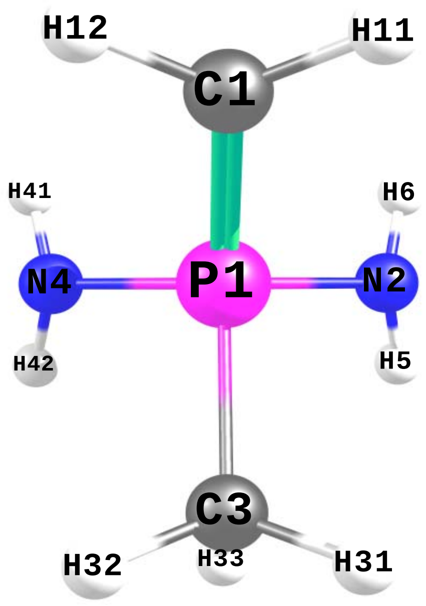

$(H_2N)_2MeP{=}CH_2$ (**P4**)
C_s-Symmetry

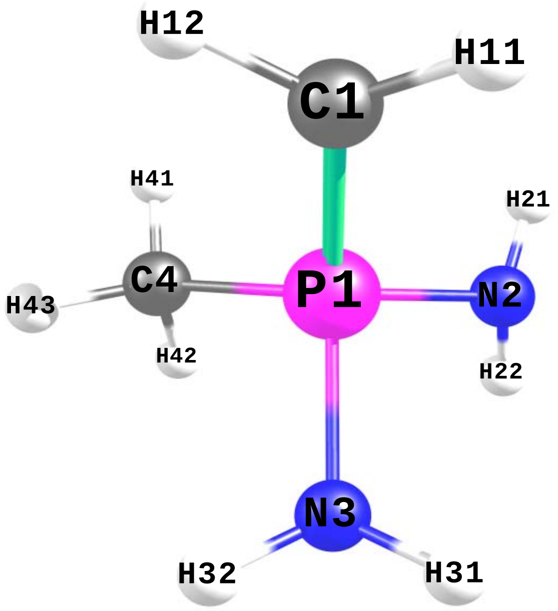

$(H_2N)_2MeP{=}CH_2$ (**P5**)
C_1-Symmetry

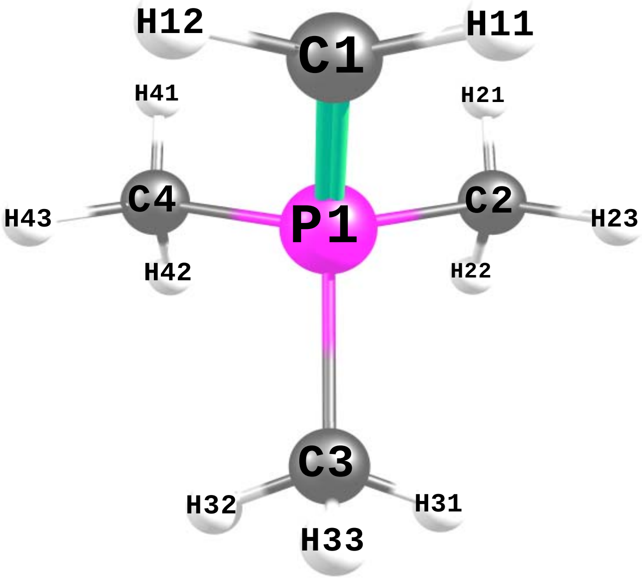

$Me_3P{=}CH_2$ (**P1**)

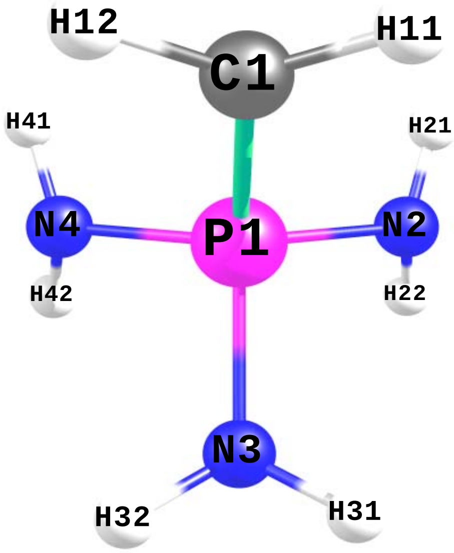

$(H_2N)_3P{=}CH_2$ (**P6**)

< to Figure 4.20 >

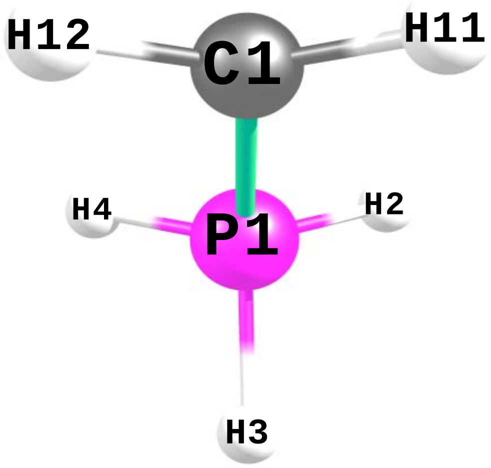

$H_3P{=}CH_2$ (**P7**)

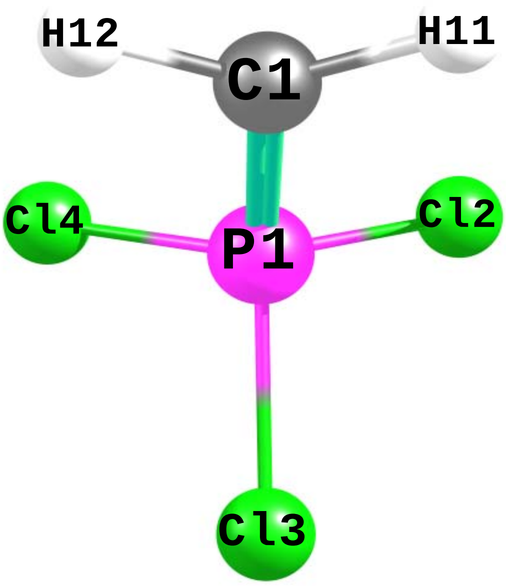

$Cl_3P{=}CH_2$ (**P8**)

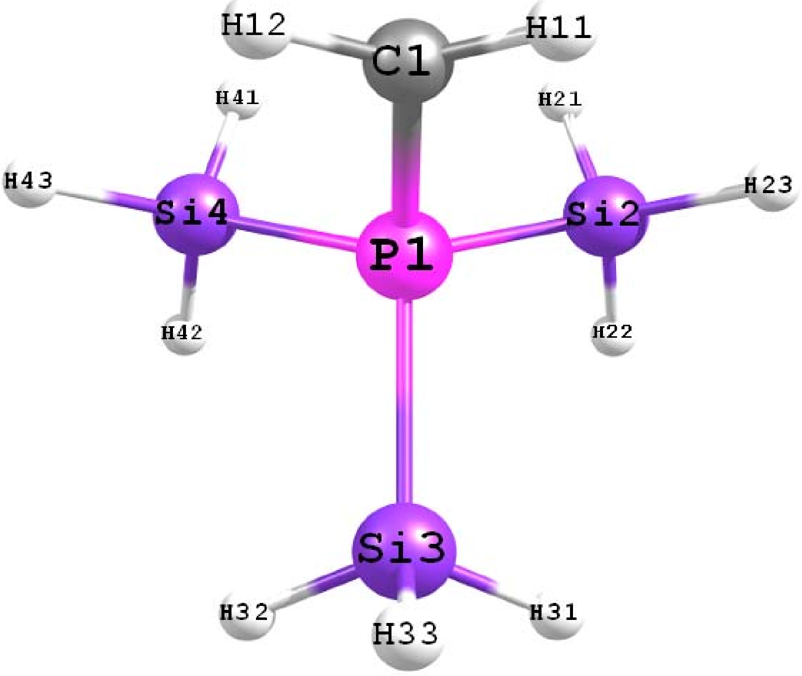

$(H_3Si)_3P{=}CH_2$ (**P9**)

Figure 4.20. Molecular models of different methylenephosphoranes obtained from quantum chemical calculations at the MP2/6–31G* level

Table 4.9. Results (pm, deg.) of Quantum Chemical Calculations at the MP2/6-31G* Level on Substituted Methylenephosphoranes. For an explanation of the numbering scheme applied here see discussion !

	$Me_3P{=}CH_2$	$(H_2N)Me_2P{=}CH_2$		$(H_2N)_2MeP{=}CH_2$		$(H_2N)_3P{=}CH_2$	$H_3P{=}CH_2$	$Cl_3P{=}CH_2$	$(H_3Si)_3P{=}CH_2$
	C_s (**P1**)	C_s (**P2**)	C_1 (**P3**)	C_s (**P4**)	C_1 (**P5**)	C_s (**P6**)	C_s (**P7**)	C_s (**P8**)	C_s (**P9**)
							H ≙ N	Cl ≙ N	Si ≙ N
P1=C1	167.9	166.7	166.5	166.0	165.8	165.5	167.6	163.8	172.6
C1–H11	108.7	108.5	108.4	108.3	108.3	108.2	108.4	108.4	108.9
C1–H12	a)	a)	108.3	a)	108.3	a)	a)	a)	a)
P1–C3	187.6		184.7	183.9					
P1–C2	182.2	181.8							
P1–C4			181.9		182.2				
P1–N3		175.9			174.0	173.0	144.0	209.3	234.2
P1–N2			170.3	169.1	168.5	168.5	140.4	201.4	225.0
C1–P1–C3	125.5		125.4	129.5					
C1–P1–C2	110.2	110.7							
C1–P1–C4			109.3		109.4				
C3–P1–C2	101.4								
C3–P1–C4			101.5						
C2–P1–C4	106.4	109.5							
C1–P1–N3		128.3			130.1	133.1	130.7	126.9	129.1
C1–P1–N2			112.6	106.8	109.5	107.5	111.4	110.7	103.8
C3–P1–N2			97.9	97.6					
N3–P1–C2		98.0							
N3–P1–C4		98.0			98.2				
N3–P1–N2					93.6	94.4	97.3	98.6	106.1
N2–P1–C4			108.7		115.8				
N2–P1–N4				119.8		121.5	105.5	109.7	106.0
P1–C1–H11	116.6	118.4	119.6	117.9	120.1	118.5	116.7	118.1	114.8
P1–C1–H12	a)	a)	117.8	a)	117.9	a)	a)	a)	a)
H11–C1–H12	115.7	116.7	117.6	118.2	117.9	118.2	116.6	119.7	113.9
Σ∠C1	348.9	353.5	355.0	354.0	355.9	355.2	350.0	355.9	353.5
P1–N3–H31		110.1			110.6	111.0			
P1–N3–H32		a)			111.2	a)			
H31–N3–H32		106.3			107.8	108.6			
Σ∠N3		326.5			329.6	330.6			
P1–N2–H21			112.4	114.8	114.9	115.2			
P1–N2–H22			117.5	118.7	117.4	116.8			
H21–N2–H22			112.4	113.3	114.3	113.8			
Σ∠N2			342.3	346.8	346.6	345.8			

a) related by symmetry

When the sum of angles at the ylidic carbon atom C1 of the alkylidenephosphorane $E_3P^{\oplus}–CR_2^{\ominus}$ deviates significantly from 360°, an increasing amount of *s* character is added to the *p* orbital filled with two non-bonding electrons, and its character changes increasingly to sp^3. Furthermore, as mentioned earlier (γ, page 153), both residues R^1 and R^2 tend decidedly towards atom E3, which is bound to phosphorus P1 and its substituents. From the NBO analysis, a double bond can initially be assumed between the atoms P1 and C1; this conception is in accordance with the *ylene* form of the phosphorane $E_3P=CH_2$. Second order perturbation analysis shows donor-acceptor interactions to be present between a bonding molecular orbital of the P=C bond and the antibonding P1–E3 orbital as well as conversely between the bonding P1–E3 orbital and the antibonding molecular orbital between P1 and C1.

In contrast, the NBO charges give values of –1.3 at atom C1 and approximately +2 at atom P1, depending on the substituents E1 to E3. These values correspond much more with the *ylidic* form $E_3P^{\oplus}–CH_2^{\ominus}$ characterized by a nonbonding electron pair at C1. The *Mulliken* charges (ca. –0.7 at C1 and approximately +1 at P1) concur with this idea. Thus one should focus the discussion on the latter form, for it represents the charge distribution much better. Based on this picture, overlap of the $\sigma_{p\rightarrow sp3}$(C1) orbital at carbon C1 with the σ^*(P1–E3) orbital of the bond P1–E3 and conversely overlapping of $\sigma^*_{p\rightarrow sp3}$(C1) with the σ(P1–E3) orbital can be assumed.

According to the Lewis model the direction of the bonding σ(P1–E3) along with the antibonding σ^*(P1–E3) orbital is given by the vector P1–E3. The atom C1 and its substituents R^1 and R^2 in contrast build a plane the normal of which points towards the σ(P1–E3) and the σ^*(P1–E3) orbitals. Both vectors form the tilt angle α; it specifies the degree to which the orbitals $\sigma_{p\rightarrow sp3}$(C1) and σ^*(P1–E3) tend towards each other in order to overlap (Figure 4.21 **a**). From quantum chemical calculations on methylenephosphoranes (Table 4.10) this value is known to be low relatively often, as for example in methylenetrisilylphosphorane (0.5°), but it can also achieve significantly larger values, as shown by the C_1-symmetrical compound $(H_2N)_2MeP=CH_2$ (23.7°), Numerous alkylidenephosphoranes with methylene groups tilted substantially in the direction described above have also been found in the literature. Depending on the groups R^1 and R^2 a strong electronic interaction between the relevant orbitals σ and σ^* arises. A few selected examples are presented in Table 4.10.

Aside from the above mentioned tilt angle α, however, a further criterion, the twist angle θ, must be included for a complete assessment of the bonding situation. It describes the degree of twisting between the direction of non-bonding electron pair at the ylidic and hence largely sp^2-hybridised carbon atom C1 and the direction of the σ^*(P1–C3) orbital characterised by its vector P1–E3. This twisting of the group $C1R^1R^2$ is shown by a Newman projection along the bond $P1^{\oplus}–C1^{\ominus}$ of the alkylidenephosphorane $E_3P^{\oplus}–CR_2^{\ominus}$ (Fig. 4.21 **b**). As the vector P1–E3 and the normal of the plane formed by atoms E3, P1 and C1 build a right angle by definition, the angle which is defined by the normals of this plane and the plane $C1R^1R^2$ containing the ylidic carbon atom C1, and the torsion angle *θ* must sum up to 90°.

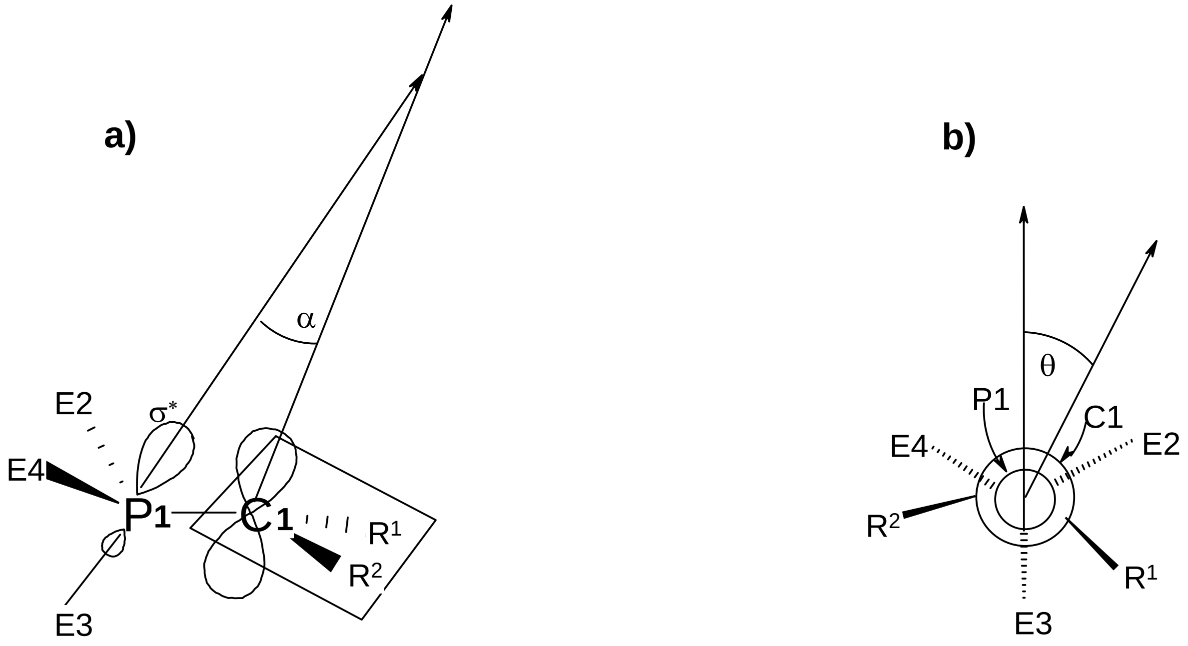

Figure 4.21. Representation of the tilt angle *α* (**a**) and the twist angle *θ* (**b**)

Table 4.10. Tilt Angles α and Twist Angles θ (°) of Several Quantum Chemically Calculated Methylenephosphoranes along with a Compilation of Selected Compounds from the Literature. For additional structural data see Table 4.5 and Table 4.9, page 132 and page 158, respectively.

Compound	α	θ	Compound	Lit.	α	θ
$Me_3P{=}CH_2$ (**P1**)	2.9	0.0	$Ph_3P{=}C(CH_2)_2$	[214]	31.5	1.7
C_s-$(H_2N)Me_2P{=}CH_2$ (**P2**)	13.2	0.0	$Ph_3P{=}C(CH_2)_3$	[215]	14.6	3.8
C_1-$(H_2N)Me_2P{=}CH_2$ (**P3**)	20.0	16.0	$^iPr_3P{=}CMe_2$	[216]	4.9	0.2
C_s-$(H_2N)_2MeP{=}CH_2$ (**P4**)	15.1	0.0	$Me_3P{=}C(PPh_2)_2$	[219]	25.8	24.7
C_1-$(H_2N)_2MeP{=}CH_2$ (**P5**)	23.7	13.9	$Ph_3P{=}C(AsPh_2)_2$	[221]	16.3	16.0
C_s-$(H_2N)_3P{=}CH_2$ (**P6**)	21.4	0.0	$Ph_3P{=}C(CN)_2$	[230]	12.6	0.0
$H_3P{=}CH_2$ (**P7**)	9.5	0.0	$Ph_3P{=}C(PCl_2)_2$	[237-239]	18.1	18.1
$Cl_3P{=}CH_2$ (**P8**)	16.3	0.0	$Ph_3P{=}C(AsCl_2)_2$	[241]	25.9	25.3
$(H_3Si)_3P{=}CH_2$ (**P9**)	0.5	0.0	$^tBu_2(Cl)P{=}CPh_2$	[245]	16.9	11.3
			$^tBu_2(Cl)P{=}CPh(SiMe_3)$	[246]	8.3	0.3

5. Tentative Extension of Present Research to Dihaloorganylarsines

5.1. Introduction

In contrast to manifold studies using different phosphorus halides as starting materials [80, 81, 87] the reactivity of 2-*tert*-butyl-1λ^3-phosphaalkyne towards compounds with an As–X bond (X = halogen) has been remaining rather unknown. Only a few research groups have worked in this field obtaining, however, some highly remarkable results. *Dautel* of our group was the first to react in his thesis [87, 88] 2-*tert*-butyl-1λ^3-phosphaalkyne with half the equimolar amount of arsenic trichloride and to prepare colourless 2,4-di-*tert*-butyl-1,3,5-trichloro-1λ^3-arsa-3λ^3,5λ^3-diphosphabicyclo[1.1.1]pentane. Unfortunately, all crystals isolated so far turned out to be disordered in that the positions of arsenic and phosphorus could not be discriminated.

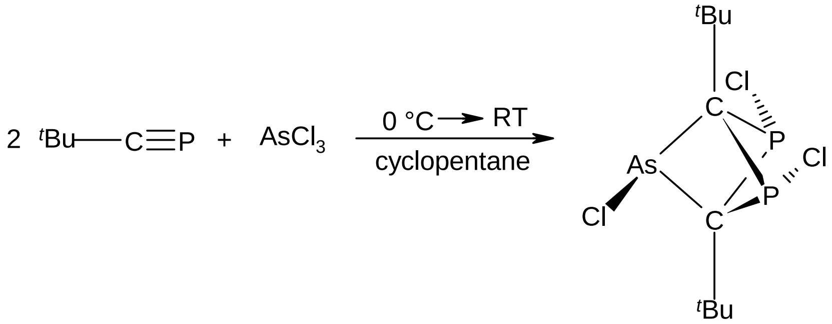

In his thesis *Merz* treated a benzene solution of 2-*tert*-butyl-1λ^3-phosphaalkyne with the tenth of an equivalent of bis(dichloroarsinyl)methane at room temperature [73]. In spite of the fact that the arsenic compound is consumed during the reaction, its function seems to be more catalytic and to initiate a tetramerization of the 1λ^3-phosphaalkyne. After a reaction time of 24 hours the already known [63, 65] highly symetrical 2,4,6,8-tetra-*tert*-butyl-1λ^3,3λ^3,5λ^3,7λ^3-tetraphosphacubane was isolated in more than 80% yield. An X-ray structure analyses showed the pale yellow crystals to be a co-crystallisate and to include one molecule of benzene per formula unit; bond lengths and angles agree very well with reported data [63, 65]. In this context, it seems worth mentioning that the oligocycle exhibits fascinating spectroscopic and structural features resulting from a unique bonding situation, in which the strong interaction of the lone electron pairs at phosphorus with the P–C σ*-antibonding orbitals of the cube reduces the nucleophilicity of the phosphorus atoms considerably [62, 63, 65, 66].

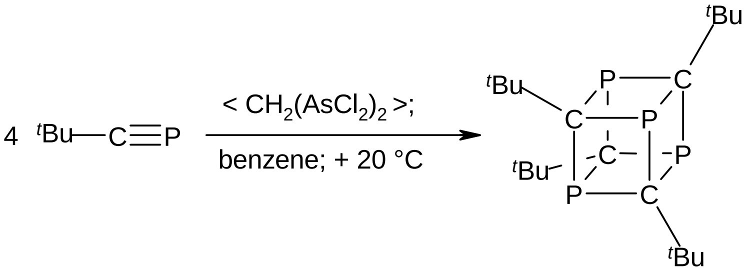

Russell et al. [182] reported the reaction of the complex 5,5-bis(η^5-cyclopentadienyl)-2,4-di-*tert*-butyl-1λ^3,3λ^3-diphospha-5-zirconia-tricyclo[2.1.0.0^{1,3}]pentane with one equivalent of arsenic(III) chloride in *n*-hexane. Within two hours at ambient temperature a yellow oily product was formed, the $^{31}P\{^1H\}$ NMR spectrum of which reveals two doublets at –42.2 and 204.8 ppm. A comparison of these values and the $^2J_{(P,P)}$ coupling constant of 47 Hz with parameters obtained from three doublets of doublets of the tricyclic cage compound (^{t}BuC)$_2$ClP$_3$ (–302.2, –121.4 and 234.7 ppm; $^1J_{(P,P)}$ = 146 and $^2J_{(P,P)}$ = 58 Hz) suggest the product to be built up analogously. Treatment with stiochometric amounts of aluminium(III) chloride in dichloromethane gave a yellow solution from which small amounts of a colourless precipitate separated when the solvent was removed slowly in vacuo. Redissolving the solid in a mixture of *n*-hexane and dichloromethane (ratio 1:3), and storing the resulting solution for 15 hours at –15 °C furnished pale yellow blocks. A single crystal X-ray diffraction analyses showed the compound to be ionic and to consist of *nido*-[3,5-^{t}Bu$_2$-1,2,4-C$_2$AsP$_2$]$^\oplus$ cations and separated [AlCl$_4$]$^\ominus$ anions.

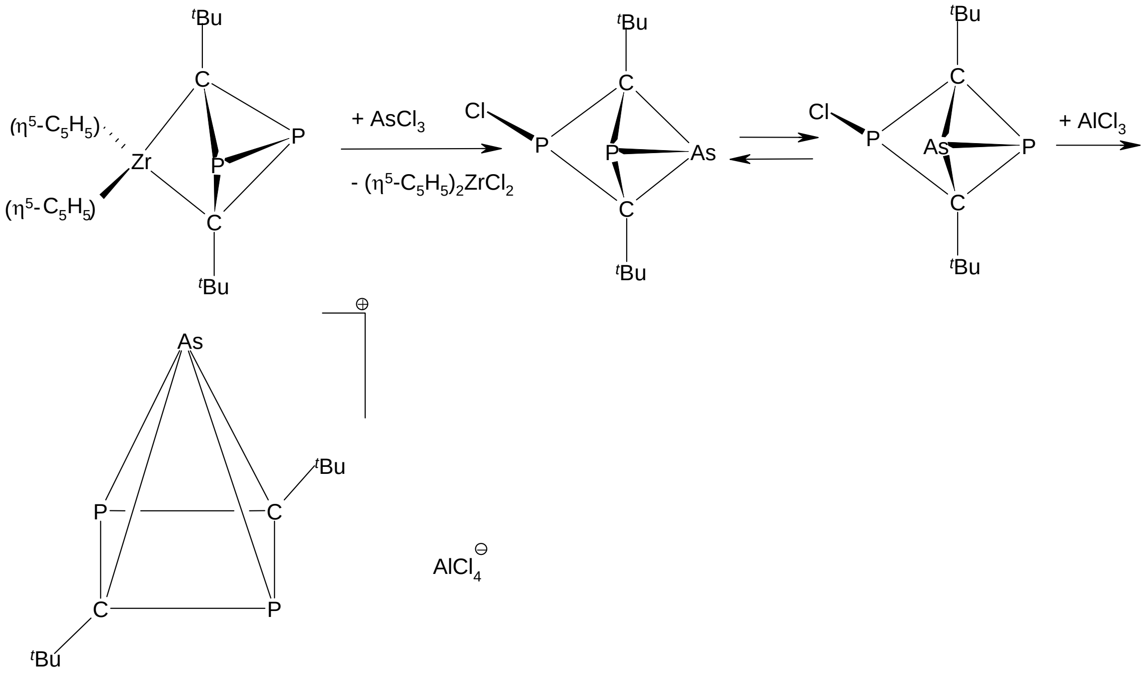

Some years ago, *Ruf* [100] of our group decided to replace the chlorine atoms of arsenic trichloride partially for diethylamino substituents and to use these arsines as starting compounds in reactions with 2-*tert*-butyl-1λ^3-phosphaalkyne. Very unexpectedly, with dichloro(diethylamino)arsine he succeeded in the preparation of an arsenic free 2,4,6-tri-*tert*-butyl-3-chloro-1-diethylamino-1$\lambda^5\sigma^4$,3$\lambda^3\sigma^3$,5$\lambda^3\sigma^2$-triphosphabicyclo[2.2.0]hexa-1,5-diene.

Within the scope of this thesis, the number of typical reactions could be enlarged by applying a series of arsines with different organyl substituents at nitrogen; syntheses as well as spectroscopic and structural properties of the 1λ^5,3λ^3,5λ^3-triphospha Dewar benzenes formed are described at full length in chapter 4.

Unlike these extensive studies on arsines with two chlorine atoms and one diorganylamino substituent bound to arsenic, only one reaction with chlorobis(diorganylamino)arsines has been performed so far. Using the diethylamino derivate *Ruf* [100] was able to isolate colourless squares of an ionic compound in 66% yield. It is built up of a 1λ^3-arsa-3λ^3,5λ^3-diphopha-7-phosphonia-homoprismane cation with a $(Et_2N)_2P$ unit bridging the carbon atoms in positions 2 and 6 and a dichlorobis(diethylamino)arsenate(III) anion.

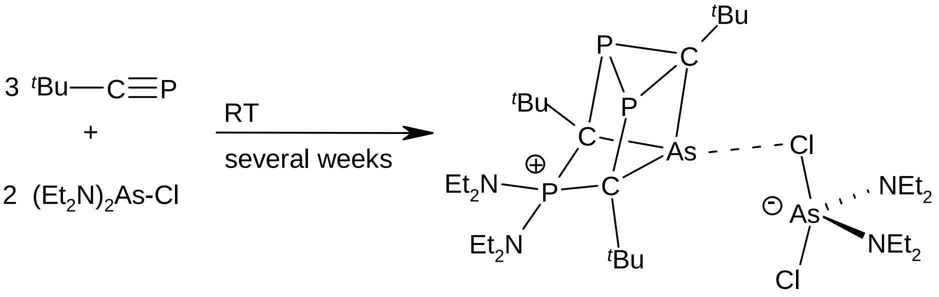

Since the formation of both the oligocycles from substituted aminochloroarsines is hardly understood, an application of vinylogous [285, 286] starting compounds such as dichloro[4-(diorganylamino)phenyl]arsines was intended in order to obtain conclusive arguments for setting up a plausible reaction mechanism. Such a procedure seems to be justified with respect to the observation of a Russian research group [287] that in the reaction of dichloro[4-(dimethylamino)phenyl]arsine with ethylmagnesium bromide not only a substitution of the two chlorine atoms but also of the complete 4-(dimethylamino)phenyl group resulting in the formation of triethylarsine is observed.

5.2. Dichloro[4-(diorganylamino)phenyl]arsine and Related Compounds

Organometallic compounds of group 15 elements may conventionally be prepared from organolithium or Grignard reagents and an easily available element(III) halide. Apart from the disadvantage that some of the halides are very sensitive against moisture, these reactions are often found to be highly exothermic. Since sometimes, however, smooth methods are required [288], syntheses such as that of [4-(dichloroarsinyl)phenyl]dimethylammonium chloride from

N,*N*-dimethylaniline and arsenic(III) chloride reported by *Michaelis* and *Rabinerson* [289] as early as 1892 deserves special attention.

From a moderately exothermic and solvent-free reaction the authors isolated a transparent, dark yellow, syrup-like product which was dissolved in water leaving behind small amounts of insoluble arsenic(III) oxide. Subsequent treatment with excess concentrated sodium hydroxide solution afforded a white precipitate first; most of it dissolved on further hydroxide addition. Thereafter, insoluble tris[4-(dimethylamino)phenyl]arsine formed by substituent exchange at arsenic (see below) could be removed by filtration; the clear filtrate which is supposed to contain the monosodium salt of [4-(dimethylamino)phenyl]arsonous acid (*i.e.* sodium hydrogen [4-(dimethylamino)phenyl]arsonite [290, 291]) was then acidified with excess hydrochloric acid. The final addition of solid anhydrous sodium carbonate to the now acidic, light green solution resulted in the formation of a slightly yellow precipitate.

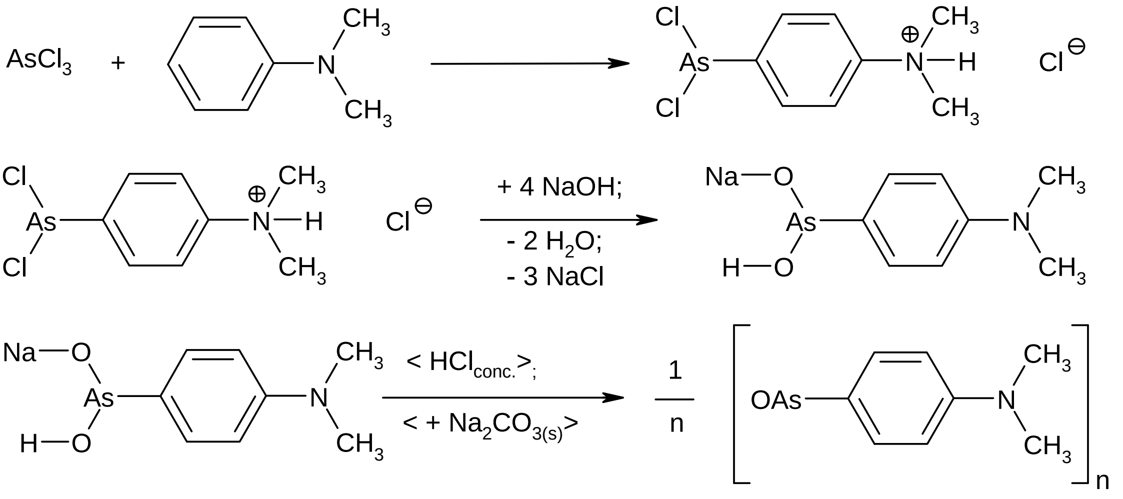

The authors assumed that the white powder obtained after careful washing and drying is [4-(dimethylamino)phenyl]oxoarsine; many compounds of such a composition are now known to be oligomeric in nature (see later). When concentrated hydrochloric acid is added to a solution of [4-(dimethylamino)phenyl]oxoarsine in dilute hydrochloric acid, after some minutes white crystals of [4-(dichloroarsanyl)phenyl]dimethylammonium chloride start to precipitate. With respect to the free base, however, it has to be pointed out that the authors were not able to convert the hydrochloride to dichloro[4-(dimethylamino)phenyl]arsine.

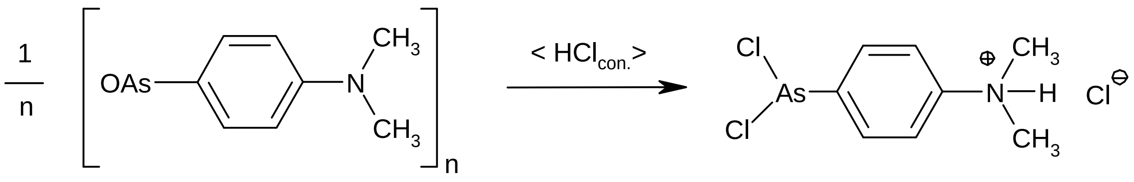

Very unexpectedly, *Michaelis* and *Rabinerson* [289] gave a nearly identical prescription for the preparation of [4-(dimethylamino)phenyl]oxoarsine and the previously mentioned tris[4-

(dimethylamino)phenyl]arsine – a compound insoluble in alkaline solution. From the high degree of similarity one might deduce that the exact reaction conditions for the exchanges of substituents at arsenic have not been known for certain and the formation of either compound may occur at random. Indeed, about fifty years later *Doak* and coworkers [292a] repeatedly failed to confirm the synthesis of [4-(dimethylamino)phenyl]oxoarsine as described by *Michaelis* and *Rabinerson* [289].

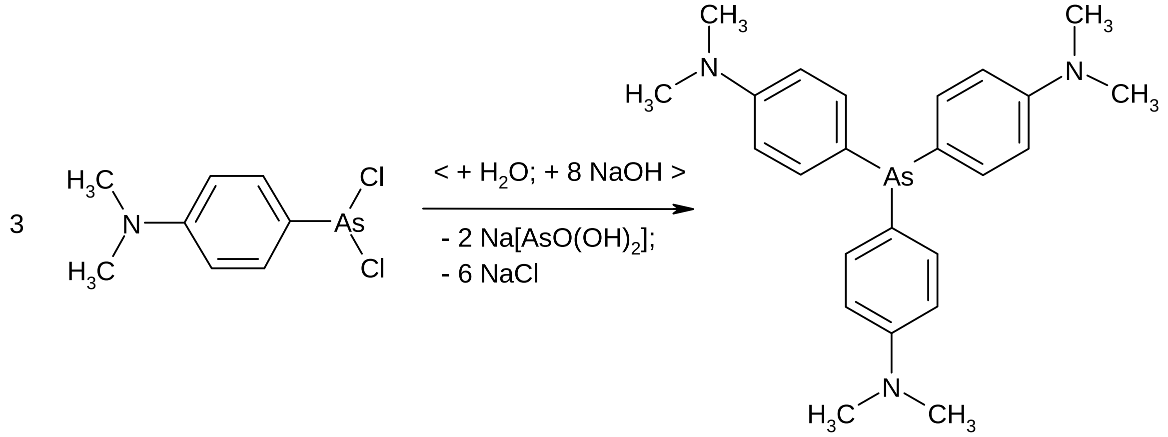

In an alternative route *Doak* et al. [292a] started with 4-(dimethylamino)aniline, made use of the *Bart* reaction and reduced the resulting [4-(dimethylamino)phenyl]arsonic acid with sulfur dioxide and a trace of potassium iodide in concentrated hydrochloric acid. Remarkably, the authors specify that at temperatures exceeding 30 °C tris[4-(dimethylamino)phenyl]arsine is the sole product. The compound is also obtained when the alkaline solution of [4-(dimethylamino)phenyl]oxoarsine is acidified.

Among different possibilities to prepare arylarsonic acids [293], by far the most widely applicable method is the *Bart* reaction. It involves the interaction of a diazonium compound with an alkaline metal arsenite(III) in the presence of copper(I) and copper(II) salts, powdered silver or copper itself. The *Bart* reaction has been improved by a number of research groups; in the *Scheller* modification [293] primary arylamines are dissolved in an alcoholic solution of sulphuric acid and arsenic(III) chloride, diazotized at 0 °C with the calculated amount of sodium nitrite in water and subsequently reacted with the arsenic(III) compound by addition of a catalytic amount of copper(I) chloride [293]. More than ten years later *Doak* et al. [292a,b] took up this method again, but changed copper(I) chloride for the corresponding bromide. After reduction and subsequent hydrolysis of the product they obtained [4-(dimethylamino)-phenyl]oxoarsine

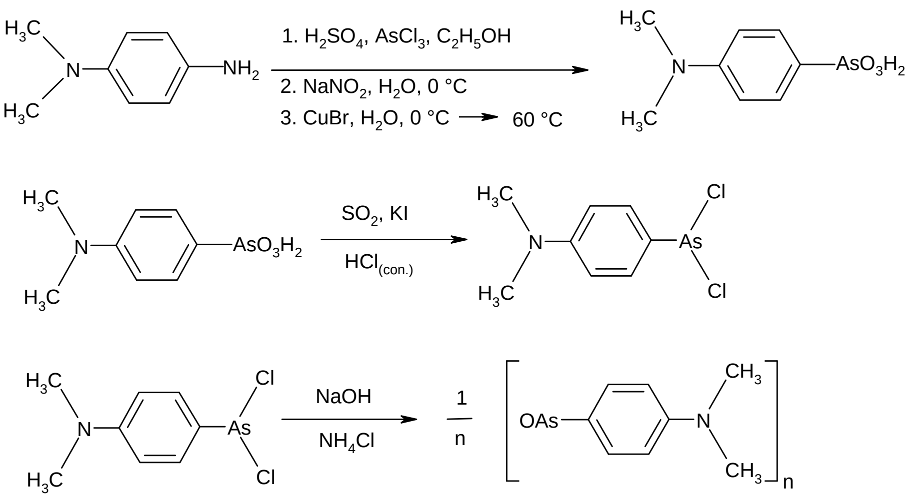

Scheme 5.1. *Bart–Scheller* Reaction modified by *Doak* et al. to prepare [4-(dimethylamino)-phenyl]arsonic acid and the corresponding oxoarsine by reduction and subsequent hydrolysis.

As far as a predictable synthesis of tris[4-(dimethylamino)phenyl]arsine is concerned, the compound could be prepared in 21% yield by *Tomaschewski* [294] reacting three equivalents of 4-dimethylaminophenyl lithium with arsenic(III) chloride at –20 °C in diethyl ether. Treatment of tris(phenylmercapto)arsine with the same lithium reagent for six hours at ambient temperature by *Wada* et al. [288] afforded the product in an essentially improved yield of 73%.

5.3. Oligomeric Organyloxoarsines

Since *Ochs* [171] and *Binder* [172] of our research group had succeeded in the isolation of hexameric dioxophenylphosphorane as solid state adducts with 1,2-dimethoxyethane and benzene, respectively, some experience on the structure of oligomeric species with P–O–P units has accumulated. We therefore were interested in an X-ray structure determination of the afore mentioned [4-(dimethylamino)phenyl]oxoarsine, realizing that only a small number of relevant reports on those compounds had been published.

The first organyloxoarsine, the methyl derivative MeAsO, was prepared as early as 1858 by *A. von Baeyer* [295]; therefore, this class of arsenic compounds is actually known for about one and a half century. By several research groups a wide variety of different syntheses [296] has been worked out so far, the most important of which are the reduction of organylarsonic acids, usually by using sulfur dioxide or very rarely thionyl chloride [297] and hydrolysis of dihaloorganylarsines or the oxidation of oligoorganyl-*cyclo*-oligoarsines. Whereas *A. von. Baeyer* still considered the methyl compound to be monomeric, *Blicke* and *Smith* [298] traced out the oligomeric character of organyloxoarsines by molecular weight determinations. As reported later [296, 299a,b,c] solutions of those compounds in organic solvents ordinarily show a dynamic equilibrium between species of different ring size, whereas polymers of formula $(RAsO)_x$ tend to be insoluble. As a consequence of different isomers to be present simultaneously, difficulties may arise to isolate suitable crystals of a single species for an X-ray structure determination. Therefore, only a limited number of compounds has been studied by this method.

Arif, *Cowly* and *Pakulski* [300] were the first to successfully isolate a tetrameric organyloxoarsine. The compound was prepared by hydrolysis of dichloromesitylarsine with a solution of excess potassium hydroxide in 1,2-dimethoxyethane and crystallized at –20 °C from *n*-hexane. Only four years later *DiMaio* and *Rheingold* [301] published the structure of the methyl derivative which was found to be a tetramer as well. The heterocycle $(H_3C{-}AsO)_4$ had been obtained in 42% yield when a chloroform solution of the polynuclear metal carbonyl complex $\{$*cyclo*-$[(H_3C{-}As)_7As]Mn(CO)_4\}Mn_2(CO)_6$, prepared at 170 °C in toluene from the starting compounds $Mn_2(CO)_{10}$ and $(H_3C{-}As)_5$ [302], was inadvertently exposed to air. Since in the absence of those metal carbonyl fragments the air oxidation of pentamethyl-*cyclo*-pentaarsine gives a variety of products characterized by a large number of ^1H NMR signals, the polynuclear metal complex is supposed to function as a template in the predominant formation of the tetramer.

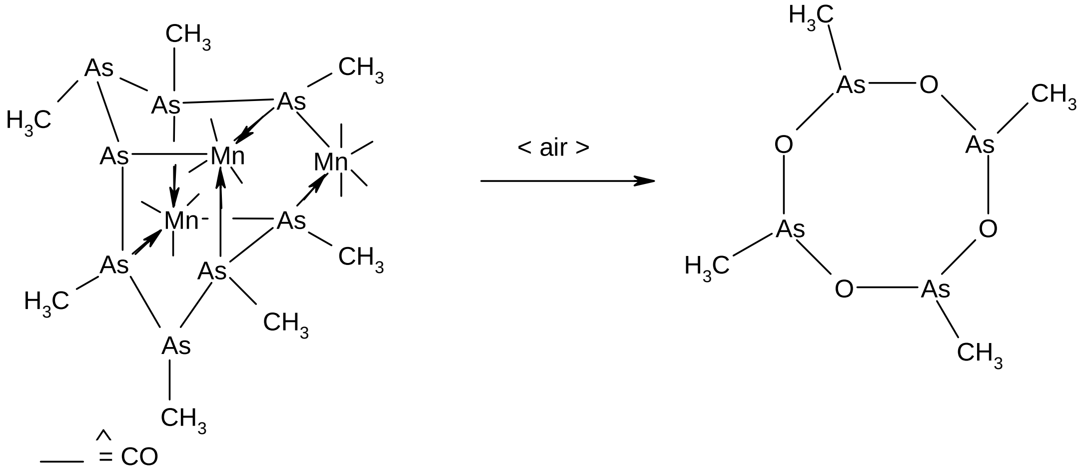

Eventually, in 1999 *Müller* and *Mühle* [303] reported the structure of tetrameric oxophenylarsine. They had taken up a synthesis already published by *Blicke* and *Smith* [298] about seventy years before. Dichlorophenylarsine, prepared by reduction of phenylarsonic acid with sulphur dioxide in concentrated hydrochloric acid, was hydrolysed with an excess of aqueous alkali and the product formed was precipitated after addition of ammonium chloride to the filtered solution. Suitable crystals could be obtained by cooling a solution of the compound in boiling *n*-octane. The X-ray structure determination confirms the results of *Blicke* and *Smith*

[298] who had already traced out the tetrameric character of the compound by cryoscopic and ebullioscopic measurements.

In 2005 *Sun*, *Patrick* and *Cullen* [304] published a previously unknown synthetic route to oligomeric organyloxoarsines. The authors started with *tert*-butyl and 3-trifluoromethylphenyl lithium, reacted these two compounds with chlorobis(dimethylamino)arsine in diethyl ether at room temperature and hydrolysed both products with an aqueous solution of sodium carbonate to give the oligomeric *tert*-butyl and 3-trifluoromethylphenyl derivative, respectively. An X-ray structure determination of (3-trifluromethylphenyl)oxoarsine showed the compound to be a tetramer in the solid state. Remarkably, the renewed interest in oligomeric organyloxoarsines comes from the observation that the methyl derivate $(H_3C–AsO)_4$ might be of importance in the chemotherapy of cancer, especially leukemia [305-311].

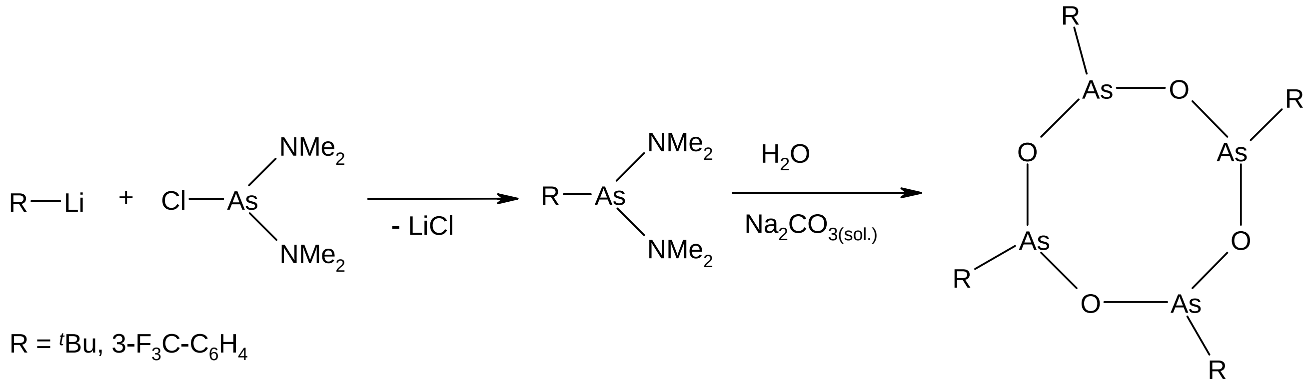

In addition to the aforementioned examples with an isolated $(As–O)_n$ heterocycle some compounds have been known, the six– or eight–membered heterocycle of which is part of a more extended oligocyclic system. With respect to this class of compounds the alkyloxoarsine $(H_2C)_3As_4O_4(CH_2)_3$ may serve as a transition. It has been prepared by *Ellermann*, *Lindner* and others [312] starting with 1,3-bis(diphenylarsinyl)propane [313]. Substitution of all phenyl groups with anhydrous hydrogen iodide furnishes the 1,3-bis(diiodoarsinyl)derivative which is hydrolyzed with concentrated aqueous ammonia in hot tetrahydrofuran. The final product could be isolated in an about 30% yield; the X-ray structure determination reveals that two neighbouring arsenic atoms in the positions 1,3 and 5,7; respectively, are brigded by 1,3-propanediyl units.

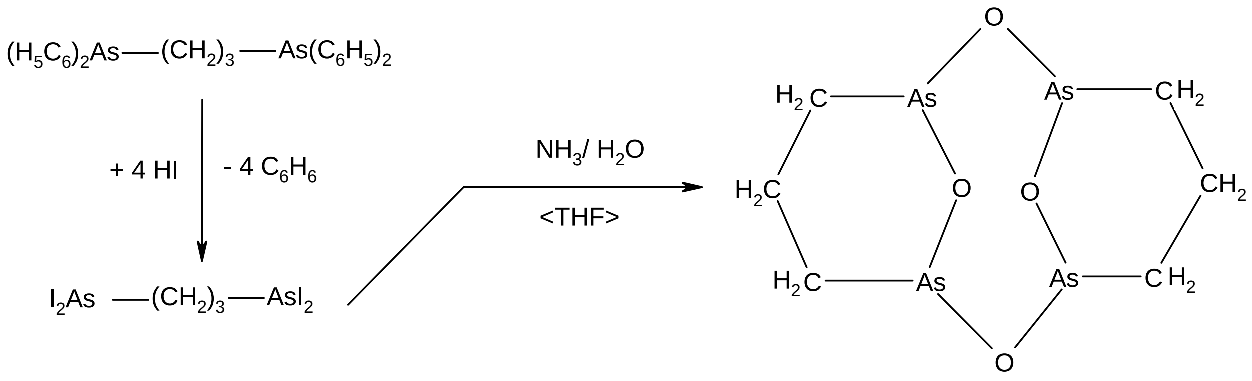

Since the adamantane like structure of the mineral arsenolite [314, 315] As_4O_6, built up of four As_3O_3 heterocycles, may serve as a reference, the molecular framework of the two following species can easily be obtained by a formal exchange of several oxygen atoms for methylene groups and an arsenic atom for an ethylidyne unit, respectively.

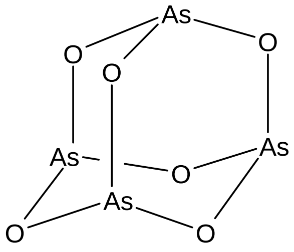

As_4O_6
<arsenolite>

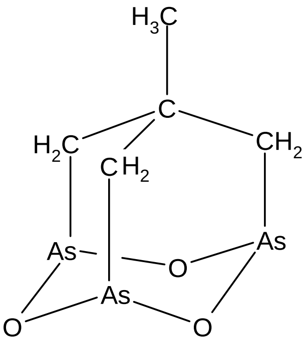

$H_3C\text{-}C[(CH_2\text{-}AsO)]_3$

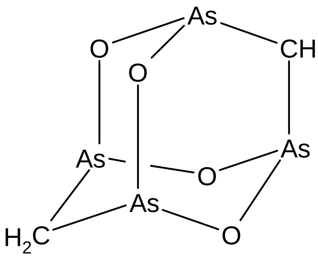

$[H_2C(AsO)_2]_2$

To prepare the compound $H_3C–C(CH_2)_3As_3O_3$ *Mills*, *Bernal* and coworkers [316] first converted 1,1,1-tris(hydroxymethyl)ethane into the corresponding tribromo derivative using phosphorus(III) bromide, introduced diphenylarsinyl substituents in a reaction with sodium diphenylarsanide in liquid ammonia and exchanged all phenyl groups for iodine using anhydrous hydrogen iodide. Reduction with sodium in tetrahydrofuran furnished the remarkable oligocycle $H_3C–C(CH_2–As)_3$ well known from *Ellermann's* elaborate work on arsenic heterocycles [317, 318]. Further reduction is supposed to open the three-membered As_3 homocycle first; in a slow reaction with the solvent tetrahydrofuran – the authors at least pretend this – the oxygen atoms are subsequently introduced.

Studying the complexing behaviour of organyloxoarsines, *Kopf*, *v. Deuten* and *Klar* [319] came across the compound $[CH_2(AsO)_2]_n$ of which a polymeric and a dimeric form had been described [320-322]. They repeated the preparation starting with bis(dichloroarsinyl)methane [320], hydrolyzed the compound with a 2 M solution of sodium hydroxide, precipitated the product by addition of the alkaline solution to an aqueous solution of excess ammonium chloride and extracted the dimer with benzene. The structure of this oligocycle may be derived from that of arsenolith by formal exchange of only two oxygen atoms for CH_2 groups.

The structure of the fascinating compound $[N(CH_2–CH_2)_3]_8(As_4O_4)_6$ has been elucidated by *Ellermann*, *Lindner* and coworkers [323, 324]. As for the first steps of the synthesis the authors followed a route already described by *Sacconi* and *Morassi* [325] but instead of the free base they reacted the ammonium salt $[H–N(CH_2–CH_2–Cl)_3]Cl$ with sodium diphenylarsanide $Na–As(C_6H_5)_2$ in liquid ammonia. Subsequently, they converted the isolated intermediate $N[CH_2–CH_2–As(C_6H_5)_2]_3$ into the hexaiodine derivative $[H–N(CH_2–CH_2–AsI_2)_3]I$ using anhydrous hydrogen iodide and treated a solution of this compound in tetrahydrofuran with concentrated aqueous ammonia. The structure of the finally isolated cryptand is best described as a cube the vertices of which are occupied by eight nitrogen atoms whereas six eight-membered $(As–O)_4$ heterocycles are placed slightly acentric on the faces.

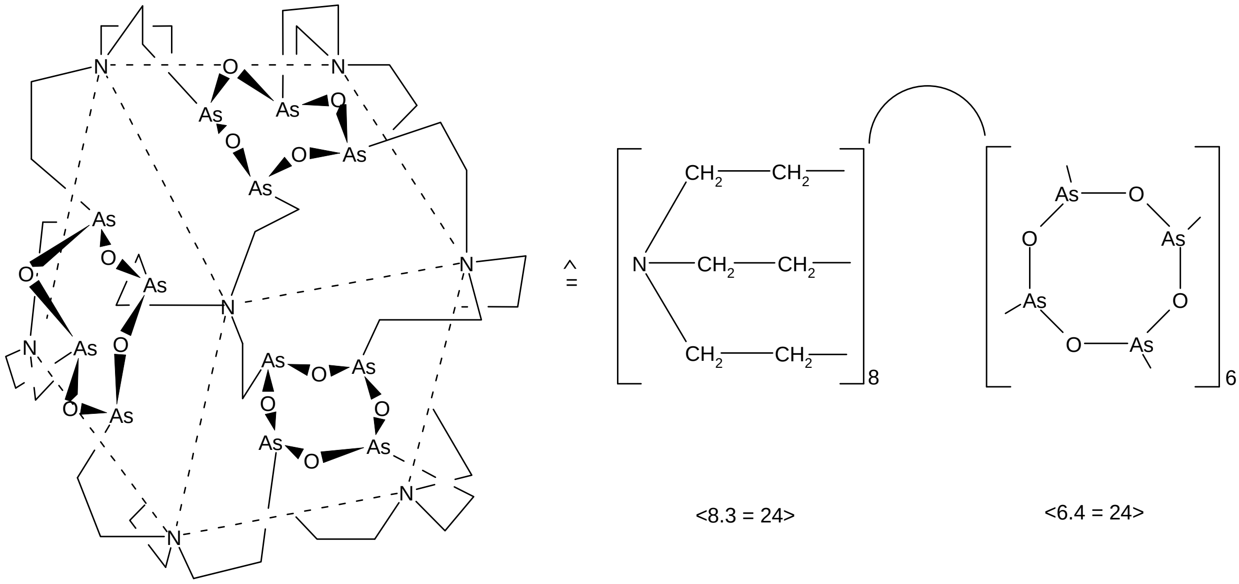

Since the heterocycles of oligomeric organyloxoarsines $(R–AsO)_n$ are composed of oxygen and arsenic atoms in an alternating sequence, these molecules may serve as ambident ligands in complexes with soft as well as hard metal centers [296]. Remarkably, the ring size is very often determined by the diameter of the metal center. For example, in the cationic sandwich complexes of the thiocyanates $[M\{cyclo\text{-}(H_3C–AsO)_n\}_2][SCN]$ ($M = Na$, $n = 4$; $M = K$, $n = 5$) the hard oxygen atoms coordinate to the hard alkali metal center, but in case of the smaller sodium cation the ligand is found to be tetrameric, whereas the larger potasium cation obviously induces a ring expansion and gives rise to the coordination of two pentamers [326, 327]. With respect to the facility to change the ring size very rapidly oligomeric organyl oxoarsines differ in their ligand properties from those of similar crown ethers considerably. Furthermore, in the reactions of the ruthenium and osmium trihalides $MCl_3 \cdot x\ H_2O$ (M = Ru, Os) with tetrameric methyloxoarsine $(H_3C–AsO)_4$, a similar ring expansion is observed, but in the ligand now tetrameric only four of the eight arsenic atoms coordinate to a transition metal cation of oxidation number two [327].

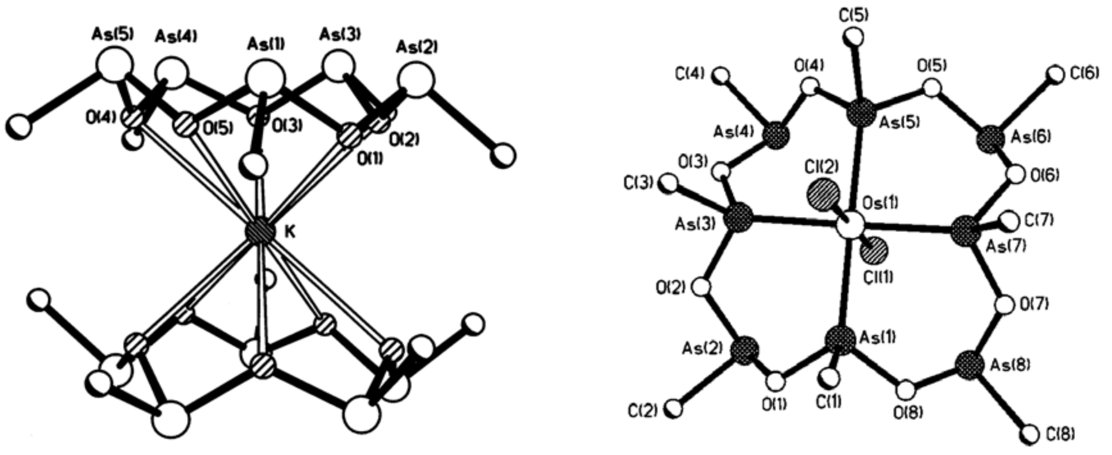

A **B**

Figure 1. Sandwich cation of the compound $[K\{$*cyclo*-$(H_3C–AsO)_5\}_2][SCN]$ [326] and molecular structure of the complex $[OsCl_2\{$*cyclo*-$(H_3C–AsO)_8\}]$ [327]

Our methods applied to prepare dichloro[4-(dimethylamino)phenyl]arsine as well as tris[4-(dimethylamino)phenyl]arsine are both based on the early studies of *Michaelis* and *Rabinerson* [289]. At first *N*,*N*-dimethylaniline and arsenic(III) chloride were reacted without a solvent and the highly viscous yellow wax obtained after a completion of the reaction at elevated temperature was dissolved in acetonitrile. Storing this solution at –13 °C afforded colourless to pale yellow crystals in about 85% yield. Without doubt, the isolation of a hydrogen chloride free compound has to be considered an essential improvement of the original procedure.

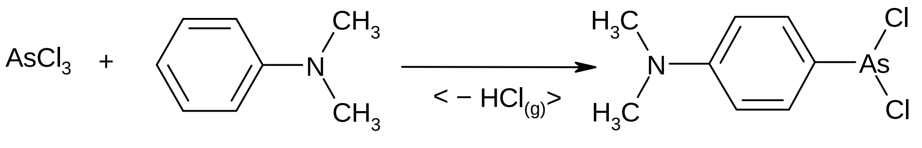

When, however, to a very dilute, filtered solution of the viscous yellow wax in cold distilled water is added slowly with stirring anhydrous sodium hydroxide until a solid starts to precipitate, at least in part a redistribution of substituents at arsenic takes place and insoluble tris[4-(dimethylamino)phenyl]arsine is formed. After allowing the suspension to stand at –13 °C overnight, the product is filtered off, dried and recrystallized from chloroform. By this procedure the triorganylarsine can be isolated in up to 46% yield.

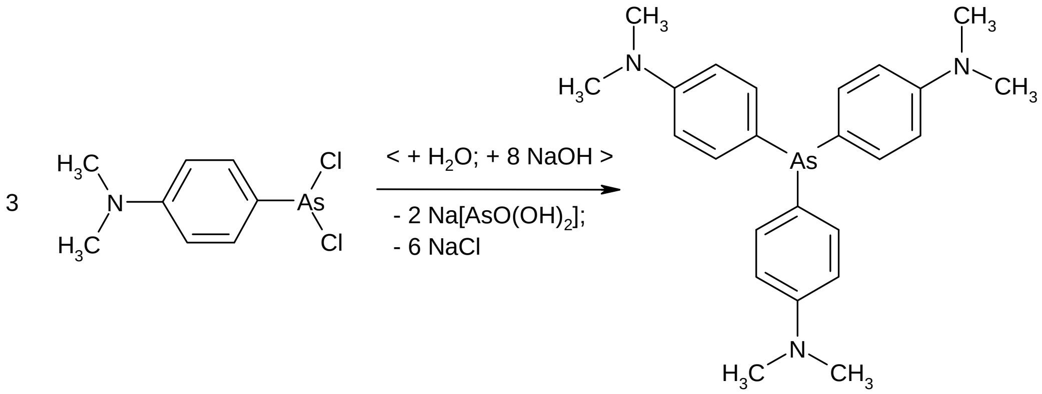

Finally, the preparation of [4-(dimethylamino)phenyl]oxoarsine from the dichloro[4-(dimethylamino)phenyl] compound or its hydrochloride as reported by *Michaelis* and *Rabinerson* [289] (see above) and the isolation of crystals suitable for an X-ray structure determination was repeatedly attempted – but always in vain; again and again, only crystals of tris[4-(dimethylamino)phenyl]arsine could be obtained by storing a solution of the crude product in chloroform at –13 °C. The compound was identified by its mass spectrum, the melting point and its X-ray structurally determined unit cell dimensions. With respect to these results our studies tally with similar experiments of *Doak* et al. [292a] who also failed to confirm the original reaction (see above). Even despite an adoption of procedures published for the preparation of oligomeric mesityl- [300] and phenyloxoarsine [303] we were not successful to obtain crystals.

5.4. NMR Characterization of Dichloro[4-(dimethylamino)phenyl]- and Tris[4-(dimethylamino)phenyl]arsine

Dichloro[4-(dimethylamino)phenyl]arsine prepared in a solvent-free reaction of the two starting compounds *N*,*N*-dimethylaniline and arsenic(III) chloride in a molar ratio of 1:1 and precipitated from an acetonitrile solution of the crude waxy product, was obtained in colourless to pale yellow plates. Its ^{1}H-NMR-spectrum shows the typical AA′XX′-pattern of a 1,4-disubstituted arene ring the four hydrogen atoms of which give rise to two doublets (^{3}J(H,H) = 8.3 Hz) at 7.54 (3,5-H) and 7.79 pm (2,6-H). The singlet at 3.1 ppm is assigned to the dimethylamino group. In the ^{13}C{^{1}H} spectrum four singlets in the arene and one in the alkyl region are noticed; they are tentatively assigned to the *ipso*-**C**–N (144.3), **C**–C–As (131.2), *ipso*-**C**–As (130.9) and **C**–C–N carbon atoms (122.0) as well as to the dimethylamino group (46.8 ppm).

Tris[4-(dimethylamino)phenyl]arsine obtained in 46% yield from an analogous solvent free reaction of the same starting compounds *N*,*N*-dimethylaniline and arsenic(III) chloride again in a ratio of 1:1, but followed by a hydrolysis of the highly viscous yellow wax formed first with sodium hydroxide and an accompanying redistribution of the substituents at arsenic, crystallizes at -13°C from a chloroform solution in colourless cuboids. As expected its NMR spectra are found to be very similar to those of the dichloro derivative:

The hydrogen atoms in 3,5- and 2,6-positions of the disubstituted arene ring become apparent as two doublets ($^3J(H,H)$ = 8.74 Hz) at 6.67 and 7.20 ppm, whereas the singlet at 2.92 ppm comes from the dimethylamino group. The singlets of the $^{13}C\{^1H\}$ spectrum at 150.4, 134.5, 126.7 (broadened), and 112.6 ppm are again tentatively assigned in an analogous way to the carbon atoms of the *ipso*-**C**–N, **C**–C–As, *ipso*-**C**-As and **C**–C–N moiety; the resonance at 40.4 ppm springs from the $(H_3C)_2N$ group.

Chemical shifts of the compounds **4** and **5** in comparison with some parameters of similar compounds, which are summarized in table 5.3.1 below.

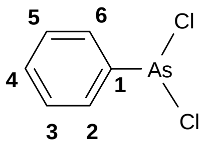

X = C_6H_5

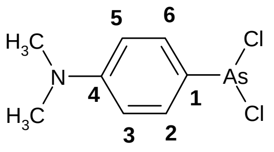

X = $(Me_2NC_6H_4)$

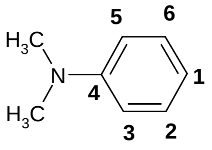

Table 5.3.1. $^{13}C\{^1H\}$ NMR Chemical Shifts of the Compounds $(4\text{-}Me_2NC_6H_4)_3As$ and $(4\text{-}Me_2NC_6H_4)AsCl_2$ in Comparsion with $C(C_6H_5)_3As$, $(C_6H_5)_2AsCl$, $(C_6H_5)AsCl_2$ and $Me_2NC_6H_5$

	$(C_6H_5)_3As$ [328]	$(C_6H_5)_2AsCl$ [328]	$(C_6H_5)AsCl_2$ [328]	$(4\text{-}Me_2NC_6H_4)_3As$	$(4\text{-}Me_2NC_6H_4)AsCl_2$	$Me_2NC_6H_5$ [329]
C(1)	139.5	142.0	145.0	126.71	130.88	116.7
C(2,6)	133.6	131.5	129.7	134.46	131.22	129.2
C(3,5)	128.5	128.6	129.0	112.64	121.95	112.3
C(4)	128.3	129.8	131.9	150.35	144.32	150.2

5.5. Discussion of the Molecular Structures of Compounds 4 and 5

5.5.1. Crystal Data, Measuring Techniques and Structural Analyses

Storing solutions of dichloro[4-(dimethylamino)phenyl]arsine (**4**) in acetonitrile and of tris[4-(dimethylamino)phenyl]arsine (**5**) in chloroform for a period of three days to two weeks at –13 °C afforded colourless to slightly yellow plates or colourless cuboids, respectively, both suitable for an X-ray structure analysis. A crystal of the approximate dimensions 0.7 x 0.5 x 0.1 mm (**4**) // 0.65 x 0.6 x 0.5 mm (**5**) was selected, covered with polyfluorinated polyether oil (*RS 3000, Riedel-de-Haën*), transferred to an automatic Syntex $P2_1$ diffractometer and cooled to a temperature of –100 ± 3 °C. A least squares fit using the positions of 38 // 35 selected reflections in a range of $9.56 < 2\theta < 24.25°$ // $15.54 < 2\theta < 25.76°$ supplied correct unit cell dimensions. The complete data set was collected with graphite monochromatized Mo-K_α-radiation at a scanning rate ranging from 4.00 to 29.30 deg min^{-1}. As derived from the unit cell parameters and the lack of systematic absences, both compounds crystallize in one of the two triclinic space groups; $P\overline{1}$, however, was chosen over $P1$ [117] on the strength of E-value statistics and a successful refinement of the structures.

Programs of the software package SHELXTL version 5.10 [118-120] were employed to solve the phase problem with statistical (direct) methods and to refine the atomic coordinates as well as at first the isotropic and subsequently the anisotropic displacement parameters of all heavier atoms by full matrix least squares calculations. Furthermore, program XP also included in this package was used for an analysis of the molecular geometry and the preparation of drawings. For the data set of compound **4**, the application of a ψ-scan absorption correction turned out to be necessary. The introduction of anisotropic displacement parameters resulted in an improvement of the R-values from 0.1087 // 0.2989 to 0.0649 // 0.1809. Finally, the positions of all hydrogen atoms could be located on a difference Fourier map; the refinement of these co-ordinates as well as their isotropic displacement parameters ended in reasonable values.

For both compounds **4** and **5**, crystallographic parameters and details of data collection have been summarized in Table 5.1; characteristic bond lengths and bond angles as well as torsion angles can be taken from Table 5.2; details concerning the least-squares planes of these molecules are given in Table 5.3. Final atomic coordinates as well as equivalent isotropic and anisotropic displacement parameters have been listed in Tables 9.5.1 and 9.6.1 of the Appendix, respectively.

In regard to the numbering scheme one should notice that the atoms of the two independent molecules **a** and **b** in the unit cell of compound **4** differ in the first integer n (n = 1 or 2) following the element symbol, whereas in compound **5** the atoms of the three substituents at the central atom As3 are characterized by the integers n = 3, 4 and 5.

Table 5.1. Crystal Data and Details of Structure Refinement for Dichloro[4-(dimethylamino)phenyl]arsine (**4**) and Tris[4-(dimethylamino)phenyl]arsine (**5**)
Diffractometer $P2_1$; wavelength 71.073 pm; temperature of measurement –100 ± 3 °C; crystal system triclinic; space group $P\overline{1}$ (No. 2 [117])

Compound	**4**	**5**
Empirical formula	$C_8H_{10}AsCl_2N$	$C_{24}H_{30}AsN_3$
Molecular weight	265.99	435.43
Melting point (°C)	112	243
Crystal size (mm)	0.7 x 0.5 x 0.1	0.65 x 0.6 x 0.5
Crystal shape	colourless plates	colourless cuboids
Determ. of unit cell dimensions:		
Number of reflections used	38	35
2θ range (min. < 2θ < max.)	$9.56° < 2\theta < 24.25°$	$15.54° < 2\theta < 25.76°$
Unit cell dimensions a (pm)	986.1(2)	984.2(2)
b (pm)	1039.6(2)	1098.7(2)
c (pm)	1135.6(2)	1120.2(2)
α (°)	79.91(3)	109.01(3)
β (°)	74.09(3)	101.95(3)
γ (°)	65.75(3)	94.76(3)
Volume (m^3)	$1018.1(4) \cdot 10^{-30}$	$1105.5(4) \cdot 10^{-30}$
Z a)	4	2
Calc. density (kg m^{-3})	$1.735 \cdot 10^3$	$1.3081 \cdot 10^3$
Calc. absorption coefficient μ (m^{-1}) b)	$3.808 \cdot 10^3$	$1.551 \cdot 10^3$
Absorption correction	ψ-scan	none
F(000)	528	456
θ-Range (°) for data collection	1.87 to 28.00	1.99 to 28.00
Limiting indices	$-11 \le h \le 13$; $-12 \le k \le 13$; $-14 \le l \le 14$	$0 \le h \le 12$; $-14 \le k \le 14$; $-14 \le l \le 14$
Scan mode c)	Wyckoff-scan	Wyckoff-scan
Scan width (°) and velocity (deg min^{-1})	1.8; 4.0 to 29.3	1.8; 5.0 to 29.3
Reflections collected	5189	5635
Unique reflections (m)	4906	5326
Reflections observed with [$I > 2\sigma(I)$] d)	4184	4827
Parameters refined (n)	297	373
Restraints	0	0
Space filling coefficient) e)	74 %	74 %
Goodness-of-fit (GOF) f)	1.048	1.054
Isotropic		
R1/wR2 f) using all data	0.1087, 0.2989	0.0839, 0.2066
R1/wR2 with [$I>2\sigma(I)$]	0.0972, 0.2873	0.0774, 0.2040

Anisotropic R1/wR2 using all data R1/wR2 with [I>2σ(I)]	 0.0649, 0.1809 0.0554, 0.1721	 0.0557, 0.1512 0.0496, 0.1486
Final R1/wR2 using all data R1/wR2 with [I>2σ(I)]	 0.0573, 0.1567 0.0478, 0.1468	 0.0407, 0.0925 0.0347, 0.0888
Indices f and g of weighting scheme w^{-1} g)	f = 0.1181; g = 0.4889	f = 0.0582; g = 0.4621
Largest diff. peak; deepest hole $(10^{-30}$ em$^{-3})$	1.162; –1.212	0.785; –0.750

a) Number of molecules in the unit cell; b) linear absorption coefficient $\mu = \Sigma\sigma_i/V_c$ [121]; c) registration of the background at the beginning and at the end of the measurement with an overall length equal to the time of measurement; d) reflections with strongly negative intensity were considered unsuitable for refinement; e) space filling or packing coefficient of the structure calculated from the Kitaigorodskii formula [122]; bond lengths are taken from Table 5.2; C–H (aliphatic) 108 pm, C–H (aromatic) 104 pm; van der Waals radii: As 200, C 180, Cl 180, N 157, H 117 pm [122,124]; f) for a definition of R-indices see Appendix, page 282; g) weighting scheme $w^{-1}= [\sigma^2(F_o)^2+(f\,P)^2+(g\,P)]$ with $P= 1/3(F_o{}^2+2F_c{}^2)$.

Table 5.2. Characteristic Bond Lengths (pm) and Bond Angles (°) as well as Torsion Angles for Dichloro[4-(dimethylamino)phenyl]arsine (**4**) and Tris[4-(dimethylamino)phenyl]arsine (**5**)

a) Bond lengths	**4 a** *m* = 1 *n* = 1	**4 b** *m* = 2 *n* = 2	Mean	**5** *m* = 3 *n* = 3	**5** *m* = 3 *n* = 4	**5** *m* = 3 *n* = 5	Mean
As*m*–C*n*1	191.9(4)	191.5(4)	191.7	195.6(2)	194.0(2)	195.0(2)	194.9
As*m*–Cl*n*1	221.5(1)	221.4(2)	220.6				
As*m*–Cl*n*2	219.3(1)	220.1(2)					
N*n*–C*n*4	135.9(5)	135.9(5)	135.9	139.7(3)	138.6(3)	138.7(3)	139.0
N*n*–C*n*7	145.3(5)	145.4(6)	145.4	145.5(4)	144.9(3)	143.9(4)	144.8
N*n*–C*n*8	145.4(6)	145.3(6)		145.7(4)	144.3(3)	144.3(4)	
C*n*1–C*n*2	139.8(5)	139.3(6)	139.5	139.2(3)	138.8(3)	139.2(3)	139.2
C*n*1–C*n*6	138.8(5)	139.9(5)		139.1(3)	139.2(3)	139.6(3)	
C*n*2–C*n*3	138.3(5)	137.5(6)	137.6	138.4(3)	138.5(3)	137.9(3)	138.3
C*n*5–C*n*6	137.1(6)	137.3(6)		138.5(3)	138.5(3)	138.2(3)	
C*n*3–C*n*4	141.3(5)	140.7(6)	141.7	140.2(3)	140.3(3)	140.4(3)	140.2
C*n*4–C*n*5	142.3(5)	142.4(5)		139.9(3)	139.8(3)	140.5(3)	

b) Bond angles	**4 a** *m* = 1 *n* = 1	**4 b** *m* = 2 *n* = 2	Mean	**5** *m* = 3 *n* = 3	**5** *m* = 3 *n* = 4	**5** *m* = 3 *n* = 5	Mean
C*n*1–As*m*–C*(n+1)*1				98.5(1)	100.2(1)		99.3
C*n*1–As*m*–C*(n+2)*1				99.3(1)			
C*n*1–As*m*–Cl*n*1	97.3(1)	98.6(1)	98.8				
C*n*1–As*m*–Cl*n*2	100.5(1)	98.9(1)					
Cl*n*1–As*m*–Cl*n*2	94.8(5)	96.5(6)	95.7				
C*n*2–C*n*1–As*m*	116.3(3)	116.5(3)	116.4	118.7(2)	119.1(2)	118.3(2)	118.7
C*n*6–C*n*1–As*m*	125.0(3)	124.7(3)	124.9	124.0(2)	123.0(2)	124.6(2)	123.9
C*n*4–N*n*–C*n*7	120.0(3)	120.1(4)	120.6	117.0(2)	118.6(2)	119.4(2)	118.4
C*n*4–N*n*–C*n*8	121.0(3)	121.3(4)		117.1(2)	118.6(2)	119.4(2)	
C*n*7–N*n*–C*n*8	118.1(4)	118.5(4)	118.3	114.0(2)	116.4(2)	117.3(3)	115.9
N*n*–C*n*4–C*n*3	121.8(3)	121.5(4)	121.4	121.7(2)	121.5(2)	121.3(2)	121.3
N*n*–C*n*4–C*n*5	121.0(3)	121.2(4)		120.8(2)	121.1(2)	121.5(2)	
C*n*2–C*n*1–C*n*6	118.5(4)	118.8(4)	118.7	117.3(2)	117.7(2)	117.0(2)	117.3
C*n*3–C*n*4–C*n*5	117.2(3)	117.3(3)	117.3	117.5(2)	117.5(2)	117.2(2)	117.4
C*n*1–C*n*2-C*n*3	120.9(4)	121.6(4)	121.0	121.9(2)	121.6(2)	122.2(2)	121.3
C*n*2-C*n*3–C*n*4	120.9(3)	120.6(4)		120.7(2)	120.8(2)	120.7(2)	
C*n*1–C*n*6–C*n*5	121.7(4)	120.2(4)		121.6(2)	121.4(2)	121.5(2)	
C*n*4–C*n*5–C*n*6	120.7(4)	121.5(4)		121.1(2)	121.0(2)	121.2(2)	
∑N[a)]	359.1	359.9	359.5	348.1	353.6	356.1	352.6

c) Torsion angles[b)]	**4 a** *m* = 1 *n* = 1	**4 b** *m* = 2 *n* = 2	**5** *m* = 3 *n* = 3	**5** *m* = 3 *n* = 4	**5** *m* = 3 *n* = 5
C*n*2–C*n*1–As*m*–Cl*n*1	–131.2(3)	–122.3(3)			
C*n*2–C*n*1–As*m*–Cl*n*2	132.5(3)	139.7(3)			
C*n*6–C*n*1–As*m*–Cl*n*1	43.4(4)	57.2(3)			
C*n*6–C*n*1–As*m*–Cl*n*2	–52.9(4)	–40.8(4)			
C*n*3–C*n*4–N*n*–C*n*7	–0.9(6)	1.8(6)	35.9(3)	14.7(3)	8.4(4)
C*n*3–C*n*4–N*n*–C*n*8	168.0(4)	–178.8(4)	176.7(3)	165.8(3)	165.8(3)
C*n*5–C*n*4–N*n*–C*n*7	178.6(4)	–178.4(4)	–145.4(3)	–167.0(2)	–173.5(3)
C*n*5–C*n*4–N*n*–C*n*8	–12.4(6)	1.0(6)	–4.7(4)	–15.9(3)	–16.1(4)

φ*n*4	C51–As3–C31–C36	81.4	C31–As3–C41–C46	90.9	C41–As3–C51–C56	89.6
φ*n*2	C51–As3–C31–C32	–101.1	C31–As3–C41–C42	–83.7	C41–As3–C51–C52	–94.6
φ*n*1	C41–As3–C31–C32	0.8	C51–As3–C41–C42	17.5	C31–As3–C51–C52	5.9
φ*n*3[c)]	EP–As3–C31–C36	–47.7	EP–As3–C41–C46	–38.5	EP–As3–C51–C56	–40.2

a) Sum of angles at nitrogen. b) The torsion angle A–B–C–D is defined as positive if, when viewed along the B–C bond, atom A must be rotated clockwise to eclipse atom D [125,126]. c) For a definition of torsion angle φ*n*3 see text on page 191 and Figure 5.4.

5.5.2. Molecular Structure of Compound 4

The X-ray structure determination of dichloro[4-(dimethylamino)phenyl]arsine (**4**) shows the compound to crystallize triclinic in the centrosymmetric space group $P\bar{1}$ and to comprise two independent molecules **a** and **b** in the asymmetric unit. Molecular models are depicted in Fig. 6.1.

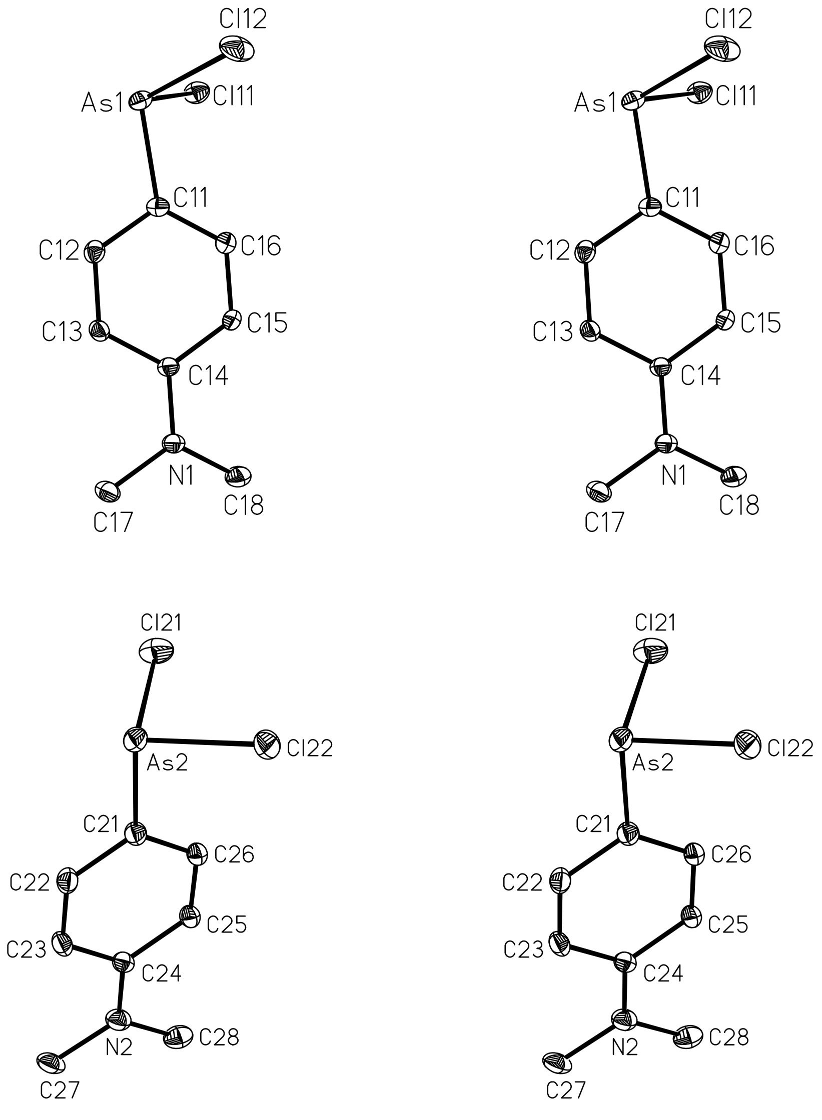

4a

4b

Figure 5.1. Stereoscopic views of both the independent molecules **a** and **b** of compound **4**. The two numbering schemes applied differ only in the first figure (n = 1 or 2) following the element symbols. Thermal ellipsoids are at 30 % probability, hydrogen atoms have been omitted for clarity.

Apart from nearly identical bond lengths and angles (Table 5.2) in molecules **a** and **b**, even the orientations of the dichloroarsinyl groups with their trigonal pyramidally coordinate arsenic atoms and the planar dimethylamino substituents in positions 1 and 4, respectively, are found to be very similar relative to the central arene rings. On the whole the geometry of both molecules approaches largely pseudosymmetry *m* in that the atoms of the total 4-dimethylaminophenyl unit form a common plane which roughly bisects the Cl*n*1–As*m*–Cl*n*2 angle (Table 5.3). Obviously the following discussion is based mainly on average values.

Table 5.3. Deviations of Atoms from the Least-Squares Planes of the Arene Rings (A_n) and Angles between these Planes and the Planes B_n formed by the Heavier Atomes of the Appropriate Dimethylamino Groups in Both Molecules of Dichloro[4-(dimethylamino)phenyl]arsine (**4a**, $n = 1$; **4b**, $n = 2$) and in Tris[4-(dimethylamino)phenyl]arsine (**5**, $n = 3, 4, 5$).
Atoms defining the least-square plane each are marked with an asterix (*).

A_n	C*n*1*	C*n*2*	C*n*3*	C*n*4*	C*n*5*	C*n*6*	As*m*	Cl*n*1	Cl*n*2	N*n*	C*n*7	C*n*8
$n = 1$	1.4	-0.7	-0.8	1.6	-1.0	-0.5	21.7$^{a)}$	183.8	-137.4	5.3	4.8	33.6
$n = 2$	0.3	-0.3	0.0	0.3	-0.3	0.0	2.5$^{b)}$	187.8	-138.0	0.4	4.4	-2.0
$n = 3$	0.4	-0.1	-0.4	0.5	-0.1	-0.3	-4.9$^{c)}$			-0.8	73.2	7.7
$n = 4$	-1.2	0.2	1.0	-1.3	0.4	0.9	-21.0$^{c)}$			-1.7	-31.9	-35.1
$n = 5$	-1.3	0.8	0.8	-1.9	1.4	0.2	-17.5$^{c)}$			-11.3	-0.1	17.1

A1 / B1 12.6°; A2 / B2 1.6°; A3 / B3 35.9°; A4 / B4 24.7°; A5 / B5 15.8°.

a) $m = 1$; b) $m = 2$; c) $m = 3$

In order to calculate the length of a polar single bond from covalent radii, differences in the electronegativity values of the two atoms concerned have to be taken into consideration. For such a correction the following methods are usually applied – the original one set up by *Schomaker* and *Stevenson* [134]:

$$d_{A\text{–}B} = r_A + r_B - c\,|x_A - x_B|$$

$d_{A\text{–}B}$ bond length; r_A, r_B covalent radius;
c individual correction factor; x_A, x_B electronegativity
(formerly *Pauling* electronegativities, nowadays mostly
Allred and *Rochow* values)

and a partially improved one published about twenty years ago by *Blom* and *Haaland* [133]:

$$d_{A\text{–}B} = r_A + r_B - c^{\backprime}\,|x_A - x_B|^m$$

$c^{\backprime} = 8.5$; $m = 1.4$ (standardized correction factors suitable for nearly all single bonds between main group elements).

Inserting covalent radii [124] of 77, 99 and 121 pm for the elements carbon, chlorine and arsenic and pertinent *Alred–Rochow* electronegativities [60] of 2.50, 2.83 and 2.20 into the *Schomaker–Stevenson* equation and applying correction factors of 8 and 4 for the As–C and As–Cl distance [124], respectively, result in calculated bond lengths of 196 and 217 pm. With the same starting parameters the method of *Blom* and *Haaland* [133] actually leads to identical values of 196 and 216 pm.

To allow, however, a careful discussion of the molecular parameters of dichloro[4-(dimethylamino)phenyl]arsine (**4**) and to obtain an answer to whether or not there is a distinct π-conjugation between the dimethylamino and the dichloroarsinyl substituent across the arene ring, a second basis will have to be created in that these values are compared with those of simple parent compounds such as arsenic(III) chloride or trimethyl– and triphenylarsine together with the heteroleptic species $(H_3C)_{3-n}AsCl_n$ and $(H_5C_6)_{3-n}AsCl_n$ (n = 1 or 2), respectively. For arsenic(III) chloride As–Cl bond lengths of 216.1 and 216.2 pm have been determined from its microwave spectrum [330] and a gas electron diffraction experiment [331]. Analogous studies on trimethylarsine reveal As–C distances of 195.9 [332] and 198 pm [333], whereas X-ray structure determinations at ambient temperature give values of 194.9 [324] and 195.7 pm [335] for triphenylarsine. Remarkably, these As–Cl and As–C bond lengths obtained from experiments tally very well with the results of *Blom* and *Haaland* [133].

Since, however, the As–Cl and As–C distances of the heteroleptic chloromethyl– and chlorophenylarsines are only partially available from the literature, quantum chemical calculations using *ab-initio* methods at the MP2/6-311++G** level or DFT methods at the B3LYP/6-311++G** level have been carried out to create a third basis and to fill the gap. Additionally, the high quality of the *ab-initio* calculations in particular allows a corroboration of experimental results. In this respect, already a short look at Table 6.4, where all relevant As–Cl and As–C bond lengths have been put together, makes evident that all values calculated by *ab-initio* methods do not deviate significantly from those experimentally determined. Unfortunately, DFT methods give somewhat longer distances for arsenic(III) chloride, trimethylarsine and both the chloromethylarsines; obviously these values are less appropriate for a comparison. But for dichlorophenyl– and chlorodiphenylarsine an excellent agreement between experimentally determined values and those calculated by DFT methods has been found. With regard to the As–C distances, however, the well-known shortening of the element carbon bond caused by a change in hybridization of the carbon atom *e.g.* from sp^3 to sp^2 is not as pronounced as expected; quite on the contrary, the mean As–C values determined for trimethyl– (195.9 pm [332]) and triphenylarsine (194.9 [334] and 195.7 pm [335]) were found to be almost identical.

Table 5.4. Bond Lengths and Angles Quantum Chemically Calculated$^{a)}$ and Experimentally Determined for the Compounds $(H_3C)_{3-n}AsCl_n$ and $(H_5C_6)_{3-n}AsCl_n$ ($n = 0 \rightarrow 3$)

Compound	As–Cl		As–C		C–As–C		C–As–Cl		Cl–As–Cl	
	calc.	exp.	calc.	exp.	calc.	exp.	calc.	exp	calc.	exp
$(H_3C)_3As$	–	–	$196.9^{b)}$ $198.9^{c)}$	195.9 [332] $198^{d)}$ [333]	$96.4^{b)}$ $97.2^{c)}$	96 [332] 96 [333]	–	–	–	–
$(H_3C)_2As–Cl$	$221.5^{b)}$ $225.4^{c)}$	–	$195.7^{b)}$ $197.9^{c)}$	–	$96.4^{b)}$ $96.9^{c)}$		$96.3^{b)}$ $97.0^{c)}$		–	–
$H_3C–AsCl_2$	$219.6^{b)}$ $223.2^{c)}$	–	$194.7^{b)}$ $197.2^{c)}$	–	–	–	$99.8^{b)}$ $100.7^{c)}$		$95.7^{b)}$ $96.4^{c)}$	–
$AsCl_3$	$218.0^{b)}$ $221.3^{c)}$	216.1 [330]	–	–	–	–	–	–	$98.9^{b)}$ $99.7^{c)}$	98.4 [330]
$(H_5C_6)_3As^{e)}$	–	–	198.1 (av.) $^{c)}$	194.9 (av.) $^{f)}$ [334] 195.7 (av.) $^{f)}$ [335]	99.9 (av.) $^{c)}$	99.7 (av.) $^{f)}$ [334] 100.1 (av.) $^{f)}$ [335]	–	–	–	–
$(H_5C_6)_2As–Cl^{g)}$	$225.7^{c)}$	$226.1^{h)}$ [336]	197.1; $197.6^{c)}$	196.6; $197.2^{h)}$ [336]	$99.5^{c)}$	$104.8^{h)}$ [336]	98.3; $99.4^{c)}$	93.5; $98.3^{h)}$ [336]	–	–
$H_5C_6–AsCl_2{}^{i)}$	$223.5^{c)}$	–	$195.9^{c)}$	–	–	–	$98.5^{c)}$	–	$98.7^{c)}$	–
$AsCl_3$	$218.0^{b)}$ $221.3^{c)}$	216.2 [331]	–	–	–	–	–	–	$98.9^{b)}$ $99.7^{c)}$	98.6 [331]

a) For details see Section 6.5.3; b) calculated by *ab-initio* methods at the MP2/6-311++G** level; c) calculated by DFT methods at the B3LYP/6-311++G** level; d) value obtained from an early GED experiment of the year 1938. e) Molecule of C_3 symmetry; f) four independent molecules in the asymmetric unit; g) molecule of point group C_1; h) values from Cambridge Structural Database; i) molecule of point group C_s

The dependence of As–Cl distances on the number of chlorine atoms at arsenic becomes apparent not only from quantum chemical calculations (Table 5.4), but also from an inspection of Table 5.5. In this compilation of different chloroarsines the parent compound arsenic(III) chloride exhibits the shortest bond length of 216.1 pm [330]. This value is followed by the range of dichloroorganylarsines opening with 218.3 pm from a gas electron diffraction experiment on dichloro(2-chlorophenyl)arsine [337] and closing with 224.0 pm from an X-ray structure analysis on dichloro(η^1-1,2,3,4,5-pentamethylcyclopentadienyl)arsine [338]. Since, however, substituted cyclopentadienyl substituents are known to be electron rich and sterically crowded, the positioning of these values at the upper end is quite understandable. In assertation to this, dichloro(η^1-1,2,3,4-tetraisopropylcyclopentadienyl)arsine exhibits As–Cl distances of 222.3 and 223.5 pm [339].

As for [bis(dichloroarsinyl)methylidene]- (**LX**) and [1-(dichloroarsinyl)ethylidene]triphenylphosphorane (**LXI**) one has to realize that only the length of the unaffected As–Cl bond can be used for a comparison. The second one is strongly elongated by a negative hyperconjugation between the free electron pair at the ylidic carbanion and the σ*(As–Cl) orbital (see Chapter 4); along with the shortened As–C distances these values have been put in brackets. A similar situation of two widely differing As–Cl distances is also come across with dichloro[8-(dimethylaminomethyl)naphthyl]arsine (**LVIII**). In this compound the nitrogen atom of the dimethylamino group interacts with arsenic and increases its coordination number to 4. As a consequence the As–Cl bond *trans* to As←N is elongated to 234.0 pm, whereas the length of the second one (220.7 pm) does not show any peculiarities. Eventually, a disorder of the dichloroarsinyl group in the solid state structure of dichloro[2,6-bis(2,4,6-triisopropylphenyl)phenyl]arsine has been found to falsify the results; hence all values obtained for the As–Cl and As–C bonds are not suitable for a comparison.

The As–Cl distances of chlorodiorganylarsines fall in a rather wide range of 218.1 to 226 pm. Since, however, trifluoromethyl substituted phenyl groups are to be supposed to shorten the As–Cl and to elongate the adjacent As–C1 bonds by still unknown reasons, the values of the first two compounds have to be negated and the virtual range might be confined to bond lengths of 223 to 226 pm. Bearing the foregoing discussion in mind the As–Cl distances in dichloroorganyl– and chlorodiorganylarsines might be fixed at standard values of 221 and 225 pm, respectively. Hence, the mean As–Cl bond length of dichloro[4-(dimethylamino)phenyl]-arsine (**4**, 220.6 pm) does not deviate from the average.

Table 5.5. Characteristic Bond Lengths (pm) and Bond Angles (°) in As–Cl Compounds
Unless otherwise stated the following parameters have been obtained from X-ray structure analyses.

Compound	As–Cl	As–C	C–As–Cl	Cl–As–Cl	Lit.
$AsCl_3$	216.1[a)]			98.4[a)]	[330]
	216.2[b)]			98.6[b)]	[331]
trans-Cl–CH=CH–$AsCl_2$[c)] exp.[d)]	219.7	189.1	101.1	99.1	[345]
calc.[e)]	223.0	194.7	96.6	99.2	
calc.[f)]	223.6	192.3	94.9	99.2	
2-Cl–C_6H_4–$AsCl_2$[c)]	218.3	195.5	98.8	96.7	[337]
$\{2,6\text{-}[2,4,6\text{-}(Me_2CH)_3H_2C_6]_2\text{-}H_3C_6\}AsCl_2$[g)]	216.4	199.0	99.5	114.3 (av.)	[342]
	213.3 (av.)		105.1 (av.)		
	208.9	202.5	100.9	115.8 (av.)	
	217.0 (av.)		100.2 (av.)		
LIX • toluene[h), i)]	219.3	198.1	98.8	99.8	[346]
	219.5		98.1		
4a	221.5	191.9	97.3	94.8	
	219.3		100.5		
4b	221.4	191.5	98.6	96.5	
	220.1		98.9		
$[\eta^1\text{-}1,2,3,4\text{-}(Me_2CH)_4HC_5]AsCl_2$	222.3	205.6		94.5	[339]
	223.5				
$(\eta^1\text{-}1,2,3,4,5\text{-}Me_5C_5)AsCl_2$	224.0	203.5	101.9	92.4	[338]
LVIII[i)]	220.7	194.0	96.1	91.3	[341]
	<234.0>[j)]		94.9		
LX[i)]	221.3	<189.2>	96.6	95.2	[340]
	<227.4> [k)]		103.2		
	222.2	<189.1>	100.5	95.1	
	<225.2> [k)]		102.5		
LXI[i)]	221.6,	<183.1>	99.1	90.9	[340]
	<237.0> [k)]		105.0		
$[2,4,6\text{-}(F_3C)_3H_2C_6]_2As\text{–}Cl$[l)] $P2_12_12_1$	219.2	202.3	100.6		[343]
		201.5	92.0		
$P2_1/a$	218.1	204.7	103.4		
		201.7	90.4		
$[2,4\text{-}(F_3C)_2H_3C_6][2,6\text{-}(F_3C)_2H_3C_6]As\text{–}Cl$	220.7	201.8	100.1		[344]
		198.8	98.8		
$[(Me_3Si)_2CH]_2As\text{–}Cl$	223.1	198.0	103.2		[347]
			97.3		
$(\eta^1\text{-}1,2,3,4,5\text{-}Me_5C_5)_2As\text{–}Cl$	223.9	203.8	98.6		[348]
		204.5	95.5		
$(H_5C_6)_2As\text{–}Cl$	226	197	96		[336]

a) Values from microwave spectra; b) combination of microwave and gas electron diffraction experiments; c) values from gas electron diffraction. d) Since nearly all experimentally determined molecular parameters (exp.) deviate considerably from those calculated quantum chemically using DFT methods at the B3LYP/6-311++G** level (calc.), the gas electron diffraction experiment should be repeated. e) Further bond lengths and angles: C=C 137.4 (exp.) *vs* 132.9 (calc.); C–Cl 172.9 *vs* 174.3 pm; C=C–As 121.0° *vs* 117.5°; C=C–Cl 123.1° *vs* 123.6°; f) calculated by *ab-initio* methods at the MP2/6-311++G** level; further bond lengths and angles: C=C 133.9; C–Cl 172.0; C=C–As 118.7°; C=C–Cl 123.5°. g) Despite severe attempts the disorder of the $AsCl_2$ group could not be resolved completely; parameters derived from more weakly populated chlorine positions have been averaged (see Appendix 9.7, pages 304-305). h) Solid state adduct with one equivalent of toluene; i) for structural formulas see next page; j) As–Cl bond *trans* to the coordinating dimethylamino group; k) elongation of one As–Cl bond due to an electronic interaction between the lone pair of the ylidic carbanion and the σ*(As–Cl) orbital; for details of negative hyperconjugation see Chapter 4. l) Chloro-bis[2,4,6-tris(trifluoromethyl)phenyl]arsine has been found to crystallize in an orthorhombic ($P2_12_12_1$) and a monoclinic space group ($P2_1/a$).

i) structural formulas of selected compounds

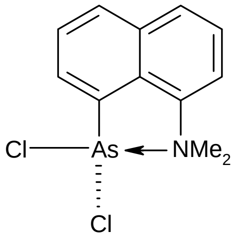

LVIII

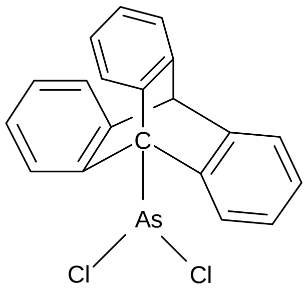

LIX

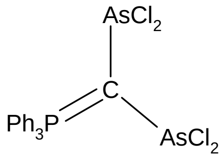

LX

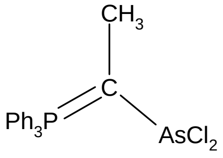

LXI

Already a short look at both the Tables 5.5 and 5.6 reveals a completely different situation for the As–C bond lengths of the two structurally independent molecules **4a** and **4b**. Both distances (191.9 and 191.5 pm) were found to be distinctly *shorter* than a standard bond length of 197 pm which might be derived as follows:

In accordance with the foregoing discussion of As–Cl values one has to realize that a number of compounds are not appropriate for a comparison. Aside from those examples already sorted out, the cyclopentadienyl derivatives characterized by rather long As–C distances of 203.5 to 205.6 pm and *trans*-dichloro(2-chlorovinyl)arsine should also be excluded. With a high degree of certainty the structural parameters of the latter compound obtained from a gas electron diffraction experiment are supposed to be incorrect especially since quantum chemical calculations using DFT methods at the B3LYP/6-311++G** level result in a much longer As–C (189.1 *vs* 194.7 pm, Table 5.5) and a shorter C=C bond (137.4 *vs* 132.9 pm; Table 5.5, – footnote[e)]); hence it were best to repeat the structure determination.

After the separation of unsuitable compounds from Table 5.5 only five chloroarsines have been left; they are dichloroorganylarsine **LIX** (198.1 pm), dichloro(8-dimethylaminonaphthyl)arsine (**LVIII**) (194.0 pm), bis[bis(trimethylsilyl)methyl]chloroarsine (198.0 pm) and chlorodiphenylarsine (197 pm) as well as dichloro(2-chlorophenyl)arsine (195.5 pm) studied by gas electron diffraction. Averaging these As–C values which in spite of very different substituents fall into a rather narrow range from 194.0 to 198.1 pm, and including the mean As–C distance obtained from the slightly varying bond lengths (194.0 to 198.1 pm) of numerous triphenylarsines of Table 5.6, result in an As–C standard of 197 pm as already specified above. Additionally, quantum chemical calculations on different methylarsines using *ab-initio* methods at the MP2/6-311++G** level furnish a sequence of similar, but slightly decreasing As–C distances starting with 196.9 pm trimethylarsine and ending with 194.7 pm for dichloromethylarsine (Table 6.4). These bond lengths are in close agreement with the standard value of 196 pm derived by *Blom* and *Haaland* [133].

Table 5.6. Selected Average Bond Lengths (pm) and Angles (°) of Various Triphenylarsines
Unless otherwise stated the molecular parameters have been obtained from X-ray structure analyses at ambient temperature.

	As–C	C–C	C–As–C	As–C–C	C–C–C	Lit.
5a)	194.9	139.2	99.3	121.3	120.0	
$(H_5C_6)_3As$d)	<194.9 195.7	137.5 137.4	99.7 100.1	120.9 120.7	120.1 120.0	[334]> [335]
$(4\text{-}Me\text{–}C_6H_4)_3As$	<196.0 195.4	140.0 137.6	102.0 99.3	120.0 121.4	120.0 120.2	[349]> [350]
$(4\text{-}Cl\text{–}C_6H_4)_3As$	195.8	137.6	99.8	120.9	120.0	[350]
$(4\text{-}MeO\text{–}C_6H_4)_3As$	196.3	137.5	98.3	121.9	120.0	[350]
$(2,4,6\text{-}Me_3H_2C_6)_3As$	197.6	139.0	107.6	120.1	120.0	[351]
$(2\text{-}Me_2NCH_2\text{–}C_6H_4)_3As$a), e)	198.2	138.6f)	98.5	120.2f)	120.2f)	[352]
$(F_5C_6)_3As$ $(F_5C_6)_3As$a)	196.0 196.3	137.6 137.8f)	100.5 100.3	121.9f) 121.7f)	120.0f) 120.0f)	[353] [354]
$(2,5\text{-}Me_2H_3C_6)_3As$	199.0	139.0	102.0	120.0	120.0	[355]
$[2,4,6\text{-}(Me_2CH)_3H_2C_6]_3As$b)	198.6	139.6f)	109.2	119.9f)	120.0f)	[356]
$[3,5\text{-}(F_3C)_2H_3C_6]_3As$c)	197.6	140.0f)	98.8	120.5f)	120.0f)	[357]
$(4\text{-}I\text{-}2,3,5,6\text{-}Me_4C_6)\text{-}(2,4,6\text{-}Me_3H_2C_6)_2As$	198.0	139.3f)	107.3	120.2f)	120.0f)	[358]
$(2\text{-}I\text{-}3\text{-}MeH_3C_6)(H_5C_6)_2As$	196.1f)	138.5f)	99.3f)	120.7f)	120.0f)	[359]

a) to c) Data collection at 173 K (a), 123 K (b) or 100 K (c); d) four independent molecules in the asymmetric unit; e) six coordinate arsenic atom in the center of a distorted octahedron owing to three intramolecular N→As contacts *trans* to three slightly elongated As–C bonds; f) values from Cambridge Structural Database

Without doubt the substantial shortening of the As–C bond between the dichloroarsinyl unit and the phenyl substituents by 5.3 pm (197 *vs.* 191.7 pm) is caused by the dimethylamino in *para*-position. Since those interactions are known to be interdependent, the geometry of the dimethylamino group and especially the distance between the nitrogen and the *ipso*-carbon atom have to be considered first and to be compared with values of parent compounds such as *N*,*N*-dimethylaniline or *N*,*N*-dimethyl-*p*-toluidine. To the best of our knowledge, however, the solid state structures of both compounds have unfortunately not yet been determined, but two electron diffraction studies of *N*,*N*-dimethylaniline have been performed. The first one published as early as 1965 [360] afforded an only rather vague molecular model in that the planes of the arene ring and the dimethylamino group had been *assumed* to be parallel and as far as bond lengths and angles are concerned, merely average values had been reported. Some years ago *Novikov*, *Samdal* and *Vilkov* [361] repeated the structure determination and achieved a substantial improvement by applying highly discriminating quantum chemical calculations in order to allow for low-frequency vibrations such as the inversion of the dimethylamino group and its torsion round the N–C_{ipso} bond. The most important results of the investigation to be mentioned in this context are the experimental corroboration of the nearly trigonal planar coordination sphere at nitrogen, a N–C_{ipso} bond length of 139.6 pm which is shortened by 6.4 pm in comparison to the N–C_{methyl} distances (146.0 pm) and slightly elongated C_{ipso}–C_{ortho} bonds (140.9 pm); further data will be found in Table 5.7.

Additionally, one can rely upon appropriate studies of solid state adducts formed by both the aniline derivatives mentioned above with acceptor molecules like hexafluorobenzene, 1,2,4,5-tetracyanobenzene and 1-cyano-3,5-dinitrobenzene. Already a short inspection of relevant publications submitted by *Dahl* as well as *Bock*, *Näther* and coworkers [362-364], however, indicates that the results of several structure determinations have to be disregarded due to low quality. Reasons might be an imperfect crystallization of the solid state adducts and twinning or disorder problems difficult to solve. Among those insufficient studies are X-ray structure analyses of the adducts between *N*,*N*-dimethylaniline [362] and *N*,*N*-dimethyl-*p*-toluidine with hexafluorobenzene [365] at ambient temperature. Furthermore, in the solid state adduct of *N*,*N*-dimethyaniline with fluoranil (2,3,5,6-tetrafluoro-*p*-chinone) [366] the donor and acceptor molecules interact to such an extend that the nitrogen atom has to renounce its trigonal planar coordination sphere and is now found in an almost ψ-tetrahedral environment characterized by a sum of angles of 347.9° (Table 5.7, on the right). The solid state adduct of *o*-sulfobenzoimide (saccharin) with *N*,*N*-dimethyl-*p*-toluidine turned out to be a salt [367]; the structure of this compound is not appropriate for a comparison.

Averaging the molecular parameters determined for the *N*,*N*-dimethylaniline part of the solid state adducts with hexafluorobenzene [362], 1,2,4,5-tetracyanobenzene [363] and 1-cyano-3,5-dinitrobenzene [364] at 120, 100 and 220 K, respectively, results in N–C distances of 138.3 and 144.3 pm from an almost sp^2-hybridized nitrogen atom ($\sum$N = 356.5°, Table 5.7) to the phenyl and methyl carbon atoms. These values are not only in a fairly good agreement with the results of the second gas electron diffraction study (139.6 and 146.0 pm [361]) but tally also very well with relevant bond lengths of 138.7 and 145.1 pm calculated quantum chemically with DFT methods at the B3LYP/6-311++G** level for the gaseous *N*,*N*-dimethylaniline molecule showing symmetry *m* and the plane of the arene ring to be parallel to that of the dimethylamino group. The strong shortening of the N–C bond to the *ipso*-carbon atom and a trigonal planar coordination sphere at nitrogen indicate an effective electronic interaction between the free electron pair and the π-system of the molecule, but all the aforementioned N–C_{ipso} distances (138.3, 139.6 and 138.7 pm) are still by about 3.5 pm longer than the bond lengths determined experimentally (135.9 pm) and calculated quantum chemically (137.6 pm) for dichloro[4-(dimethylamino)phenyl]arsine (**4**) (Table 5.7).

Table 5.7. Characteristic Bond Lengths (pm) and Angles (°) of the $(H_3C)_2N–C_6H_x$ Fragment Ascertained for Several Solid State Adducts of *N*,*N*-Dimethylaniline and *N*,*N*-Dimethyl-*p*-toluidine as well as Respective Values Calculated with DFT Methods at the B3LYP/6-311++G** Level in Comparsion with Relevant Parameters of Dichloro[4-(dimethylamino)phenyl]arsine (**4**)

One should be aware that the results of some X-ray structure determinations are not appropriate for a comparison; these values have been placed at the right side of the table. The following numbering scheme has been applied:

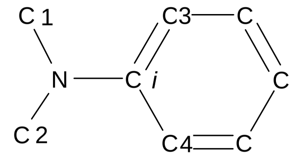

	DMA•HFB$^{a)b)}$ [362]	DMA•TCB$^{a)}$ [363]	DMA•CDNB$^{a)}$ [364]	Mean	DMA$^{c)}$ [361]	**4**(av.) exp.	**4** calc.	DMA$^{a)d)}$ calc.	DMT• HFB$^{a)}$ [365]	DMA• FA$^{a)}$ [366]
N–C*i*	138.5(4)	138.4(2)	137.9(2)	138.3	139.6	135.9	137.6	138.7	136.7(9)	137(2)
N–C1	142.8(5)	144.8(2)	144.2(2)	144.3	146.0	145.4	145.5	145.1	144.0(9)	141(3)
N–C2	144.0(4)	145.1(2)	144.8(2)		146.0		145.6			139(3)
C*i*–C3	141.3(4)	140.5(2)	139.9(2)	140.1	140.9	139.5	141.4	141.4	139.8(9)	140(3)
C*i*–C4	138.6(4)	140.1(2)	139.7(2)		140.9		141.9			
C1–N–C2	119.3(3)	115.2(2)	116.4(2)	117.0	117.4	118.3	119.0	115.8	116.2(2)	109.1(2)
C*i*–N–C1	120.0(3)	118.8(2)	121.1(2)	120.0	121.3	120.6	120.0	120.1	121.9(8)	119.2(1)
C*i*–N–C2	118.8(3)	119.2(2)	120.8(2)	119.6	121.3		120.3	124.1	121.9(8)	119.6(2)
C3–C*i*–C4	118.0(3)	117.8(2)	117.7(2)	117.8	117.5	117.3	117.4	116.8	116.7(8)	117.0(2)
∑N$^{e)}$	358.1	353.2	358.3	356.5	360.0	359.5	359.3	360.0	360.0	347.9

a) *N*,*N*-Dimethylaniline (DMA), hexafluorobenzene (HFB), 1,2,4,5-tetracyanobenzene (TCB), 1-cyano-3,5-dinitrobenzene (CDNB), *N*,*N*-dimethyl-*p*-toluidine (DMT), fluoranil (FA). b) Results of an earlier X-ray structure determination at ambient temperature [362] are highly incorrect and therefore not appropriate for discussion. c) Values from gas electron diffraction experiment; d) molecular symmetry *m*; e) sum of angles at nitrogen.

Since the unusual bond shortenings are supposed to be an indication of the "phenylogous" principle well-known in preparative organic chemistry but up to now hardly understood theoretically, this topic will be discussed in detail in Chapter 5.5.4 which necessarily is enlarged by sophisticated quantum chemical calculations.

As expected all bond lengths and angles unaffected by the π-conjugation of compound **4** do not deviate significantly from standard values. This observation applies for both the outer substituents chlorine and methyl at the arsenic and nitrogen atom, respectively. The average values of the angles Cl–As–Cl (95.7°) and C–As–Cl (98.8°, Table 5.2.) correspond very well with relevant parameters determined for arsenic(III) chloride (98.4°) and chlorodiphenylarsine (93.5° and 98.3°, Table 5.4.). Additionally, quantum chemical calculations on dichlorophenylarsine reveal very similar values of 98.7° and 98.5° for the angles Cl–As–Cl and C–As–Cl, respectively (Table 5.4.). Furthermore, the structural data of the dimethylamino groups of compound **4** and *N*,*N*-dimethylaniline [361] are also found to be very similar. The average N–C_{methyl} bond lengths are almost identical (145.4 *vs* 146.0 pm) and the mean values of the angles C_{methyl}–N–C_{methyl} (118.3°) and C_{methyl}–N–C_{phenyl} (120.6°) determined for compound **4** do not differ substantially from those of *N*,*N*-dimethylaniline (117.4° and 121.3°, repectively; Table 5.7.). In this context, however, one should notice that for these two angles the results of quantum chemical calculations on *N*,*N*-dimethylaniline tally less satisfactorily with experimentally determined values than they did before.

The packing of the two crystallographically different dichloro[4-(dimethylamino)phenyl]arsine molecules **4a** and **4b** in the unit cell is depicted in stereoscopic view in Figure 5.2. An inspection of intermolecular distances reveals two short arsenic…chlorine contacts of 362.6 (As1…Cl11) and 369.0 pm (As1…Cl22) as well as a short arsenic…nitrogen contact of 348.2 pm (As…N1). Since these distances do not deviate substantially from the relevant sums of van-der-Waals radii (As…Cl 380, As…N 357 pm [122,124]), strong intermolecular interactions which might increase the coordination number of arsenic, have to be cluded. Taking into account an analogous sum of 380 pm for arsenic and carbon, the same conclusion holds for several short arsenic···carbon contacts found in a range from 357.9 (As2…C23) or 361.1 pm (As…C14) and 375.6 (As2…C17) to 378.4 pm (As…C22).

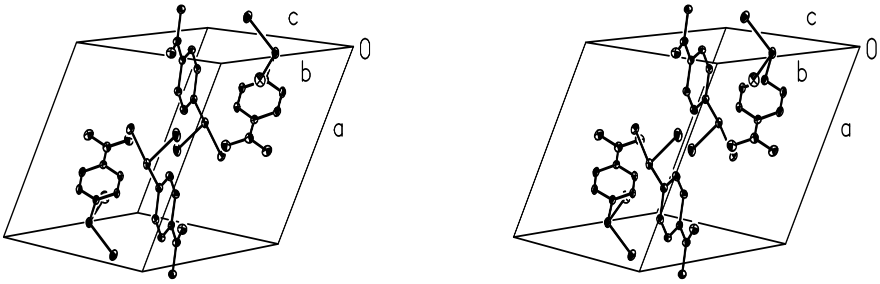

Figure 5.2. Packing of the two crystallographically independent dichloro[4-(dimethylamino)phenyl]arsine molecules **4a** and **4b** in stereoscopic view
The unit cell comprises four molecules. Thermal ellipsoids are at 30 % probability, hydrogen atoms have been omitted for clarity.

5.5.3. Molecular Structure of Compound 5

Since the heteroleptic compound dichloro[4-(dimethylamino)phenyl]arsine (**4**) differs from the homoleptic tris[4-(dimethylamino)phenyl] derivative (**5**) merely by exchange of two 4-(dimethylamino)phenyl substituents for chlorine, a comparsion of appropriate bond lengths and angles obtained from X-ray structure analyses of these two substituted phenylarsines, will open an additional chance of pointing out the unexpected electronic interaction between the dichloroarsinyl group and the π-system of the 4-(dimethylamino)phenyl unit of molecule **4** elaborated in detail in the preceding chapter. At first, however, a molecular model of compound **5** will be depicted stereoscopically in Figure 5.3. As already indicated by a sum of angles at arsenic of 298.0° and individual C–As–C values varying only slightly between 98.5 and 100.2° (Table 5.2.), the central atom is found in a trigonal pyramidal environment (see below). Previous to a necessary but rather difficult analysis of the molecular conformation, however, the following discussion will focus first on the bonding situation at the dimethylamino groups and the As–C distances.

As the sums of angles at the nitrogen atoms N4 and N5 amount to values of 353.6° and 356.1°, respectively, and hence deviate significantly from the value of nitrogen atom N3 (348.1°, Table 5.2.), only two of three dimethylamino groups are considered to be almost planar. The third one is found in an environment which has to be classified as intermediate between trigonal planar and trigonal pyramidal. Since for amines the barrier of a pyramidal inversion at nitrogen is well known to be rather low, crystal packing effects may easily account for the different geometry. Furthermore, the angles between the least-squares planes of the arene rings A_n and the dimethylamino groups B_n ($n = 3 \rightarrow 5$, Table 5.3.) fall into a rather wide range from 35.9° (A3 / B3) to 15.8° (A5 / B5). Differing distances of the two carbon atoms Cn7 and Cn8 to the least-squares planes A_n of the arene rings give additional information about the twist of the dimethylamino groups (Table 5.3.); the difference in these two values is highest again for the two carbon atoms C37 and C38 at nitrogen atom N3.

Irrespective of these minor deviations the structural data of the dimethylamino groups of compound **5** correspond very well with parameters obtained for *N*,*N*-dimethylaniline by gas electron diffraction [361]. Especially the length of the characteristic N–C$_{phenyl}$ bond which in comparsion to the average N–C$_{methyl}$ distance of 144.8 pm is shortened to 139.0 pm owing to π-conjugation with the arene ring, tallies with the appropriate value of the aniline derivative (139.6 pm, Table 5.7). Moreover, nearly identical N–C$_{phenyl}$ and N–C$_{methyl}$ distances of 138.7 and 145.4 pm, respectively, obtained from quantum chemical calculations on *N*,*N*-dimethylaniline, can also be taken for a comparsion (Table 5.7.).

The structural similarity between tris[4-(dimethylamino)phenyl]arsine (**5**) and a standard compound such as *N*,*N*-dimethylaniline holds not only for the outer part of the molecule, as elaborated just above but also for its arsenic centre. For comparison numerous triphenylarsine derivatives along with triphenylarsine itself have been compiled in Table 5.6. Despite various substituents at the arene rings the average As–C bond lengths fall into a rather small range from 195.4 pm obtained for tris(4-methylphenyl)arsine to 199.0 pm for the tris(2,5-dimethylphenyl) derivative. One, however, should note that the results of some older X-ray structure analyses on triphenylarsine itself [334] and tris(4-methylphenyl)arsine [349] are not accurate enough as to be taken for comparsion; these values have been put in brackets.

The series of average As–C distances starts with tris[4-(dimethylamino)phenyl]arsine (**5**; 194.9 pm) but is immediately followed by the almost identical value of triphenylarsine (195.7 pm) crystallizing with four independent molecules in the asymmetric section of the unit cell. As expected, methyl groups or even bulkier substituents in positions 2 and 6 of the arene rings cause an elongation of the average As–C distances up to values of 198.6 or 199.0 pm published *e.g.* for tris(2,4,6-triisopropylphenyl)arsine or tris(2,5-dimethylphenyl)arsine, respectively. Tris[2-(dimethylaminomethyl)phenyl]arsine, however, has to be regarded as an exception as three dimethylamino groups additionally coordinate at the arsenic atom and increase its coordination number to 6 (As–C 198.2 pm). Parallel to the As–C bond elongation a widening of the C–As–C angles up to 107.6° in tris(2,4,6-trimethylphenyl)arsine is observed.

As a summary, the following results have to be pointed out: The X-ray structure analysis of tris[4-(di-methylamino)phenyl]arsine (**5**) clearly demonstrates that the unusual shortening of the N–C$_{phenyl}$ as well as the As–C$_{phenyl}$ bond lengths are restricted to dichloro [4-(dimethylamino)phenyl]arsine (**4**) and disapper completely or at least largely when the highly electronegative chlorine atoms at arsenic are replaced by 4-(dimethylamino)phenyl substituents.

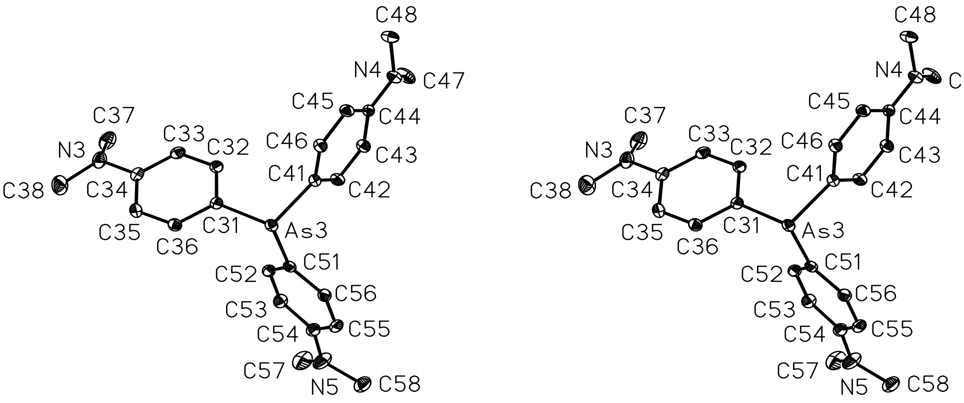

Figure 5.3. Molecular model of compound **5** in stereoscopic view
Thermal ellipsoids are at 30% probability; hydrogen atoms have been omitted for clarity.

In order to allow a straightforward conformational analysis of compound **5** the phenyl carbon atoms in *ortho* position to the arsenic atom which are located closer to the nonbonding electron pair (EP; free coordination site of the distorted tetrahedron at arsenic) are attributed the designation Cn6 (n = 3, 4, 5) (Figure 5.3). According to the rules set up by *Cahn*, *Ingold* and *Prelog* [368] the torsion angle EP–As3–Cn1–Cn6 (φn3, Figure 5.4.) has to be used to define the partial conformation of an individual As3–Cn1 bond. Since, however, the position of the pseudoatom EP cannot be established, the values of φn3 cannot be determined directly and have to be calculated from the relevant torsion angles φn4, φn2 and φn1 (Table 5.2.c, Figure 5.4.) by applying the formula

$$\varphi n3 : \varphi(\mathrm{EP{-}As3{-}C}n1\mathrm{{-}C}n6) = -\left[180 - |\varphi n4| - \tfrac{1}{2}\left(|\varphi n2| + |\varphi n1|\right)\right]$$

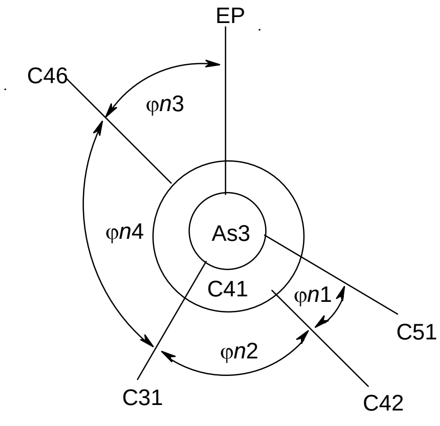

As3 in front of C41

Figure 5.4. Newman projection to specify the partial conformation of the individual As3–Cn1 bond. The bond As3–C41 has been selected as an example.

The calculation results in torsion angles φ*n*3 of –47.7°, –38.5° and –40.2° (Table 5.2.c). These values indicate a negative synclinal [369] partial conformation at all As3–C*n*1 bonds and hence a helical chirality of the molecule concerned (Figure 5.3). Since the angles φ*n*3 are found to be very similar, a high degree of molecular C_3 pseudosymmetry is achieved. Furthermore, the planes of the arene rings form an right-handed propeller; by the centres of inversion of space group $P\overline{1}$ the enantiomeric molecule is generated (Figure 5.5.).

The packing of molecule (**5**) in the unit cell is illustrated in Figure 5.5. An inspection of tris[4-(dimethylamino)phenyl]arsine intermolecular distances does not reveal any values exceeding the sum of appropriate van-der Waals radii.

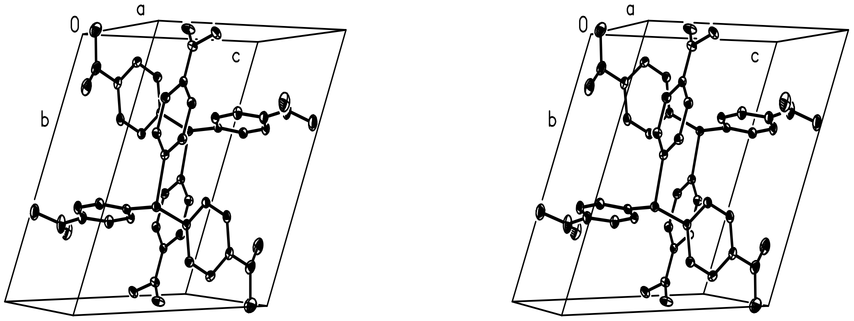

Figure 5.5. Packing of tris[4-(dimethylamino)phenyl]arsine (**5**) in stereoscopic view. The unit cell comprises two enantiomeric molecules. Thermal ellipsoids are at 30% probability, hydrogen atoms have been omitted for clarity.

5.4. Reactions of 2-*tert*-Butyl-1λ³-phosphaalkyne with Dichloro[4-(dimethylamino)-phenyl]arsine

Combined solutions of one equivalent of dichloro[4-(dimethylamino)phenyl]arsine and slightly more than three equivalents of 2-*tert*-butyl-1λ³-phosphaalkyne in acetonitrile were allowed to warm up to room temperature from –78 °C. After removing a small amounts of an insoluble precipitate, the red-coloured filtrate showed different $^{31}P\{^1H\}$ NMR signals (Figure 5.6). Attempts to isolate any product were unsuccessful. Furthermore, the reaction was carried out in different solvents (such as dichloromethane, tetrahydrofuran and acetonitrile) but all attempts to isolate a crystalline product were unsuccessful.

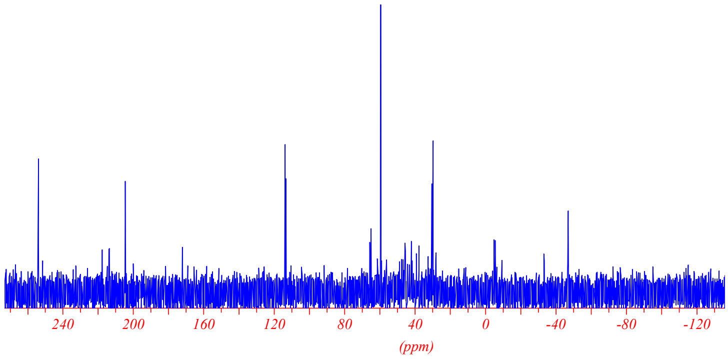

Figure 5.6. $^{31}P\{^{1}H\}$ NMR spectrum of an d_8-toluene solution from dichloro[4-(dimethylamino)phenyl]arsine and 2-*tert*-butyl-1λ^3-phosphaalkyne

5.5.4. Quantum Chemical Calculations on Various Substituted Dichlorophenylarsines

In the molecular structure of dichloro[4-(dimethylamino)phenyl]arsine (**4**), unusual changes in bond lengths have been noticed. Compared with standard values which, however, have to be corrected [370] to 144 and 194 pm for the N_{sp2}–C_{sp2} and As–C_{sp2} single bond, respectively, the distances between the *ipso*-carbon atoms and nitrogen as well as arsenic are both shortened to values of 135.9 and 191.9 pm. Additionally, relatively large fluctuations in the C–C bond lengths from 137.1 to 142.3 pm within the arene ring (Table 5.2) suggest substantial substituent effects.

To throw light on the aforementioned problems quantum chemical calculations were performed [253] in particular with regard to population analyses on a *natural bond orbital* (NBO) basis. By such a procedure information on the allocation of atomic charges as well as the significance of donor-acceptor interactions between Lewis-type natural bond orbitals is easily available. For all compounds to be studied NBO analyses were accomplished by use of the hybrid density functional method B3LYP [371] and the basis set 6-311++G** [372]. From the *canonical molecular orbitals* initially obtained by these calculations, *natural bond orbitals* (NBOs) are derived applying mathematical algorithms to receive representations of two- or three-center bonds and for lone pairs.

As for dichloro[4-(dimethylamino)phenyl]arsine (**4**) NBO analyses were performed using the results of the X-ray structure determination as well as molecular parameters supplied by quantum chemical calculations. In the case of the experimentally based NBO analysis the atomic coordinates of the non-hydrogen atoms were directly adopted from the last stage of the crystal structure refinement, whereas standard values of 109 and 108 pm had to be ascribed to the C–H bond lengths of the methyl groups and the arene ring, respectively. Without doubt the initially most important result of these quantum chemical studies was the close agreement in the molecular parameters obtained from the solid state structure analysis and from calculations on the gaseous compound (Figure 5.5.4.1 **a**) and **b**); Table 5.5.4.1). The only major deviation worth to be mentioned are differences of 5.4 and 3.1 pm in the As–Cl bond lengths (221.5 *vs* 224.6; 219.3 *vs* 224.7 pm), whereas the distances between arsenic or nitrogen and the *ipso*-carbon atoms C1 and C4, respectively, are found to be rather similar (191.9 *vs* 193.5; 135.9 *vs* 137.6 pm).

By analogy to *N*,*N*-dimethylaniline [361] the aforementioned shortening of the N–C_{ipso} bond to 135.9 pm can be attributed to an electronic interaction between the lone pair at nitrogen and the antibonding π^* orbitals of the adjacent C_{ipso}–C_{ortho} bonds; on an average these two distances are significantly elongated by 1.7 pm (Table 5.2) with respect to the standard value (140 pm).

Quite obviously the interaction is intensified by structural features such as the trigonal planar coordination sphere at nitrogen (Table 5.2 b) and an almost perfect co-planarity of the arene ring with the dimethylamino group; in both the crystallographically independent molecules **4a** and **4b** the deviations come up to 12.6° and 1.6° only (Table 5.3). The sp^2-hybridization of the nitrogen atom is also reflected in the results of the NBO hybridization analysis; *s* and *p* character of all bonding orbitals involved vary only slightly between 0.3111 and 0.3695 and between 0.6298 and 0.6895, respectively. This type of hybridization also implies an almost pure *p* character of the lone pair (0.9939). In this context one should point out that quantum chemical calculations on the gaseous aniline molecule itself reveal a non-planar coordination sphere at nitrogen; the sum of angles (343.4°) is found to be intermediate between the values of an sp^2- and an sp^3-hybridization (Fig. 5.5.4.1 **i**). Experimental and theoretical studies have been summarized in the publication of *Novikov* et al. [361].

Further donor-acceptor interactions in the dichloro[4-(dimethylamino)phenyl]arsine (**4**) molecule are restricted to donating effects within the arene ring; in particular, one has to emphasize that such an interaction cannot be observed for bonds at the arsenic atom. Therefore, an NBO charge analysis was performed to account for the significant shortening of the As–C_{ipso} bond to 191.9 pm. It results in a high positive charge of 0.963 to be allocated to the arsenic atom (Fig. 5.5.4.1 **a**), whereas the adjacent *ipso* carbon atom exhibits a rather high negative charge of –0.468. In comparison to values of –0.404 and –0.260 calculated for the *ipso*-carbon atom of dichlorophenylarsine (**c**) and the hydrogen bonded *para* carbon atom of *N*,*N*-dimethylaniline (**d**), respectively, a considerable increase in negative charge has to be noticed, whereas the positive charge at the arsenic atom of dichlorophenylarsine (0.974; **c**) turned out to be almost unchanged. The unusual shortening of the As–C_{ipso} bond in dichloro[4-(dimethylamino)phenyl]arsine (**4**) may therefore be essentially traced back to the unexpectedly high difference of 1.431 elementary charges and an enhanced electronic attraction between arsenic and *ipso* carbon atom.

The electronic situation specified above can best be described in the sense of a push-pull effect in that the dimethylamino substituents induces (pushes) a negative charge at (to) the *para* carbon atom and this charge is additionally increased by (pulled to) the dichloroarsinyl group. In our opinion the As–C_{ipso} bond length might be appropriate to serve as an indicator for this effect; its size should depend on the Hammett constants [373] of the substituents. Since results of structure determinations on dichlorophenylarsines with different substituents in *para* position to the Cl_2As group are not available, quantum chemical calculations were performed to obtain the necessary data.

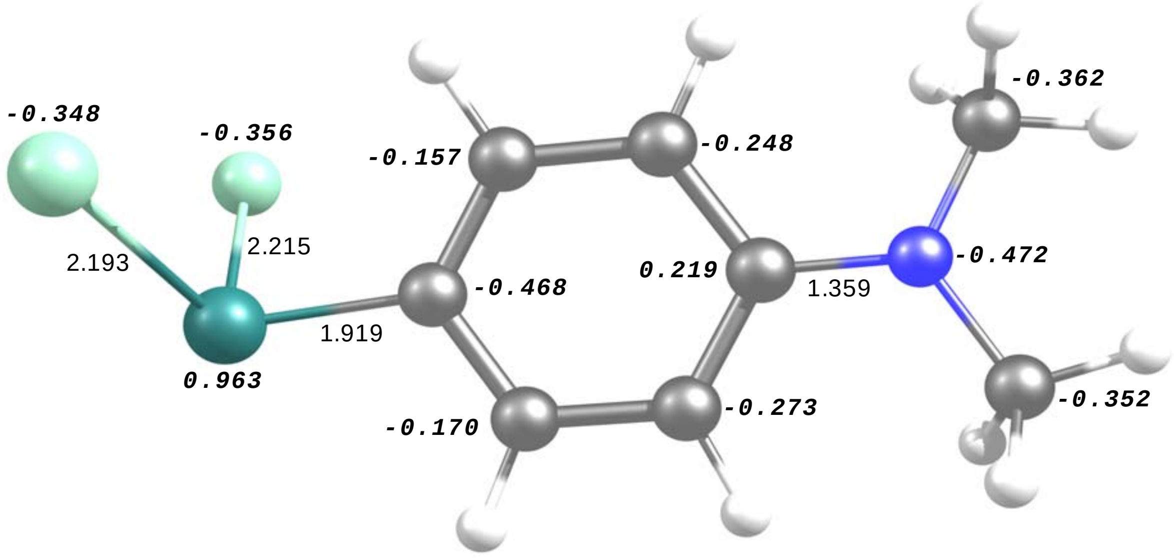

a) Dichloro[4-(dimethylamino)phenyl]arsine (experimentally)

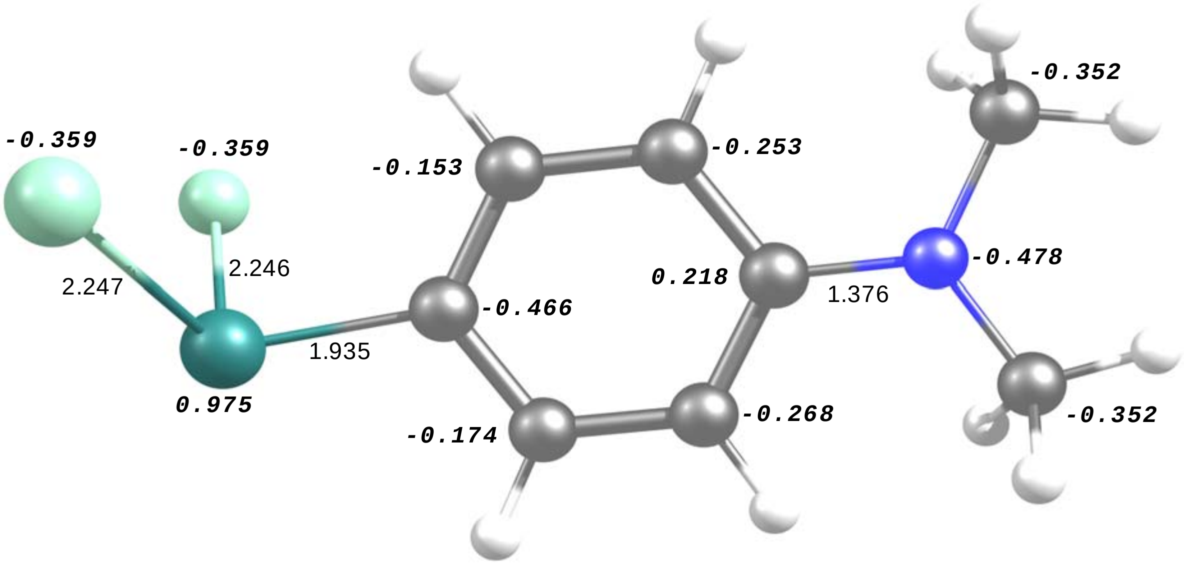

b) Dichloro[4-(dimethylamino)phenyl]arsine (calculated)

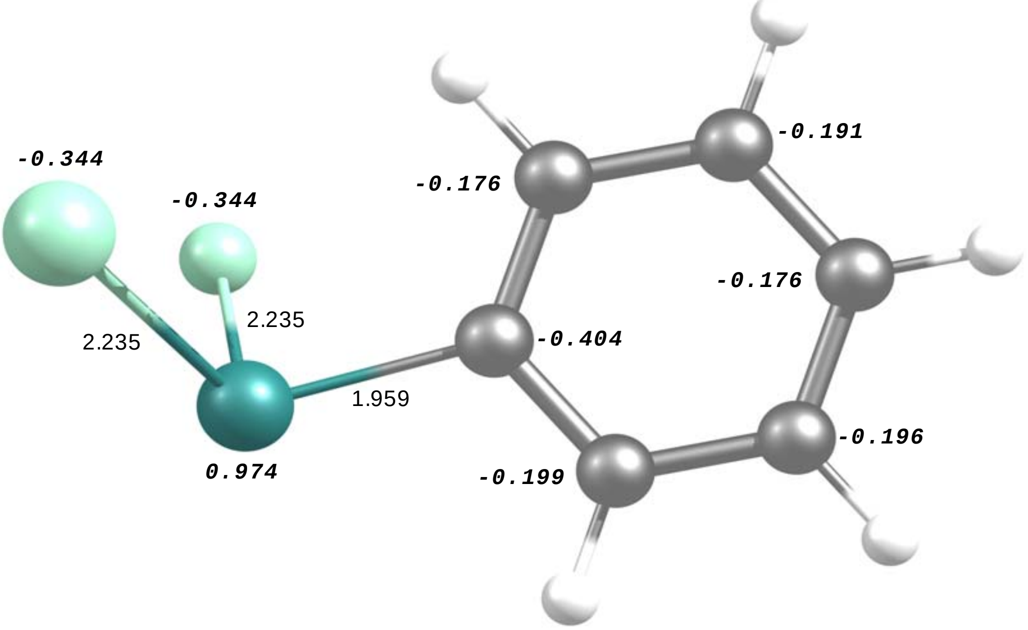

c) Dichlorophenylarsine (calculated)

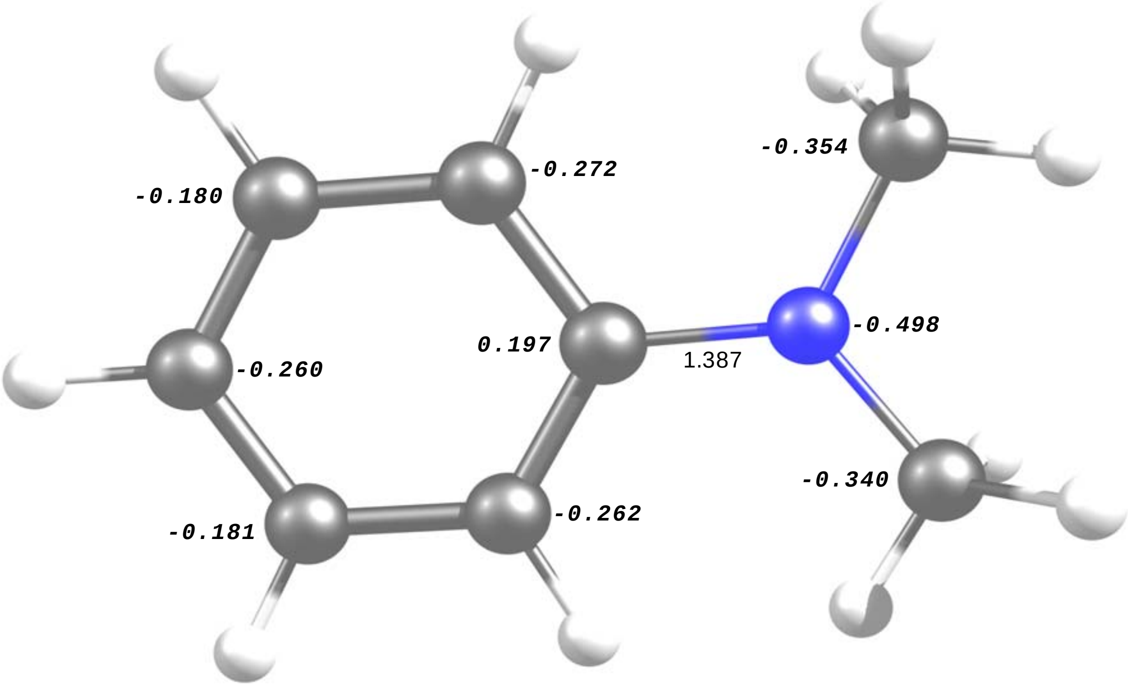

d) Dimethylaniline (calculated)

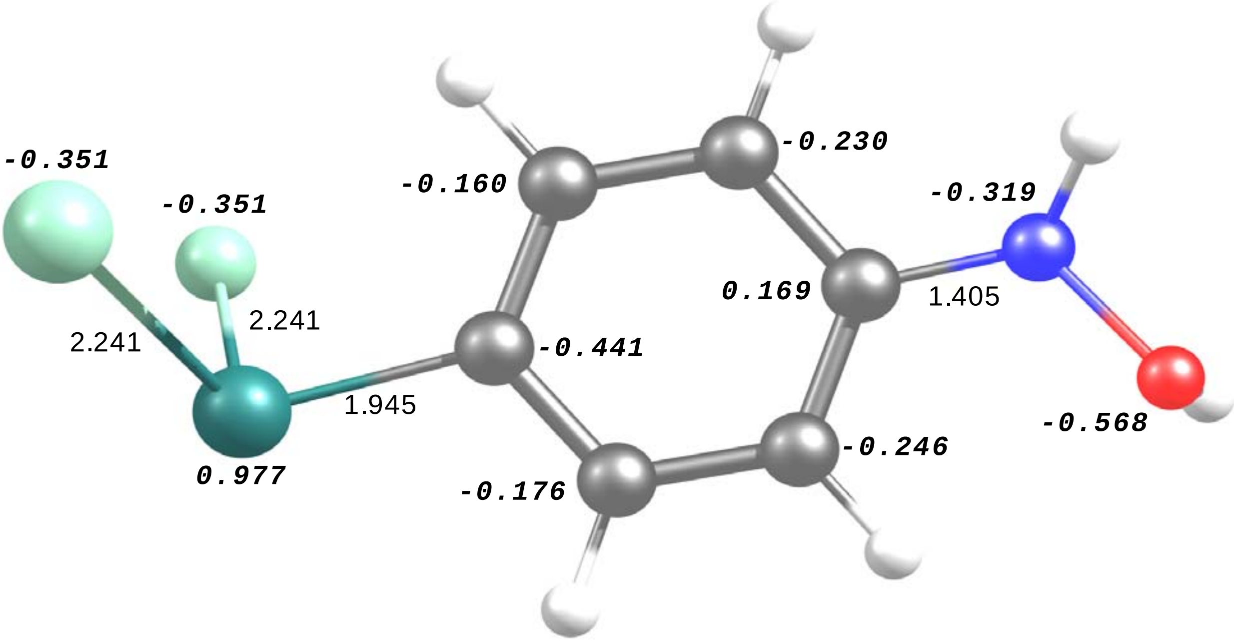

e) Dichloro[4-(hydroxylamino)phenyl]arsine (calculated)

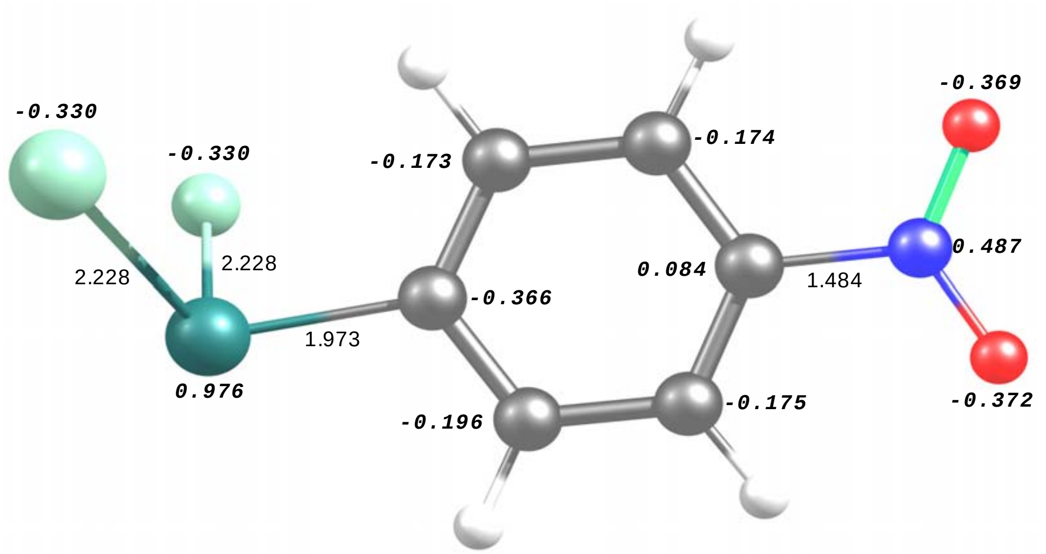

f) Dichloro(4-nitrophenyl)arsine (calculated)

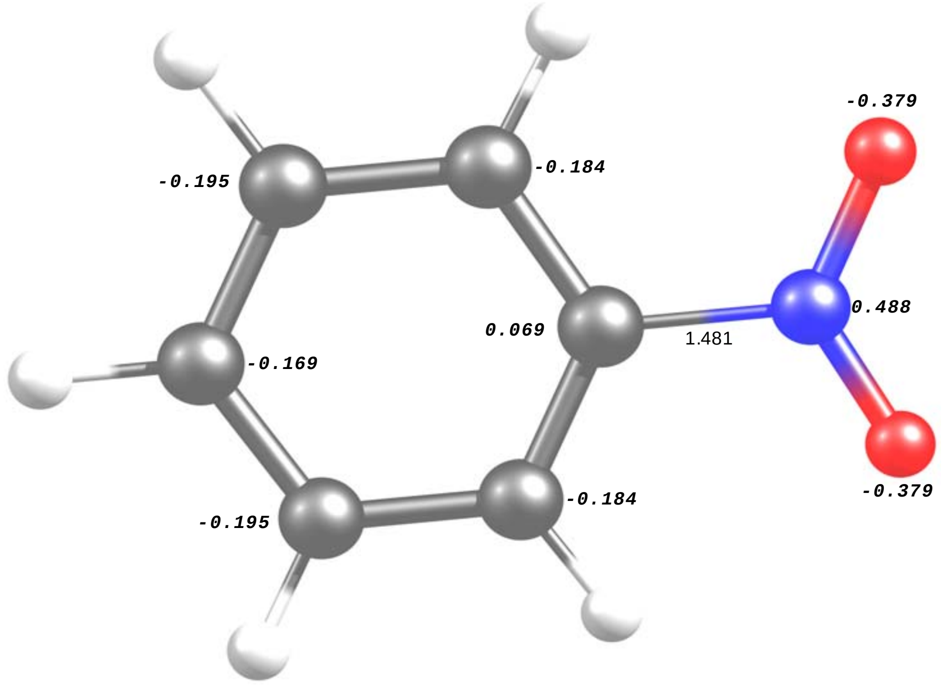

g) Nitrobenzene (calculated)

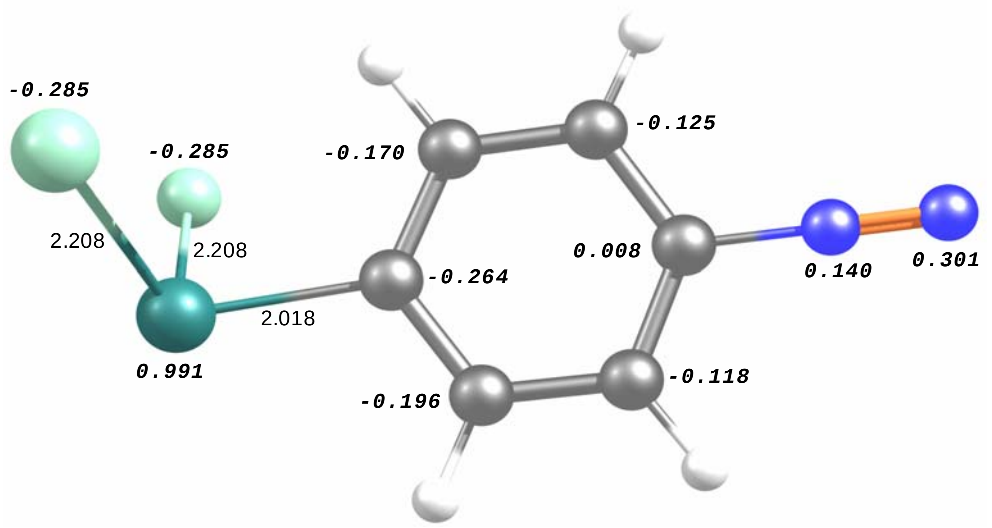

h) Dichloro(4-diazoniumphenyl)arsine Cation (calculated)

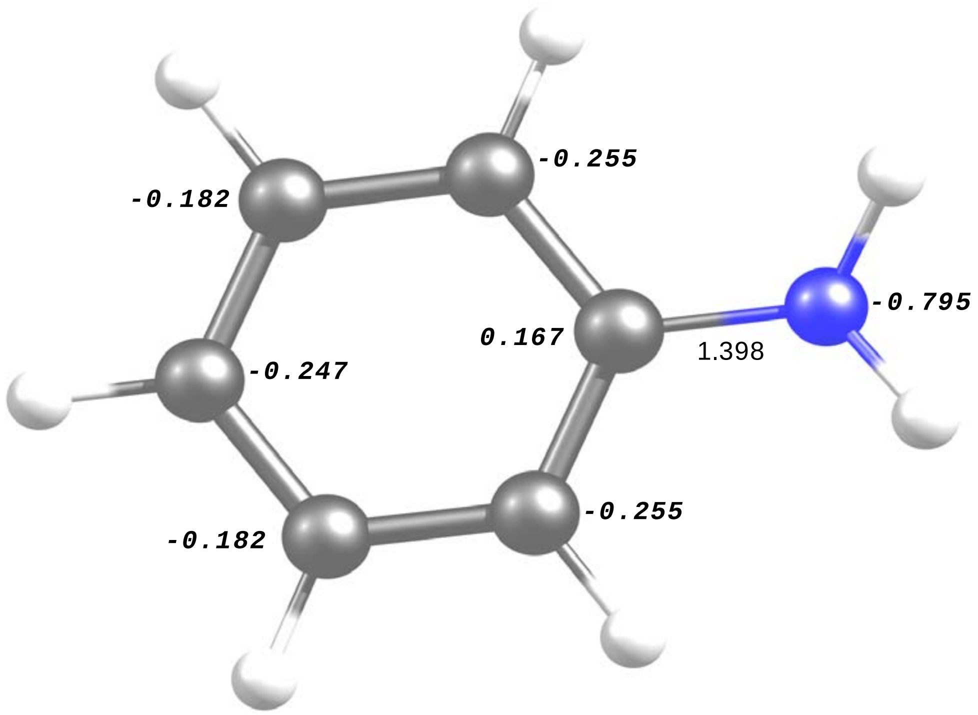

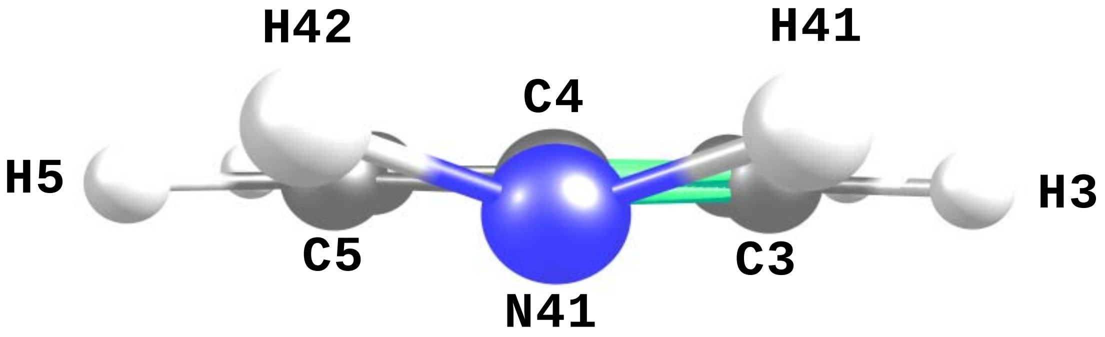

(Molecule in side-view)

i) Aniline (calculated)

Figure 5.5.4.1. Molecular models of different dichlorophenylarsines and related compounds together with bond lengths (standard figures) and NBO charges (*italic figures*) calculated quantum chemically at the B3LYP/6-311++G** level of theory:
a) and **b**) 4-$Me_2N–C_6H_4–AsCl_2$; **c**) $C_6H_5–AsCl_2$; **d**) $Me_2N–C_6H_5$; **e**) 4-HO(H)N–$C_6H_4–AsCl_2$; **f**) 4-$O_2N–C_6H_4–AsCl_2$; **g**) $O_2N–C_6H_5$; **h**) $[4\text{-}N_2–C_6H_4–AsCl_2]^{\oplus}$ Cation; **i**) $H_2N–C_6H_5$ (C4–N4–H41 115.6°; C4–N4–H42 115.6°; H41–N4–H42 112.2°; $\sum$(N4) = 343.4°; C2–C1–C6 (α) 118.9°; C3–C4–C5 (β) 118.6°)

Table 5.5.4.1. Correlation between Hammett Constants σ_p and Molecular Properties of Some Dichlorophenylarsines 4-X$_p$–C$_6$H$_4$–AsCl$_2$
The values of the table illustrate the correlation between the Hammett constants σ_p of various substituents X$_p$ *in para* position to the Cl$_2$As group and molecular properties such as characteristic bond lengths, bond angles and elementary charges Q of the two *ipso* carbon atoms in position 1 (As–C1) and 4 together with appropriate charge differences ΔQ. In addition to the endocyclic angles α and β at the atoms C1 and C4, respectively, their differences Δ_α and Δ_β to the values of unsubstituted dichlorophenylarsine or benzene are given. For comparison relevant data of *N*,*N*-dimethylaniline, aniline itself and nitrobenzene have been included.

Compound	As–C1	As–Cl	Cl–As–C1	Cl–As–Cl	C2–C1–C6 (α) / Δ_α	Q_{C1}	$\Delta Q_{As–C1}$	C4–N	C3–C4–C5 (β) / Δ_β	Q_{C4}	$\Delta Q_{C4–N}$	σ_p [257]
Cl$_2$As–C$_6$H$_4$–NMe$_2$ (exp.)	191.9	220.4 (av.)	98.9 (av.)	94.8	118.5 / –	-0.468	1.431	135.9	117.2 / –	0.219	0.691	-0.83
Cl$_2$As–C$_6$H$_4$–NMe$_2$ (calc.)	193.5	224.6 (av.)	99.2	97.6	118.4 / -1.7	-0.466	1.441	137.6	117.4 / -2.8	0.218	0.696	-0.83
Cl$_2$As–C$_6$H$_4$–N(H)OH	194.5	224.1	98.8	98.1	119.1 / -1.0	-0.441	1.418	140.5	119.7 / -0.5	0.169	0.488	-0.34
Cl$_2$As–C$_6$H$_4$–H	195.9	223.5	98.5	98.7	120.1 / ±0.0	-0.404	1.378	–	120.2 / ±0.0	-0.176	–$^{a)}$	0.00
Cl$_2$As–C$_6$H$_4$–NO$_2$	197.3	222.8	97.7	99.2	120.3 / +0.2	-0.366	1.342	148.4	122.5 / +2.3	0.084	0.403	0.78
[Cl$_2$As–C$_6$H$_4$–N≡N]$^{\oplus}$	201.8	220.8	95.0 (av.)	100.6	120.6 / +0.5	-0.264	1.255	137.9	124.0 / +3.8	0.008	0.132	1.91
C$_6$H$_5$–NMe$_2$	–	–	–	–	118.1 / -1.9$^{b)}$	-0.260	–	138.7	116.8 / -3.2$^{b)}$	0.197	0.695	-0.83
C$_6$H$_5$–NH$_2$	–	–	–	–	118.9 / -1.1$^{b)}$	-0.247	–	139.8	118.6 / -1.4$^{b)}$	0.167	0.962	-0.66
C$_6$H$_5$–NO$_2$	–	–	–	–	120.3 / +0.3$^{b)}$	-0.169	–	148.1	122.3 / +2.3$^{b)}$	0.069	0.419	0.78

a) $\Delta Q_{C4–H}$ = 0.384; b) difference to the C–C–C angles of benzene (120.0°)

Table 5.5.4.2. Influence of Various Substituents X_p on the C–C Bond Lengths[a] of Some Dichlorophenylarsines 4-X_p–C_6H_4–$AsCl_2$
The compounds are arranged as to an increase of the Hammett constants σ_p of the substituents X_p *in para* position to the Cl_2As group. For a better comparison data of *N*,*N*-dimethylaniline, aniline itself and nitrobenzene have been included. In addition to the distances, differences Δ to appropriate values of unsubstituted dichlorophenylarsine (above) or benzene (below), respectively, are given.

Compound	C4–C3 / $\Delta_{C4–C3}$	C4–C5 / $\Delta_{C4–C5}$	C3–C2 / $\Delta_{C3–C2}$	C5–C6 / $\Delta_{C5–C6}$	C2–C1 / $\Delta_{C2–C1}$	C6–C1 / $\Delta_{C6–C1}$	σ_p [257]
$Cl_2As–C_6H_4–NMe_2$ (exp.)	141.0 / +1.3[b]	142.4 / + 3.2[b]	137.9 / -1.1[b]	137.2 / -2.4[b]	139.6 / -0.3[b]	139.4 / -0.4[b]	-0.83
$Cl_2As–C_6H_4–NMe_2$ (calc.)	141.9 / +2.2	141.4 / +2.2	138.2 / -0.8	138.8 / -0.8	140.1 / +0.2	140.0 / +0.2	-0.83
$Cl_2As–C_6H_4–N(H)OH$	140.7 / +1.0	139.7 / +0.5[c]	138.3 / -0.7	139.2 / -0.4[c]	140.1 / +0.2	139.8 / ±0.0[c]	-0.34
$Cl_2As–C_6H_4–H$	139.7 / ±0.0	139.2 / ±0.0	139.0 / ±0.0	139.6 / ±0.0	139.9 / ±0.0	139.8 / ±0.0	0.00
$Cl_2As–C_6H_4–NO_2$	139.3 / -0.4	138.8 / -0.4	138.9 / -0.1	139.4 / -0.2	139.9 / ±0.0	139.8 / ±0.0	0.78
$[Cl_2As–C_6H_4–N{\equiv}N]^{\oplus}$	140.9 / +1.2	140.4 / +1.2	138.2 / -0.8	138.7 / -0.9	140.4 / +0.5	140.2 / +0.4	1.91
$C_6H_5–NMe_2$	141.4 / +1.9	141.4 / +1.9	139.1 / -0.4	139.0 / - 0.5	139.2 / -0.3	139.4 / -0.1	-0.83
$C_6H_5–NH_2$	140.3 / +0.8	140.3 / +0.8	140.3 / -0.4	139.1 / -0.4	139.5 / ±0.0	139.5 / ±0.0	-0.66
$C_6H_5–H$	139.5 / ±0.0	139.5 / ±0.0	139.5 / ±0.0	19.5 / ±0.0	139.5 / ±0.0	139.5 / ±0.0	0.00
$C_6H_5–NO_2$	139.1 / -0.4	139.1 / -0.4	139.1 / -0.4	139.1 / -0.4	139.5 / ±0.0	139.5 / ±0.0	0.78

a) Numbering scheme of the arene ring

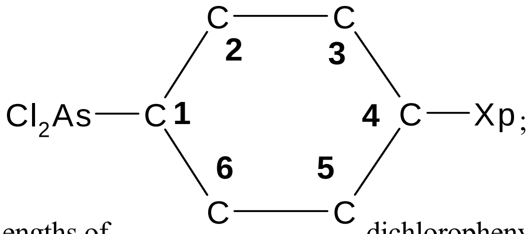

; b) average C–C bond lengths adopted from Table 6.2.; difference values obtained in comparison with calculated bond lengths of dichlorophenylarsine; c) N–OH side of the arene ring

a)

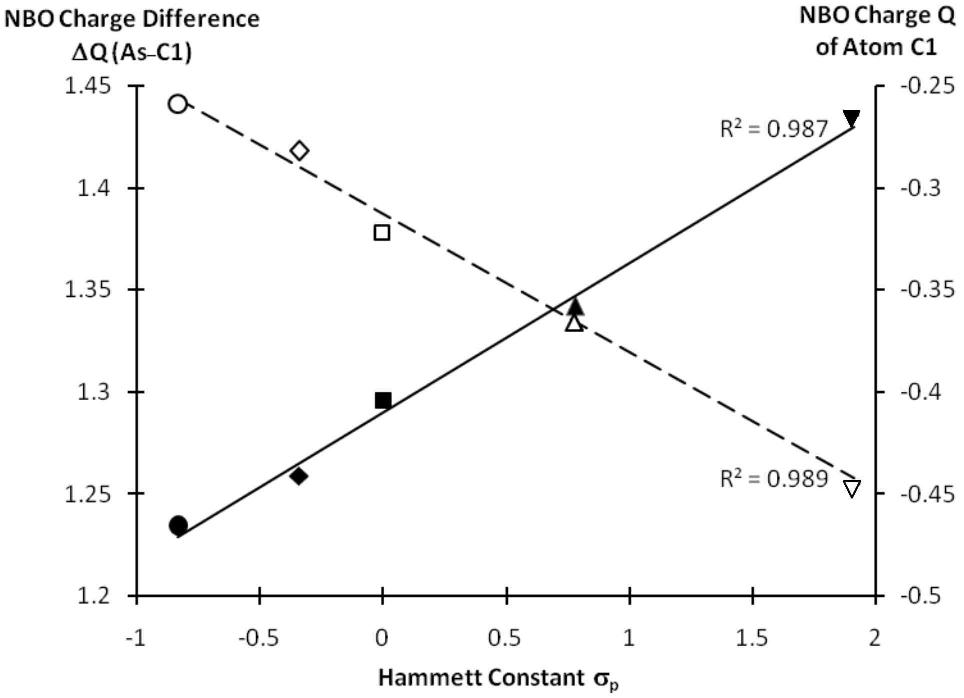

b)

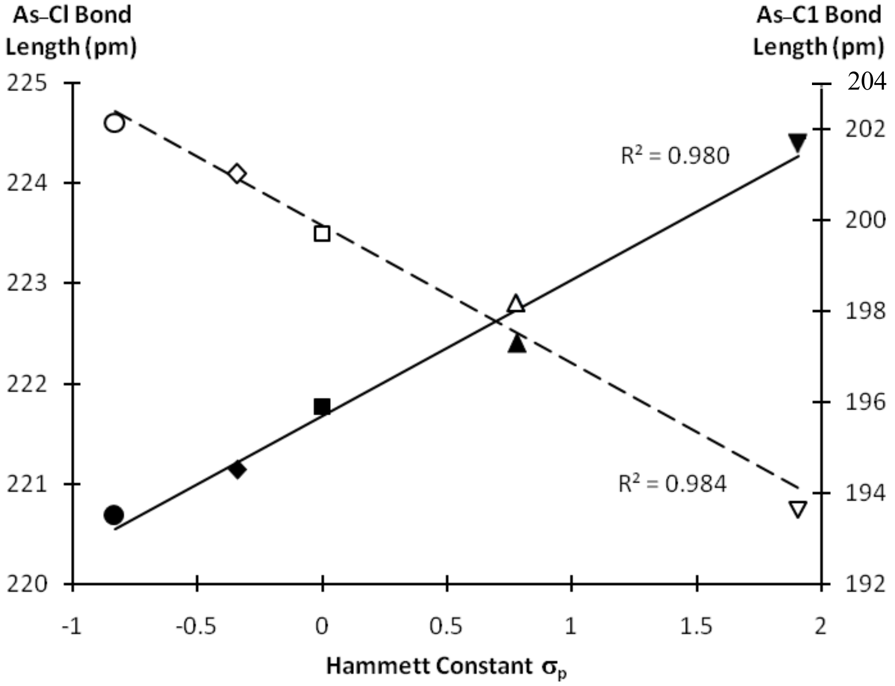

Figure 5.5.4.2. Correlation between the Hammett constant σ_p of the substituent X_p (● NMe_2; ♦ N(H)OH; ■ H; ▲ NO_2; ▼ $N_2^{\oplus}$) in *para* position to the $AsCl_2$ group and
a) the NBO charge difference $\Delta Q_{As–C1}$ (left, dashed line and open symbol) together with the NBO charge Q of atom C1 (right) and
b) the As–Cl (left, dashed line and open symbol) as well as the As–C1 bond length (right) of several dichlorophenylarsines $4\text{-}X_p–C_6H_4–AsCl_2$

a)

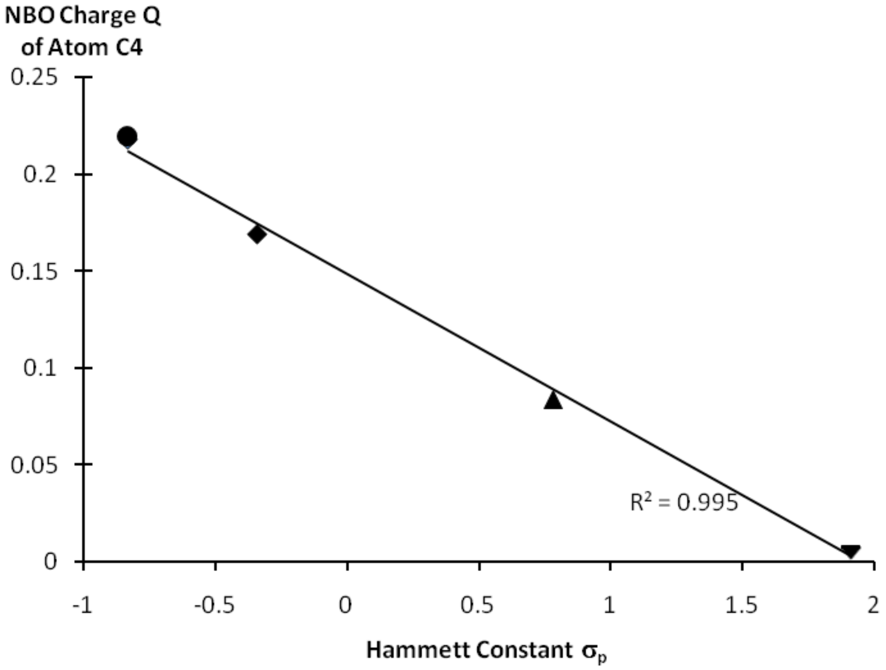

b)

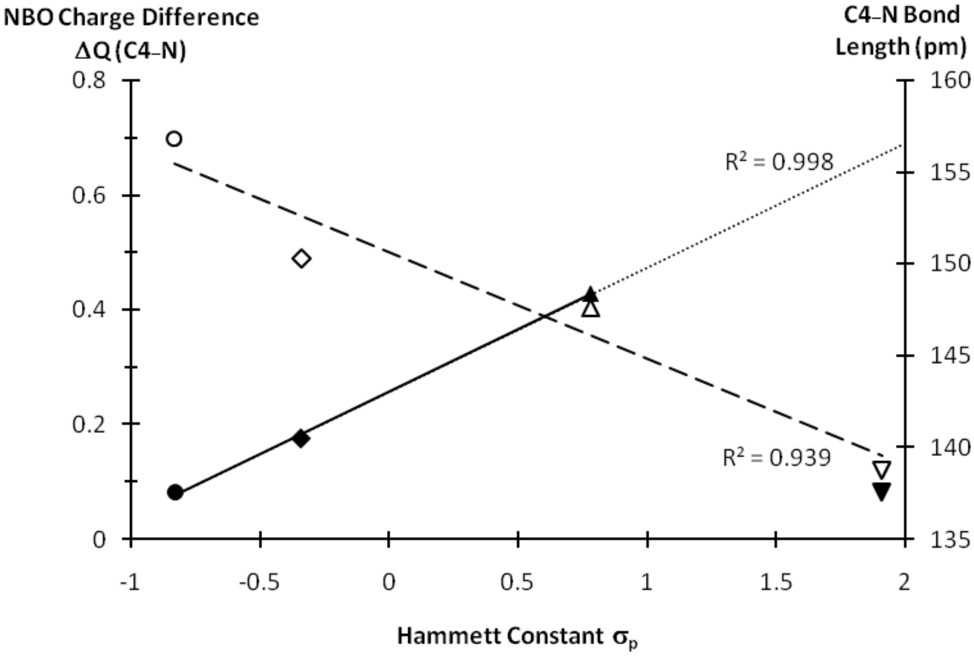

Figure 5.5.4.3. Correlation between the Hammett constant σ_p of the substituent X_p (● NMe_2; ♦ N(H)OH; ▲ NO_2; ▼ $N_2^{\oplus}$) in *para* position to the $AsCl_2$ group and
a) the NBO charge of atom C4 together with
b) the appropriate $\Delta Q_{(C4–N)}$ charge difference (left, dashed line and open symbol) and the C4–N bond length (right) of several dichlorophenylarsines 4-X_p–C_6H_4–$AsCl_2$. It should be noted that in the calculation of the correlation coefficient $R^2 = 0.998$ the value of the $N_2^{\oplus}$ substituent (C4–N 137.9 pm) has not been taken into account.

From the great variety of suitable substituents four typical nitrogen containing species were selected to comprise a Hammett constant range as wide as possible, from highly negative to highly positive values. The hydrogen atom, by definition, serves as a substituent with a reference value σ_p of 0.0; other substituents of these studies are the dimethylamino (NMe_2, –0.83), the hydroxylamino (N(H)OH, –0.34), the nitro (NO_2, 0.78) and the cationic diazonium groups ($N_2^{\oplus}$, 1.91). To allow, however, a more authoritative interpretation of the results obtained from quantum chemical calculations, compounds without a Cl_2As unit such as *N*,*N*-dimethylaniline, aniline itself, benzene, and nitrobenzene have also been included.

At first, molecular models of all compounds mentioned above along with their characteristic bond lengths and NBO charges of the non-hydrogen atoms are depicted in Figure 5.5.4.1. As for the group of dichlorophenylarsine derivatives $4\text{-}X_p\text{–}C_6H_4\text{–}AsCl_2$ and the non-substituted dichlorophenylarsine (X_p = H), the graphical representation of the results (Table 5.5.4.1) in Figure 5.5.4.2 demonstrates an excellent correlation between the Hammett constants σ_p of the corresponding substituents X_p and the NBO charges of the carbon atom C1 adjacent to arsenic as well as the associated NBO charge differences ΔQ of the atoms As and C1. The correlation coefficients R^2 obtained here and further below come up to a very high value of 0.980 or are found to be even better.

Whereas the dimethylamino substituent induces the highest NBO charge of –0.466 and the cationic diazonium group causes the lowest negative charge (–0.264) at atom C1, the NBO charge differences $\Delta Q_{As\text{–}C1}$ correspondingly decreases from 1.431 to 1.255 (Table 5.5.4.1). As to be expected, this decrease involves a substantial elongation of the As–C1 distance from 193.5 pm in the *N*,*N*-dimethylamino derivative to 201.8 pm in the cationic diazonium compound. By analogy to this correlation, a slight but continuous shortening of the average As–Cl bond from 224.6 to 220.8 pm can be noticed.

In keeping with different electronegativities of the elements carbon and arsenic, the quantum chemical calculations on all dichlorophenylarsine derivatives investigated here result in negative NBO charges at the carbon atoms of the As–C1 bonds and positive charges at arsenic. As already discussed above, however, the effect of the *para* substituents on these values is much more apparent for the carbon than for the arsenic atom. At the opposite side of the arene ring the situation is found to be partially reverse inasmuch as the nitrogen atoms of the C4–N bonds can be characterized by negative or positive NBO charges, depending on the substituents (NMe_2 and N(H)OH *vs* NO_2 and $N_2^{\oplus}$, Figure 5.5.4.1) with their various groups or atoms. Irrespective of the algebraic sign of charge at nitrogen, the NBO charges of the carbon atom C4 are invariably positive but their magnitude changes drastically from 0.218 in the dimethylamino derivative to values near zero in the nitro compound (0.084) and the cationic diazonium derivative (0.008). This decrease of NBO charges is accompanied by an analogous change in the appropriate NBO charge difference ΔQ_{C4-N} from 0.696 to 0.132 (Table 5.5.4.1). Again, a very tight correlation of these two parameters with the Hammet constants σ_p of the substituents is observed (Figure 6.5.4.3); in both cases the correlation coefficient comes up to an extremely high or at least a satisfactory value of 0.998 and 0.939, respectively.

To achieve, however, a correlation of similar quality between the Hammett constants σ_p of the substituents X_p and the increasing bond lengths C4–N (Figure 5.5.4.3b) or between the bond lengths C4–N and the NBO charge differences ΔQ_{C4-N} (Table 5.5.4.1), the cationic diazonium group $N_2^{\oplus}$ has to be omitted from the list of substituents. Based on the corresponding Hammett constant of this substituent ($\sigma_p = 1.91$), a distance C4–N can be extrapolated to a value of 155.3 pm, but, in fact, it amounts to 137.9 pm only. This unexpected phenomenon can be interpreted by additional strong donor-acceptor interactions between the cationic diazonium group and the π-system of the arene ring; usually, resonance structures as given in Scheme 5.5.4.1, are taken in order to describe this effect with formulas. For other substituents, NBO second-order perturbation analyses do not indicate such interactions of a comparable magnitude.

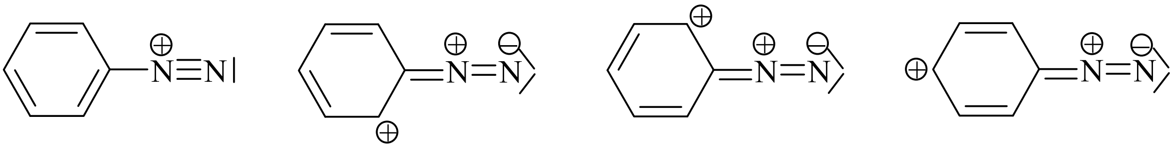

Scheme 5.5.4.1. Resonance structures of the phenyldiazonium cation

The Hammett constants σ_p of the substituents X_p not only correlate tightly with the lengths of the bonds C4–N, As–C1 and As–Cl but have also an effect on the C–C distances of the arene ring. To eliminate, however, the superimposing but rather small effect of the Cl_2As group on these bond lengths, relevant values of unsubstituted dichlorophenylarsine (X_p = H) are taken as a reference. In the case of bond lengths calculated additionally for *N*,*N*-dimethylaniline, aniline itself and nitrobenzene, the C–C distance of benzene (139.5 pm) is used for a comparison.

As demonstrated by the compilation of data in Table 5.5.4.2, the influence of the substituents X_p on the C–C bond lengths and the appropriate differences Δ obtained by comparison with the corresponding reference value, is relatively weak and diminishes with increasing distance. Nevertheless, analogous correlation between the Hammett constants σ_p and the lengths of nearly all C–C bonds is noticed again but as before the diazonium cation ($X_P = N_2^{\oplus}$) has to be excluded from this discussion due to its conspicuously deviating values. Distances and differences do not follow the correlation outlined above; in contrast to the highly positive

Hammett constant σ_p of the $N_2^{\oplus}$ group (1.91), the data are rather found to be extremely similar to those of dichloro[4-(dimethylamino)phenyl]arsine, the dimethylamino substituent of which is characterized by a fairly negative σ_p value of -0.83. Additional strong donor-acceptor interactions between the diazonium group and the π-system of the arene ring already mentioned above are supposed to account for these deviations, too.

Furthermore, in the dichlorophenylarsine derivatives $4\text{-}X_p\text{–}C_6H_4\text{–}AsCl_2$ the substituents X_p give rise to an unusual alternation of elongated and shortened C–C distances in the arene rings. Starting with the para position C4, one first notices a change from positive (Δ_{C4-C3} and Δ_{C4-C5}) to negative difference values (Δ_{C3-C2} and Δ_{C5-C6}, Table 5.5.4.2); they are subsequently followed by the values Δ_{C2-C1} and Δ_{C6-C1} which are found to be positive again. The phenomenon of alternating bond lengths can best be realized with the dimethylamino derivative (Figure 5.5.4.4); already for the nitro derivative and for nitrobenzene, a compound which has been incorporated for comparison, most difference values turn out to be much smaller and as a consequence the data are less convincing.

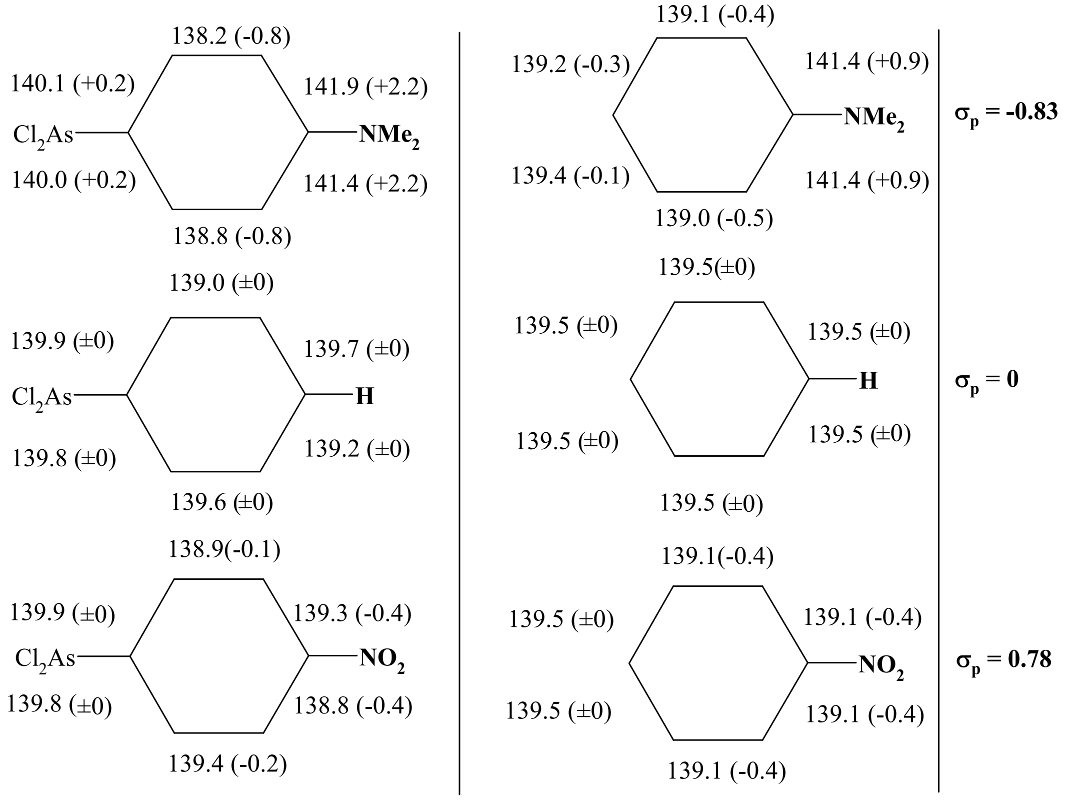

Figure 5.5.4.4. Correlation between the Hammett constants σ_p (on the right) of the substituents X_p or X and the C–C distances of the arene rings calculated quantum chemically for two typical substituted dichlorophenylarsine derivatives $Cl_2As\text{–}C_6H_4\text{–}4\text{–}X_p$ (on the left) in comparison with the corresponding phenyl compounds $C_6H_5\text{–}X$ (intermediate columm; X_p or X = NMe_2, NO_2).
To demonstrate the characteristic influence of the substituents X_p or X, difference values Δ more evident than the individual distances have been determined by using the C–C bond lengths of unsubstituted dichlorophenylarsine or benzene (X_p or X = H), respectively, as references; the difference values Δ are given in brackets.

In contrast to the distinctly alternating C–C bond lengths just discussed for dichloro[4-(dimethylamino)phenyl]arsine, quantum chemical calculations on the related compound *N*,*N*-dimethylaniline (Figure 5.5.4.4) result in an only slight elongation of the two distances C3–C4 and C4–C5 adjacent to the dimethylamino group, whereas the four remaining bonds are found to be almost identical but somewhat shortened with respect to benzene (139.5 pm). Hence, the difference values Δ changes the algebraic sign only once; subsequent to a distinct alteration from positive (0.9) to negative (–0.4), the values Δ_{C1-C2} and Δ_{C1-C6} stay negative and turn out to be very small. In addition to this result one should realize indeed that for dichloro[4-(dimethylamino)phenyl]arsine the difference values of the bonds C1–C2 and C1–C6 adjacent to the Cl_2As group are found to be positive (0.2) when obtained on the basis of quantum chemical calculations but to be negative (–0.4; Table 5.5.4.2) when determined with the average distances of the crystal structure analysis (Table 5.2).

Though an overinterpretation of these data and the difference values Δ in particular has to be avoided, the salient alternation of elongated, shortened and again, elongated C–C bond lengths of dichloro[4-(dimethylamino)phenyl]arsine quite evident from the results of the crystal structure analysis (Table 5.2.) and confirmed by quantum chemical calculations (Table 5.5.4.2), is in accordance with the so-called “phenylogous” principle [285]. Along with the well–known “vinylogous” principle [286] which it can be attributed to, these two heuristic rules are often applied in organic chemistry. They allow an understanding why for a group of similar compounds which differ from a parent compound just by insertion of a vinylene or phenylene unit into the primary element element bond, an almost identical reactivity is observed with our studies the “phenylogous” principle has been transferred for the first time to bond lengths.

Finally, the correlation between the Hammett constant σ_p of the *para* substituent X_p and the two endocyclic angles α (C6–C1–C2) and β (C3–C4–C5) has also been inspected (Figure 5.5.4.5). As evidenced by a rather high correlation coefficient R^2 of 0.947, the parameter σ_p has a strong effect on the magnitude of angle β the vertex of which is carbon atom C4 directly bonded to the substituent X_p, whereas the interrelation between α and σ_p is rather poor ($R^2 = 0.774$). In this context one should remember an investigation of *Domenicano* et al. [374] published more than thirty years ago. The authors analyzed the influence of various substituents on the endocyclic C–C–C bond angles of phenyl derivatives. These initial studies were supplemented by theoretical aspects from *Coulson* [375, 376] some years later. At the moment our results obtained from quantum chemical calculations, do not form a broad enough basis that would enable us to make any definitive statement.

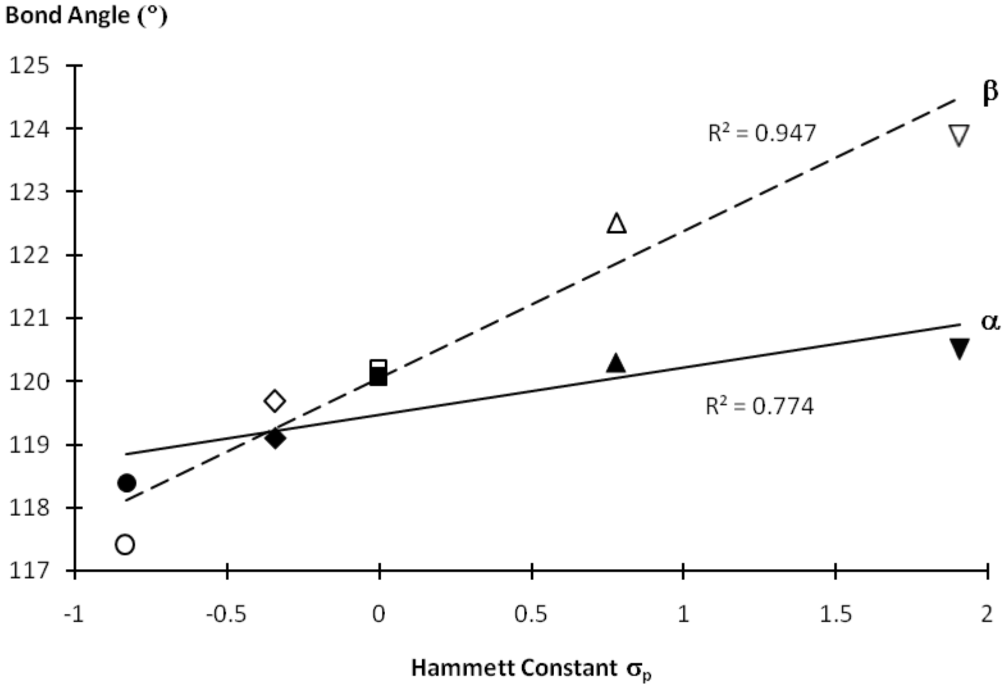

Figure 5.5.4.5. Correlation between the Hammett constant σ_p of the substituent X_p (● NMe_2; ♦ N(H)OH; ■ H; ▲ NO_2; ▼ $N_2^{\oplus}$) in *para* position to the $AsCl_2$ group and the endocyclic angles C2–C1–C6 (α**)** and C3–C4–C5 (β; dashed line and open symbols) of several dichlorophenylarsines 4-X_p–C_6H_4–$AsCl_2$

6. Experimental Section

6.1. General Considerations

All manipulations of air- and moisture-sensitive materials were performed by applying standard Schlenk techniques under an atmosphere of argon (purity > 99.998%), which was freed from of oxygen with BTS catalyst [347] and dried with P_4O_{10}. All glassware was evacuated to $1 \cdot 10^{-3}$ mbar and filled afterwards with argon, reactions and distillations were carried out under argon atmosphere. Reagents were purchased from *Aldrich Chemical Co.* in 95 – 99.5% purity or synthesized according to published procedures.

n-Pentane, cyclopentane and *n*-hexane were distilled from $LiAlH_4$; chloroform, dichloromethane and acetonitrile were dried and purified by distillation from CaH_2. Ethanol was dried and purified by distillation from magnesium. Diethyl ether, benzene, toluene, tetrahydrofuran and 1,2-dimethoxyethane were refluxed over sodium/benzophenone and distilled under argon prior to use [378]. Phosphorus(III) halides (Cl, Br) as well as arsenic(III) chloride were treated overnight at room temperature with aluminium turnings to remove hydrogen halide, subsequently filtered and fractionated [378]. Chlorotrimethylsilane and 2,2-dimethylpropionyl chloride were freshly distilled under argon prior to use. Red phosphorus was purified by refluxing overnight with distilled H_2O, allowed to settle and washed several times with boiling water until the washings were neutral, then washed several times with ethanol, transferred to a flask, dried at 100 °C after evaporation of the solvent in vacuo and stored under argon. Incrustations were removed from sodium and potassium under petroleum ether, water was used to cover white phosphorus (P_4). 1-Adamantoyl chloride, sodium hydroxide, sodium carbonate, concentrated hydrochloric acid (37%), lithium tetrahydridoaluminate, calcium hydride, potassium hydroxide and magnesium were used as received without further purification. Dimethylaluminum chloride and diethylaluminum chloride were purchased from *Aldrich* (packaged under nitrogen in poly-coated Sure/Seal^{TM} bottles) as 1 M solution in *n*-hexane. *n*-Butyl lithium was purchased from *Aldrich* (packaged under nitrogen in 100 mL and 1 L poly-coated Sure/Seal^{TM} bottles) as a 1.6 M solution in *n*-hexane. Dimethylamine and isopropylmagnesium chloride were purchased from *Aldrich* (packaged under nitrogen in poly-coated Sure/Seal^{TM} bottles) as a 2 M solution in THF.

Di-*tert*-butylchlorophosphine, chlorodiisopropylphosphine, chlorodiethylphosphine, chlorodimethylphosphine, chlorodiphenylphosphine and dichlorophenylphosphine were freshly distilled, the purity of all phosphines was checked by measuring their $^{31}P\{^1H\}$ NMR spectra before use. Diethylamine, *N*-methylisopropylamine, *N*-ethylmethylamine, and *N*,*N*-dimethylaniline were dried over potassium hydroxide and distilled before use.

All NMR samples were prepared in 5 mm or 10 mm tubes which were flame-sealed under argon; all deuterated solvents were dried and distilled as described for the pertinent non-deuterated solvent. All nuclear resonance spectra were obtained by applying Fourier transform techniques; the following instruments of the company *Bruker Analytische Meßtechnik GmbH*, *Rheinstetten* were used:

AM 200 (^{1}H: 200.132, ^{13}C: 50.323, ^{31}P: 81.015, ^{29}Si: 39.761, ^{27}Al: 52.148 MHz)
AC 250 (^{1}H: 250.133, ^{13}C: 62.897, ^{31}P: 101.256 MHz), and
AM 400 (^{1}H: 400.137, ^{13}C: 100.614, ^{31}P: 161.977, ^{29}Si: 79.495, ^{15}N: 40.561 MHz)

Standard deuterated solvents were used as follows:

^{1}H NMR: d_6-benzene (internal; $\delta(C_6D_5H) = 7.15$ ppm); $CDCl_3$ (internal; $\delta(CHCl_3) = 7.24$ ppm); d_3-CD_3CN (internal; $\delta(CD_2HCN) = 1.94$ ppm); CD_2Cl_2 (internal; $\delta(CDHCl_2) = 5.32$ ppm); d_8-toluene (internal; $\delta(C_7D_7H) = 7.09$ ppm); d_6-dimethylsulfoxide (internal; $\delta(CD_3S\ (O)CD_2H) = 2.49$ ppm).

^{13}C NMR: d_6-benzene (internal; $\delta = 128.00$ ppm); $CDCl_3$ (internal; $\delta = 77.00$ ppm); d_3-CD_3CN (internal; $\delta(\mathbf{C}D_3) = 1.30$ ppm); CD_2Cl_2 (internal; $\delta = 53.80$ ppm); d_8-toluene (internal; δ(ipso-C) = 137.5 ppm); d_6-dimethylsulfoxide (internal; $\delta = 39.5$ ppm)

Other standards:

^{31}P NMR: 85 % aqueous solution of H_3PO_4, external; $\delta = 0.00$ ppm.
^{29}Si NMR: tetramethylsilane, external; $\delta = 0.00$ ppm.
^{15}N NMR: nitromethane, external; $\delta = 0.00$ ppm.
^{27}Al NMR: acetylacetonatoaluminium(III), saturated solution in C_6D_6, external; $\delta = 0.00$ ppm.

All the NMR measurements were obtained at room temperature unless otherwise stated. Chemical shifts are reported in δ (ppm) with positive values for downfield and negative values for upfield; couplings constant are reported in Hz. For the multiplicity of the resonance signals, the following abbreviations were used:

s: singlet, d: doublet, t: triplet, q: quartet, m: multiplet, dd: doublet of doublets, dt: doublet of triplets, ddd: doublet of doublet of doublets.

FT-IR-spectra were recorded from Nujol mulls between CsBr plates at a *Perkin-Elmer Paragon* 1000 PC IR spectrophotometer of the company *Perkin-Elmer, Shelton, Connecticut, USA*.

Raman spectra were taken from crystalline samples in capillaries, which were sealed under vacuum, on a *Dilor ISA XY 500* instrument, *Lille*, *France.* The following abbreviations for intensities and line shapes are used:

vw: very weak, w: weak, m: medium, s: strong, vs: very strong, br: broad, sh: shoulder.

Melting points (uncorrected) were determined at a conventional apparatus (*apparatus B-545* of the company *Buechi, Flawil, Switzerland*) with samples sealed in capillaries under argon.

Mass spectra were obtained at a mass spectrometer *MAT 711* of the company *Varian, Palo Alto, California*, *USA*.

Elemental analyses were carried out with the ICP AES analysing technique at a *Perkin-Elmer Series II Analyzer 2400*, with Optima 3000 *Perkin-Elmer, Shelton, Connecticut, USA*.

Single crystals were separated directly from solution at room temperature under argon and covered with polyfluorinated polyether oil (*RS 3000, Riedel-de-Haën*) in order to protect them from atmospheric moisture and oxygen. The oil 'freezes' at reduced temperatures and holds the crystal static in the X-ray beam. Oxidation of the compounds by atmospheric oxygen during the X-ray data collection does not take place since the crystals are cooled down to –100 ± 3 °C in a stream of nitrogen [379]. Intensities were collected on the four-circle diffractometers P21 (*Syntex, Cupertino, USA*) and P4 (*Siemens Analytical X-ray Instruments Inc., Madison, Wisconsin, USA.*) using graphite monochromatized Mo-K_{α}-radiation (λ = 71.073 pm).

For the treatment of data and the subsequent refinement of the structure model the determination of structures by applying statistical methods software packages SHELXTL, version 5.10 was employed. The sub-program XP served for an analysis of the molecular geometry and the preparation of the drawings [118-120].

6.2. Tris(trimethylsilyl)phosphine

7.2.1. First method

Sodium/potassium alloy (Na 52.2 g, 2.27 mol; K 66.5 g, 170 mmol) was added dropwise over a period of 1h to the vigorously stirred emulsion of 37g (120 mmol) white phosphorus in 1,2-dimethoxyethane (2 L) at 60 °C, and the mixture was heated at reflux for 24 h. A slight excess of freshly distilled chlorotrimethylsilane (475 mL, 406.6 g, 374 mmol) was added carefully to the phosphide suspension while stirring and refluxing. After 24 h the mixture was filtered and the residue was washed several times with a total of two litres of 1,2-dimethoxyethane. Finally, the solvent was distilled off at atmospheric pressure, and the remaining tris(trimethylsilyl)phosphine was purified by vacuum distillation.

Yield 77% (230 g, 920 mmol); bp. 30–35 °C/10^{-3} mbar.

6.2.1. Second method

1,2-Dimethoxyethane (1.5 L) was added to stirred sodium/potassium alloy (Na 17.10 g, 744 mmol; K 21.74 g, 556 mmol). After the emulsion had been heated under reflux for 4 h, during which its colour changed to purple, it was cooled down to room temperature. Red phosphorus (13.42 g, 433 mmol) was added under stirring at room temperature, and the mixture was heated at reflux for 24 h. The suspension was cooled to room temperature; a slight excess of freshly distilled chlorotrimethylsilane (174 mL, 148.8 g, 137 mmol) was added under vigorous stirring within 1 h and thereafter the mixture was heated at reflux for 24 h. After filtration, the residue was washed several times with a total of 1 L of 1,2-dimethoxyethane. Finally, the solvent was distilled off at atmospheric pressure, and the remaining tris(trimethylsilyl)phosphine was purified by vacuum distillation.

Yield 78% (85 g , 340 mmol); bp. 30–35 °C/10^{-3} mbar.

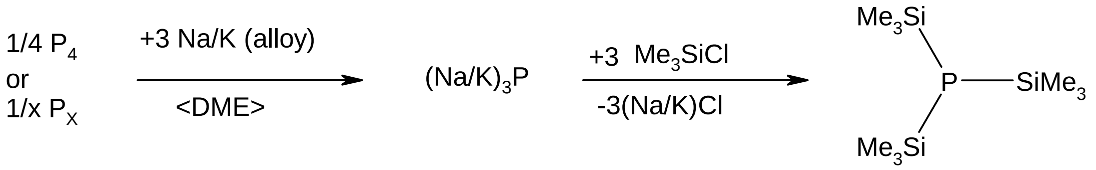

Characterization

NMR (solution in C_6D_6):

$^{31}P\{^1H\}$ (101.256 MHz): δ = –251.50 ppm (s with ^{13}C and ^{29}Si satellites, $^1J_{(P,Si)}$ = 26.70 Hz, $^2J_{(P,C)}$ = 11.44 Hz)

$^{29}Si\{^1H\}$ (39.761 MHz): δ = 2.68 ppm (d, $^1J_{(Si,P)}$ = 27.47 Hz)

$^{13}C\{^1H\}$ (62.896 MHz): δ = 4.40 ppm (d with ^{29}Si satellites, $^1J_{(C,Si)}$ = 49.48 Hz, $^2J_{(C,P)}$ = 11.26 Hz)

^1H (250.133 MHz): δ = 0.284 ppm (d with ^{13}C and ^{29}Si satellites, $^1J_{(H,C)}$ = 119.77 Hz, $^2J_{(H,Si)}$ = 6.58 Hz, $^3J_{(H,P)}$ = 4,45 Hz)

6.3. [2,2-Dimethyl-1-(trimethylsiloxy)propylidene]trimethylsilylphosphine

A solution of freshly distilled 2,2-dimethylpropionyl chloride (38 mL, 37.2 g, 309 mmol; 10% excess) in *n*-pentane (100 mL) was added dropwise with stirring to a solution of 81 mL (69.9 g, 280 mmol) tris(trimethylsilyl)phosphane in *n*-pentane (200 mL) at room temperature. The reaction mixture was stirred for 24 h and the reaction progress was followed by NMR spectroscopy in order to ensure complete consumption of tris(trimethylsilyl)phosphine and to avoid further substitution. Thereafter the solvent was removed under high vacuum, and the residue was distilled at a pressure of 10^{-3} mbar to afford *E*/*Z*-isomeric [2,2-dimethyl-1-(trimethylsiloxy)propylidene]trimethylsilylphosphine as a yellow oil.

Yield 88% (65 g, 250 mmol); bp. 45–48 °C/10^{-3} mbar.

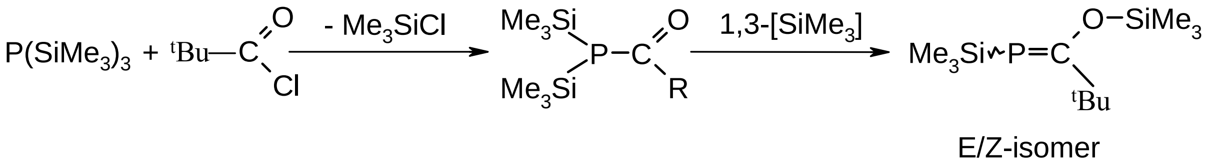

Characterization

NMR (solution in C_6D_6; values refer to the *Z*-isomer, if not otherwise stated)

$^{31}P\{^{1}H\}$ (101.256 MHz): δ = 116.64 (s with ^{29}Si satellites, $^{1}J_{(Si,P)}$ = 51.50 Hz, $^{3}J_{(Si,P)}$ = 3.05 Hz, *Z*-isomer); δ = 103.74 ppm (s, *E*-isomer)

$^{29}Si\{^{1}H\}$ (39.761 MHz): δ = –4.87, (d with ^{13}C satellites, $^{1}J_{(Si,P)}$ = 52.26, $^{1}J_{(Si,C)}$ = 48.90 (P**Si**C)), δ = 13.82 ppm, (d with ^{13}C satellites, $^{3}J_{(Si,P)}$ = 3.06, $^{1}J_{(Si,C)}$ = 57.50 Hz (O**Si**C))

$^{13}C\{^{1}H\}$ (62.896 MHz): δ = 1.48 (d, $^{2}J_{(C,P)}$ = 9.47 (PSi**C**)), δ = 2.60 (s, OSi**C**), δ = 30.59 (d, $^{3}J_{(C,P)}$ = 13.16 (PCC**C**)), δ = 45.33 (d, $^{2}J_{(C,P)}$ = 24.73 (PC**C**)), 225.70 ppm (d, $^{1}J_{(C,P)}$ = 79.98 Hz (P=**C**)).

^{1}H (250.133 MHz): δ = 0.23 (s, **H**$_3$CSiO), δ = 0.33 (d, $^{3}J_{(H,P)}$ = 3.90 (**H**$_3$CSiP)), δ = 1.26 ppm (d, $^{4}J_{(H,P)}$ = 1.60 Hz ((**H**$_3$C)$_3$C)).

6.4. 2,2-Dimethylpropylidynephosphine

50.0 g (190 mmol) of [2,2-dimethyl-1-(trimethylsiloxy)propylidene]trimethylsilylphosphine were added dropwise to 10 g of granular sodium hydroxide over a period of 2 h. Thereafter the pressure within the system was reduced to 10 mbar, and the catalyst was heated to 140–160 °C with an oil bath. All volatile compounds were collected at –196 °C and separated later by fractional distillation under normal pressure (100 cm spinning band column).

Yield 68% (13 g, 130 mmol); bp. 55–60 °C.

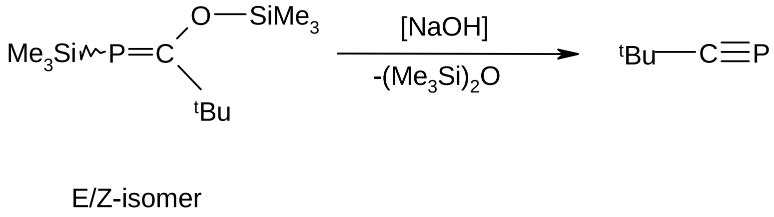

Characterization

NMR (solution in C_6D_6)

$^{31}P\{^1H\}$ (101.256 MHz): δ = –68.50 (s) ppm

$^{13}C\{^1H\}$ (62.896 MHz): δ = 31.57 ($^3J_{(C,P)}$ = 5.69, (PCC**C**)); δ = 36.45 ($^2J_{(C,P)}$ = 17.89, (PC**C**)); δ = 184,60 ppm ($^1J_{(C,P)}$ = 37.88 Hz (P≡**C**)).

^1H (250.133 MHz): δ = 1.10 ppm (d, $^4J_{(H,P)}$ = 0.92 Hz, 9H).

6.5. Lithium bis(trimethylsilyl)phosphinide•bis(tetrahydrofuran)

153 mL (245 mmol) of a 1.6 M solution of *n*-butyllithium in *n*-hexane were added to a stirred solution of 73 mL (63.0 g, 250 mmol) of tris(trimethylsilyl)phosphine in 300 mL of THF over a period of 2 h at 0 °C. The reaction mixture was allowed to warm up to room temperature and stirring was continued for 8 h. All volatile compounds were removed under reduced pressure at room temperature, and the brown residue was covered with 400 mL of *n*-pentane. Under stirring 20 mL of THF were added slowly to the suspension until complete dissolution had been achieved. When, thereafter, the solution was cooled and stored at –30 °C, lithium bis(trimethylsilyl)phosphinide•bis(tetrahydrofuran) precipitated as colourless to pale yellow crystals. The still cold liquid phase was carefully separated from the solid with a pipette, and the remaining solvent was removed under vacuum. The exact THF content of the solid (1.89 equivalents per formula unit) has to be determined by its ^1H NMR spectrum.

Yield 76% (60 g, 187 mmol).

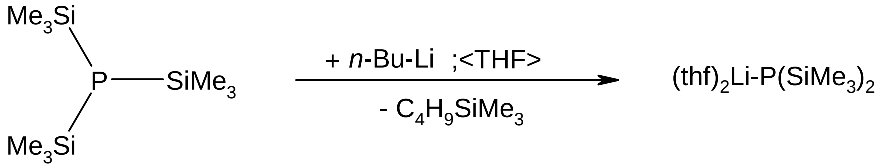

Characterization

NMR (solution in C_6D_6):

$^{31}P\{^1H\}$ (101.256 MHz): δ = –297.6 ppm (s)

$^{29}Si\{^1H\}$ (79.495 MHz): δ = 1.63 ppm (d, $^1J_{(Si,P)}$ = 27.61 Hz)

$^{13}C\{^1H\}$ (50.323 MHz): δ = 7.53 (d, **C**H_3–Si; $^2J_{(C,P)}$ = 10.11 Hz); δ = 25.43 (s, **C**H_2, THF); δ = 68.53 ppm (s, **C**H_2–O, THF)

^1H (250.133 MHz): δ = 0.533 (d, C**H**$_3$–Si, $^3J_{(H,P)}$ = 4.0 Hz); δ = 1.383 (m, C**H**$_2$, THF); δ = 3.69 ppm (m, C**H**$_2$–O, THF)

6.6. [(Adamant-1-yl)(trimethylsiloxy)methylidene]trimethylsilylphosphine

35.0 g of lithium bis(trimethylsilyl)phosphinide • 1.89 tetrahydrofuran (109 mmol) in cyclopentane (100 mL) were added slowly to a stirred solution of 1-adamantoyl chloride (21.7 g, 109 mmol) in cyclopentane (100 mL) at –40 °C. The reaction mixture was allowed to warm up to room temperature and stirring was continued for 30 min. The cyclopentane solution was filtered to remove insoluble lithium chloride and most of the solvent was removed under reduced pressure. After cooling the solution for 12 h to –30 °C, [(adamant-1-yl)(trimethylsiloxy)methylidene]trimethylsilylphosphine separated as a viscous oil, which solidifies in the refrigerator. Further purification of the yellowish compound was accomplished by recrystallisation from *n*-pentane.

Yield 89% (33 g, 96.9 mmol); mp. 56–58 °C.

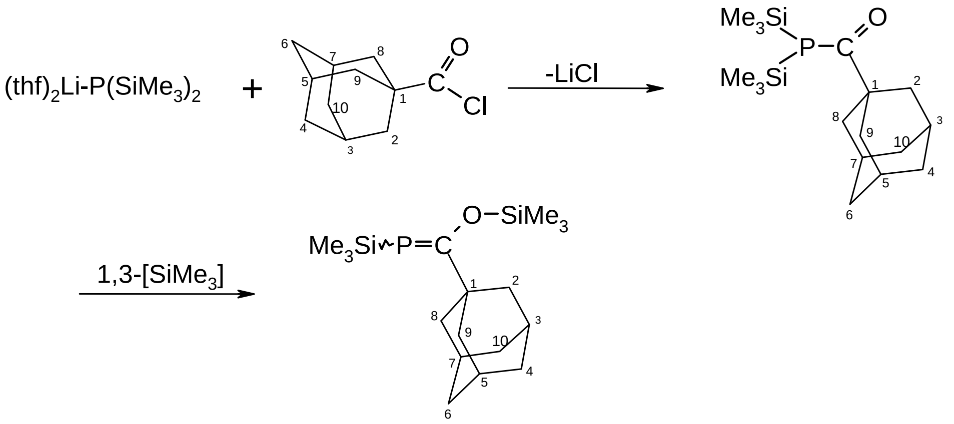

Characterization

NMR (solution in C_6D_6: refer to the *Z*-isomer, if not otherwise stated)

$^{31}P\{^{1}H\}$ (101.256 MHz): δ = 122.61 (s with ^{29}Si satellites, $^{1}J_{(Si,P)}$ = 53.41 Hz, *Z*-isomer); δ = 104.32 ppm (s, *E*-isomer)

$^{29}Si\{^{1}H\}$ (79.495 MHz): δ = –5.30 (d with ^{13}C satellites, $^{1}J_{(Si,P)}$ = 52.32, $^{1}J_{(Si,C)}$ = 48.29 (P**Si**C)); δ = 13.20 ppm (d with ^{13}C satellites, $^{3}J_{(Si,P)}$ = 3.09, $^{1}J_{(Si,C)}$ = 60.86 Hz (O**Si**C))

^{1}H (250.133 MHz): δ = 0.279 (s, $\mathbf{H_3}$CSiO, 9H); δ = 0.357 (d, $^{3}J_{(H,P)}$ = 3.88 Hz, $\mathbf{H_3}$CSiP, 9H); δ = 1.45–1.97 ppm (m, 15 $H_{adamantyl}$).

$^{13}C\{^{1}H\}$ (62.896 MHz): δ = 1.37 (d, $^{2}J_{(C,P)}$ = 9.47 (PSi**C**)); δ = 2.58 (s, (OSi**C**)); δ = 29.11 (d, $^{4}J_{(C,P)}$ = 2.10, **C**-3, **C**-5, **C**-7); δ = 36.87 (s, **C**-4, **C**-6, **C**-10); δ = 41.91 (d, $^{3}J_{(C,P)}$ = 14.21, **C**-2, **C**-8, **C**-9); δ = 47.48 (d, $^{2}J_{(C,P)}$ = 22.10, **C**-1); δ = 226.83 ppm (d, $^{1}J_{(C,P)}$ = 79.45 Hz, (P=**C**)).

6.7. Adamant-1-ylmethylidynephosphine

To a solution of [(adamant-1-yl)(trimethylsiloxy)methylidene]trimethylsilylphosphine (6.81 g, 20 mmol) in 1,2-dimethoxyethane (20 mL) was added with stirring a catalytic amount of solid sodium hydroxide(15 mg). When after one hour the colour of the solution had changed to orange-red, stirring was continued for 24 hours. Thereafter, all volatile compounds and the solvent were removed from the still orange-red solution at room temperature under vacuum. Sublimation of the residue in vacuum furnished the 1λ^3-phosphaalkyne as colourless crystals. Yield 70% (2.5 g, 14 mmol); mp. 68–70 °C.

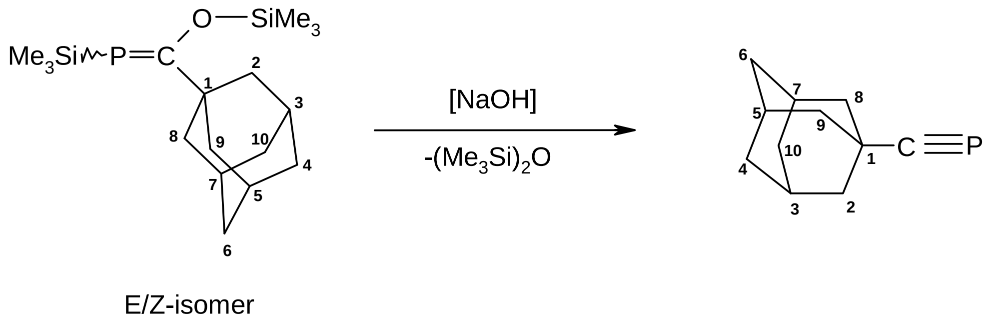

Characterization

NMR (solution in C_6D_6):

$^{31}P\{^1H\}$ (101.256 MHz): $\delta = -67.3$ (s) ppm

$^{13}C\{^1H\}$ (62.896 MHz): $\delta = 28.33$ (s, **C**-3, **C**-5, **C**-7); $\delta = 35.92$ (s, **C**-4, **C**-6, **C**-10); $\delta = 38.51$ (d, $^2J_{(C,P)} = 18.31$, **C**-1); $\delta = 43.10$ (d, $^3J_{(C,P)} = 5.6$, **C**-2, **C**-8, **C**-9); $\delta = 184.18$ (d, $^1J_{(C,P)} = 38.15$ Hz, (P≡**C**)).

^1H (250.133 MHz): $\delta = 1.45$–2.02 ppm (m, $15H_{adamantyl}$).

6.8. Procedures for the Preparation of the Complexes Dialkyl[1,1-bis(alkylchloroalanyl)organylmethyl]phosphine•Dialkylchloroalane (1/1)

*6.8.1. Dimethyl[1,1-bis(methylchloroalanyl)*tert*-butylmethyl]phosphine•Dimethylchloroalane(1/1)* ***(1a)***

2-*tert*-Butyl-1λ^3-phosphaalkyne (0.70 g, 7 mmol) was added to a stirred 1 M solution (23 mL, 23 mmol) of dimethylaluminium chloride in *n*-hexane at –78 °C. When the reaction mixture had been allowed to warm up to room temperature, stirring was continued for 12 hours. The solution slowly turned yellow, and a colourless solid precipitated. Solvent and excess dimethylaluminium chloride were removed without filtration very slowly over six days under reduced pressure. The residue was washed with cold *n*-hexane and the compound was isolated in 83% yield (2.2 g, 5.8 mmol). Colourless crystals were obtained by recrystallisation (25 °C/–60 °C; 3 weeks) from toluene.

Characterization

Melting point: 118 °C

Elemental analysis: $C_{11}H_{27}Al_3Cl_3P$; calc.: C 34.99%, H 7.21%, Cl 28.17%, P 8.21%

found: C 34.71%, H 7.22%, Cl 28.10%, P 7.81%

Molar mass (cryoscopic in benzene [380]): 370.0 g mol^{-1} (calc. 377.6 g mol^{-1})

NMR (solution in d_6-benzene):

$^{31}P\{^1H\}$ (161.977 MHz):

High-Field Signals:

$\delta = -39.8$ (s, br); –37.1 (s, br); –35.21 ppm (s, br) (intensity ratio 1:7:1; **P**).

Low-Field Signals:

$\delta = -5.8$ (s), –4.0 ppm (s) (intensity ratio 1:4; **P**).

$^{13}C\{^1H\}$ (100.614 MHz):

$\delta = -7.4$ ppm (br, s, Al–**C**H_3).

$\delta = -2.3$ ppm (br, s, Al–**C**H_3).

$\delta = 16.2$ (d, $^1J_{(C,P)} = 26.2$ Hz; P(**C**$H_3)_2$); 15.9 ppm (d, $^1J_{(C,P)} = 25.0$ Hz; P(**C**$H_3)_2$) (intensity ratio 1:3).

$\delta = 35.50$ (d, $^3J_{(C,P)} = 7.1$ Hz; C(**C**$H_3)_3$); 35.40 ppm (d, $^3J_{(C,P)} = 6.1$ Hz; C(**C**$H_3)_3$) (intensity ratio 1:3).

$\delta = 39.00$ (d, $^2J_{(C,P)} = 11.2$ Hz; **C**$(CH_3)_3$); 38.60 ppm (d, $^2J_{(C,P)} = 10.7$ Hz; **C**$(CH_3)_3$) (intensity ratio 1:3).

$\delta = 12.5$ (s), 13.3 (s), $\delta = 27.2$ (s), 30.1 ppm (s); unidentified.

P**C**Al_2 undetected.

^1H (250.133 MHz):

$\delta = -0.25$ (br, s, Al–C**H**$_3$); –0.1 (s, Al–C**H**$_3$); –0.07 (br, s, Al–C**H**$_3$); 0.025 (s, Al–C**H**$_3$); 0.15 ppm (s, Al–C**H**$_3$) (intensity ratio 33:23:29:8:1).

$\delta = 0.96$ (d, $^2J_{(P,H)} = 7.60$ Hz; P(C**H**$_3)_2$); 1.05 ppm (d, $^2J_{(P,H)} = 7.80$ Hz; P(C**H**$_3)_2$) (intensity ratio 1:3) and also 0.70 – 0.86 ppm weak doublets.

$\delta = 1.16$ (s; C(C**H**$_3)_3$); 1.08 ppm (s; C(C**H**$_3)_3$) (Intensity ratio 1:3).

$\delta = 1.4$ ppm (s); unidentified.

$^{27}Al\{^1H\}$ (52.148 MHz): 168.0 ppm (singlet, very broad, **Al**, $W_{1/2} = 4432$ Hz)

Table 6.1. Molecular Mass and Characteristic Fragments from the mass spectrum of ($C_{11}H_{27}Al_3Cl_3P$) (70 eV, sample temperature 360 K, source temperature 420 K)

Signal (m/z)	Rel. Int. (%)	Classification	Signal (m/z)	Rel. Int. (%)	Classification
367	0.8	$\{M - CH_3\}^+$ ($^{37}Cl_3$)	271	21.5	$\{M - (CH_3)_{-}CH_3)_2AlCl\}^+$ ($^{35}Cl\,^{37}Cl$)
365	6.2	$\{M - CH_3\}^+$ ($^{35}Cl\,^{37}Cl_2$)	269	33.4	$\{M - (CH_3)_{-}CH_3)_2AlCl\}^+$ ($^{35}Cl_2$)
363	18.3	$\{M - CH_3\}^+$ ($^{35}Cl_2\,^{37}Cl$)	266	13.9	$\{M - CH_3AlCl_2\}^+$ (^{37}Cl)
361	19.1	$\{M - CH_3\}^+$ ($^{35}Cl_3$)	264	41.2	$\{M - CH_3AlCl_2\}^+$ (^{35}Cl)
345	1.7	$\{M - Cl\}^+$ ($^{37}Cl_2$)	251	21.0	$\{M - Cl - (CH_3)_2AlCl\}^+$ (^{37}Cl)
343	5.9	$\{M - Cl\}^+$ ($^{35}Cl\,^{37}Cl$)	249	67.4	$M - Cl - (CH_3)_2AlCl\}^+$ (^{35}Cl)
341	8.7	$\{M - Cl\}^+$ ($^{35}Cl_2$)	157	73.8	$\{(CH_3)_3CCP(CH_3)_2Al\}^+$
288	2.0	$\{M - (CH_3)_2AlCl\}^+$ ($^{37}Cl_2$)	79	6.1	$\{CH_3AlCl\}^+$(^{37}Cl)
286	11.3	$\{M - (CH_3)_2AlCl\}^+$ ($^{35}Cl\,^{37}Cl$)	77	19.0	$\{CH_3AlCl\}^+$(^{35}Cl)
284	17.7	$\{M - (CH_3)_2AlCl\}^+$ ($^{35}Cl_2$)	57	100.1	$\{C(CH_3)_3\}^+$
273	3.6	$\{M - (CH_3)_{--}CH_3)_2AlCl\}^+$ ($^{37}Cl_2$)	27	13.9	$\{Al\}^+$

IR (Nujol mull between CsBr disks; $\tilde{\nu}$ [cm^{-1}]): 1396(w), 1301(w), 1286(w), 1198(s), 1181(s), 1029(vw), 939(s), 889(vw), 868(vw), 837(m), 765(m), 680(vs), 581(w), 535(vw), 451(m).

Raman (crystalline solid in glass capillary*; $\tilde{\nu}$ [cm^{-1}])*: 1468(vw), 1435(vw), 1412(vw), 1196(w), 1188(m), 937(vw), 914(vw), 890(vw), 870(vw), 837(vw), 767(vw), 720(w), 693(s), 663(w), 614(w), 582(s), 536(w), 452(vw), 423(w), 392(vw), 355(vw), 330(vs), 294(vs), 275(s), 258(w), 229(m), 201(s), 182(s), 155(vs), 127(vs).

X-ray structure analysis: Chapter 2 (page 50).

6.8.2. *Diethyl[bis(ethylchloroalanyl)*tert*-butylmethyl]phosphine•Diethylchloroalane(1/1)* ***(1b)***

2-*tert*-Butyl-1λ^3-phosphaalkyne (0.833 g , 8.33 mmol) was added to a stirred 1 M solution (25 mL, 25 mmol) of diethylaluminium chloride in *n*-hexane at –78 °C. When the reaction mixture had been allowed to warm up to room temperature, stirring was continued for four days, during which time the solution turned yellow. Solvent and excess diethylaluminium chloride were removed without filtration very slowly over six days under reduced pressure. The viscous yellow oil was washed with cold *n*-hexane and the compound was precipitated in 81% yield (3.1 g, 6.71 mmol). Colourless crystals were obtained by recrystallisation (25 °C/–60 °C; 3 weeks) from toluene.

Characterization

Melting point: 129 °C.

Elemental analysis: $C_{17}H_{39}Al_3Cl_3P$ calc.: C 44.22%, H 8.51%; Cl 23.03%, P 6.71%

found: C 44.14%, H 8.24%, Cl 23.27%, P 5.78%

Molar mass (cryoscopic in benzene [380]): 453.0 g mol^{-1} (calc. 461.78 g mol^{-1})

NMR (solution in *d_6*-benzene):

$^{31}P\{^1H\}$ (101.256 MHz):

High-Field Signals:

δ = –11.6 (s, br); –8.5 (s, br); δ = –5.4 (s, br); –1.5 (s, br); –0.24 ppm (s, br) (intensity ratio 52:131:666:117:117; **P**).

Low-Field Signals:

δ = 23.5 (s); 24.0 (s); 25.7 (s, br); 26.3 ppm (s); 26.6 (s); 27.0 ppm (s) (intensity ratio 3:19:49:6:6:1); **P**).

$^{13}C\{^1H\}$ (62.896 MHz):

δ = 3.7 ppm (br, Al–**C**H_2–CH_3).

δ = 7.5 ppm (br, Al–**C**H_2–CH_3).

δ = 8.5 (s, Al–CH_2–**C**H_3); 8.6 ppm (s, Al–CH_2–**C**H_3) (intensity ratio 1:5).

δ = 9.40 ppm (d, $^2J_{(C,P)}$ = 2.10 Hz, P–CH_2–**C**H_3).

δ = 11.3 (s, Al–CH_2–**C**H_3); 11.5 (s, Al–CH_2–**C**H_3) ppm (intensity ratio 1:5).

δ = 24.1 ppm (d, $^1J_{(C,P)}$ = 21.6 Hz, P-**C**H_2–CH_3).

δ = 36.3 (d, $^3J_{(C,P)}$ = 6.8 Hz; C(**C**H_3)$_3$); 36.1 ppm (d, $^3J_{(C,P)}$ = 6.3 Hz; C(**C**H_3)$_3$)) (Intensity ratio 1:5).

δ = 38.50 (d, $^2J_{(C,P)}$ = 10.5 Hz; **C**(CH_3)$_3$); 38.3 ppm (d, $^2J_{(C,P)}$ = 10.0 Hz; **C**(CH_3)$_3$) (Intensity ratio 1:5).

δ = 27.3 ppm (s), 30.3 ppm (s); unidentified.

P**C**Al_2 undetected.

^1H (250.133 MHz):

δ = 0.43 and 0.46 ppm (highest resonance at 0.45 ppm) (two overlapping quartet (1:4:6:4:1); $^3J_{(H,H)}$ = 8.03; Al–C**H**$_2$–CH_3, 8H).

δ =0.89 ppm (dt, $^3J_{(H,H)}$ = 7.6 Hz, $^3J_{(P,H)}$ = 18.4 Hz; P–CH_2–C**H**$_3$, 6H).

δ = 1.18 (s; C(C**H**$_3$)$_3$); 1.11 ppm (s; C(C**H**$_3$)$_3$, 9H) (Intensity ratio 1: 6).

δ = 1.27 ppm (t, $^3J_{(H,H)}$ = 8.03 Hz; Al-CH_2-C**H**$_3$, 12H).

δ = 1.55 – 1.77 ppm (m, P–C**H**$_2$–CH_3, 4H).

δ = 2.1 (s), 1.4 (s), 0.79 ppm (s); unidentified.

$^{27}Al\{^1H\}$ (52.148 MHz): 177.0 ppm (singlet, very broad, **Al**, $W_{1/2}$ = 4380 Hz).

Table 6.2. Molecular Mass and Characteristic Fragments from the Mass Spectrum of ($C_{17}H_{39}Al_3Cl_3P$) (70 eV, sample temperature 400 K, source temperature 420 K)

Signal (m/z)	Rel. Int. (%)	Classification	Signal (m/z)	Rel. Int. (%)	Classification
437	3.7	$\{M - C_2H_5\}^+ (^{37}Cl_3)$	185	91.7	$\{(CH_3)_3CCP(C_2H_5)_2Al\}^+$
435	32.0	$\{M - C_2H_5\}^+ (^{35}Cl\ ^{37}Cl_2)$	101	8.4	$\{PCC(CH_3)_3 + H\}^+$
433	97.4	$\{M - C_2H_5\}^+ (^{35}Cl_2\ ^{37}Cl)$	99	8.1	$\{PCC(CH_3)_3 - H\}^+$
431	100.0	$\{M - C_2H_5\}^+ (^{35}Cl_3)$	93	12.6	$\{C_2H_5AlCl\}^+(^{37}Cl)$
429	1.7	$\{M - Cl\}^+ (^{37}Cl_2)$	91	41.0	$\{C_2H_5AlCl\}^+(^{35}Cl)$
427	7.5	$\{M - Cl\}^+ (^{35}Cl\ ^{37}Cl)$	90	3.5	$\{(C_2H_5)_2PH\}^+$
425	11.2	$\{M - Cl\}^+ (^{35}Cl_2)$	89	6.5	$\{(C_2H_5)_2P\}^+$
344	5.0	$\{M - (C_2H_5)_2AlCl\}^+ (^{37}Cl_2)$	85	93.7	$\{PCC(CH_3)_2\}^+$
342	25.2	$\{M - (C_2H_5)_2AlCl\}^+ (^{35}Cl\ ^{37}Cl)$	69	4.7	$\{CC(CH_3)_3\}^+$
340	33.7	$\{M - (C_2H_5)_2AlCl\}^+ (^{35}Cl_2)$	61	11.6	$C_2H_5PH\}^+$
336	10.9	$\{M - C_2H_5AlCl_2\}^+ (^{37}Cl)$	60	1.1	$\{C_2H_5P\}^+$
334	24.6	$\{M - C_2H_5AlCl_2\}^+ (^{35}Cl)$	59	5.3	$\{C_2H_4P\}^+$
315	3.3	$\{M - (C_2H_5)\_C_2H_5)_2AlCl\}^+ (^{37}Cl_2)$	57	59.0	$\{C(CH_3)_3\}^+$
313	6.1	$\{M - (C_2H_5)\_C_2H_5)_2AlCl\}^+ (^{35}Cl\ ^{37}Cl)$	55	5.4	$\{C(CH_3)_3 - 2H\}^+$
311	10.6	$\{M - (C_2H_5)\_C_2H_5)_2AlCl\ \}^+ (^{35}Cl_2)$	41	15.6	$\{C(CH_3)_2 - H\}^+$
307	16.7	$\{M - Cl - (C_2H_5)_2AlCl\}^+ (^{37}Cl)$	29	24.9	$\{(C_2H_5)\}^+$
305	47.0	$M - Cl - (C_2H_5)_2AlCl\}^+ (^{35}Cl)$	27	42.8	$\{Al\}^+$

IR (Nujol mull between CsBr disks; $\tilde{\nu}$ [cm^{-1}]): 1404(vs), 1290(vw), 1229(s), 1187(vs), 1035(vw), 1026(s), 985(vs), 957(s), 925(s), 901(s), 828(m), 778(m), 730(m), 696(m), 620(m; br), 539(m), 453(m).

X-ray structure analysis: Chapter 2 (page 50).

6.8.3. Dimethyl[bis(methylchloroalanyl)-1-adamantylmethyl]phosphine•Dimethylchloroalane(1/1) (1c)

2-(1-admantyl)-1λ^3-phosphaalkyne (0.60 g, 3.367 mmol) in *n*-hexane (10 mL) was added to a stirred 1 M solution (10.1 mL, 10.1 mmol) dimethylaluminium chloride in *n*-hexane at –78 °C. When the reaction mixture had been allowed to warm up to room temperature, stirring was continued for five days. The solution slowly turned yellow. Without filtration solvent and excess dimethylaluminium chloride were removed very slowly within six days under reduced pressure. The residue was washed with cold *n*-hexane and the compound was precipitated in 78% yield (1.2 g, 2.63 mmol). Colourless crystals were obtained by recrystallisation (25 °C/–60 °C; 2 weeks) from a 1:1 mixture of *n*-hexane and cyclopentane.

Characterization

Melting point: 133 °C.

Elemental analysis: $C_{17}H_{33}Al_3Cl_3P$ calc.: C 44.80%, H 7.30%, Cl 23.34%, P 6.80%
found: C 45.10%, H 7.35%, Cl 23.88%, P 6.67%

Molar mass (cryoscopic in benzene [380]): 449.0 g mol^{-1} (calc. 455.73 g mol^{-1})

NMR (solution in *d*$_6$-benzene):

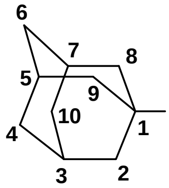

$^{31}P\{^1H\}$ (101.256 MHz):

High-Field Signals:

δ = –43.5 (s, br); –42.6 (s, br); –41.9.6 (s, br); –39.1 (s, br); –37.4 ppm (s, br); (intensity ratio 1:2:6:31:8; **P**).

Low-Field Signals:

δ = –7.6 (s); –6.0 ppm (s), (intensity ratio 2:6; **P**).

$^{13}C\{^1H\}$ (62.896 MHz):

δ = –7.1 (br, s, Al–CH$_3$).

δ = –1.3 ppm (br, s, Al–**C**H$_3$).

δ = 17.08 (d, $^1J_{(P,C)}$ = 24.2 Hz; P(**C**H$_3$)$_2$); 16.94 ppm (d, $^1J_{(P,C)}$ = 24.6 Hz; P(CH$_3$)$_2$) (intensity ratio 1:4).

δ = 29.62 (d); 29.67 (d); 29.73 (d); 29.80 (d) (major signal), 29.95 ppm (d), ($^4J_{(P,C)}$ = 1.5, 3.0, 1.1, 0.93, 0.93 Hz, respectively; every signal represents (**C**3, **C**5, **C**7) of different isomers).

δ = 36.09 (s); 36.14 (s); 36.30 (s) (major signal); 36.38 (s); 36.54 ppm (s) (intensity ratio 1:1:4:2:1), respectively, every signal represents (**C**4, **C**6, **C**10) of different isomers).

δ = 42.0 (d); 42.2 ppm (d) ($^2J_{(P,C)}$ = 10.4, 10.6 Hz, respectively; every signal represents (**C**1) of different isomers).

δ = 46.4 (d); 46.5 (d); 46.8 (d); 46.9 (d); 47.0 (d) ($^3J_{(P,C)}$ = 4.1, 5.0, 3.5, 3.2, 4.1 Hz, respectively; every signal represents (**C**2, **C**8, **C**9) of different isomers).

δ = 13.3 (s), 14.3 (s), δ = 26.1 (s), 27.2 (s), 28.8 ppm (s); unidentified.

P**C**Al$_2$ undetected.

^1H (200.133 MHz):

δ = –0.23 (s, br; Al–C**H**$_3$); δ = –0.04 (s; Al–C**H**$_3$); δ = 0.01 (s, br; Al–C**H**$_3$); δ = 0.1 (s, Al–C**H**$_3$); δ = 0.15 ppm (s, Al–C**H**$_3$) (intensity ratio: 14:4:20:4:1).

δ = 0.74 (d); 0.84 (d); 0.85 (d); 0.95 (d); 1.02 (d); 1.05 (d); 1.16 (d); 1.27 (d); 1.29 ppm (d) ($^2J_{(P,H)}$ = 8.1, 6.4, 6.4, 5.6, 6.2, 7.5, 7.7, 8.9, 8.7 Hz) (intensity ratio 1:1:1:2:2:3:12:5:5, respectively; every signal represents P(C**H**$_3$)$_2$ of different isomers).

δ = 1.39 – 2.0 ppm (m, H$_{\mathrm{adamantyl}}$).

$^{27}Al\{^1H\}$ (52.148 MHz): 140 ppm (Singlet, very broad, **Al**, $W_{1/2}$ = 4400 Hz).

Table 6.3. Molecular Mass and Characteristic Fragments from the Mass Spectrum of ($C_{17}H_{33}Al_3Cl_3P$) (70 eV, sample temperature 410 K, source temperature 410 K)

Signal (m/z)	Rel. Int. (%)	Classification	Signal (m/z)	Rel. Int. (%)	Classification
445	1.0	$\{M - CH_3\}^+ (^{37}Cl_3)$	342	9.8	$\{M - CH_3AlCl_2\}^+ (^{35}Cl)$
443	1.5	$\{M - CH_3\}^+ (^{35}Cl\ ^{37}Cl_2)$	329	1.0	$\{M - Cl - (CH_3)_2AlCl\}^+ (^{37}Cl)$
441	2.5	$\{M - CH_3\}^+ (^{35}Cl_2\ ^{37}Cl)$	327	2.9	$M - Cl - (CH_3)_2AlCl\}^+ (^{35}Cl)$
439	2.4	$\{M - CH_3\}^+ (^{35}Cl_3)$	235	13.4	$\{(C_{10}H_{15})CP(CH_3)_2Al\}^+$
423	2.7	$\{M - Cl\}^+ (^{37}Cl_2)$	210	100.0	$\{(CH_3)_2PCH_2(C_{10}H_{15})\}^+$
421	0.8	$\{M - Cl\}^+ (^{35}Cl\ ^{37}Cl)$	135	23.1	$\{C_{10}H_{15}\}^+$
419	1.1	$\{M - Cl\}^+ (^{35}Cl_2)$	93	20.9	$\{C_7H_9\}^+$
366	2.6	$\{M - (CH_3)_2AlCl\}^+ (^{37}Cl_2)$	91	18.9	$\{C_7H_7\}^+$
364	8.9	$\{M - (CH_3)_2AlCl\}^+ (^{35}Cl^{37}Cl)$	79	20.0	$\{C_6H_7\}^+$
362	14.3	$\{M - (CH_3)_2AlCl\}^+ (^{35}Cl_2)$	79	10.5	$\{CH_3AlCl\}^+(^{37}Cl)$
351	0.2	$\{M - (CH_3) - CH_3)_2AlCl\}^+ (^{37}Cl_2)$	77	34.0	$\{CH_3AlCl\}^+(^{35}Cl)$
349	1.9	$\{M - (CH_3) - CH_3)_2AlCl\}^+ (^{35}Cl^{37}Cl)$	62	50.4	$\{(CH_3)_2PH\}^+$
347	6.3	$\{M - (CH_3) - CH_3)_2AlCl\}^+ (^{35}Cl_2)$	61	5.4	$\{(CH_3)_2P\}^+$
344	3.7	$\{M - CH_3AlCl_2\}^+ (^{37}Cl)$	27	12.7	$\{Al\}^+$

IR (Nujol mull between CsBr disks; $\tilde{\nu}$ [cm^{-1}]): 2360(w), 1558(w), 1538(w), 1400(s), 1358(s), 1344(s), 1318(w), 1306(s), 1287(s), 1258(w), 1000(vs; br), 1103(vs), 1066(vs), 986(m), 937(s; br), 873(w), 866(m), 803(m), 785(m), 721(m; br), 683(br), 583(m), 469(m), 453(m), 438(m), 418(w), 404(w), 401(w), 410(w), 400(w).

X-ray structure analysis: Chapter 2 (page 50).

6.8.4. *Diethyl[bis(ethylchloroalanyl)-1-adamantylmethyl]phosphine•Diethylchloroalane(1/1)* **(1d)**

A similar procedure to that described for **7.8.3** was used here, except that 1M solution (10.1 mL, 10.1 mmol) of diethylaluminium chloride was employed instead of dimethylaluminium chloride. The residue was washed with cold *n*-hexane and the compound was precipitated in 80% yield (1.45 g, 2.69 mmol). Colourless crystals were obtained by recrystallisation (25 °C/–60 °C; 2 weeks) from a 1:1 mixture of *n*-hexane and cyclopentane.

Characterization

Melting point: 149 °C

Elemental analysis: $C_{23}H_{45}Al_3Cl_3P$ Calc.: C 51.17%; H 8.40%; Cl 19.70%, P 5.74%

Found: C 50.96%; H 8.14%; Cl 19.20%, P 5.62%

Molar mass (cryoscopic in benzene [380]): 531.0 g.mol^{-1} (calc. 539.89 g.mol^{-1})

NMR (solution in d_6-benzene):

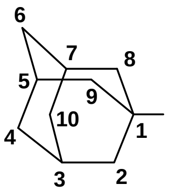

$^{31}P\{^{1}H\}$ (101.256 MHz):

High-Field Signals:

δ = –10.2 (s, br); –7.0 (s, br), –2.6 (s, br); –1.2 (s, br) ppm (intensity ratio 7:97:88:92; **P**).

Low-Field Signals:

δ = 22.2 (s); 23.1 (s); 24.6 (s, br); 25.8 ppm (s) (intensity ratio 2:4:17:1; **P**).

$^{13}C\{^{1}H\}$ (62.896 MHz):

δ = 3.6 ppm (s, br, Al–**C**H_2–CH_3).

δ = 8.4 ppm (s, br, Al–**C**H_2–CH_3).

δ = 8.70 (s; Al–CH_2–**C**H_3); 8.9 ppm (s; Al–CH_2–**C**H_3) (intensity ratio 3:1).

δ = 9.4 ppm (d, $^{2}J_{(C,P)}$ = 2.04 Hz; P–CH_2–**C**H_3).

δ = 11.80 (s; Al–CH_2–**C**H_3); 12.8 ppm (s; Al–CH_2–**C**H_3) (intensity ratio 3:1).

δ = 22.8 (d); 23.9 (d); 25.0 ppm (major) (d) ($^{1}J_{(C,P)}$ = 24.4, 25.4, 21.4 Hz, respectively; every signal represents P–**C**H_2–CH_3 of different isomers).

δ = 29.90 (major) (d); 30.1 (d); 30.2 ppm (d) ($^{4}J_{(C,P)}$ = 2.5, 2.04, 1.78 Hz, respectively; every signal represents (**C**3, **C**5, **C**7) of different isomers).

δ = 36.02 (s); 36.2 (s); 36.3 ppm (s) (intensity ratio 3:1:3, respectively; every signal represents (**C**4, **C**6, **C**10) of different isomers).

δ = 41.4 (major) (d); 41.8 (d); 41.9 ppm (d) ($^{2}J_{(C,P)}$ =10.4, 13.0, 13.7 Hz, respectively; every signal represents (**C**1) of different isomers).

δ = 47.0 (d); 47.5 (d); 48.2 ppm (d) ($^{3}J_{(P,C)}$ = 6.4, 5.1, 6.1 Hz, respectively; every signal represents (**C**2, **C**8, **C**9) of different isomers).

δ = 26.1 ppm (s); unidentified.

P**C**Al_2 undetected.

^{1}H (250.133 MHz):

δ = 0.46 ppm (q, $^{3}J_{(H,H)}$ = 8.03 Hz; 2 x Al–C**H_2**–CH_3, 4H).

δ = 0.55 ppm (q, $^{3}J_{(H,H)}$ = 8.03 Hz, 2 x Al–C**H_2**–CH_3; 4H).

δ = 0.91 ppm (dt, $^{3}J_{(H,H)}$ = 7.50 Hz, $^{3}J_{(P,H)}$ = 18.1 Hz, 2 x P–CH_2–C**H_3**, 6H).

δ = 1.31 ppm (dt, $^{3}J_{(H,H)}$ = 8.03 Hz, $^{4}J_{(H,P)}$ = 1.37 Hz, Al–CH_2–C**H_3**, 6H).

δ = 1.32 ppm (t, $^{3}J_{(H,H)}$ = 8.03 Hz, Al–CH_2–C**H_3**, 6H).

δ = 1.45 – 2.2 ppm (m, br, $H_{adamantyl}$, 15H).

δ = 1.61 – 1.80 ppm (m, 2 x P–C**H_2**–CH_3, 4H).

δ = 0.1 – 1.1 ppm very broad signals, 0.79 (s) ; unidentified.

$^{27}Al\{^1H\}$ (52.148 MHz): 149 ppm (singlet, very broad, **Al**, $W_{1/2} = 4526$ Hz).

Table 6.4. Characteristic masses ($C_{23}H_{45}Al_3Cl_3P$) from the mass spectrum (70 eV, sample temperature 415 K, source temperature 430 K)

Signal (m/z)	Rel. Int. (%)	Classification	Signal (m/z)	Rel. Int. (%)	Classification
515	0.46	$\{M - C_2H_5\}^+ (^{37}Cl_3)$	328	100.0	$\{(C_{10}H_{15})CP(C_2H_5)_3AlClH\}^+(^{35}Cl)$
513	4.12	$\{M - C_2H_5\}^+ (^{35}Cl\ ^{37}Cl_2)$	301	31.60	$\{(C_{10}H_{15})CP(C_2H_5)_2AlClH\}^+(^{37}Cl)$
511	9.85	$\{M - C_2H_5\}^+ (^{35}Cl_2\ ^{37}Cl)$	299	90.20	$\{(C_{10}H_{15})CP(C_2H_5)_2AlClH\}^+(^{35}Cl)$
509	10.95	$\{M - C_2H_5\}^+ (^{35}Cl_3)$	263	65.96	$\{(C_{10}H_{15})CP(C_2H_5)_2Al\}^+$
507	0.66	$\{M - Cl\}^+ (^{37}Cl_2)$	238	48.65	$\{(C_2H_5)_2PCH_2(C_{10}H_{15})\}^+$
505	1.06	$\{M - Cl\}^+ (^{35}Cl\ ^{37}Cl)$	135	75.15	$\{C_{10}H_{15}\}^+$
503	2.53	$\{M - Cl\}^+ (^{35}Cl_2)$	93	12.51	$\{C_2H_5AlCl\}^+(^{37}Cl)$
422	7.42	$\{M - (C_2H_5)_2AlCl\}^+ (^{37}Cl_2)$	91	42.89	$\{C_2H_5AlCl\}^+(^{35}Cl)$
420	41.92	$\{M - (C_2H_5)_2AlCl\}^+ (^{35}Cl\ ^{37}Cl)$	93	26.11	$\{C_7H_9\}^+$
418	58.19	$\{M - (C_2H_5)_2AlCl\}^+ (^{35}Cl_2)$	91	34.65	$\{C_7H_7\}^+$
414	1.79	$\{M - C_2H_5AlCl_2\}^+ (^{37}Cl)$	90	34.65	$\{(C_2H_5)_2PH\}^+$
412	3.07	$\{M - C_2H_5AlCl_2\}^+ (^{35}Cl)$	89	1.94	$\{(C_2H_5)_2P\}^+$
393	4.83	$\{M - (C_2H_5) - C_2H_5)_2AlCl\}^+ (^{37}Cl_2)$	79	32.17	$\{C_6H_7\}^+$
391	8.60	$\{M - (C_2H_5) - C_2H_5)_2AlCl\}^+ (^{35}Cl^{37}Cl)$	61	11.82	$C_2H_5PH\}^+$
389	12.87	$\{M - (C_2H_5) - C_2H_5)_2AlCl\}^+ (^{35}Cl_2)$	60	1.90	$\{C_2H_5P\}^+$
385	2.44	$\{M - Cl(C_2H_5)_2AlCl\}^+ (^{37}Cl)$	59	5.71	$\{C_2H_4P\}^+$
383	4.22	$M - Cl - (C_2H_5)_2AlCl\}^+ (^{35}Cl)$	29.0	30.86	$\{(C_2H_5)\}^+$
330	28.97	$\{(C_{10}H_{15})CP(C_2H_5)_3AlClH\}^+(^{37}Cl)$	27	42.31	$\{Al\}^+$

IR (Nujol mull between CsBr disks; $\tilde{\nu}$ [cm^{-1}]): 2681(w), 1406(w), 1344(w), 1306(m), 1254(w), 1189(w), 1105(m), 1066(m), 1034(w), 985(m), 943(w), 917(s), 838(vs), 818(m), 800(s), 785(s), 724(vs), 697(s), 664(m), 648(m), 638(m), 623(w), 556(w), 536(w), 504(w), 455(m).

X-ray structure analysis: Chapter 2 (page 50).

6.9. Bromodiphenylphosphine [381]

Chlorodiphenylphosphine (21 mL, 25.81 g, 117 mmol, δ $^{31}P\{H\}$ = + 82.80 ppm in C_6D_6) was mixed with 3.7 mL (10.55 g, 38.95 mmol) of phosphorus (III) bromide (δ $^{31}P\{H\}$ = + 227.3 ppm in C_6D_6), and the mixture was heated without solvent under reflux with stirring for 24 hours in oil bath to 200 °C. The phosphorus(III) chloride (δ $^{31}P\{H\}$ = + 219.2 ppm in C_6D_6) was distilled off at atmospheric pressure. $^{31}P\{^1H\}$ NMR was showed the remaining residue contained both chloro- and bromo-diphenylphosphine δ $^{31}P\{H\}$ = + 82.80 ppm, + 73.32 ppm in C_6D_6) respectively. Finally the Bromodiphenylphosphine was distilled off and purified by vacuum distillation (100 cm spinning band column) and the compound was isolated in 68% yield (21 g, 67.9 mmol).

$$3\ Ph_2PCl + PBr_3 \longrightarrow 3\ Ph_2PBr + PCl_3$$

Characterization

Boiling point: 100 °C / 1 • 10^{-3} mbar.

Elemental analysis: $C_{12}H_{10}BrP$ Calc.: C 54.37%; H 3.80%

Found: C 54.10%; H 3.69%

NMR (solution in C_6D_6):

$^{31}P\{^1H\}$ (101.256 MHz):

δ = 73.32 ppm (s)

^1H (200.132 MHz):

δ = 6.99-7.05 ppm (m, **H**(phenyl); 6H)

δ = 7.46-7.59 ppm (m, **H**(phenyl); 4H)

$^{13}C\{^1H\}$ (50.323 MHz):

δ = 137.60 ppm (d, $^1J_{(C,P)}$ = 36.84 Hz; *ipso*-**C**)

δ = 130.48 ppm (s; *para*-**C**)

δ = 128.84 ppm (d, $^3J_{(C,P)}$ = 6.52 Hz; *meta*-**C**)

δ = 132.90 ppm (d, $^2J_{(C,P)}$ = 24.00 Hz; *ortho*-**C**)

6.10. Chlorophenylisopropylphosphine [382]

A solution of 55 mL (110 mmol) of 2 M isopropylmagnesiumchloride in THF was added to a stirred solution of 13.6 mL (17.943 g, 100 mmol) of dichlorophenylphosphine (δ $^{31}P\{H\}$ = + 161.5 ppm in C_6D_6) in 500 mL diethyl ether over a period of 4 h at –78 °C. The reaction mixture was allowed to warm to ambient temperature and stirring was continued for 8 hours, and the mixture was then refluxed for 90 minutes. The solution was filtered off and the filtrate was evaporated at atmospheric pressure to remove the solvents and the residue purified by vacuum distillation and the compound was isolated in 67% yield (12 g, 64.3 mmol).

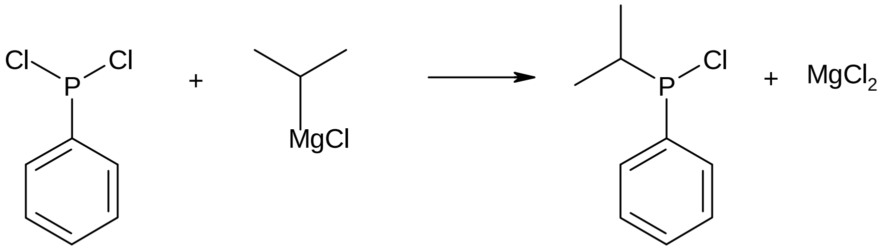

Characterization

Boiling point: 50 °C / 2 • 10^{-2} mbar.

Elemental analysis: $C_9H_{12}ClP$ calc.: C 57.92%; H 6.48%; Cl 19.00%; P 16.60%

found: C 57.65%; H 6.49%; Cl 18.65%; P 16.44%

NMR (solution in C_6D_6)

$^{31}P\{^1H\}$ (101.256 MHz):

δ = 102.55 ppm (s)

^{1}H (250.133 MHz):

δ = 0.76 ppm (dd, $^{3}J_{(H,P)}$ = 16.75 Hz, $^{3}J_{(H,H)}$ = 6.88 Hz; **H**$_3$C–CH–P; 3H)

δ = 1.04 ppm (dd, $^{3}J_{(H,P)}$ = 14.00 Hz, $^{3}J_{(H,H)}$ = 6.88 Hz; **H**$_3$C–CH–P; 3H)

δ = 1.93 ppm (dsptet, $^{2}J_{(H,P)}$ = 4.13 Hz, $^{3}J_{(H,H)}$ = 6.88 Hz; H$_3$C–C**H**–P; 1H)

δ = 7.12–7.17 ppm (m, **H**(phenyl); 3H)

δ = 7.48–7.57 ppm (m, **H**(phenyl); 2H)

$^{13}C\{^{1}H\}$ (62.896 MHz):

δ = 17.61 ppm (d, $^{2}J_{(C,P)}$ = 20.52 Hz ; H$_3$**C**–CH–P)

δ = 18.01 ppm (d, $^{2}J_{(C,P)}$ = 14.74 Hz ; H$_3$**C**–CH–P)

δ = 34.49 ppm (d, $^{1}J_{(C,P)}$ = 26.84 Hz ; H$_3$C–**C**H–P)

δ = 128.77 ppm (d, $^{3}J_{(C,P)}$ = 7.89 Hz; *meta*-**C**)

δ = 130.71 ppm (s; *para*-**C**)

δ = 131.61 ppm (d, $^{2}J_{(C,P)}$ = 25.25 Hz; *ortho*-**C)**

δ = 138.01 ppm (d, $^{1}J_{(C,P)}$ = 36.31 Hz; *ipso*-**C**)

6.11. Procedures for the Preparation of Several 2,4-Di-*tert*-butyl-3,3-diorganyl-1λ^3,5λ^3-diphospha-3-phosphonia-tricyclo[2.1.0.0^{2,5}]pentane Halides.

6.11.1. *2,4-Di-*tert*-butyl-3,3-dimethyl-1λ^3,5λ^3-diphospha-3-phosphonia-tricyclo[2.1.0.0^{2,5}]pentane chloride* (**2a)**

A solution of chlorodimethylphosphine (0.24g, 2.50 mmol, δ $^{31}P\{H\}$ = + 96.0 ppm in C_6D_6) in cyclopentane (10 mL) was added dropwise to a stirred solution (0.51 g, 5.1 mmol) in cyclopentane (10 mL) of 2-*tert*-butyl-1λ^3-phosphaalkyne at –70 °C over a period of 30 minutes. When the reaction mixture had been allowed to warm up to room temperature, stirring was continued for four days. The solution slowly turned yellow-brown, and a colourless solid precipitated. Without filtration solvent was removed under reduced pressure at room temperature to give the crude product as a yellow-brown solid. The residue was dried under vacuum for several hours, and then 10 mL of toluene was added to the residue and the mixture refluxed with stirring for 4 hours, after which the mixture changed colour from yellow-brown to yellow-orange. The mixture was then allowed to settle overnight in a refrigerator at 4°C and then the yellow-orange solution was removed by a pipette, and the residue was dried under vacuum for several hours. Colourless crystals were obtained by recrystallisation (25 °C/–60 °C, 3-4 weeks) from dichloromethane (10 mL). The crystals were dried several times under vacuum at 10^{-3} mbar and then the compound was isolated in 77% yield (0.6 g, 1.91 mmol).

Characterization

Melting point: 157°C (dec.).

Elemental analysis: $C_{12}H_{24}ClP_3 \bullet 0.2CH_2Cl_2$; calc.: C 46.71%; H 7.84%; Cl 15.82%; P 29.62%

found: C 45.96%; H 8.37%; Cl 15.59%; P 28.81%

NMR (solution in $CDCl_3$)

$^{31}P\{^1H\}$ (101.256 MHz):

$\delta = -264.07$ ppm (d, $^2J_{(P1/P5,P3)} = 10.81$ Hz; **P1**/**P5**)

$\delta = 104.02$ ppm (t, $^2J_{(P1/P5,P3)} = 10.81$ Hz; **P3**)

^1H (250.133 MHz):

$\delta = 1.02$ ppm (s, **H**$_3$C–C–C–P3/P1,P5; 18H)

$\delta = 3.08$ ppm (d, $^2J_{(H,P3)} = 12.85$ Hz; **H**$_3$C–P3; 6H)

$\delta = 5.27$ ppm (s; C**H**$_2$Cl$_2$)

$^{13}C\{^1H\}$ (62.896 MHz):

$\delta = 18.7$ ppm (dt, $^1J_{(C,P3)} = 32.89$ Hz, $^3J_{(C,P1\ \mathrm{and}\ P5)} = 4.89$ Hz; H$_3$**C**–P3)

$\delta = 30.12$ ppm (pseudo-quintet–equal to dt, $^3J_{(C,P3)} = 5.1$ Hz, $^3J_{(C,P1\ \mathrm{and}\ P5)} = 2.42$ Hz; H$_3$**C**–C–C–P3/P1 and P5)

$\delta = 31.69$ ppm (t, $^2J_{(C,P1\ \mathrm{and}\ P5)} = 4.83$ Hz; H$_3$C–**C**–C–P3/P1 and P5)

$\delta = 48.11$ ppm (dt, $^1J_{(C,P3)} = 59.51$ Hz, $^1J_{(C,P1\ \mathrm{and}\ P5)} = 42.09$ Hz; H$_3$C–C–**C**–P3//P1 and P5)

$\delta = 53.38$ ppm (s; **C**H$_2$Cl$_2$)

Table 6.5. Molecular Mass and Characteristic Fragments from the Mass Spectrum of ($C_{12}H_{24}P_3Cl$) (70 eV, Sample Temperature 440 K, Source Temperature 420 K)

Signal (m/z)	Rel. Int. (%)	Classification	Signal (m/z)	Rel. Int. (%)	Classification
296	5.2	$\{M\}^+ (^{35}Cl)$	129	2.7	$\{P_2CC(CH_3)_3 - 2\,H\}^+$
297	2.2	$\{M\}^+ (^{13}C)$	115	3.5	$\{(CH_3PCC(CH_3)_3\}^+$
298	4.1	$\{M\}^+ (^{37}Cl)$	101	11.3	$\{PCC(CH_3)_3 + H\}^+$
299	0.6	$\{M\}^+ (^{13}C)$	100	19.6	$\{PCC(CH_3)_3\}^+$
283	4.7	$\{M - CH_3\}^+$	99	4.7	$\{PCC(CH_3)_3 - H\}^+$
281	12.0	$\{M - CH_3\}^+$	85	35.9	$\{PCC(CH_3)_2\}^+$
261	100.0	$\{M - Cl\}^+$	83	4.9	$\{PCC(CH_3)_2 - 2\,H\}^+$
205	14.7	$\{M + H - Cl - C(CH_3)_3\}^+$	69	38.2	$\{CC(CH_3)_3\}^+$
203	6.1	$\{M - H - Cl - C(CH_3)_3\}^+$	62	4.8	$\{(CH_3)_2PH\}^+$
185	3.4	$\{(CH_3)P[CC(CH_3)_3]_2 + H\}^+$	61	22.3	$\{(CH_3)_2P\}^+$
184	1.6	$\{(CH_3P[CC(CH_3)_3]_2\}^+$	57	34.8	$\{C(CH_3)_3\}^+$
169	26.6	$\{P[CC(CH_3)_3]_2\}^+$	55	22.9	$\{C(CH_3)_3 - 2H\}^+$
161	14.6	$\{(CH_3)_2P_3C_2CH_2\}^+$	47	18.4	$\{CH_3PH\}^+$
146	14.4	$\{CH_3P_3C_2CH_2\}^+$	46	5.3	$\{CH_3P\}^+$
145	2.1	$\{CH_3P_3C_2CH\}^+$	45	16.5	$\{CH_2P\}^+$
134	12.5	$\{(CH_3)P_3CCH_2\}^+$	41	79.6	$\{C(CH_3)_2 - H\}^+$
131	3.4	$\{P_2CC(CH_3)_3\}^+$			

IR (Nujol mull between CsBr disks; $\tilde{\nu}$ *[cm^{-1}])*: 870(m), 814(w,b), 722(vs), 698(m), 637(mw), 565(w), 534(w), 457(w, b), 412(m(w)).

Raman (crystalline solid in glass capillary; $\tilde{\nu}$ *[cm^{-1}])*: 940(vw), 932(w(m)), 871(mw), 815m(w), 699(mw), 697(mw), 637(mw), 611(w), 568(vs), 534(m(w), 412m(s), 396m(w).

X-ray structure analysis: Chapter 3 (page 83).

6.11.2. *2,4-Di-*tert*-butyl-3,3-diethyl-1λ^3,5λ^3-diphospha-3-phosphonia-tricyclo[2.1.0.0^{2,5}]pentane chloride* (**2b**)

A similar procedure to that described for **6.12.1** was used here, except that chlorodiethylphosphine (0.31 g, 2.5 mmol, δ ^{31}P{H} = + 118.5 ppm in C_6D_6) was employed instead of chlorodimethylphosphine. Colourless crystals were obtained by recrystallisation (25 °C/–60 °C; 3-4 weeks) from dichloromethane. The crystals were dried several times under vacuum at 10^{-3} mbar and then the compound was isolated in 74% yield (0.6 g, 1.85 mmol).

Characterization

Melting point: 168 °C (dec.).

Elemental analysis: $C_{14}H_{28}ClP_3$ calc.: C 51.78%; H 8.69%; Cl 10.92%; P 28.61%.
found: C 51.51%; H 8.42%; Cl 10.50%; P 28.00%.

NMR (solution in $CDCl_3$)

$^{31}P\{^1H\}$ (101.256 MHz):

δ = –286.52 ppm (d, $^2J_{(P1/P5,P3)}$ = 1.5 Hz; **P1**/**P5**)

δ = 119.50 ppm (t, $^2J_{(P1/P5,P3)}$= 1.5 Hz; **P3**)

^1H (250.133 MHz):

δ = 1.03 ppm (s, **H**$_3$C–C–C–P3/P1, P5; 18H)

δ = 1.63 ppm (dt, $^3J_{(H,H)}$ = 7.43 Hz, $^3J_{(H,P3)}$ =17.60 Hz; **H**$_3$C–CH$_2$–P3; 6H)

δ = 3.43 ppm (dq, $^3J_{(H,H)}$ = 7.43 Hz, $^2J_{(H, P3)}$ =11.82 Hz; H$_3$C–C**H**$_2$–P3; 4H)

δ = 5.08 ppm (s; C**H**$_2$Cl$_2$)

$^{13}C\{^1H\}$ (100.614MHz):

δ = 8.84 ppm (dt, $^2J_{(C,P3)}$ = 5.72 Hz, $^4J_{(C,P1\text{ and }P5)}$ = 2.86 Hz; H$_3$**C**–CH$_2$–P3//P1 and P5)

δ = 26.59 ppm (dt, $^1J_{(C,P3)}$ = 26.91 Hz, $^3J_{(C,P1\text{ and }P5)}$ = 3.82 Hz; H$_3$C–**C**H$_2$–P3//P1 and P5)

δ = 30.30 ppm (pseudo-quintet–equal to dt, $^3J_{(C,P3)}$ = 5.09 Hz, $^3J_{(C,P1\text{ and }P5)}$ = 2.65 Hz; H$_3$**C**–C–C–P3//P1 and P5)

δ = 31.47 ppm (t, $^2J_{(C,P1\text{ and }P5)}$ = 4.93 Hz; H$_3$C–**C**–C–P1 and P5)

δ = 40.82 ppm (dt, $^1J_{(C,P3)}$ = 52.45 Hz, $^1J_{(C,P1\text{ and }P5)}$ = 41.80 Hz; H$_3$C–C–**C**–P3//P1 and P5)

δ = 53.29 ppm (s; **C**H$_2$Cl$_2$)

Table 6.6. Molecular Mass and Characteristic Fragments from the Mass Spectrum of ($C_{14}H_{28}P_3Cl$) (70 eV, Sample Temperature 470 K, Source Temperature 460 K)

Signal (m/z)	Rel. Int. (%)	Classification	Signal (m/z)	Rel. Int. (%)	Classification
324	12.0	$\{M\}^+(^{35}Cl)$	129	3.0	$\{P_2CC(CH_3)_3 - 2\ H\}^+$
325	2.2	$\{M\}^+(^{13}C)$	117	1.5	$\{(C_2H_5PCC(CH_3)_3\}^+$
326	3.9	$\{M\}^+(^{37}Cl)$	101	5.7	$\{PCC(CH_3)_3 + H\}^+$
327	0.6	$\{M\}^+(^{13}C)$	100	1.6	$\{PCC(CH_3)_3\}^+$
311	8.4	$\{M - CH_3\}^+$	99	12.2	$\{PCC(CH_3)_3 - H\}^+$
309	26.4	$\{M - CH_3\}^+$	90	1.1	$\{(C_2H_5)_2PH\}^+$
289	100.0	$\{M\text{- }Cl\}^+$	89	6.7	$\{(C_2H_5)_2P\}^+$
233	3.6	$\{M + H - Cl - C(CH_3)_3\}^+$	85	10.6	$\{PCC(CH_3)_2\}^+$
231	19.5	$\{M - H - Cl - C(CH_3)_3\}^+$	83	5.3	$\{PCC(CH_3)_2 - 2\ H\}^+$
189	5.8	$\{(C_2H_5)_2P_3C_2CH_2\}^+$	69	13.4	$\{CC(CH_3)_3\}^+$
177	1.6	$\{(C_2H_5)_2P_3CCH_2\}^+$	61	10.1	$C_2H_5PH\}^+$
169	12.7	$\{P[CC(CH_3)_3]_2\}^+$	60	3.0	$\{C_2H_5P\}^+$
160	3.5	$\{C_2H_5P_3C_2CH_2\}^+$	59	6.2	$\{C_2H_4P\}^+$
159	6.4	$\{C_2H_5P_3C_2CH\}^+$	57	18.4	$\{C(CH_3)_3\}^+$
132	5.8	$\{P_2CC(CH_3)_3 + 1\ H\}^+$	55	14.8	$\{C(CH_3)_3 - 2H\}^+$
131	10.4	$\{P_2CC(CH_3)_3\}^+$	41	29.4	$\{C(CH_3)_2 - H\}^+$
130	6.8	$\{P_2CC(CH_3)_3 - 1\ H\}^+$	29	9.9	$\{C_2H_5\}^+$

IR (Nujol mull between CsBr disks; $\tilde{\nu}$ [cm^{-1}]): 933(w), 871(s), 814(vw), 721(m(w)), 714(ms), 706(ms), 633(mw), 568(vw),m 528(w, b), 409(mw).

Raman (crystalline solid in glass capillary; $\tilde{\nu}$ [cm^{-1}]): 934(mw,b), 929(mw,b), 872(mw), 831(mw), 814(m(w)), 726(vs), 709(s), 694(s(vs)), 633(mw), 569(vs), 534(m(w)), 384(s).

X-ray structure analysis: Chapter 3 (page 83).

6.11.3. *2,4-Di-*tert*-butyl-3-isopropyl-3-phenyl-1λ^3,5λ^3-diphospha-3-phosphonia-tricyclo[2.1.0.0^{2,5}]pentane chloride* (**2c**)

A similar procedure to that described for 6.12.1 was used here, except that chloroisopropylphenylphosphine (0.47 g, 2.5 mmol, $\delta\ ^{31}P\{H\}$ = + 102.55 ppm in C_6D_6) was employed instead of chlorodimethylphosphine. Colourless crystals were obtained by recrystallisation (25 °C/–13 °C; one week) from dichloromethane. The crystals were dried several times under vacuum at 10^{-3} mbar and then the compound was isolated in 79% yield (0.76 g, 1.96 mmol).

Characterization

Melting point: 184 °C (dec.).

Elemental analysis: $C_{19}H_{30}ClP_3$ calc.: C 59.00%; H 7.82%; Cl 9.17%; P 24.02%.

found: C 58.91%; H 8.09%; Cl 8.92%; P 23.96%.

NMR (solution in $CDCl_3$)

$^{31}P\{^1H\}$ (101.256 MHz):

$\delta = -289.57$ ppm (d) $^1J_{(P1,P5)} = 172.2$ Hz, **P1** or **P5**)

$\delta = -278.28$ ppm (d) $^1J_{(P1,P5)} = 172.2$ Hz, **P1** or **P5**)

$\delta = 110.63$ Hz (s; **P3**)

^1H (250.1329 MHz):

$\delta = 0.84$ ppm (s, $\mathbf{H}_3$C–C–C–P1 and P5; 18H)

$\delta = 1.60$ ppm (dd, $^3J_{(H,H)} = 6.88$ Hz, $^3J_{(H,P3)} = 17.90$ Hz; $\mathbf{H}_3$C–CH–P3; 6H)

$\delta = 4.90$–5.05 ppm (m, H_3C–C**H**–P3; 1H)

$\delta = 5.17$ ppm (s, C$\mathbf{H}_2$Cl$_2$)

$\delta = 7.54$–7.72 ppm (m, **H**(phenyl); 3H)

$\delta = 8.56$–8.65 ppm (m, **H**(phenyl); 2H)

$^{13}C\{^1H\}$ (50.323 MHz):

$\delta = 17.80$ ppm (dd, $^2J_{(C,P3)} = 4.6$ Hz, $^4J_{(C,P1\ or\ P5)} = 2.03$ Hz; H_3**C**–CH–P3//P1 or P5)

$\delta = 30.52$ ppm (pseudo-quintet–equal to dt, $^3J_{(C,P3)} = 5.60$ Hz, $^3J_{(C,P1\ and\ P5)} = 3.05$ Hz; H_3**C**–C–C–P3//P1 and P5)

$\delta = 31.00$ ppm (ddd, $^1J_{(C,P3)} = 23.90$ Hz, $^3J_{(C,P1\ or\ P5)} = 5.09$ Hz, $^3J_{(C,P1\ or\ P5)} = 1.53$ Hz; H_3C–**C**H–P3//P1, P5)

$\delta = 31.48$ ppm (t, $^2J_{(C,P1\ and\ P5)} = 4.58$ Hz; H_3C–**C**–C–P1 and P5)

$\delta = 42.93$ ppm (dt, $^1J_{(C,P3)} = 51.54$ Hz, $^1J_{(C,P1\ and\ P5)} = 41.71$ Hz; H_3C–C–**C**–P3//P1 and P5)

$\delta = 53.31$ ppm (s; **C**H$_2$Cl$_2$)

$\delta = 124.82$ ppm (ddd, $^1J_{(C,P3)} = 53.28$ Hz, $^3J_{(C,P1\ or\ P5)} = 6.23$ Hz, $^3J_{(C,P1\ or\ P5)} = 2.05$ Hz; *ipso*-**C**)

$\delta = 130.21$ (d, $^3J_{(C,P3)} = 10.68$ Hz; *meta*-**C**)

$\delta = 132.64$ ppm (dd, $^2J_{(C,P3)} = 8.91$ Hz, $^4J_{(C,\ P1\ or\ P5)} = 4.33$ Hz; *ortho*-**C**)

$\delta = 135.27$ ppm (d, $^4J_{(C,P3)} = 3.06$ Hz; *para*-**C**)

Table 6.7. Molecular Mass and Characteristic Fragments from the Mass Spectrum of ($C_{19}H_{30}P_3Cl$) (70 eV, Sample Temperature 470 K, Source Temperature 440 K)

Signal (m/z)	Rel. Int. (%)	Classification	Signal (m/z)	Rel. Int. (%)	Classification
386	14.8	$\{M\}^+$ (^{35}Cl)	151	30.7	$\{(C_6H_5)(C_3H_7)P\}^+$
387	4.4	$\{M\}^+$(^{13}C)	131	45.9	$\{P_2CC(CH_3)_3\}^+$
388	5.9	$\{M\}^+$ (^{37}Cl)	129	9.7	$\{P_2CC(CH_3)_3 - 2\ H\}^+$
389	1.3	$\{M\}^+$(^{13}C)	108	35.3	$\{C_6H_5P\}^+$
373	14.4	$\{M - CH_3\}^+$	107	21.7	$\{C_6H_4P\}^+$
371	41.8	$\{M - CH_3\}^+$	101	8.1	$\{PCC(CH_3)_3 + H\}^+$
351	99.7	$\{M - Cl\}^+$	100	9.7	$\{PCC(CH_3)_3\}^+$
295	16.9	$\{M + H - Cl - C(CH_3)_3\}^+$	99	44.4	$\{PCC(CH_3)_3 - H\}^+$
293	18.9	$\{M - H - Cl - C(CH_3)_3\}^+$	85	26.8	$\{PCC(CH_3)_2\}^+$

251	15.2	$\{(C_6H_5)(C_3H_7)P_3C_2CH_2\}^+$	83	17.5	$\{PCC(CH_3)_2 - 2\ H\}^+$
246	6.7	$\{(C_6H_5P[CC(CH_3)_3]_2\}^+$	77	29.3	$\{C_6H_5\}^+$
239	6.5	$\{(C_6H_5)(C_3H_7)P_3CCH_2\}^+$	74	2.6	$\{(C_3H_7)P\}^+$
213	12.8	$\{(C_3H_7)P[CC(CH_3)_3]_2 + H\}^+$	69	38.1	$\{CC(CH_3)_3\}^+$
208	23.6	$\{C_6H_5P_3C_2CH_2\}^+$	57	58.5	$\{C(CH_3)_3\}^+$
207	8.3	$\{C_6H_5P_3C_2CH\}^+$	55	16.1	$\{C(CH_3)_3 - 2H\}^+$
177	32.1	$\{(C_6H_5PCC(CH_3)_3\}^+$	43	49.1	$\{(C_3H_7)\}^+$
169	59.1	$\{P[CC(CH_3)_3]_2\}^+$	42	9.3	$\{(C_3H_6)\}^+$
152	13.9	$\{(C_6H_5)(C_3H_7)PH\}^+$	41	100.0	$\{C(CH_3)_2 - H\}^+$

IR (Nujol mull between CsBr disks; $\tilde{\nu}$ [cm^{-1}]): 994(m), 880(ms), 857(s-vs), 814(mw), 713(mw), 708(w), 703(w), 674(s), 630(ms), 575(m), 560(m), 532(mw), 512(m), 505(mw), 422(mw).

Raman (crystalline solid in glass capillary; $\tilde{\nu}$ [cm^{-1}]): 993(s), 931(mw), 883(vw), 859(mw), 825((m)w), 813(mw), 674(ms,b), 629(mw), 612(m), 576(vs), 561(ms), 532(mw), 510(s), 487(m), 422(ms).

X-ray structure analysis: Chapter 3 (page 83)

6.11.4. *2,4-Di-*tert*-butyl-3,3-diphenyl-1λ^3,5λ^3-diphospha-3-phosphonia-tricyclo[2.1.0.0^{2,5}]pentane chloride* **(2d.1)**

A similar procedure to that described for 6.12.1 was used here, except that chlorodiphenylphosphine (0.45 g, 2.5 mmol, δ $^{31}P\{H\}$ = + 82.80 ppm in C_6D_6) was employed instead of chlorodimethylphosphine. Colourless crystals were obtained by recrystallisation (25 °C/–13 °C; one week) from dichloromethane. The crystals were dried several times under vacuum at 10^{-3} mbar and then the compound was isolated in 80% yield (0.80 g, 1.90 mmol).

Characterization

Melting point: 196 °C.

Elemental analysis: $C_{22}H_{28}ClP_3$ calc.: C 62.80%; H 6.71%; Cl 8.42%; P 22.08%.

found: C 63.16%; H 6.80%; Cl 8.21%; P 21.62 %.

NMR (solution in $CDCl_3$)

$^{31}P\{^1H\}$ (101.256 MHz):

δ = –281.93 ppm (d, $^2J_{(P1/P5,P3)}$ = 4.14 Hz; **P1**/**P5**)

δ = 85.14 (t, $^2J_{(P1/P5,P3)}$ = 4.14 Hz; **P3**)

^1H (250.133 MHz):

δ = 0.74 ppm (s, **H**$_3$C–C–C–P3/P1, P5; 18H)

δ = 5.16 ppm (s; C**H**$_2$Cl$_2$)

δ = 7.69–7.80 ppm (m, **H**(phenyl); 6H)

δ = 7.81–8.17 ppm (m, **H**(phenyl); 4H)

$^{13}C\{^1H\}$ (62.896 MHz):

δ = 30.38 ppm (pseudo-quintet–equal to dt, $^3J_{(C,P3)}$ = 5.26 Hz, $^3J_{(C,P1\ \text{and}\ P5)}$ = 2.63 Hz; H_3**C**–C–C–P3//P1 and P5)

δ = 32.05 ppm (t, $^2J_{(C,P1\ \text{and}\ P5)}$ = 4.74 Hz; H_3C–**C**–C–P3//P1 and P5)

δ = 47.59 ppm (dt, $^1J_{(C,P3)}$ = 58.23 Hz, $^1J_{(C,P1\ \text{and}\ P5)}$ = 43.28Hz; H_3C–C–**C**–P3//P1 and P5)

δ = 53.26 ppm (s; **C**H_2Cl_2)

δ = 124.24 ppm (dt, $^1J_{(C,P3)}$ = 58.58 Hz, $^3J_{(C,P1\ \text{and}\ P5)}$ = 4.74 Hz; *ipso*-**C**)

δ = 130.39 (d, $^3J_{(C,P3)}$ = 11.05 Hz; *meta*-**C**)

δ = 132.98 ppm (d, $^2J_{(C,P3)}$ = 9.99 Hz; *ortho*-**C**)

δ = 136.20 ppm (d, $^4J_{(C,P3)}$ = 3.15 Hz; *para*-**C**)

Table 6.8. Molecular Mass and Characteristic Fragments from the Mass Spectrum of ($C_{22}H_{28}P_3Cl$) (70 eV, Sample Temperature 470 K, Source Temperature 440 K)

Signal (m/z)	Rel. Int. (%)	Classification	Signal (m/z)	Rel. Int. (%)	Classification
423	1.9	$\{M\}^+(^{13}C)$	169	20.4	$\{P[CC(CH_3)_3]_2\}^+$
421	6.1	$\{M\}^+(^{13}C)$	131	4.8	$\{P_2CC(CH_3)_3\}^+$
422	9.0	$\{M\}^+(^{37}Cl)$	129	6.4	$\{P_2CC(CH_3)_3 - 2\,H\}^+$
420	23.0	$\{M\}^+(^{35}Cl)$	108	12.1	$\{C_6H_5P\}^+$
407	24.4	$\{M - CH_3\}^+$	107	13.2	$\{C_6H_4P\}^+$
405	76.2	$\{M - CH_3\}^+$	99	14.8	$\{PCC(CH_3)_3 - H\}^+$
385	100.0	$\{M - Cl\}^+$	85	9.4	$\{PCC(CH_3)_2\}^+$
285	4.7	$\{(C_6H_5)_2P_3C_2CH_2\}^+$	77	6.0	$\{C_6H_5\}^+$
247	9.3	$\{(C_6H_5P[CC(CH_3)_3]_2 + H\}^+$	69	5.4	$\{CC(CH_3)_3\}^+$
185	49.4	$\{(C_6H_5)_2P\}^+$	57	11.9	$\{C(CH_3)_3\}^+$
183	64.4	$\{(C_6H_4)_2P\}^+$	55	6.9	$\{C(CH_3)_3 - 2H\}^+$
177	6.0	$\{(C_6H_5PCC(CH_3)_3\}^+$	41	23.1	$\{C(CH_3)_2 - H\}^+$

IR (Nujol mull between CsBr disks; $\tilde{\nu}$ [cm^{-1}]): 997(sh), 992(m), 938(w,b), 893(vvw), 895(s), 815((m)w), 726(w,b), 698(mw), 631(ms), 615(w), 588(s), 570(m), 529(w), 513(ms), 507(s-vs), 481(ms), 407(m,b).

Raman (crystalline solid in glass capillary; $\tilde{\nu}$ [cm^{-1}]): 999(ms), 993(m), 939(w), 857(w-vw), 815(w), 727(vs), 709(s), 693(s), 631(w,b), 614(mw), 587(vvs), 587(vvs)?, 530(mw), 512(m), 408(mw), 405(sh).

X-ray structure analysis: Chapter 3 (page 83).

6.11.5. *2,4-Di-*tert*-butyl-3,3-diphenyl-1λ^3,5λ^3-diphospha-3-phosphonia tricyclo[2.1.0.0^{2,5}]pentane bromide* **(2d.2)**

A similar procedure to that described for 6.12.1 was used here, except that bromodiphenylphosphine (0.663 g, 2.50 mmol, δ $^{31}P\{H\}$ = + 73.32 ppm in C_6D_6) was employed instead of chlorodimethylphosphine. Colourless crystals were obtained by recrystallisation (25 °C/–13 °C; one week) from dichloromethane. The crystals were dried several times under vacuum at 10^{-3} mbar and then the compound was isolated in 73 % yield (0.85 g, 1.82 mmol).

Characterization

Melting point: 243 °C.

Elemental analysis: $C_{22}H_{28}BrP_3 \cdot 0.8\ CH_2Cl_2$;

calc.: C 51.36%; H 5.60%; Br 14.98%; Cl 10.6%; P 17.42%
found: C 51.94%; H 5.92%; Br 15.07%; Cl 9.92%; P 17.16%

NMR (solution in C_6D_6)

$^{31}P\{^1H\}$ (101.256 MHz):

δ = –280.82 ppm (d, $^2J_{(P1/P5,P3)}$ = 4.45 Hz; **P1/P5**)

δ = 85.02 (t, $^2J_{(P3/P1,P5)}$ = 4.45 Hz; **P3**)

^1H NMR (200.1323 MHz):

δ = 0.85 ppm (s, **H**$_3$C–C–C–P3/P1, P5; 18H)

δ = 5.25 ppm (s; C**H**$_2$Cl$_2$)

δ = 7.74–7.89 ppm (m, **H**(phenyl); 6H)

δ = 8.23–8.32 ppm (m, **H**(phenyl); 4H)

$^{13}C\{^1H\}$ (50.323 MHz):

δ = 30.68 ppm (pseudo-quintet–equal to dt, $^3J_{(C,P3)}$ = 5.47 Hz, $^3J_{(C,P1\ \mathrm{and}\ P5)}$ = 2.73 Hz; H$_3$**C**–C–C–P3//P1 and P5)

δ = 32.38 ppm (dt, $^2J_{(C,\ P3)}$ = 0.96, $^2J_{(C,P1\ \mathrm{and}\ P5)}$ = 5.06 Hz; H$_3$C–**C**–C–P3//P1 and P5)

δ = 47.95 ppm (dt, $^1J_{(C,P3)}$ = 57.81 Hz, $^1J_{(C,P1\ \mathrm{and}\ P5)}$ = 43.41 Hz; H$_3$C–C–**C**–P3//P1 and P5)

δ = 53.41 ppm (s; **C**H$_2$Cl$_2$)

δ = 124.60 ppm (dt, $^1J_{(C,P3)}$ = 58.21 Hz, $^3J_{(C,P1\ \mathrm{and}\ P5)}$ = 4.54 Hz; *ipso*-**C**)

δ = 130.62 (d, $^3J_{(C,P3)}$ = 11.34 Hz; *meta*-**C**)

δ = 133.38 ppm (d, $^2J_{(C,P3)}$ = 10.10 Hz; *ortho*-**C)**

δ = 136.31 ppm (d, $^4J_{(C,P3)}$ = 3.09 Hz; *para*-**C)**

Table 6.9. Molecular Mass and Characteristic Fragments from the Mass Spectrum of ($C_{22}H_{28}P_3Br$) (70 eV, Sample Temperature 500 K, Source Temperature 440 K)

Signal (m/z)	Rel. Int. (%)	Classification	Signal (m/z)	Rel. Int. (%)	Classification
467	0.3	$\{M\}^+(^{13}C)$	177	10.9	$\{(C_6H_5PCC(CH_3)_3\}^+$
465	0.4	$\{M\}^+(^{13}C)$	169	17.3	$\{P[CC(CH_3)_3]_2\}^+$
466	1.1	$\{M\}^+(^{81}Br)$	131	9.5	$\{(P_2CC(CH_3)_3\}^+$
464	1.1	$\{M\}^+(^{79}Br)$	129	5.8	$\{P_2CC(CH_3)_3 - 2\ H\}^+$
451	0.7	$\{M - CH_3\}^+$	108	11.6	$\{C_6H_5P\}^+$
449	0.6	$\{M - CH_3\}^+$	107	8.7	$\{C_6H_4P\}^+$
385	100.0	$\{M\text{- }Br\}^+$	100	2.9	$\{PCC(CH_3)_3\}^+$
329	4.6	$\{M + H - Br - C(CH_3)_3\}^+$	99	13.7	$\{PCC(CH_3)_3 - H\}^+$
285	5.8	$\{(C_6H_5)_2P_3C_2CH_2\}^+$	85	6.7	$\{PCC(CH_3)_2\}^+$
273	3.5	$\{(C_6H_5)_2P_3CCH_2\}^+$	77	6.0	$\{C_6H_5\}^+$

247	7.0	$\{(C_6H_5P[CC(CH_3)_3]_2 + H\}^+$	69	8.1	$\{CC(CH_3)_3\}^+$
207	3.4	$\{C_6H_5P_3C_2CH\}^+$	57	11.3	$\{C(CH_3)_3\}^+$
185	59.7	$\{(C_6H_5)_2P\}^+$	55	3.6	$\{C(CH_3)_3 - 2H\}^+$
183	43.3	$\{(C_6H_4)_2P\}^+$	41	17.6	$\{C(CH_3)_2 - H\}^+$

IR (Nujol mull between CsBr disks; $\tilde{\nu}$ *[cm^{-1}])*: 996(sh), 994(m), 942(w,b), 891(vw), 858(s,b), 814(m(w)), 726(w,b), 698(mw), 629(ms), 615(w), 587(s), 569(m), 569(m), 527(w), 512(m), 505(mw), 406(mb).

Raman (crystalline solid in glass capillary; $\tilde{\nu}$ *[cm^{-1}])*: 999(ms), 993(m), 935(w), 858(w), 815(w), 631(w,b), 614(mw), 587(vvs), 587(vvs), 529(mw), 513(ms), 506(vs), 480(ms), 408(mw), 406(sh).

X-ray structure analysis: Chapter 3 (pages 83).

6.11.6. *2,4-Di-*tert*-butyl-3,3-diisopropyl-1λ^3,5λ^3-diphospha-3-phosphonia-tricyclo[2.1.0.0^{2,5}]pentane chloride* **(2e)**

A similar procedure to that described for 6.12.1 was used here, except that chlorodiisopropylphosphine (0.381 g, 2.5 mmol, δ ^{31}P{H} = + 134.5 ppm in C_6D_6) was employed instead of chlorodimethylphosphine and refrigeratoion at different temperatures did not crystallize the oily crude product even after a long period.

Characterization

NMR (solution in $CDCl_3$)

^{31}P{^{1}H} (101.256 MHz):

$\delta = -285.81$ ppm (d, $^{2}J_{(P1/P5,P3)} = 1.3$ Hz; **P1/P5**)

$\delta = 130.45$ ppm (t, $^{2}J_{(P3/P1,P5)} = 1.3$ Hz; **P3**)

^{1}H (250.133 MHz):

$\delta = 0.69$ ppm (s; **H**$_3$C–C–C–P3/P1,P5; 18H)

$\delta = 1.40$ ppm (dd, $^{3}J_{(H,H)} = 7.07$ Hz, $^{3}J_{(H,P3)} = 16.3$ Hz; **H**$_3$C–CH–P3; 12H)

$\delta = 2.9$–3.2 ppm (m; H$_3$C–C**H**–P3; 2H)

^{13}C{^{1}H} (50.323 MHz):

$\delta = 17.60$ ppm (dt, $^{2}J_{(C,\ P3)} = 5.2$ Hz, $^{4}J_{(C,\ P1\ \mathrm{and}\ P5)} = 2.48$ Hz; H$_3$**C**–CH–P3//P1 and P5)

$\delta = 29.97$ ppm (pseudo-quintet–equal to dt, $^{3}J_{(C,P3)} = 4.55$ Hz, $^{3}J_{(C,P1\ \mathrm{and}\ P5)} = 3.10$ Hz; H$_3$**C**–C–C–P3//P1 and P5)

$\delta = 30.36$ ppm (t, $^{2}J_{(C,P1\ \mathrm{and}\ P5)} = 5.36$ Hz, H$_3$C–**C**–C–P1 and P5)

$\delta = 31.65$ ppm (dt, $^{1}J_{(C,P3)} = 20.21$ Hz, $^{3}J_{(C,P1\ \mathrm{and}\ P5)} = 3.71$ Hz; H$_3$C–**C**H–P3//P1 and P5)

$\delta = 37.99$ ppm (dt, $^{1}J_{(C,P3)} = 45.78$ Hz, $^{1}J_{(C,P1\ \mathrm{and}\ P5)} = 41.45$ Hz; H$_3$C–C–**C**–P3//P1 and P5)

IR (Nujol mull between CsBr disks; $\tilde{\nu}$ [cm^{-1}]): 885(m), 871(s), 815(mw), 715(mw), 710(w), 635(s), 633(mw), 576(m), 535(w), 460(w), 412(mw).

6.11.7. *Reaction with Chloro-di-*tert-*butylphosphine*

A mixture of chloro-di-t-butylphosphine (0.452 g, 2.5 mmol, δ $^{31}P\{H\}$ = + 145.8 ppm in C_6D_6) and 2-*tert*-butyl-1λ^3-phosphaalkyne (0.51 g, 5 mmol) did not react in different solvents at different temperatures.

6.12. General procedure for the preparation of mixed dialkylamino chloro arsine compounds

The $(R^{`}R^{``}N)_nAsCl_{3-n}$ compounds (*n* = 1, 2) were prepared by treating $AsCl_3$ in *n*-pentane solution with an appropriate amount of $R^{`}R^{``}NH$ according to the literature procedure for mixed dimethylamino- and diethylamino-chloroarsine derivatives [383] with some modifications.

$$2\,n\,R`R``NH + AsCl_3 \xrightarrow{n\text{-pentane}} R`R``NAsCl_{3-n} + n\,[R`R``NH_2]Cl_{(s)}$$

6.12.1. Dimethylaminodichloroarsine

A solution of 100 mL (200 mmol) of 2 M $(CH_3)_2NH$ in THF was added to a stirred solution of 8.4 mL (18.06 g, 100 mmol) arsenic(III) chloride in *n*-pentane (250 mL) over a period of 2 hours at –78 °C. The reaction mixture was allowed to warm to room temperature and stirring was continued for 24 hours at this temperature. After filtration of the precipitate and distillation of the solvents under reduced pressure at room temperature, the remaining residue was purified by vacuum distillation to give a viscous oil.

Yield 74% (14.0 g, 73.74 mmol); 74%; bp. 48–52 °C/ 13 mbar.

Characterization

Elemental analysis: $C_2H_6AsCl_2N$ calc.: C 12.65%; H 3.18%; N 7.38%
found: C 12.75%; H 3.12%; N 7.11%

NMR (solution in C_6D_6)
^1H (250.133 MHz):
δ = 2.45 ppm (s, C**H**$_3$)
$^{13}C\{^1H\}$ (62.896 MHz):

δ = 38.49 ppm (s, **C**H_3)

6.12.2. Bis(dimethylamino)chloroarsine

A solution of 300 mL (600 mmol) of 2 M $(CH_3)_2NH$ in THF was added to a stirred solution of 12.6 mL (27.2 g, 150 mol) arsenic(III) chloride in *n*-pentane (250 mL) over a period of 2 hours at –78 °C and then continued in a similar manner to that described for **6.12.1.** to give a viscous oil.

Yield 77% (23.0 g, 115.85 mmol); bp. 68–70 °C/ 20 mbar.

Characterization

Elemental analysis: $C_4H_{12}AsClN_2$ calc.: C 24.20%; H 6.09%; N 14.11%
found: C 24.10%; H 6.21%; N 13.67%

NMR (solution in C_6D_6)

^{1}H (250.133 MHz):

δ = 2.50 ppm (s; C**H**$_3$)

$^{13}C\{^{1}H\}$ (62.896 MHz):

δ = 39.68 ppm (s; **C**H_3)

6.12.3. Diethylaminodichloroarsine

Diethyamine (31 mL, 21.92 g, 300 mmol) in *n*-pentane (250 mL) was added to a stirred solution of 12.6 mL (27.1 g, 150 mmol) of arsenic(III) chloride in *n*-pentane (250 mL) over a period of 2 h at –30 °C and then continued in a similar manner to that described for **6.12.1.** to give a viscous oil.

Yield 55% (17.88 g, 82 mmol); bp.35–37 °C / 10^{-2} mbar

Characterization

Elemental analysis: $C_4H_{10}AsCl_2N$ calc.: C 22.04%; H 4.62%; N 6.43%
found: C 21.92%; H 4.60%; N 6.40%

NMR (solution in C_6D_6):

^{1}H (250.133 MHz):

δ = 0.89 ppm (t, $^{3}J_{(H,H)}$ = 7.10 Hz; 6H)

δ = 3.02 ppm (q, $^{3}J_{(H,H)}$ = 7.10 Hz; 4H)

$^{13}C\{^{1}H\}$ (62.896 MHz):

δ = 15.00 ppm (s; **C**H_3)

δ = 42.60 ppm (s; **C**H_2)

6.12.4. Bis(diethylamino)chloroarsine

Diethyamine (62 mL, 43.83 g, 600 mmol) in *n*-pentane (250 mL) was added to a stirred solution of 12.6 ml (27.1 g, 150 mmol) of arsenic (III) chloride in *n*-pentane (250 mL) over a period of 2 h at –30 °C and then continued in a similar manner to that described for **6.12.1.** to give a viscous oil.

Yield 61% (18.34 g, 72 mmol); bp. 35–37 °C / 10^{-2} mbar

Characterization

Elemental analysis: $C_8H_{20}AsClN_2$ calc.: C 37.74%; H 7.92%; N 11.00%

found: C 37.71%; H 7.74%; N 10.99%

NMR (solution in C_6D_6):

^1H (250.133 MHz):

$\delta = 0.810$ ppm (t, $^3J_{(H,H)} = 7.20$ Hz; 12H)

$\delta = 3.11$ ppm (q, $^3J_{(H,H)} = 7.20$ Hz; 8H)

$^{13}C\{^1H\}$ (62.896 MHz):

$\delta = 15.60$ ppm (s; $\mathbf{C}H_3$)

$\delta = 43.20$ ppm (s; $\mathbf{C}H_2$)

6.12.5. *N*-Ethylmethylaminodichloroarsine

N-Ethylmethylamine (20.4 mL, 14.04 g, 240 mmol) in *n*-pentane (250 mL) was added to a stirred solution of 10.0 ml (21.5 g, 120 mmol) of arsenic(III) chloride *n*-pentane (250 mL) over a period of 2 h at –78 °C and then continued in a similar manner to that described for **6.12.1.** to give a viscous oil.

Yield 74% (18.0 g, 88.27 mmol); bp. 36–37 °C / 10^{-2} mbar

Characterization

Elemental analysis: $C_3H_8AsCl_2N$ calc.: C 17.67%; H 3.95%; N 6.87%

found: C 18.00%; H 4.14%; N 6.83%

NMR (solution in C_6D_6)

^1H (250.133 MHz):

$\delta = 0.88$ ppm (t, $^3J_{(H,H)} = 7.10$ Hz; $C\mathbf{H}_3$–CH_2–N; 3H)

$\delta = 2.58$ ppm (s, $C\mathbf{H}_3$–N; 3H)

$\delta = 2.86$ ppm (q, $^3J_{(H,H)} = 7.10$ Hz; CH_3–$C\mathbf{H}_2$–N; 2H)

$^{13}C\{^1H\}$ (62.896 MHz):

δ = 14.40 ppm (s; **C**H_3–CH_2–N)

δ = 34.75 pmm (s; **C**H_3–N)

δ = 46.63 ppm (s; CH_3–**C**H_2–N)

6.12.6. Bis(*N*-ethylmethylamino)chloroarsine

N-Ethylmethylamine (15.1 mL, 10.39 g, 175.8 mmol) in *n*-pentane (250 mL) was added to a stirred solution of 3.7 ml (7.96 g, 43.9 mmol) of arsenic(III) chloride in *n*-pentane (250 ml) over a period of 2 h at –78 °C and then continued in a similar manner to that described for **6.12.1.** to give a viscous oil.

Yield 80% (8.0 g, 35.31 mmol); bp. 45–46 °C / 10^{-2} mbar

Characterization

Elemental analysis: $C_6H_{16}AsClN_2$ calc.: C 31.81%; H 7.12%; N 12.36%
found: C 31.81%; H 7.40%; N 12.30%

NMR (solution in C_6D_6)

^1H (250.133 MHz):

δ = 0.95 ppm (t, $^3J_{(H,H)}$ = 7.10 Hz; C**H**$_3$–CH_2–N; 6H)

δ = 2.55 ppm (s, C**H**$_3$–N; 6H)

δ = 2.87 ppm (q, $^3J_{(H,H)}$ = 7.10 Hz; CH_3–C**H**$_2$–N; 4H)

$^{13}C\{^1H\}$ (62.896 MHz):

δ = 14.44 ppm (s; **C**H_3–CH_2–N)

δ = 35.75 ppm (s; **C**H_3–N)

δ = 46.90 ppm (s; CH_3–**C**H_2–N)

6.12.7. *N*-Methylisopropylaminodichloroarsine

N-Methylisopropylamine (25.2 mL, 17.69 g, 242 mmol) in *n*-pentane (250 mL) was added to a stirred solution of 10.0 ml (21.5 g, 120 mmol) of arsenic(III) chloride in *n*-pentane (250 mL) over a period of 2 h at –78 °C and then continued in a similar manner to that described for **6.12.1.** to give a viscous oil.

Yield 73% (19.0 g, 87.2 mmol); bp. 36–37 °C / 10 mbar

Characterization

Elemental analysis: $C_4H_{10}AsCl_2N$ calc.: C 22.04%; H 4.62%; N 6.43%
found: C 22.11%; H 4.83%; N 6.25%

NMR (solution in C_6D_6)

^1H (250.133 MHz):

δ = 0.91 ppm (d, $^3J_{(H,H)}$ = 6.70 Hz; C**H**$_3$–CH–N; 6H)

δ = 2.58 ppm (s, C**H**$_3$–N; 3H)

δ = 3.41 ppm (sept; $^3J_{(H,H)}$ = 6.70 Hz; CH$_3$–C**H**–N;1H)

$^{13}C\{^1H\}$ (62.896 MHz):

δ = 21.61 pmm (s; **C**H$_3$–CH–N)

δ = 29.55 ppm (s; **C**H$_3$–N)

δ = 52.17 ppm (s; CH$_3$–**C**H–N)

6.12.8. Bis(*N*-methylisopropylamino)chloroarsine

N-Methylisopropylamine (14.0 mL, 9.83 g, 134.4 mmol) in *n*-pentane (250 ml) was added to a stirred solution of 2.80 ml (6.02 g, 33.21 mmol) of arsenic(III) chloride in *n*-pentane (250 mL) over a period of 2 h at –78 °C and then continued in a similar manner to that described for **6.12.1.** to give a viscous oil.

Yield 77% (6.5 g, 25.53 mmol); bp. 48–50 °C / 10 mbar

Characterization

Elemental analysis: $C_8H_{20}AsClN_2$ calc.: C 37.74%; H 7.92%; N 11.00%

found: C 37.50%; H 8.06%; N 10.69%

NMR (solution in C_6D_6)

^1H (250.133 MHz):

δ = 1.00 ppm (d, $^3J_{(H,H)}$ = 6.70 Hz; C**H**$_3$–CH–N; 12H)

δ = 2.54 ppm (s, C**H**$_3$–N; 6H)

δ = 3.41 ppm (sept, $^3J_{(H,H)}$ = 6.70 Hz; CH$_3$–C**H**–N; 2H)

$^{13}C\{^1H\}$ (62.896 MHz):

δ = 21.42 pmm (s; **C**H$_3$–CH–N)

δ = 30.23 ppm (s; **C**H$_3$–N)

δ = 51.19 ppm (s; CH$_3$–**C**H–N)

6.13. Procedures for the preparation of 2,4,6-Tri-*tert*-butyl-3-chloro-1-dialkylamino-1$\lambda^5\sigma^4$,3$\lambda^3\sigma^3$,5$\lambda^3\sigma^2$-triphosphabicyclo[2.2.0]hexa-1,5-dienes

6.13.1. *2,4,6-Tri-*tert*-butyl-3-chloro-1-dimethylamino-1$\lambda^5\sigma^4$,3$\lambda^3\sigma^3$,5$\lambda^3\sigma^2$-triphosphabicyclo[2.2.0]hexa-1,5-diene*

To a stirred solution of 2-*tert*-butyl-1λ^3-phosphaalkyne (1.50 g, 15 mmol) in cyclopentane (10 mL) at –78 °C was added dropwise a solution of dimethylaminodichloroarsine (0.993 g, 5 mmol) in cyclopentane (10 mL). After the mixtures had been allowed to warm up slowly to room temperature, the reactions took about five days to reach completion. Thereafter, insoluble products were filtered off to leave a red filtrate from which the solvent was removed under reduced pressure at room temperature to leave a viscous red oil, which crystallized without solvent after two months at –13 °C to furnish 7.13.1 as red crystals in 63% yield (1.2 g, 3.159 mmol).

Characterization

Boiling point: 133.0 °C (dec.).

Elemental analysis: $C_{17}H_{33}ClNP_3$ calc.: C 53.76%; H 8.76%; N 3.69%.
found: C 53.74%; H 8.84%; N 3.54%.

Molar mass (Cryoscopic in benzene [380]): 372.0 g mol^{-1} (calc. 379.83 g mol^{-1})

NMR (solution in C_6D_6)

$^{31}P\{H\}$ (101.256 MHz):

$\delta = 51.10$ ppm (t, $^2J_{(P,P)} = 11.40$ Hz; **P1**)

$\delta = 278.90$ ppm (d, $^2J_{(P,P)} = 11.40$ Hz; **P3/P5**).

^1H (250.133 MHz):

$\delta = 1.06$ ppm (s, C**H**$_3$–C–C–P1; 9H)

$\delta = 1.37$ ppm (s, C**H**$_3$–C–C–P3/P5; 18H)

$\delta = 2.35$ ppm (d, $^3J_{(P,H)} = 9.40$ Hz; C**H**$_3$–N; 6H)

$^{13}C\{H\}$ (100.614 MHz):

$\delta = 29.50$ ppm (dt, $^2J_{(C,P)} = 9.70$ Hz, $^2J_{(C,P)} = 5.40$ Hz; CH$_3$–**C**–C4)

$\delta = 32.80$ ppm (dd, $^2J_{(C,P)} = 11.10$ Hz, $^2J_{(C,P)} = 6.30$ Hz; CH$_3$–**C**–C2/C6)

$\delta = 33.20$ ppm (dt, $^3J_{(C,P)} = 7.80$ Hz, $^3J_{(C,P)} = 4.75$ Hz; **C**H$_3$–C–C4)

$\delta = 35.80$ ppm (dd, $^3J_{(C,P)} = 5.50$ Hz, $^3J_{(C,P)} = 2.70$ Hz; **C**H$_3$–C–C2/C6)

$\delta = 39.20$ ppm (d, $^2J_{(C,P)} = 3.20$ Hz; **C**H$_3$–N)

$\delta = 64.30$ ppm (dt, $^1J_{(C,P)} = 57.90$ Hz, $^1J_{(C,P)} = 32.60$ Hz; **C4**)
$\delta = 139.10$ ppm (m; $^1J_{(C2/C4,P1)} = 32.1$; **C2/C6**)
$^{15}N\{^1H\}$ (40.561 MHz): $\delta = -257.5$ ppm (singlet).

Table 6.10. Molecular Mass and Characteristic Fragments from the Mass Spectrum of ($C_{17}H_{33}ClNP_3$) (70 eV, Sample Temperature 370 K, Source Temperature 410 K)

Signal (m/z)	Rel. Int. (%)	Classification	Signal (m/z)	Rel. Int. (%)	Classification
485	0.5	$\{(C_4H_9\text{-}C{\equiv}P)_5 - CH_3\}^+$	264	23.7	$\{M - PCC(CH_3)_3 - CH_3\}^+$
442	0.4	$\{(C_4H_9\text{-}C{\equiv}P)_5 - C_4H_9\}^+$	169	68.8	$\{P[CC(CH_3)_3]_2\}^+$
382	4.8	$\{M\}^+(^{13}C)$	110	100.0	$\{(CH_3)_2NP + Cl\}^+$
381	17.6	$\{M\}^+(^{37}Cl)$	112	29.7	$\{(CH_3)_2NP + Cl\}^+$
380	9.1	$\{M\}^+(^{13}C)$	101	7.9	$\{PCC(CH_3)_3 + H\}^+$
379	45.5	$\{M\}^+(^{35}Cl)$	100	8.0	$\{PCC(CH_3)_3\}^+$
366	20.0	$\{M - CH_3\}^+$	99	25.5	$\{PCC(CH_3)_3 - H\}^+$
364	59.1	$\{M - CH_3\}^+$	85	27.3	$\{PCC(CH_3)_2\}^+$
344	30.2	$\{M- Cl\}^+$	75	35.9	$\{C_2H_6NP\}^+$
337	2.9	$\{M - N(CH_3)_2\}^+$	69	33.2	$\{CC(CH_3)_3\}^+$

335	8.6	$\{M - N(CH_3)_2\}^+$	57	47.5	$\{C(CH_3)_3\}^+$
300	6.8	$\{M - N(CH_3)_2 - Cl\}^+$	55	21.6	$\{C(CH_3)_3 - 2H\}^+$
281	7.1	$\{M - PCC(CH_3)_3\}^+$	44	95.7	$\{N(CH_3)_2\}^+$
279	18.0	$\{M - PCC(CH_3)_3\}^+$	41	71.5	$\{C(CH_3)_2 - H\}^+$
266	9.0	$\{M - PCC(CH_3)_3 - CH_3\}^+$			

IR (Nujol mull between CsBr disks; $\tilde{\nu}$ *[cm^{-1}])*: 1392(w), 1365(vs), 1295(s), 1228(s), 1215(s), 1171(m), 1116(w), 1036(w), 979(vs), 918(m), 816(m), 788(w), 769(w), 756(w), 723(s), 702(w), 626(m), 563(m), 533(m), 461(w), 328(w), 325(w).

X-ray structure analysis: Chapter 4 (page 126).

6.13.2. *2,4,6-Tri-*tert*-butyl-3-chloro-1-diethylamino-1$\lambda^5\sigma^4$,3$\lambda^3\sigma^3$,5$\lambda^3\sigma^2$-triphosphabicyclo[2.2.0]hexa-1,5-diene*

To a stirred solution of 2-*tert*-butyl-1λ^3-phosphaalkyne (1.0 g, 10 mmol) in cyclopentane (10 mL) at –78 °C was added dropwise a solution of diethylaminodichloroarsine (0.719 g, 3.3 mmol) in *n*-pentane (5 mL) and then continued in a similar manner to that described for 7.13.1 to leave a viscous red oil, which crystallized without solvent after three months at –13°C to furnish **6.13.2** as red crystals in 44% yield (0.62 g, 1.5 mmol).

Characterization

Boiling point: 143.7°C (dec.).

Elemental analysis: $C_{19}H_{37}ClNP_3$ calc.: C 55.95%; H 9.14%; N 3.43%

found: C 55.68%; H 9.04%; N 3.33%

Molar mass (Cryoscopic in benzene [380]): 400.0 g mol^{-1} (calc. 407.88 g mol^{-1})

NMR (solution in C_6D_6)

$^{31}P\{H\}$ (161.977 MHz):

δ = 52.00 ppm (t, $^2J_{(P,P)}$ = 12.7 Hz; **P1**)

δ = 280.90 ppm (d, $^2J_{(P,P)}$ = 12.7 Hz; **P3**/**P5**).

^1H (400.134 MHz):

δ = 0.73 ppm (t, $^3J_{(H,H)}$ = 7.20 Hz; C**H**$_3$–CH$_2$–N; 6H)

δ = 1.08 ppm (s, C**H**$_3$–C–C4; 9H)

δ = 1.37 ppm (s, C**H**$_3$–C–C2/C6; 18H)

δ = 2.96 ppm (m, br, CH$_3$–C**H**$_2$–N; 4H)

$^{13}C\{H\}$ (50.323 MHz):

δ = 13.10 ppm (d, $^3J_{(C,P)}$ = 3.1 Hz; **C**H$_3$–CH$_2$–N)

δ = 29.40 ppm (dt, $^2J_{(C,P)}$ = 9.70 Hz, $^2J_{(C,P)}$ = 5.70 Hz; CH$_3$–**C**–C4)

δ = 33.10 ppm (dd, $^2J_{(C,P)}$ = 11.20 Hz, $^2J_{(C,P)}$ = 6.30 Hz; CH$_3$–**C**–C2/C6)

δ = 33.40 ppm (dt, $^3J_{(C,P)}$ = 7.70 Hz, $^3J_{(C,P)}$ = 4.90 Hz; **C**H$_3$–C–C4)

δ = 36.00 ppm (dd, $^3J_{(C,P)}$ = 5.70 Hz, $^3J_{(C,P)}$ = 2.60 Hz; **C**H_3–C–C2/C6)

δ = 40.60 ppm (d, $^2J_{(C,P)}$ = 3.40 Hz; CH_3–**C**H_2–N)

δ = 64.50 ppm (dt, $^1J_{(C,P)}$ = 57.20 Hz, $^1J_{(C,P)}$ = 32.00 Hz; **C4**)

δ = 138.50 ppm (m, $^1J_{(C2/C4,P1)}$ = 30.9 Hz; **C2**/**C6**)

$^{15}N\{^1H\}$ (40.561 MHz): δ = – 264.5 ppm (singlet).

Table 6.11. Characteristic Masses ($C_{19}H_{37}ClNP_3$) from the Mass Spectrum (70 eV, Sample Temperature 470 K, Source Temperature 460 K)

Signal (m/z)	Rel. Int. (%)	Classification	Signal (m/z)	Rel. Int. (%)	Classification
500	0.4	$\{(^t\mathrm{BuC{\equiv}P})_5\}^+$	169	45.15	$\{P[CC(CH_3)_3]_2\}^+$
485	0.3	$\{(^t\mathrm{BuC{\equiv}P})_5\text{–}\mathrm{Me}\}^+$	140	30.35	$\{C_4H_{10}NP + Cl\}^+$
442	1.1	$\{(^t\mathrm{BuC{\equiv}P})_5\text{–}{}^t\mathrm{Bu}\}^+$	138	100.0	$\{C_4H_{10}NP + Cl\}^+$
410	6.18	$\{M\}^+(^{13}C)$	103	10.30	$\{C_4H_{10}NP\}^+$
409	13.33	$\{M\}^+(^{37}Cl)$	101	6.80	$\{PCC(CH_3)_3 + H\}^+$
408	10.70	$\{M\}^+(^{13}C)$	100	4.92	$\{PCC(CH_3)_3\}^+$
407	43.5	$\{M\}^+(^{35}Cl)$	99	13.55	$\{PCC(CH_3)_3 - H\}^+$
394	11.69	$\{M - CH_3\}^+$	85	15.11	$\{PCC(CH_3)_2\}^+$
392	34.08	$\{M - CH_3\}^+$	72	40.55	$\{NC_4H_{10}\}^+$
372	18.60	$\{M - Cl\}^+$	69	23.78	$\{CC(CH_3)_3\}^+$
337	6.08	$\{M - N(C_4H_{10}\}^+$	57	38.77	$\{C(CH_3)_3\}^+$
335	16.40	$\{M - N(C_4H_{10}\}^+$	55	17.62	$\{C(CH_3)_3 - 2H\}^+$
294	4.13	$\{M - PCC(CH_3)_3 - CH_3\}^+$	41	32.39	$\{C(CH_3)_2 - H\}^+$
292	11.10	$\{M - PCC(CH_3)_3 - CH_3\}^+$	29	9.67	$\{(C_2H_5)\}^+$

IR (Nujol mull between CsBr disks; $\tilde{\nu}$ [cm^{-1}]): 2482(s), 2389(m), 1343(s), 1288(s), 1189(vs), 1166(vs), 1099(s), 1074(m), 1058(s), 1008(vs), 956(m), 920(s), 897(vs), 629(sh), 608(s), 567(w), 460(m), 429(m), 382(vs), 326(br,s).

X-ray structure analysis: Chapter 4 (page 126).

6.13.3. *2,4,6-Tri-*tert*-butyl-3-chloro-1-N-methylisopropylamino-$1\lambda^5\sigma^4,3\lambda^3\sigma^3,5\lambda^3\sigma^2$-triphosphabicyclo-[2.2.0]hexa-1,5-diene*

To a stirred solution of 2-*tert*-butyl-1λ^3-phosphaalkyne (0.75 g, 7.5 mmol) in cyclopentane (10 mL) at –78 °C was added dropwise a solution of N-methylisopropylaminodichloroarsine (0.545 g, 2.5 mmol) in cyclopentane (10 mL) and then continued in a similar manner to that described for 7.13.1 to leave a viscous red oil. The residue was taken up in a small amount of benzene, and cooled to 8°C to furnish **6.13.4** as red crystals after four weeks in 67% yield (0.68 g, 1.67 mmol).

Characterization

Boiling point: 151.5 °C (dec.).

Elemental analysis: $C_{19}H_{37}ClNP_3$ calc.: C 55.95%; H 9.18%; N 3.43%
found: C 55.70%; H 8.97%; N 3.47%

Molar mass (Cryoscopically in benzene [380]): 401.0 g mol^{-1} (calc. 407.89 g mol^{-1})

NMR (solution in C_6D_6):

$^{31}P\{H\}$ (101.256 MHz):

$\delta = 50.94$ ppm (t, $^2J_{(P,P)} = 13.36$ Hz; **P1**)

$\delta = 281.80$ ppm (br; **P3/P5**)

^1H (250.133 MHz):

$\delta = 0.81$ ppm (d, $^3J_{(H,H)} = 6.66$Hz; $C\mathbf{H}_3$–CH–N; 6H)

$\delta = 1.10$ ppm (s, $C\mathbf{H}_3$–C–C4; 9H)

$\delta = 1.37$ ppm (s, $C\mathbf{H}_3$–C–C2/C6; 18H)

$\delta = 2.28$ ppm (d, $^3J_{(P,H)} = 9.86$ Hz; $C\mathbf{H}_3$–N; 3H)

$\delta = 3.85 - 4.0$ ppm (m; 1H)

$^{13}C\{^1H\}$ (62.896 MHz):

$\delta = 20.00$ ppm (d, $^3J_{(C,P)} = 2.00$ Hz; $\mathbf{C}H_3$–CH–N)

$\delta = 28.80$ ppm (d, $^2J_{(C,P)} = 4.60$ Hz; $\mathbf{C}H_3$–N)

$\delta = 29.60$ ppm (dt, $^2J_{(C,P)} = 9.70$ Hz, $^2J_{(C,P)} = 6.10$ Hz; CH_3–**C**–C4)

$\delta = 32.40$ ppm (dd, $^2J_{(C,P)} = 11.10$ Hz, $^2J_{(C,P)} = 6.20$ Hz; CH_3–**C**–C2/C6)

$\delta = 33.40$ ppm (dt, $^3J_{(C,P)} = 9.20$ Hz, $^3J_{(C,P)} = 7.60$ Hz; $\mathbf{C}H_3$–C–C4)

$\delta = 36.10$ ppm (dd, $^3J_{(C,P)} = 6.90$ Hz, $^3J_{(C,P)} = 2.80$ Hz; $\mathbf{C}H_3$–C–C2/C6)

$\delta = 48.70$ ppm (d, $^2J_{(C,P)} = 2.00$ Hz; CH_3–**C**H–N)

$\delta = 64.90$ ppm (dt, $^1J_{(C,P)} = 57.90$ Hz, $^1J_{(C,P)} = 32.10$ Hz; **C4**)

$\delta = 138.80$ ppm (m; $^1J_{(C2/C4,P1)} = 31.6$ Hz; **C2**/**C6**)

$^{15}N\{^1H\}$ (40.561 MHz): $\delta = -260.0$ ppm (singlet).

Table 6.12. Characteristic Masses ($C_{19}H_{37}ClNP_3$) from the Mass Spectrum (70 eV, Sample Temperature 400 K, Source Temperature 410 K)

Signal (m/z)	Rel. Int. (%)	Classification	Signal (m/z)	Rel. Int. (%)	Classification
410	3.98	$\{M\}^+(^{13}C)$	140	30.66	$\{(CH_3)(C_3H_7)NP + Cl\}^+$
409	8.58	$\{M\}^+(^{37}Cl)$	138	100.0	$\{(CH_3)(C_3H_7)NP + Cl\}^+$
408	6.89	$\{M\}^+(^{13}C)$	103	14.23	$\{(C_3H_7)(CH_3)NP\}^+$
407	28.01	$\{M\}^+(^{35}Cl)$	101	7.09	$\{PCC(CH_3)_3 + H\}^+$
394	7.90	$\{M - CH_3\}^+$	100	5.49	$\{PCC(CH_3)_3\}^+$
392	22.98	$\{M - CH_3\}^+$	99	14.37	$\{PCC(CH_3)_3 - H\}^+$
372	18.72	$\{M - Cl\}^+$	85	15.51	$\{PCC(CH_3)_2\}^+$
366	2.76	$\{M - (C_3H_7)\}^+$	72	42.83	$\{N(CH_3)(C_3H_7)\}^+$
364	7.48	$\{M - (C_3H_7)\}^+$	69	18.89	$\{CC(CH_3)_3\}^+$
337	5.21	$\{M - N(CH_3)(C_3H_7)\}^+$	57	38.24	$\{C(CH_3)_3\}^+$
335	14.05	$\{M - N(CH_3)(C_3H_7)\}^+$	55	13.34	$\{C(CH_3)_3 - 2H\}^+$
294	2.20	$\{M - PCC(CH_3)_3 - CH_3\}^+$	43	22.80	$\{(C_3H_7)\}^+$
292	5.92	$\{M - PCC(CH_3)_3 - CH_3\}^+$	42	14.56	$\{(C_3H_6)\}^+$
169	42.15	$\{P[CC(CH_3)_3]_2\}^+$	41	34.39	$\{C(CH_3)_2 - H\}^+$

IR (Nujol mull between CsBr disks; $\tilde{\nu}$ [cm^{-1}]): 2726(m), 1412(w), 1366(vs), 1307(w), 1272(w), 1228(s), 1171(m), 1119(w), 1272(w), 1228(s), 1171(m), 1119(w), 1038(s), 962(s), 922(m), 856(w), 813(w), 781(w), 722(s), 668(w), 619(m), 564(m), 529(w), 461(m), 458(m), 440(m), 431(w), 426(w), 420(w), 413(w), 409(w), 406(w), 404(w), 402(w).

X-ray structure analysis: Chapter 4 (page 126)

6.12.4. *2,4,6-Tri*-tert-*butyl-3-chloro-1-N-ethylmethylamino-1*$\lambda^5\sigma^4$*,3*$\lambda^3\sigma^3$*,5*$\lambda^3\sigma^2$*-triphosphabicyclo-[2.2.0]hexa-1,5-diene*

To a stirred solution of 2-*tert*-butyl-1λ^3-phosphaalkyne (0.75 g, 7.5 mmol) in cyclopentane (10 mL) at –78 °C was added dropwise a solution of *N*-methylethylaminodichloroarsine (0.51 g, 2.5 mmol) in cyclopentane (10 mL) and then continued in a similar manner to that described for 7.13.1 to leave a viscous red oil. The residue was taken up in a small amount of toluene, and cooled to – 60 °C to furnish **6.12.4** as red crystals after five weeks in 65% yield (0.64 g, 1.625 mmol).

Characterization

Boiling point: 137.8 °C (dec.).

Elemental analysis: $C_{18}H_{35}ClNP_3$ calc.: C 54.89%; H 8.96%; N 3.56%

found: C 54.68%; H 8.97%; N 3.30%

Molar mass (Cryoscopic in benzene [380]): 387.6 g.mol^{-1} (calc. 393.86 g.mol^{-1})

NMR (solution in C_6D_6)

$^{31}P\{H\}$ (101.256 MHz):

δ = 51.95 ppm (t, $^2J_{(P,P)}$ = 13.10 Hz; **P1**)

δ = 279.20 ppm (br; **P3/P5**).

^1H (250.133 MHz):

δ = 0.71 ppm (t, $^3J_{(H,H)}$ = 7.11Hz; C**H**$_3$–CH$_2$–N; 3H)

δ = 1.04 ppm (s, C**H**$_3$–C–C–P1; 9H)

δ = 1.35 ppm (s, C**H**$_3$–C–C–P3/P5; 18H)

δ = 2.27 ppm (d, $^3J_{(P,H)}$ = 10.32 Hz; C**H**$_3$–N; 3H)

δ = 3.22 ppm (m, br, CH$_3$–C**H**$_2$–N; 2H)

$^{13}C\{H\}$ (50.323 MHz):

δ = 13.10 ppm (d, $^3J_{(C,P)}$ = 5.2 Hz; **C**H$_3$–CH$_2$–N)

δ = 29.50 ppm (dt, $^2J_{(C,P)}$ = 9.70 Hz, $^2J_{(C,P)}$ = 5.60 Hz; CH$_3$–**C**–C4)

δ = 32.80 ppm (dd, $^2J_{(C,P)}$ = 11.10 Hz, $^2J_{(C,P)}$ = 6.30 Hz; CH$_3$–**C**–C2/C6)

δ = 33.20 ppm (dt, $^3J_{(C,P)}$ = 9.50 Hz, $^3J_{(C,P)}$ = 7.90 Hz; **C**H$_3$–C–C4)

δ = 35.60 ppm (d, $^2J_{(C,P)}$ = 3.10 Hz; **C**H$_3$–N)

δ = 36.00 ppm (dd, $^3J_{(C,P)}$ = 6.20 Hz, $^3J_{(C,P)}$ = 2.50 Hz; **C**H_3–C–C2/C6)

δ = 45.40 ppm (d, $^2J_{(C,P)}$ = 2.50 Hz; CH_3–**C**H_2–N)

δ = 64.10 ppm (dt, $^1J_{(C,P)}$ = 56.70 Hz, $^1J_{(C,P)}$ = 32.30 Hz; **C4**)

δ = 138.50 ppm (m; $^1J_{(C2/C4,P1)}$ = 33.7 Hz; **C2**/**C6**)

$^{15}N\{^1H\}$ (40.561 MHz): δ = – 263.0 ppm (singlet).

Table 6.13. Characteristic Masses ($C_{18}H_{35}ClNP_3$) from the Mass Spectrum (70 eV, Sample Temperature 390 K, Source Temperature 410 K)

Signal (m/z)	Rel. Int. (%)	Classification	Signal (m/z)	Rel. Int. (%)	Classification
442	0.61	$\{(C_4H_9\text{-}C{\equiv}P)_5{-}C_4H_9\}^+$	126	30.67	$\{(CH_3)(C_2H_5)NP + Cl\}^+$
400	0.31	$\{(C_4H_9\text{-}C{\equiv}P)_5{-}C_4H_9\}^+$	124	100.0	$\{(CH_3)(C_2H_5)NP + Cl\}^+$
396	3.94	$\{M\}^+(^{13}C)$	101	4.19	$\{PCC(CH_3)_3 + H\}^+$
395	13.37	$\{M\}^+(^{37}Cl)$	100	5.14	$\{PCC(CH_3)_3\}^+$
394	8.73	$\{M\}^+(^{13}C)$	99	14.33	$\{PCC(CH_3)_3 - H\}^+$
393	39.77	$\{M\}^+(^{35}Cl)$	89	12.17	$\{(C_2H_5)(CH_3)NP\}^+$
380	15.84	$\{M - CH_3\}^+$	85	15.80	$\{PCC(CH_3)_2\}^+$
378	47.15	$\{M - CH_3\}^+$	69	14.43	$\{CC(CH_3)_3\}^+$
358	17.34	$\{M - Cl\}^+$	58	39.26	$\{N(CH_3)(C_2H_5)\}^+$
337	4.70	$\{M - N(CH_3)(C_2H_5)\}^+$	57	22.47	$\{C(CH_3)_3\}^+$
335	10.65	$\{M - N(CH_3)(C_2H_5)\}^+$	55	9.30	$\{C(CH_3)_3 - 2H\}^+$
280	5.45	$\{M - PCC(CH_3)_3 - CH_3\}^+$	41	30.00	$\{C(CH_3)_2 - H\}^+$
278	16.17	$\{M - PCC(CH_3)_3 - CH_3\}^+$	29	8.64	$\{(C_2H_5)\}^+$
169	38.90	$\{P[CC(CH_3)_3]_2\}^+$			

IR (Nujol mull between CsBr disks; $\tilde{\nu}$ [cm^{-1}]): 2435(m), 2410(m), 2259(s), 1334(s), 1394(s), 1377(N), 1365(vs), 1334(w), 1273(w), 1222(vs), 1165(s), 1089(w), 1059(w), 1037(w), 1000(vs), 931(vs), 875(w), 766(m), 723(m), 668(w), 560(m), 460(m), 431(m), 411(w).

X-ray structure analysis: Chapter 4 (page 126).

6.14. Preparation of Dichloro[4-(dimethylamino)phenyl]arsine

It is recommended that the preparation be carried out free of solvent under an atmosphere of argon.

9.5 mL (9.1 g, 75 mmol) of *N*,*N*-dimethylaniline are added dropwise within 20 min with stirring at 0 °C to 6.3 mL (13.6 g, 75 mmol) of arsenic(III) chloride. Gaseous hydrogen chloride is evolved and the solution gradually takes on a yellow colour. While stirring is continued for 50 to 60 min, the mixture is heated in a water bath to complete the reaction. After 4 h cooling to ambient temperature the previously liquid product starts to solidify and becomes a highly viscous yellow wax. It is repeatedly placed under vacuum to remove all volatile materials and finally dissolved in 50 mL of acetonitrile. Storing the solution for several days at –13 °C affords colourless to pale yellow crystals of dichloro[4-(dimethylamino)phenyl]arsine.

Yield 85% (17.0 g, 63.9 mmol); mp. 112 °C

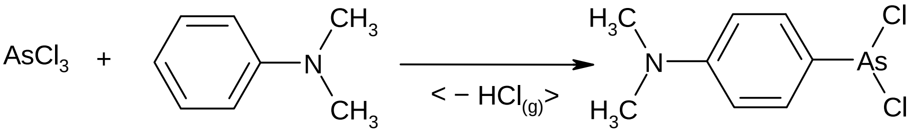

Characterization

Elemental analysis: $C_8H_{10}AsCl_2N$ Calc.: C 36.12%; H 3.79%; N 5.27%; Cl 26.66%.
Found: C 35.82%; H 3.65%; N 5.08%; Cl 26.74%.

NMR (solution in CD_3CN)

^1H (250.134 MHz): δ = 3.02 (s, $C\mathbf{H}_3$–N; 6H); δ = 7.54 (d, $C_6\mathbf{H}_4$; $^3J_{(H,H)}$ = 8.30, 2H); δ = 7.82 ppm (d, $C_6\mathbf{H}_4$; $^3J_{(H,H)}$ =8.30 Hz, 2H)

$^{13}C\{^1H\}$ (62.896 MHz): δ = 46.78 (s, $\mathbf{C}H_3$–N); δ = 122.0 (s, **C**-C-N); δ = 130.88 (s, slightly broadened, *ipso*-**C**-As); δ = 131.22 (s, **C**-C-As); δ = 144.32 ppm (s, *ipso*-**C**-N).

Table 6.14. Molecular Mass and Characteristic Fragments from the Mass Spectrum of $C_8H_{10}AsCl_2N$ (70 eV, Sample Temperature 300 K, Source Temperature 500 K)

Signal (m/z)	Rel. Int. (%)	Classification	Signal (m/z)	Rel. Int. (%)	Classification
269	1.0	$\{M\}^+$	230	16.3	$\{M – Cl\}^+$
268	0.7	$\{M\}^+$	195	1.8	$\{AsC_6H_4N(CH_3)_2\}^+$
267	6.1	$\{M\}^+$	122	6.1	$\{C_6H_5N(CH_3)_2 + H\}^+$
266	1.5	$\{M\}^+$	121	71.4	$\{C_6H_5N(CH_3)_2\}^+$
265	8.7	$\{M\}^+$	120	100	$\{C_6H_4N(CH_3)_2\}^+$
232	5.1	$\{M – Cl\}^+$			

IR (Nujol mull between CsBr disks; $\tilde{\nu}$ [cm^{-1}]): 1591 (vs), 1201 (m), 1082 (vs), 1127 (m), 1065 (m), 1014 (m), 993 (m), 832 (s), 807 (s), 722 (vs), 632 (m), 604 (s), 575 (w), 548 (vs), 514 (s), 502 (w), 381 (s, br), 366 (s, br).

X-ray structure analysis: Chapter 5 (page 177)

6.15. Preparation of Tris[4-(dimethylamino)phenyl]arsine

It is recommended that the preparation be carried out free of solvent under an atmosphere of argon.

9.5 mL (9.1 g, 75 mmol) of *N*,*N*-dimethylaniline are added dropwise within 20 min with stirring at ambient temperature to 6.3 mL (13.6 g, 75 mmol) of arsenic(III) chloride. Gaseous hydrogen chloride is evolved and after 3 h the previously liquid product has become a highly viscous yellow wax. With vigorous stirring it is dissolved in 300 mL of cold distilled water. To the solution, from which insoluble material has been removed by filtration, are slowly added with stirring 85 g (2.13 mol) of anhydrous sodium hydroxide until a solid starts to precipitate. The suspension thus formed is allowed to stand overnight at –13 °C, then the insoluble product is filtered off. After adhering solvent has been removed with repeated evaporation the solid is recrystallized from 15 mL of chloroform. Cooling to –13 °C affords colourless cuboids of tris[4-(dimethylamino)phenyl]arsine.

Yield 46 % (5.0 g, 11.5 mmol); mp. 243 °C

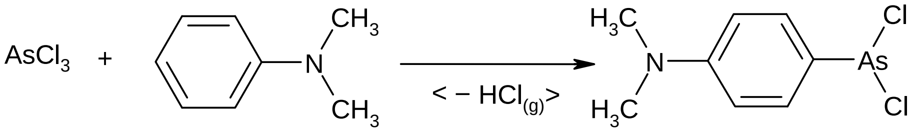

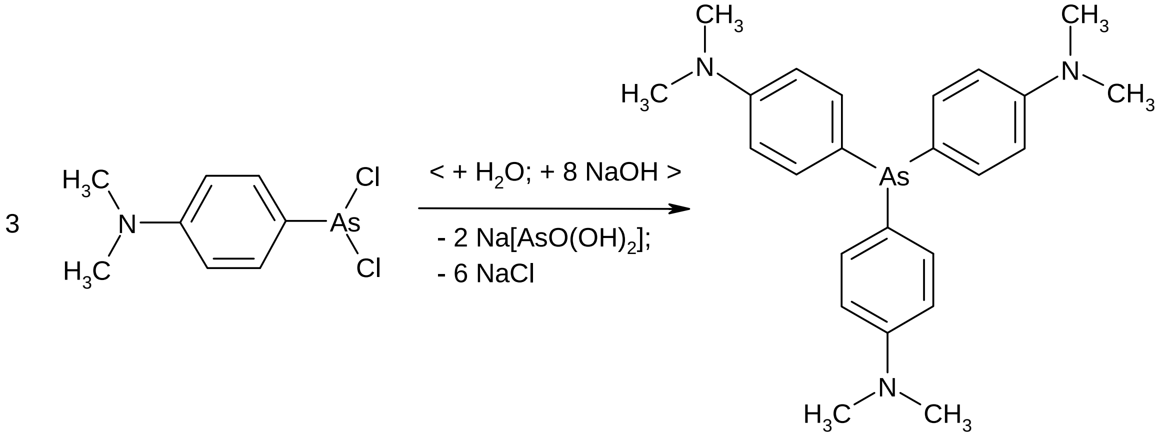

Characterization

Elemental analysis: $C_{24}H_{30}AsN_3$ Calc.: C 66.20%; H 6.94%; N 9.65%

Found: C 65.99%; H 6.85%; N 9.52%

NMR (solution in $CDCl_3$)

^{1}H (250.134 MHz): δ = 2.92 (s, C**H**$_3$–N; 18H); δ = 6.67 (d, C_6**H**$_4$; $^{3}J_{(H,H)}$ = 8.74 Hz, 6H); δ = 7.20 ppm (d, C_6**H**$_4$; $^{3}J_{(H,H)}$ =8.74 Hz, 6H).

$^{13}C\{^{1}H\}$ (50.323 MHz): δ = 40.38 (s, **C**H$_3$–N); δ = 112.64 (s, **C**-C-N); δ = 126.71 (s, slightly broadened, *ipso*-**C**-As); δ = 134.46 (s, **C**-C-As); δ = 150.35 ppm (s, *ipso*-**C**-N).

Table 6.14. Molecular Mass and Characteristic Fragments of $C_{24}H_{30}AsN_3$ from the Mass Spectrum (70 eV, Sample Temperature 460 K, Source Temperature 400 K)

Signal (m/z)	Rel. Int. (%)	Classification	Signal (m/z)	Rel. Int. (%)	Classification
437	0.8	$\{M\}^+$	241	17.0	$\{C_{16}H_{20}N_2\}^+(^{13}C)$
436	5.4	$\{M\}^+(^{13}C)$	240	100	$\{C_{16}H_{20}N_2\}^+$
435	21.0	$\{M\}^+$	197	1.0	$\{AsC_6H_4N(CH_3)_2\}^+(^{13}C)$
395.7	0.8	As_4O_6	196	2.6	$\{AsC_6H_4N(CH_3)_2\}^+(^{13}C)$
316	0.8	$\{M - C_6H_4N(CH_3)_2\}^+(^{13}C)$	195	24.1	$\{AsC_6H_4N(CH_3)_2\}^+$
315	4.9	$\{M - C_6H_4N(CH_3)_2\}^+$	121	1.2	$\{C_6H_5N(CH_3)_2\}^+$
242	1.6	$\{C_{16}H_{20}N_2\}^+$	120	3.1	$\{C_6H_4N(CH_3)_2\}^+$

IR (Nujol mull between CsBr disks; $\tilde{\nu}$ [cm^{-1}]): 3547 (w), 2664 (m), 2336 (w), 2086 (w), 1918 (w), 1890 (w), 1752 (w), 1701 (w), 1624 (w), 1591 (vs), 1546 (m), 1497 (vs), 1198 (vs), 1166 (vs), 1088 (s), 1049 (vs), 1000 (s), 942 (vs), 885 (m), 807 (vs), 755 (s), 722 (vs), 663 (w), 628 (w), 570 (w), 522 (vs).

X-ray structure analysis: Chapter 5 (page 177)

6.16. Preparation of [4-(Dimethylamino)phenyl]oxoarsine

The title compound was prepared by several methods.

6.16.1. Method I

It is recommended that the reaction be carried out free of solvent and – at least initially – under an atmosphere of argon.

19 mL (18.2 g, 150 mmol) of *N*,*N*-dimethylaniline are added dropwise within 20 min with stirring at 0 °C to 12.6 mL (27.2 g, 150 mmol) of arsenic(III) chloride. Gaseous hydrogen chloride is evolved and the solution gradually takes on a yellow colour. While stirring is continued for 30 to 40 min, the mixture is heated in a water bath to complete the reaction. After cooling to ambient temperature the previously liquid product starts to solidify and within 3 h it becomes a highly viscous yellow wax.

The subsequent procedure may now be performed under aerobic conditions. The product is dissolved with vigorous stirring in about 700 mL of cold distilled water; during this operation a very unpleasant smell of unknown origin is noticed. While stirring is being continued, 55 g of anhydrous sodium hydroxide are added slowly until the solution has just become basic as shown by litmus paper. After filtration in order to remove insoluble material it is treated with about 100 mL of a concentrated (37%) solution of hydrochloric acid until an acidic reaction against litmus is observed. Subsequent addition of about 60 g of anhydrous sodium carbonate to the now pale green solution results in the precipitation of a colourless solid. After the suspension had been stored for 12 to 14 h at 8 °C in the refrigerator, the product is filtered off, washed with cold water, and dried by removing adhering solvent under reduced pressure.

Yield 47% (15.0 g, 71 mmol); mp. 77 °C

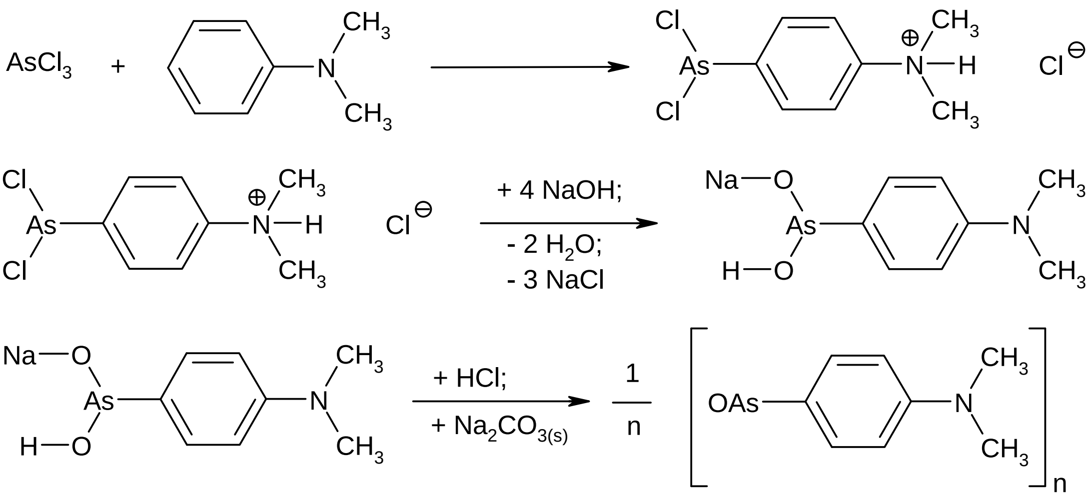

Characterization

Elemental analysis: $C_8H_{10}AsNO$ Calc.: C 45.52%; H 4.77%; N 6.64%

Found: C 46.38%; H 4.74%; N 6.69%

NMR (solution in $CDCl_3$)

^1H (200.132 MHz): $\delta = 2.97$ (s, $C\mathbf{H}_3$–N; 6H); $\delta = 6.75$ (d, $C_6\mathbf{H}_4$; $^3J_{(H,H)} = 8.05$, 2H); $\delta = 7.63$ ppm (d, $C_6\mathbf{H}_4$; $^3J_{(H,H)} = 8.05$ Hz, 2H).

$^{13}C\{^1H\}$ (50.323 MHz): $\delta = 40.26$ (s, $\mathbf{C}H_3$–N); $\delta = 111.93$ (s, **C**-C-N); $\delta = 130.86$ (s, slightly broadened, *ipso*-**C**-As); $\delta = 136.83$ (s, **C**-C-As); $\delta = 151.83$ ppm (s, *ipso*-**C**-N)

6.16.2. Method II

The subsequent procedure follows the orginal synthesis of 2,4,6,8-tetraphenyl-2λ^3,4λ^3,6λ^3,8λ^3-tetraarsa-1,3,5,7-tetraoxaocane (tetrameric phenyloxoarsine) from dichlorophenylarsine as published in 1930 by *Blicke* and *Smith* [298] and successfully repeated recently by *Müller* and *Mühle* [303].

5.0 g (18.8 mmol) of dichloro[4-(dimethylamino)phenyl]arsine are added, portion by portion, with concerted cooling and vigorous stirring to 16 mL of a 10% aqueous solution of sodium hydroxide (40 mmol). The clear alkaline reaction mixture is neutralized by addition of 2.0 g of ammonium chloride, whereupon the crude product precipitates as a colourless powder. Attempts to recystallize [4-(dimethylamino)phenyl]oxoarsine from boiling *n*-octane failed.

Yield 45% (1.8 g, 8.53 mmol); mp. 78 – 80 °C

Characterization

Elemental analysis: $C_8H_{10}AsNO$ Calc.: C 45.52%; H 4.77%; N 6.64%

Found: C 46.40%; H 5.01%; N 6.73%

NMR (solution in $CDCl_3$): see method I

6.16.3. Method III

The subsequent procedure follows the orginal synthesis of 2,4,6,8-tetramesityl-2λ^3,4λ^3,6λ^3,8λ^3-tetraarsa-1,3,5,7-tetraoxaocane (tetrameric mesityloxoarsine) from dichloromesitylarsine published by *Cowley* et al. [300].

5.0 g (18.8 mmol) of dichloro[4-(dimethylamino)phenyl]arsine in 10 mL of 1,2-dimethoxyethane (DME) is added drop by drop at 10 to 15 °C to a vigorously stirred solution of 2.2 g (39.2 mmol) of potassium hydroxide in 10 mL of 1,2-dimethoxyethane. Stirring is continued for 12 h; then the solvent is removed under reduced pressure. After extraction of the remaining residue with cold chloroform the solution is evaporated to dryness, leaving a colourless product. Attempts to recystallize [4-(dimethylamino)phenyl]oxoarsine from *n*-hexane failed.

Yield 76% (3.0 g, 14.21 mmol); mp. 80 °C

Characterization:

Elemental analysis: $C_8H_{10}AsNO$ Calc.: C 45.52%; H 4.77%; N 6.64%

Found: C 46.37%; H 5.00%; N 6.55%

NMR (solution in $CDCl_3$): see method I

Clear chloroform solutions of [4-(dimethylamino)phenyl]oxoarsine prepared by different methods as described before (I: 5.0 g in 10 mL; II: 1.0 g in 3.0 mL; III: 2.0 g in 5 mL) were stored at –13 °C in a refrigerator. After one week colourless crystals had precipitated which were collected and characterized by their lattice parameters ($P\bar{1}$; a = 985.5(2), b = 1098.2 (2), c = 1116.2 (2) pm; α = 108.71(3)°, β = 101.67(3)°, γ = 94.92(3)°; V = 1105.7 (4) x 10^{-30} m^3 at –100 ± 3°C) and their melting points. A comparsion with data given in chapter 6 showed the solid to be tris[4-(dimethylamino)phenyl]arsine. The compound has very probably been formed by a rearrangement of the corresponding [4-(dimethylamino)phenyl]oxoarsine. A similar reaction has been reported by *Doak* et al. [292a].

Yield 0.05 to 0.25 g; mp. 243 °C

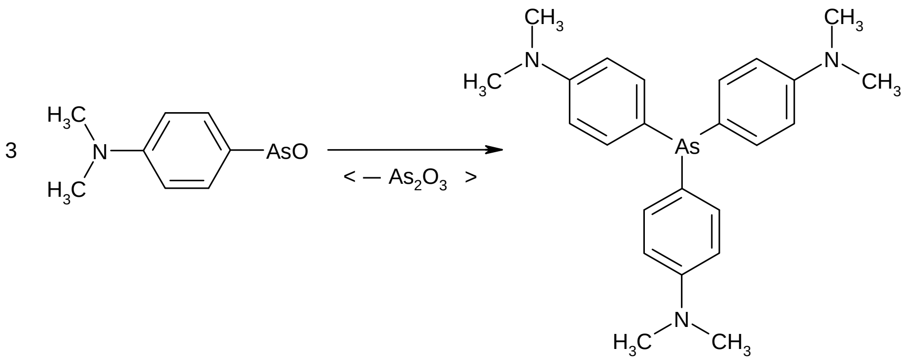

6.17. Preparation of Dimethyl[4-(dichloroarsanyl)phenyl)phenylammonium Chloride

Slow addition of 20 mL of concentrated (37%) hydrochloric acid (8.7 g, 239.5 mmol) to a stirred solution of 5.0 g (23.7 mmol) of [4-(dimethylamino)phenyl]oxoarsine in 10 mL of dilute hydrochloric acid (0.365 g, 10.0 mmol) results in the precipitation of the ammonium salt. The product is filtered off and the adhering solvent is removed under reduced pressure at ambient temperature.

Yield 85 % (6.1g, 20.71mmol); mp. 117.5 °C

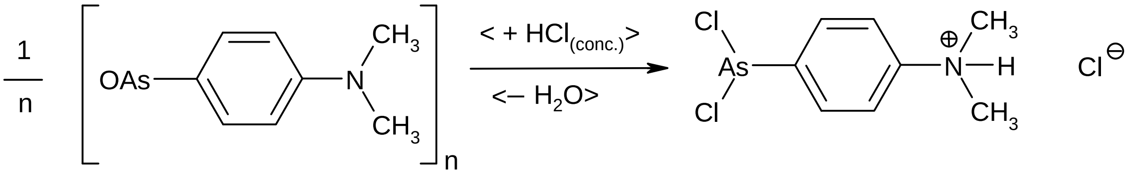

Characterization

Elemental analysis: $C_8H_{11}AsCl_3N$ Calc.: C 31.77%; H 3.67%; N 4.63%; Cl 35.16%.

Found: C 32.56%; H 3.79%; N 4.72%; Cl 34.89%.

NMR (solution in d_6-DMSO)

^1H (250.134 MHz): δ = 3.10 (s, C**H**$_3$–N; 6H); δ = 7.49 – 8.03 ppm ((m, C$_6$**H**$_4$) + H–N$^{\oplus}$)

$^{13}C\{^1H\}$ (62.896 MHz): δ = 46.0 (s, **C**H$_3$–N); δ = 121.2 (s, **C**-C-N); δ = 129.8 (s, slightly broadened, *ipso*-**C**-As); δ = 130.3 (s, **C**-C-As); δ = 143.4 ppm (s, *ipso*-**C**-N).

Mass spectrum: identical with the mass spectrum of dichloro[4-(dimethylamino)phenyl]arsine

6.18. Reaction of 2-*tert*-Butyl-1λ^3-phosphaalkyne with Dichloro[4-(dimethylamino)phenyl]arsine

Dichloro[4-dimethylamino)phenyl)]arsine (1.0 g, 3.76 mmol) and 2-*tert*-butyl-1λ^3-phosphaalkyne (1.13 g, 11.28 mmol), each dissolved in 50 mL of acetonitrile, are combined at –78 °C. The reaction mixture is vigorously stirred and allowed to warm up to room temperature. Within four days the solution takes on a yellow and later on a red colour. Insoluble material is filtered off and the filtrate is evaporated under reduced pressure at ambient temperature. The remaining dark red liquid contains several products, but a crystalline compound could not be separated. Repeating the reaction in different solvents such as dichloromethane or tetrahydrofuran was as before unsuccessful.

7. Summary

The reactions of $1\lambda^3$-phosphaalkynes R–C≡P with halides of main-group elements very often result in complicated cage compounds. Based on detailed investigations by several co-workers of our group, a general reaction scheme may now be outlined explaining even the formation of rather complicated cage structures (Scheme 7.1).

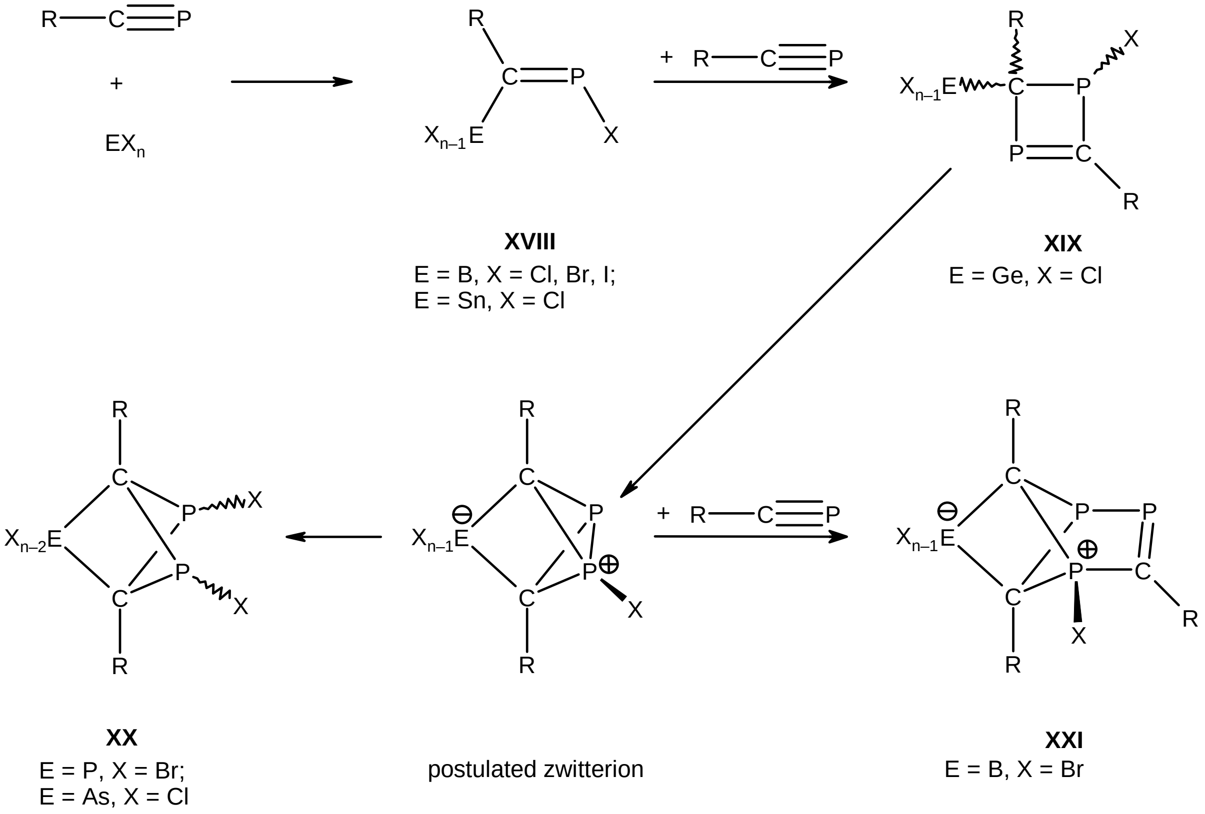

Scheme 7.1. Some complicated organophosphorus cage compounds from $1\lambda^3$-phospaalkynes and various halides of group 13 and group 15 elements.

The research of my thesis is based on earlier studies of *Dautel*, *Löw* and *Ruf* of *Becker's* group and deals with reactions between $1\lambda^3$-phospaalkynes and dialkylaluminium chlorides, halodiorganylphosphines or dichloro(dialkylamino)arsines in order to study the influence of alkyl and aryl groups in various mixed organyl halides of group 13 and group 15 elements on reaction routes and molecular structures. My research started with mixtures of 2-*tert*-butyl- or 2-(1-adamantyl)-$1\lambda^3$-phosphaalkyne and slightly more than three equivalents of different dialkylaluminium chlorides. When they were allowed to warm up to room temperature, the 1:2 insertion products, bridged by a third chloroalane molecule, precipitated in high yields. In these compounds (**1a-1d**), dative bonding between phosphorus or chlorine as a donor atom and aluminium as an acceptor atom results in a bicyclic system.

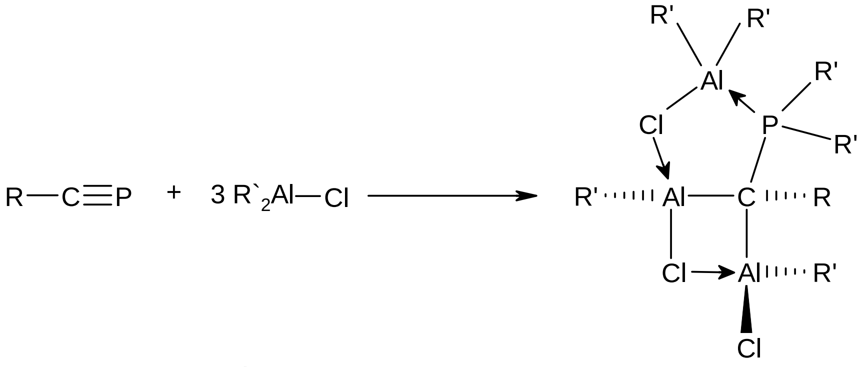

1a : R = *tert*-butyl, R\` = methyl;
1b : R = *tert*-butyl, R\` = ethyl;
1c : R = 1-adamantyl, R\` = methyl;
1d : R = 1-adamantyl, R\` = ethyl

The $^{31}P\{^{1}H\}$ NMR spectra of all compounds dissolved in d_6-benzene indicate the presence of several isomers in solution. Signals at high and also at low field are observed with different intensity ratios at ambient temperature as well as at 80 °C in d_8-toluene. The occurrence of two well separated shift regions observed are caused by either complexed or uncomplexed phosphorus atoms; this phenomenon can be explained by a competition between both the Lewis-basic centres phosphorus and chlorine for the Lewis acidic aluminium centre. From the broadening of the high field signals one can deduce that they originate from phosphorus atoms coordinated to aluminium. The broadening is at least partly a consequence of the quadrupole interaction between phosphorus and aluminium nuclei (^{27}Al: s = 5/2, electric quadrupole moment $Q_b = 0.1402(10) \cdot 10^{-28}$ m^2, 100% natural abundance). The $^{27}Al\{^{1}H\}$ NMR spectra of the complexes **1a**-**1d** dissolved in d_6-benzene as well show very broad singlets between 177 and 140 ppm. As can be taken from the literature data this region is attributed to four-coordinated aluminium.

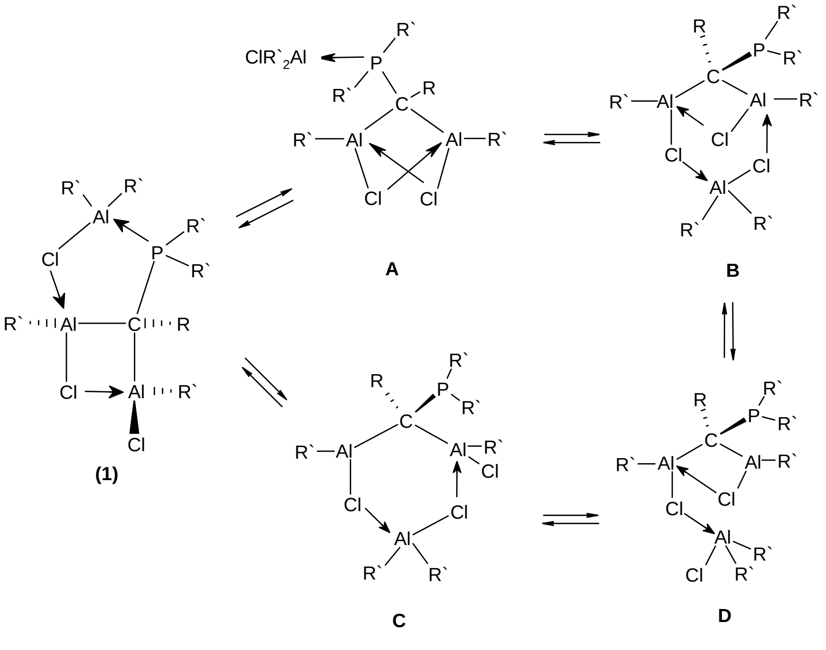

For all compounds crystal structures (Table 7.1) were obtained from colourless, cuboid-shaped single crystals.

Table 7.1. Crystal Data of the Complexes Dialkyl[bis(alkylchloroalanyl)organylmethyl]-phosphine•Dialkylchloroalane (1/1) (**1a**, **1b**, **1c**, and **1d**)

Compound	^{t}Bu/Me$_2$ **1a**	^{t}Bu/Et$_2$ **1b**	Ad/Me$_2$ **1c•C$_5$H$_{10}$(2/1)**	Ad/Et$_2$ **1d**
Crystal system	Monoclinic	Monoclinic	Triclinic	Monoclinic
Space group	$P2_1/c$	$P2_1/n$	$P\bar{1}$	$P2_1/c$
Z	4	4	4 + 2[a)]	4
R1	0.0451	0.0471	0.0791	0.0626

[a)] Four molecules of compound **1c** and two molecules of cyclopentane.

The molecules consist of two fused four- and five-membered rings. As a main result one has to emphasize that the $1\lambda^3$-phospaalkyne reacts at the Al–C bond of the starting material, whereas the Al–Cl moiety remains intact. Since only one of the two Al–C bonds of a molecule is involved in this insertion reaction, each P≡C unit is converted to an R`$_2$P–CAl$_2$ fragment. The heterocycle finally isolated, however, is a molecular complex of the underlying insertion compound and a third equivalent of dialkylaluminium chloride. The addition of the C–Al moiety to the P≡C group is in accordance with the polarity of the bonds involved; subsequent steps in the formation of the final complex are mostly a consequence of the Lewis acidity of the aluminium centres. The four- and the five-membered rings both contain two chlorine-bridged aluminium atoms (figure 7.1.). The chlorine bridge between the atoms Al3 and Al1 is slightly more symmetrical than that between Al1 and Al6. In the four-membered ring the two aluminium atoms Al1 and Al6 approach each other at an average distance of 289.1 pm which tallies the element-element distance (286.3 pm) in aluminium metal.

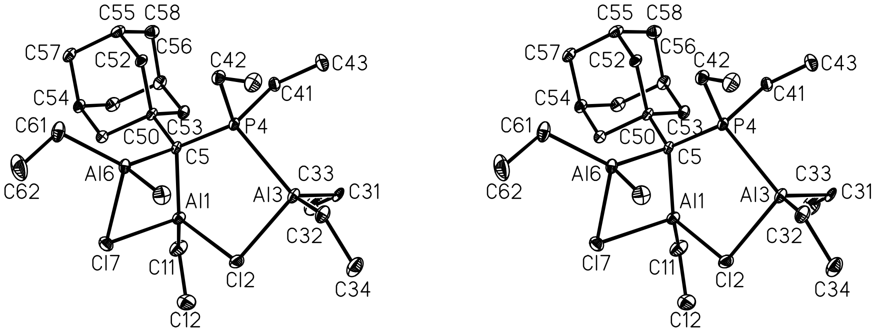

Figure 7.1. Stereoscopic view of a molecular model of compound **1d**. Thermal ellipsoids are at 30% probability; hydrogen atoms are omitted for clarity. The atoms C51, C59, C44, and Cl61 have not been labeled.

With halodiorganylphosphines, however, only one phosphorus–halogen bond is available for an initial insertion into the P≡C unit of a $1\lambda^3$–phosphaalkyne; hence, subsequent reactions and a variation of the mechanism outlined in Scheme 7.1 have to be taken into consideration. At first, a transannular attack of the R^1R^2P group at the *sp*^{2}-hybridized carbon atom of the still undetectable 1,2-dihydro-$1\lambda^3$,$3\lambda^3$-diphosphete is expected to occur as before, but in contrast to Scheme 7.1 it is now supposed to be nucleophilic. Subsequently, the former P=C double bond changes into a transannular P–P single bond and the postulated intermediate specified in Scheme 7.2, stabilizes by elimination of a halide anion to give the $1\lambda^3$,$5\lambda^3$-diphospha-$3\lambda^5$-phosphoniotricyclo[2.1.0.0^{2,5}]pentane cation.

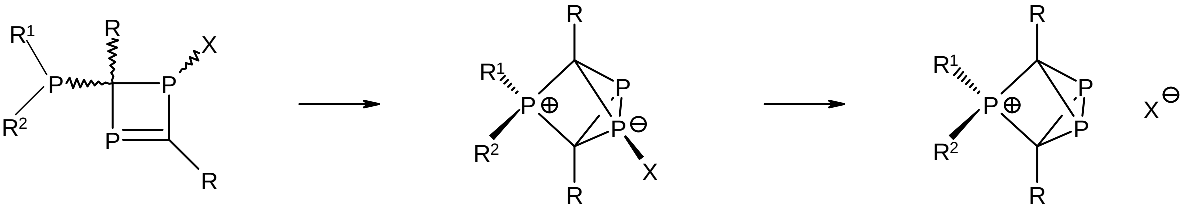

$1\lambda^3$,$3\lambda^3$-diphosphete

postulated intermediate

R = *tert*-butyl;
R^1, R^2 = organyl

Scheme 7.2. Postulated mechanism to explain the formation of the 3,3-diorganyl-$1\lambda^3$,$5\lambda^3$-diphospha-$3\lambda^5$-phosphoniotricyclo[2.1.0.0^{2,5}]pentane cation.

In the cation derived from chloro(isopropyl)phenyl phosphine the two phosphorus atoms of the P–P unit are magnetically inequivalent; as a consequence the $^{13}C\{^1H\}$ NMR spectrum reveals a doublet of doublets of doublets for the quaternary carbon atoms of the oligocycle. The $^{31}P\{^1H\}$ spectrum is characterized by a singlet for the positively charged phosphorus and two doublets at relatively high field with a $^1J_{PP}$ coupling constant of 172.7 Hz for the P–P unit. The ionic compounds were recrystallized from dichloromethane and isolated as colourless needles; they form solid state adducts with one or two molecules of solvent per formula unit, depending upon the substituents R^1 and R^2 (methyl, ethyl, *iso*-propyl, and phenyl) at phosphorus (Table.7.2). Most average bond lengths and angles are found as expected; the mean P–P distance of 213.0 pm, however, is shortened, and the mean P–C distance of 189.7 pm is elongated with respect to the relevant standard values.

Quantum chemical calculations were performed on the hydrogen substituted phosphonium and phosphenium cations in order to ascertain optimized structural data and relative energies for different isomers (Fig.7.3). As for the phosphonium cation ($[H_2P(CH)_2P_2]^{\oplus}$) the conventional trigonal bipyramidal framework of point group C_{2v} represents the absolute minimum on the potential energy surface. Remarkably, the P–P bond is found to be shortened to 216.8 pm, whereas the adjacent P–C bond is elongated to 191.5 pm. Both distances are only slightly longer than the average bond lengths obtained from crystal structure analysis.

Table 7.2. Crystal Data of Compounds **2a** to **2d** 3,3-Diorganyl-1λ^3,5λ^3-diphospha-3-phosphoniatricyclo[2.1.0.0^{2,5}]pentane Cations **2a** to **2d**

Compound[a]	**Me/Me/Cl (2a)**	**Et/Et/Cl (2b)**	**Ph/^{i}Pr/Cl (2c)**	**Ph/Ph/Cl (2d.1)**	**Ph/Ph/Br (2d.2)**
Crystal system	Triclinic	Triclinic	Monoclinic	Monoclinic	Monoclinic
Space group	$P\bar{1}$	$P\bar{1}$	$P2_1/c$	$P2_1/n$	$P2_1/n$
Z[b]	2 + 2	4 + 8	4 + 8	4 + 4	4 + 4
R1	0.1053	0.0683	0.0627	0.0698	0.0889

[b] Solid state adducts with one or two molecules of dichloromethane per formula unit; b) number of ionic species and dichloromethane molecules in the unit cell, respectively.

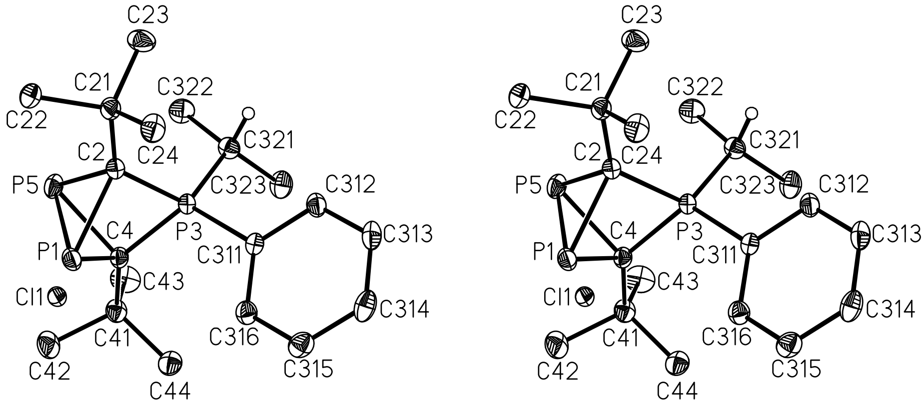

Figure 7.2. Stereoscopic view of cation and anion in the solid state adduct **2c•CH$_2$Cl$_2$** (**1/2**). Thermal ellipsoids are at 30% probability; hydrogen atoms and co-crystallizing dichloromethane molecules have been omitted for clarity but the CH–hydrogen atom of the isopropyl group is shown.

At the phosphonium group, however, the calculated (178.5 pm) and experimentally determined (179.1 pm) P–C distances do not differ. To our surprise the absolute minimum in energy of the trigonal bipyramidal framework is followed by a second one which has to be attributed to the so-called housene structure of point group C_1 showing a somewhat higher energy value + 77.9 kJ mol^{-1}.

Quite a reverse situation is encountered for the phosphenium cation $[P(CH)_2P_2]^{\oplus}$. Here the pseudo square-based pyramidal *nido* structure of point group C_{2v} known from *Russell's* tetrachloroaluminate(III) compound [181] is found to be the only minimum on the potential energy surface. Calculated P–P and P–C bond lengths compare very well with the average of experimentally determined data. A phosphenium cation with a trigonal bipyramidal framework of point group C_{2v} is higher in energy by only 35.7 kJ mol^{-1}, but due to one imaginary frequency it has to be considered the structure of a transition state. The opened housene structure corresponds neither to a minimum nor to a saddle point on the potential energy surface.

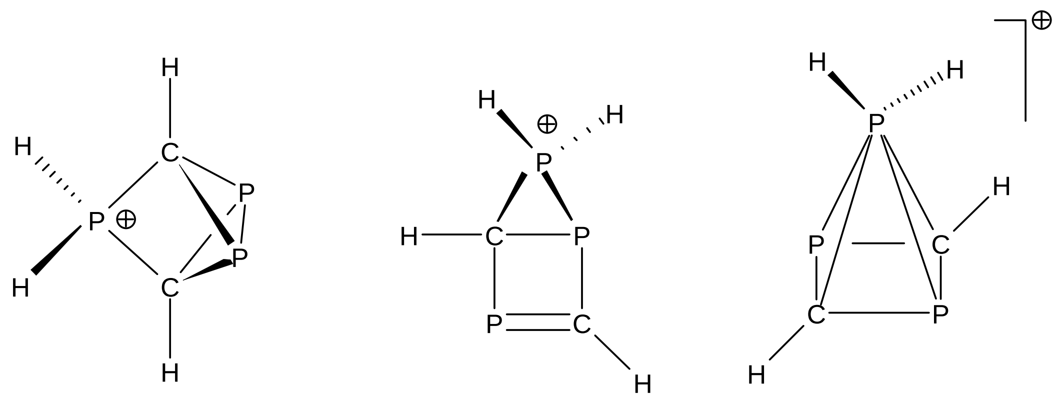

trigonal
bipyramidal structure
(C_{2v})

opened housene
structure
(C_1)

pseudo square-based
pyramidal structure
(C_2)

pseudo square-based
pyramidal *nido* structure
(C_{2v})

trigonal bipyramidal
structure
(C_{2v})

Figure 7.3. Structural isomers of the $[H_2P(CH)_2P_2]^{\oplus}$ (above) and $[P(CH)_2P_2]^{\oplus}$ cation (below) obtained from quantum chemical calculations.

In the pseudo square-based pyramidal *nido* structure (point group C_{2v}) of the phosphenium cation $[P(CH)_2P_2]^{\oplus}$ the *s*-orbital and all *p*-orbitals of the apical four-coordinate phosphorus atom are used to form two P–C and two P–P bonds. Further addition of two hydrogen atoms to entail the phosphonium cation $[H_2P(CH)_2P_2]^{\oplus}$ of point group symmetry C_2 not only increases the coordination number of the apical phosphorus atom to six but also requires two electrons and two orbitals for P–H bonding. These are no longer available to the bonding system within the *nido* structure; as a consequence its energy increases to +246.6 kJ mol^{-1} and the cation rearranges to give the conventional structure.

The reactions between 1λ^3-phosphaalkynes and dichloro(diorganylamino)arsines in a molar ratio of 3:1, performed in cyclopentane at ambient temperature, take quite a different route. To explain the underlying mechanism, one, however, has to realize first that the As–N and the P–N bonds differ in energy by values of about 582(126) and 617(21) kJ per mole. As a consequence, the insertion of the $P\equiv C$ unit into one of the two As–Cl bonds is immediately followed by a transfer of the diorganylamino group from arsenic to phosphorus. Subsequently, the arsenic component of the starting material is completely lost, probably as a precipitate of insoluble "arsenic(I) chloride," and an ylidic $1\lambda^5,3\lambda^3,5\lambda^3$-triphospha Dewar benzene is formed by further addition of $1\lambda^3$-phosphaalkyne molecules (Figure 7.4.).

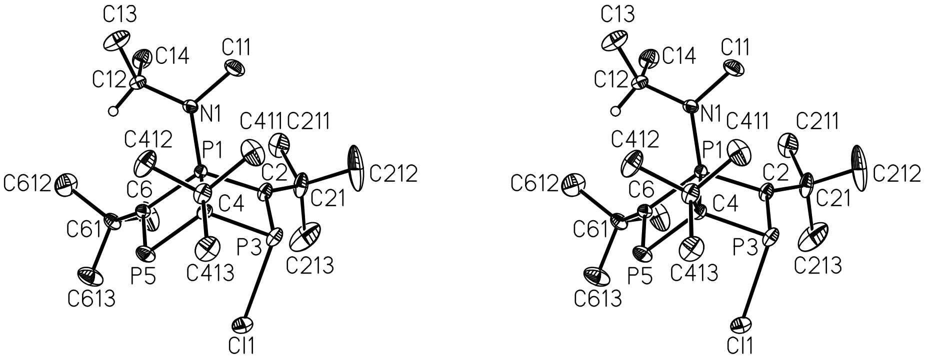

Figure 7.4. Molecule of compound **3c** in stereoscopic view. Thermal ellipsoids are at 30% probability; only the CH-hydrogen atom of the isopropyl group is shown.

From these reactions compounds **3a** to **3d** differing by their substituents at nitrogen were isolated as deep red, cuboid-shaped single crystals. X-ray structure analyses (Table 7.3.) reveal molecules which are characterized by an ylidic and a regular P–C double bond of almost equal length [$P1^{\oplus}$–$C2^{\ominus}_{av.}$ 172.2 pm, P5–$C6_{av.}$ 169.6 pm]. In addition to these two characteristic features the average bond length P3–C2 is found to be considerably shortened to a value of 172.7 pm, whereas the adjacent phosphorus–chlorine bond P3–Cl1 is strongly elongated to 245.5 pm. The bonding situation encountered here makes the rapid 1,3-migration of the chlorine atom between the two phosphorus atoms P3 and P5 (Figure 7.5.a) – as derived from the $^{31}P\{H\}$ NMR spectra – quite understandable.

We could not yet establish, however, the existence of isolated halide anions in solution or isolate derivatives with separate cations.

The formation of an ylidic $P^{\oplus}$—$C^{\ominus}$ bond in compounds **3a** to **3b** gives a straightforward explanation why the adjacent P–Cl bond is found to be strongly elongated. As can already be taken from the expresion "ylidic," the sp^2-hybridized carbon atom C2 has to be considered a carbanion, whereas the positive charge is located at the four coordinate phosphorus atom P1. An electronic interaction between the free electron pair at carbon and the empty σ*(P–Cl) orbital not only shortens the bond C2–P3 but also elongates the bond P3–Cl1 by about 60 pm with respect to the standard value of 204.3 pm (Figure 7.5.b).

Table 7.3. Crystal Data of Several $1\lambda^5,3\lambda^3,5\lambda^3$-triphospha Dewar Benzenes (**3a** to **3d**)

Compound	Me_2N **3a**	Et_2N **3b**	Me^iPrN **3c**	MeEtN **3d**
Crystal system	Monoclinic	Triclinic	Monoclinic	Monoclinic
Space group	$P2_1/c$	$P\bar{1}$	$P2_1/n$	$P2_1/n$
Z	4	4	4	4
R1	0.0816	0.0598	0.0445	0.0859

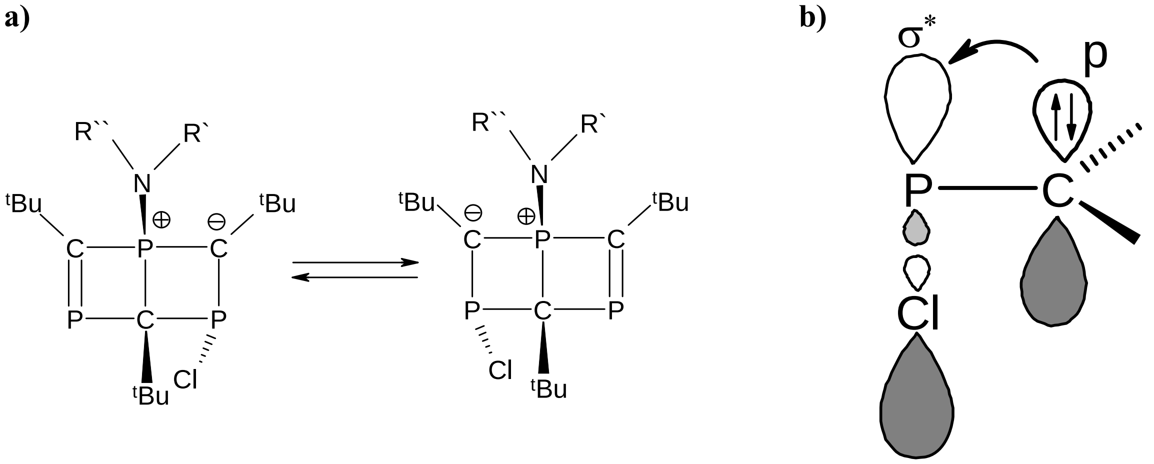

electronic interaction between the free electron pair at carbon and the σ*(P–Cl) orbital

Figure 7.5. Rapid 1,3-chlorine exchange in compounds **3a** to **3b** (a) as a consequence of the strong elongation of the P–Cl bond (b)

In order to corroborate the experimental results, to acquire information to what extend bond lengths may vary in a series of similar compounds, and to obtain a deeper understanding of the theoretical background, quantum chemical calculations on several (dimethylamino)-methylphosphines were performed first. Later on, these studies were extended to various types of methylenephosphoranes such as the homoleptic species $Me_3P{=}CH_2$ and $(H_2N)_3P{=}CH_2$ as well as the heteroleptic derivatives $(H_2N)Me_2P{=}CH_2$ and $(H_2N)_2MeP{=}CH_2$. In this series of compounds, however, the dimethylamino substituent of the previously studied phosphines have been exchanged for the parent NH_2 group in order to save computing time. Moreover, the compounds $H_3P{=}CH_2$, $Cl_3P{=}CH_2$ and $(H_3Si)_3P{=}CH_2$ were included into the calculations. A comparison of structural data obtained from a greater number of methylenephosphoranes with one, two, or three amino groups at phosphorus indicate an unexpected correlation between the conformation of the molecules and their bond lengths and angles. Particularly, a strong elongation of the P–N distance, a widening of the C=P–N angle and an sp^3-hybridisation of the nitrogen atom occur when the P–N bond concerned and the vector of the free electron pair at the ylidic carbon atom are found in an ecliptic position.

In order to widen the scope of different starting materials, reactions of $1\lambda^3$-phosphaalkynes with dichloro[4-(dimethylamino)phenyl]arsine (**4**) were also taken into consideration. This compound differs from a dichloro(diorganylamino)arsine just by insertion of a phenyl unit into the As–N bond. In keeping with the so-called "phenylogous principle" it is expected to be of similar reactivity. Along with tris[4-(dimethylamino)phenyl]arsine (**5**) the dichloro derivative **4** could be obtained in high yield directly from *N*,*N*-dimethylaniline and arsenic(III) chloride according to the modified preparation of *Michaelis* and *Rabinerson* [289].

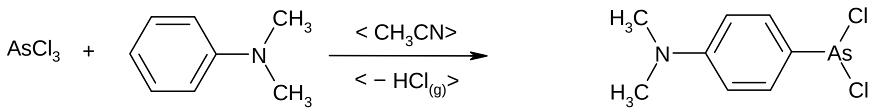

4

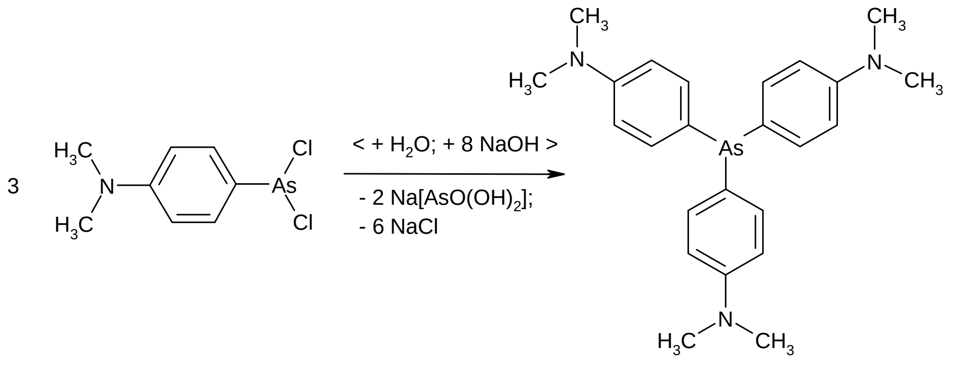

5

Dichloro[4-(dimethylamino)phenyl]arsine (**4**) crystallizes from acetonitrile in colourless plates. The X-ray structure analysis ($P\bar{1}$, triclinic, Z = 4; R1 = 0.0478) revealed two crystallographically independent molecules in the asymmetric part of the unit cell (Figure 7.7.). The average As–Cl bond (220.6 pm) is found to be slightly longer than that of arsenic(III) chloride (216.1 or 216.2 pm), but to be rather similar to that in the orthorhombic modification of chlorobis[2,4,6-tris(trifluoromethyl)phenyl]arsine (219.2 pm). Mean As–C_{aryl} (191.7 pm) and C_{aryl}–N bond lengths (135.9 pm) suggest extended electronic interactions between the dichloroarsanyl group, the π-electron system of the arene ring and the nitrogen lone pair. In both molecules the nitrogen atoms are found in a planar coordination sphere; the sums of bond angles vary only slightly between 359.1° for **4a** and 359.9° for **4b**. In contrast to these observations, sums of bond angles of 292.7° for **4a** and 293.98° for **4b** indicate a pyramidal coordination sphere at arsenic.

4a

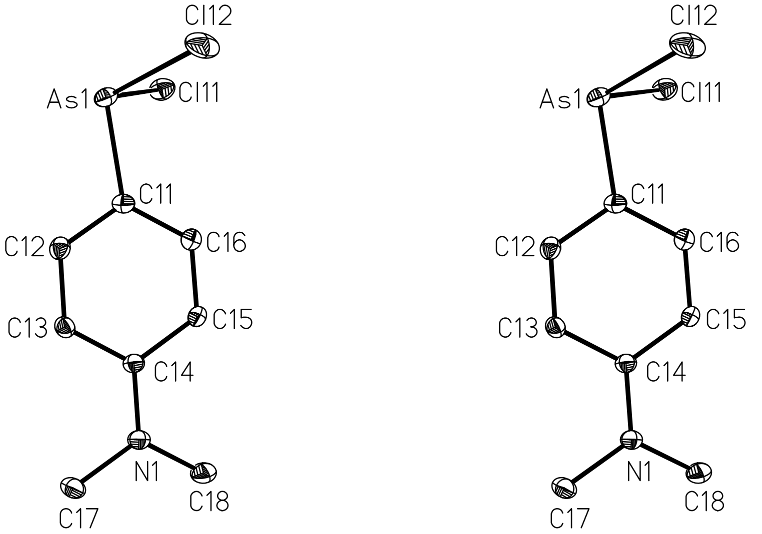

4b

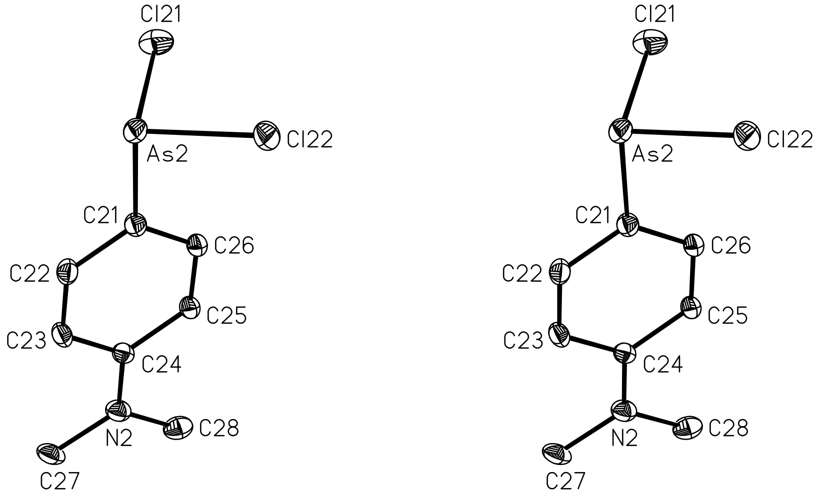

Figure 7.7. Stereoscopic view of both independent molecules **a** and **b** of compound **4**. Thermal ellipsoids are at 30 % probability, hydrogen atoms are omitted for clarity.

Apart from the molecular parameters already discussed, the structure of dichloro[4-(dimethylamino)phenyl]arsine (**4**) attracts attention by unusual changes in bond lengths. Compared with standard values which, however, have to be corrected to 144 and 194 pm for the N_{sp2}–C_{sp2} and As–C_{sp2} single bond, respectively, the distances between the *ipso* carbon atoms and nitrogen as well as arsenic are both additionally shortened to values of 135.9 and 191.9 pm. Furthermore, relatively large fluctuations in the C–C bond lengths from 137.1 to 142.3 pm within the arene ring suggest substantial substituent effects.

Quantum chemical calculations were performed on several *para* substituted dichlorophenyl arsine compounds in order to ascertain optimized structural data and to shed some light onto these phenomena. Indeed, the aforementioned shortening of the N–C_{ipso} bond to 135.9 pm can only in part be attributed to the well-known electronic interaction between the lone pair at nitrogen and the antibonding π^* orbitals of the adjacent C_{ipso}–C_{ortho} bonds – on an average, these two distances are significantly elongated by 1.7 pm with respect to the standard value (140 pm). Furthermore, this interaction is intensified by structural features such as the trigonal planar coordination sphere at nitrogen and an almost perfect co-planarity of the arene ring with the dimethylamino group; in both crystallographically independent molecules **4a** and **4b** the deviations come up to 12.6° and 1.6° only. An NBO charge analysis of the dichloro[4-(dimethylamino)phenyl]arsine (**4**) molecule, however, does reveal that even the *ipso* carbon atom at arsenic exhibits an *increased electron density*. Hence, the unusual shortening of the As–C_{ipso} bond may essentially be traced back to the unexpectedly high difference of 1.431 elementary charges and an enhanced electronic attraction between the arsenic and the *ipso* carbon atoms.

The electronic situation traced out for dichloro[4-(dimethylamino)phenyl]arsine (**4**) can best be described in the sense of a push-pull effect in that the dimethylamino substituent induces (pushes) a negative charge at (to) the *para* carbon atom and this charge is additionally increased by (pulled to) the dichloroarsinyl group. In our opinion, the As–C_{ipso} bond length might be appropriate to serve as an indicator for this effect; its size should depend on the Hammett constants of the substituents. Since structure determinations of dichlorophenyl arsines with different substituents in *para* position to the Cl_2As group are not available, quantum chemical calculations were performed to obtain the necessary data.

From the great variety of suitable substituents, four typical nitrogen containing species were selected to comprise a Hammett constant range as wide as possible, from highly negative to highly positive values. The hydrogen atom, by definition, serves as a substituent with a reference value σ_p of 0.0; other substituents of these studies are the dimethylamino (NMe_2, –0.83), the hydroxylamino (N(H)OH, –0.34), the nitro (NO_2, 0.78) and the cationic diazonium group ($N_2^{\oplus}$, 1.91). To allow, however, a more authoritative interpretation of these theoretical results, compounds without a Cl_2As unit such as aniline, *N*,*N*-dimethylaniline, benzene, and nitrobenzene have also been included.

Correlations between the Hammett constant σ_p and various molecular properties of some dichlorophenylarsines 4-X_p–C_6H_4–$AsCl_2$, such as elementary charges Q at the two *ipso* carbon atoms in positions 1 (As–C1) and 4 (C4–N), together with the appropriate charge differences ΔQ as well as the lengths of the As–Cl, As–C1 or C4–N bonds have been studied; for nearly all properties, high correlation coefficients R^2 between 0.939 and 0.998 were obtained.

Furthermore, the parameter σ_p has also a strong effect ($R^2 = 0.947$) on the magnitude of the angle β, the vertex of which is carbon atom C4 directly bonded to the substituent X_p. In contrast to this result the interrelation between the constant σ_p and angle α, the vertex of which is carbon atom C1, is rather poor ($R^2 = 0.774$).

Though an overinterpretation of structural data and difference values in particular has to be avoided, the salient alternation of elongated, shortened and again elongated C–C bond lengths in the dichloro[4-(dimethylamino)phenyl]arsine molecule, quite evident from the results of the crystal structure analysis and confirmed by quantum chemical calculations, is in accordance with the so-called "phenylogous" principle. Along with the well–known "vinylogous" principle, which it can be associated with, these two heuristic rules are often applied in organic chemistry. They allow an understanding why for a group of similar compounds which differ from a parent compound just by insertion of a vinylene or phenylene unit into the primary element–element bond, an almost identical reactivity is observed. With our studies, the "phenylogous" principle has been applied to bond lengths for the first time.

Tris[4-(dimethylamino)phenyl]arsine (**5**) ($P\overline{1}$, triclinic, Z = 4; R1 = 0.0347) crystallizes from chloroform in colourless cuboids. The X-ray structure analysis (Figure 7.8.) reveals bond lengths and angles at arsenic (As–C 194.9 pm, C–As–C 99.3°, As–C–C 121.3°) as to be expected and obtained for similar compounds such as triphenyl arsine or triphenyl arsine derivatives. The sums of angles at two of the nitrogen atoms amount to values of 353.6° and 356.1° and deviate significantly from the value of the third (348.1°). Hence, two of three dimethylamino groups are found to be almost planar, whereas the third group shows a coordination sphere which has to be classified as an intermediate between trigonal planar and trigonal pyramidal.

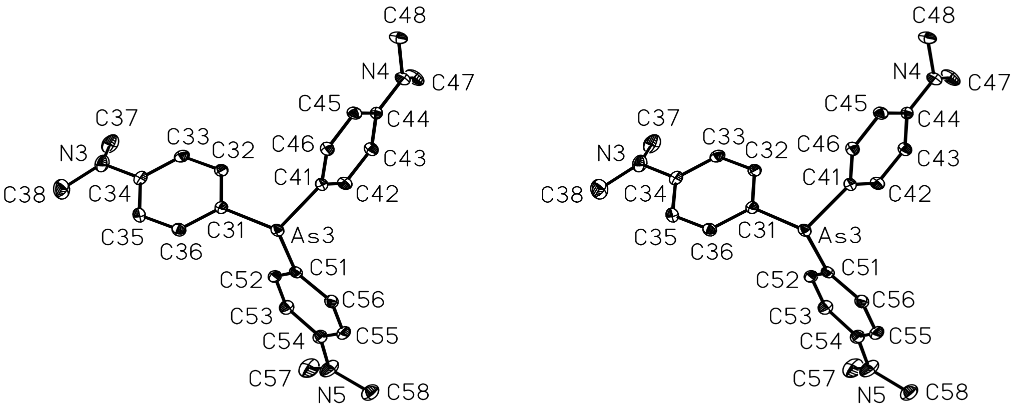

Figure 7.8. Stereoscopic views of compound **5**.
Thermal ellipsoids are at 30% probability, hydrogen atoms are omitted for clarity. The chiral molecule given here forms a right-handed propeller.

The molecule shows a high degree of C_3 pseudosymmetry; the sum of angles at arsenic amounts to 298.0°. The average C_{aryl}–N bond length (139.0 pm) suggests an interaction of the nitrogen lone pair with the π-system of the arene ring but it turns out to be much weaker than in dichloro[4-(dimethylamino)phenyl]arsine (**4**).

Up to now the reaction of dichloro[4-(dimethylamino)phenyl]arsine (**4**) with $1\lambda^3$-phosphaalkynes did not produce suitable results. By changing the solvent and the reaction conditions, however, the formation and isolation of crystalline material will at least be expected.

8. Zusammenfassung

Die Reaktionen von 1λ^3-Phosphaalkinen mit den Halogeniden der Hauptgruppenelemente führen sehr häufig zu komplizierten Oligocyclen. Aufgrund vorausgehender, ausführlicher Untersuchungen von Mitgliedern unserer Arbeitsgruppe kann ein allgemeiner Reaktionsmechanismus formuliert werden (Schema 8.1).

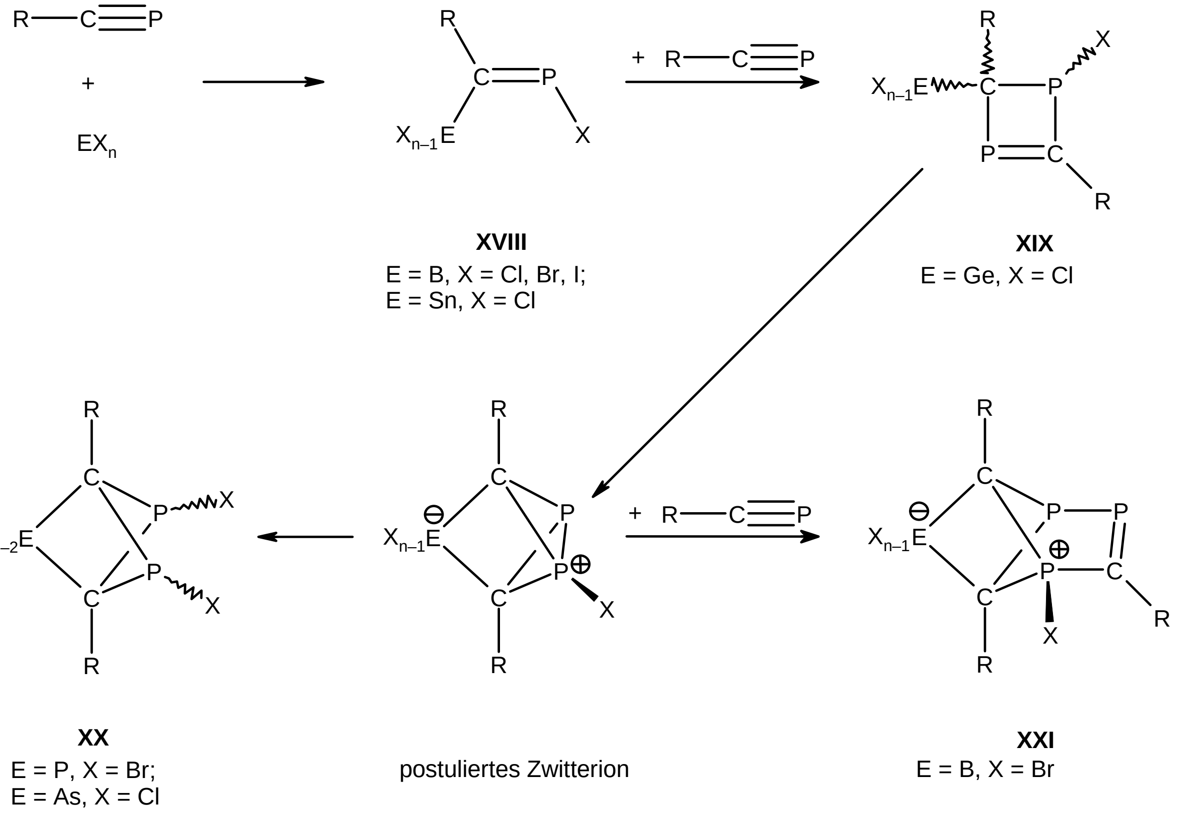

Schema 8.1. Bildung phosphororganischer Oligocyclen aus 1λ^3-Phosphaalkinen und Halogniden der Gruppen 13 und 15

Die hier vorliegende Dissertation schließt an frühere Unversuchungen von *Dautel*, *Löw* und *Ruf* aus der Arbeitsgruppe *Becker* an und beschäftigt sich mit Reaktionen von 1λ^3-Phosphaalkinen mit Dialkylchloralanen, Halogendiorganylphosphanen, Dichlor(dialkylamino)- sowie dem Dichlor[4-(dimethylamino)phenyl]arsan. Ziel war es, die Einflüsse von Alkyl- und Arylsubstituenten aus heteroleptischhen Organylelementhalogeniden der Gruppen 13 und 15 auf den Reaktionsweg, die spektroskopischen Eigenschaften und die Strukturen der Reaktionsprodukte zu klären. Lässt man zuvor gekühlte Lösungen von 2-*tert*-Butyl- oder 2-(1-Adamantyl)-1λ^3-phosphaalkin und etwas mehr als drei Äquivalenten Chlordialkylalan langsam auf Zimmertemperatur erwärmen, so setzt unter Insertion sowohl der ursprünglichen P≡C– und der daraus hervorgehenden jede P=C–Gruppe in jeweils eine der beiden Al–C-Bindungen des Halogenids eine Reaktion ein und es entstehen die 1:2-Insertionsprodukte mit einem $Al_2C–PR_2$-Fragment. Nach Komplexierung mit einem dritten Äquivalent Chloroalan scheiden sie sich in hoher Ausbeute als farblose Niederschläge ab. In diesen Verbindungen (**1a-1d**) stellt Phosphor oder Chlor das Donor- und Aluminium das Akzeptoratom dar; dadurch kommt es zur Ausbildung bicyclischer Addukte.

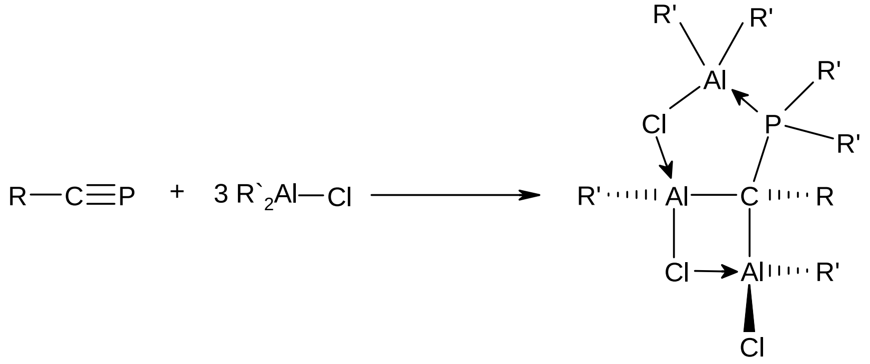

1a : R = *tert*-Butyl, R` = Methyl;
1b : R = *tert*-Butyl, R` = Ethyl;
1c : R = 1-Adamantyl, R ` = Methyl;
1d : R = 1-Adamantyl, R` = Ethyl

Bereits die ^{31}P{^{1}H}-NMR-Spektren der Verbindungen in d_6-Benzol weisen bereits auf das Vorliegen verschiedener, am Ende dieses Absatzes zusammengestellter Isomere in Lösung hin. Unterschiedlich intensive Signale werden sowohl ein einem Hoch- als auch in einen Tieffeldbereich bei Zimmertemperatur sowie bei 80 °C in d_8-Toluol beobachtet. Das Auftreten zweier derartiger Bereiche der chemischen Verschiebungen ist auf Aluminium-komplexierte und unkomplexierte Phosphoratome zürckzuführen; dabei konkurrieren die beiden Lewis-basischen Zentren Phosphor und Chlor um das Lewis-saure Zentrum Aluminium. Aus der Verbreiterung der Hochfeldsignale man kann ableiten, daß diese von den Aluminium-komplexierten Phosphoratomen herrühren, denn die Verbreiterung ist zumindest teilweise auf die große Quadrupol-Wechselwirkung mit den Aluminiumkernen (^{27}Al: s = 5/2, elektrisches Quadrupolmoment Q_b = 0.1402(10) • 10^{-28} m^{2}, 100% natürliche Häufigkeit) zurückzuführen. Die ^{27}Al{^{1}H}-NMR-Spektren von Lösungen in d_6-Benzol weisen sehr breite Signale zwischen 140 und 177 ppm auf. Ein derartiger Bereich der chemischen Verschiebung ist nach Literaturangeben als Hinweis auf die Koordinationszahl vier der Aluminiumatome zum werten.

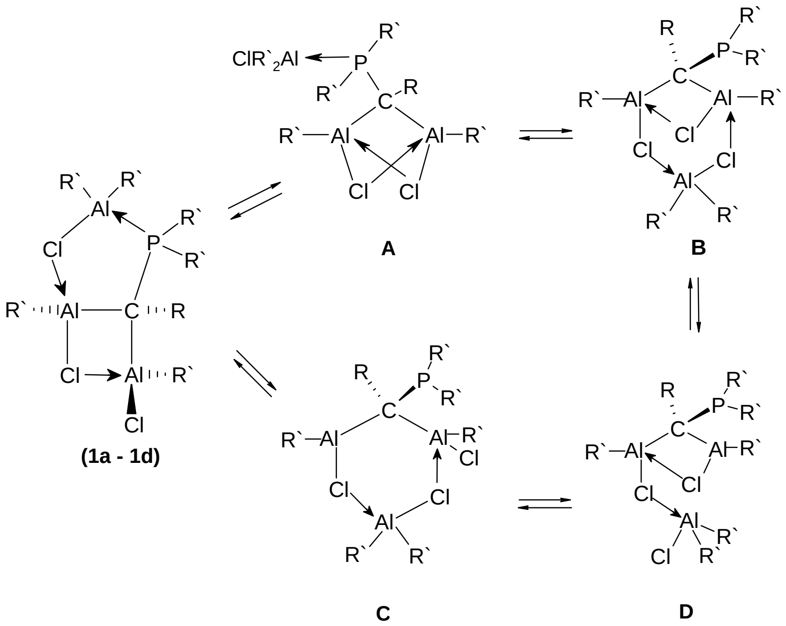

Röntgensstrukturanalysen wurden an farblosen, quaderförmigen Einkristallen der Verbindungen **1a** bis **1d** durchgeführt; die Kristalldaten sind in Tabelle 8.1 zusammengestellt.

Tabelle 8.1. Kristalldaten der Dialkyl[bis(alkylchloralanyl)organylmethyl]phosphane•Dialkylchloralan(1/1) (**1a**, **1b**, **1c**, and **1d**)

Verbindung	^{t}Bu/Me$_2$ **1a**	^{t}Bu/Et$_2$ **1b**	Ad/Me$_2$ **1c•C$_5$H$_{10}$(2/1)**	Ad/Et$_2$ **1d**
Kristallsystem	monoklin	monoklin	triklin	monoklin
Raumgruppe	$P2_1/c$	$P2_1/n$	$P\overline{1}$	$P2_1/c$
Z	4	4	4 + 2[a)]	4
R1	0,0451	0,0471	0,0791	0,0626

[a)] Vier Moleküle **1c** und zwei Moleküle Cyclopentan

Nach den Ergbnissen der Strukturbestimmung bauen sich die Bicyclen aus einem vier- und einem fünfgliedrigen Ring auf. In diesem Zusammenhang ist besonders hervorzuheben, dass das 1λ^3-Phosphaalkin an der Al–C Bindung der Ausgangsverbindung reagiert, während die Al–Cl-Gruppe intakt bleibt. Da sich aber jeweils nur eine dieser beiden Al–C Bindungen eines Moleküls an dieser Insertion beteiligt, wird jede P≡C–Einheit in ein R\`$_2$P–CAl$_2$-Fragment umgewandelt. Der schließlich isolierte Bicyclus ist dann jedoch ein Komplex des Primärprodukts mit einem dritten Äquivalent Dialkylchloralan. Die Addition der C–Al-Einheit an die P≡C-Gruppe folgt der Polarität der betroffenen Bindungen; die anschließenden Schritte bis hin zur Bildung des dann kristallin isolierten Komplexes rühren überwiegend von der Lewis-Acidität der Aluminiumatome her. Sowohl der vier- als auch der fünfgliedrige Ring enthalten jeweils zwei über Chlor verbrückte Aluminiumatome (Abb. 8.1.); dabei ist die zwischen den Atomen Al3 und Al1 ausgebildete Chlorbrücke etwas symmetrischer als die

Brücke zwischen Al1 und Al6. Im viergliedrigen Ring nähern sich die beiden Aluminiumatome Al1 und Al6 bis auf einen mitleren Abstand von 289,1 pm; im Vergleich dazu beträgt der Element–Element-Abstand im elementaren Aluminium 286,3 pm.

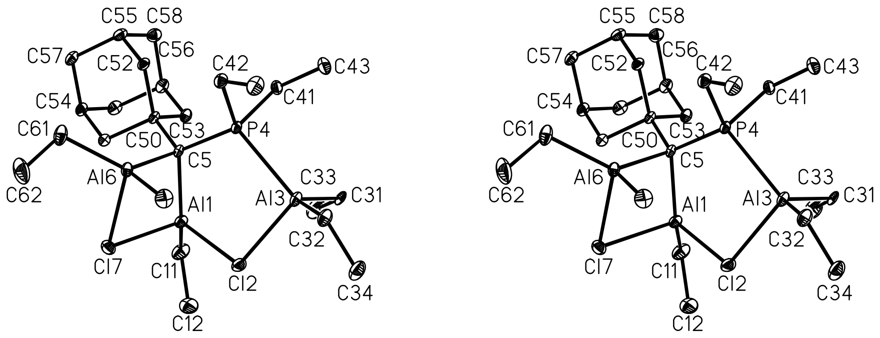

Abbildung 8.1. Stereoskopische Darstellung eines Molekülmodells von Verbindung **1d**. Die Auslenkungsellipsoide wurden auf 30% skaliert. Auf die Darstellung der Wasserstoffatome wurde der Übersichtlichkeit halber verzichtet. Die Atome C51, C59, C44 und Cl61 wurden nicht bezeichnet.

Da im Gegensatz zu Phosphor(III) bromid mit drei P–Br-Bindungen bei den Umsetzungen der Halogendiorganylphosphane nur eine Phosphor–Halogen-Bindung für die zunächst einsetzende Insertion der P≡C-Einheit eines 1λ^3-Phosphaalkins und nachfolgende Reaktionen zur Verfügung steht, muss eine Abwandlung des zu Beginn der Einleitung angegebenen Reaktionsschemas (Schema 8.1) in Betracht gezogen werden. Zwar ist zunächst wiederum ein transannularer Angriff der R^1R^2P-Gruppe am *sp*^{2}-hybridisierten Kohlenstoffatom des bislang nicht nachweisbaren 1,2-Dihydro-1λ^3,3λ^3-diphosphets zur erwarten; im Gegensatz zu Schema 8.1 wäre hier aber ein nucleophiler Angriff zu formulieren – dies käme einer *Umpolung* gleich. Die in Schema 8.2 postulierte Zwischenstufe stabilisiert sich dann unter Freigabe eines Halogenid-Anions und Ausbildung des entsprechenden 3,3-Diorganyl-1λ^3,5λ^3-diphospha-3λ^5-phosphonia-tricyclo[2.1.0.0^{2,5}]pentan-Kations.

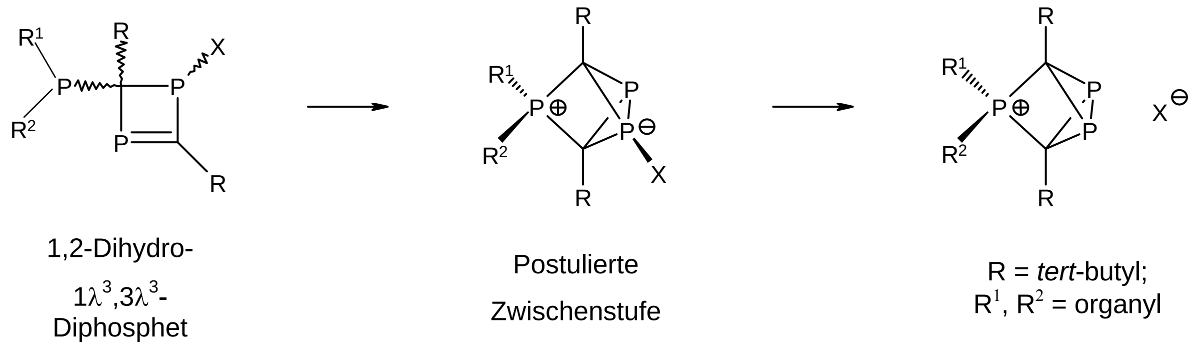

Schema 8.2. Postulierter Mechanismus für die Bildung von 3,3-Diorganyl-1λ^3,5λ^3-diphospha-3λ^5-phosphonia-tricyclo[2.1.0.0^{2,5}]pentan-Kationen

Im Isopropylphenylphosphonium-Derivat sind die beiden Phosphoratome der P–P-Einheit chemisch nicht äquivalent; daher zeigt sich das quartäre Kohlenstoffatom des Oligocyclus im $^{13}C\{^1H\}$-NMR-Spektrum als Dublett von Dublett von Dubletts. Das $^{31}P\{^1H\}$-NMR-Spektrum weist ein Singulett für das positiv geladene Phosphoratom sowie zwei Dubletts mit einer Kopplungskonstanten von $^1J_{PP}$ =172,7 Hz für die P–P Einheit bei vergleichsweise hohem Feld auf. Die Kristallstrukturen aller Verbindungen (Tabelle 8.2) wurden an farblosen nadelförmigen, aus Dichlormethan algeschiederen Einkristallen bestimmt; sie enthalten je nach Subtituent am positiv geladenen Phosphoratom (R^1, R^2: Methyl, Ethyl, *Iso*-propyl, und Phenyl) stets ein oder zwei Moleküle des Lösungsmittels pro Formeleinheit. Die mittleren Bindungslängen und –winkel entsprechen zumeist erwarteten Werten; Der P–P-Abstand ist aber bei einem Mittel von 213,0 pm gegenüber dem Standard verkürzt; die P–C-Abstände zwischen P–P-Einheit und apikalem Kohlenstoffatom mit 189,7 pm hingegen verlängert.

Nachdem etwa zeitgleich zu den hier beschriebenen Untersuchengen *Green*, *Russell* et al. Synthese und Struktur eines Tetrachloroaluminats mit einem sehr ähnlichen Phosphenium-Kation der Zusammensehung $[2,4\text{-}{}^tBu_2C_2P_3]^\oplus$ publizierten, wurden quantenchemische Berechnungen an den wasserstoffsubstituierten Kationen $[H_2P(CH)_2P_2]^\oplus$ und $[P(CH)_2P_2]^\oplus$ durchgeführt, um optimierte Strukturdaten und relative Energien für unterschiedliche Isomere zu ermitteln (Abb. 8.3). Im Falle des Phosphoniumkations ($[H_2P(CH)_2P_2]^\oplus$) stellt die trigonal-bipyramidale Struktur der Punktgruppe C_{2v} das absolute Minimum auf der Energiehyperfläche dar. Bemerkenswerterweise erhält man auch hier eine auf 216,8 pm verkürzt P–P Bindung, während sich die benachbarten P–C-Abstände auf 191,5 pm verlängern. Beide Werte entsprechen den kristallstrukturanalytisch ermittelten Bindungslängen. Auch in der Phosphoniumgruppe unterscheiden sich zu 178,5 pm die berechneten und die zu 179,1 pm experimentell bestimmten P–C-Abstände kaum. Zu unserer Überraschung folgt dem absoluten Energieminimum des trigonal-bipyramidalen Gerüstes ein zweites lokales Minimum, das der sogenannten Housene-Struktur der Punktgruppe C_1 zugeschrieben werden muß. Im Vergleich zur ersten Struktur weist die zweite einen Energierenunterschied von nur + 77,9 kJ mol^{-1} auf.

Beim $[P(CH)_2P_2]^\oplus$-Kation trifft man die umgekehrte Situation an: Hier stellt die pseudo-quadratisch pyramidale *nido*-Struktur (Punkt-Gruppe C_{2v}) des von *Russells* Tetrachloroaluminat(III) her bekannten Kations [181] das einzige Minimum auf der Energiehyperfläche dar. Berechnete P–P- und P–C-Bindungslängen stimmen sehr gut mit den experimentell bestimmeten Mittelwerten überein. Zwar liegt ein Phosphenium-Kation mit einem trigonal-bipyramidalen Gerüst der Punktgruppe C_{2v} energetisch um nur 35,7 kJ mol^{-1} über dem absoluten Minimum; diese Struktur stellt aber, da die Rechnung eine imaginäre Frequenz aufweist, lediglich einen Übergangszustand dar. Die offene Housene-Struktur entspricht hier weder einem Minimum noch einem Sattelpunkt auf der Energiehyperfläche.

Tabelle 8.2. Kristalldaten der 3,3-Diorganyl-1λ^3,5λ^3-diphospha-3-phosphonia-tricyclo[2.1.0.0^{2,5}]-pentan-Halogenide **2a** bis **2d.**

Verbindung[a)]	**Me/Me/Cl 2a**	**Et/Et/Cl 2b**	**Ph/^{i}Pr/Cl 2c**	**Ph/Ph/Cl 2d.1**	**Ph/Ph/Br 2d.2**
Kristallsystem	triklin	triklin	monoklin	monoklin	monoklin
Raumgruppe	$P\bar{1}$	$P\bar{1}$	$P2_1/c$	$P2_1/n$	$P2_1/n$
Z[b)]	2 + 2	4 + 8	4 + 8	4 + 4	4 + 4
R1	0,1053	0,0683	0,0627	0,0698	0,0889

[a)] Festkörperaddukte mit einem oder zwei Molekülen Dichlormethan pro Formeleinheit;

[b)] Zahl der Ionenpaare und der Dichlormethan-Moleküle in der Elementarzelle.

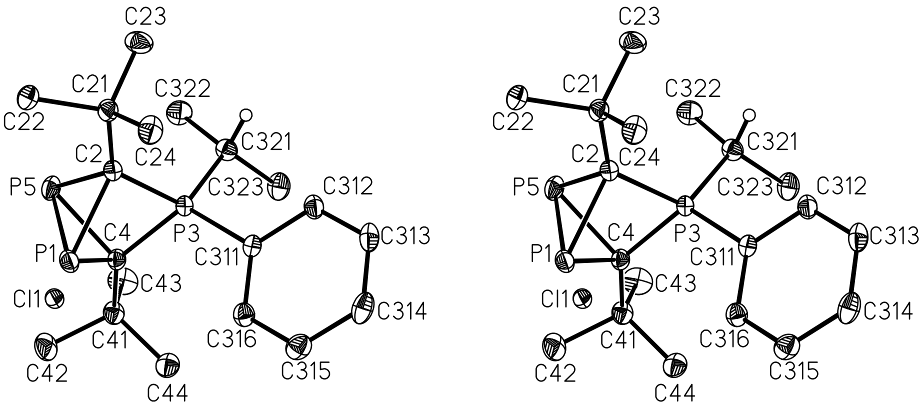

Abbildung 8.2. Stereoskopische Darstellung von Kation und Anion aus Verbindung **2c**. Die Auslenkungsellipsoide wurden auf 30 % skaliert. Auf die Darstellung der Wasserstoffatome wurde mit Ausnahme des tertiären Wasserstoffatoms der Isopropylgruppe sowie der Dichlormethan-Moleküle der Übersichtlichkeit halber verzichtet.

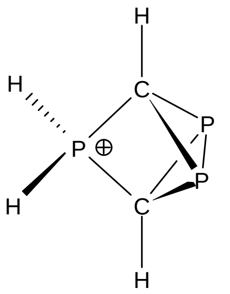

trigonal-
bipyramidale Struktur
(C_{2v})

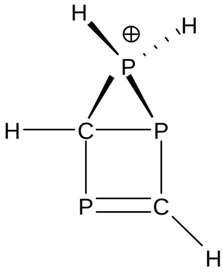

offene Housene-
Struktur
(C_1)

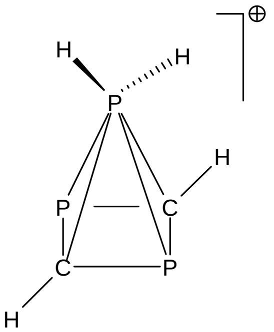

pseudo-quadratisch-
pyramidale Struktur
(C_2)

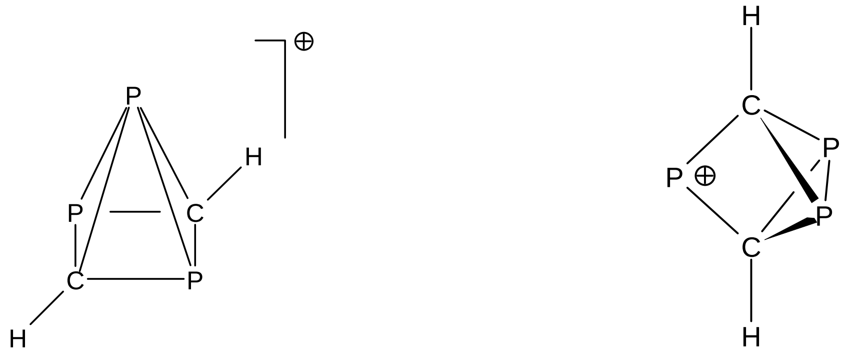

pseudo-quadratisch-
pyramidale *nido*-Struktur
(C_{2v})

trigonal-bipyramidale
Struktur
(C_{2v})

Abbildung 8.3. Strukturelle Isomere des $[H_2P(CH)_2P_2]^{\oplus}$- (oben) und des $[P(CH)_2P_2]^{\oplus}$-Kations (unten).

In der pseudo-quadratisch-pyramidalen *nido*-Struktur (Punktgruppe C_{2v}) des Phosphenium-Kations $[P(CH)_2P_2]^{\oplus}$ werden sowohl das *s*- als auch alle *p*-Orbitale des apicalen vierfach koordinieren Phosphoratoms zur Bildung von zwei P–C- und zwei P–P-Bindungen sowie zur Ausbildung eines nach außen gerichteten und mit zwei Elektronen besetzten *sp*-Hybridorbitals herangezogen. Durch Hinzufügen von zwei Wasserstoffatomen erhält man das Phosphoniumkation $[H_2P(CH)_2P_2]^{\oplus}$ mit C_2-Symmetrie, wobei nicht nur die Koordinationszahl des apicalen Phosphoratoms auf sechs steigt, sondern auch zwei Elektronen und zwei Orbitale zur sp^3-Hybridisierung und zur Bildung zweier P–H-Bindungen zur Verfügung gestellt werden müssen. Diese stehen nicht mehr für Bindungen innerhalb der *nido*-Struktur zur Verfügung; als Folge davon erhöht sich die Energie des Kations auf + 246,6 kJ mol^{-1}, und es lagert sich daraufhin in die energetisch günstigere trigonal-bipyramidale Struktur um.

Die Umsetzungen von $1\lambda^3$-Phosphaalkinen mit Dichlor(diorganylamino)arsanen bei Zimmertemperatur führen zu völlig anderen Reaktionsprodukten. Allerdings sollte man hier zunächst anmerken, dass sich die As–N- und die P–N-Bindungsdissoziationsenergie mit 582(126) und 617(21) kJ·mol^{-1} unterscheiden. Als Folge kommt es im laufe der sehr unüberichtliden und von den Zwischenstufen her bislang nicht verstandenen Umsetzung zu einer Wanderung der Dialkylamino-Gruppe vom Arsen- zum Phosphoratom. Die aus Ansätzen von 2-*tert*-Butyl-$1\lambda^3$-phosphaalkin und Dichlor(dialkylamino)arsanen im Molverhältnis 1:3 bei Zimmertemperatur in Cyclopentan isolierten $1\lambda^5,3\lambda^3,5\lambda^3$-Triphospha-dewarbenzol-Derivate (Abbildung 8.4.) fallen in hohen Ausbeuten an. Allerdings geht der Arsenanteil vermutlich als unlöslicher, polymerer Niederschlag von Arsen(I)chlorid vollständig verloren.

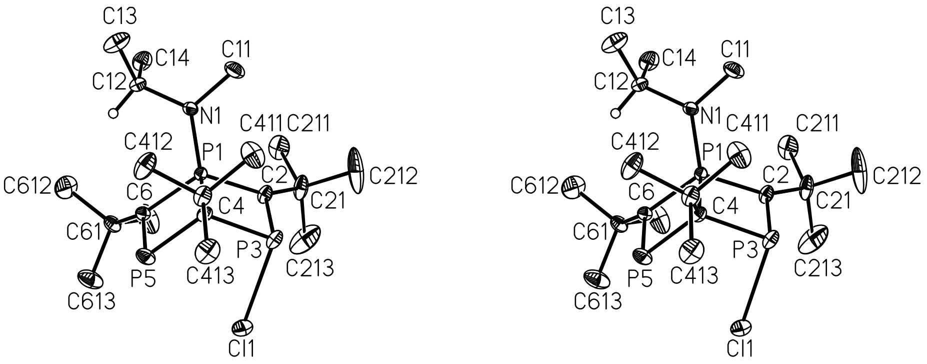

Abbildung 8.4. Stereoskopische Darstellung eines Molekülmodells von Verbindung **3c**. Die Auslenkungsellipsoide wurden auf 30% skaliert. Auf die Darstellung der Wasserstoffatome wurde mit Ausnahme des tertiären Wasserstoffatoms der Isopropylgruppe der Übersichtlichkeit halber verzichtet.

Man erhält die Verbindungen **3a** bis **3d** mit einem Dimethylamino-, Diethylamino-, Isopropylmethylamino- und Ethylmethylamino-Substituenten am Stickstoffatom als tiefrote, quaderförmige Einkristalle. Röntgenstrukturanalysen (Tabelle 8.3.) zeigen Moleküle, welche durch eine ylidische und eine herkömmliche P–C-Doppelbindung mit nahezu der gleichen Länge gekennzeichnet sind (P1$^{\oplus}$—C2$^{\ominus}_{\text{av.}}$ 172,2 pm; P5–C6$_{\text{av.}}$ 169,6 pm). Zusätzlich zu diesen zwei charakteristischen Abständen findet man eine mittlere Bindungslänge P3–C2 von nur 172,7 pm; sie ist gegenüber dem Standard für eine P–C-Einfachbindung von 183 pm stark verkürzt, während der benachbarte Phosphor–Chlor-Abstand P3–Cl1 auf 245,5 pm stark verlängert ist. Die hier angetroffene Bindungssituation macht den schnellen Austausch des Chloratoms zwischen den beiden durch zwei Bindungen getrennten Phosphoratomen P3 und P5 (Abbildung 8.5.a) – wie er aus den ^{31}P{H}-NMR-Spektren abzuleiten ist – leicht verständlich. Allerdings konnten wir bislang weder die Existenz freier Halogenid-Ionen in Lösung nachweisen noch Derivate mit separierten Ionenpaaren isolieren.

Tabelle 8.3. Kristalldaten der Dialkylamino-1$\lambda^5\sigma^4$,3$\lambda^3\sigma^3$,5$\lambda^3\sigma^2$-Triphospha-dewarbenzole, **3a** bis **3d**

Verbindung	Me$_2$N **3a**	Et$_2$N **3b**	Me^{i}PrN **3c**	MeEtN **3d**
Kristallsystem	monoklin	triklin	monoklin	monoklin
Raumgruppe	$P2_1/c$	$P\bar{1}$	$P2_1/n$	$P2_1/n$
Z	4	4	4	4
R1	0,0816	0,0598	0,0445	0,0859

Das Auftreten der ylidischen Bindung P1$^{\oplus}$—C2$^{\ominus}$ in den Verbindungen **3a** bis **3d** liefert eine einfache Erklärung, warum die angrenzende P–Cl Bindung in starken Maße verlängert ist. Wie man bereits aus dem Begriff „ylidisch“ ableiten kann, muß das *sp*^{2}-hybridisierte Kohlenstoffatom C2 als Carbanion angesprochen werden, während die positive Ladung am vierfach koordinierten Phosphoratom P1 lokalisiert ist. Eine elektronische Wechselwirkung zwischen dem freien Elektronpaar des Carbanions und dem leeren σ*(P–Cl)-Orbital im Sinne einer negativen Hyperkonjugation verkürzt nicht nur die Bindung C2–P3, sondern verlängert auch die Bindung

P3–Cl1 um bis zu 60 pm in Bezug auf einen mit 204,3 pm angegebenen Standard (Abbildung 8.5.b).

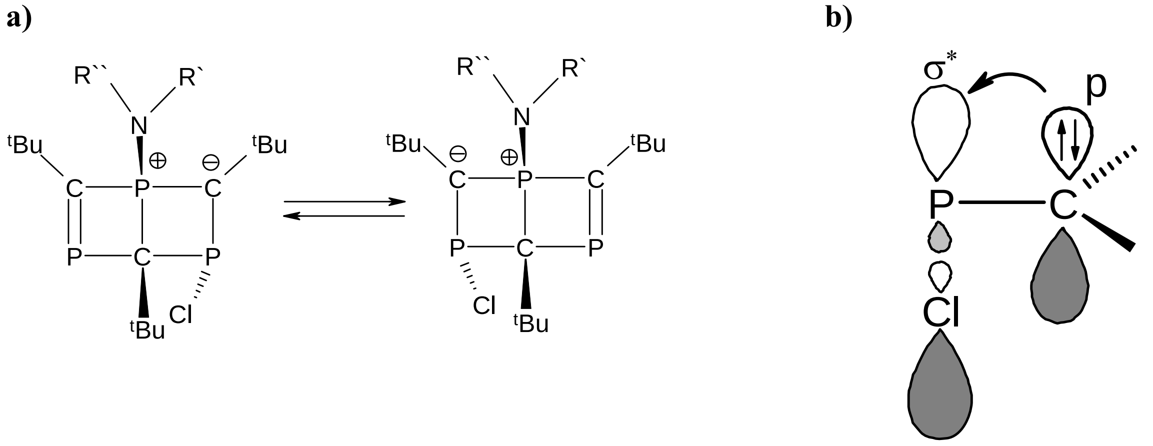

Abbildung 8.5. Schneller 1,3-Austausch des Chloratoms in den Verbindungen **3a** bis **3d** (a) als Folge der starken Verlängerung der P–Cl-Bindung (b). Die Verlängerung ist eine Folge der Wechselwirkung zwischen dem freien Elektronenpaar am Kohlenstoffatom C2 und dem σ*(P–Cl) Orbital.

Um die experimentellen Ergebnisse nachzuvollziehen und um Informationen darüber zu erhalten, wie stark Bindungslängen in einer Reihe von ähnlichen Verbindungen varierren können, und um ein besseres Verständnis des gesamten theoretischen Hintergrundes zu gewinnen, wurden quantenchemische Berechnungen zunächst an verschiedenen (Dimethylamino)methylphosphanen $Me_{3-x}(Me_2N)_xP$ ($x = 0 \rightarrow 3$) durchgeführt. Im Folgenden wurden dann diese theoretischen Untersuchungen auf unterschiede Methylenphosphorane, der Zusammensetzung $Me_{3-x}(NH2)_xP{=}CH_2$ ($x = 0 \rightarrow 3$) ausgedehnt. In diesen Verbindungen musste jedoch, um Rechenzeit zu sparen, der Dimethylamino-Substituent der Phosphane gegen die NH_2-Gruppe in den Phosphornes ausgetauscht werden. Zudem wurden die Verbindungen $H_3P{=}CH_2$, $Cl_3P{=}CH_2$ und $(H_3Si)_3P{=}CH_2$ mit in die Berechnungen eingeschlossen. Ein Vergleich der strukturellen Daten aus einer größeren Anzahl von Methylenphosphoranen mit einer, zwei oder drei Aminogruppen am Phosphor zeigen einen unerwarteten Zusammenhang zwischen der Molekülkonformation und den Bindungslängen und -winkeln. Besonders stark treten die starke Verlängerung des P–N-Abstandes, eine Aufweitung des C=P–N Winkels und eine *sp*^{3}-Hybridisierung des betreffenden Stickstoffatoms in den Vordergrund, wenn die P–N-Bindung und der Vektor des freien Elektronpaares am ylidischen Kohlenstoffatom in einer ekliptischen Position zueinander angeordnet sind.

Um den brauchbaren Bereich der Edukte zu erweitern, wurden Reaktionen der 1λ^3-Phosphaalkine mit Dichlor[4-(dimethylamino)phenyl]arsan (**4**) in Betrachtung gezogen. Diese Verbindung unterscheidet sich von einem Dichlor(diorganylamino)arsan lediglich durch Einschub einer Phenyl-Einheit in die As–N-Bindung, so dass nach dem sogenannten "Phenylogie-Prinzip" [285] einer vergleichbaren Reaktivität ausgegangen werden kann. Zusammen mit Tris[4-(dimethylamino)phenyl]arsan (**5**) konnte das Dichlor-Derivat **4** in hoher Ausbeute direkt aus *N,N*-Dimethylanilin und Arsen(III)-chlorid entsprechend einer abgewandelten Vorschrift von *Michaelis* und *Rabinerson* [289] erhalten werden.

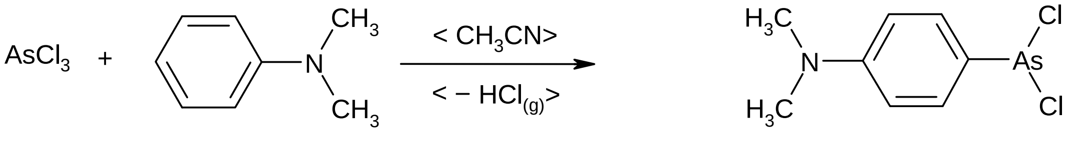

4

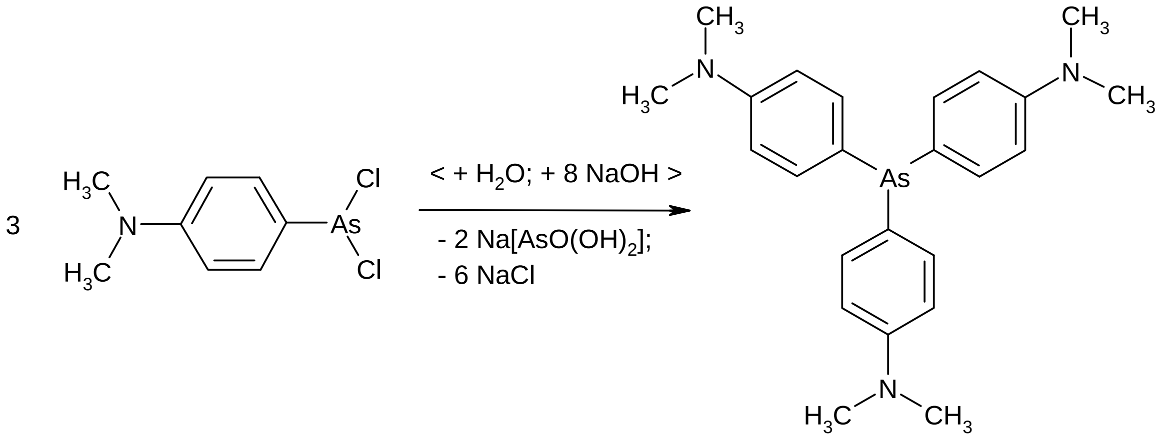

5

Dichlor[4-(dimethylamino)phenyl]arsan (**4**) kristallisiert aus Acetonitril in farblosen Plättchen. Die Röntgenstrukturanalyse ($P\bar{1}$, triklin, Z = 4; R1 = 0,0478) zeigt zwei kristallographisch unabhängige Moleküle in der asymmetrischen Einheit der Elementarzelle (Abbildung 8.7). Der mittlere As–Cl-Abstand (220,6 pm) ist gegenüber dem am Arsen(III)chlorid zu 216,1 [330] bzw. 216,2 pm [331] ermittelten Wert zwar etwas verlängert, entspricht aber der an der orthorhombischen Modifikation des Chlorbis[2,4,6-tris(trifluoromethyl)phenyl]arsans (219,2 pm) bestimmten Bindungslänge [343]. Demgegenüber lassen jedoch die mittlere As–C_{aryl}-(191,7 pm) und C_{aryl}–N-Bindungslänge (135,9 pm) auf eine unerwartet starke elektronische Wechselwirkung zwischen der Dichlorarsanyl-Gruppe, dem π-Elektronensystem des Arenringes und dem a priori freien Elektronenpaar am Stickstoffatom schließen. In beiden Molekülen weist das Stickstoffatom eine trigonal-planare Umgebung auf; die Summe der Bindungswinkel schwankt nur wenig zwischen 359,1° in **4a** und 359,9° in **4b**. Im Gegensatz zu diesen Befunden zeigt die Summe der Bindungswinkel an den Arsenatomen mit 292,7° in **4a** und 294,0° in **4b** eine eindeutig pyramidale Koordination an.

4a

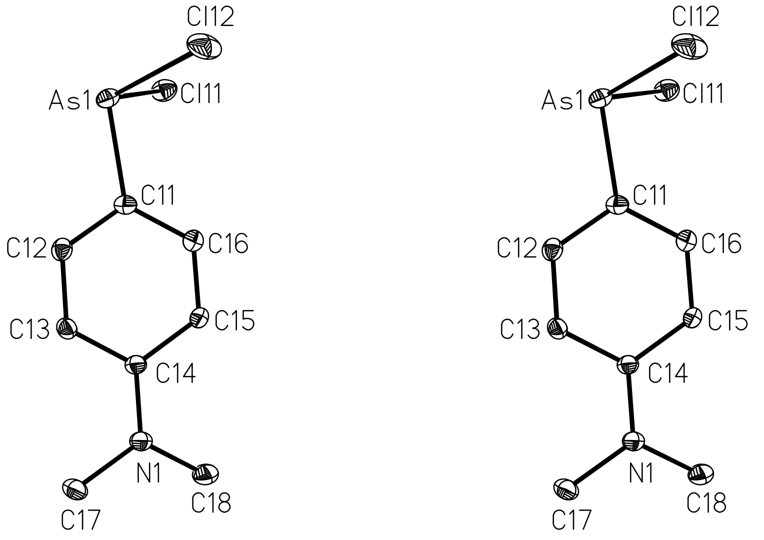

4b

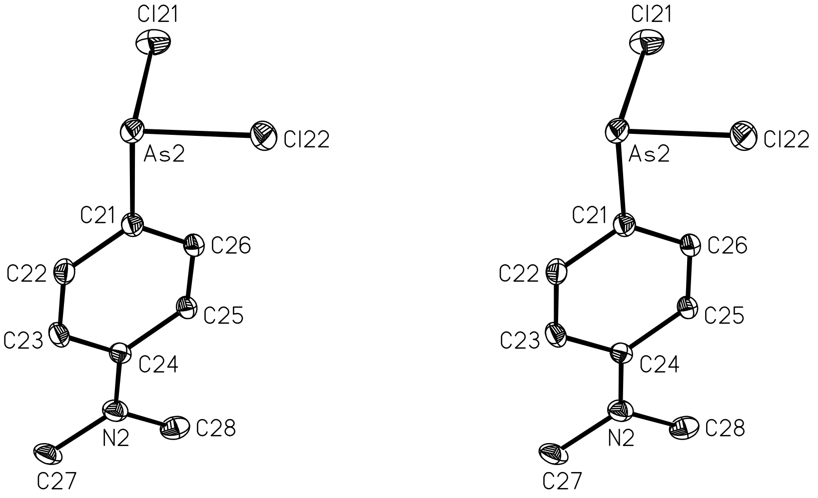

Abbildung 8.7. Stereoskopische Darstellung der beiden kristallographisch unabhängigen Moleküle von Verbindung **4.** Die Auslenkungsellipsoide wurden auf 30% skaliert. Auf die Darstellung der Wasserstoffatome wurde der Übersichtlichkeit halber verzichtet.

Über obigen Hinweis auf eine unerwartet stake elektronische Wechselwirkung und die damit verbundenen Bindungsverkürzungen hinaus erfordert die Struktur des Dichlor[4-(dimethylamino)phenyl]arsans (**4**) weitere Aufmerksamkeit und eine zusätzliche sorgfältige Diskussion, denn im Vergleich zu den auf 144 und 194 pm korrigierten Standardwerten für eine N_{sp2}–C_{sp2}- bzw. As–C_{sp2}-Bindung sind die Abstände zwischen den *ipso*-Kohlenstoff- und dem Stickstoff- sowie dem Arsenatom auf Werte von 135,9 und 191,9 pm signifikant verkürzt. Außerdem weisen verhältnismäßig große Änderungen in der Abfolge der $\mathrm{C}\overset{..}{-}\mathrm{C}$-Bindungslängen zwischen 137,1 und 142,3 pm innerhalb des Arenringes auf erhebliche Substituenteneffekte hin. Quantenchemische Berechnungen wurden an mehreren *para*-substituierten Dichlorphenylarsan-Derivaten durchgeführt, um optimierte Strukturdaten zu ermitteln und um die angeprochenen Phänomene näher zu beleuchten. In der Tat kann die bereits erwähnte Verkürzung der N–C_{ipso}-Bindung auf 135,9 pm nur teilweise auf die bekannte elektronische Wechselwirkung zwischen dem a priori nichtbindenden Elektronenpaar am Stickstoffatom und dem antibindenden π^*-Orbital der beiden benachbarten C_{ipso}–C_{ortho}–Bindungen, die dadurch um durchschnittlich 1,7 pm gegenüber den Standard (140 pm) deutlich verlängert sind, zurückgeführt werten. Auch zustätzliche strukturelle Gegebenheiten wie die den Effekt verstärkende trigonal-planare Umgebung am Stickstoffatom und eine nahezu vollständige Koplanarität des Arenringes mit der Dimethylamino-Gruppe – in beiden kristallographisch unabhängigen Molekülen **4a** und **4b** betragen die Abweichungen lediglich 12.6° bzw. 1.6°– reichen zur Erklärung nicht aus.

Eine NBO-Ladungsanalyse am Dichlor[4-(dimethylamino)phenyl]arsan-Molekül (**4**) zeigt jedoch recht unwartet, dass das dem Arsen benachbarte *ipso*-Kohlenstoffatom eine erhöhte Elektronendichte aufweist. Demzufolge kann die ungewöhnliche Verkürzung der As–C_{ipso}-Bindung im Wesentlichen auf den ebenfalls unerwartet hohen Ladungsunterschied von 1,431 und einer damit erhöhten Coulomb-Anziehung zwischen dem Arsen- und dem *ipso*-Kohlenstoffatom zurückgeführt werden. Die im Dichlor[4-(dimethylamino)phenyl]arsan (**4**) angetroffene elektronische Situation kann demnach im Sinne eines Push-Pull-Effekts insofern gut beschrieben werden, als der Dimethylamino Substituent eine negative Ladung am *ipso*-Kohlenstoffatom induziert (push) und diese Ladung durch die Dichlorarsanyl-Gruppe zusätzlich erhöht wird (pull). Unserer Ansicht nach sollte die As–C_{ipso}-Bindungslänge ein geeignetes Maß für diesen Effekt darstellen; ihr Wert sollte dabei von der Hammett-Konstanten σ_p des Substituenten abhängen. Da Strukturparameter von Dichlorphenylarsanen mit unterschiedlichen Substituenten in *para*-Position zur Cl_2As-Gruppe nicht zugänglich sind, wurden quantenchemische Berechnungen durchgeführt, um die notwendigen Daten zu erhalten.

Aus der großen Zahl geeigneter Stickstoff-Substituenten wurden vier Substituenten ausgewählt, die einen möglichst großen Bereich der Hammett-Konstanten σ_p von stark negativen bis zu stark positiven Werten abdecken. Wasserstoff dient per Definition als Substituent mit einem Bezugswert σ_p von 0,0; andere Substituenten dieser Untersuchung waren die Dimethylamino- (NMe_2; –0,83), die Hydroxylamino- (N(H)OH; –0,34), die Nitro- (NO_2; 0,78) sowie die kationische Diazoniumgruppe ($N_2^{\oplus}$; 1,91). Um jedoch die theoretischen Ergebnisse weiter zu untermauern, bot es sich an, auch Verbindungen ohne Cl_2As-Einheit wie Anilin, *N,N*-Dimethylanilin, Benzol und Nitrobenzol einzubeziehen. Untersucht wurden dabei Korrelationen zwischen den Hammett-Konstanten σ_p und molekularen Eigenschaften von Dichlorphenylarsanen 4-X_p–C_6H_4–$AsCl_2$ wie den Elementarladungen Q an den beiden *ipso*-Kohlenstoffatomen in Position 1 (As–C1) und 4 (C4–N) mit den zugehörigen Ladungsunterscheiden ΔQ sowie den

Längen der As–Cl-, As–C1- und C4–N Bindung; für fast alle Eigenschaften ließen sich hohe Korrelationskoeffizienten R^2 zwischen 0,939 und 0,998 erhalten. Darüberhinaus hat der Parameter σ_p einen starken Einfluß (R^2 = 0,947) auf die Größe des endocyclischen C–C–C-Winkels β, mit dem direkt an den Substituenten X_p gebundenen Kohlenstoffatom C4 als Spitze. Im Gegensatz dazu erweist sich die Korrelation zwischen den Konstanten σ_p und dem C–C–C-Winkel α mit dem Kohlenstoffatom C1 in der Spitze als ziemlich schwach (R^2 = 0,774).

Obwohl eine Überinterpretation von strukturellen Daten und insbesondere von Differenzwerte grundsätzlich vermieden werden muss, stimmt der auffällige Wechsel zwischen verlängerten, verkürzten und wiederum verlängerten C–C-Bindunglängen im Arenring des Dichlor[4-(dimethyl-amino)phenyl]arsan-Moleküls, wie er als Resultat aus der Kristallstrukturanalyse hervorgeht und durch quantenchemische Berechnungen betätigt wurde, mit dem sogenannten "Phenylogie-Prinzip" überein. Zusammen mit dem in unmittelbarer Beziehung damit stehen dem "Vinylogie-Prinzip" wird es als heuristische Regel in der organischen Chemie häufig angewendet. Diese Regeln beinhalten, dass ähnliche Verbindungen, die sich von einer Stammverbindung durch Einfügen einer Vinylen- oder Phenylen-Einheit in die ursprüngliche Element–Element-Bindung unterscheiden, eine nahezu identische Reaktivität wie die Stammverbindung aufweisen. Mit den hier vorliegenden Untersuchungen wurde das "Phenylogie-Prinzip" zum ersten Mal auf Bindungslängen und-winkel angewandt.

Tris[4-(dimethylamino)phenyl]arsan (**5**) ($P\overline{1}$, triklin, Z = 4; R1 = 0,0347) kristallisiert aus Chloroform in farblosen Quadern. Die Röntgenstrukturanalyse (Abbildung 8.8) ergibt die zu erwartenden Bindungslängen und -winkel am Arsenatom (As–C 194,9 pm, C–As–C 99,3°, As–C–C 121,3°) und gleichen damit weitgehend Werten ähnlicher Verbindungen wie Triphenylarsan oder substituierter Triphenylarsane. Die Winkelsummen an zwei der drei Stickstoffatomen betragen 353,6° und 356,1° und weichen damit erheblich vom dritten Wert ab (348,1°), so dass zwei nahezu planare Dimethylamino-Gruppen vorlügen, während das dritte Stickstoffatom eine zwischen trigonal-planar und trigonal-pyramidal einzustufende Koordinationsphäre aufweist.

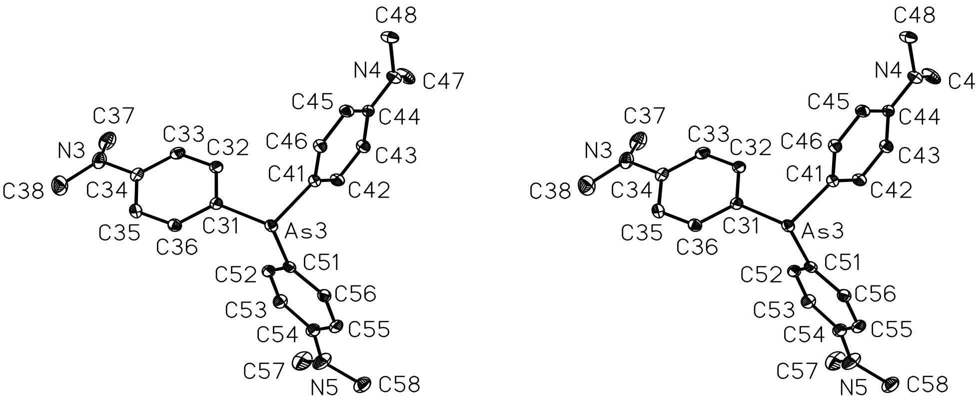

Abbildung 7.8. Stereoskopische Darstellung des Molekülmodells von Verbindung **5**. Die Auslenkungsellipsoide wurden auf 30 % skaliert. Auf die Darstellung der Wasserstoffatome wurde der Übersichtlichkeit halber verzichtet. Das hier gezeigte chirale Molekül bildet einen rechtshändigen Propeller.

Die Moleküle von Verbindung **5** zeigen einen hohen Grad an C_3-Pseudosymmetrie; die Winkelsumme am Arsenatom beträgt 298,0°. Die mittlere C_{aryl}–N-Bindungslänge (139,0 pm) weist zwar auf eine Wechselwirkung zwischen dem freien Elektronenpaar am Stickstoffatom und dem π-System des Arenringes hin; diese ist aber offensichtlich wesentlich schwächer als im Dichlor[4-(dimethylamino)phenyl]arsan (**4**).

Bislang lieferte die Reaktion von Dichlor[4-(dimethylamino)phenyl]arsan (**4**) mit $1\lambda^3$-Phosphaalkinen keine verwertbaren Resultate. Durch Variation des Lösungsmittels und der Reaktionsbedingungen sollte aber die Bildung und Isolierung kristalliner Produkte doch noch möglich sein.

9. Appendix

9.1. General Crystallographic Information

Four-circle diffractometer $P2_1$ (Syntex, Cupertino, USA) and P4 (Siemens Analytical X-ray Instruments Inc., Madison, Wisconson, USA); Mo-K_α radiation with graphite monochromator (λ = 71.073 nm); control of intensity and orientation by two measurements after a period of 98 reflections; registration of the background at the beginning and at the end of the measurement with an overall duration equal to the time of measurement; application of the software package program SHELXTL, version 5.10 from the company Bruker AXS Inc., Madison, Wisconsin [118-120] for the treatment of data, determination of structures with statistical methods and subsequent refinements: calculation of the quality factors R1 and wR2 using measured values with $F > 4\sigma\,(F_o)$; scattering factors for the neutral atoms C, Al, P, As, Cl and Br from D. T. Cromer and J. B. Man [384] and for the hydrogen atoms from R. F. Stewart, E. R. Davidson and W. T. Simpson [385]; full-matrix least squares refinement on F^2; several cycles of refinement with complete matrix and following difference Fourier synthesis; minimizing of the function $\Sigma w\,(F_o^2 - F_c^2)^2$. The quality factors are defined by the following formulas with m (number of reflections) and n (number of parameters):

$$R = R_1 = \frac{\sum \left| F_o - |F_c| \right|}{\sum F_o} \qquad wR = \sqrt{\frac{\sum w\left(F_o - |F_c|\right)^2}{\sum w F_o^2}}$$

$$wR_2 = \sqrt{\frac{\sum w\left(F_o^2 - F_c^2\right)^2}{\sum w\left(F_o^2\right)^2}} \qquad GOF = \sqrt{\frac{\sum w\left(F_o^2 - F_c^2\right)^2}{(m-n)}}$$

The anisotropic displacement parameters U_{ij} ($10^{-23}m^2$) refer to the expression: $e[-2\pi^2 (a^{*2} h^2 U_{11} + b^{*2} k^2 U_{22} + c^{*2} l^2 U_{33} + 2b^* c^* k\, l\, U_{23} + 2a^* c^* h\, l\, U_{13} + 2\, a^* b^* h\, k\, U_{12})]$; the equivalent isotropic parameters U_{eq} ($10^{-23}m^2$) are calculated from the anisotropic values applying the formula $U_{eq} = 1/3\ \Sigma_i\, \Sigma_j U_{ij}\, a_i^*\, a_j^*\, \mathbf{a_i . a_j}$ (**a** is real-cell and a^* reciprocal-cell length [386a]. Therefore the equivalent isotropic U_{eq} value is defined as one-third of the trace of the orthogonalized U_{ij} tensor [386b].

9.2. Dialkyl[1,1-bis(alkylchloroalanyl)organylmethyl]phosphine•Dialkylchloroalane(1/1) complexes 1a to 1d.

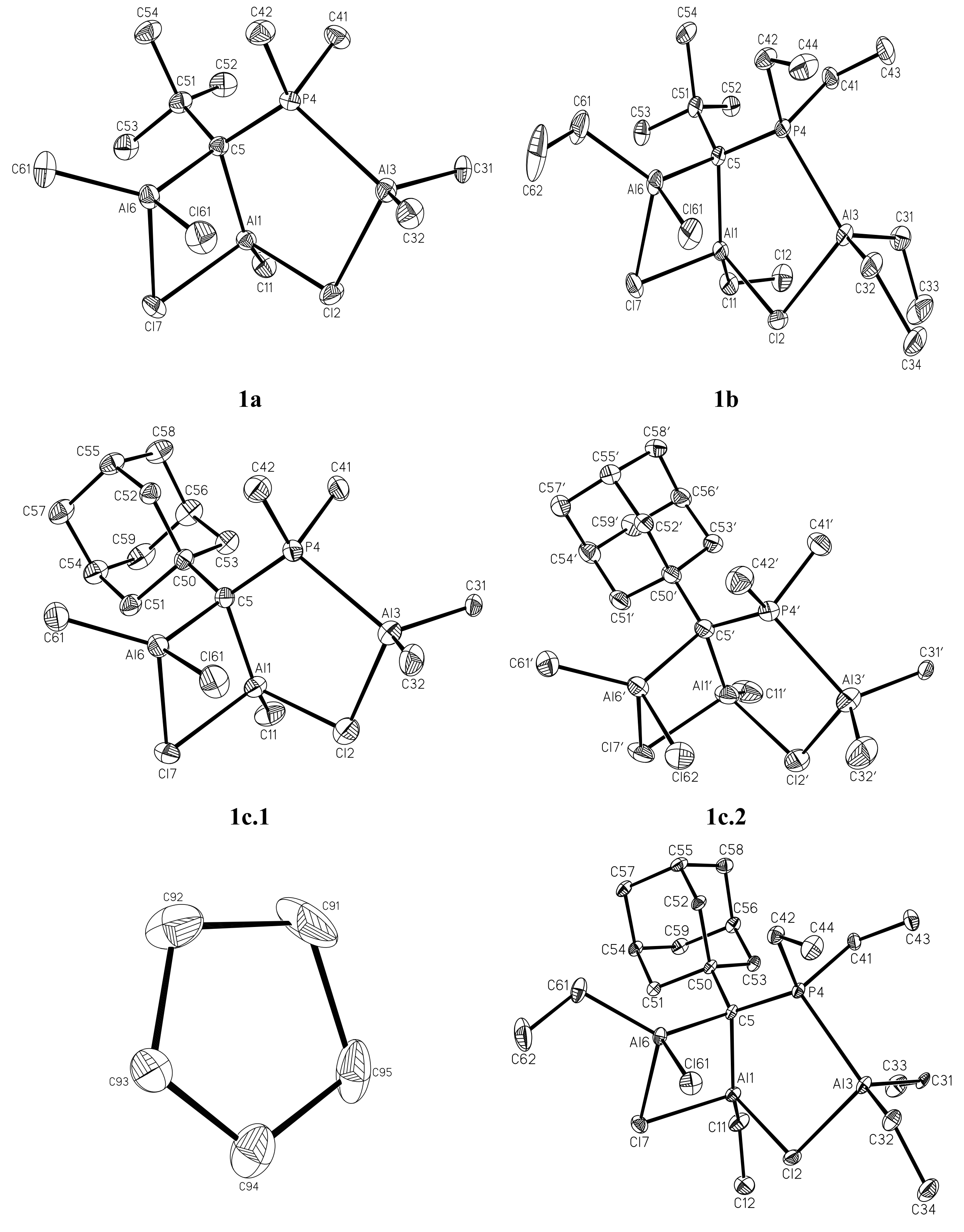

1a **1b**

1c.1 **1c.2**

cyclopentane **1d**

Figure 9.2.1. Molecular structures of **1a-1d**. Thermal ellipsoids are at 30% probability and at 5% for only co-crystallizing cyclopentane. Hydrogen atoms are omitted for clarity.

Table 9.2.1. Atomic Coordinates and Equivalent Isotropic Displacement Parameters as well as Anisotropic Displacement Parameters, with Estimated Standard Deviations in Parentheses

Parameters for 1a

Atom	$X/a\cdot10^4$	$Y/b\cdot10^4$	$Z/c\cdot10^4$	U_{eq}	U_{11}	U_{22}	U_{33}	U_{23}	U_{13}	U_{12}
Al1	7851(1)	3276(1)	2210(1)	26(1)	22(1)	28(1)	28(1)	-2(1)	7(1)	3(1)
Cl2	6061(1)	2972(1)	77(1)	39(1)	27(1)	43(1)	45(1)	-21(1)	5(1)	3(1)
Al3	3655(1)	3249(1)	481(1)	27(1)	23(1)	27(1)	30(1)	-1(1)	2(1)	2(1)
P4	4773(1)	3809(1)	2647(1)	24(1)	24(1)	26(1)	24(1)	-1(1)	9(1)	2(1)
C5	6890(3)	3856(1)	3038(3)	23(1)	24(1)	26(1)	20(1)	-2(1)	4(1)	0(1)
Al6	7464(1)	4305(1)	1359(1)	29(1)	29(1)	29(1)	28(1)	2(1)	7(1)	-4(1)
Cl7	9324(1)	3727(1)	828(1)	36(1)	29(1)	46(1)	38(1)	1(1)	16(1)	0(1)
C11	9042(3)	2718(1)	3231(4)	42(1)	35(1)	40(1)	53(2)	10(1)	12(1)	10(1)
C31	2917(3)	2662(1)	1485(3)	30(1)	28(1)	23(1)	37(1)	3(1)	3(1)	-7(1)
C32	2399(3)	3529(1)	-1471(3)	36(1)	33(1)	40(2)	32(1)	1(1)	1(1)	2(1)
C41	4016(4)	3564(1)	4304(4)	41(1)	41(2)	51(2)	36(1)	2(1)	21(1)	-1(1)
C42	3783(4)	4406(1)	2382(4)	39(1)	36(1)	33(1)	46(2)	-3(1)	9(1)	12(1)
C51	7840(3)	3991(1)	4787(3)	32(1)	34(1)	38(1)	22(1)	-5(1)	1(1)	1(1)
C52	7740(4)	3597(1)	6033(3)	44(1)	50(2)	55(2)	25(1)	4(1)	3(1)	7(2)
C53	9609(3)	4044(1)	4809(4)	42(1)	35(1)	53(2)	32(1	-6(1)	4(1)	0(1)
C54	7275(4)	4486(1)	5355(4)	43(1)	49(2)	45(2)	33(1)	-16(1	5(1)	1(1)
Cl61	5730(1)	4295(1)	-853(1)	45(1)	48(1)	51(1)	33(1)	7(1)	6(1)	0(1)
C61	8479(5)	4944(1)	1696(5)	48(1)	49(2)	35(2)	58(2)	4(2)	7(2)	-12(1)

Atom	$X/a\cdot10^4$	$Y/b\cdot10^4$	$Z/c\cdot10^4$	U_{eq}	Atom	$X/a\cdot10^4$	$Y/b\cdot10^4$	$Z/c\cdot10^4$	U_{eq}
H111	8346	2499	3656	63	H423	4120(50)	4624(16)	3190(50)	75(13)
H112	9897	2832	4104	63	H521	8520(40)	3674(12)	7080(40)	53(10)
H113	9487	2539	2448	63	H522	6690(40)	3603(12)	6160(40)	43(9)
H311	2568	2408	673	45	H523	7910(50)	3331(14)	5650(50)	65(12)
H312	2037	2755	1955	45	H531	10030(40)	3724(11)	4560(40)	36(8)
H313	3784	2534	2321	45	H532	9810(40)	4305(13)	4130(40)	51(10)
H321	1580(60)	3349(18)	-2000(60)	105(17)	H533	10150(40)	4118(13)	5870(50)	59(10)
H322	2000(40)	3856(14)	-1330(50)	61(11)	H541	7850(50)	4611(14)	6370(50)	65(11)
H323	2970(50)	3588(16)	-2170(50)	80(14)	H542	7300(40)	4790(11)	4550(40)	39(8)
H411	4220(40)	3786(12)	5160(40)	43(9)	H543	6150(40)	4483(11)	5390(40)	39(8)
H412	2850(40)	3555(11)	3930(40)	41(8)	H611	9390(60)	4958(18)	2390(70)	102(18)
H413	4380(40)	3268(13)	4700(40)	51(10)	H612	8800(50)	5021(16)	910(50)	73(14)
H421	4020(50)	4577(15)	1550(50)	67(12)	H613	7830(50)	5167(16)	1870(50)	78(14)
H422	2660(40)	4344(11)	2070(40)	41(8)					

Parameters for 1b

Atom	$X/a\cdot10^4$	$Y/b\cdot10^4$	$Z/c\cdot10^4$	U_{eq}	U_{11}	U_{22}	U_{33}	U_{23}	U_{13}	U_{12}
Al1	8260(1)	2722(1)	-163(1)	25(1)	26(1)	27(1)	23(1)	1(1)	3(1)	1(1)
Cl2	9619(1)	3651(1)	550(1)	33(1)	31(1)	34(1)	33(1)	-2(1)	7(1)	-10(1)
Al3	7870(1)	3903(1)	1483(1)	26(1)	31(1)	20(1)	26(1)	1(1)	0(1)	-3(1)
P4	6266(1)	2707(1)	1304(1)	21(1)	23(1)	21(1)	20(1)	0(1)	0(1)	-2(1)
C5	6891(2)	2141(1)	514(1)	21(1)	23(1)	20(1)	21(1)	0(1)	-1(1)	0(1)
Al6	8791(1)	1466(1)	918(1)	29(1)	30(1)	23(1)	34(1)	1(1)	-6(1)	5(1)
Cl7	10255(1)	1794(1)	-121(1)	38(1)	30(1)	41(1)	44(1)	-4(1)	7(1)	9(1)
C11	7914(3)	3159(2)	-1186(1)	36(1)	42(1)	44(1)	24(1)	5(1)	6(1)	2(1)
C12	6880(5)	3896(2)	-1248(2)	51(1)	67(2)	44(2)	43(2)	17(1)	2(1)	6(2)
C31	6584(4)	4771(2)	1006(2)	43(1)	41(2)	28(1)	60(2)	16(1)	7(1)	6(1)
C32	9204(3)	4084(2)	2438(1)	34(1)	41(1)	31(1)	29(1)	-2(1)	-2(1)	-9(1)
C33	7537(5)	5431(2)	704(3)	61(1)	68(2)	34(2)	80(3)	23(2)	-8(2)	-5(2)
C34	10121(4)	4860(2)	2454(2)	44(1)	53(2)	34(1)	43(1)	-9(1)	1(1)	-14(1)
C41	4207(3)	3105(2)	1158(1)	32(1)	23(1)	35(1)	37(1)	-6(1)	3(1)	2(1)
C42	6119(3)	2074(2)	2150(1)	32(1)	41(1)	31(1)	23(1)	5(1)	3(1)	-9(1)
C43	3722(4)	3541(2)	1860(2)	45(1)	36(1)	52(2)	48(2)	-16(1)	10(1)	6(1)
C44	6788(4)	2434(2)	2901(1)	43(1)	54(2)	52(2)	21(1)	5(1)	0(1)	-19(1)
C51	5566(3)	1641(1)	32(1)	26(1)	30(1)	24(1)	23(1)	-2(1)	-3(1)	-1(1)

C52	4382(3)	2153(2)	-462(1)	31(1)	27(1)	36(1)	28(1)	0(1)	-5(1)	-3(1)
C53	6366(3)	1112(2)	-532(2)	35(1)	42(1)	31(1)	31(1)	-8(1)	-5(1)	1(1)
C54	4611(3)	1113(2)	535(2)	35(1)	40(1)	30(1)	35(1)	0(1)	-4(1)	-13(1)
Cl61	10258(1)	2026(1)	1830(1)	41(1)	39(1)	40(1)	41(1)	2(1)	-15(1)	-1(1)
C61	8820(5)	329(2)	1056(2)	53(1)	58(2)	27(1)	72(2)	7(1)	-8(2)	8(1)
C62	10299(8)	13(2)	1489(3)	84(2)	124(4)	38(2)	82(3)	-7(2)	-45(3)	34(2)

Atom	X/a·10^4	Y/b·10^4	Z/c·10^4	U_{eq}	Atom	X/a·10^4	Y/b·10^4	Z/c·10^4	U_{eq}
H111	7440(40)	2787(18)	-1511(17)	35(7)	H432	2680(50)	3770(20)	1800(20)	68(11)
H112	8980(40)	3290(20)	-1339(18)	44(9)	H433	4540(40)	3920(20)	2030(20)	51(10)
H121	6750(50)	4120(30)	-1760(20)	73(12)	H441	7920(30)	2585(17)	2892(15)	30(7)
H122	7420(40)	4290(20)	-940(20)	53(10)	H442	6520(50)	2100(30)	3310(20)	75(12)
H123	5670(60)	3820(30)	-1140(30)	81(13)	H443	6200(50)	2930(30)	3010(20)	76(13)
H311	5760(60)	4570(30)	610(30)	103(17)	H521	3620(30)	1849(17)	-771(16)	34(7)
H312	6170(60)	4890(30)	1260(30)	76(17)	H522	4950(40)	2400(20)	-790(20)	50(10)
H321	9920(40)	3660(20)	2529(18)	44(8)	H523	3800(40)	2470(20)	-140(20)	51(9)
H322	8460(40)	4070(19)	2858(18)	38(8)	H531	6900(30)	1407(17)	-892(16)	30(7)
H331	8180(60)	5190(30)	230(30)	115(18)	H532	5510(40)	800(20)	-788(18)	49(9)
H332	6780(70)	5890(40)	530(30)	140(20)	H533	7110(40)	810(20)	-272(19)	46(9)
H333	8510(50)	5620(30)	990(20)	72(13)	H541	5290(30)	759(17)	807(16)	33(7)
H341	10810(40)	4920(20)	2020(20)	49(9)	H542	3870(40)	857(19)	233(18)	44(8)
H342	9370(40)	5290(20)	2440(20)	58(10)	H543	4000(40)	1410(20)	890(20)	59(10)
H343	10880(50)	4930(30)	2960(30)	80(13)	H611	8650(60)	20(30)	590(30)	104(16)
H411	3470(30)	2681(17)	1046(16)	35(7)	H612	8010(70)	150(30)	1260(30)	120(20)
H412	4190(30)	3485(17)	712(16)	32(7)	H621	10680(80)	230(40)	1950(40)	140(20)
H421	6730(30)	1598(17)	2056(15)	26(7)	H622	10300(60)	-560(30)	1530(30)	107(17)
H422	4910(40)	1909(19)	2166(18)	40(8)	H623	11250(120)	200(60)	1260(60)	260(60)
H431	3740(50)	3210(30)	2260(30)	80(14)					

Parameters for 1c•C$_5$H$_{10}$(2/1)

Atom	X/a·10^4	Y/b·10^4	Z/c·10^4	U_{eq}	U_{11}	U_{22}	U_{33}	U_{23}	U_{13}	U_{12}
Al1	999(1)	3427(1)	1653(1)	36(1)	42(1)	36(1)	35(1)	-18(1)	-3(1)	-7(1)
Cl2	2465(1)	2852(1)	850(1)	57(1)	61(1)	60(1)	61(1)	-35(1)	16(1))	-21(1)
Al3	3860(1)	3726(1)	777(1)	39(1)	42(1)	36(1)	41(1)	-20(1)	6(1)	-8(1)
P4	2832(1)	4607(1)	1733(1)	31(1)	32(1)	29(1)	30(1)	-11(1)	5(1)	-8(1)
C5	1540(4)	4162(3)	2286(3)	27(1)	26(2)	28(2)	28(2)	-12(2)	1(2)	-6(2)
Al6	1965(1)	2967(1)	3372(1)	31(1)	33(1)	28(1)	30(1)	-9(1)	2(1)	-5(1)
Cl7	893(1)	2091(1)	2941(1)	41(1)	47(1)	32(1)	46(1)	-14(1)	1(1)	-14(1)
C11	-294(6)	3657(5)	956(5)	56(2)	62(4)	57(4)	61(4)	-30(3)	-24(3)	-5(3)
C31	3855(3)	4643(3)	-543(2)	13(1)	19(2)	17(2)	0(1)	4(1)	6(1)	-3(1)
C32	5251(5)	2884(4)	1145(4)	48(1)	49(3)	46(3)	45(3)	-19(3)	15(3)	-5(3)
C41	2659(5)	5835(4)	946(4)	44(1)	51(3)	34(3)	42(3)	-11(2)	13(2)	-13(2)
C42	3716(5)	4674(4)	2549(4)	43(1)	34(3)	53(3)	50(3)	-26(3)	1(2)	-12(2)
C50	520(4)	4846(3)	2565(3)	30(1)	26(2)	31(2)	31(2)	-14(2)	0(2)	-2(2)
C51	-421(4)	4271(4)	3114(4)	36(1)	29(2)	45(3)	41(3)	-24(2)	4(2)	-9(2)
C52	855(4)	5338(3)	3170(3)	31(1)	29(2)	32(2)	34(2)	-15(2)	1(2)	-4(2)
C53	-4(5)	5641(4)	1718(4)	39(1)	39(3)	40(3)	39(3)	-15(2)	-9(2)	3(2)
C54	-1442(4)	4907(4)	3397(4)	44(1)	26(2)	59(4)	57(4)	-34(3)	6(2)	-8(2)
C55	-162(4)	5963(4)	3469(4)	38(1)	34(3)	39(3)	48(3)	-25(2)	-3(2)	2(2)
C56	-1017(5)	6275(4)	2010(4)	48(1)	38(3)	48(3)	56(4)	-21(3)	-19(3)	15(2)
C57	-1059(5)	5349(4)	4018(4)	46(1)	32(3)	59(4)	55(3)	-36(3)	3(2)	-2(2)
C58	-643(5)	6744(4)	2603(4)	48(1)	44(3)	44(3)	61(4)	-30(3)	-11(3)	9(2)
C59	-1915(5)	5671(5)	2547(5)	53(2)	28(3)	72(4)	73(4)	-47(4)	-10(3)	9(3)
Cl61	3613(1)	2232(1)	3130(1)	48(1)	40(1)	41(1)	51(1)	-10(1)	2(1)	4(1)

C61	1730(5)	2818(4)	4668(4)	44(1)	50(3)	42(3)	34(3)	-11(2)	2(2)	-7(2)
Al1'	5738(2)	2893(1)	6106(1)	45(1)	40(1)	33(1)	69(1)	-23(1)	-13(1)	-2(1)
Cl2'	4961(1)	3109(1)	7448(1)	59(1)	49(1)	47(1)	87(1)	-37(1)	6(1)	-3(1)
Al3'	4827(2)	1575(1)	8459(1)	50(1)	45(1)	51(1)	58(1)	-30(1)	5(1)	-2(1)
P4'	5980(1)	778(1)	7480(1)	37(1)	34(1)	35(1)	46(1)	-20(1)	2(1)	-7(1)
C5'	6571(4)	1582(4)	6413(4)	37(1)	28(2)	33(3)	54(3)	-21(2)	-1(2)	-6(2)
Al6'	7933(1)	1981(1)	6716(1)	38(1)	32(1)	36(1)	53(1)	-21(1)	-3(1)	-9(1)
Cl7'	7307(1)	3606(1)	5913(1)	50(1)	57(1)	33(1)	68(1)	-19(1)	-12(1)	-14(1)
C11'	4700(7)	3647(5)	5187(6)	75(2)	70(5)	47(4)	115(7)	-33(4)	-42(5)	8(3)
C31'	3246(5)	1440(5)	8458(6)	58(2)	31(3)	48(3)	93(5)	-28(4)	7(3)	-3(3)
C32'	5386(7)	1365(7)	9639(5)	75(2)	79(5)	100(6)	58(4)	-58(4)	11(4)	-19(5)
C41'	5020(5)	68(4)	7349(4)	50(1)	57(4)	48(3)	52(3)	-21(3)	6(3)	-24(3)
C42'	7043(5)	-168(4)	8124(4)	50(1)	51(3)	43(3)	49(3)	-12(3)	-3(3)	1(3)
C50'	6881(4)	1261(3)	5545(4)	33(1)	31(2)	27(2)	42(3)	-12(2)	-4(2)	-7(2)
C51'	7489(5)	2014(4)	4762(4)	40(1)	40(3)	30(3)	51(3)	-12(2)	-5(2)	-12(2)
C52'	7663(4)	302(3)	5760(3)	31(1)	31(2)	30(2)	34(2)	-12(2)	-1(2)	-9(2)
C53'	5838(4)	1172(4)	5140(4)	37(1)	33(3)	35(3)	47(3)	-18(2)	-3(2)	-7(2)
C54'	7832(5)	1724(4)	3913(4)	45(1)	50(3)	41(3)	43(3)	-10(2)	0(3)	-17(3)
C55'	8007(4)	20(4)	4896(4)	36(1)	36(3)	33(3)	38(3)	-14(2)	-2(2)	-4(2)
C56'	6166(5)	888(4)	4282(4)	41(1)	37(3)	40(3)	51(3)	-19(3)	-8(2)	-9(2)
C57'	8625(5)	783(4)	4160(4)	41(1)	37(3)	46(3)	45(3)	-20(3)	2(2)	-11(2)
C58'	6949(5)	-69(4)	4529(4)	40(1)	46(3)	38(3)	45(3)	-22(2)	0(2)	-11(2)
C59'	6773(5)	1646(4)	3532(4)	47(1)	52(3)	44(3)	43(3)	-10(3)	-11(3)	-8(3)
Cl62	7760(1)	2019(1)	8092(1)	59(1)	57(1)	71(1)	61(1)	-35(1)	-2(1)	-17(1)
C61'	9502(5)	1611(5)	6377(5)	51(2)	36(3)	63(4)	64(4)	-33(3)	-2(3)	-11(3)
C91	8267(14)	1170(20)	713(17)	245(13)	104(12)	380(40)	240(30)	-130(30)	-102(15)	63(17)
C92	8677(16)	470(16)	1499(11)	181(8)	160(16)	290(20)	114(11)	-70(14)	3(11)	-103(17)
C93	9847(13)	570(14)	1443(12)	182(8)	121(12)	217(19)	147(14)	23(13)	-46(10)	-32(12)
C94	10254(17)	1102(13)	616(11)	169(7)	220(20)	164(15)	114(12)	-28(11)	-25(13)	-49(14)
C95	9370(20)	1557(11)	97(12)	190(10)	290(30)	112(11)	175(16)	4(10)	-147(19)	-50(14)

Atom	$X/a\cdot10^4$	$Y/b\cdot10^4$	$Z/c\cdot10^4$	U_{eq}	Atom	$X/a\cdot10^4$	$Y/b\cdot10^4$	$Z/c\cdot10^4$	U_{eq}
H11A	-258	4231	411	83	H31F	3055	1630	7823	87
H11B	-990	3741	1340	83	H32D	4753	1479	10069	113
H11C	-286	3113	765	83	H32E	5919	1803	9547	113
H31A	4162	4294	-961	19	H32F	5765	709	9890	113
C31B	4320	5130	-628	19	H41D	5418	-335	7004	75
C31C	3082	4947	-678	19	H41E	4386	489	7017	75
H32A	5806	2970	613	72	H41F	4739	-332	7957	75
H32B	5110	2224	1391	72	H42D	7378	-571	7762	75
H32C	5540	3031	1620	72	H42E	6687	-554	8707	75
H41A	2287	6254	1283	66	H42F	7632	116	8247	75
H41B	2199	5900	458	66	H51C	6983	2631	4590	48
H41C	3400	6011	676	66	H51D	8168	2097	4985	48
H42A	3338	5153	2815	65	H52C	7276	-195	6237	37
H42B	4440	4850	2230	65	H52D	8348	342	6008	37
H42C	3845	4054	3040	65	H53C	5426	688	5612	45
H51A	-664	3959	2736	44	H53D	5327	1787	4977	45
H51B	-125	3767	3672	44	H54B	8229	2223	3432	54
H52A	1183	4848	3721	37	H55B	8517	-604	5062	43
H52B	1437	5735	2822	37	H56B	5471	831	4048	49
H53A	573	6037	1353	47	H57C	9307	843	4399	50
H53B	-249	5349	1325	47	H57D	8861	604	3608	50
H54A	-2035	4511	3747	53	H58C	6557	-566	5002	48
H55A	84	6266	3862	46	H58D	7159	-254	3979	48
C56A	-1331	6778	1450	57	H59C	6270	2265	3357	56
H57A	-1708	5743	4228	55	H59D	6985	1463	2980	56
H57B	-744	4841	4565	55	H61D	9635	939	6441	76
H58A	-1292	7160	2783	58	H61E	9973	1711	6780	76
H58B	-61	7139	2250	58	H61F	9695	1997	5738	76

H59A	-2577	6076	2729	64	H91A	7752	1689	868	294
H59B	-2161	5374	2158	64	H91B	7858	908	386	294
H61A	2160	3236	4787	65	H92A	8606	-167	1508	217
H61B	1986	2157	5039	65	H92B	8264	565	2058	217
H61C	928	2988	4830	65	H93A	9937	855	1898	218
H11D	4108	3283	5215	112	H93B	10304	-70	1617	218
H11E	5107	3809	4576	112	H94A	10781	696	321	203
H11F	4361	4231	5305	112	H94B	10666	1572	676	203
H31D	2753	1846	8760	87	H95A	9472	1413	-477	228
H31E	3145	776	8789	87	H95B	9300	2253	-64	228

Parameters for 1d

Atom	X/a·10^4	Y/b·10^4	Z/c·10^4	U_{eq}	U_{11}	U_{22}	U_{33}	U_{23}	U_{13}	U_{12}
Al1	7709(1)	9391(1)	6398(1)	19(1)	18(1)	16(1)	25(1)	4(1)	10(1)	1(1)
Cl2	9435(1)	8775(1)	6363(1)	26(1)	22(1)	32(1)	28(1)	5(1)	14(1)	6(1)
Al3	10297(1)	8319(1)	7913(1)	20(1)	13(1)	21(1)	29(1)	1(1)	9(1)	3(1)
P4	8399(1)	8360(1)	8285(1)	16(1)	11(1)	16(1)	20(1)	3(1)	5(1)	1(1)
C5	7169(3)	8867(2)	7350(2)	15(1)	9(1)	14(2)	21(2)	0(1)	5(1)	0(1)
Al6	6194(1)	8072(1)	6362(1)	18(1)	15(1)	15(1)	23(1)	-1(1)	4(1)	-1(1)
Cl7	6229(1)	8807(1)	5092(1)	26(1)	28(1)	28(1)	20(1)	3(1)	6(1)	-1(1)
C11	7844(5)	10448(2)	6054(3)	33(1)	34(2)	23(2)	50(3)	8(2)	23(2)	1(2)
C12	8454(5)	10576(3)	5329(4)	39(1)	46(3)	37(3)	38(2)	1(2)	19(2)	-21(2)
C31	11351(3)	9189(2)	8611(2)	19(1)	10(2)	21(2)	29(2)	-4(1)	9(1)	-8(1)
C32	11063(4)	7354(2)	7798(3)	25(1)	20(2)	22(2)	36(2)	0(2)	11(2)	4(2)
C33	10863(5)	9994(3)	8302(4)	41(1)	37(3)	31(2)	60(3)	-7(2)	23(2)	-8(2)
C34	12136(4)	7439(3)	7432(4)	36(1)	22(2)	42(3)	46(3)	-10(2)	16(2)	3(2)
C41	9031(3)	8843(2)	9452(2)	21(1)	17(2)	26(2)	18(2)	-2(1)	3(1)	1(2)
C42	7775(3)	7473(2)	8608(3)	22(1)	19(2)	20(2)	27(2)	5(1)	8(1)	-1(1)
C43	10007(4)	8347(3)	10207(3)	31(1)	24(2)	38(2)	23(2)	4(2)	1(2)	5(2)
C44	8632(4)	6784(2)	8768(3)	32(1)	28(2)	23(2)	45(2)	9(2)	13(2)	3(2)
C50	6255(3)	9385(2)	7644(2)	16(1)	12(2)	15(2)	23(2)	2(1)	8(1)	0(1)
C51	5169(3)	9685(2)	6742(2)	18(1)	17(2)	17(2)	21(2)	0(1)	8(1)	0(1)
C52	5650(3)	8968(2)	8259(2)	19(1)	16(2	18(2)	25(2)	5(1)	9(1)	-1(1)
C53	6935(3)	10108(2)	8186(2)	19(1)	16(2)	16(2)	25(2)	-1(1)	7(1)	-1(1)
C54	4258(3)	10200(2)	7005(3)	21(1)	15(2)	21(2)	28(2)	7(1)	8(1)	6(1)
C55	4756(3)	9489(2)	8525(3)	23(1)	20(2)	25(2)	30(2)	6(1)	15(2)	4(2)
C56	6035(3)	10625(2)	8453(3)	23(1)	21(2)	19(2)	30(2)	-3(1)	11(2)	0(1)
C57	3689(3)	9757(2)	7617(3)	23(1)	16(2)	21(2)	34(2)	4(2)	12(2)	2(2)
C58	5488(4)	10180(2)	9073(3)	26(1)	26(2)	27(2)	29(2)	0(2)	14(2)	4(2)
C59	4966(4)	10888(2)	7551(3)	25(1)	24(2)	17(2)	36(2)	5(2)	14(2)	7(2)
Cl61	7362(1)	7136(1)	6255(1)	31(1)	32(1)	23(1)	37(1)	-1(1)	13(1)	8(1)
C61	4463(4)	7719(2)	6053(3)	31(1)	20(2)	21(2)	43(2)	1(2)	4(2)	-6(2)
C62	3916(6)	7357(4)	5067(4)	57(2)	49(3)	57(4)	44(3)	-2(3)	-8(2)	-26(3)

Atom	X/a·10^4	Y/b·10^4	Z/c·10^4	U_{eq}	Atom	X/a·10^4	Y/b·10^4	Z/c·10^4	U_{eq}
H111	8300(50)	10750(30)	6680(40)	50(15)	H442	8270(50)	6370(30)	8870(30)	41(13)
H112	7130(60)	10640(30)	5830(40)	63(19)	H443	9340(60)	6980(30)	9210(40)	57(17)
H121	8450(50)	11120(30)	5140(30)	40(13)	H511	4740(30)	9300(20)	6330(20)	8(8)
H122	9330(60)	10410(30)	5610(40)	51(15)	H512	5520(40)	9950(20)	6360(20)	13(9)
H123	8130(50)	10360(30)	4800(40)	49(15)	H521	6320(40)	8790(20)	8850(30)	16(9)
H311	11484	9135	9290	23	H522	5180(40)	8540(20)	7930(30)	23(10)
H312	12184	9142	8560	23	H531	7630(40)	9960(20)	8800(30)	25(11)
H321	10390(50)	6970(30)	7320(40)	56(16)	H532	7310(40)	10360(20)	7820(20)	13(9)
H322	11350(50)	7180(30)	8430(40)	41(13)	H541	3650(40)	10390(20)	6460(30)	14(9)
H331	11370(50)	10460(30)	8630(30)	48(14)	H551	4390(40)	9210(20)	8950(30)	27(11)
H332	10660(50)	10080(30)	7630(40)	58(17)	H561	6500(40)	11070(20)	8830(20)	14(9)
H333	10130(60)	10040(30)	8420(40)	61(17)	H571	3220(40)	9360(20)	7310(30)	14(9)
H341	11800(50)	7620(30)	6780(40)	47(14)	H572	3090(40)	10080(20)	7730(30)	29(11)
H342	12420(60)	6960(40)	7340(40)	66(18)	H581	4930(40)	10510(30)	9270(30)	32(12)

H343	12750(60)	7710(30)	7850(40)	60(17)	H582	6140(50)	10000(30)	9720(40)	49(14)
H411	9420(40)	9340(20)	9390(30)	21(10)	H591	5270(40)	11190(20)	7150(30)	28(11)
H412	8330(50)	8920(30)	9660(30)	39(13)	H592	4380(40)	11210(30)	7710(30)	33(12)
H421	7610(40)	7550(20)	9170(30)	19(10)	H611	4490(50)	7360(30)	6630(40)	43(13)
H422	6970(40)	7330(30)	8070(30)	35(12)	H612	3990(50)	8110(30)	6090(30)	38(13)
H431	10410(50)	8650(30)	10750(40)	43(14)	H621	3770(50)	7720(30)	4530(40)	59(17)
H432	9620(50)	7850(30)	10360(40)	49(14)	H622	4410(60)	6900(40)	4990(40)	70(20)
H433	10610(50)	8170(30)	10020(40)	49(15)	H623	2930(70)	7130(40)	4880(50)	90(20)
H441	8790(40)	6650(30)	8160(30)	35(12)					

9.3. 2,4-di-tert-Butyl-3,3-diorganyl-1λ^3,5λ^3-diphospha-3-phosphonia-tricycle[2.1.0.0^{2,5}]pentane halides

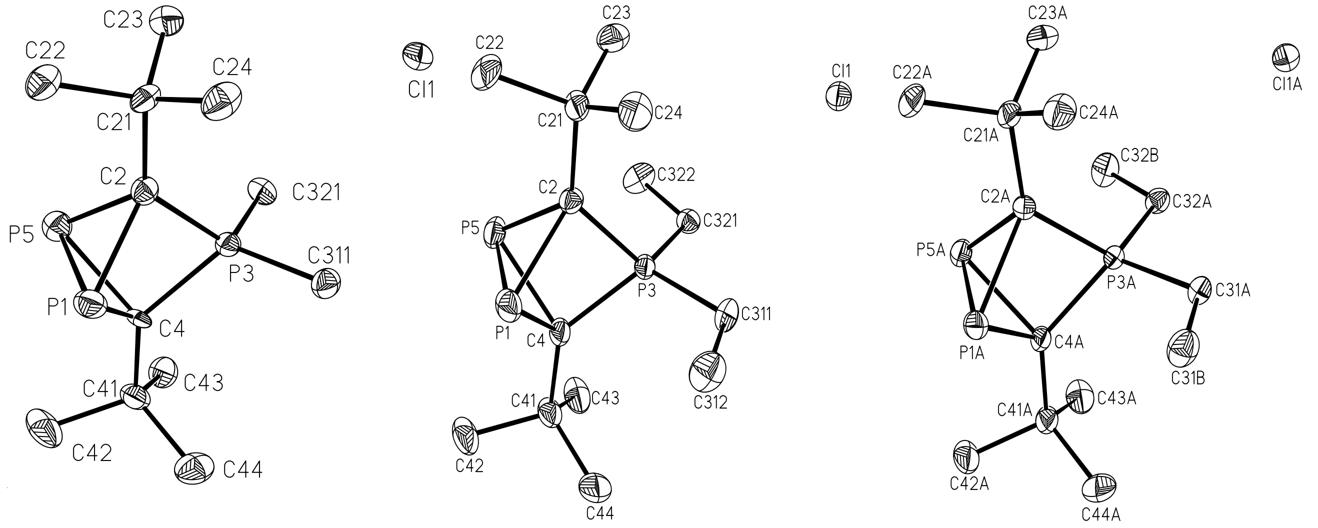

2a•CH$_2$Cl$_2$(1/1) **2b•CH$_2$Cl$_2$(2/4)**

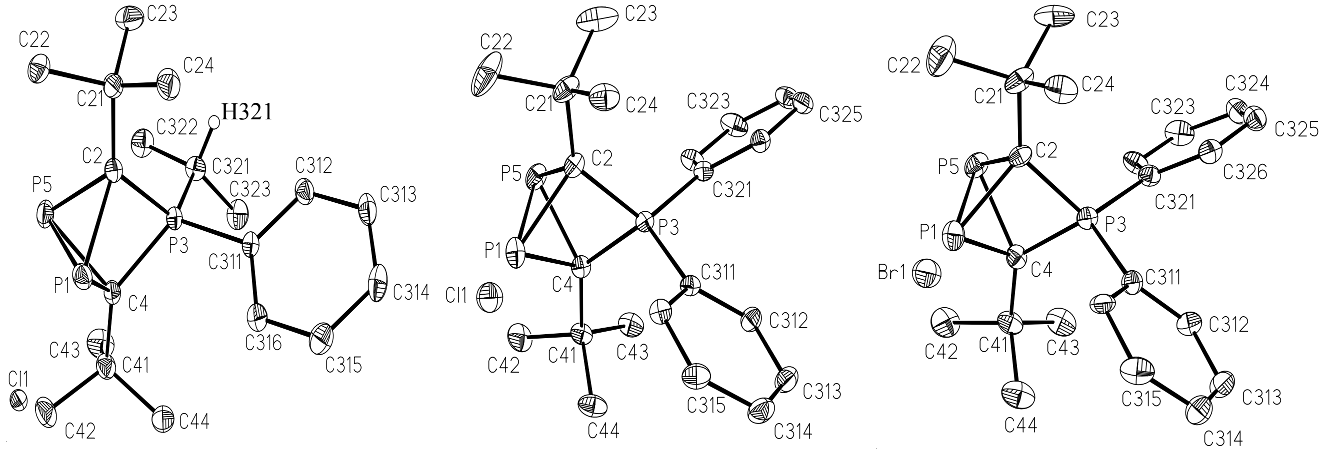

2c•CH$_2$Cl$_2$(1/2) **2d.1•CH$_2$Cl$_2$(1/1)** **2d.2•CH$_2$Cl$_2$(1/1)**

Figure 9.3.1. Structures of the cation and anion in the co-crystallisates **2a – 2d• x CH$_2$Cl$_2$**. Thermal ellipsoids are at 30 % probability. Hydrogen atoms and the co-crystallizing dichloromethane molecules have been omitted for clarity; only the CH– hydrogen atom of the isopropyl group is shown

Table 9.3.1. Atomic Coordinates and Equivalent Isotropic Displacement Parameters as well as Anisotropic Displacement Parameters with Estimated Standard Deviations in Parentheses

Parameters for 2a•CH$_2$Cl$_2$(1/1)

Atom	X/a·10^4	Y/b·10^4	Z/c·10^4	U_{eq}	U_{11}	U_{22}	U_{33}	U_{23}	U_{13}	U_{12}
P1	-481(3)	6035(2)	2778(2)	39(1)	35(1)	31(1)	47(1)	11(1)	1(1)	5(1)
C2	708(9)	7774(7)	2428(6)	28(1)	27(4)	32(3)	24(3)	4(3)	2(3)	8(3)
P3	2430(2)	7907(2)	3399(2)	27(1)	33(1)	25(1)	27(1)	3(1)	3(1)	12(1)
C4	1790(10)	6154(6)	2889(6)	30(2)	46(4)	12(3)	32(4)	5(2)	4(3)	5(3)
P5	1147(3)	6471(2)	1362(2)	38(1)	49(1)	35(1)	30(1)	-1(1)	-1(1)	15(1)
C21	-128(9)	8805(7)	2098(6)	30(2)	33(4)	36(4)	23(3)	5(3)	-2(3)	14(3)
C22	-1644(12)	8086(9)	1227(8)	47(2)	49(5)	53(5)	41(5)	7(4)	-12(4)	20(4)
C23	1147(12)	9897(8)	1498(7)	45(2)	62(6)	38(4)	35(4)	11(3)	1(4)	13(4)
C24	-656(12)	9418(10)	3187(7)	46(2)	54(5)	62(5)	35(4)	8(4)	10(4)	35(5)

C311	2227(11)	8381(8)	4918(7)	37(2)	49(5)	36(4)	32(4)	4(3)	5(3)	21(4)
C321	4467(9)	8884(7)	3024(7)	32(2)	29(4)	25(3)	44(4)	4(3)	5(3)	9(3)
C41	2479(11)	5084(7)	3196(7)	37(2)	43(4)	24(3)	41(4)	4(3)	2(3)	8(3)
C42	1588(13)	3799(9)	2413(10)	62(3)	62(7)	31(4)	91(8)	-8(5)	-22(6)	18(4)
C43	4367(11)	5510(9)	2978(7)	43(2)	45(5)	46(5)	41(4)	2(4)	0(4)	19(4)
C44	2287(13)	4861(10)	4509(8)	52(2)	70(7)	51(5)	49(5)	14(4)	10(5)	35(5)
Cl1	3842(3)	11893(2)	4240(2)	42(1)	55(1)	31(1)	44(1)	2(1)	-9(1)	20(1)
C6	4000(20)	7302(13)	-1658(11)	83(4)	124(12)	69(8)	67(7)	13(6)	10(8)	46(8)
Cl61	2915(7)	8432(6)	-1418(6)	83(2)	81(4)	79(4)	103(4)	36(3)	34(3)	36(3)
Cl6A	3880(20)	8759(12)	-801(14)	103(5)	161(16)	55(6)	99(10)	26(7)	73(10)	36(9)
Cl62	4864(11)	6920(11)	-476(7)	125(4)	86(6)	270(13)	50(3)	10(7)	-5(4)	104(7)
Cl6B	4361(19)	6283(12)	-511(15)	52(3)	50(7)	66(5)	45(5)	10(4)	14(5)	25(5)

Atom	$X/a\cdot10^4$	$Y/b\cdot10^4$	$Z/c\cdot10^4$	U_{eq}	Atom	$X/a\cdot10^4$	$Y/b\cdot10^4$	$Z/c\cdot10^4$	U_{eq}
H221[a)]	-1266	7721	525	70	H32A	5297	8679	3495	49
H222	-2185	8714	1019	70	H32B	4593	9817	3174	49
H223	-2424	7376	1597	70	H32C	4610	8681	2199	49
H231	1384	9528	745	68	H421[a)]	2136	3147	2527	93
H232	2162	10243	1990	68	H422	1626	3983	1597	93
H233	699	10607	1381	68	H423	442	3457	2622	93
H241	-1301	8724	3641	69	H431	4840	4882	3281	65
H242	-1326	9952	2968	69	H432	4914	6386	3375	65
H243	319	9974	3654	69	H433	4523	5529	2143	65
H31A[b)]	2871	8006	5407	56	H441	2594	4090	4665	78
H31B	1069	8054	5103	56	H442	1143	4720	4701	78
H31C	2631	9340	5064	56	H443[c)]	3004	5635	4984	78

a) *tert*-Butyl substituents; b) methyl group at P3; c) due to the disorder of the co-crystallizing dichloromethane molecule calculation of the CH_2-hydrogen positions not reasonable

Parameters for 2b•CH_2Cl_2(2/4)

Atom	$X/a\cdot10^4$	$Y/b\cdot10^4$	$Z/c\cdot10^4$	U_{eq}	U_{11}	U_{22}	U_{33}	U_{23}	U_{13}	U_{12}
P1	7304(2)	563(1)	9784(1)	41(1)	54(1)	36(1)	30(1)	5(1)	13(1)	2(1)
C2	7674(4)	1963(4)	9532(3)	28(1)	27(2)	28(2)	26(2)	-3(2)	3(2)	5(2)
P3	8140(1)	1618(1)	8624(1)	24(1)	24(1)	25(1)	23(1)	1(1)	4(1)	3(1)
C4	6918(5)	480(4)	8715(3)	32(1)	34(3)	31(3)	28(2)	-2(2)	11(2)	-1(2)
P5	5952(1)	1273(1	9250(1	39(1)	29(1)	44(1)	38(1)	-8(1)	12(1)	-2(1)
C21	8148(5)	2939(4)	10089(3)	34(1)	38(3)	35(3)	24(2)	-4(2)	8(2)	-2(2)
C22	7359(6)	2836(5)	10771(3)	51(2)	58(4)	56(4)	30(3)	-16(3)	16(3)	2(3)
C23	8013(6)	3908(4)	9705(3)	45(1)	55(4)	39(3)	40(3)	-7(2)	6(3)	12(3)
C24	9534(5)	3042(5)	10357(3)	47(1)	39(3)	53(4)	40(3)	-8(3)	-3(2)	2(3)
C311	9726(4)	1465(4)	8581(3)	35(1)	25(2)	46(3)	36(3)	3(2)	7(2)	11(2)
C312	10192(6)	791(5)	9144(4)	52(2)	48(3)	63(4)	51(4)	13(3)	0(3)	27(3)
C321	7900(5)	2403(4)	7872(3)	29(1)	32(2)	27(2)	25(2)	0(2)	1(2)	6(2)
C322	6642(6)	2710(5)	7786(3)	46(1)	50(3)	55(4)	37(3)	-1(3)	-3(2)	26(3)
C41	6387(6)	-514(4)	8195(3)	42(1)	49(3)	31(3)	38(3)	-5(2)	13(2)	-7(2)
C42	5316(7)	-1201(5)	8566(4)	60(2)	68(4)	43(3)	53(4)	-8(3)	20(3)	-21(3)
C43	5883(6)	-247(5)	7434(3)	55(2)	63(4)	50(4)	35(3)	-11(3)	10(3)	-16(3)
C44	7420(7)	-1097(5)	8080(4)	61(2)	80(5)	32(3)	67(4)	-11(3)	25(4)	3(3)
Cl1	10710(1)	4399(1)	8364(1)	35(1)	32(1)	38(1)	33(1)	-6(1)	4(1)	3(1)
P1A	7546(1)	5627(1)	4905(1)	33(1)	45(1)	30(1)	26(1)	5(1)	10(1)	9(1)
C2A	7739(4)	6971(3)	4551(3)	25(1)	26(2)	21(2)	26(2)	0(2)	5(2)	3(2)
P3A	8257(1)	6567(1)	3670(1)	22(1)	24(1)	22(1)	22(1)	1(1)	4(1)	6(1)
C4A	7160(4)	5386(4)	3838(3)	28(1)	29(2)	24(2)	28(2)	-2(2)	10(2)	4(2)
P5A	6076(1)	6136(1)	4303(1)	32(1)	30(1)	30(1)	36(1)	-2(1)	12(1)	4(1)
C21A	8105(5)	8002(4)	5049(3)	30(1)	31(2)	27(2)	30(2)	-6(2)	9(2)	3(2)
C22A	7310(6)	7929(4)	5720(3)	47(2)	62(4)	38(3)	37(3)	-12(2)	24(3)	5(3)
C23A	7896(6)	8879(4)	4593(3)	43(1)	57(4)	25(3)	48(3)	-2(2)	12(3)	12(2)
C24A	9518(5)	8225(4)	5338(3)	42(1)	38(3)	40(3)	41(3)	-12(2)	2(2)	2(2)

C31A	9887(4)	6545(4)	3643(3)	29(1)	27(2)	31(2)	31(2)	2(2)	7(2)	10(2)
C31B	10506(5)	6067(5)	4281(3)	43(1)	37(3)	52(3)	45(3)	7(3)	4(2)	20(3)
C32A	7899(5)	7210(4)	2860(3)	30(1)	34(3)	31(3)	27(2)	4(2)	3(2)	14(2)
C32B	6547(5)	7350(5)	2720(3)	44(1)	42(3)	59(4)	36(3)	12(3)	1(2)	23(3)
C41A	6732(5)	4322(4)	3393(3)	35(1)	39(3)	29(3)	36(3)	-3(2)	14(2)	3(2)
C42A	5709(7)	3638(4)	3802(4)	56(2)	70(4)	31(3)	60(4)	-8(3)	33(3)	-9(3)
C43A	6212(6)	4441(5)	2603(3)	49(2)	51(4)	41(3)	41(3)	-13(2)	5(3)	-10(3)
C44A	7865(6)	3825(5)	3354(4)	54(2)	65(4)	31(3)	66(4)	-9(3)	14(3)	13(3)
Cl1A	10871(1)	9289(1)	3446(1)	33(1)	36(1)	29(1)	33(1)	-2(1)	6(1)	6(1)
C6	13251(6)	3854(5)	9515(3)	52(2)	43(3)	69(4)	44(3)	-7(3)	-6(3)	19(3)
Cl61	13178(3)	2552(2)	9642(2)	108(1)	130(2)	71(2)	131(2)	10(1)	14(2)	37(2)
Cl62	14562(2)	4393(2)	9048(1)	84(1)	67(1)	129(2)	39(1)	-6(1)	2(1)	-5(1)
C6A	6649(8)	11051(6)	5332(4)	66(2)	81(5)	71(5)	51(4)	-4(3)	-12(4)	35(4)
Cl6A	6078(2)	12040(2)	5793(1)	93(1)	88(2)	132(2)	70(1)	-26(1)	4(1)	64(2)
Cl6B	6450(3)	11078(2)	4356(1)	101(1)	168(3)	112(2)	51(1)	14(1)	14(1)	89(2)
C7	8371(8)	5736(7)	7852(4)	69(2)	74(5)	94(6)	46(4)	3(4)	8(3)	33(4)
Cl71	7268(2)	5994(2)	8406(1)	85(1)	83(1)	130(2)	56(1)	10(1)	19(1)	50(1)
Cl72	7780(3)	5394(2)	6908(1)	109(1)	190(3)	119(2)	39(1)	4(1)	6(1)	83(2)
C7A	11278(7)	9257(6)	7201(4)	68(2)	74(5)	90(6)	56(4)	17(4)	13(4)	45(4)
Cl7A	12471(3)	10058(3)	7826(2)	125(1)	80(2)	128(2)	159(3)	3(2)	3(2)	17(2)
Cl7B	10497(4)	8214(2)	7616(2)	131(1)	159(3)	74(2)	170(3)	45(2)	43(2)	29(2)

Atom	$X/a\cdot10^4$	$Y/b\cdot10^4$	$Z/c\cdot10^4$	U_{eq}	Atom	$X/a\cdot10^4$	$Y/b\cdot10^4$	$Z/c\cdot10^4$	U_{eq}
H221 a) b)	7413	2208	10996	76	H22A b)	6428	7779	5539	70
H222	6492	2809	10605	76	H22B	7531	8581	6032	70
H223	7682	3426	11137	76	H22C	7471	7382	6012	70
H231	8538	3988	9295	67	H23A	7015	8759	4416	65
H232	8272	4512	10066	67	H23B	8388	8906	4168	65
H233	7146	3833	9514	67	H23C	8151	9530	4905	65
H241	10032	3152	9937	70	H24A	10017	8273	4916	63
H242	9633	2415	10569	70	H24B	9669	7669	5624	63
H243	9812	3624	10735	70	H24C	9749	8871	5656	63
H31A c)	10995	677	9020	78	H31F c)	11387	6136	4216	65
H31B	9590	133	9121	78	H31G	10096	5341	4270	65
H31C	10284	1139	9645	78	H31H	10424	6422	4757	65
H31D	9795	1169	8076	42	H31I	9971	6166	3169	34
H31E	10293	2153	8655	42	H31J	10367	7257	3635	34
H32A	6614	3109	7360	69	H32F	6450	7645	2249	66
H32B	6548	3122	8236	69	H32G	6381	7808	3123	66
H32C	5967	2092	7709	69	H32H	5960	6684	2700	66
H32D	8567	3037	7944	34	H32I	8472	7895	2905	36
H32E	7999	2028	7400	34	H32J	8083	6821	2416	36
H421 b)	5639	-1350	9052	89	H42A b)	5002	3956	3831	84
H422	4986	-1843	8252	89	H42B	6053	3570	4304	84
H423	4652	-841	8627	89	H42C	5433	2960	3528	84
H431	6556	193	7211	82	H43A	6857	4880	2358	73
H432	5220	112	7503	82	H43B	5499	4752	2627	73
H433	5555	-878	7106	82	H43C	5951	3768	2321	73
H441	8080	-675	7836	91	H44A	8513	4267	3114	80
H442	7071	-1739	7770	91	H44B	7604	3155	3068	80
H443	7763	-1245	8561	91	H44C	8189	3742	3857	80
H61 d)	13303	4245	10004	62	H71 d)	8701	5171	8041	83
H62	12483	3909	9223	62	H72	9067	6348	7884	83
H6AA	7540	11140	5496	80	H7AA	10682	9656	7029	82
H6AB	6199	10379	5467	80	H7AB	11644	9013	6764	82

a) Molecule 1 left side, molecule 2 right side; b) *tert*-butyl substituents; c) ethyl group at P3; d) dichloromethane molecules

Parameters for 2c•CH_2Cl_2(1/2)

Atom	X/a·10^4	Y/b·10^4	Z/c·10^4	U_{eq}	U_{11}	U_{22}	U_{33}	U_{23}	U_{13}	U_{12}
P1	1684(1)	7351(1)	1690(1)	30(1)	28(1)	36(1)	26(1)	0(1)	9(1)	5(1)
C2	1552(2)	6739(4)	628(2)	25(1)	24(1)	28(1)	25(1)	0(1)	6(1)	1(1)
P3	2474(1)	6067(1)	710(1)	23(1)	22(1)	24(1)	25(1)	1(1)	7(1)	0(1)
C4	2284(2)	5566(4)	1649(2)	27(1)	24(1)	30(2)	27(1)	3(1)	7(1)	-2(1)
P5	1276(1)	5153(1)	1259(1)	33(1)	26(1)	37(1)	38(1)	7(1)	9(1)	-5(1)
C21	1059(2)	7577(4)	-17(2)	29(1)	24(1)	36(2)	27(1)	3(1)	5(1)	5(1)
C22	302(2)	7761(5)	210(2)	37(1)	24(1)	49(2)	37(2)	-2(2)	5(1)	5(2)
C23	991(2)	6611(6)	-760(2)	44(1)	39(2)	58(3)	31(2)	-7(2)	-2(2)	18(2)
C24	1372(2)	9172(5)	-149(3)	38(1)	35(2)	40(2)	42(2)	13(2)	8(2)	4(2)
C311	3128(2)	7593(4)	654(2)	25(1)	22(1)	24(1)	30(2)	1(1)	7(1)	0(1)
C312	3367(2)	7872(4)	-49(2)	31(1)	27(1)	36(2)	30(2)	3(1)	9(1)	3(1)
C313	3849(2)	9082(5)	-103(2)	36(1)	31(2)	40(2)	42(2)	8(2)	16(1)	-1(1)
C314	4097(2)	9995(4)	528(3)	40(1)	32(2)	29(2)	59(2)	6(2)	15(2)	-6(1)
C315	3854(2)	9732(4)	1224(2)	37(1)	35(2)	30(2)	45(2)	-6(2)	6(2)	-3(1)
C316	3369(2)	8537(4)	1286(2)	30(1)	31(2)	28(2)	32(2)	1(1)	9(1)	-1(1)
C321	2657(2)	4558(4)	48(2)	32(2)	32(2)	28(2)	31(2)	-3(1)	7(1)	5(1)
C322	2131(2)	3177(5)	-4(3)	42(1)	47(2)	31(2)	47(2)	-10(2)	7(2)	-6(2)
C323	3452(2)	4006(5)	217(3)	42(1)	35(2)	40(2)	53(2)	-1(2)	14(2)	11(2)
C41	2713(2)	4716(4)	2338(2)	33(1)	34(2)	35(2)	32(2)	8(1)	7(1)	1(1)
C42	2305(3)	4871(6)	3025(3)	47(1)	47(2)	61(3)	36(2)	18(2)	13(2)	0(2)
C43	2783(3)	3001(5)	2146(3)	50(1)	66(3)	32(2)	50(2)	11(2)	3(2)	6(2)
C44	3472(2)	5420(5)	2553(2)	39(1)	33(2)	44(2)	37(2)	11(2)	1(1)	5(2)
Cl1	2658(1)	-733(1)	3163(1)	35(1)	31(1)	43(1)	30(1)	1(1)	6(1)	3(1)
C6	4530(3)	-473(6)	3786(3)	57(1)	38(2)	66(3)	67(3)	4(2)	12(2)	-14(2)
Cl61	4845(1)	1454(2)	3767(1)	75(1)	49(1)	62(1)	117(1)	1(1)	23(1)	-10(1)
Cl62	4919(1)	-1690(2)	3161(1)	66(1)	45(1)	73(1)	79(1)	-7(1)	6(1)	-3(1)
C7	877(3)	4261(6)	-2332(2)	51(1)	51(2)	64(3)	36(2)	-7(2)	2(2)	-14(2)
Cl71	578(1)	2664(2)	-1850(1)	73(1)	66(1)	92(1)	67(1)	21(1)	33(1)	-1(1)
Cl72	755(1)	3924(1)	-3326(1)	60(1)	84(1)	54(1)	38(1)	-2(1)	0(1)	-16(1)

Atom	X/a·10^4	Y/b·10^4	Z/c·10^4	U_{eq}	Atom	X/a·10^4	Y/b·10^4	Z/c·10^4	U_{eq}
H221[a)]	360(30)	8300(60)	680(30)	52(13)	H32C	2230(30)	2500(60)	-450(30)	68(15)
H222	100(30)	6790(60)	290(30)	49(13)	H33A	3780(20)	4860(50)	200(20)	37(11)
H223	-10(30)	8260(60)	-190(30)	68(16)	H33B	3580(30)	3330(60)	720(30)	63(15)
H231	680(20)	7100(50)	-1120(25)	37(10)	H33C	3560(30)	3420(60)	-230(30)	62(14)
H232	1410(30)	6520(70)	-940(30)	73(17)	H421[a)]	2300(20)	5910(60)	3160(20)	40(11)
H233	800(30)	5540(70)	-7000(30)	76(18)	H422	2560(30)	4400(60)	3500(30)	52(13)
H241	1080(20)	9700(50)	-560(20)	33(10)	H423	1830(30)	4390(60)	2900(30)	70(16)
H242	1420(20)	9730(50)	290(20)	35(10)	H431	3020(30)	2380(60)	2590(30)	56(13)
H243	1870(20)	9090(50)	-330(30)	48(12)	H432	2290(30)	2440(70)	1980(30)	71(16)
H312[b)]	3180(20)	7350(50)	-520(20)	41(11)	H433	3030(30)	2800(60)	1720(30)	71(16)
H313	3970(20)	9190(40)	-610(20)	30(9)	H441	3760(20)	4810(50)	2950(20)	40(11)
H314	4410(30)	10810(60)	480(30)	51(13)	H442	3440(30)	6440(60)	2720(30)	59(14)
H315	4030(20)	10340(50)	1660(20)	38(11)	H443	3730(30)	5410(60)	2120(30)	57(14)
H316	3199(19)	8340(40)	1730(20)	23(8)	H61[c)]	3970(30)	-520(60)	3530(30)	68
H321[c)]	2550(20)	5030(50)	-440(20)	39(11)	H62	4740(30)	-1290(60)	4160(30)	68
H32A	2190(30)	2640(60)	470(30)	63(15)	H71	400(30)	5130(60)	-2500(30)	61
H32B	1660(30)	3450(60)	-150(30)	53(13)	H72	1370(30)	4410(60)	-2140(30)	61

a) *tert*-Butyl substituents; b) phenyl substituent; c) isopropyl substituent; d) dichloromethane molecules

Parameters for 2d.1•CH_2Cl_2(1/1)

Atom	X/a·10^4	Y/b·10^4	Z/c·10^4	U_{eq}	U_{11}	U_{22}	U_{33}	U_{23}	U_{13}	U_{12}
P1	1957(1)	2556(1)	520(1)	35(1)	26(1)	36(1)	41(1)	-8(1)	2(1)	3(1)
C2	2748(3)	1607(2)	1031(2)	28(1)	26(1)	31(2)	27(1)	-5(1)	7(1)	-5(1)
P3	4421(1)	1841(1)	811(1)	21(1)	24(1)	19(1)	21(1)	-3(1)	4(1)	-2(1)
C4	3809(3)	2838(2)	984(2)	25(1)	30(1)	24(1)	23(1)	-5(1)	4(1)	-1(1)
P5	2835(1)	2483(1)	1819(1)	34(1)	37(1)	35(1)	33(1)	-10(1)	15(1)	-4(1)

C21	2014(4)	813(2)	1121(2)	36(1)	39(2)	35(2)	37(2)	-8(1)	15(1)	-15(1)
C22	492(5)	988(4)	1142(4)	73(2)	48(3)	69(3)	112(5)	-34(3)	44(3)	-32(2)
C23	2692(7)	378(3)	1915(3)	62(2)	96(4)	55(3)	34(2)	2(2)	10(2)	-39(3)
C24	2087(4)	269(2)	377(2)	38(1)	52(2)	27(2)	35(2)	-4(1)	7(2)	-10(2)
C311	4789(3)	1668(2)	-219(2)	22(1)	28(1)	20(1)	19(1)	-1(1)	4(1)	-2(1)
C312	6147(3)	1731(2)	-360(2)	28(1)	25(1)	33(2)	28(1)	-1(1)	5(1)	-3(1)
C313	6429(4)	1692(2)	-1161(2)	36(1)	33(2)	42(2)	36(2)	3(1)	13(1)	-3(1)
C314	5362(4)	1591(2)	-1831(2)	37(1)	47(2)	42(2)	24(2)	1(1)	13(1)	-1(2)
C315	4014(4)	1526(2)	-1698(2)	33(1)	41(2)	36(2)	21(1)	1(1)	1(1)	-5(1)
C316	3714(3)	1565(2)	-890(2)	26(1)	26(1)	27(1)	25(1)	-2(1)	2(1)	-3(1)
C321	5848(3)	1456(2)	1538(2)	24(1)	26(1)	23(1)	22(1)	0(1)	2(1)	-4(1)
C322	6329(4)	1864(2)	2282(2)	32(1)	45(2)	25(2)	24(1)	-2(1)	-2(1)	-2(1)
C323	7427(4)	1553(2)	2833(2)	42(1)	56(2)	35(2)	29(2)	2(1)	-11(2)	-6(2)
C324	8034(4)	837(2)	2653(2)	38(1)	37(2)	36(2)	38(2)	11(2)	-7(1)	-2(1)
C325	7551(4)	415(2)	1935(2)	34(1)	32(2)	27(2)	41(2)	7(1)	6(1)	1(1)
C326	6458(3)	723(2)	1372(2)	28(1)	29(1)	27(2)	26(1)	-2(1)	5(1)	-1(1)
C41	4409(4)	3675(2)	873(2)	29(1)	40(2)	19(1)	27(1)	-4(1)	3(1)	-2(1)
C42	3520(5)	4306(2)	1216(3)	46(1)	64(3)	25(2)	49(2)	-9(2)	14(2)	7(2)
C43	5880(4)	3735(2)	1354(3)	40(1)	46(2)	29(2)	41(2)	-2(2)	-2(2)	-11(2)
C44	4387(5)	3818(2)	-61(2)	41(1)	65(3)	29(2)	26(2)	0(1)	2(2)	-6(2)
Cl1	73(1)	1539(1)	-1466(1)	37(1)	31(1)	40(1)	38(1)	6(1)	3(1)	-1(1)
C6	4066(8)	1472(4)	4105(4)	92(2)	112(5)	63(4)	82(4)	19(3)	-36(4)	-17(3)
Cl61	3444(2)	1474(1)	5043(2)	124(1)	95(1)	104(2)	190(3)	31(2)	70(2)	20(1)
Cl62	5179(2)	645(1)	4056(1)	94(1)	91(1)	104(1)	93(1)	7(1)	31(1)	-9(1)

Atom	X/a·10^4	Y/b·10^4	Z/c·10^4	U_{eq}	Atom	X/a·10^4	Y/b·10^4	Z/c·10^4	U_{eq}
H221[a]	80(70)	490(40)	1270(40)	90(20)	H323	7640(50)	1910(30)	3300(30)	57(14)
H222	-10(80)	1260(50)	690(50)	107	H324	8730(40)	670(30)	3030(30)	43(12)
H223	470(70)	12600(40)	1730(40)	90(20)	H325	7900(40)	-40(30)	1850(30)	37(11)
H231	2190(60)	-90(40)	2040(40)	85(19)	H326	6170(40)	440(30)	900(30)	37(11)
H232	2470(60)	690(40)	2410(40)	78(18)	H421[a]	2520(50)	4320(30)	880(30)	55(14)
H233	3660(60)	240(40)	1960(40)	80(20)	H422	3840(50)	4850(30)	1100(30)	56(14)
H241	1580(40)	-250(30)	460(30)	36(11)	H423	3640(70)	4290(40)	1770(40)	100(20)
H242	3030(40)	120(30)	350(30)	38(11)	H431	6450(50)	3270(30)	1110(30)	55(14)
H243	1610(40)	490(20)	-140(30)	33(10)	H432	5920(40)	3680(20)	1980(30)	30(10)
H312[b]	6860(40)	1800(20)	80(30)	33(10)	H433	6280(50)	4210(30)	1210(30)	59(14)
H313	7370(50)	1760(30)	-1210(30)	47(12)	H441	3460(50)	3850(30)	-320(30)	47(12)
H314	5600(40)	1490(30)	-2360(30)	37(11)	H442	4900(50)	3390(30)	-250(30)	46(12)
H315	3320(50)	1450(30)	-2160(30)	41(11)	H443	4830(50)	4320(30)	-160(30)	62(15)
H316	2770(40)	1560(30)	-830(30)	36(11)	H61[c]	4558	1971	4052	110
H322	5990(40)	2320(30)	2440(30)	32(10)	H62	3301	1442	3646	110

a) *tert*-Butyl substituents; b) phenyl substituents; c) dichloromethane molecule

Parameters for 2d.2•CH$_2$Cl$_2$(1/1)

Atom	X/a·10^4	Y/b·10^4	Z/c·10^4	U_{eq}	U_{11}	U_{22}	U_{33}	U_{23}	U_{13}	U_{12}
P1	1986(3)	2529(1)	528(2)	38(1)	35(1)	37(1)	43(1)	-6(1)	7(1)	2(1)
C2	2796(8)	1599(5)	1043(5)	28(2)	31(4)	32(4)	23(4)	-3(3)	11(3)	-4(4)
P3	4421(2)	1845(1)	796(1)	26(1)	31(1)	24(1)	23(1)	-5(1)	6(1)	-3(1)
C4	3793(8)	2838(5)	974(5)	30(2)	38(5)	25(4)	26(4)	-7(3)	6(4)	1(4)
P5	2871(2)	2473(1)	1818(2)	37(1)	42(1)	36(1)	36(1)	-9(1)	16(1)	-6(1)
C21	2114(9)	798(5)	1149(6)	39(2)	41(5)	41(5)	40(5)	-6(4)	19(5)	-15(4)
C22	649(10)	947(6)	1217(8)	66(3)	47(6)	51(6)	106(10)	-21(6)	30(7)	-7(5)
C23	2804(11)	377(6)	1944(5)	55(3)	79(8)	55(6)	29(5)	12(5)	2(5)	-29(6)
C24	2161(10)	241(5)	400(5)	41(2)	52(6)	37(5)	30(5)	1(4)	-2(5)	-7(4)
C311	4761(8)	1669(4)	-229(5)	28(2)	34(4)	23(4)	27(4)	-2(3)	8(4)	1(3)
C312	6076(8)	1778(5)	-397(5)	34(2)	31(5)	36(5)	34(5)	1(4)	5(4)	-4(4)
C313	6317(10)	1734(5)	-1204(6)	42(2)	49(6)	38(5)	44(6)	2(4)	22(5)	-1(4)
C314	5295(10)	1609(5)	-1852(6)	42(2)	55(6)	45(6)	28(5)	-3(4)	13(5)	4(5)

C315	3987(10)	1526(5)	-1704(5)	39(2)	50(6)	39(5)	27(5)	1(4)	1(4)	-9(5)
C316	3701(8)	1551(5)	-893(5)	31(2)	29(4)	35(4)	30(4)	10(4)	9(4)	-2(4)
C321	5836(8)	1476(5)	1498(5)	29(2)	35(4)	28(4)	22(4)	0(4)	1(4)	-3(4)
C322	6296(9)	1871(5)	2255(5)	37(2)	47(6)	28(4)	33(5)	-1(4)	0(5)	-1(4)
C323	7390(10)	1567(6)	2797(6)	47(2)	55(6)	46(6)	33(5)	1(5)	-11(5)	-10(5)
C324	8007(10)	859(5)	2611(6)	44(2)	41(5)	34(5)	54(6)	4(5)	1(5)	2(4)
C325	7534(9)	443(5)	1881(6)	38(2)	32(5)	30(5)	51(6)	3(4)	3(5)	-1(4)
C326	6464(8)	758(5)	1338(5)	34(2)	39(5)	34(5)	28(5)	-5(4)	9(4)	-3(4)
C41	4343(9)	3673(5)	853(5)	36(2)	50(5)	22(4)	34(5)	-1(4)	4(4)	-3(4)
C42	3471(11)	4303(5)	1197(7)	58(3)	83(8)	22(5)	75(8)	-10(5)	27(7)	4(5)
C43	5803(10)	3751(5)	1279(6)	49(3)	57(7)	31(5)	54(6)	-5(4)	-1(5)	-13(5)
C44	4295(11)	3827(5)	-86(6)	50(3)	77(8)	34(5)	37(6)	-7(4)	2(6)	-10(5)
Br1	30(1)	1517(1)	-1438(1)	39(1)	35(1)	41(1)	39(1)	9(1)	4(1)	-2(1)
C6	3963(19)	1433(8)	4139(8)	126(6)	239(17)	60(9)	62(9)	7(7)	-26(11)	18(11)
Cl61	3460(6)	1446(3)	5057(4)	179(2)	144(5)	140(5)	280(7)	46(4)	115(5)	35(4)
Cl62	5186(4)	637(3)	4070(3)	118(2)	108(3)	144(4)	107(3)	15(3)	30(3)	-16(3)

Atom	X/a·10^4	Y/b·10^4	Z/c·10^4	U$_{eq}$	Atom	X/a·10^4	Y/b·10^4	Z/c·10^4	U$_{eq}$
H221a)	231	445	1335	99	H323	7710	1842	3290	56
H222	186	1166	700	99	H324	8746	659	2978	53
H223	597	1326	1660	99	H325	7935	-43	1760	46
H231	2391	-144	1991	82	H326	6151	480	845	40
H232	2703	703	2420	82	H421a)	3774	4836	1077	87
H233	3750	306	1920	82	H422	3546	4236	1790	87
H241	1685	-253	470	61	H423	2542	4235	940	87
H242	3089	119	361	61	H431	6175	4250	1114	73
H243	1741	508	-102	61	H432	6321	3303	1120	73
H312b)	6786	1880	37	40	H433	5838	3747	1874	73
H313	7200	1791	-1310	50	H441	4614	4366	-168	75
H314	5480	1579	-2394	50	H442	3379	3772	-370	75
H315	3285	1452	-2150	47	H443	4863	3440	-306	75
H316	2815	1490	-795	37	H61c)	4366	1953	4043	151
H322	5863	2339	2392	44	H62	3183	1354	3706	151

a) *tert*-Butyl substituents; b) phenyl substituents; c) dichloromethane molecule

9.4. 2,4,6-*Tri*-tert-butyl-3-chloro-1-dialkylamino-1$\lambda^5\sigma^4$,3$\lambda^3\sigma^3$,5$\lambda^3\sigma^2$-triphosphabicyclo[2.2.0]hexa-1,5-dienes

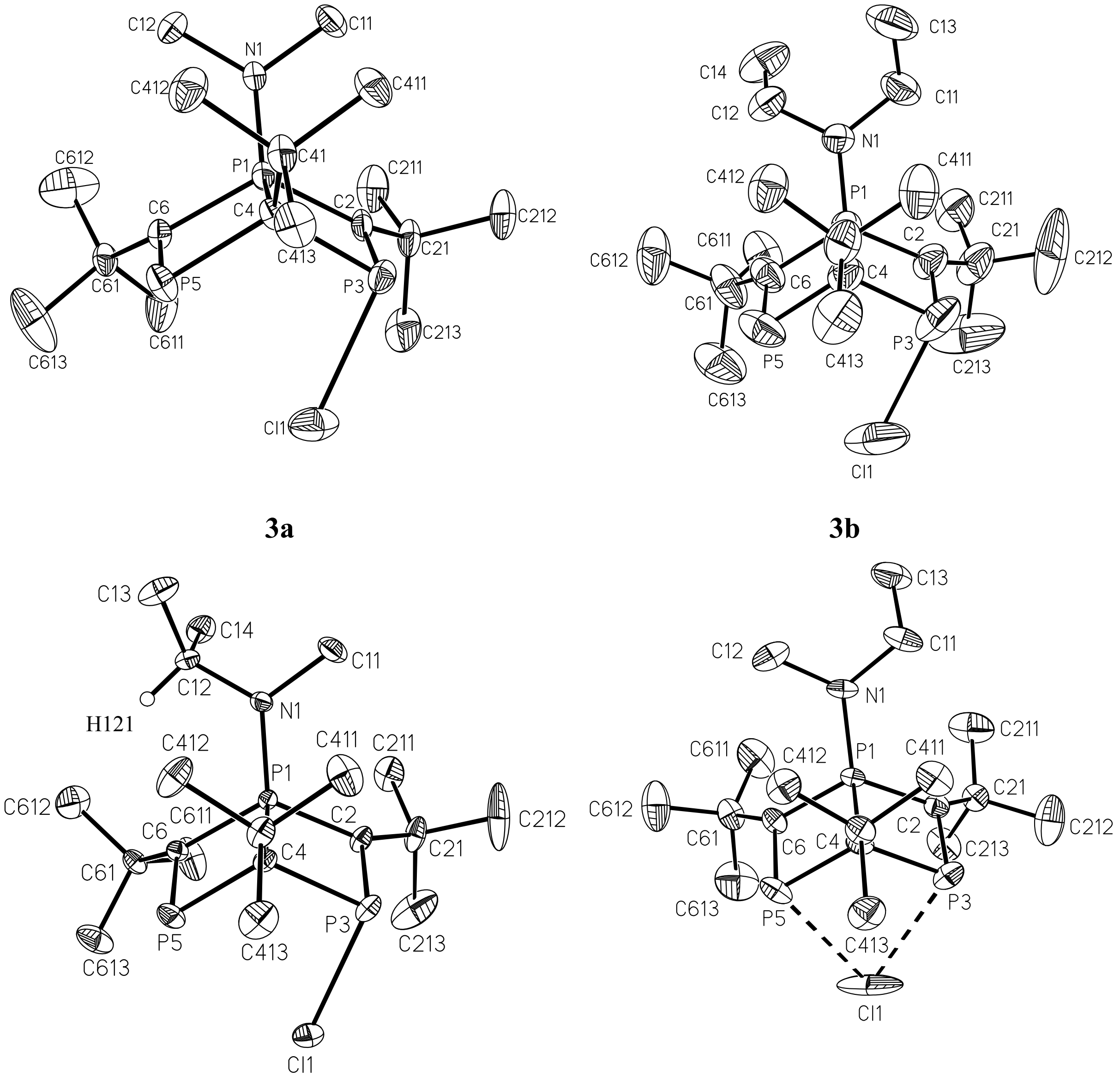

3a **3b**

3c **3d**

Figure 9.4.1. Molecular structures of **3a-3d.** Thermal ellipsoids are at 30 % probability. Hydrogen atoms have been omitted for clarity; only the CH– hydrogen atom of the isopropyl group is shown.

Table 9.4.1. Atomic Coordinates and Equivalent Isotropic Displacement Parameters as well as Anisotropic Displacement Parameters, with Estimated Standard Deviations in Parentheses

Parameters for 3a

Atom	$X/a\cdot10^4$	$Y/b\cdot10^4$	$Z/c\cdot10^4$	U_{eq}	U_{11}	U_{22}	U_{33}	U_{23}	U_{13}	U_{12}
Cl1	2525(2)	-764(2)	1527(1)	68(1)	89(1)	53(1)	55(1)	14(1)	-13(1)	-11(1)
P1	2759(1)	3359(1)	907(1)	28(1)	20(1)	35(1)	29(1)	-1(1)	3(1)	0(1)
C2	1575(4)	2816(6)	1288(2)	35(1)	18(2)	50(3)	36(2)	2(2)	5(2)	1(2)
P3	1376(1)	1090(2)	916(1)	37(1)	30(1)	47(1)	34(1)	0(1)	3(1)	-11(1)
C4	2580(4)	1664(5)	423(2)	31(1)	24(2)	34(2)	34(2)	-3(2)	-1(2)	4(2)
P5	4105(1)	1065(2)	785(1)	42(1)	29(1)	46(1)	49(1)	-7(1)	-5(1)	8(1)
C6	4242(4)	2733(6)	1178(2)	33(1)	22(2)	39(3)	39(3)	2(2)	4(2)	-1(2)
N1	2702(3)	5089(5)	637(2)	33(1)	22(2)	38(2)	39(2)	3(2)	4(2)	0(2)
C21	989(4)	3418(7)	1851(2)	44(1)	25(2)	72(4)	38(3)	-6(3)	10(2)	-5(2)
C211	1411(7)	4985(11)	2057(4)	66(2)	51(4)	91(6)	59(4)	-34(5)	21(3)	-5(4)
C212	-357(5)	3459(11)	1650(4)	65(2)	31(3)	98(6)	70(4)	-25(5)	20(3)	-8(4)

C213	1274(7)	2302(13)	2417(3)	73(2)	62(5)	121(8)	40(3)	4(4)	24(3)	-4(5)
C41	2273(4)	1513(6)	-306(2)	36(1)	26(2)	50(3)	32(2)	-7(2)	4(2)	-1(2)
C411	1090(5)	2282(8)	-528(3)	46(1)	39(3)	61(4)	37(3)	-3(3)	-4(2)	10(3)
C412	3228(6)	2260(9)	-638(3)	55(2)	51(4)	76(5)	38(3)	-4(3)	14(3)	-12(3)
C413	2173(6)	-147(7)	-482(3)	49(1)	47(3)	51(4)	47(3)	-15(3)	3(3)	2(3)
C61	5190(4)	3196(6)	1725(2)	37(1)	24(2)	50(3)	35(2)	-4(2)	-2(2)	-2(2)
C611	4644(8)	3154(19)	2337(4)	99(4)	46(4)	212(14)	39(4)	-10(6)	-3(3)	-27(6)
C612	5649(12)	4759(12)	1649(6)	108(5)	130(9)	91(7)	84(6)	14(6)	-57(7)	-61(7)
C613	6192(8)	2083(14)	1779(6)	108(4)	56(5)	131(9)	119(8)	-65(7)	-48(5)	34(5)
C11	1568(5)	5884(7)	457(3)	47(1)	34(3)	44(3)	60(4)	4(3)	-7(3)	11(3)
C12	3693(5)	5853(8)	402(3)	49(1)	39(3)	50(4)	60(4)	15(3)	16(3)	-7(3)

Atom	$X/a\cdot10^4$	$Y/b\cdot10^4$	$Z/c\cdot10^4$	U_{eq}	Atom	$X/a\cdot10^4$	$Y/b\cdot10^4$	$Z/c\cdot10^4$	U_{eq}
H111[a)]	1650(50)	6900(60)	680(20)	32(13)	H413	460(60)	1800(70)	-330(30)	56
H112	910(60)	5210(80)	570(30)	64(19)	H421	3320(60)	3370(80)	-520(30)	61(19)
H113	1420(60)	6160(70)	-50(30)	57	H422	3150(70)	2240(90)	-1050(40)	80(20)
H121	3880(60)	6780(80)	600(30)	53(18)	H423	3970(70)	1940(80)	-470(30)	65
H122	3560(60)	6220(70)	-50(30)	59	H431	2960(70)	-600(80)	-360(30)	70(20)
H123	4460(60)	5210(70)	500(30)	59	H432	1690(60)	-660(80)	-270(30)	60(20)
H211[b)]	1130(50)	5230(70)	2440(30)	46(16)	H433	2060(50)	-210(70)	-990(30)	58
H212	1210(60)	5600(70)	1740(30)	50(20)	H611	4100(90)	4050(100)	2300(50)	100(30)
H213	2420(80)	4790(100)	2160(40)	110(30)	H612	5080(90)	3540(110)	2680(50)	120(30)
H221	-650(60)	4340(80)	1270(40)	70(20)	H613	4270(100)	2350(130)	2400(50)	119
H222	-740(70)	3840(80)	2030(40)	80(20)	H621	6320(110)	5110(150)	2030(60)	162
H223	-570(60)	2390(80)	1600(30)	54(18)	H622	5840(130)	4960(170)	1310(70)	162
H231	2150(80)	2000(90)	2550(40)	90(30)	H623	5090(120)	5260(170)	1620(80)	162
H232	1120(80)	2740(100)	2700(40)	87	H631	6890(70)	2270(90)	2070(40)	80(20)
H233	1020(60)	1130(80)	2320(30)	60(20)	H632	5840(100)	740(130)	1790(60)	140(40)
H411	1190(50)	3320(70)	-450(30)	45(16)	H633	6410(100)	1570(140)	1520(60)	129
H412	930(50)	2060(70)	-950(30)	49(16)					

a) Methyl groups at N1; b) *tert*-butyl substituents

Parameters for 3b

Atom	$x/a\cdot10^4$	$y/b\cdot10^4$	$z/c\cdot10^4$	U_{eq}	U_{11}	U_{22}	U_{33}	U_{23}	U_{13}	U_{12}
Cl1	2116(2)	14243(1)	8538(1)	168(1)	153(1)	194(2)	104(1)	3(1)	2(1)	-103(1)
P1	-682(1)	12315(1)	6989(1)	57(1)	56(1)	62(1)	52(1)	20(1)	7(1)	-3(1)
C2	-187(5)	13259(3)	6659(2)	78(1)	99(3)	69(2)	66(2)	23(2)	20(2)	-11(2)
P3	-185(2)	14049(1)	7587(1)	108(1)	161(1)	66(1)	94(1)	10(1)	55(1)	-28(1)
C4	-883(4)	13065(2)	7963(2)	70(1)	83(3)	66(2)	59(2)	16(2)	17(2)	-8(2)
P5	539(1)	12556(1)	8520(1)	97(1)	72(1)	158(1)	54(1)	28(1)	3(1)	2(1)
C6	599(4)	11837(3)	7585(2)	74(1)	55(2)	111(3)	63(2)	39(2)	11(2)	8(2)
N1	-1896(3)	11551(2)	6330(2)	67(1)	65(2)	70(2)	60(2)	21(1)	1(1)	-7(1)
C21	423(6)	13421(3)	5927(3)	103(2)	150(5)	84(3)	82(3)	31(2)	46(3)	-15(3)
C211	202(6)	12581(3)	5212(3)	105(2)	135(4)	113(4)	79(3)	35(3)	46(3)	4(3)
C212	-298(12)	14144(5)	5622(5)	235(5)	479(17)	143(6)	189(7)	126(6)	193(10)	123(8)
C213	2016(8)	13724(7)	6228(4)	229(6)	214(8)	314(11)	106(5)	0(6)	71(5)	-166(8)
C41	-2222(5)	13198(3)	8339(3)	78(1)	94(3)	71(2)	80(3)	28(2)	34(2)	12(2)
C411	-3326(5)	13576(3)	7795(3)	103(2)	124(4)	86(3)	117(4)	40(3)	42(3)	43(3)
C412	-2867(5)	12289(3)	8425(3)	88(1)	83(3)	88(3)	113(3)	44(3)	45(2)	19(2)
C413	-1764(6)	13879(3)	9213(3)	109(2)	151(5)	94(3)	88(3)	15(3)	53(3)	10(3)
C61	1709(5)	11201(4)	7403(3)	101(2)	64(3)	173(5)	96(3)	73(4)	27(2)	47(3)
C611	1802(13)	10930(10)	6510(6)	110(4)	91(7)	160(10)	108(8)	55(7)	46(6)	61(7)
C612	1320(11)	10283(7)	7647(9)	136(4)	111(8)	151(9)	215(14)	125(10)	77(8)	70(7)
C613	3173(9)	11622(10)	7927(8)	142(4)	61(6)	217(14)	143(10)	53(9)	0(6)	19(7)
C61’	1180(20)	10427(17)	6688(12)	217(16)	230(30)	330(40)	121(16)	40(20)	62(17)	220(30)
C62’	2360(20)	11041(14)	8187(8)	151(7)	140(16)	220(20)	137(14)	91(15)	36(12)	111(15)
C63’	2880(20)	11830(20)	7160(20)	252(18)	117(15)	410(50)	380(40)	300(40)	140(20)	120(20)
C11	-2960(4)	11807(4)	5710(3)	96(1)	79(3)	130(4)	72(3)	40(30)	-12(2)	-7(3)
C12	-2173(5)	10617(2)	6418(3)	83(1)	90(3)	63(2)	88(3)	13(2)	20(2)	-11(2)

C13	-4490(5)	11571(4)	5788(3)	128(2)	65(3)	189(6)	117(4)	50(4)	-18(3)	-6(3)
C14	-2188(6)	9890(3)	5613(3)	128(2)	147(5)	87(3)	124(4)	-16(3)	47(4)	-28(3)
Cl1A	4562(4)	8984(4)	6520(4)	125(2)	139(4)	145(4)	92(2)	54(3)	-7(2)	24(2)
P1A	5522(2)	7507(3)	8069(2)	76(2)	68(3)	81(3)	79(3)	12(2)	24(2)	18(2)
C2A	6511(9)	8535(7)	8184(7)	55(2)	47(4)	65(5)	52(4)	10(3)	14(3)	4(3)
P3A	6563(3)	8408(3)	7166(3)	96(2)	93(4)	106(4)	88(3)	23(3)	22(3)	5(3)
C4A	5598(8)	7184(7)	6964(6)	69(3)	71(5)	72(5)	59(4)	7(4)	19(4)	1(4)
P5A	3614(2)	7128(1)	6688(1)	89(1)	54(1)	120(2)	75(1)	8(1)	-6(1)	7(1)
C6A	3631(5)	7331(3)	7722(3)	71(2)	47(3)	72(4)	84(4)	3(3)	18(3)	2(3)
N1A	6080(4)	6917(6)	8723(6)	47(3)	60(6)	38(4)	39(4)	5(3)	9(4)	-3(4)
C20A	6916(8)	9411(6)	8878(5)	63(2)	76(6)	54(4)	59(4)	15(3)	19(4)	4(4)
C21A	6968(14)	9240(7)	9733(6)	115(6)	207(15)	58(7)	59(6)	-14(4)	14(7)	13(7)
C22A	8333(7)	9868(5)	8826(5)	92(2)	76(5)	76(5)	100(5)	-11(4)	15(4)	-10(4)
C23A	5818(7)	10072(4)	8771(4)	83(2)	80(5)	59(4)	99(5)	7(3)	9(4)	11(3)
C40A	6227(6)	6400(6)	6452(4)	78(3)	84(5)	93(7)	46(4)	-3(4)	23(4)	2(5)
C41A	7862(6)	6543(6)	6771(5)	92(2)	69(5)	103(6)	85(5)	-16(4)	28(5)	10(4)
C42A	5646(9)	5487(5)	6566(6)	86(3)	85(6)	75(5)	81(5)	-13(4)	23(5)	17(4)
C43A	5967(10)	6394(7)	5547(4)	111(3)	120(8)	147(9)	52(4)	2(5)	18(5)	10(6)
C60A	2367(5)	7481(6)	8111(5)	87(8)	52(12)	82(11)	105(11)	-17(8)	30(8)	-7(7)
C61A	2771(10)	7806(11)	9072(5)	202(7)	123(9)	340(20)	132(9)	-6(11)	79(8)	78(11)
C62A	1230(10)	6733(8)	7818(9)	234(10)	104(9)	187(13)	340(20)	-99(14)	142(12)	-74(9)
C63A	1774(13)	8311(9)	7859(10)	232(9)	227(17)	212(16)	350(20)	115(17)	191(18)	159(14)
C11A	7569(5)	7061(4)	9148(3)	67(2)	65(4)	69(4)	63(3)	18(3)	1(3)	4(3)
C12A	5176(6)	6137(4)	8831(4)	77(2)	91(5)	60(4)	78(4)	16(3)	25(4)	-4(3)
C13A	8320(11)	6212(12)	9014(10)	99(5)	107(8)	83(10)	107(10)	22(8)	15(6)	37(7)
C14A	5120(20)	6220(11)	9732(11)	118(6)	158(14)	100(11)	104(8)	34(8)	50(8)	-15(9)
Cl1B	5432(3)	884(4)	3342(4)	63(1)	51(2)	73(2)	75(2)	38(2)	9(1)	15(1)
P1B	4438(2)	2500(2)	1924(2)	28(1)	26(2)	28(2)	26(2)	3(1)	6(2)	-5(2)
C2B	4021(9)	2681(7)	2892(7)	60(3)	63(7)	58(6)	61(7)	11(5)	29(5)	2(5)
P3B	3463(2)	1585(2)	2836(2)	39(1)	45(3)	46(2)	27(2)	14(2)	11(2)	0(2)
C4B	3727(11)	1299(7)	1692(6)	46(3)	47(6)	49(6)	47(6)	20(5)	14(4)	11(4)
P5B	5544(2)	984(1)	1602(1)	63(1)	53(1)	54(1)	79(2)	13(1)	13(1)	11(1)
C6B	6079(5)	2106(3)	1736(3)	59(2)	60(5)	65(5)	56(5)	17(4)	13(4)	15(4)
N1B	3877(7)	3175(7)	1352(6)	72(7)	70(12)	76(11)	74(11)	15(8)	29(9)	22(8)
C20B	4210(8)	3496(6)	3642(6)	73(4)	82(8)	58(7)	69(8)	-1(5)	17(6)	6(6)
C21B	5026(12)	4334(6)	3486(8)	84(4)	99(10)	48(6)	90(8)	-10(5)	25(8)	-3(6)
C22B	2795(14)	3760(7)	3822(8)	121(5)	148(14)	104(10)	105(10)	-11(8)	77(11)	2(9)
C23B	5081(16)	3279(7)	4388(5)	143(7)	211(19)	97(9)	76(8)	-2(7)	-57(10)	33(11)
C40B	2495(8)	714(5)	1019(5)	61(3)	68(8)	44(5)	61(6)	0(4)	15(6)	-6(5)
C41B	1090(7)	1047(6)	1152(6)	72(2)	45(5)	79(6)	83(6)	14(5)	0(4)	-4(4)
C42B	2729(13)	696(9)	159(6)	63(4)	68(6)	67(9)	49(6)	14(6)	11(5)	-19(6)
C43B	2410(11)	-289(5)	1085(6)	76(3)	99(8)	46(5)	77(6)	8(4)	19(6)	-3(5)
C60B	7587(6)	2526(6)	1878(6)	87(15)	40(20)	90(20)	150(20)	60(17)	31(17)	15(14)
C61B	7710(10)	3501(6)	1769(9)	114(5)	77(8)	81(7)	186(14)	42(8)	38(9)	-24(6)
C62B	8460(10)	1965(7)	1421(11)	147(7)	88(10)	94(9)	240(20)	-24(11)	94(12)	-4(7)
C63B	8220(11)	2667(10)	2821(7)	141(6)	77(8)	181(15)	139(13)	48(12)	-26(8)	-37(9)
C11B	2689(7)	3675(5)	1521(4)	66(2)	74(6)	65(5)	61(5)	17(4)	14(4)	21(4)
C12B	4283(8)	3142(4)	538(4)	63(2)	69(5)	58(5)	71(5)	26(4)	25(4)	15(4)
C13B	1447(14)	3516(17)	780(10)	77(5)	108(10)	82(13)	60(8)	32(10)	36(7)	45(9)
C14B	4720(20)	4076(13)	447(14)	83(6)	74(8)	91(13)	111(14)	64(13)	31(8)	21(8)

Atom	x/a·10^3	y/b·10^3	z/c·10^3	U$_{eq}$	Atom	x/a·10^3	y/b·10^3	z/c·10^3	U$_{eq}$
H111[a) b)]	-2854	11498	5153	115	H22B	8593	10430	9258	138
H112	-2771	12458	5776	115	H22C	8268	9991	8291	138
H121	-3079	10539	6579	99	H23A	5765	10198	8237	124
H122	-1448	10534	6860	99	H23B	6100	10631	9205	124
H131	-5115	11814	5414	192	H23C	4907	9798	8803	124
H132	-4586	11831	6351	192	H41A	8251	6023	6495	138
H133	-4729	10920	5647	192	H41B	8072	6615	7363	138
H141	-2313	9296	5709	191	H41C	8270	7080	6653	138

H142	-1307	9978	5439	191	H42A	4649	5357	6334	128
H143	-2953	9937	5185	191	H42B	5806	5517	7151	128
H211[c]	-793	12401	4989	158	H42C	6119	5014	6286	128
H212	598	12097	5405	158	H43A	4967	6294	5324	167
H213	661	12705	4784	158	H43B	6403	5913	5244	167
H221	-1298	13944	5449	352	H43C	6366	6969	5494	167
H222	71	14252	5158	352	H61A	3291	7374	9281	303
H223	-128	14698	6065	352	H61B	1927	7855	9296	303
H231	2455	13678	5755	344	H61C	3346	8390	9240	303
H232	2412	13339	6555	344	H62A	1295	6358	6200	351
H233	2182	14344	6564	344	H62B	1299	6376	7275	351
H411	-4146	13642	8040	154	H62C	339	6967	7783	351
H412	-3592	13163	7246	154	H63A	1752	8246	7277	347
H413	-2933	14159	7757	154	H63B	2370	8863	8184	347
H421	-3654	12380	8696	132	H63C	832	8335	7962	347
H422	-2167	12041	8751	132	H11C[a][b]	3038	4322	1709	79
H423	-3186	11873	7880	132	H11D	2342	3506	1975	79
H431	-2588	14032	9432	164	H12C	3490	2836	89	75
H432	-1240	14423	9170	164	H12D	5062	2787	486	75
H433	-1179	13607	9580	164	H13D	685	3819	961	115
H6’A	594	9985	6844	325	H13E	1132	2874	561	115
H6’B	1960	10158	6496	325	H13F	1745	3755	353	115
H6’C	630	10625	6249	325	H14D	5009	4021	-76	125
H6’D	1642	10827	8445	226	H14E	5490	4387	897	125
H6’E	2890	11599	8552	226	H14F	3932	4418	463	125
H6’F	2989	10590	8084	226	H21D[c]	5981	4226	3460	126
H6’G	2973	12447	7502	377	H21E	5034	4863	3934	126
H6’H	2594	11830	6580	377	H21F	4570	4431	2968	126
H6’I	3771	11606	7238	377	H22D	2230	3239	3878	181
H611	914	10601	6181	166	H22E	2310	3969	3371	181
H612	2534	10550	6440	166	H22F	2953	4238	4332	181
H613	2020	11466	6330	166	H23D	4570	2785	4520	214
H621	435	9968	7300	204	H23E	5262	3807	4858	214
H622	1240	10424	8222	204	H23F	5962	3107	4259	214
H623	2049	9903	7565	204	H41D	1107	1663	1111	109
H631	3137	11761	8509	213	H41E	950	1023	1696	109
H632	3469	12171	7788	213	H41F	331	633	734	109
H633	3836	11198	7814	213	H42D	2709	1295	77	95
H11A[a][b]	7624	7302	9743	81	H42E	1996	277	-250	95
H11B	8076	7520	8959	81	H42F	3633	505	101	95
H12A	5540	5576	8606	92	H43D	1573	-643	714	115
H12B	4224	6101	8515	92	H43E	2377	-297	1648	115
H13A	9313	6384	9247	148	H43F	3230	-543	934	115
H13B	8185	5926	8426	148	H61D	7551	3473	1185	171
H13C	7934	5792	9284	148	H61E	8639	3816	2039	171
H14A	4445	5739	9765	178	H61F	7015	3822	2016	171
H14B	4843	6799	9972	178	H62D	8204	1940	839	221
H14C	6038	6175	10033	178	H62E	8323	1360	1490	221
H21A	7720	8890	9847	172	H62F	9437	2220	1630	221
H21B	6083	8908	9739	172	H63D	8444	2097	2916	211
H21C	7132	9812	10152	172	H63E	7542	2891	3145	211
H22A	9037	9472	8896	138	H63F	9065	3101	2984	211

a) Molecule 1 as well as molecule 2 is strongly disordered and decomposes into symbol model A and B; b) ethyl groups at N1; c) *tert*-butyl substituents.

Parameters for **3b** see Thesis of R. Ruf [100].

Parameters for 3c

Atom	$X/a\cdot10^4$	$Y/b\cdot10^4$	$Z/c\cdot10^4$	U_{eq}	U_{11}	U_{22}	U_{33}	U_{23}	U_{13}	U_{12}
Cl1	7199(1)	8408(1)	871(1)	42(1)	35(1)	48(1)	43(1)	4(1)	7(1)	-12(1)
P1	3752(1)	7849(1)	2012(1)	18(1)	17(1)	18(1)	19(1)	-1(1)	0(1)	0(1)
C2	5058(2)	8237(1)	2702(2)	26(1)	21(1)	23(1)	32(1)	-9(1)	-4(1)	2(1)

P3	6320(1)	7679(1)	2178(1)	28(1)	19(1)	25(1)	40(1)	-6(1)	-4(1)	0(1)
C4	4926(2)	7161(1)	1466(2)	22(1)	18(1)	20(1)	27(1)	-4(1)	1(1)	2(1)
P5	4545(1)	7666(1)	302(1)	31(1)	35(1)	35(1)	24(1)	0(1)	9(1)	8(1)
C6	3375(2)	8248(1)	844(2)	23(1)	24(1)	25(1)	21(1)	1(1)	2(1)	-3(1)
N1	2414(2)	7581(1)	2588(1)	25(1)	21(1)	34(1)	21(1)	5(1)	3(1)	1(1)
C21	5240(3)	8922(2)	3425(2)	39(1)	37(2)	34(1)	45(2)	-21(1)	-18(1)	9(1)
C211	3888(4)	9276(2)	3710(3)	50(1)	54(2)	45(2)	49(2)	-25(2)	-1(2)	11(2)
C212	5973(8)	8586(4)	4290(4)	101(3)	141(5	85(4	74(3	-53(3)	-77(4)	63(4)
C213	6082(5)	9605(3)	2997(5)	82(2)	58(3)	48(2)	142(5)	-51(3)	8(3)	-17(2)
C41	4988(3)	6219(1)	1467(2)	29(1)	30(1)	20(1)	36(1)	-6(1)	-3(1)	2(1)
C411	5170(4)	5889(2)	2472(3)	49(1)	76(3)	26(2)	43(2)	4(1)	-5(2)	3(2)
C412	3703(3)	5868(2)	1018(3)	47(1)	36(2)	30(2)	74(2)	-18(2)	-10(2)	-2(1)
C413	6189(3)	5958(2)	882(3)	45(1)	40(2)	33(2)	61(2)	-13(1)	4(2)	12(1)
C61	2689(3)	8999(2)	412(2)	29(1)	38(1)	26(1)	24(1)	7(1)	2(1)	4(1)
C611	2853(6)	9718(2)	1078(3)	63(1)	111(4)	30(2)	47(2)	-2(1)	-16(2)	17(2)
C612	1187(4)	8861(3)	186(3)	58(1)	43(2)	60(2)	71(2)	28(2)	-9(2)	12(2)
C613	3344(4)	9200(2)	-523(2)	54(1)	64(2)	56(2)	44(2)	25(2)	16(2)	17(2)
C11	2552(3)	7268(2)	3558(2)	40(1)	40(2)	50(2)	29(1)	16(1)	7(1)	6(1)
C12	1017(2)	7610(2)	2183(2)	30(1)	21(1)	39(1)	31(1)	4(1)	3(1)	-6(1)
C13	304(4)	6794(2)	2228(3)	54(1)	36(2)	44(2)	81(3)	-8(2)	12(2)	-13(1)
C14	207(3)	8271(2)	2667(2)	42(1)	26(1)	50(2)	52(2)	2(2)	2(1)	9(1)

Atom	X/a·10^4	Y/b·10^4	Z/c·10^4	U$_{eq}$	Atom	X/a·10^4	Y/b·10^4	Z/c·10^4	U$_{eq}$
H111[a)]	2320(30)	6695(19)	3560(20)	41(8)	H411	4470(40)	6000(20)	2860(30)	55(10)
H112	3450(30)	7324(18)	3810(20)	41(8)	H412	6050(40)	6090(20)	2800(20)	58(10)
H113	2010(40)	7570(20)	3990(30)	55(10)	H413	5300(40)	5290(20)	2480(30)	73(12)
H121[b)]	1100(20)	7768(14)	1541(17)	17(6)	H421	3740(40)	5240(20)	1010(30)	74(12)
H131	790(40)	6360(20)	1970(20)	56(10)	H422	2970(40)	6030(20)	1370(20)	55(10)
H132	-500(40)	6840(20)	1890(30)	70(12)	H423	3540(30)	6050(20)	350(30)	56(10)
H133	180(40)	6610(30)	2870(30)	87(15)	H431	6290(30)	5360(20)	880(20)	51(9)
H141	-540(40)	8350(20)	2410(20)	53(10)	H432	7000(40)	6150(20)	1180(20)	54(10)
H142	750(30)	8820(20)	2650(20)	53(9)	H433	6080(40)	6130(20)	270(30)	69(12)
H143	30(30)	8108(19)	3320(20)	49(9)	H611	2450(40)	9620(20)	1680(30)	59(10)
H211[c)]	3360(40)	8890(20)	4040(30)	75(13)	H612	3820(40)	9800(20)	1180(30)	69(13)
H212	4080(30)	9740(20)	4210(20)	60(10)	H613	2410(40)	10190(30)	790(30)	86(13)
H213	3400(50)	9530(30)	3150(30)	100(15)	H621	1120(40)	8370(20)	-300(30)	72(12)
H221	6130(50)	9020(30)	4770(30)	99(15)	H622	860(40)	9310(20)	-180(20)	58(10)
H222	6760(50)	8300(30)	4210(30)	108(17)	H623	680(50)	8860(30)	780(40)	124(19)
H223	5460(50)	8220(30)	4600(40)	100(20)	H631	4370(40)	9299(19)	-440(20)	48(9)
H231	6170(40)	10060(30)	3480(30)	79(12)	H632	2950(40)	9700(20)	-820(30)	77(12)
H232	7020(60)	9350(30)	2930(40)	121(19)	H633	3240(40)	8690(30)	-1040(30)	86(13)
H233	5500(70)	9840(40)	2590(50)	160(30)					

a) Methyl group at N1; b) isopropyl substituent at N1; c) *tert*-butyl substituents

Parameters for 3d

Atom	X/a·10^4	Y/b·10^4	Z/c·10^4	U$_{eq}$	U$_{11}$	U$_{22}$	U$_{33}$	U$_{23}$	U$_{13}$	U$_{12}$
Cl1	1175(3)	3644(2)	2641(2)	123(1)	189(3)	109(2)	72(1)	64(1)	-74(2)	-79(2)
P1	1648(1)	2287(1)	4868(1)	28(1)	35(1)	28(1)	22(1)	3(1)	0(1)	-5(1)
C2	-58(5)	2578(3)	4666(3)	36(1)	37(3)	38(3)	34(3)	1(2)	-1(2)	-3(2)
P3	299(2)	3603(1)	4406(1)	47(1)	47(1)	35(1)	58(1)	6(1)	-14(1)	0(1)
C4	2119(5)	3374(3)	4713(3)	36(1)	42(3)	33(3)	33(3)	7(2)	4(2)	-6(2)
P5	3187(2)	3036(1)	3680(1)	49(1)	59(1)	50(1)	37(1)	2(1)	15(1)	-16(1)
C6	2768(5)	2028(3)	3946(4)	39(1)	41(3)	41(3)	33(3)	-5(2)	7(2)	-4(2)
N1	1909(5)	1711(3)	5806(3)	40(1)	58(3)	38(2)	23(2)	8(2)	-4(2)	-5(2)
C21	-1382(6)	2115(3)	4451(4)	44(1)	39(3)	47(3)	44(3)	-4(2)	-6(2)	-7(2)
C211	-1567(9)	1344(5)	5038(6)	88(3)	87(6)	97(6)	81(5)	24(5)	-23(4)	-59(5)
C212	-2572(8)	2711(5)	4569(8)	95(3)	52(5)	86(6)	148(9)	-47(6)	-9(5)	0(4)
C213	-1358(7)	1841(5)	3422(5)	68(2)	61(4)	92(5)	49(4)	-15(4)	-8(3)	-26(4)

C41	2786(6)	3968(3)	5407(4)	39(1)	41(3)	33(3)	43(3)	-1(2)	1(2)	-10(2)
C411	1841(7)	4099(4)	6265(4)	53(2)	63(4)	48(3)	47(3)	-12(3)	2(3)	-14(3)
C412	4162(6)	3633(4)	5745(4)	51(2)	43(3)	50(3)	61(4)	-3(3)	-12(3)	-13(3)
C413	3005(7)	4820(3)	4941(5)	55(2)	59(4)	33(3)	73(4)	4(3)	-4(3)	-10(3)
C61	3072(6)	1227(4)	3395(4)	50(2)	50(4)	54(4)	45(3)	-18(3)	5(3)	-9(3)
C611	2293(10)	503(4)	3787(6)	88(3)	121(7)	49(4)	96(6)	-30(4)	35(5)	-10(4)
C612	4579(8)	1065(6)	3383(7)	94(3)	59(5)	106(7)	117(7)	-57(6)	7(4)	5(5)
C613	2643(11)	1364(6)	2353(6)	103(3)	141(9)	112(7)	56(5)	-33(5)	-7(5)	-5(6)
C11	1009(7)	1742(4)	6613(4)	57(2)	83(5)	60(4)	28(3)	2(3)	2(3)	-24(3)
C12	3268(7)	1370(4)	6004(5)	64(2)	75(5)	57(4)	60(4)	8(3)	-25(3)	9(4)
C13	817(9)	829(5)	6987(5)	81(2)	117(7)	70(5)	56(4)	19(4)	17(4)	-2(5)

Atom	$X/a\cdot10^4$	$Y/b\cdot10^4$	$Z/c\cdot10^4$	U_{eq}	Atom	$X/a\cdot10^4$	$Y/b\cdot10^4$	$Z/c\cdot10^4$	U_{eq}
H111[a)]	131	1976	6437	69	H412	2276	4470	6701	79
H112	1406	2091	7097	69	H413	1673	3573	6563	79
H121[b)]	3184	797	6191	96	H421	4750	3539	5217	77
H122	3687	1683	6499	96	H422	4025	3118	6074	77
H123	3825	1404	5452	96	H423	4579	4032	6157	77
H131[a)]	315	842	7564	121	H431	3568	4753	4396	83
H132	1697	581	7092	121	H432	3448	5189	5374	83
H133	322	507	6534	121	H433	2137	5049	4762	83
H211[c)]	-773	996	4981	133	H611	2599	393	4413	132
H212	-2359	1044	4827	133	H612	2447	20	3405	132
H213	-1688	1501	5681	133	H613	1335	632	3795	132
H221	-2597	2908	5203	143	H621	5045	1544	3136	141
H222	-3411	2427	4427	143	H622	4767	590	2996	141
H223	-2462	3175	4152	143	H623	4891	959	4008	141
H231	-2213	1581	3266	101	H631	2939	897	1984	155
H232	-626	1451	3328	101	H632	3061	1864	2121	155
H233	-1220	2319	3029	101	H633	1666	1414	2315	155
H411	989	4337	6064	79					

a) Ethyl group at N1; b) methyl group at N1; c) *tert*-butyl substituents

9.5. Dichloro[4-(dimethylamino)phenyl)]arsine (4)

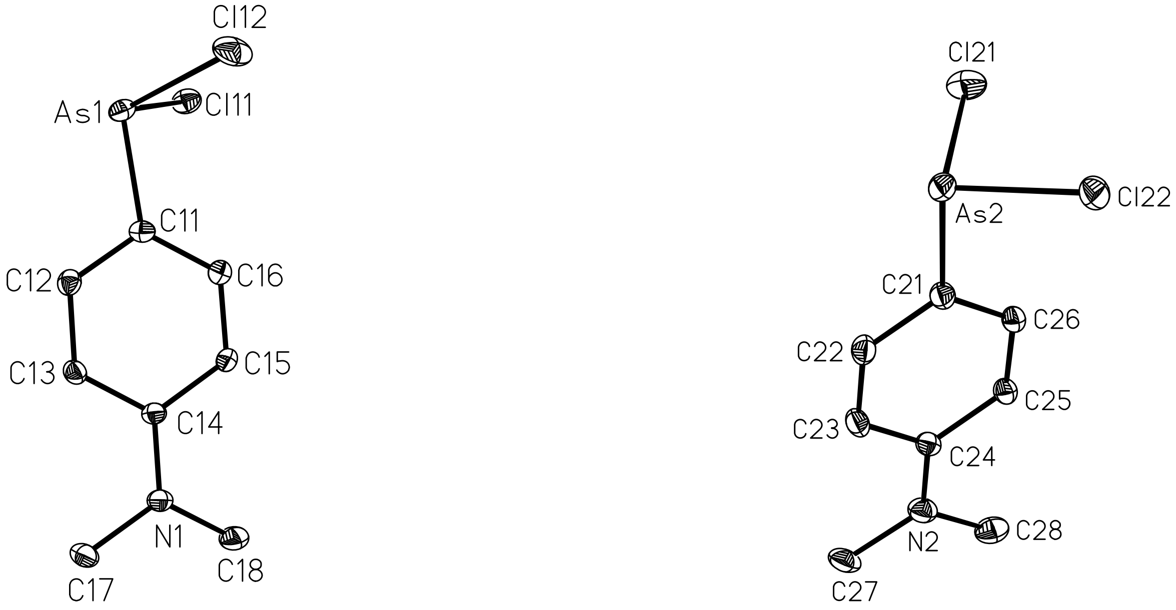

4 a **4 b**

Figure 9.5.1. Molecular structure (**4**) of two independent molecules **a** and **b**. Thermal ellipsoids are at 30% probability, hydrogen atoms are omitted for clarity

Table 9.5.1. Atomic Coordinates and Equivalent Isotropic Displacement Parameters as well as Anisotropic Displacement Parameters, with Estimated Standard Deviations in Parentheses.

Parameters for 4

Atom	X/a·10^4	Y/b·10^4	Z/c·10^4	U_{eq}	U_{11}	U_{22}	U_{33}	U_{23}	U_{13}	U_{12}
As1	5414(1)	8781(1)	3278(1)	26(1)	30(1)	19(1)	27(1)	2(1)	-10(1)	-7(1)
Cl11	3919(1)	8866(1)	5141(1)	34(1)	34(1)	28(1)	32(1)	-3(1)	-4(1)	-7(1)
Cl12	3904(2)	8416(1)	2388(1)	48(1)	47(1	46(1	54(1	-10(1)	-32(1)	-6(1)
N1	10238(4)	2968(4)	4196(3)	28(1)	22(2)	22(2)	33(2)	2(1)	-3(1)	-5(1)
C11	6858(4)	6884(4)	3477(3)	25(1)	23(2)	22(2)	26(2)	0(1)	-8(1)	-5(1)
C12	8400(4)	6688(4)	3113(3)	25(1)	28(2)	26(2)	22(2)	2(1)	-6(1)	-13(2)
C13	9526(4)	5395(4)	3335(3)	24(1)	20(2)	27(2)	25(2)	2(1)	-4(1)	-9(1)
C14	9151(4)	4236(4)	3939(3)	23(1)	22(2)	19(2)	24(2)	-2(1)	-5(1)	-5(1)
C15	7579(4)	4445(4)	4262(4)	27(1)	23(2	20(2	38(2	2(2)	-4(2)	-10(1)
C16	6483(4)	5738(4)	4035(4)	28(1)	25(2)	25(2)	34(2)	3(2)	-8(2)	-11(2)
C17	11839(4)	2771(5)	3831(4)	30(1)	21(2)	31(2)	34(2)	-1(2)	-7(2)	-5(2)
C18	9826(5)	1881(5)	5017(5)	38(1)	31(2)	27(2)	47(3)	10(2)	-13(2)	-7(2)
As2	-441(1)	7728(1)	-1249(1)	30(1)	33(1)	30(1)	26(1)	-4(1)	-11(1)	-9(1)
Cl22	-2132(1)	9052(1)	218(1)	40(1)	36(1)	34(1)	37(1)	-7(1)	-10(1)	1(1)
Cl21	603(2)	9278(2)	-2142(1)	48(1)	56(1)	46(1)	43(1)	12(1)	-15(1)	-24(1)
N2	4430(4)	3746(4)	1475(3)	33(1)	32(2)	27(2)	34(2)	3(1)	-10(1)	-7(1)
C21	1063(4)	6556(4)	-337(4)	26(1)	26(2)	25(2)	27(2)	-4(1)	-7(1)	-7(2)
C22	1763(5)	5128(5)	-565(4)	29(1)	34(2)	29(2)	27(2)	-8(2)	-6(2)	-13(2)
C23	2874(5)	4192(4)	23(4)	29(1)	30(2)	21(2)	32(2)	-7(2)	-1(2)	-8(2)
C24	3335(4)	4653(4)	883(3)	24(1)	21(2)	22(2)	26(2)	0(1)	-2(1)	-7(1)
C25	2603(4)	6113(4)	1115(4)	25(1)	28(2)	23(2)	27(2)	-4(1)	-7(1)	-11(2)
C26	1500(4)	7038(4)	518(3)	25(1)	28(2)	23(2)	26(2)	-4(1)	-7(1)	-9(2)
C27	5189(6)	2268(5)	1200(5)	39(1)	36(2)	23(2)	44(3)	6(2)	-5(2)	-3(2)
C28	4882(6)	4221(6)	2381(5)	40(1)	37(2)	45(3)	36(2)	8(2)	-15(2)	-14(2)

Atom	X/a·10^3	Y/b·10^3	Z/c·10^3	U$_{eq}$	Atom	X/a·10^3	Y/b·10^3	Z/c·10^3	U$_{eq}$
H12	873(7)	735(7)	276(6)	54(18)	H22	148(5)	477(5)	-113(4)	28(12)
H13	1048(5)	539(5)	308(4)	16(10)	H23	328(6)	325(6)	-12(5)	37(14)
H15	730(6)	382(6)	465(5)	40(15)	H25	285(6)	643(6)	170(5)	37(14)
H16	542(6)	582(6)	425(5)	36(13)	H26	105(5)	800(5)	72(4)	27(12)
H171	1216(6)	309(6)	301(6)	41(14)	H271	454(7)	171(7)	137(6)	56(18)
H172	1239(7)	183(7)	403(5)	52(19)	H272	581(7)	183(7)	172(6)	47(16)
H173	1210(8)	332(8)	423(7)	70(20)	H273	571(7)	222(6)	33(6)	44(15)
H181	918(7)	216(7)	587(6)	47(16)	H281	522(7)	496(7)	203(6)	52(17)
H182	932(7)	150(6)	468(5)	40(15)	H282	570(8)	339(8)	273(6)	61(19)
H183	1060(9)	114(9)	511(7)	80(20)	H283	407(7)	456(7)	306(6)	54(18)

9.6. Tris[4-(dimethylamino)phenyl]arsine (5).

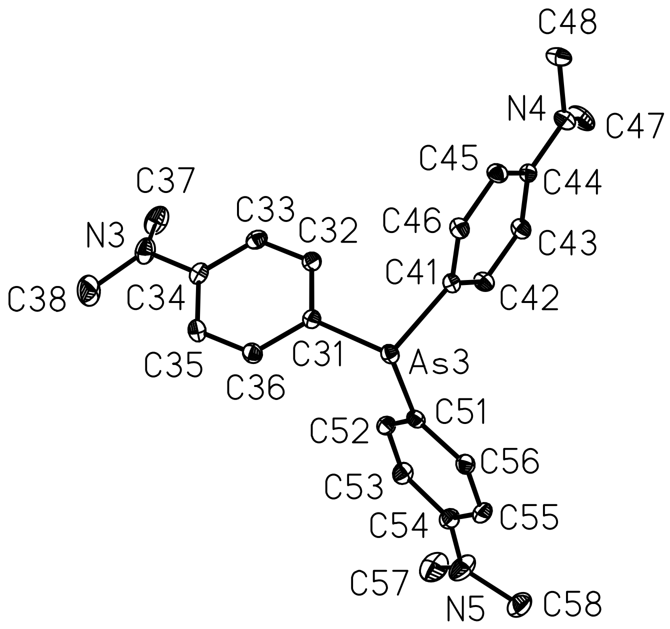

Figure 9.6.1. Molecular structure (**5**). Thermal ellipsoids are at 30 % probability, hydrogen atoms are omitted for clarity.

Table 9.6.1. Atomic Coordinates and Equivalent Isotropic Displacement Parameters as well as Anisotropic Displacement Parameters, with Estimated Standard Deviations in Parentheses

Parameters for 5

Atom	X/a·10^4	Y/b·10^4	Z/c·10^4	U$_{eq}$	U$_{11}$	U$_{22}$	U$_{33}$	U$_{23}$	U$_{13}$	U$_{12}$
As3	2432(1)	3606(1)	6391(1)	23(1)	26(1)	20(1)	24(1)	8(1)	10(1)	2(1)
N3	2102(2)	1337(2)	489(2)	39(1)	47(1)	43(1)	24(1)	6(1)	12(1)	0(1)
N4	2773(2)	9343(2)	6784(2)	31(1)	35(1)	23(1)	37(1)	12(1)	10(1)	7(1)
N5	8416(2)	2903(3)	8775(2)	51(1)	38(1)	79(2)	34(1)	19(1)	5(1)	21(1)
C31	2376(2)	2943(2)	4533(2)	23(1)	22(1)	24(1)	23(1)	8(1)	6(1)	2(1)
C32	2186(2)	1600(2)	3889(2)	28(1)	33(1)	24(1)	28(1)	10(1)	7(1)	0(1)
C33	2100(2)	1061(2)	2568(2)	30(1)	33(1)	24(1)	28(1)	4(1)	8(1)	1(1)
C34	2201(2)	1860(2)	1826(2)	27(1)	23(1)	34(1)	22(1)	8(1)	5(1)	1(1)
C35	2375(2)	3209(2)	2469(2)	28(1)	25(1)	34(1)	28(1)	16(1)	5(1)	2(1)
C36	2464(2)	3732(2)	3792(2)	25(1)	24(1)	25(1)	27(1)	10(1)	5(1)	1(1)
C38	1999(5)	-73(3)	-85(3)	60(1)	93(3)	50(2)	32(1)	3(1)	24(2)	10(2)
C37	2957(4)	2068(4)	-42(3)	49(1)	51(2)	66(2)	29(1)	16(1)	14(1)	-2(1)
C41	2596(2)	5452(2)	6654(2)	22(1)	24(1)	20(1)	23(1)	6(1)	7(1)	3(1)
C42	1381(2)	6002(2)	6500(2)	26(1)	21(1)	24(1)	30(1)	7(1)	6(1)	2(1)
C43	1426(2)	7278(2)	6538(2)	27(1)	22(1)	26(1)	33(1)	9(1)	6(1)	8(1)

C44	2711(2)	8064(2)	6743(2)	24(1)	29(1)	22(1)	20(1)	7(1)	6(1)	5(1)
C45	3937(2)	7521(2)	6939(2)	27(1)	23(1)	24(1)	34(1)	9(1)	7(1)	1(1)
C36	3874(2)	6240(2)	6887(2)	26(1)	20(1)	24(1)	34(1)	10(1)	7(1)	5(1)
C48	1494(3)	9762(3)	6284(3)	39(1)	47(1)	32(1)	44(1)	21(1)	9(1)	15(1)
C47	4074(3)	10011(3)	6720(3)	45(1)	48(2)	23(1)	70(2)	20(1)	23(1)	4(1)
C51	4385(2)	3502(2)	7102(2)	23(1)	28(1)	19(1)	25(1)	9(1)	10(1)	5(1)
C52	4818(2)	3697(2)	8425(2)	29(1)	39(1)	26(1)	24(1)	8(1)	13(1)	10(1)
C53	6147(3)	3547(2)	8991(2)	33(1)	42(1)	37(1)	20(1)	10(1)	7(1)	10(1)
C54	7117(2)	3157(2)	8239(2)	32(1)	32(1)	35(1)	29(1)	10(1)	5(1)	8(1)
C55	6700(2)	2998(2)	6912(2)	32(1)	33(1)	37(1)	27(1)	10(1)	14(1)	8(1)
C56	5367(2)	3164(2)	6364(2)	27(1)	33(1)	27(1)	22(1)	10(1)	9(1)	6(1)
C57	9435(3)	2641(4)	8009(4)	61(1)	34(2)	88(3)	56(2)	20(2)	9(1)	23(2)
C58	8936(4)	3358(4)	10175(3)	52(1)	51(2)	61(2)	37(1)	14(1)	-5(1)	15(2)

Atom	$X/a \cdot 10^3$	$Y/b \cdot 10^3$	$Z/c \cdot 10^3$	U_{eq}	Atom	$X/a \cdot 10^3$	$Y/b \cdot 10^3$	$Z/c \cdot 10^3$	U_{eq}
H32	206(3)	101(3)	435(2)	28(6)	H482	81(3)	968(3)	677(3)	39(8)
H33	202(3)	16(3)	219(3)	38(7)	H483	113(4)	927(4)	539(4)	72(12)
H35	242(3)	376(3)	200(3)	31(7)	H471	398(3)	1082(3)	678(3)	45(8)
H36	263(3)	462(3)	416(3)	40(8)	H472	485(4)	1011(3)	751(3)	50(9)
H381	291(3)	-30(3)	29(3)	38(8)	H473	441(4)	957(4)	603(4)	79(13)
H382	111(5)	-50(4)	8(4)	89(14)	H52	417(3)	401(2)	899(2)	28(6)
H383	189(5)	-30(4)	-99(5)	88(14)	H53	635(3)	363(3)	984(3)	38(7)
H371	392(4)	213(4)	27(4)	64(11)	H55	726(3)	278(3)	637(3)	34(7)
H372	281(3)	164(3)	-99(4)	55(9)	H56	515(3)	303(3)	547(3)	33(7)
H373	272(4)	288(4)	7(4)	60(11)	H571	974(4)	345(4)	777(3)	59(10)
H42	54(3)	553(3)	642(2)	27(6)	H572	1026(4)	252(4)	850(4)	62(10)
H43	60(3)	759(3)	641(3)	30(7)	H573	904(4)	194(4)	722(4)	69(11)
H45	481(3)	799(3)	711(3)	42(8)	H581	835(4)	308(3)	1063(4)	58(10)
H46	469(3)	592(3)	698(3)	30(7)	H582	972(5)	310(4)	1040(4)	79(13)
H481	170(3)	1064(3)	642(2)	25(6)	H583	899(5)	442(5)	1065(4)	92(14)

9.7. Dichloro(2,6-bis[2,4,6-tri-isopropylphenyl]phenyl)arsine [342].

The disorder of the C–AsCl_2 group in the solid state structure of dichloroterphenylarsine can partially be resolved with the assumption of four molecules as shown below. *Isopropyl* groups and hydrogen atoms have been omitted for clarity.

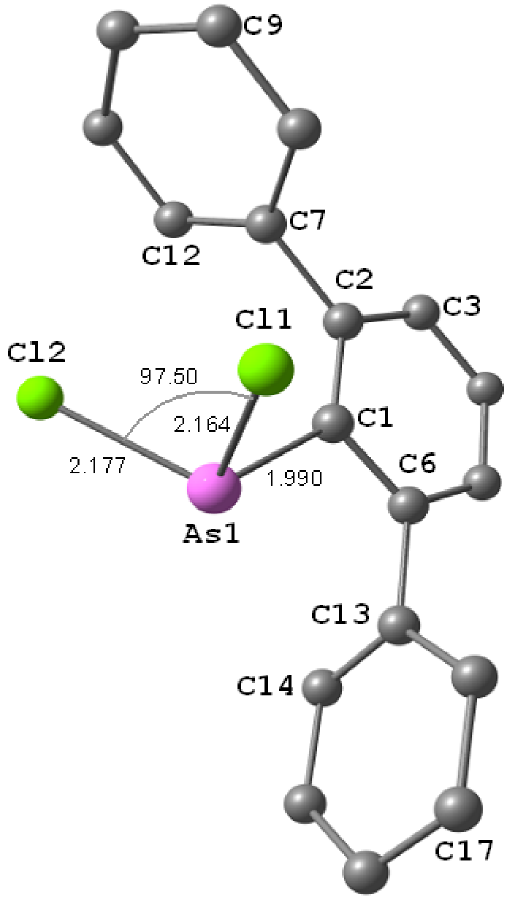

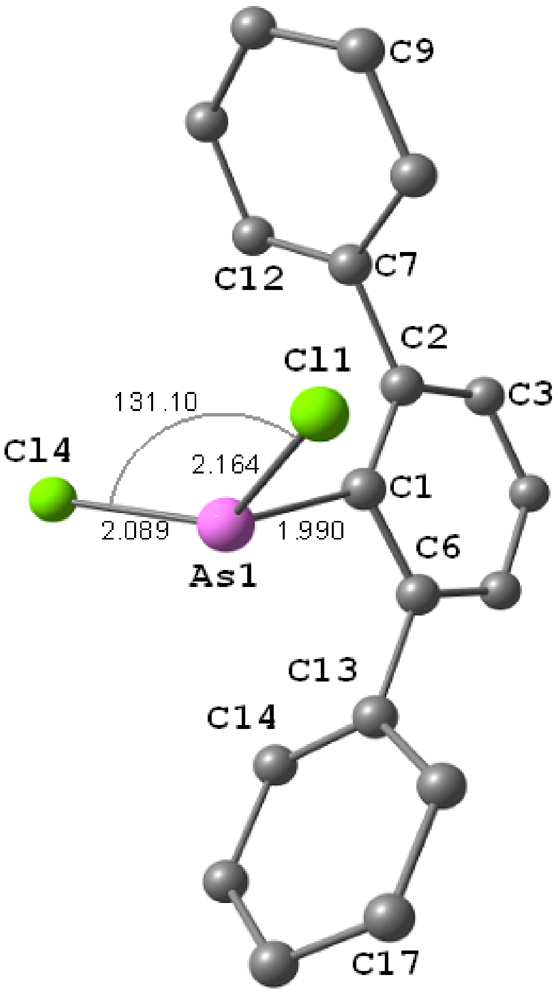

…..

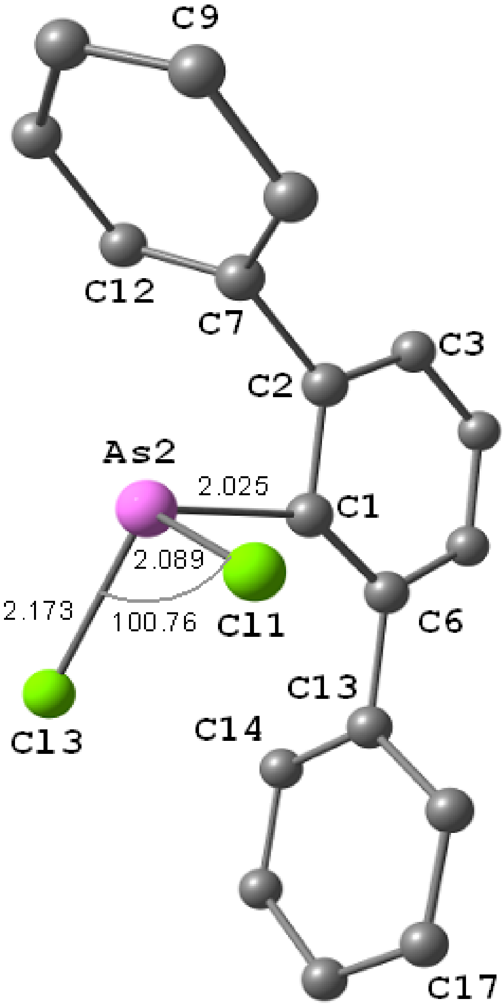
C9
C12
C7
C3
C2
As2
2.025
C1
2.089
2.173
100.76
Cl1
C6
C13
Cl3
C14
C17

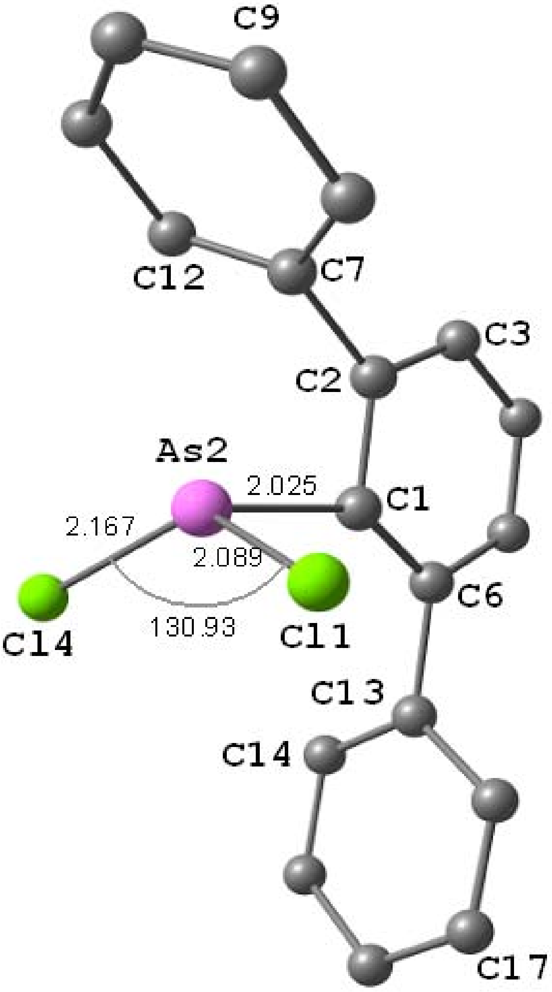
C9
C12
C7
C3
C2
As2
2.025
C1
2.167
2.089
C6
Cl4
130.93
Cl1
C13
C14
C17

……

9.8. Optimized Cartesian Coordinates and Total Energies [Hartree] for All Species Reported of Chapter 3.

1 Hartree = 627.5095 kcal = 2627.26 kJ
Coordinates X, Y, Z in Angstroms

$[H_2P(CH)_2P_2]^{\oplus}$ (C_{2v}, minimum)
E(RB+HF-LYP) = -1102.45174177
zero-point energy = 0.055524

Atom	X	Y	Z
15	0.000000	1.083981	-0.969408
15	0.000000	-1.083981	-0.969408
15	0.000000	0.000000	1.505793
1	0.000000	1.125615	2.361460
1	0.000000	-1.125615	2.361460
6	1.134520	0.000000	0.128339
1	2.216672	0.000000	0.116182
6	-1.134520	0.000000	0.128339
1	-2.216672	0.000000	0.116182

$[H_2P(CH)_2P_2]^{\oplus}$ (C_1, minimum)
E(RB+HF-LYP) = -1102.41994678
zero-point energy = 0.053385

Atom	X	Y	Z
15	-1.494760	-0.494002	-0.337337
1	-2.769585	-0.830271	0.167135
1	-1.200305	-1.231884	-1.499018
15	-0.249341	1.299424	0.270969
15	1.517700	-0.781737	0.046769
6	-0.156501	-0.492756	0.894210
1	-0.388955	-0.802677	1.908191
6	1.166621	0.705499	-0.694596
1	1.694159	1.233107	-1.480012

$[H_2P(CH)_2P_2]^{\oplus}$ (C_2, first-order saddle point)
E(RB+HF-LYP) = -1102.35449040
zero-point energy = 0.052146

Atom	X	Y	Z
15	0.000000	0.000000	1.236442
1	-0.305142	1.049250	2.149208
1	0.305142	-1.049250	2.149208
15	-1.393111	0.037857	-0.553717
15	-1.393111	-0.037857	-0.553717
6	0.000000	1.157186	-0.460104
1	0.022708	2.234869	-0.356150
6	0.000000	-1.157186	-0.460104
1	-0.022708	-2.234869	-0.356150

$[P(CH)_2P_2]^{\oplus}$ (C_{2v}, square-pyramidal, minimum)
E(RB+HF-LYP) = -1101.24272304
zero-point energy = 0.036087

Atom	**X**	**Y**	**Z**
15	0.000000	0.000000	1.303002
15	-1.401720	0.000000	-0.496674
15	1.401720	0.000000	-0.496674
6	0.000000	1.139710	-0.344226
1	0.000000	2.220390	-0.257053
6	0.000000	-1.139710	-0.344226
1	0.000000	-2.220390	-0.257053

$[P(CH)_2P_2]^{\oplus}$ (C_{2v}, trigonal bipyramidal, first-order saddle point)
E(RB+HF-LYP) = -1101.22848524
zero-point energy = 0.035454

Atom	**X**	**Y**	**Z**
15	-1.065390	0.000000	-0.900280
15	1.065390	0.000000	-0.900280
15	0.000000	0.000000	1.590004
6	0.000000	1.139457	0.228233
1	0.000000	2.221994	0.209772
6	0.000000	-1.139457	0.228233
1	0.000000	-2.221994	0.209772

[**2c** calc tricycl]$^{\oplus}$ (C_1, minimum)
E(RB+HF-LYP) = -1766.18341017
zero-point energy = 0.450475

Atom	**X**	**Y**	**Z**
15	1.004961	0.567451	-1.843298
6	0.371967	1.466446	-0.265489
6	-0.248417	2.866473	-0.271428
6	0.614498	3.800265	-1.145274
1	0.661416	3.460246	-2.183784
1	1.636286	3.888675	-0.765077
1	0.180706	4.802694	-1.151338
6	-0.301578	3.431843	1.162673
1	-0.741606	4.431793	1.150880
1	-0.919164	2.815821	1.822707
1	0.696701	3.515132	1.599552
6	-1.675750	2.808162	-0.855542
1	-2.103043	3.813365	-0.886279
1	-1.674945	2.413227	-1.874528
1	-2.340870	2.186169	-0.252406
15	-0.134541	-0.093902	0.536403
6	-1.750204	-0.739528	-0.016232
6	-2.897310	-0.523460	0.766644
1	-2.835416	-0.032494	1.729536
6	-4.145788	-0.936444	0.313041
1	-5.021746	-0.764369	0.926955
6	-4.268240	-1.570762	-0.922184

1	-5.241420	-1.895462	-1.270806
6	-3.137683	-1.787439	-1.706401
1	-3.226898	-2.281810	-2.666311
6	-1.886186	-1.371556	-1.261154
1	-1.022236	-1.552400	-1.884639
6	-0.149621	-0.151131	2.399992
1	-0.992955	0.503799	2.649572
6	1.110104	0.441864	3.050889
1	1.994757	-0.165049	2.852949
1	1.307524	1.464763	2.730949
1	0.963396	0.460539	4.133825
6	-0.456201	-1.561831	2.939253
1	-1.364607	-1.993257	2.519104
1	0.368847	-2.251237	2.752420
1	-0.586857	-1.499074	4.022329
6	1.362638	-0.626051	-0.371189
6	2.127074	-1.954208	-0.475737
6	3.180623	-1.842740	-1.598680
1	2.720648	-1.656212	-2.573046
1	3.735405	-2.780561	-1.673857
1	3.908125	-1.049993	-1.403225
6	2.857760	-2.255336	0.849725
1	3.422775	-3.185887	0.757847
1	3.564047	-1.462076	1.107518
1	2.161655	-2.380079	1.681258
6	1.168895	-3.116603	-0.802842
1	1.727090	-4.055425	-0.830842
1	0.698207	-2.988413	-1.780184
1	0.381100	-3.227245	-0.052552
15	2.241818	1.072921	-0.155032

[**2c** calc housene]$^{\oplus}$ (C_1, minimum)
E(RB+HF-LYP) = -1766. 15076038
zero-point energy = 0.448857

Atom	**X**	**Y**	**Z**
6	0.189460	1.184268	0.257330
6	-0.536378	2.551071	0.278232
6	0.477178	3.635429	-0.152822
1	0.880773	3.435072	-1.149691
1	1.313412	3.723110	0.545502
1	-0.021349	4.606843	-0.189209
6	-1.004848	2.832315	1.720460
1	-1.455828	3.825857	1.781645
1	-1.757994	2.108385	2.045180
1	-0.173545	2.804612	2.430606
6	-1.734945	2.619321	-0.686752
1	-2.129363	3.638110	-0.695682
1	-1.441388	2.374354	-1.711553

1	-2.548867	1.958361	-0.393046
15	-0.600666	-0.488429	0.312970
6	-2.334643	-0.623358	-0.212143
6	-3.364987	-0.474793	0.730625
1	-3.144712	-0.246581	1.767643
6	-4.690936	-0.602550	0.331699
1	-5.484349	-0.482563	1.059653
6	-4.997550	-0.880861	-1.001046
1	-6.032224	-0.980205	-1.307087
6	-3.977364	-1.034687	-1.937122
1	-4.214698	-1.257001	-2.970538
6	-2.645889	-0.908470	-1.548340
1	-1.859078	-1.034503	-2.282130
6	-0.376175	-1.793485	1.646697
1	-1.305069	-1.640785	2.209663
6	0.799102	-1.662818	2.617078
1	1.755236	-1.849836	2.130583
1	0.839612	-0.686432	3.101791
1	0.669059	-2.416450	3.399096
6	-0.437856	-3.178098	0.977646
1	-1.310687	-3.295689	0.332956
1	0.461111	-3.373347	0.389660
1	-0.500169	-3.938940	1.759590
15	0.742586	0.197734	-1.306251
15	1.955223	1.070763	1.000863
6	2.303305	0.063590	-0.320270
6	3.557800	-0.668598	-0.728054
6	4.646831	-0.504536	0.348953
6	3.241949	-2.168703	-0.931908
6	4.066351	-0.073375	-2.065980
1	4.336713	-0.929921	1.307528
1	5.560246	-1.017214	0.038745
1	4.898909	0.547955	0.506646
1	2.463458	-2.321291	-1.686056
1	4.137192	-2.692506	-1.275977
1	2.918502	-2.639222	0.000186
1	4.302574	0.987952	-1.960999
1	4.974300	-0.595310	-2.378289
1	3.328660	-0.183795	-2.865850

```
-----------------------------------------------------------------------------
```

nido-$[P(CH)_2P_2]^{\oplus}$

```
-----------------------------------------------------------------------------
     Molecular Orbital Coefficients
                           25        26        27        28        29
                        (B2)--O   (A1)--O   (B1)--O   (B2)--O   (B1)--O
     EIGENVALUES --    -0.59133  -0.53029  -0.51867  -0.51501  -0.46433
   1 1   P  1S          0.00000   0.03425   0.00000   0.00000   0.00000
   2        2S          0.00000  -0.15659   0.00000   0.00000   0.00000
   3        2PX         0.00000   0.00000  -0.16361   0.00000  -0.07328
   4        2PY         0.08130   0.00000   0.00000  -0.15126   0.00000
   5        2PZ         0.00000  -0.15577   0.00000   0.00000   0.00000
   6        3S          0.00000   0.37692   0.00000   0.00000   0.00000
   7        3PX         0.00000   0.00000   0.44430   0.00000   0.19756
   8        3PY        -0.21206   0.00000   0.00000   0.39678   0.00000
   9        3PZ         0.00000   0.42125   0.00000   0.00000   0.00000
  10        4S          0.00000   0.25498   0.00000   0.00000   0.00000
  11        4PX         0.00000   0.00000   0.13503   0.00000   0.11524
  12        4PY        -0.02783   0.00000   0.00000   0.13991   0.00000
  13        4PZ         0.00000   0.12322   0.00000   0.00000   0.00000
  14        5XX         0.00000  -0.01170   0.00000   0.00000   0.00000
  15        5YY         0.00000  -0.00111   0.00000   0.00000   0.00000
  16        5ZZ         0.00000  -0.03746   0.00000   0.00000   0.00000
  17        5XY         0.00000   0.00000   0.00000   0.00000   0.00000
  18        5XZ         0.00000   0.00000  -0.06111   0.00000   0.00162
  19        5YZ         0.05187   0.00000   0.00000  -0.04533   0.00000
  20 2   P  1S          0.00000  -0.01043   0.01969   0.00000  -0.01080
  21        2S          0.00000   0.04155  -0.08718   0.00000   0.05467
  22        2PX         0.00000  -0.04682   0.06382   0.00000  -0.14725
  23        2PY         0.06958   0.00000   0.00000   0.06374   0.00000
  24        2PZ         0.00000   0.08282   0.12401   0.00000   0.04951
  25        3S          0.00000  -0.12976   0.22480   0.00000  -0.10047
  26        3PX         0.00000   0.11503  -0.17072   0.00000   0.39599
  27        3PY        -0.17433   0.00000   0.00000  -0.17269   0.00000
  28        3PZ         0.00000  -0.22118  -0.33453   0.00000  -0.13290
  29        4S          0.00000  -0.03563   0.10500   0.00000  -0.22247
  30        4PX         0.00000   0.06154  -0.07768   0.00000   0.09933
  31        4PY        -0.01207   0.00000   0.00000  -0.04113   0.00000
  32        4PZ         0.00000  -0.06070  -0.12481   0.00000  -0.06978
  33        5XX         0.00000   0.01141  -0.00229   0.00000   0.01394
  34        5YY         0.00000  -0.00069   0.00841   0.00000   0.03508
  35        5ZZ         0.00000  -0.01201  -0.02942   0.00000  -0.03777
  36        5XY        -0.04347   0.00000   0.00000  -0.03310   0.00000
  37        5XZ         0.00000  -0.03921  -0.03152   0.00000   0.00212
  38        5YZ        -0.01807   0.00000   0.00000   0.03958   0.00000
  39 3   P  1S          0.00000  -0.01043  -0.01969   0.00000   0.01080
  40        2S          0.00000   0.04155   0.08718   0.00000  -0.05467
  41        2PX         0.00000   0.04682   0.06382   0.00000  -0.14725
  42        2PY         0.06958   0.00000   0.00000   0.06374   0.00000
  43        2PZ         0.00000   0.08282  -0.12401   0.00000  -0.04951
  44        3S          0.00000  -0.12976  -0.22480   0.00000   0.10047
  45        3PX         0.00000  -0.11503  -0.17072   0.00000   0.39599
  46        3PY        -0.17433   0.00000   0.00000  -0.17269   0.00000
  47        3PZ         0.00000  -0.22118   0.33453   0.00000   0.13290
  48        4S          0.00000  -0.03563  -0.10500   0.00000   0.22247
  49        4PX         0.00000  -0.06154  -0.07768   0.00000   0.09933
  50        4PY        -0.01207   0.00000   0.00000  -0.04113   0.00000
  51        4PZ         0.00000  -0.06070   0.12481   0.00000   0.06978
  52        5XX         0.00000   0.01141   0.00229   0.00000  -0.01394
  53        5YY         0.00000  -0.00069  -0.00841   0.00000  -0.03508
  54        5ZZ         0.00000  -0.01201   0.02942   0.00000   0.03777
  55        5XY         0.04347   0.00000   0.00000   0.03310   0.00000
```

```
56        5XZ          0.00000   0.03921  -0.03152   0.00000   0.00212
57        5YZ         -0.01807   0.00000   0.00000   0.03958   0.00000
58 4   C  1S           0.01857  -0.01118   0.00000   0.02838   0.00000
59        2S          -0.02913   0.01774   0.00000  -0.07405   0.00000
60        2PX          0.00000   0.00000   0.04277   0.00000  -0.25741
61        2PY          0.34416  -0.02511   0.00000   0.08084   0.00000
62        2PZ         -0.05824  -0.20322   0.00000   0.30276   0.00000
63        3S          -0.13360   0.01898   0.00000  -0.07727   0.00000
64        3PX          0.00000   0.00000   0.00369   0.00000  -0.18336
65        3PY          0.18237  -0.03044   0.00000   0.01924   0.00000
66        3PZ         -0.04487  -0.13111   0.00000   0.23062   0.00000
67        4XX         -0.01095  -0.00395   0.00000  -0.01251   0.00000
68        4YY          0.01683  -0.00119   0.00000   0.00070   0.00000
69        4ZZ         -0.00899   0.00036   0.00000   0.01336   0.00000
70        4XY          0.00000   0.00000  -0.00360   0.00000   0.01192
71        4XZ          0.00000   0.00000   0.01821   0.00000   0.00489
72        4YZ          0.01069   0.01328   0.00000  -0.00728   0.00000
73 5   H  1S           0.20393  -0.01314   0.00000   0.03684   0.00000
74        2S           0.14261   0.00301   0.00000   0.03765   0.00000
75 6   C  1S          -0.01857  -0.01118   0.00000  -0.02838   0.00000
76        2S           0.02913   0.01774   0.00000   0.07405   0.00000
77        2PX          0.00000   0.00000   0.04277   0.00000  -0.25741
78        2PY          0.34416   0.02511   0.00000   0.08084   0.00000
79        2PZ          0.05824  -0.20322   0.00000  -0.30276   0.00000
80        3S           0.13360   0.01898   0.00000   0.07727   0.00000
81        3PX          0.00000   0.00000   0.00369   0.00000  -0.18336
82        3PY          0.18237   0.03044   0.00000   0.01924   0.00000
83        3PZ          0.04487  -0.13111   0.00000  -0.23062   0.00000
84        4XX          0.01095  -0.00395   0.00000   0.01251   0.00000
85        4YY         -0.01683  -0.00119   0.00000  -0.00070   0.00000
86        4ZZ          0.00899   0.00036   0.00000  -0.01336   0.00000
87        4XY          0.00000   0.00000   0.00360   0.00000  -0.01192
88        4XZ          0.00000   0.00000   0.01821   0.00000   0.00489
89        4YZ          0.01069  -0.01328   0.00000  -0.00728   0.00000
90 7   H  1S          -0.20393  -0.01314   0.00000  -0.03684   0.00000
91        2S          -0.14261   0.00301   0.00000  -0.03765   0.00000
                          30        31        32        33        34
                       (A1)--V   (B1)--V   (B2)--V   (B2)--V   (A1)--V
   EIGENVALUES --     -0.28179  -0.25123  -0.23861  -0.21927  -0.18306
 1 1   P  1S          -0.01090   0.00000   0.00000   0.00000  -0.02608
 2        2S           0.04903   0.00000   0.00000   0.00000   0.13209
 3        2PX          0.00000  -0.18807   0.00000   0.00000   0.00000
 4        2PY          0.00000   0.00000   0.11912  -0.15233   0.00000
 5        2PZ         -0.07055   0.00000   0.00000   0.00000  -0.17602
 6        3S          -0.12238   0.00000   0.00000   0.00000  -0.25653
 7        3PX          0.00000   0.53527   0.00000   0.00000   0.00000
 8        3PY          0.00000   0.00000  -0.33368   0.44674   0.00000
 9        3PZ          0.20759   0.00000   0.00000   0.00000   0.53068
10        4S          -0.31173   0.00000   0.00000   0.00000  -0.79959
11        4PX          0.00000   0.56659   0.00000   0.00000   0.00000
12        4PY          0.00000   0.00000  -0.44937   0.49324   0.00000
13        4PZ          0.21839   0.00000   0.00000   0.00000   0.96261
14        5XX          0.07433   0.00000   0.00000   0.00000  -0.08536
15        5YY         -0.05847   0.00000   0.00000   0.00000   0.03273
16        5ZZ         -0.02064   0.00000   0.00000   0.00000   0.05185
17        5XY          0.00000   0.00000   0.00000   0.00000   0.00000
18        5XZ          0.00000   0.04865   0.00000   0.00000   0.00000
19        5YZ          0.00000   0.00000  -0.08733   0.06121   0.00000
20 2   P  1S           0.00148   0.00380   0.00000   0.00000   0.00620
21        2S          -0.01391  -0.01418   0.00000   0.00000  -0.01151
22        2PX         -0.02565   0.03267   0.00000   0.00000   0.00959
23        2PY          0.00000   0.00000   0.09562   0.10753   0.00000
24        2PZ         -0.15397  -0.13465   0.00000   0.00000   0.00535
```

```
25        3S      -0.00986   0.05450   0.00000   0.00000   0.13491
26        3PX      0.08190  -0.09534   0.00000   0.00000  -0.03265
27        3PY      0.00000   0.00000  -0.27514  -0.31519   0.00000
28        3PZ      0.43125   0.38426   0.00000   0.00000  -0.03159
29        4S       0.21027   0.00023   0.00000   0.00000  -0.09937
30        4PX      0.12748  -0.12281   0.00000   0.00000  -0.21418
31        4PY      0.00000   0.00000  -0.39498  -0.37005   0.00000
32        4PZ      0.45690   0.38483   0.00000   0.00000   0.14612
33        5XX      0.00497   0.01771   0.00000   0.00000   0.04232
34        5YY      0.01257   0.02870   0.00000   0.00000   0.02461
35        5ZZ     -0.01155  -0.04878   0.00000   0.00000  -0.08263
36        5XY      0.00000   0.00000   0.06740   0.05222   0.00000
37        5XZ     -0.04125  -0.01089   0.00000   0.00000   0.00027
38        5YZ      0.00000   0.00000   0.01829  -0.03472   0.00000
39 3   P  1S       0.00148  -0.00380   0.00000   0.00000   0.00620
40        2S      -0.01391   0.01418   0.00000   0.00000  -0.01151
41        2PX      0.02565   0.03267   0.00000   0.00000  -0.00959
42        2PY      0.00000   0.00000   0.09562   0.10753   0.00000
43        2PZ     -0.15397   0.13465   0.00000   0.00000   0.00535
44        3S      -0.00986  -0.05450   0.00000   0.00000   0.13491
45        3PX     -0.08190  -0.09534   0.00000   0.00000   0.03265
46        3PY      0.00000   0.00000  -0.27514  -0.31519   0.00000
47        3PZ      0.43125  -0.38426   0.00000   0.00000  -0.03159
48        4S       0.21027  -0.00023   0.00000   0.00000  -0.09937
49        4PX     -0.12748  -0.12281   0.00000   0.00000   0.21418
50        4PY      0.00000   0.00000  -0.39498  -0.37005   0.00000
51        4PZ      0.45690  -0.38483   0.00000   0.00000   0.14612
52        5XX      0.00497  -0.01771   0.00000   0.00000   0.04232
53        5YY      0.01257  -0.02870   0.00000   0.00000   0.02461
54        5ZZ     -0.01155   0.04878   0.00000   0.00000  -0.08263
55        5XY      0.00000   0.00000  -0.06740  -0.05222   0.00000
56        5XZ      0.04125  -0.01089   0.00000   0.00000  -0.00027
57        5YZ      0.00000   0.00000   0.01829  -0.03472   0.00000
58 4   C  1S      -0.00543   0.00000  -0.07970  -0.03197  -0.05599
59        2S       0.03659   0.00000   0.14633   0.05908   0.05831
60        2PX      0.00000  -0.08918   0.00000   0.00000   0.00000
61        2PY      0.00116   0.00000  -0.11817  -0.04116  -0.11555
62        2PZ     -0.21987   0.00000   0.14662  -0.26431   0.22728
63        3S      -0.11315   0.00000   0.70794   0.27296   0.81401
64        3PX      0.00000  -0.13944   0.00000   0.00000   0.00000
65        3PY      0.03447   0.00000  -0.15749  -0.05979  -0.27854
66        3PZ     -0.22974   0.00000   0.17812  -0.37186   0.40349
67        4XX      0.01062   0.00000  -0.01327  -0.01691   0.00173
68        4YY      0.00365   0.00000   0.00851   0.00097   0.00265
69        4ZZ     -0.01429   0.00000  -0.00474   0.00660  -0.01867
70        4XY      0.00000  -0.00021   0.00000   0.00000   0.00000
71        4XZ      0.00000  -0.00889   0.00000   0.00000   0.00000
72        4YZ      0.00381   0.00000  -0.00644   0.00226   0.00903
73 5   H  1S       0.00540   0.00000   0.00585  -0.01476  -0.02149
74        2S       0.00548   0.00000  -0.03592  -0.01873  -0.00435
75 6   C  1S      -0.00543   0.00000   0.07970   0.03197  -0.05599
76        2S       0.03659   0.00000  -0.14633  -0.05908   0.05831
77        2PX      0.00000  -0.08918   0.00000   0.00000   0.00000
78        2PY     -0.00116   0.00000  -0.11817  -0.04116   0.11555
79        2PZ     -0.21987   0.00000  -0.14662   0.26431   0.22728
80        3S      -0.11315   0.00000  -0.70794  -0.27296   0.81401
81        3PX      0.00000  -0.13944   0.00000   0.00000   0.00000
82        3PY     -0.03447   0.00000  -0.15749  -0.05979   0.27854
83        3PZ     -0.22974   0.00000  -0.17812   0.37186   0.40349
84        4XX      0.01062   0.00000   0.01327   0.01691   0.00173
85        4YY      0.00365   0.00000  -0.00851  -0.00097   0.00265
86        4ZZ     -0.01429   0.00000   0.00474  -0.00660  -0.01867
87        4XY      0.00000   0.00021   0.00000   0.00000   0.00000
```

```
  88        4XZ          0.00000  -0.00889   0.00000   0.00000   0.00000
  89        4YZ         -0.00381   0.00000  -0.00644   0.00226  -0.00903
  90 7   H  1S           0.00540   0.00000  -0.00585   0.01476  -0.02149
  91        2S           0.00548   0.00000   0.03592   0.01873  -0.00435
---------------------------------------------------------------------------
```

nido-$[H_2P(CH)_2P_2]^{\oplus}$

```
---------------------------------------------------------------------------
     Molecular Orbital Coefficients
                           26        27        28        29        30
                         (A)--O    (B)--O    (B)--O    (B)--O    (B)--O
     EIGENVALUES --     -0.58409  -0.56646  -0.52088  -0.45817  -0.42467
   1 1   P  1S          -0.00150   0.00000   0.00000   0.00000   0.00000
   2        2S          -0.00120   0.00000   0.00000   0.00000   0.00000
   3        2PX          0.00000   0.03294  -0.17886  -0.03813  -0.00417
   4        2PY          0.00000  -0.02988  -0.03852  -0.00892  -0.00881
   5        2PZ          0.06357   0.00000   0.00000   0.00000   0.00000
   6        3S          -0.04500   0.00000   0.00000   0.00000   0.00000
   7        3PX          0.00000  -0.08772   0.48612   0.10037   0.01008
   8        3PY          0.00000   0.07498   0.10210   0.02425   0.02072
   9        3PZ         -0.17122   0.00000   0.00000   0.00000   0.00000
  10        4S           0.11815   0.00000   0.00000   0.00000   0.00000
  11        4PX          0.00000  -0.02646   0.18736   0.10069  -0.01304
  12        4PY          0.00000   0.03886   0.03768   0.00914   0.10185
  13        4PZ         -0.08593   0.00000   0.00000   0.00000   0.00000
  14        5XX          0.04456   0.00000   0.00000   0.00000   0.00000
  15        5YY         -0.01506   0.00000   0.00000   0.00000   0.00000
  16        5ZZ         -0.02407   0.00000   0.00000   0.00000   0.00000
  17        5XY          0.00236   0.00000   0.00000   0.00000   0.00000
  18        5XZ          0.00000  -0.00046  -0.05106   0.01879   0.02518
  19        5YZ          0.00000   0.06676   0.00489  -0.00623  -0.14580
  20 2   H  1S          -0.06715   0.08524   0.01779  -0.00633  -0.15307
  21        2S          -0.07092   0.08620   0.02203  -0.00511  -0.27822
  22 3   H  1S          -0.06715  -0.08524  -0.01779   0.00633   0.15307
  23        2S          -0.07092  -0.08620  -0.02203   0.00511   0.27822
  24 4   P  1S           0.02934  -0.00189   0.01685  -0.01296   0.00071
  25        2S          -0.13230   0.00806  -0.07424   0.06328  -0.00318
  26        2PX          0.10916   0.00333   0.03960  -0.15808   0.00997
  27        2PY         -0.00859   0.08711   0.01414   0.00770   0.03062
  28        2PZ         -0.05190  -0.01413   0.12099   0.02284  -0.03083
  29        3S           0.31197  -0.02256   0.19358  -0.12940   0.00698
  30        3PX         -0.27193  -0.00800  -0.10598   0.42638  -0.02631
  31        3PY          0.02207  -0.22312  -0.03780  -0.02145  -0.08738
  32        3PZ          0.13299   0.03676  -0.32437  -0.05894   0.08606
  33        4S           0.23692  -0.00026   0.07875  -0.20950   0.01166
  34        4PX         -0.03940   0.00426  -0.06128   0.12964  -0.00750
  35        4PY          0.00368  -0.02178  -0.00750  -0.00813  -0.06198
  36        4PZ          0.03897   0.01141  -0.10768  -0.02805   0.03595
  37        5XX         -0.04553  -0.00287   0.00114   0.01205   0.00045
  38        5YY          0.00411  -0.00043   0.01421   0.03400  -0.00383
  39        5ZZ          0.02843   0.00612  -0.03552  -0.03069   0.00590
  40        5XY          0.00379  -0.05276  -0.00804  -0.00277  -0.00682
  41        5XZ          0.01902   0.00293  -0.02827   0.00755   0.00626
  42        5YZ          0.00054  -0.00274   0.00712   0.00449   0.05502
  43 5   P  1S           0.02934   0.00189  -0.01685   0.01296  -0.00071
  44        2S          -0.13230  -0.00806   0.07424  -0.06328   0.00318
  45        2PX         -0.10916   0.00333   0.03960  -0.15808   0.00997
  46        2PY          0.00859   0.08711   0.01414   0.00770   0.03062
  47        2PZ         -0.05190   0.01413  -0.12099  -0.02284   0.03083
  48        3S           0.31197   0.02256  -0.19358   0.12940  -0.00698
  49        3PX          0.27193  -0.00800  -0.10598   0.42638  -0.02631
  50        3PY         -0.02207  -0.22312  -0.03780  -0.02145  -0.08738
  51        3PZ          0.13299  -0.03676   0.32437   0.05894  -0.08606
```

```
52        4S           0.23692   0.00026  -0.07875   0.20950  -0.01166
53        4PX          0.03940   0.00426  -0.06128   0.12964  -0.00750
54        4PY         -0.00368  -0.02178  -0.00750  -0.00813  -0.06198
55        4PZ          0.03897  -0.01141   0.10768   0.02805  -0.03595
56        5XX         -0.04553   0.00287  -0.00114  -0.01205  -0.00045
57        5YY          0.00411   0.00043  -0.01421  -0.03400   0.00383
58        5ZZ          0.02843  -0.00612   0.03552   0.03069  -0.00590
59        5XY          0.00379   0.05276   0.00804   0.00277   0.00682
60        5XZ         -0.01902   0.00293  -0.02827   0.00755   0.00626
61        5YZ         -0.00054  -0.00274   0.00712   0.00449   0.05502
62 6   C  1S           0.04446   0.03247   0.00898   0.00257   0.00233
63        2S          -0.07874  -0.06208  -0.02047  -0.00611  -0.02021
64        2PX         -0.01864   0.01478  -0.01544  -0.25560   0.01975
65        2PY          0.13122   0.32693   0.03021   0.01251  -0.01435
66        2PZ          0.09961   0.03387   0.04184   0.02963   0.35876
67        3S          -0.20589  -0.17107  -0.03173  -0.01026   0.05445
68        3PX         -0.01063   0.00778  -0.03218  -0.17412   0.01456
69        3PY          0.12299   0.16669   0.01430   0.00889  -0.04233
70        3PZ          0.04650   0.01648   0.03178   0.02574   0.30763
71        4XX          0.01081  -0.01331  -0.00255  -0.00133  -0.00731
72        4YY         -0.00881   0.01319   0.00032   0.00012   0.00056
73        4ZZ          0.00445  -0.00250   0.00225   0.00110   0.01138
74        4XY          0.00056  -0.00015   0.00015   0.01271  -0.00018
75        4XZ         -0.00040  -0.00169   0.01559  -0.00038  -0.00357
76        4YZ         -0.00373   0.00813  -0.00048  -0.00060  -0.01158
77 7   H  1S           0.03182   0.18590   0.01315   0.00627   0.00817
78        2S          -0.00994   0.14375   0.01239   0.00573  -0.00003
79 8   C  1S           0.04446  -0.03247  -0.00898  -0.00257  -0.00233
80        2S          -0.07874   0.06208   0.02047   0.00611   0.02021
81        2PX          0.01864   0.01478  -0.01544  -0.25560   0.01975
82        2PY         -0.13122   0.32693   0.03021   0.01251  -0.01435
83        2PZ          0.09961  -0.03387  -0.04184  -0.02963  -0.35876
84        3S          -0.20589   0.17107   0.03173   0.01026  -0.05445
85        3PX          0.01063   0.00778  -0.03218  -0.17412   0.01456
86        3PY         -0.12299   0.16669   0.01430   0.00889  -0.04233
87        3PZ          0.04650  -0.01648  -0.03178  -0.02574  -0.30763
88        4XX          0.01081   0.01331   0.00255   0.00133   0.00731
89        4YY         -0.00881  -0.01319  -0.00032  -0.00012  -0.00056
90        4ZZ          0.00445   0.00250  -0.00225  -0.00110  -0.01138
91        4XY          0.00056   0.00015  -0.00015  -0.01271   0.00018
92        4XZ          0.00040  -0.00169   0.01559  -0.00038  -0.00357
93        4YZ          0.00373   0.00813  -0.00048  -0.00060  -0.01158
94 9   H  1S           0.03182  -0.18590  -0.01315  -0.00627  -0.00817
95        2S          -0.00994  -0.14375  -0.01239  -0.00573   0.00003
                          31        32        33        34        35
                        (A)--V    (A)--V    (B)--V    (B)--V    (B)--V
   EIGENVALUES --     -0.26886  -0.25855  -0.25580  -0.22059  -0.11920

 1 1   P  1S           0.02489   0.03931   0.00000   0.00000   0.00000
 2        2S          -0.11490  -0.19563   0.00000   0.00000   0.00000
 3        2PX          0.00000   0.00000  -0.17140  -0.01380   0.01256
 4        2PY          0.00000   0.00000  -0.02455  -0.02331  -0.03232
 5        2PZ          0.08036   0.05509   0.00000   0.00000   0.00000
 6        3S           0.27736   0.39890   0.00000   0.00000   0.00000
 7        3PX          0.00000   0.00000   0.48415   0.03787  -0.10268
 8        3PY          0.00000   0.00000   0.06965   0.08036   0.10035
 9        3PZ         -0.22921  -0.15088   0.00000   0.00000   0.00000
10        4S           0.61920   1.05052   0.00000   0.00000   0.00000
11        4PX          0.00000   0.00000   0.64377   0.07244   0.55712
12        4PY          0.00000   0.00000   0.05921  -0.00869   0.20775
13        4PZ         -0.46555  -0.25688   0.00000   0.00000   0.00000
14        5XX         -0.04983   0.11154   0.00000   0.00000   0.00000
15        5YY          0.04927  -0.06849   0.00000   0.00000   0.00000
```

```
16          5ZZ    -0.00392  -0.07198   0.00000   0.00000   0.00000
17          5XY     0.00605   0.01709   0.00000   0.00000   0.00000
18          5XZ     0.00000   0.00000   0.07491   0.00839   0.13841
19          5YZ     0.00000   0.00000   0.02378  -0.01176   0.00050
20 2   H    1S     -0.03971  -0.12959   0.00197   0.01371  -0.02219
21          2S     -0.03471  -0.43882   0.03238   0.02407  -0.12677
22 3   H    1S     -0.03971  -0.12959  -0.00197  -0.01371   0.02219
23          2S     -0.03471  -0.43882  -0.03238  -0.02407   0.12677
24 4   P    1S     -0.00323  -0.00758   0.00422   0.00148   0.02706
25          2S      0.02045   0.02310  -0.02171  -0.00659  -0.11678
26          2PX     0.02449  -0.01279   0.02328  -0.00225  -0.07864
27          2PY    -0.00181  -0.00276  -0.00987   0.14053   0.00257
28          2PZ     0.15481  -0.01188  -0.14020  -0.01018  -0.01708
29          3S     -0.01561  -0.12949   0.03944   0.01759   0.33504
30          3PX    -0.07848   0.04196  -0.06473   0.00724   0.27429
31          3PY     0.00542   0.00918   0.02825  -0.40767  -0.00841
32          3PZ    -0.43550   0.03962   0.40081   0.03014   0.07990
33          4S     -0.25869   0.07891   0.15862   0.03627   1.09617
34          4PX    -0.12195   0.15567  -0.03105   0.01186   0.85752
35          4PY     0.00301  -0.00124   0.04161  -0.54971   0.03290
36          4PZ    -0.49810  -0.02045   0.42936   0.03821   0.10473
37          5XX    -0.01161  -0.03047   0.01545   0.00488   0.01640
38          5YY    -0.01457  -0.01476   0.02180  -0.00354  -0.08315
39          5ZZ     0.02279   0.05885  -0.03883  -0.00172   0.08858
40          5XY    -0.00020   0.00129  -0.00721   0.08632  -0.01120
41          5XZ     0.04134  -0.02384  -0.00655  -0.00035   0.03389
42          5YZ    -0.00072  -0.00513  -0.00689  -0.01384  -0.00355
43 5   P    1S     -0.00323  -0.00758  -0.00422  -0.00148  -0.02706
44          2S      0.02045   0.02310   0.02171   0.00659   0.11678
45          2PX    -0.02449   0.01279   0.02328  -0.00225  -0.07864
46          2PY     0.00181   0.00276  -0.00987   0.14053   0.00257
47          2PZ     0.15481  -0.01188   0.14020   0.01018   0.01708
48          3S     -0.01561  -0.12949  -0.03944  -0.01759  -0.33504
49          3PX     0.07848  -0.04196  -0.06473   0.00724   0.27429
50          3PY    -0.00542  -0.00918   0.02825  -0.40767  -0.00841
51          3PZ    -0.43550   0.03962  -0.40081  -0.03014  -0.07990
52          4S     -0.25869   0.07891  -0.15862  -0.03627  -1.09617
53          4PX     0.12195  -0.15567  -0.03105   0.01186   0.85752
54          4PY    -0.00301   0.00124   0.04161  -0.54971   0.03290
55          4PZ    -0.49810  -0.02045  -0.42936  -0.03821  -0.10473
56          5XX    -0.01161  -0.03047  -0.01545  -0.00488  -0.01640
57          5YY    -0.01457  -0.01476  -0.02180   0.00354   0.08315
58          5ZZ     0.02279   0.05885   0.03883   0.00172  -0.08858
59          5XY    -0.00020   0.00129   0.00721  -0.08632   0.01120
60          5XZ    -0.04134   0.02384  -0.00655  -0.00035   0.03389
61          5YZ     0.00072   0.00513  -0.00689  -0.01384  -0.00355
62 6   C    1S      0.01791   0.03125   0.00991  -0.08071   0.01049
63          2S     -0.05232  -0.01768  -0.01661   0.14212  -0.01491
64          2PX    -0.00112  -0.00678  -0.06742   0.00998   0.26281
65          2PY     0.02844   0.09774   0.01814  -0.11372   0.00449
66          2PZ     0.14028  -0.28938  -0.05338  -0.07025  -0.03586
67          3S     -0.03587  -0.47837  -0.08713   0.72357  -0.14661
68          3PX    -0.00235  -0.00295  -0.08149   0.01845   0.72297
69          3PY     0.02021   0.18519   0.02495  -0.15785   0.00169
70          3PZ     0.13020  -0.39816  -0.06241  -0.10611  -0.07048
71          4XX    -0.00883   0.00105   0.00157  -0.02090  -0.00019
72          4YY    -0.00527  -0.00232  -0.00126   0.00672  -0.00109
73          4ZZ     0.01580   0.00844   0.00000   0.00003   0.00331
74          4XY     0.00003   0.00020   0.00013   0.00143   0.02638
75          4XZ     0.00060   0.00161  -0.01144  -0.00054  -0.00149
76          4YZ    -0.00247   0.00169   0.00159  -0.00278  -0.00005
77 7   H    1S      0.00026   0.01723  -0.00179  -0.00710  -0.00125
78          2S     -0.00974  -0.01607   0.00461  -0.04289   0.02327
```

```
  79 8   C  1S          0.01791   0.03125  -0.00991   0.08071  -0.01049
  80        2S         -0.05232  -0.01768   0.01661  -0.14212   0.01491
  81        2PX         0.00112   0.00678  -0.06742   0.00998   0.26281
  82        2PY        -0.02844  -0.09774   0.01814  -0.11372   0.00449
  83        2PZ         0.14028  -0.28938   0.05338   0.07025   0.03586
  84        3S         -0.03587  -0.47837   0.08713  -0.72357   0.14661
  85        3PX         0.00235   0.00295  -0.08149   0.01845   0.72297
  86        3PY        -0.02021  -0.18519   0.02495  -0.15785   0.00169
  87        3PZ         0.13020  -0.39816   0.06241   0.10611   0.07048
  88        4XX        -0.00883   0.00105  -0.00157   0.02090   0.00019
  89        4YY        -0.00527  -0.00232   0.00126  -0.00672   0.00109
  90        4ZZ         0.01580   0.00844   0.00000  -0.00003  -0.00331
  91        4XY         0.00003   0.00020  -0.00013  -0.00143  -0.02638
  92        4XZ        -0.00060  -0.00161  -0.01144  -0.00054  -0.00149
  93        4YZ         0.00247  -0.00169   0.00159  -0.00278  -0.00005
  94 9   H  1S          0.00026   0.01723   0.00179   0.00710   0.00125
  95        2S         -0.00974  -0.01607  -0.00461   0.04289  -0.02327
---------------------------------------------------------------------------
```

Tricyclo-[P(CH)$_2$P$_2$]$^{\oplus}$

```
---------------------------------------------------------------------------
     Molecular Orbital Coefficients
                           25        26        27        28        29
                        (B2)--O   (B1)--O   (A1)--O   (A2)--O   (A1)--O
     EIGENVALUES --    -0.58506  -0.52190  -0.51768  -0.51468  -0.44966
   1 1   P  1S          0.00000   0.02582  -0.01856   0.00000   0.00200
   2        2S          0.00000  -0.11300   0.09004   0.00000  -0.00604
   3        2PX         0.00000   0.05170  -0.15706   0.00000   0.06357
   4        2PY         0.05443   0.00000   0.00000   0.12305   0.00000
   5        2PZ         0.00000   0.09434   0.01415   0.00000  -0.12431
   6        3S          0.00000   0.29531  -0.18627   0.00000   0.03426
   7        3PX         0.00000  -0.13696   0.42374   0.00000  -0.17463
   8        3PY        -0.13935   0.00000   0.00000  -0.32243   0.00000
   9        3PZ         0.00000  -0.24666  -0.03650   0.00000   0.33249
  10        4S          0.00000   0.14931  -0.20043   0.00000  -0.04615
  11        4PX         0.00000  -0.06008   0.11092   0.00000  -0.11404
  12        4PY        -0.00968   0.00000   0.00000  -0.09673   0.00000
  13        4PZ         0.00000  -0.09808  -0.02978   0.00000   0.13009
  14        5XX         0.00000   0.00516   0.05411   0.00000  -0.02123
  15        5YY         0.00000   0.00029  -0.00090   0.00000   0.02580
  16        5ZZ         0.00000  -0.02816  -0.02580   0.00000  -0.00999
  17        5XY        -0.02981   0.00000   0.00000  -0.00963   0.00000
  18        5XZ         0.00000  -0.00618   0.00809   0.00000   0.03169
  19        5YZ        -0.02423   0.00000   0.00000  -0.04864   0.00000
  20 2   P  1S          0.00000  -0.02582  -0.01856   0.00000   0.00200
  21        2S          0.00000   0.11300   0.09004   0.00000  -0.00604
  22        2PX         0.00000   0.05170   0.15706   0.00000  -0.06357
  23        2PY         0.05443   0.00000   0.00000  -0.12305   0.00000
  24        2PZ         0.00000  -0.09434   0.01415   0.00000  -0.12431
  25        3S          0.00000  -0.29531  -0.18627   0.00000   0.03426
  26        3PX         0.00000  -0.13696  -0.42374   0.00000   0.17463
  27        3PY        -0.13935   0.00000   0.00000   0.32243   0.00000
  28        3PZ         0.00000   0.24666  -0.03650   0.00000   0.33249
  29        4S          0.00000  -0.14931  -0.20043   0.00000  -0.04615
  30        4PX         0.00000  -0.06008  -0.11092   0.00000   0.11404
  31        4PY        -0.00968   0.00000   0.00000   0.09673   0.00000
  32        4PZ         0.00000   0.09808  -0.02978   0.00000   0.13009
  33        5XX         0.00000  -0.00516   0.05411   0.00000  -0.02123
  34        5YY         0.00000  -0.00029  -0.00090   0.00000   0.02580
  35        5ZZ         0.00000   0.02816  -0.02580   0.00000  -0.00999
  36        5XY         0.02981   0.00000   0.00000  -0.00963   0.00000
  37        5XZ         0.00000  -0.00618  -0.00809   0.00000  -0.03169
  38        5YZ        -0.02423   0.00000   0.00000   0.04864   0.00000
```

```
39 3   P  1S         0.00000   0.00000   0.01824   0.00000   0.00800
40        2S         0.00000   0.00000  -0.07812   0.00000  -0.04489
41        2PX        0.00000  -0.13626   0.00000   0.00000   0.00000
42        2PY        0.10118   0.00000   0.00000   0.00000   0.00000
43        2PZ        0.00000   0.00000  -0.09842   0.00000  -0.14628
44        3S         0.00000   0.00000   0.21352   0.00000   0.05962
45        3PX        0.00000   0.36327   0.00000   0.00000   0.00000
46        3PY       -0.25498   0.00000   0.00000   0.00000   0.00000
47        3PZ        0.00000   0.00000   0.25471   0.00000   0.40178
48        4S         0.00000   0.00000   0.12656   0.00000   0.23885
49        4PX        0.00000   0.13700   0.00000   0.00000   0.00000
50        4PY       -0.02605   0.00000   0.00000   0.00000   0.00000
51        4PZ        0.00000   0.00000   0.10276   0.00000   0.09653
52        5XX        0.00000   0.00000   0.00707   0.00000   0.03709
53        5YY        0.00000   0.00000  -0.00519   0.00000  -0.03963
54        5ZZ        0.00000   0.00000  -0.00986   0.00000  -0.00670
55        5XY        0.00000   0.00000   0.00000   0.04059   0.00000
56        5XZ        0.00000  -0.05087   0.00000   0.00000   0.00000
57        5YZ        0.05725   0.00000   0.00000   0.00000   0.00000
58 4   C  1S         0.02448   0.00000  -0.00008   0.00000   0.00783
59        2S        -0.04278   0.00000   0.00743   0.00000  -0.02893
60        2PX        0.00000   0.20187   0.00000   0.32537   0.00000
61        2PY        0.35014   0.00000   0.00898   0.00000   0.00782
62        2PZ       -0.04068   0.00000  -0.12874   0.00000  -0.22318
63        3S        -0.14748   0.00000   0.01859   0.00000   0.00965
64        3PX        0.00000   0.12770   0.00000   0.24423   0.00000
65        3PY        0.18728   0.00000   0.01002   0.00000  -0.01469
66        3PZ       -0.01541   0.00000  -0.07142   0.00000  -0.17812
67        4XX       -0.00550   0.00000  -0.01141   0.00000   0.01086
68        4YY        0.01633   0.00000   0.00380   0.00000  -0.00374
69        4ZZ       -0.01328   0.00000   0.01065   0.00000  -0.00668
70        4XY        0.00000  -0.01314   0.00000  -0.01014   0.00000
71        4XZ        0.00000   0.00988   0.00000  -0.00958   0.00000
72        4YZ       -0.00158   0.00000   0.00943   0.00000   0.01006
73 5   H  1S         0.20461   0.00000   0.01044   0.00000  -0.00929
74        2S         0.14270   0.00000   0.00584   0.00000  -0.00401
75 6   C  1S        -0.02448   0.00000  -0.00008   0.00000   0.00783
76        2S         0.04278   0.00000   0.00743   0.00000  -0.02893
77        2PX        0.00000   0.20187   0.00000  -0.32537   0.00000
78        2PY        0.35014   0.00000  -0.00898   0.00000  -0.00782
79        2PZ        0.04068   0.00000  -0.12874   0.00000  -0.22318
80        3S         0.14748   0.00000   0.01859   0.00000   0.00965
81        3PX        0.00000   0.12770   0.00000  -0.24423   0.00000
82        3PY        0.18728   0.00000  -0.01002   0.00000   0.01469
83        3PZ        0.01541   0.00000  -0.07142   0.00000  -0.17812
84        4XX        0.00550   0.00000  -0.01141   0.00000   0.01086
85        4YY       -0.01633   0.00000   0.00380   0.00000  -0.00374
86        4ZZ        0.01328   0.00000   0.01065   0.00000  -0.00668
87        4XY        0.00000   0.01314   0.00000  -0.01014   0.00000
88        4XZ        0.00000   0.00988   0.00000   0.00958   0.00000
89        4YZ       -0.00158   0.00000  -0.00943   0.00000  -0.01006
90 7   H  1S        -0.20461   0.00000   0.01044   0.00000  -0.00929
91        2S        -0.14270   0.00000   0.00584   0.00000  -0.00401
                       30        31        32        33        34
                    (B1)--V   (B2)--V   (B1)--V   (A2)--V   (A1)--V
   EIGENVALUES --   -0.32448  -0.24157  -0.23290  -0.19961  -0.16406
 1 1   P  1S         0.00129   0.00000   0.00593   0.00000  -0.01767
 2        2S        -0.00760   0.00000  -0.02917   0.00000   0.08337
 3        2PX       -0.04293   0.00000  -0.12571   0.00000   0.07702
 4        2PY        0.00000   0.10912   0.00000  -0.14740   0.00000
 5        2PZ       -0.09592   0.00000   0.11614   0.00000   0.07614
 6        3S         0.00497   0.00000   0.05905   0.00000  -0.18904
 7        3PX        0.12389   0.00000   0.36436   0.00000  -0.26476
```

```
 8        3PY         0.00000  -0.30726   0.00000   0.43369   0.00000
 9        3PZ         0.27001   0.00000  -0.32749   0.00000  -0.21948
10        4S          0.10619   0.00000   0.26828   0.00000  -0.50722
11        4PX         0.14018   0.00000   0.48988   0.00000  -0.33250
12        4PY         0.00000  -0.41232   0.00000   0.55628   0.00000
13        4PZ         0.16638   0.00000  -0.38455   0.00000  -0.60288
14        5XX        -0.01280   0.00000  -0.05755   0.00000  -0.07969
15        5YY         0.02323   0.00000   0.03778   0.00000   0.04796
16        5ZZ        -0.00136   0.00000   0.02315   0.00000   0.01302
17        5XY         0.00000   0.03853   0.00000  -0.04031   0.00000
18        5XZ         0.00512   0.00000   0.03968   0.00000   0.08270
19        5YZ         0.00000   0.06604   0.00000  -0.05730   0.00000
20 2   P  1S         -0.00129   0.00000  -0.00593   0.00000  -0.01767
21        2S          0.00760   0.00000   0.02917   0.00000   0.08337
22        2PX        -0.04293   0.00000  -0.12571   0.00000  -0.07702
23        2PY         0.00000   0.10912   0.00000   0.14740   0.00000
24        2PZ         0.09592   0.00000  -0.11614   0.00000   0.07614
25        3S         -0.00497   0.00000  -0.05905   0.00000  -0.18904
26        3PX         0.12389   0.00000   0.36436   0.00000   0.26476
27        3PY         0.00000  -0.30726   0.00000  -0.43369   0.00000
28        3PZ        -0.27001   0.00000   0.32749   0.00000  -0.21948
29        4S         -0.10619   0.00000  -0.26828   0.00000  -0.50722
30        4PX         0.14018   0.00000   0.48988   0.00000   0.33250
31        4PY         0.00000  -0.41232   0.00000  -0.55628   0.00000
32        4PZ        -0.16638   0.00000   0.38455   0.00000  -0.60288
33        5XX         0.01280   0.00000   0.05755   0.00000  -0.07969
34        5YY        -0.02323   0.00000  -0.03778   0.00000   0.04796
35        5ZZ         0.00136   0.00000  -0.02315   0.00000   0.01302
36        5XY         0.00000  -0.03853   0.00000  -0.04031   0.00000
37        5XZ         0.00512   0.00000   0.03968   0.00000  -0.08270
38        5YZ         0.00000   0.06604   0.00000   0.05730   0.00000
39 3   P  1S          0.00000   0.00000   0.00000   0.00000   0.01409
40        2S          0.00000   0.00000   0.00000   0.00000  -0.03914
41        2PX        -0.21893   0.00000   0.01213   0.00000   0.00000
42        2PY         0.00000   0.10710   0.00000   0.00000   0.00000
43        2PZ         0.00000   0.00000   0.00000   0.00000   0.00807
44        3S          0.00000   0.00000   0.00000   0.00000   0.25254
45        3PX         0.60764   0.00000  -0.04049   0.00000   0.00000
46        3PY         0.00000  -0.31617   0.00000   0.00000   0.00000
47        3PZ         0.00000   0.00000   0.00000   0.00000  -0.03701
48        4S          0.00000   0.00000   0.00000   0.00000   0.06629
49        4PX         0.45793   0.00000   0.03029   0.00000   0.00000
50        4PY         0.00000  -0.41383   0.00000   0.00000   0.00000
51        4PZ         0.00000   0.00000   0.00000   0.00000   0.03003
52        5XX         0.00000   0.00000   0.00000   0.00000  -0.02595
53        5YY         0.00000   0.00000   0.00000   0.00000  -0.04592
54        5ZZ         0.00000   0.00000   0.00000   0.00000   0.06892
55        5XY         0.00000   0.00000   0.00000   0.07582   0.00000
56        5XZ         0.03027   0.00000   0.00941   0.00000   0.00000
57        5YZ         0.00000  -0.06904   0.00000   0.00000   0.00000
58 4   C  1S          0.00000  -0.08715   0.00000   0.00000  -0.06501
59        2S          0.00000   0.15774   0.00000   0.00000   0.07710
60        2PX        -0.14818   0.00000  -0.18095   0.28353   0.00000
61        2PY         0.00000  -0.12800   0.00000   0.00000  -0.11153
62        2PZ         0.00000  -0.07334   0.00000   0.00000  -0.21585
63        3S          0.00000   0.74717   0.00000   0.00000   0.86976
64        3PX        -0.11082   0.00000  -0.20117   0.43966   0.00000
65        3PY         0.00000  -0.17728   0.00000   0.00000  -0.29366
66        3PZ         0.00000  -0.06890   0.00000   0.00000  -0.46900
67        4XX         0.00000  -0.00641   0.00000   0.00000  -0.01309
68        4YY         0.00000   0.00833   0.00000   0.00000   0.00320
69        4ZZ         0.00000  -0.01412   0.00000   0.00000  -0.00818
70        4XY         0.00439   0.00000   0.00042  -0.00469   0.00000
```

```
  71        4XZ          0.01710   0.00000   0.00562   0.01668   0.00000
  72        4YZ          0.00000   0.00316   0.00000   0.00000  -0.01610
  73 5   H  1S           0.00000  -0.00059   0.00000   0.00000  -0.02816
  74        2S           0.00000  -0.03487   0.00000   0.00000  -0.02103
  75 6   C  1S           0.00000   0.08715   0.00000   0.00000  -0.06501
  76        2S           0.00000  -0.15774   0.00000   0.00000   0.07710
  77        2PX         -0.14818   0.00000  -0.18095  -0.28353   0.00000
  78        2PY          0.00000  -0.12800   0.00000   0.00000   0.11153
  79        2PZ          0.00000   0.07334   0.00000   0.00000  -0.21585
  80        3S           0.00000  -0.74717   0.00000   0.00000   0.86976
  81        3PX         -0.11082   0.00000  -0.20117  -0.43966   0.00000
  82        3PY          0.00000  -0.17728   0.00000   0.00000   0.29366
  83        3PZ          0.00000   0.06890   0.00000   0.00000  -0.46900
  84        4XX          0.00000   0.00641   0.00000   0.00000  -0.01309
  85        4YY          0.00000  -0.00833   0.00000   0.00000   0.00320
  86        4ZZ          0.00000   0.01412   0.00000   0.00000  -0.00818
  87        4XY         -0.00439   0.00000  -0.00042  -0.00469   0.00000
  88        4XZ          0.01710   0.00000   0.00562  -0.01668   0.00000
  89        4YZ          0.00000   0.00316   0.00000   0.00000   0.01610
  90 7   H  1S           0.00000   0.00059   0.00000   0.00000  -0.02816
  91        2S           0.00000   0.03487   0.00000   0.00000  -0.02103
---------------------------------------------------------------------------
```

Tricyclo-[$H_2P(CH)_2P_2$]$^{\oplus}$

```
---------------------------------------------------------------------------
     Molecular Orbital Coefficients
                           26        27        28        29        30
                        (B1)--O   (A1)--O   (A2)--O   (B2)--O   (A1)--O
     EIGENVALUES --     -0.57079  -0.52533  -0.50138  -0.46661  -0.45084
   1 1   P  1S           0.00000   0.02584   0.00000  -0.02158   0.00531
   2        2S           0.00000  -0.12389   0.00000   0.09535  -0.02517
   3        2PX          0.08294   0.00000  -0.12002   0.00000   0.00000
   4        2PY          0.00000  -0.12028   0.00000   0.06106  -0.11659
   5        2PZ          0.00000   0.05932   0.00000  -0.11600  -0.12844
   6        3S           0.00000   0.25619   0.00000  -0.24721   0.05953
   7        3PX         -0.20897   0.00000   0.31014   0.00000   0.00000
   8        3PY          0.00000   0.31472   0.00000  -0.16318   0.32071
   9        3PZ          0.00000  -0.15138   0.00000   0.30894   0.33806
  10        4S           0.00000   0.28186   0.00000  -0.14225   0.01633
  11        4PX         -0.02298   0.00000   0.08936   0.00000   0.00000
  12        4PY          0.00000   0.04536   0.00000  -0.08937   0.15628
  13        4PZ          0.00000  -0.01511   0.00000   0.11147   0.13541
  14        5XX          0.00000  -0.00425   0.00000   0.00636   0.01872
  15        5YY          0.00000  -0.03382   0.00000  -0.00971  -0.04560
  16        5ZZ          0.00000   0.01369   0.00000   0.02777   0.00973
  17        5XY          0.04486   0.00000  -0.01193   0.00000   0.00000
  18        5XZ         -0.02687   0.00000   0.04811   0.00000   0.00000
  19        5YZ          0.00000   0.03692   0.00000  -0.01168  -0.03142
  20 2   P  1S           0.00000   0.02584   0.00000   0.02158   0.00531
  21        2S           0.00000  -0.12389   0.00000  -0.09535  -0.02517
  22        2PX          0.08294   0.00000   0.12002   0.00000   0.00000
  23        2PY          0.00000   0.12028   0.00000   0.06106   0.11659
  24        2PZ          0.00000   0.05932   0.00000   0.11600  -0.12844
  25        3S           0.00000   0.25619   0.00000   0.24721   0.05953
  26        3PX         -0.20897   0.00000  -0.31014   0.00000   0.00000
  27        3PY          0.00000  -0.31472   0.00000  -0.16318  -0.32071
  28        3PZ          0.00000  -0.15138   0.00000  -0.30894   0.33806
  29        4S           0.00000   0.28186   0.00000   0.14225   0.01633
  30        4PX         -0.02298   0.00000  -0.08936   0.00000   0.00000
  31        4PY          0.00000  -0.04536   0.00000  -0.08937  -0.15628
  32        4PZ          0.00000  -0.01511   0.00000  -0.11147   0.13541
  33        5XX          0.00000  -0.00425   0.00000  -0.00636   0.01872
  34        5YY          0.00000  -0.03382   0.00000   0.00971  -0.04560
```

```
35         5ZZ        0.00000   0.01369   0.00000  -0.02777   0.00973
36         5XY       -0.04486   0.00000  -0.01193   0.00000   0.00000
37         5XZ       -0.02687   0.00000  -0.04811   0.00000   0.00000
38         5YZ        0.00000  -0.03692   0.00000  -0.01168   0.03142
39 3   P   1S         0.00000   0.00808   0.00000   0.00000  -0.01518
40         2S         0.00000  -0.03888   0.00000   0.00000   0.06012
41         2PX        0.05048   0.00000   0.00000   0.00000   0.00000
42         2PY        0.00000   0.00000   0.00000   0.00221   0.00000
43         2PZ        0.00000   0.07426   0.00000   0.00000  -0.05782
44         3S         0.00000   0.08218   0.00000   0.00000  -0.19861
45         3PX       -0.12964   0.00000   0.00000   0.00000   0.00000
46         3PY        0.00000   0.00000   0.00000  -0.00539   0.00000
47         3PZ        0.00000  -0.20023   0.00000   0.00000   0.16796
48         4S         0.00000   0.12763   0.00000   0.00000  -0.09958
49         4PX       -0.01067   0.00000   0.00000   0.00000   0.00000
50         4PY        0.00000   0.00000   0.00000   0.10770   0.00000
51         4PZ        0.00000  -0.10613   0.00000   0.00000  -0.00781
52         5XX        0.00000   0.03627   0.00000   0.00000  -0.05054
53         5YY        0.00000  -0.01794   0.00000   0.00000   0.03600
54         5ZZ        0.00000  -0.02813   0.00000   0.00000   0.01954
55         5XY        0.00000   0.00000   0.04414   0.00000   0.00000
56         5XZ        0.03563   0.00000   0.00000   0.00000   0.00000
57         5YZ        0.00000   0.00000   0.00000  -0.10134   0.00000
58 4   H   1S         0.00000  -0.06540   0.00000  -0.10275   0.05495
59         2S         0.00000  -0.07032   0.00000  -0.19648   0.11167
60 5   H   1S         0.00000  -0.06540   0.00000   0.10275   0.05495
61         2S         0.00000  -0.07032   0.00000   0.19648   0.11167
62 6   C   1S         0.02326   0.02668   0.00000   0.00000  -0.00718
63         2S        -0.03959  -0.05125   0.00000   0.00000  -0.00100
64         2PX        0.33973   0.05180   0.00000   0.00000  -0.02136
65         2PY        0.00000   0.00000   0.32986   0.24772   0.00000
66         2PZ        0.06944   0.18496   0.00000   0.00000  -0.12923
67         3S        -0.14867  -0.17151   0.00000   0.00000   0.07097
68         3PX        0.18560   0.07769   0.00000   0.00000  -0.05699
69         3PY        0.00000   0.00000   0.25045   0.15590   0.00000
70         3PZ        0.05526   0.10805   0.00000   0.00000  -0.10190
71         4XX        0.01584  -0.01022   0.00000   0.00000  -0.00036
72         4YY       -0.00668   0.00815   0.00000   0.00000   0.01455
73         4ZZ       -0.01289   0.00279   0.00000   0.00000  -0.01694
74         4XY        0.00000   0.00000  -0.01013  -0.01420   0.00000
75         4XZ       -0.00374  -0.01222   0.00000   0.00000   0.00411
76         4YZ        0.00000   0.00000  -0.00780   0.00449   0.00000
77 7   H   1S         0.20071  -0.00494   0.00000   0.00000  -0.00873
78         2S         0.14456  -0.02738   0.00000   0.00000   0.01103
79 8   C   1S        -0.02326   0.02668   0.00000   0.00000  -0.00718
80         2S         0.03959  -0.05125   0.00000   0.00000  -0.00100
81         2PX        0.33973  -0.05180   0.00000   0.00000   0.02136
82         2PY        0.00000   0.00000  -0.32986   0.24772   0.00000
83         2PZ       -0.06944   0.18496   0.00000   0.00000  -0.12923
84         3S         0.14867  -0.17151   0.00000   0.00000   0.07097
85         3PX        0.18560  -0.07769   0.00000   0.00000   0.05699
86         3PY        0.00000   0.00000  -0.25045   0.15590   0.00000
87         3PZ       -0.05526   0.10805   0.00000   0.00000  -0.10190
88         4XX       -0.01584  -0.01022   0.00000   0.00000  -0.00036
89         4YY        0.00668   0.00815   0.00000   0.00000   0.01455
90         4ZZ        0.01289   0.00279   0.00000   0.00000  -0.01694
91         4XY        0.00000   0.00000  -0.01013   0.01420   0.00000
92         4XZ       -0.00374   0.01222   0.00000   0.00000  -0.00411
93         4YZ        0.00000   0.00000   0.00780   0.00449   0.00000
94 9   H   1S        -0.20071  -0.00494   0.00000   0.00000  -0.00873
95         2S        -0.14456  -0.02738   0.00000   0.00000   0.01103
                        31        32        33        34        35
                      (B1)--V   (B2)--V   (A2)--V   (B1)--V   (A1)--V
```

```
     EIGENVALUES --    -0.24114  -0.21794  -0.17809  -0.15495  -0.14571
   1 1   P  1S          0.00000  -0.00656   0.00000   0.00000  -0.01097
   2        2S          0.00000   0.03093   0.00000   0.00000   0.06230
   3        2PX         0.08894   0.00000  -0.14680   0.08174   0.00000
   4        2PY         0.00000  -0.12628   0.00000   0.00000  -0.07645
   5        2PZ         0.00000  -0.11439   0.00000   0.00000   0.06385
   6        3S          0.00000  -0.07000   0.00000   0.00000  -0.07752
   7        3PX        -0.24827   0.00000   0.42940  -0.22622   0.00000
   8        3PY         0.00000   0.36033   0.00000   0.00000   0.25278
   9        3PZ         0.00000   0.31941   0.00000   0.00000  -0.18166
  10        4S          0.00000  -0.23360   0.00000   0.00000  -0.43040
  11        4PX        -0.29192   0.00000   0.57541  -0.49888   0.00000
  12        4PY         0.00000   0.47817   0.00000   0.00000   0.36584
  13        4PZ         0.00000   0.38013   0.00000   0.00000  -0.51823
  14        5XX         0.00000  -0.03736   0.00000   0.00000   0.02288
  15        5YY         0.00000   0.05291   0.00000   0.00000  -0.05060
  16        5ZZ         0.00000  -0.01776   0.00000   0.00000   0.00740
  17        5XY        -0.01936   0.00000   0.03933  -0.07764   0.00000
  18        5XZ         0.04984   0.00000  -0.05530   0.04524   0.00000
  19        5YZ         0.00000   0.03881   0.00000   0.00000  -0.08991
  20 2   P  1S          0.00000   0.00656   0.00000   0.00000  -0.01097
  21        2S          0.00000  -0.03093   0.00000   0.00000   0.06230
  22        2PX         0.08894   0.00000   0.14680   0.08174   0.00000
  23        2PY         0.00000  -0.12628   0.00000   0.00000   0.07645
  24        2PZ         0.00000   0.11439   0.00000   0.00000   0.06385
  25        3S          0.00000   0.07000   0.00000   0.00000  -0.07752
  26        3PX        -0.24827   0.00000  -0.42940  -0.22622   0.00000
  27        3PY         0.00000   0.36033   0.00000   0.00000  -0.25278
  28        3PZ         0.00000  -0.31941   0.00000   0.00000  -0.18166
  29        4S          0.00000   0.23360   0.00000   0.00000  -0.43040
  30        4PX        -0.29192   0.00000  -0.57541  -0.49888   0.00000
  31        4PY         0.00000   0.47817   0.00000   0.00000  -0.36584
  32        4PZ         0.00000  -0.38013   0.00000   0.00000  -0.51823
  33        5XX         0.00000   0.03736   0.00000   0.00000   0.02288
  34        5YY         0.00000  -0.05291   0.00000   0.00000  -0.05060
  35        5ZZ         0.00000   0.01776   0.00000   0.00000   0.00740
  36        5XY         0.01936   0.00000   0.03933   0.07764   0.00000
  37        5XZ         0.04984   0.00000   0.05530   0.04524   0.00000
  38        5YZ         0.00000   0.03881   0.00000   0.00000   0.08991
  39 3   P  1S          0.00000   0.00000   0.00000   0.00000   0.00337
  40        2S          0.00000   0.00000   0.00000   0.00000   0.02395
  41        2PX         0.12983   0.00000   0.00000  -0.08437   0.00000
  42        2PY         0.00000   0.01497   0.00000   0.00000   0.00000
  43        2PZ         0.00000   0.00000   0.00000   0.00000  -0.02919
  44        3S          0.00000   0.00000   0.00000   0.00000   0.17450
  45        3PX        -0.38249   0.00000   0.00000   0.24985   0.00000
  46        3PY         0.00000  -0.05375   0.00000   0.00000   0.00000
  47        3PZ         0.00000   0.00000   0.00000   0.00000   0.07497
  48        4S          0.00000   0.00000   0.00000   0.00000  -0.54924
  49        4PX        -0.68833   0.00000   0.00000   0.77648   0.00000
  50        4PY         0.00000   0.08702   0.00000   0.00000   0.00000
  51        4PZ         0.00000   0.00000   0.00000   0.00000   0.94252
  52        5XX         0.00000   0.00000   0.00000   0.00000  -0.02011
  53        5YY         0.00000   0.00000   0.00000   0.00000  -0.10346
  54        5ZZ         0.00000   0.00000   0.00000   0.00000   0.12513
  55        5XY         0.00000   0.00000  -0.08321   0.00000   0.00000
  56        5XZ        -0.12418   0.00000   0.00000   0.12978   0.00000
  57        5YZ         0.00000  -0.00050   0.00000   0.00000   0.00000
  58 4   H  1S          0.00000  -0.00705   0.00000   0.00000   0.00610
  59        2S          0.00000  -0.04119   0.00000   0.00000  -0.19827
  60 5   H  1S          0.00000   0.00705   0.00000   0.00000   0.00610
  61        2S          0.00000   0.04119   0.00000   0.00000  -0.19827
  62 6   C  1S         -0.08841   0.00000   0.00000  -0.01309  -0.08025
```

```
63          2S          0.15108   0.00000   0.00000   0.03687   0.08026
64          2PX        -0.12830   0.00000   0.00000  -0.01710  -0.12692
65          2PY         0.00000  -0.17156  -0.27639   0.00000   0.00000
66          2PZ         0.03708   0.00000   0.00000  -0.31367  -0.08963
67          3S          0.78729   0.00000   0.00000   0.06262   1.28147
68          3PX        -0.17306   0.00000   0.00000  -0.01054  -0.48282
69          3PY         0.00000  -0.20132  -0.44668   0.00000   0.00000
70          3PZ         0.11506   0.00000   0.00000  -0.54928  -0.18491
71          4XX         0.00565   0.00000   0.00000   0.00604   0.00812
72          4YY        -0.00739   0.00000   0.00000  -0.00443  -0.01982
73          4ZZ        -0.01660   0.00000   0.00000   0.00756  -0.01324
74          4XY         0.00000   0.00059   0.00469   0.00000   0.00000
75          4XZ        -0.00100   0.00000   0.00000   0.00937  -0.00940
76          4YZ         0.00000   0.00611  -0.01843   0.00000   0.00000
77 7   H    1S         -0.00380   0.00000   0.00000   0.00688  -0.01997
78          2S         -0.03583   0.00000   0.00000  -0.02620   0.05885
79 8   C    1S          0.08841   0.00000   0.00000   0.01309  -0.08025
80          2S         -0.15108   0.00000   0.00000  -0.03687   0.08026
81          2PX        -0.12830   0.00000   0.00000  -0.01710   0.12692
82          2PY         0.00000  -0.17156   0.27639   0.00000   0.00000
83          2PZ        -0.03708   0.00000   0.00000   0.31367  -0.08963
84          3S         -0.78729   0.00000   0.00000  -0.06262   1.28147
85          3PX        -0.17306   0.00000   0.00000  -0.01054   0.48282
86          3PY         0.00000  -0.20132   0.44668   0.00000   0.00000
87          3PZ        -0.11506   0.00000   0.00000   0.54928  -0.18491
88          4XX        -0.00565   0.00000   0.00000  -0.00604   0.00812
89          4YY         0.00739   0.00000   0.00000   0.00443  -0.01982
90          4ZZ         0.01660   0.00000   0.00000  -0.00756  -0.01324
91          4XY         0.00000  -0.00059   0.00469   0.00000   0.00000
92          4XZ        -0.00100   0.00000   0.00000   0.00937   0.00940
93          4YZ         0.00000   0.00611   0.01843   0.00000   0.00000
94 9   H    1S          0.00380   0.00000   0.00000  -0.00688  -0.01997
95          2S          0.03583   0.00000   0.00000   0.02620   0.05885
```

9.9. Optimized Cartesian Coordinates and Total Energies [Hartrees] for All Species Reported of Chapter 4.

1 Hartree = 627.5095 kcal/mol = 2627.26 kJ/mol
ZPE = zero point energy correction
Coordinates X, Y, Z in Angstroms

$(Me_2N)_3P$, C_s symmetry (minimum)
EUMP2 = -743.12204769072; ZPE = 0.227795

Atom	X	Y	Z
P1	0.000000000	0.747167000	0.000000000
N2	0.639640000	0.029999000	-1.425317000
N3	-1.518105000	-0.134066000	0.000000000
N4	0.639640000	0.029999000	1.425317000
C21	0.655675000	-1.405088000	-1.674052000
H212	1.582393000	-1.878871000	-1.316295000
H213	-0.198227000	-1.866411000	-1.177305000
H211	0.577249000	-1.590674000	-2.752925000
C22	1.740927000	0.732325000	-2.068913000
H223	2.725891000	0.372940000	-1.732059000
H222	1.685967000	0.591185000	-3.155432000
H221	1.669046000	1.801584000	-1.855266000
C31	-2.326053000	0.121617000	-1.197038000
H313	-3.192233000	-0.548078000	-1.181369000
H311	-2.697516000	1.158801000	-1.245826000
H312	-1.739970000	-0.078109000	-2.093253000
C32	-2.326053000	0.121617000	1.197038000
H322	-1.739970000	-0.078109000	2.093253000
H321	-2.697516000	1.158801000	1.245826000
H323	-3.192233000	-0.548078000	1.181369000
C41	0.655675000	-1.405088000	1.674052000
H411	0.577249000	-1.590674000	2.752925000
H413	-0.198227000	-1.866411000	1.177305000
H412	1.582393000	-1.878871000	1.316295000
C42	1.740927000	0.732325000	2.068913000
H422	1.685967000	0.591185000	3.155432000
H423	2.725891000	0.372940000	1.732059000
H421	1.669046000	1.801584000	1.855266000

$(Me_2N)_2MeP$, C_s symmetry (minimum)
EUMP2 = -648.76708414068; ZPE = 0.209740

Atom	X	Y	Z
P1	-0.000005000	0.284417000	-0.902828000
N2	-1.438387000	-0.128886000	-0.034976000
N4	1.438403000	-0.129050000	-0.035097000
C42	1.990739000	-1.447198000	-0.329136000
H422	3.078610000	-1.429164000	-0.190235000
H423	1.581611000	-2.235848000	0.322649000
H421	1.778582000	-1.707925000	-1.368251000
C41	1.714986000	0.270559000	1.338273000

H413	1.325507000	1.269746000	1.536392000
H412	1.283574000	-0.425078000	2.074728000
H411	2.799996000	0.296543000	1.497719000
C21	-1.714742000	0.270547000	1.338495000
H212	-1.283572000	-0.425434000	2.074763000
H213	-1.324836000	1.269521000	1.536855000
H211	-2.799733000	0.296940000	1.498012000
C22	-1.991092000	-1.446843000	-0.329182000
H223	-1.582118000	-2.235701000	0.322447000
H222	-3.078947000	-1.428547000	-0.190191000
H221	-1.779086000	-1.707460000	-1.368355000
C3	0.000110000	2.107273000	-0.653608000
H33	0.000135000	2.447378000	0.384616000
H31	0.887879000	2.514111000	-1.143651000
H32	-0.887636000	2.514193000	-1.143624000

(Me$_2$N)Me$_2$P, C$_s$ symmetry (minimum)
EUMP2 = -554.41026738897; ZPE = 0.163121

Atom	**X**	**Y**	**Z**
P1	0.000000000	0.871718000	0.000000000
N3	0.349308000	-0.868741000	0.000000000
C31	1.103155000	-1.259600000	1.194744000
H313	1.277945000	-2.339522000	1.157088000
H311	2.081130000	-0.756359000	1.281744000
H312	0.521187000	-1.048148000	2.094051000
C32	1.103155000	-1.259600000	-1.194744000
H322	0.521187000	-1.048148000	-2.094051000
H321	2.081130000	-0.756359000	-1.281744000
H323	1.277945000	-2.339522000	-1.157088000
C2	-1.218180000	0.904271000	1.388749000
H23	-1.898709000	0.049608000	1.327914000
H22	-0.716803000	0.898447000	2.358911000
H21	-1.797183000	1.830652000	1.324827000
C4	-1.218180000	0.904271000	-1.388749000
H43	-1.898709000	0.049608000	-1.327914000
H41	-1.797183000	1.830652000	-1.324827000
H42	-0.716803000	0.898447000	-2.358911000

(Me$_2$N)Me$_2$P, C$_1$ symmetry (minimum)
EUMP2 = -554.41484239221; ZPE = 0.162905

Atom	**X**	**Y**	**Z**
P1	0.633905000	0.269177000	-0.630890000
N3	-0.918962000	-0.320620000	-0.145837000
C32	-2.058301000	0.389203000	-0.719459000
H321	-2.938515000	-0.263621000	-0.697281000
H322	-2.311126000	1.313143000	-0.173471000
H323	-1.842982000	0.646843000	-1.758201000
C31	-1.172898000	-0.718422000	1.232260000
H313	-0.334989000	-1.298289000	1.623926000
H312	-1.347356000	0.139706000	1.901061000

H311	-2.063868000	-1.355778000	1.263430000
C2	1.688958000	-1.207454000	-0.298580000
H23	1.654623000	-1.551231000	0.739703000
H22	1.376363000	-2.025145000	-0.951845000
H21	2.727143000	-0.956260000	-0.537346000
C4	1.207829000	1.340444000	0.772943000
H43	1.191206000	0.833607000	1.743022000
H41	2.234719000	1.663311000	0.573147000
H42	0.585410000	2.237775000	0.835083000

Me_3P, C_{3v} symmetry (minimum)
EUMP2 = -460.06869679115; ZPE = 0.116361

Atom	**X**	**Y**	**Z**
P1	0.000026000	-0.000035000	-0.602713000
C2	1.571664000	-0.427096000	0.278091000
H23	1.459070000	-0.396571000	1.367320000
H22	1.896945000	-1.430305000	-0.011123000
H21	2.359839000	0.273674000	-0.011019000
C4	-0.415936000	1.574587000	0.278053000
H43	-0.386160000	1.461784000	1.367281000
H41	0.290308000	2.357846000	-0.011095000
H42	-1.416867000	1.906851000	-0.011124000
C3	-1.155759000	-1.147451000	0.278077000
H33	-1.073022000	-1.065199000	1.367305000
H32	-2.187162000	-0.927346000	-0.011147000
H31	-0.943158000	-2.180456000	-0.011028000

$(H_2N)Me_2P=CH_2$, C_s symmetry (minimum)
EUMP2= -515.21566774092; ZPE = 0.131127

Atom	**X**	**Y**	**Z**
P1	0.000000000	0.152125000	0.000000000
C1	-0.400480000	1.770637000	0.000000000
H12	-0.290382000	2.329175000	0.923921000
H11	-0.290382000	2.329175000	-0.923921000
C2	-0.650089000	-0.671166000	-1.484422000
H23	-0.255336000	-0.175859000	-2.376287000
H22	-0.350095000	-1.720117000	-1.502887000
H21	-1.737270000	-0.586701000	-1.501834000
C4	-0.650089000	-0.671166000	1.484422000
H43	-0.255336000	-0.175859000	2.376287000
H41	-1.737270000	-0.586701000	1.501834000
H42	-0.350095000	-1.720117000	1.502887000
N3	1.601594000	-0.574046000	0.000000000
H32	2.129480000	-0.263193000	0.817827000
H31	2.129480000	-0.263193000	-0.817827000

$(H_2N)Me_2P=CH_2$, C_1 symmetry (minimum)
EUMP2 = -515.21452814182; ZPE = 0.130915

Atom	X	Y	Z
P1	0.106322000	-0.081080000	-0.065891000
N2	-0.577925000	-1.031013000	1.170437000
C1	1.402345000	-0.824392000	-0.800518000
H1	1.264480000	-1.784393000	-1.285612000
H2	2.210879000	-0.195721000	-1.154013000
H22	-1.532598000	-1.349486000	1.041573000
H21	0.041532000	-1.776708000	1.472698000
C3	-1.462571000	0.410772000	-0.908012000
H32	-1.896248000	-0.452652000	-1.421236000
H31	-1.237055000	1.172728000	-1.658049000
H33	-2.198710000	0.814425000	-0.204456000
C4	0.647611000	1.502381000	0.645866000
H43	0.898244000	2.211148000	-0.147738000
H42	-0.152368000	1.922358000	1.259312000
H41	1.528176000	1.339025000	1.268807000

$(H_2N)_2MeP=CH_2$, C_s symmetry (minimum)
EUMP2 = -531.25631108873; ZPE = 0.120448

Atom	X	Y	Z
P1	-0.039889000	0.129380000	0.000000000
N4	-0.549887000	-0.548158000	1.463539000
C1	-0.549887000	1.709072000	0.000000000
H12	-0.486071000	2.261473000	0.928811000
H11	-0.486071000	2.261473000	-0.928811000
H42	-0.243814000	-1.485864000	1.698552000
H41	-1.520477000	-0.372075000	1.699314000
N2	-0.549887000	-0.548158000	-1.463539000
H22	-0.243814000	-1.485864000	-1.698552000
H21	-1.520477000	-0.372075000	-1.699314000
C3	1.669829000	-0.549219000	0.000000000
H32	2.194496000	-0.193467000	0.888887000
H31	2.194496000	-0.193467000	-0.888887000
H33	1.688818000	-1.645749000	0.000000000

$(H_2N)_2MeP=CH_2$, C_1 symmetry (minimum)
EUMP2 = -531.25792721587; ZPE = 0.120557

Atom	X	Y	Z
P1	0.050313000	0.117167000	-0.059715000
N3	-0.959821000	-1.001867000	-0.929000000
N2	-1.199246000	0.626128000	0.950169000
C1	0.894913000	1.435787000	-0.603103000
H11	0.366862000	2.280635000	-1.028903000
H12	1.932524000	1.294125000	-0.880101000
H22	-1.837473000	-0.082250000	1.295576000
H21	-0.934291000	1.319339000	1.639457000
H31	-1.719673000	-0.508549000	-1.398006000

H32	-0.427369000	-1.502372000	-1.639880000
C4	1.210273000	-1.088187000	0.661359000
H43	1.841962000	-1.518861000	-0.120948000
H41	1.852154000	-0.597755000	1.393819000
H42	0.652969000	-1.897244000	1.136992000

$Me_3P=CH_2$ (minimum)
EUMP2 = -499.17092883541; ZPE = 0.142026

Atom	**X**	**Y**	**Z**
P1	0.000000000	0.166158000	0.000000000
C1	-0.360261000	1.805792000	0.000000000
H12	-0.160115000	2.347913000	0.920116000
H11	-0.160115000	2.347913000	-0.920116000
C2	-0.735240000	-0.640800000	-1.459215000
H23	-0.297250000	-0.220829000	-2.368945000
H22	-0.546046000	-1.717518000	-1.447263000
H21	-1.809587000	-0.452048000	-1.471110000
C4	-0.735240000	-0.640800000	1.459215000
H43	-0.297250000	-0.220829000	2.368945000
H41	-1.809587000	-0.452048000	1.471110000
H42	-0.546046000	-1.717518000	1.447263000
C3	1.725331000	-0.571248000	0.000000000
H33	2.448278000	0.247465000	0.000000000
H32	1.905087000	-1.186262000	0.887002000
H31	1.905087000	-1.186262000	-0.887002000

$(H_2N)_3P=CH_2$ (minimum)
EUMP2 = -547.30202648738; ZPE = 0.110315

Atom	**X**	**Y**	**Z**
N4	-0.131623000	-1.469618000	0.732632000
P1	0.115678000	-0.000042000	-0.053353000
N2	-0.130673000	1.469575000	0.732704000
N3	-1.434782000	0.000419000	-0.821589000
C1	1.665438000	-0.000567000	-0.633006000
H41	0.612061000	-1.753748000	1.358778000
H42	-1.061125000	-1.640032000	1.099217000
H21	0.613312000	1.754674000	1.358012000
H22	-1.060354000	1.642441000	1.097607000
H31	-1.552115000	0.827007000	-1.404780000
H32	-1.553446000	-0.827350000	-1.402834000
H11	2.076889000	0.928007000	-1.007322000
H12	2.076537000	-0.929597000	-1.006581000

$H_3P=CH_2$ (minimum)
EUMP2 = -381.63116067190; ZPE = 0.053242

Atom	**X**	**Y**	**Z**
P1	0.477820000	-0.000002000	0.006794000
C1	-1.197240000	-0.000003000	-0.061180000
H12	-1.695888000	-0.922518000	0.213859000
H11	-1.695863000	0.922534000	0.213835000

H2	1.017795000	1.118254000	-0.649076000
H3	1.372275000	-0.000012000	1.135676000
H4	1.017818000	-1.118213000	-0.649128000

$Cl_3P=CH_2$ (minimum)
EUMP2 = -1758.8089880288; ZPE = 0.031357

Atom	**X**	**Y**	**Z**
P1	0.000075000	-0.166069000	0.392962000
C1	0.000354000	-0.909031000	1.852874000
H12	0.937410000	-0.969801000	2.393600000
H11	-0.936104000	-0.969676000	2.394623000
Cl2	-1.646526000	-0.657737000	-0.657474000
Cl3	-0.001125000	1.895165000	0.032471000
Cl1	1.647384000	-0.655975000	-0.657343000

$(H_3Si)_3P=CH_2$ (minimum)
EUMP2 = -1252.1193727851; ZPE = 0.104784

Atom	**X**	**Y**	**Z**
P1	0.000000000	0.433909000	0.000000000
C1	0.584398000	2.057575000	0.000000000
H11	0.382516000	2.615659000	0.912950000
H12	0.382516000	2.615659000	-0.912950000
Si4	0.986629000	-0.493439000	-1.797349000
Si3	-2.210169000	-0.341741000	0.000000000
Si2	0.986629000	-0.493439000	1.797349000
H43	0.712054000	0.408404000	-2.941435000
H41	2.438438000	-0.588561000	-1.524004000
H42	0.422710000	-1.843417000	-2.061803000
H31	-2.517074000	-1.154822000	1.210838000
H32	-2.517074000	-1.154822000	-1.210838000
H33	-3.066916000	0.872056000	0.000000000
H21	2.438438000	-0.588561000	1.524004000
H22	0.422710000	-1.843417000	2.061803000
H33	0.712054000	0.408404000	2.941435000

9.10. Optimized Cartesian Coordinates and Total Energies [Hartrees] for All Species Reported of Chapter 5.

1 Hartree = 627.5095 kcal/mol = 2627.26 kJ/mol

ZPE = zero point energy correction
Coordinates X, Y, Z in Angstroms

Dichloro[(4-dimethylamino)phenyl]arsine; experimental geometry; population analysis only, no structure optimization
E(RB+HF-LYP) = -3522.09513592

Atom	X	Y	Z
As1	-2.085020000	-0.633498000	-0.260363000
Cl2	-2.490601000	1.240586000	-1.368404000
Cl3	-2.900424000	0.095151000	1.640701000
C1	-0.210354000	-0.345611000	0.030426000
C6	0.637111000	-1.411430000	-0.287880000
C2	0.358644000	0.857814000	0.424022000
C5	2.011072000	-1.262230000	-0.248901000
H6	0.292775000	-2.385056000	-0.603926000
C3	1.718167000	1.028991000	0.472885000
H2	-0.260741000	1.683855000	0.740910000
C4	2.597934000	-0.028031000	0.108463000
H5	2.553423000	-2.151511000	-0.534270000
H3	2.099269000	2.014936000	0.694409000
N4	3.945685000	0.149516000	0.116276000
C42	4.825077000	-0.953749000	-0.230162000
C41	4.525094000	1.477749000	0.232263000
H421	4.597565000	-1.895062000	0.270107000
H423	5.846394000	-0.602282000	-0.083598000
H422	4.735858000	-1.285931000	-1.264471000
H412	4.212058000	2.219427000	-0.502599000
H411	4.365595000	1.915164000	1.217823000
H413	5.614619000	1.456735000	0.207919000

Dichloro[(4-dimethylamino)phenyl]arsine, B3LYP/6-311++G**, minimum
E(RB+HF-LYP) = -3522.10593138; ZPE = 0.165062

Atom	X	Y	Z
As1	-2.100295000	-0.676113000	-0.035446000
Cl1	-2.713694000	0.739709000	-1.667835000
Cl2	-2.742630000	0.584877000	1.709397000
C1	-0.200622000	-0.307333000	-0.002918000
C6	0.647162000	-1.420511000	-0.041856000
C2	0.376374000	0.968162000	0.049109000
C5	2.027651000	-1.276688000	-0.026224000

H6	0.233234000	-2.424102000	-0.087462000
C3	1.749499000	1.127339000	0.065241000
H2	-0.255992000	1.848227000	0.074756000
C4	2.619574000	0.006296000	0.034298000
H5	2.642466000	-2.164859000	-0.061611000
H3	2.153077000	2.129535000	0.100367000
N4	3.985703000	0.164344000	0.065181000
C42	4.856283000	-0.993620000	-0.070402000
C41	4.571504000	1.496642000	0.028472000
H421	4.676729000	-1.722384000	0.726803000
H423	5.893014000	-0.670515000	0.003586000
H422	4.723978000	-1.500440000	-1.035191000
H412	4.327559000	2.032489000	-0.897953000
H411	4.234183000	2.103664000	0.874597000
H413	5.654544000	1.410023000	0.094714000

Dichloro(4-nitrophenyl)arsine; B3LYP/6-311++G**; C_s, minimum
E(RB+HF-LYP) = -3592.65761837; ZPE = 0.094852

Atom	X	Y	Z
C1	-0.460121000	-0.405487000	0.000543000
C6	0.321562000	-1.564222000	0.002095000
C2	0.147396000	0.854256000	-0.001083000
H6	-0.141860000	-2.545642000	0.003374000
H2	-0.455993000	1.753813000	-0.002276000
C5	1.712152000	-1.473912000	0.002008000
C3	1.532264000	0.957060000	-0.001201000
H5	2.339868000	-2.354224000	0.003193000
H3	2.029246000	1.917418000	-0.002465000
C4	2.289982000	-0.211865000	0.000340000
As1	-2.412676000	-0.685950000	0.000714000
Cl1	-2.908196000	0.672199000	1.695417000
Cl2	-2.907592000	0.666852000	-1.698444000
N4	3.770529000	-0.104757000	0.000180000
O42	4.412214000	-1.146341000	0.001880000
O41	4.255290000	1.018012000	-0.001657000

Dichloro(4-diazoniumphenyl)arsine; minimum; C_s
B3LYP/6-311++G**
E(RB+HF-LYP) = -3496.70578442; ZPE = 0.090731

Atom	X	Y	Z
As1	1.753543000	-0.082991000	0.663245000
Cl1	2.189825000	1.768458000	-0.457295000
Cl2	2.185986000	-1.603503000	-0.878408000

C1	-0.233367000	-0.039397000	0.310410000
C6	-1.084209000	-0.208971000	1.411817000
C2	-0.760311000	0.153449000	-0.976603000
C5	-2.461424000	-0.189095000	1.252773000
H6	-0.679391000	-0.357766000	2.407137000
C3	-2.126923000	0.179850000	-1.180184000
H2	-0.098351000	0.284536000	-1.824260000
C4	-2.948922000	0.006799000	-0.049582000
H5	-3.135973000	-0.317284000	2.090231000
H3	-2.555102000	0.327170000	-2.164017000
H41	-4.315769000	0.031411000	-0.232191000
N42	-5.412224000	0.051734000	-0.382234000

Dichloro[(4-hydroxyamino)phenyl]arsine; minimum; C_1
B3LYP/6-311++G**
E(RB+HF-LYP) = -3518.66286919; ZPE = 0.113588

Atom	**X**	**Y**	**Z**
As1	1.746380000	0.009641000	-0.717132000
Cl1	2.481476000	-1.673257000	0.567064000
Cl2	2.428726000	1.711318000	0.570954000
C1	-0.129748000	-0.020538000	-0.203704000
C6	-1.052438000	-0.045075000	-1.253121000
C2	-0.598963000	-0.013843000	1.117263000
C5	-2.422943000	-0.068051000	-1.004599000
H6	-0.711275000	-0.042857000	-2.284453000
C3	-1.957537000	-0.034599000	1.374816000
H2	0.101063000	0.010304000	1.944109000
C4	-2.882365000	-0.064800000	0.314267000
H5	-3.132354000	-0.070883000	-1.820020000
H3	-2.313772000	-0.034754000	2.400040000
N41	-4.246580000	-0.165646000	0.633961000
H41	-4.493906000	0.377977000	1.454593000
O42	-5.113273000	0.246083000	-0.412845000
H42	-5.657535000	-0.532675000	-0.579728000

Dichlorophenylarsine; B3LYP/6-311++G**; C_s, minimum
E(RB+HF-LYP) = -3388.09825360; ZPE = 0.092636

Atom	**X**	**Y**	**Z**
As1	-1.035444000	-0.152429000	-0.699176000
Cl1	-1.736622000	1.769799000	0.199668000
Cl2	-1.747332000	-1.550141000	0.892790000
C4	0.848199000	-0.048480000	-0.170163000
C6	1.773329000	-0.269192000	-1.194876000
C2	1.290963000	0.224876000	1.127948000
C5	3.141389000	-0.217063000	-0.923074000
H6	1.437079000	-0.481897000	-2.205527000
C3	2.654857000	0.275790000	1.393408000
H2	0.575643000	0.396227000	1.923745000
C4	3.579836000	0.055231000	0.369531000
H5	3.857259000	-0.388549000	-1.718732000
H3	2.999650000	0.487491000	2.399190000
H4	4.641929000	0.096290000	0.583154000

Chlorodiphenylarsine; B3LYP/6-311++G**; C_1; minimum
E(RB+HF-LYP) = -3159.54772754; ZPE = 0.181668

Atom	**X**	**Y**	**Z**
As1	0.068668000	1.051472000	-0.754670000
Cl1	0.130072000	2.479501000	0.991568000
C11	1.488229000	-0.181244000	-0.162304000
C16	2.749825000	0.002412000	-0.740238000
C12	1.300341000	-1.209650000	0.767089000
C15	3.814030000	-0.826694000	-0.388533000
H16	2.906007000	0.795506000	-1.464978000
C13	2.364593000	-2.037728000	1.116313000
H12	0.327184000	-1.366778000	1.216972000
C14	3.621034000	-1.847530000	0.540073000
H15	4.788601000	-0.676355000	-0.839340000
H13	2.213396000	-2.833122000	1.837813000
H14	4.446485000	-2.495145000	0.813849000
C21	-1.519370000	-0.010956000	-0.249250000
C26	-1.953824000	-0.936338000	-1.206106000
C22	-2.241051000	0.141157000	0.935918000
H26	-1.413710000	-1.055822000	-2.141251000
H22	-1.923390000	0.865516000	1.675910000
C25	-3.083767000	-1.716680000	-0.969836000
C23	-3.376133000	-0.637319000	1.166852000
H25	-3.409147000	-2.433472000	-1.715574000
H23	-3.931264000	-0.513032000	2.090143000
C24	-3.797366000	-1.567479000	0.218801000
H24	-4.680666000	-2.169104000	0.401248000

Triphenylarsine; minimum; C$_3$
B3LYP/6-311++G**
E(RB+HF-LYP) = -2930.99511771; ZPE = 0.098241

As1	-0.004713000	0.004410000	-1.204290000
C11	0.724245000	1.598390000	-0.280265000
C16	0.148015000	2.181569000	0.852432000
C12	1.867083000	2.185868000	-0.837121000
C15	0.712636000	3.322711000	1.424249000
H16	-0.743310000	1.749798000	1.292425000
C13	2.435965000	3.320595000	-0.261340000
H12	2.318304000	1.757052000	-1.726740000
C14	1.858320000	3.892174000	0.871818000
H15	0.255320000	3.765267000	2.302746000
H13	3.323871000	3.761510000	-0.701291000
H14	2.295537000	4.778632000	1.317754000
C21	1.016988000	-1.419845000	-0.279612000
C22	0.970068000	-2.700467000	-0.844517000
C26	1.799075000	-1.211927000	0.860708000
H22	0.381915000	-2.876575000	-1.740038000
H26	1.858108000	-0.225862000	1.306392000
C23	1.673675000	-3.757569000	-0.269830000
C25	2.510112000	-2.268521000	1.431628000
H23	1.624328000	-4.744713000	-0.716435000
H25	3.113561000	-2.093841000	2.315965000
C24	2.446857000	-3.542669000	0.870455000
H24	3.000592000	-4.362053000	1.315218000
C31	-1.745236000	-0.167813000	-0.273097000
C32	-2.835241000	0.508523000	-0.835083000
C36	-1.950350000	-0.950153000	0.867606000
H32	-2.699060000	1.106172000	-1.731284000
H36	-1.122864000	-1.491482000	1.311126000
C33	-4.100790000	0.421856000	-0.257284000
C35	-3.219155000	-1.043943000	1.441317000
H33	-4.934462000	0.954517000	-0.701849000
H35	-3.364659000	-1.655554000	2.325318000
C34	-4.295350000	-0.356748000	0.882969000
H34	-5.280621000	-0.431600000	1.329563000

Trimethylarsine; B3LYP/6-311++G**; C$_{3v}$; minimum
E(RB+HF-LYP) = -2355.66297617; ZPE=0.110144

Atom	**X**	**Y**	**Z**
As1	-0.000017000	0.000136000	-0.473988000
C1	-1.716693000	-0.137466000	0.521248000

H11	-2.362066000	0.697439000	0.241411000
H12	-2.217484000	-1.067013000	0.243724000
H13	-1.553832000	-0.122883000	1.601299000
C2	0.977417000	-1.417800000	0.521007000
H21	2.032100000	-1.391186000	0.240290000
H22	0.887342000	-1.281336000	1.600970000
H23	0.572484000	-2.393358000	0.245074000
C3	0.739358000	1.555020000	0.521361000
H22	0.663851000	1.409055000	1.601240000
H21	1.787284000	1.690913000	0.247061000
H23	0.190381000	2.455373000	0.238851000

Trimethylarsine; MP2/6-311++G**; C_{3v}; minimum
E(RHF) = -2353.02974043; ZPE=0.111876

Atom	**X**	**Y**	**Z**
As1	-0.000001000	-0.000003000	-0.478369000
C1	1.212726000	-1.183370000	0.523889000
H11	1.010546000	-2.224595000	0.258503000
H12	2.248684000	-0.955720000	0.258514000
H13	1.077555000	-1.051481000	1.601728000
C2	0.418472000	1.641937000	0.523883000
H21	-0.296651000	2.425283000	0.258506000
H22	0.371839000	1.458937000	1.601723000
H23	1.421292000	1.987447000	0.258496000
C3	-1.631195000	-0.458559000	0.523889000
H32	-1.449388000	-0.407452000	1.601728000
H31	-2.431819000	0.237165000	0.258511000
H33	-1.952044000	-1.469541000	0.258508000

Chlorodimethylarsine; B3:YP/6-311++G**; C_s, minimum
E(RB+HF-LYP) = -2775.99529633; ZPE = 0.074813

Atom	**X**	**Y**	**Z**
As1	-2.124734000	-0.222571000	0.472945000
Cl1	-2.515653000	0.776505000	-1.509365000
C2	-0.388560000	-1.041733000	-0.009102000
H22	0.364620000	-0.258283000	-0.093533000
H21	-0.104564000	-1.722501000	0.798501000
H23	-0.460338000	-1.590600000	-0.948059000
C1	-3.241669000	-1.826004000	0.157724000

H12	-4.292785000	-1.537687000	0.173795000
H13	-2.998929000	-2.292679000	-0.796935000
H11	-3.053780000	-2.529739000	0.973751000

Chlorodimethylarsine; MP2/6-311++G**; C_s; minimum
E(RHF) = -2772.94746706; ZPE = 0.076022

Atom	X	Y	Z
As1	0.345601000	0.000000000	-0.503063000
Cl1	-1.745758000	-0.000003000	0.225508000
C2	0.973281000	-1.458517000	0.641295000
H21	0.553863000	-2.403549000	0.290361000
H23	2.064814000	-1.505198000	0.567033000
H22	0.678201000	-1.286747000	1.678561000
C1	0.973274000	1.458520000	0.641294000
H11	0.553824000	2.403546000	0.290381000
H12	0.678224000	1.286732000	1.678566000
H13	2.064803000	1.505229000	0.567005000

Dichloromethylarsine; B3LYP/6-311++G**; C_s, minimum
E(RB+HF-LYP) = -3196.32243937; ZPE = 0.039262

Atom	X	Y	Z
As1	-0.243469000	0.593683000	0.000000000
Cl1	-0.243469000	-0.830928000	1.717877000
Cl2	-0.243469000	-0.830928000	-1.717877000
C1	1.697973000	0.937300000	0.000000000
H11	1.936099000	1.517966000	0.893605000
H12	2.252382000	0.000293000	0.000000000
H13	1.936099000	1.517966000	-0.893605000

Dichloromethylarsine; MP2/6-311++G**; C_s, minimum
E(RHF) = -3192.85655914 ; ZPE = 0.040091

Atom	X	Y	Z
As1	-0.241508000	0.594767000	0.000000000
Cl1	-0.241508000	-0.819541000	1.680156000
Cl2	-0.241508000	-0.819541000	-1.680156000
C1	1.681921000	0.894002000	0.000000000
H11	1.940514000	1.467081000	0.894396000
H12	2.208489000	-0.061099000	0.000000000
H13	1.940514000	1.467081000	-0.894396000

Trichloroarsine; B3LYP/6-311++G**; C_{3v}; minimum
E(RB+HF-LYP) = -3616.64471553; ZPE = 0.003669

Atom	**X**	**Y**	**Z**
As1	0.000000000	0.000000000	0.632470000
Cl1	0.000000000	1.952624000	-0.409245000
Cl2	-1.691022000	-0.976312000	-0.409245000
Cl3	1.691022000	-0.976312000	-0.409245000

Trichloroarsine; MP2/6-311++G**; C_{3v}; minimum
E(RHF) = -3612.75722107; ZPE = 0.003964

Atom	**X**	**Y**	**Z**
As1	0.000000000	0.000000000	0.635684000
Cl1	0.000000000	1.912505000	-0.411325000
Cl2	-1.656278000	-0.956253000	-0.411325000
Cl3	1.656278000	-0.956253000	-0.411325000

Trans-chlorovinyldichloroarsine; minimum; C_s
B3LYP/6-311++G**
E(RB+HF-LYP) = -3694.02888497; ZPE = 0.035668

Atom	**X**	**Y**	**Z**
As1	-2.416499000	-1.502601000	-0.107885000
Cl1	-2.945297000	-0.146318000	1.581230000
Cl2	-2.618160000	-0.061088000	-1.797264000
C1	-0.484078000	-1.355852000	0.083402000
H1	-0.027636000	-0.375334000	0.157545000
C2	0.215897000	-2.484532000	0.116710000
H2	-0.216283000	-3.475797000	0.044512000
Cl21	1.950281000	-2.540045000	0.282541000

Trans-chlorovinyldichloroarsine; minimum; C_s
MP2; SDD for As atom; 6-311++G** for other atoms
E(RHF) = -1461.46863597; ZPE = 0.036022

Atom	**X**	**Y**	**Z**
As1	-0.779051000	-0.000091000	0.648043000
Cl1	-1.647008000	1.702639000	-0.512864000
Cl2	-1.648405000	-1.701859000	-0.513087000
C1	0.899229000	-0.000679000	-0.289756000
H1	0.889198000	-0.000770000	-1.376190000
C2	2.032933000	-0.000295000	0.422705000

H2	2.054997000	-0.000135000	1.509181000
Cl21	3.599619000	-0.000207000	-0.286761000

Benzene, minimum, D_{6h}
B3LYP/6-311++G**
E(RB+HF-LYP) = -232.311304360; ZPE = 0.100077

Atom	X	Y	Z
C6	-1.207799000	0.697309000	0.000000000
C5	0.000000000	1.394633000	0.000000000
C1	-1.207836000	-0.697350000	0.000000000
H5	-0.000026000	2.479041000	0.000000000
H1	-2.146951000	-1.239554000	0.000000000
C4	1.207837000	0.697351000	0.000000000
C2	-0.000001000	-1.394633000	0.000000000
H4	2.146952000	1.239555000	0.000000000
H2	0.000025000	-2.479041000	0.000000000
C3	1.207794000	-0.697307000	0.000000000
H3	2.146910000	-1.239526000	0.000000000
H6	-2.146880000	1.239509000	0.000000000

Dimethylaniline; B3LYP/6-311++G**; C_s, minimum
E(RB+HF-LYP) = -366.311389535; ZPE = 0.171838

Atom	X	Y	Z
C1	-0.422337000	-2.640603000	0.000000000
C6	-1.497491000	-1.753440000	0.000000000
C2	0.865302000	-2.111318000	0.000000000
H6	-2.513713000	-2.133570000	0.000000000
H2	1.724576000	-2.773833000	0.000000000
C5	-1.301367000	-0.377426000	0.000000000
C3	1.081138000	-0.736838000	0.000000000
H5	-2.175095000	0.258949000	0.000000000
H3	2.099611000	-0.374853000	0.000000000
C4	0.000000000	0.175237000	0.000000000
N4	0.239472000	1.541761000	0.000000000
H1	-0.584673000	-3.711542000	0.000000000
C42	-0.803920000	2.550498000	0.000000000
H422	-1.791608000	2.100875000	0.000000000
H423	-0.734934000	3.189922000	0.888605000
H421	-0.734934000	3.189922000	-0.888605000
C41	1.601971000	2.042246000	0.000000000

H412	2.159144000	1.719868000	0.889102000
H411	2.159144000	1.719868000	-0.889102000
H413	1.576405000	3.131936000	0.000000000

Nitrobenzene; B3LYP/6-311++G**; C_{2v}, minimum
E(RB+HF-LYP) = -436.874703949; ZPE = 0.102601

Atom	**X**	**Y**	**Z**
C1	-2.515469000	-0.000013000	-0.000002000
C6	-1.821182000	-1.210178000	-0.000060000
C2	-1.821215000	1.210167000	0.000060000
H6	-2.362415000	-2.148714000	-0.000102000
H2	-2.362477000	2.148699000	0.000101000
C5	-0.429802000	-1.218706000	-0.000053000
C3	-0.429833000	1.218712000	0.000056000
H5	0.135340000	-2.140409000	-0.000083000
H3	0.135290000	2.140424000	0.000088000
C4	0.241436000	0.000001000	0.000002000
N4	1.722315000	0.000008000	0.000000000
O22	2.290864000	-1.084510000	0.000141000
O21	2.290861000	1.084520000	-0.000144000
H1	-3.599355000	-0.000030000	-0.000005000

Aniline; minimum; C_s
B3LYP/6-311++G**
E(RB+HF-LYP) = -287.687732923; ZPE = 0.116519

Atom	**X**	**Y**	**Z**
C1	-0.423268000	-2.628208000	-0.026857000
C2	-1.499668000	-1.741820000	-0.004393000
C6	0.873010000	-2.114494000	-0.001988000
H2	-2.515517000	-2.121501000	-0.023270000
H6	1.723417000	-2.787567000	-0.019029000
C3	-1.289047000	-0.367353000	0.041375000
C5	1.094258000	-0.741656000	0.043729000
H3	-2.136288000	0.311078000	0.064170000
H5	2.108699000	-0.355897000	0.068282000
C4	0.013702000	0.152843000	0.064685000
N41	0.229668000	1.530425000	0.167407000

H1	-0.591107000	-3.697846000	-0.063028000
H42	1.128574000	1.856862000	-0.155275000
H41	-0.526227000	2.115997000	-0.155810000

10. References

[1] H. Albers, *Angew.Chem.*,1950, **62**, 451.

[2] T. E. Gier, *J. Am. Chem. Soc.*,1961, **83**, 1769.

[3] S. Haber, P. Le Floch, F. Mathey, *J. Chem. Soc., Chem. Commun.*, 1992, 1799.

[4] P. Le Floch, F. Mathey, *J. Chem. Soc., Chem. Commun.*, 1993, 1295.

[5] P. Le Floch, F. Mathey in: *Synthetic Methods of Organometallic and Inorganic Chemistry* (Hrsg.: W.A. Herrmann), **Vol. 3**: Phosphorus, Arsenic, Antimony, and Bismuth, edited by H.H. Karsch, Georg Thieme Verlag, Stuttgart. 1996, page. 8.

[6] M. J. Hopkinson, H. W. Kroto, J. F. Nixon, N. P. C. Simmons, *J. Chem. Soc., Chem. Commun.*, 1976, 513.

[7] T. A. Cooper, H. W. Kroto, J. F. Nixon, O. Ohashi, *J. Chem. Soc. Chem. Commun.*, 1980, 333.

[8] E. P. O. Fuchs, M. Hermesdorf, W. Schnurr, W. Rösch, H. Heydt, M. Regitz, P. Binger, *J. Organomet. Chem.*, 1988, **338**, 329.

[9] B. Pellerin, J. M. Denis, J. Perrocheau, R. Carrié, *Tetrahedron. Lett.*, 1986, **27**, 5723.

[10] J. C. T. R. Burckett-St. Laurent, T. A. Cooper, H. W. Kroto, J. F. Nixon, O. Ohashi, K. Ohno, *J. Mol. Struct.*, 1982, **79**, 215.

[11] M. J. Hopkinson, H. W. Kroto, J. F. Nixon, N. P. C. Simmons, *Chem. Phys. Lett.*, 1976, **42**, 460.

[12] M. Hermesdorf, M. Birkel, H. Heydt, M. Regitz, *Phosphorus Sulfur Silicon*, 1989, **46**, 31.

[13] J. C. Guillemin, T. Janati, P. Guenot, P. Savignac, J. M. Denis, *Angew. Chem.*, 1991, **103**, 191; *Angew. Chem., Int. Ed. Engl.*, 1991, **30**, 196.

[14] S. Haber, P. Le Floch, F. Mathey, *Phosphorus Sulfur and Silicon*, 1993, **75**, 225.

[15] J. C. Guillemin, T. Janati, J. M. Denis, *J. Chem. Soc., Chem. Commun.*, 1992, 415.

[16] J. C. Guillemin, P. Savignac, J. M. Denis, *Inorg. Chem.*, 1991, **30**, 2170.

[17] R. Appel, G. Westerhaus, *Angew. Chem.*, 1981, **93**, 215; *Angew. Chem., Int. Ed. Engl.*, 1981, **20**, 197.

[18] R. Appel, A. Westerhaus, *Tetrahedron. Lett.*, 1981, **22**, 2159.

[19] M. Regitz and others, *unpublished results*, Kaiserslautern, 1989 cited in W. Fiedler, O. Löber, U. Bergsträßer, M. Regitz, *Eur. J. Org. Chem.*, 1999, 363.

[20] E. Niecke, A. Ruban, M. Raab in: *Science of Synthesis*: Houben-Weyl Methods of Molecular Transformations, **Volume 27**, Category 4: Compounds with Two Carbon-Heteroatom Bonds, edited by A. Padwa, Georg Thieme Verlag Stuttgart. New York, 2004, page 937.

[21] D. J. Berger, P. P. Gaspar, P. Le Floch, F. Mathey, *Organometallics*, 1996, **15**, 4904.

[22] G. David, E. Niecke, M. Nieger, J. Radseck, *J. Am. Chem. Soc.,* 1994, **116**, 2191.

[23] J-. C. Guillemin; T. Janati, J-. M. Denis, *J. Org. Chem*., 2001, **66**, 7864.

[24] G. Becker, G. Gresser, W. Uhl, *Z. Naturforsch.*, 1981, **36b**, 16.

[25] R. Appel, F. Knoll, I. Ruppert, *Angew. Chem.*, 1981, **93**, 771; *Angew. Chem., Int. Ed. Engl.*, 1981, **20**, 731.

[26] M. Regitz in: *Methoden der Organischen Chemie (Houben – Weyl). Bd. E1, Organische Phosphor-Verbindungen I*, Georg Thieme Verlag Stuttgart New York, 1982, Page. 23.

[27] E. A. Ishmaeva, I. I. Patsanovskii, *Russ. Chem. Rev*., 1985, **54**, 243.

[28] T. Allspach, M. Regitz, G. Becker, W. Becker, *Synthesis*, 1986, 31.

[29] W. Rösch, U. -J. Vogelbacher, T. Allspach, M. Regitz, *J. Organomet. Chem.*, 1986, **306**, 39.

[30] G. Märkl, H. Sejpka, *Tetrahedron. Lett.*, 1986, **27**, 171.

[31] M. Regitz, P. Binger, *Angew. Chem.*, 1988, **100**, 1541; *Angew. Chem., Int. Ed. Engl.*, 1988, **27**, 1484.

[32] L. N. Markovskii; V. D. Romanenko, *Tetrahedron.*, 1989, **45**, 6019.

[33] G. Becker, H. Schmidt, G. Uhl, W. Uhl, *Inorg. Synth*., 1990, **27**, 243.

[34] M. Regitz, *Chem. Rev.*, 1990, **90**, 191.

[35] M. Regitz in: *Multiple Bonds and Low Coordination in Phosphorus Chemistry*, edited by M. Regitz, O. J. Scherer, Georg Thieme, Stuttgart, 1990, page 58.

[36] M. J. Maah, J. F. Nixon in: The Chemistry of Organophosphorus Compounds, **Volume 1**, edited by F. R. Hartley, John Wiley & Sons, New York, 1990, Chapter 9, Page 255.

[37] A. C. Gaumont, J. M. Denis, *Chem. Rev.*, 1994, **94**, 1413.

[38] A. Mack, E. Pierron, T. Allspach, U. Bergsträßer, M. Regitz, *Synthesis*, 1998, 1305.

[39] K. B. Dillon, F. Mathey, J. F. Nixon, Phosphorus: *The Carbon Copy, From Organophosphorus to Phospha-organic Chemistry*, J. Wiley & Sons, Chichester, 1998, page 40.

[40] L. D. Quin, G. S. Quin, *A Guide To Organphosphorus Chemistry*, J. Wiley & Sons, Chichester, 2000, Page 307.

[41] U. Bergsträßer in: *Science of Synthesis*: Houben-Weyl Methods of Molecular Transformations, **Volume 19**, Category 3: Compounds with Four and Three Carbon-Heteroatom Bonds, edited by S.-I. Murahashi, Georg Thieme Verlag Stuttgart. New York, 2004, page 427.

[42] H. H. Karsch, F. Bienlein, T. Rupprich, F. Uhlig, E. Herrmann and M. Scheer in: *Synthetic Methods of Organometallic and Inorganic Chemistry* (Hrsg.: W.A. Herrmann), **Vol. 3**: Phosphorus, Arsenic, Antimony, and Bismuth, edited by H. H. Karsch, Georg Thieme Verlag, Stuttgart. 1996, page. 58.

[43] J. S. Figueroa, C. C. Cummins, *J. Am. Chem. Soc.*, 2004, **126**, 13916.

[44] H. W. Kroto, J. F. Nixon, N. P. C. Simmons, *J. Mol. Spectroscopy.*, 1980, **82**, 185.

[45] H. W. Kroto, J. F. Nixon, N. P. C. Simmons, N. P. C. Westwood, *J. Am. Chem. Soc.*, 1978, **100**, 446.

[46] H. E. Hosseini, H. W. Kroto, J. F. Nixon, S. Brownstein, J. R. Morton, K. F. Preston, *J. Chem, Soc. Chem. Commun.*, 1979, 653.

[47] G. Heckmann, G. Becker and H. Kraft, *Magn. Reson. Chem.*, 1999, **37**, 667.

[48] H. Kraft, *Ph.d. Thesis*, Universität Stuttgart, 2000.

[49] G. Becker, W. Schwarz, N. Seidler, M. Westerhausen, *Z. Anorg. Allg. Chem.*, 1992, **612**, 72.

[50] G. Becker, G. Heckmann, K. Hübler, W. Schwarz, *Z. Anorg. Allg. Chem.*, 1995, **621**, 34.

[51] G. Becker, K. Hübler, *Z. Anorg. Allg. Chem.*, 1994, **620**, 405.

[52] M. Finze, E. Bernhardt, H. Willner, C. W. Lehmann, *Angew. Chem.*, 2004, **116**, 4254; *Angew. Chem., Int. Ed. Engl.*, 2004, **43**, 4160.

[53] F. E. Hahn, D. Le Van, M. C. Moyes, T. von Fehren, R. Fröhlich, E.-U. Würthwein, *Angew. Chem.*, 2001, **113**, 3241; *Angew. Chem., Int. Ed. Engl.*, 2001, **40**, 3144.

[54] J. Grobe, D. Le Van, F. Immel, B. Krebs, M. Läge, *Chem. Ber.*, 1996, **129**, 1271.

[55] L. N. Markovskii, G. N. Koidan, A. P. Marchenko, V. D. Romanenko, M. I. Povolotskii, A. M. Pinchuk, *J. Gen. Chem. USSR*, 1989, **59**, 1912.

[56] A. N. Chernega, G. N. Koidan, A. P. Marchenko, A. A. Korkin, *Heteroatom Chem.*, 1993, **4**, 365.

[57] J. Grobe, D. Le Van, B. Lüth, M. Hegemann, Chem. Ber., 1990, **123**, 2317.

[58] G. Becker, M. Böhringer, R. Gleiter, K. –H. Pfeifer, J. Grobe, D. Le Van, M. Hegemann, *Chem. Ber.*, 1994, **127**, 1041.

[59] G. Becker, H. Brombach, S. T. Horner, E. Niecke, W. Schwarz, R. Sreubel, E. –U. Würthwein, *Inorg. Chem.*, 2005, **44**, 3080.

[60] A. L. Allred, E. G. Rochow, *J. Inorg. Nucl. Chem.*, 1958, **5**, 264.

[61] R. Hoffmann, *Angew. Chem.*, 1982, **94**, 725; *Angew. Chem., Int. Ed. Engl.*, 1982, **21**, 711.

[62] M. Hofmann, P. Schleyer, M. Regitz, *Eur. J. Org. Chem.*, 1999, 3291.

[63] T. Wettling, B. Geißler, R. Schneider, S. Barth, P. Binger, M. Regitz, *Angew. Chem.*, 1992 **104**, 761; *Angew. Chem. Int. Ed. Engl.*, 1992, **31**, 758.

[64] B. Geißler, S. Barth, U. Bergsträßer, M. Slany, J. Durkin, P.B. Hitchcock, M. Hofmann, P. Binger, J. F. Nixon, P. v. R. Schleyer, M. Regitz, *Angew. Chem.*, 1995, **107**, 485; *Angew. Chem. Int. Ed. Engl.*, 1995, **34**, 484.

[65] T. Wettling, J. Schneider, O. Wagner, C.G. Kreiter, M. Regitz. *Angew. Chem.*, 1989,**101**, 1035; *Angew. Chem. Int. Ed. Engl.*, 1989, **28**, 1013

[66] M. Regitz, T. Wettling, B. Breit, M. Birkel, B. Geißler, U. Bergsträßer, S. Barth, P. Binger, *Phosphorus Sulfur Silicon and Realted Elements*, 1993, **76**, 1.

[67] F. Tabellion, C. Peters, U. Fischbeck, M. Regitz, F. Preuss, *Chem. Eur. J.*, 2000, **6**, 4558.

[68] P. Binger, S. Leininger, J. Stannek, P. Gabor, R. Mynott, J. Bruckmann, C. Krüger, *Angew. Chem.*, 1995, **107**, 2411; *Angew. Chem. Int. Engl.*, 1995, **34**, 2227.

[69] M. M. Al-Ktaifani, W. Bauer, U. Bergsträßer, B. Breit, M. D. Francis, F. W. Heinemann, P. B. Hitchcock, A. Mack, J. F. Nixon, H. Pritzkow, M. Regitz, M. Zeller, U. Zenneck, *Chem, Eur. J.*, 2002, **8**, 2622.

[70] J. F. Nixon, *Chem. Soc. Rev.*, 1995, **24**, 319.

[71] J. F. Nixon, *Chem. Rev.*, 1988, **88**, 1327.

[72] D. A. Wann, S. L. Hinchley, K. B. Borisenko, H. E. Robertson, M. D. Francis, J. F. Nixon, D. W. H. Rankin, *Dalton Trans.*, 2005, 1972.

[73] K. W. Merz, *PhD. Thesis*, Universität Stuttgart, 1995.

[74] A. Mack, B. Breit, T. Wettling, U. Bergsträßer, S. Leininger, M. Regitz, *Angew. Chem.*, 1997, **109**, 1396; *Angew. Chem. Int. Ed. Engl.*, 1997, **36**, 1337.

[75] M. Regitz, A. Hoffmann, U. Bergsträßer, *Modern Acetylene Chemistry*, P. J. Stang, F. Diederich, (Hrsgg.); VCH, Weinheim. 1995, Page. 173.

[76] D. Hu, H. Schäufele, H. Pritzkow, U. Zenneck, *Angew. Chem.*, 1989, **101**, 929; *Angew. Chem. Int. Ed. Engl.*, 1989, **28**, 900.

[77] U. Zenneck, *Angew.Chem.*, 1990, **102**, 171; *Angew. Chem. Int. Ed. Engl.*, 1990, **29**, 126.

[78] R. Bartsch, P. B. Hitchcock, J.F. Nixon, *J. Organomet. Chem.*, 1989, **375**, C31.

[79] V. Caliman, P. B. Hitchcock, J. F. Nixon, M. Hofmann, P. V. R. Schleyer, *Angew. Chem.*, 1994. 106, 2284; *Angew. Chem. Int. Ed. Engl.*, 1994, **33**, 2202.

[80] G. Becker, W. Becker, R. Knebl, H. Schmidt, U. Weeber, M. Westerhausen, *Nova Acta Leopoldina Neue Folge Nr. 264.*, 1985, **59**, 55.

[81] G. Becker, W. Becker, R. Knebl, H. Schmidt, A. Hildenbrand and M. Westerhausen. *Phosphorus Sulfur.*, 1987, **30**, 349.

[82] G. Becker, J. Dautel, R. Knebl, R. Löw, R. Ruf, J. Schüler, in W. Siebert (ed.), *Advances in Boron Chemistry (Proceedings of the Ninth International Meeting on Boron Chemistry),* Special Publication No. 201, The Royal Society of Chemistry, Cambridge. 1997, page. 248.

[83] K. S. Fongers, H. Hogeveen, R. F. Kingma, *Tetahedron lett.*, 1983, **24**, 643.

[84] R. Breslow, L. A. Deuring., *Tetrahedron Lett.*, 1984, **25**, 1345.

[85] S. Lochschmidt, F. Mathey, A. Schmidpeter, *Tetrahedron Lett.*, 1986, **27**, 2635.

[86] J. M. Vural, S. A. Weissman, S. G. Baxter, A. H. Cowley, C. M. Nunn., *J. Chem. Soc., Chem. Commun.*, 1988, 462.

[87] R. Knebl , *PhD. Thesis,* Universität Stuttgart, 1988.

[88] a) J. Dautel, *Ph.d. Thesis,* Universität Stuttgart, 1992.

b) J. Otto, *Ph.d. Thesis*, Universität Stuttgart, 1996.

[89] M. E. Fessler, J. T. Spencer, J. F. Lomax, R. N. Grimes, *Inorg. Chem.*, 1988, **27**, 3069.

[90] N. S. Hosmane, R. N. Grimes, *Inorg. Chem.*, 1979, **18**, 3294.

[91] R. E. Williams, *Inorg. Chem.*, 1971, **10**, 210.

[92] T. L. Heying, J. W. Ager Jr., S. L. Clark, D. J. Mangold, H. L. Goldstein, M. Hillman, R. J. Polak, J. W. Szymanski, *Inorg. Chem.*, 1963, **2**, 1089.

[93] F. Meyer, P. Paetzold, U. Englert, *Chem. Ber.*, 1994, **127**, 93.

[94] R. W. Miller, J. T. Spencer, *Organometallics*, 1996, **15**, 4293.

[95] P. N. Condick, M. A. Fox, R. Greatrex, C. Jones, D. L. Ormsby., *Chem. Commun.*, 2002, 1448.

[96] A. S. Ionkin, SN Ignat'eva, B. A. Arbuzov, *Izv. Akad. Nauk SSSR, Ser. Khim.*, 1990, 1452.

[97] R. Köster in: *Methoden der Organischen Chemie (Houben – Weyl), Organobor-Verbindungen I*, Georg Thieme Verlag Stuttgart New York, 1982, Page. 467.

[98] J. B. Koster, G. J. Timmermans, H. van Bekkum, *Synthesis*, 1971, 139.

[99] H. Hogeveen, R. F. Kingma, D. M. Kok, *J. Org. Chem.*, 1982, **47**, 989.

[100] R. Ruf, *Ph.d. Thesis,* Universität Stuttgart, 2000.

[101] B. Breit, U. Bergsträßer, G. Maas, M. Regitz, *Angew. Chem.*, 1992, **104**, 1043; *Angew. Chem. Int. Ed. Engl.*, 1992, **31**, 1055.

[102] B. Breit, M. Regitz, *Chem. Ber.*, 1996, **129**, 489.

[103] K. K. Laali, B. Geissler, M. Regitz, J. J. Houser, *J. Org. Chem.*, 1995, **60**, 6362.

[104] B. Breit, A. Hoffmann, U. Bergstäßer, L. Ricard, F. Mathey, M. Regitz, *Angew. Chem.*, 1994, **106**, 1541; *Angew. Chem., Int. Ed. Engl.*, 1994, **33**, 1491.

[105] A. Hoffmann, B. Breit, M. Regitz, *Chem. Ber./Recueil.*, 1997, **130**, 255.

[106] A. Hoffmann, A. Mack, R. Goddard, P. Binger, M. Regitz, *Eur. J. Inorg. Chem.*, 1998, **11**, 1597.

[107] J. F. Nixon, *Coordination Chemistry Reviews.*, 1995, **145**, 201.

[108] J. Renner, U. Bergsträßer, P. Binger, M. Regitz, *Eur. J. Inorg. Chem.*, 2000, 2337.

[109] D. E. Hibbs, C. Jones, A. F. Richards, *J. Chem. Soc., Dalton Trans.*, 1999, 3531.

[110] A. M. Arif, A. R. Barron, A. H. Cowley, S. W. Hall, *J. Chem. Soc., Chem. Commun.*, 1988, 171; S. Ito, H. Sugiyama, M. Yoshifuji, *Chem. Commun.*, 2002, 1744.

[111] J. E. Dean (ed.), *Lange's Handbook of Chemistry.*, 15th ed., McGraw-Hill, INC., New York. 1999, Bond dissociation energies, section 4, page 4.41,Table 4.11.

[112] R. Löw, *Ph.d. Thesis,* Universität Stuttgart, 2000.

[113] a) D. Sundholm, J. Olsen, *Phys. Rev. Lett.*, 1992, **68**, 927.
b) R. Benn, E. Jansen, H. Lehmkuhl, A. Rufinska, *J. Organomet. Chem.*, 1987, **333**, 155.

[114] A. Kuczkowski, S. Schulz, M. Nieger, P. R. Schreiner, *Organometallics*, 2002, **21**, 1408.

[115] J. P. van Linthoudt, E. V. van den Berghe, G. P. van der Kelen, *Spectrochim. Acta, Part A*, 1980, **36**, 315.

[116] J. P. van Linthoudt, E. V. van den Berghe, G. P. van der Kelen, *spectrochim. Acta, Part A.*, 1979, **35**, 1307.

[117] Theo. Hahn, (editor.) *International Tables for Crystallography*, volume A, Space-Group symmetry, 1st ed., published for the International Union of Crystallography by D. Reidel Publishing Company, Boston, 1983.

[118] G. M. Sheldrick, *Acta Crystallogr., Sect. A.*, 1990, **46**, 467.

[119] G. M. Sheldrick, *shelx 97, Program for Crystal Structure Refinement*, University of Göttingen, Germany., 1997.

[120] *Software packages SHELXTL, Version 5.10.* Bruker AXS Inc., Madison, Wisconsin, USA. 1997.

[121] J. A. Ibers, W.C. Hamilton (editor.), *International Tables for X-Ray Crystallography*, **Vol.4**, published for the International Union of Crystallography, Kynoch Press, Birmingham (UK). 1974, page. 47.

[122] A. I. Kitaigorodskii, *Organic Chemical Crystallography*; Consultant's Bureau, 1st ed., New York, 1961, chapter 1, page 1, chapter 3, page 65. (English Translation of the Russian Original Published by Press of the Academy of Sciences of the USSR, Moscow, 1955).

[123] A. J. Downs (editor), A. J. Downs in: *Chemistry of Aluminium, Gallium, Indium and Thallium*, Chapman & Hall: London, 1993, page 1.

[124] L. Pauling, The Nature of the Chemical Bond, 3rd edn., Cornell University Press, Ithaca, NY, 1960.; L. Pauling, *Die Nature der chemischen Bindung*; 2nd repr. Of the 3rd ed., Verlag Chemie, Weinheim., Kapitel 7, page 214, 1976.

[125] R. S. Cahn, C. Sir Ingold, V. Prelog, *Angew. Chem.*, 1966, **78**, 413; *Angew. Chem. Int. Ed. Engl.*, 1966, **5**, 385.

[126] H. J. Geise, C. Altona, C. Rombers, *Tetrahedron*, 1967, **23**, 439.

[127] H. Schmidbaur, S. Lauteschläger, G. Müller, *J. Organomet. Chem.*, 1985, **281**,33.

[128] R. D. Rogers, W. J. Cook, J. L. Atwood, *Inorg. Chem.*, 1979, **18**, 279.

[129] M. R. Churchill, H. J. Wasserman, *Inorg. Chem.*, 1981, **20**, 4119.

[130] G. Allegra, G. Peredo, I. Immirzi, *Makromol. Chem*., 1963, **61**, 69.

[131] W. Uhl, A. Vester, W. Hiller, *Z. Anorg. Allg. Chem.*, 1990, **589**, 175.

[132] A. Haaland: *In Coordination Chemistry of Aluminium*, edited by G. H. Robinson, VCH: New York, 1993, Chapter 1, Page 1.

[133] R. Blom, A. Haaland, *J. Mol. Struct*., 1985, **128**, 21

[134] V. Schomaker, D. P. Stevenson, *J. Am. Chem. Soc*., 1941, **63**, 37.

[135] Q. Shen, *Disseration*, 1973, Oregen State University, Corvallis, Oregon, cited in: A. F. Wells., *Structural Inorganic Chemistry*, fifth edition; Oxford: Clarendon press. 1984(Reprinted with corrections 1986), page. 444.

[136] R. J. Wehmschulte, P. P. Power, *Inorg. Chem.*, 1996, **35**, 3262.

[137] A. Haaland, *J. Mol. Struct.*, 1983, **97**, 115.

[138] J. C. Huffman, W. E. Streib, *J. Chem. Soc. D*: *Chem. Commun.*, 1971, 911.

[139] A. Almenningen, L. Fernholt, A. Haaland, J. Weidlein, *J. Organomet. Chem.*, 1978, **145**, 109.

[140] L. E. Sutton (ed.) in *Table of interatomic distances and configuration in molecules and ions*, Supplement 1956-1959, Special publication No. 18, Chemical Society, London, UK. 1965.

[141] R. J. Wehmschulte, K. Ruhlandt-Senge, P. P. Power, *Inorg. Chem.*, 1994, **33**, 3205.

[142] C. C. Wang, M. Zaheeruddin, L. H. Spinar, *J. Inorg. Nucl. Chem.,* 1963, **25**, 326.

[143] R. L. Wells, A. T. McPhall, J. A. Laske, P. S. White, *Polyhedron*, 1994, **13**, 2737.

[144] M. D. Fryzuk, G. R. Giesbrecht, G. Olvsson, S. J. Rettig, *Organometallics*, 1996, **15**, 4832.

[145] D. A. Atwood, L. Contreras, A. H. Cowley, R. A. Jones, M. A. Mardones, *Organometallics.*, 1993, **12**, 17.

[146] A. H. Cowley, R. A. Jones, M. A. Mardones, J. L. Atwood, S. G. Bott, *Angw. Chem.*, 1990, **102**, 1504; *Angew. Chem., Int. Ed. Engl.*, 1990, **29**, 1409.

[147] M. A. Petrie, P. P. Power, *J. Chem. Soc. Dalton Trans.*, 1993, 1737.

[148] H. H. Karsch, A. Appelt, F. H. Köhler, G. Müller, *Organometallics*, 1985, **4**, 231.

[149] A. Haaland, J. Hougen, H. V. Volden, G. Hanika, H. H. Karsch, *J. Organomet. Chem.*, 1987, **322**, C24.

[150] a) R. L. Wells, A. T. McPhail, M. F. Self, J. A. Laske, *Organometallics*, 1993, **12**, 3333.

b) E. Hey-Hawkins, M. F. Lappert, J. L. Atwood, S. G. Bott, *J. Chem. Soc. Dalton. Trans.*, 1991, 939.

[151] R. L. Wells, E. E. Foos, A. L. Rheingold, G. P. A. Yap, L. M. Liable-Sands, P. S. White, *Organometallics*, 1998, **17**, 2869.

[152] J. F. Janik, E. N. Duesler, W. F. McNamara, M. Westerhausen, R. T. Paine, *Organometallics*, 1989, **8**, 506.

[153] E. Niecke, M. Leuer, M. Nieger, *Chem. Ber.*, 1989, **122**, 453.

[154] J. A. Laske. Cooke; H. Rahbarnooli, A. T. McPhail, R. L. Wells, *Polyhedron*, 1996, **15**, 3033.

[155] F. R. Bennett, F. M. Elms, M. G. Gardiner, G. A. Koutsantonis, C. L. Raston, N. K. Roberts, *Organometallics*, 1992, **11**, 1457.

[156] F. M. Elms, M. G. Gardiner, G. A. Koutsantoris, C. L. Raston, J. L. Atwood, K. D. Robinson, *J. Organomet. Chem.*, 1993, **449**, 45.

[157] S. A. Sangokoya, W. T. Pennington, G. H. Robinson, *J. Organomet. Chem.*, 1990, **385**, 23.

[158] S. A. Sangokoya, B. Lee, M. F. Self, W. T. Pennington, G. H. Robinson, *Polyhedron,* 1989, **8**, 1497.

[159] M. D. Haaly, D. A. Wierda, A. R. Barron., *Organometallics*, 1988, **7**, 2543.

[160] D. C. Bradley, H. Chudzynska, M. M. Faktor, D. M. Frigo, M. B. Hursthouse, B. Hussain, L. M. Smith., *Polyhedron*, 1988, **7**, 1289.

[161] D. A. Wierda, A. R. Barron., *Polyhedron*, 1989, **8**, 831.

[162] G. H. Robinson, M. F. Self, S. A. Sangokoya, W. T. Pennington., *J. Cryst. Spectr. Res.*, 1988, **18**, 285.

[163] C. N. McMahon, A. R. Baron, *J. Chem. Cryst.*, 1997, **27**, 195.

[164] Radii of 130 pm and 110 pm were used for aluminium and phosphorus: J. E. Huheey, E. A. Keiter, R. L. Keiter, *Inorganic Chemistry: Principles of Structure and Reactivity*, Fourth Edition, HaperCollins College Publishers, chapter 8, page 290, 1993. The Al–P bond length may be estimated by using the empirical formula of Modified *Schomaker-Stevenson* rule by *Blom* and *Haaland*, which gives a value of 236.0 pm. For further discussion see references [132-134].

[165] *The Cambridge Structural Database (CSD)*, associated software systems (including ConQuest 1.9 *Ver.* 5.28) and documentation are proprietary products in which the rights are held by the Cambridge Crystallographic Data Centre (CCDC) located at 12 Union Road, Cambridge 2007, CB2 1EZ UK.

[166] D. G. Gilheany in: *The Chemistry of Organophosphorus Compounds*, **Volume 2**, edited by F. R. Hartley, John Wiley & Sons, New York, 1992, Chapter 1, Page 1.

[167] D. G. Gilheany in: *The Chemistry of Organophosphorus Compounds*, **Volume 1**, edited by F. R. Hartley, John Wiley & Sons, New York, 1990, Chapter 2, Page 9.

[168] D. G. Gilheany in: *The Chemistry of Organophosphorus Compounds*, **Volume 3**, edited by F. R. Hartley, John Wiley & Sons, New York, 1994, Chapter 1, Page 1.

[169] J. J. Daly, *J. Chem. Soc. (Resumed)*, 1964, 3799.

[170] G. Bandoli, G. Bortolozzo, D. A. Clemente, U. Croatto, C. Panattoni; *J. Chem. Soc. (A)*, 1970, 2778

[171] R. Ochs, *Ph.d. Thesis*, Universität Stuttgart, 2004.

[172] R. Binder, *Wissenschftliche Arbeit Zur Staatsprüfung Für das Lehramt an Gymnasien*, Universität Stuttgart, 2005.

[173] a) L. S. Bartell, L. O. Brockway, *J. Chem. Phys*., 1960, **32**, 512.

b) B. Beagley, A. R. Medwid, *J. Mol. Struct*., 1977, **38**, 229.

[174] H. Schmidbauer, W. Tronich, *Chem. Ber*., 1968, **101**, 595.

[175] R. Allmann In: *Homoatomic Rings, Chains and Macromolecules of Main-Group Elements*, edited by A. L. Rheingold, Elsvier Scientific Publishing Company, Amsterdam, 1977, Chapter 2, Page 33.

[176] P. Binger, B. Biedenbach, S. Leininger, M. Regitz in: *Synthetic Methods of Organometallic and Inorganic Chemistry* (Hrsg.: W.A. Herrmann), **Vol. 3**: Phosphorus, Arsenic, Antimony, and Bismuth, edited by H. H. Karsch, Georg Thieme Verlag, Stuttgart. 1996, page. 175.

[177] B. Geißler, T.Wettling, S. Barth, P. Binger, M. Regitz, *Synthesis*, 1994, 1337.

[178] M. Regitz, U. Bergsträßer, *Polish J. Chem*., 1999, **73**, 135.

[179] P. Binger, B. Biedenbach, C. Krüger, M. Regitz, *Angew. Chem*., 1987, **99**, 798; *Angew. Chem. Int. Ed. Engl*., 1987, **26**, 764.

[180] P. Binger, T. Wettling, R. Schneider, F. Zurmühlen, U. Bergsträßer, J. Hoffmann, G. Maas, M. Regitz, *Angew. Chem*., 1991, 103, 208; *Angew. Chem., Int. Ed.*, 1991, **30**, 207.

[181] J. M. Lynam, M. C. Copsey, M. Green, J. C. Jeffery, J. E. McGrady, C. A. Russell, J. M. Slattery, A. C. Swain, *Angew. Chem.,* 2003, **115**, 2884; *Angew. Chem. Int. Ed. Engl*., 2003, **42**, 2778.

[182] a) *"Novel Structure, Bonding and Reactivity for Pnictogens in Low Coordinate Environments – is Phosphorus a Carbon Copy ?"*, a Lecture give at the University of Stuttgart in 16.01.2006 by C. Russell.; b) C. Fish, M. Green, J. C. Jeffery, R. J. Kilby, J. M. Lynam, J. E.

McGrady, D. A. Pantazis, C. A. Christopher, C. E. Willans, *Angew. Chem.*, 2006, **118**, 6837; *Angew. Chem. Int. Ed. Engl.*, 2006, **45**, 6685; c) C. Fish, M. Green, J. C. Jeffery, R. J. Kilby, J. M. Lynam, J. E. McGrady, D. A. Pantazis, C. A. Russell, C. E. Willans, *Chem. Commun.*, 2006, 1375.

[183] C. Fish, M. Green, J. C. Jeffery, R. J. Kilby, J. M. Lynam, C. A. Russel, C. E. Willans, *Organometallics*, 2005, **24**, 5789.

[184] R. Bartsch, J. F. Nixon, *Polyhedron*, 1989, **8**, 2407.

[185] G. P. Schiemenz, S. Pörksen, P. M. Dominiak, K. Wozniak, *Z. Naturforsch.*, 2002, **57b**, 8.

[186] R. R. Randle, D. H. Whiffen, *Molecular Spectroscopy*, Institute of Petroleum, London, 1955, pp. 111-123 cited in D. H. Whiffen, *J. Chem, Soc. (Resumed)*, 1956, 1350 or in G. B. Deacon, R. A. Jones, P. E. Rogasch, *Aust. J. Chem.*, 1963, **16**, 360.

[187] N. Walker, D. Stuart; *Acta. Cryst.*, 1983, **A 39**, 158.

[188] O. Mundt, H. Riffel, G. Becker, A. Simon; *Z. Natur-forsch.*, 1988, **43B**, 952.

[189] A. R. Barron, A. H. Cowley, S. W. Hall, C. M. Nunn; *Angew. Chem.*, 1988, **100**, 873; *Angew. Chem., Int. Ed. Engl.*, 1988, **27**, 837.

[190] a) M. D. Francis, P. B. Hitchcock; *Organometallics*, 2003, **22**, 2891; b) C. Fish, M. Green, R. J. Kilby, J. M. Lynam, J. E. McGrady, D. A. Pantazis, C. A. Russell, A. C. Whitwood, C. E. Willans, *Angew. Chem.*, 2006, **118**, 3710; *Angew. Chem. Int. Ed*, 2006, **45**, 3628

[191] R. Appel, B. Niemann, M. Nieger, *Angew. Chem.* 1988, 100, 957.; *Angew. Chem. Int. Ed*, 1988, **27**, 957.

[192] E. Niecke, O. Altmeyer, M. Nieger, *J. Chem. Soc., Chem. Commun.*, 1988, 945.

[193] W. G. Haije, J. A. L. Dobbelaar, W. J. A. Maaskant; *Acta. Cryst. C.*, 1986, **42**, 1485.

[194] M. Z. Bani-Fwaz, G. Becker, M. Niemeyer, private communication, 2007, calculated structures by using **Gaussian 03**, Revision A.1, M. J. Frisch, G. W. Trucks, H. B. Schlegel, G. E. Scuseria, M. A. Robb, J. R. Cheeseman, J. A. Montgomery, Jr., T. Vreven, K. N. Kudin, J. C. Burant, J. M. Millam, S. S. Iyengar, J. Tomasi, V. Barone, B. Mennucci, M. Cossi, G. Scalmani, N. Rega, G. A. Petersson, H. Nakatsuji, M. Hada, M. Ehara, K. Toyota, R. Fukuda,

J. Hasegawa, M. Ishida, T. Nakajima, Y. Honda, O. Kitao, H. Nakai, M. Klene, X. Li, J. E. Knox, H. P. Hratchian, J. B. Cross, C. Adamo, J. Jaramillo, R. Gomperts, R. E. Stratmann, O. Yazyev, A. J. Austin, R. Cammi, C. Pomelli, J. W. Ochterski, P. Y. Ayala, K. Morokuma, G. A. Voth, P. Salvador, J. J. Dannenberg, V. G. Zakrzewski, S. Dapprich, A. D. Daniels, M. C. Strain, O. Farkas, D. K. Malick, A. D. Rabuck, K. Raghavachari, J. B. Foresman, J. V. Ortiz, Q. Cui, A. G. Baboul, S. Clifford, J. Cioslowski, B. B. Stefanov, G. Liu, A. Liashenko, P. Piskorz, I. Komaromi, R. L. Martin, D. J. Fox, T. Keith, M. A. Al-Laham, C. Y. Peng, A. Nanayakkara, M. Challacombe, P. M. W. Gill, B. Johnson, W. Chen, M. W. Wong, C. Gonzalez, and J. A. Pople, Gaussian, Inc., Pittsburgh PA, 2003.

[195] K. Wade, *J. Chem. Soc. Chem. Commun.*, 1971, 792.; G. Olah, K. Wade, R. E. Williams, *Electron Deficient Boron and Carbon Clusters*, Wiley Interscience Publication, 1991, Chapter 1, Page. 5.

[196] G. Anderson, J. C. Green, M. D. Francis, *Organometallics*, 2003, **22**, 2897.

[197] Pauling electronegativities were taken from reference [124], Kapital 3, page 61.

[198] P. Binger, S. leininger, M. Regitz, U. Bergsträßer, J. Bruckmann, C. Krüger, *J. Organomet. Chem.*, 1997, **529**, 215.

[199] R. Gleiter, H. Lange, P. Binger, J. Stannek, C. Krüger, J. Bruckmann, U. Zenneck, S. Kummer, *Eur. J. Inorg. Chem.*, 1998, 1619.

[200] F. Tabellion, C. Peters, U. Fischbeck, M. Regitz, F. Preuss, *Chem. Eur. J.*, 2000, **6**, 4558

[201] F. Tabellion, A. Nachbauer, S. Leininger, C. Peters, M. Regitz, F. Preuss, *Angew. Chem.*, 1998, **110**, 1318; *Angew. Chem. Int. Ed.*, 1998, **37**, 1233.

[202] A. Mack, F. Tabellion, C. Peters, A. Nachbauer, U. Bergsträsser, F. Preuss, M. Regitz, *Phosohorus, Sulfur and Silicon*, 1999, **144**, 261.

[203] R. Milczarek, W. Rüssler, P. Binger, K. Jonas, K. Angermund, C. Krüger, M. Regitz, *Angew. Chem.* 1987, **99**, 957; *Angew. Chem. Int. Ed. Engl.*, 1987, **26**, 908.

[204] E. E. Van Tamelen, S. P. Pappas, *J. Am. Chem. Soc.*, 1962, **84**, 3789.

[205] I. Gutman and J. H. Potgieter, *J. Chem. Educ.*, 1994, **71**, 222.

[206] A. Mack, S. Danner, U. Bergsträßer, H. Heydt, M. Regitz, *J. Organomet. Chem.*, 2002, **643**, 409.

[207] C. H. Youder, C. D. Jr., Schaeffer, *Introduction to Multinuclear NMR: Theory and application*, Benjaamin-Cummings. Pub. Co. Inc., 1987, pages 138 and 173.

[208] H. Günther, *NMR-Spektroskopie*, 2nd ed., Thieme Verlag, Stuttgart. 1983, Page.155.

[209] E. D. Becker, *High Resolution NMR*, 2nd ed., Academic Press, New York. 1980, page 150.

[210] a) H. Beckmann, G. Grossmann, G. Ohms, *Magn. Reson. Chem.*, 1992, **30**, 860.

b) R. Radeglia, *J. F. Prakt. Chemie.*, 1989, **331**, 863.

[211] N. W. Mitzel, D. H. Brown, S. Parsons, P. T. Brain, C. R. Pulham, D. W. H. Rankin, *Angew. Chem.*, 1998, **110**, 1767; *Angew. Chem. Int. Ed.*, 1998, **37**, 1670.

[212] N. W. Mitzel, B. A. Smart, Karl-Heinz. Dreihäupl, D. W. H. Rankin, H. Schmidbaur, *J. Am. Chem. Soc.*, 1996, **118**, 12673.

[213] H. Schmidbaur, J. Jeong, A. Schier, W. Graf, D.L. Wilkinson, G. Müller, *New J. Chem.*, 1989, **13**, 341.

[214] H. Schmidbaur, A. Schier, B. Milewski-Mahrla, U. Schubert, *Chem. Ber.*, 1982, **115**, 722.

[215] H. Schmidbaur, A. Schier, D. Neugebauer, *Chem. Ber.*, 1983, **116**, 2173.

[216] H. Schmidbaur, A. Schier, C. M. F. Frazȁo, G. Müller, *J. Am. Chem. Soc.*, 1986, **108**, 976.

[217] N. W. Mitzel, A. Schier, H. Beruda, H. Schmidbaur, *Chem. Ber.*, 1992, **125**, 1053.

[218] H. Schmidbaur, B. Milewski-Mahrla, G. Müller, C. Krüger, *Organometallics.*, 1984, **3**, 38.

[219] H. Schmidbaur, W. Graf, G. Müller, *Angew. Chem.*; 1988, **100**, 439; *Angew. Chem., Int. Ed.*, 1988, **27**, 417.

[220] H. Schmidbaur, U. Deschler, B. Milewski-Mahrla, *Chem. Ber.*, 1983, **116**, 1393.

[221] H. Schmidbaur, P. Nusstein, G. Muller, *Z. Naturforsch., B: Chem. Sci.*, 1984, **39**, 1456.

[222] T. Berclaz, G. Bernardinelli, M. Geoffroy, G. Rao, Z. Tancic, *Radiat. Phys. Chem.*, 1999, **56**, 539.

[223] P. D. Boyle, *Acta Crystallogr., Sect. C: Cryst. Struct. Commun.*, 1996, **52**, 2859.

[224] V. S. Brovarets, A. V. Golovchenko, V. N. Sviripa, K. V. Zyuz`, A. V. Chernega, B. S. Drach, *Russ. J. Gen. Chem.*, 2004, **74**, 1434.

[225] E. C. Spencer, B. Kalyanasundari, M. B. Mariyatra, J. A. K. Howard, K. Panchanatheswaran, *Inorg. Chim. Acta.*, 2006, **359**, 35.

[226] S. Husebye, E. A. Meyers, R. A. Zingaro, A. L. Braga, J. V. Comasseto, N. Petragnani, *Acta Crystallogr., Sect. C: Cryst. Struct. Commun.*, 1986, **42**, 90.

[227] F. S. Stephens, *J. Chem. Soc. (Resumed)*, 1965, 5658.

[228] F. Castaneda, C. Aliaga, C. A. Bunton, M. T. Garland, R. Baggio, *Acta Crystallogr., Sect. C: Cryst. Struct. Commun.*, 2005, **61**, o496.

[229] F. Castaneda, C. A. Terraza, M. T. Garland, C. A. Bunton, R. F. Baggio, *Acta Crystallogr., Sect. C. Struct. Commun.*, 2001, **57**, 180.

[230] R. Richter, H. Hartung, S. Deresch, J. Kaiser, *Z. Anorg. Allg. Chem.*, 1980, **469**, 179.

[231] P. J. Wheatley, *J. Chem. Soc.*, 1965, 5785.

[232] R. A. Aitken, M. J. Drysdale, G. Ferguson, A. J. Lough, *J. Chem. Soc., Perkin Trans. 1*, 1998, 875.

[233] H. Schmidbaur, C. Zybill, C. Kruger, H.-J. Kraus, *Chem. Ber.*, 1983, **116**, 1955.

[234] H. J. R. de Boer, O. S. Akkermann, F. Bickelhaupt, G. Erker, P. Czisch, R. Mynott, J. M. Wallis, C. Krüger, *Angew. Chem.*, 1986, **98**, 641; *Angew. Chem., Int. Ed.*, 1986, **25**, 639.

[235] G. Erker, P. Czisch, R. Mynott, Yi-Hung Tsay, C. Kruger, *Organometallics*, 1985, **4**, 1310.

[236] G. Erker, P. Czisch, C. Kruger, J. M. Wallis, *Organometallics*, 1985, **4**, 2059.

[237] A. Schmidpeter, H. Noth, G. Jochem, H.-P. Schrodel, K. Karaghiosoff, *Chem. Ber.*, 1995, **128**, 379.

[238] G. Jochem, *Ph.d Disseration*, Durch Ylidsubstituenten Stabilisierte Verbindungen des niederkoordinierten Phosphors, Fakultät für Chemie und Pharamazie der Ludwig-Maximilians-Universität München, 1994, UB Stuttgart Diss. 1994/4989.

[239] H-P. Schrödel, *Ph.d Disseration*, Phosphoniosubstituierte PC-Ringe und –Käfige aus der Kondensation von Dihalogenphosphino(trimethylsilyl)methylenphosphoranen, Fakultät für Chemie und Pharamazie der Ludwig-Maximilians-Universität München, 1997, UB Stuttgart Diss. 1997/3282.

[240] G. Jochem, F. Breitsameter, A. Schier, A. Schmidpeter, *Heteroat. Chem.*, 1996, **7**, 239.

[241] F. Breitsameter, A. Schmidpeter, H. Noth, *Chem.-Eur. J.*, 2000, **6**, 3531.

[242] M. A. Howells, R. D. Howells, N. C. Baenziger, D. J. Burton, *J. Am. Chem. Soc.*, 1973, **95**, 5366.

[243] G. E. Hardy, W. C. Kaska, B. P. Chandra, J. I. Zink, *J. Am. Chem. Soc.*, 1981, **103**, 1074.

[244] G. Fritz, W. Schick, W. Hönle, H. G. V. Schnering, *Z. Anorg. Allg. Chem.*, 1984, **511**, 95.

[245] H. Grützmacher, H. Pritzkow, *Angew. Chem.* 1992, 104, 92; *Angew. Chem. Int. Ed.*, 1992, **31**, 99.

[246] a) U. Heim, H. Pritzkow, U. Fleischer, H. Grützmacher, *Angew. Chem.*, 1993, **105**, 1400; *Angew. Chem. Int. Ed.*, 1993, **32**, 1359.

b) U. Heim, H. Pritzkow, U. Fleischer, H. Grützmacher, M. Sanchez, R. Re`au, G. Betrand, *Chem. Eur. J.*, 1996, **2**, 68

[247] D. G. Gilheany, *Chem. Rev.*, 1994, **94**, 1339 and references cited therein.

[248]a) A. G. Orpen, L. Brammer, F. H. Allen, O. Kennard, D. G. Watson, R. Taylor, *J. Chem. Soc. Dalton Trans.*, 1989, S1; b) F. H. Allen, O. Kennard, D. G. Watson, L. Brammer, A. G. Orpen, R. Taylor, *J. Chem. Soc., Perkin Trans. II.*, 1987, S1.

[249] A. Tarassoli, R. C. Haltiwanger, A. D. Norman, *Inorg. Chem.*, 1982, **21**, 2684.

[250] L. V. Vilkov, L. C. Kaikin, V. V. Evdokimov, *Zh. Struct. Khim.*, 1972, **13**, 9.

[251] M. F. Lappert, J. B. Pedley, B. T. Wilkins, O. Stelzer, E. Unger, *J. Chem. Soc., Dalton Trans.*, 1975, 1207.

[252] A. H. Cowley, M. J. S. Dewar, D. W. Goodman, J. R. Schweiger, *J. Am. Chem. Soc.*, 1973, **95**, 6506.

[253] M. Z. Bani-Fwaz, G. Becker, R. Ruf, private communication, 2007, calculated structures by using **Gaussian 98** (Revision A.7), M. J. Frisch, G. W. Trucks, H. B. Schlegel, G. E. Scuseria, M. A. Robb, J. R. Cheeseman, V. G. Zakrzewski, J. A. Montgomery, R. E. Stratmann, J. C. Burant, S. Dapprich, J. M. Millam, A. D. Daniels, K. N. Kudin, M. C. Strain, O. Farkas, J. Tomasi, V. Barone, M. Cossi, R. Cammi, B. Mennucci, C. Pomelli, C. Adamo, S. Clifford, J. Ochterski, G. A. Petersson, P. Y. Ayala, Q. Cui, K. Morokuma, D. K. Malick, A. D. Rabuck, K. Raghavachari, J. B. Foresman, J. Cioslowski, J. V. Ortiz, B. B. Stefanov, G. Liu, A. Liashenko, P. Piskorz, I. Komaromi, R. Gomperts, R. L. Martin, D. J. Fox, T. Keith, M. A. Al-Laham, C. Y. Peng, A. Nanayakkara, C. Gonzalez, M. Challacombe, P. M. W. Gill, B. G. Johnson, W. Chen, M. W. Wong, J. L. Andres, M. Head-Gordon, E. S. Replogle and J. A. Pople, Gaussian, Inc., Pittsburgh PA, 1998.

[254] I. Shevchenko, V. Andrushko, E. Lork, G-V. Röschenthaler, *Eur. J. Inorg. Chem.*, 2002, 2985.

[255] D. Martin, H. Gornitzka, A. Baceiredo, G. Bertrand, *Eur. J. Inorg. Chem.*, 2005, 2619.

[256] K-H. Dreihäupl, K. Angermaier, J. Riede, H. Schmidbaur, *Chem. Ber.*, 1994, **127**, 1599.

[257] R. Schröck, K-H. Dreihäupl, A. Sladek, K. Angermair, H. Schmidbaur, *Chem. Ber.*, 1996, **129**, 495.

[258] S. G-Granda, R. S-Garci´a, K. Bieger, *Acta Cryst. Sec. C: Cryst. Struct. Commun.*, 1996, **C52**, 2857.

[259] J. Barluenga, M. Toma´s, K. Bieger, S. G-Granda, R. S-Garci´a, *J. Organomet. Chem.*, 1997, **529**, 233.

[260] E. D-Ayoub, S. Sole´, H. Gornitzka, A. B. Rozhenko, W. W. Schoeller, D. Bourissou, G. Bertrand, *J. Am. Chem. Soc.*, 2003, **125**, 124.

[261] R. Appel, U. Baumeister, F. Knoch, *Chem. Ber.*, 1983, **116**, 2275.

[262] Z. Wang, G. Zhang, I. Guzei, J. G. Verkade, *J. Org. Chem.*, 2001, **66**, 3521.

[263] T. Ka´rpa´ti, T. Veszpre´mi, N. Thirupathi, X. Liu, Z. Wang, A. Ellern, L. Nyula´szi, J. G. Verkade, *J. Am. Chem. Soc.*, 2006, **128**, 1500.

[264] J. W. Goerge *in Progress in Inorganic Chemistry*, Vol. II, (edited by: F. A. Cotton), Interscience Publishers Intc., New York. 1960, Page. 33.

[265]V. A. Naumov, O. A. Kataeva, *J. Structural. Chem.*, 1983, **24**, 312.

[266] G. Frenking, F. Marschner, H. Goetz, *Phosphorus and Sulfur.*, 1980, **8**, 337.

[267] S. Chitsaz, H. Folkerts, J. Grebe, T. Grob, K. Harms, W. Hiller, M. Krieger, W. Massa, J. Merle, M. Mohlen, B. Neumuller, K. Dehnicke, *Z. Anorg. Allg. Chem.*, 2000, **626**, 775.

[268] F. Weller, D. Nuszhar, K. Dehnicke, F. Gingl, J. Strahle, *Z. Anorg. Allg. Chem.*, 1991, **602**, 7.

[269] E. Pohl, H. J. Gosink, R. Herbst-Irmer, M. Noltemeyer, H. W. Roesky, G. M. Sheldrick, *Acta Crystallogr., Sect. C: Cryst. Struct. Commun.*, 1993, **49**, 1280.

[270] A. Dietrich, B. Neumuller, K. Dehnicke, *Z. Anorg. Allg. Chem.*, 2000, **626**, 1837.

[271] P. Molina, C. López-Leonardo, J. LIamas-Botia, C. Foces-Foces, C. Fernandez-Castaño, *J. Chem. Soc. Chem. Commun.*, 1995, 1387.

[272] C. Imrie, T. A. Modro, P. H. Van Rooyen, C. C. P. Wagener, K. Wallace, *J. Phys. org. Chem.*, 1995, **8**, 41.

[273] L. Chiche, H. Christol, *J. Chem. Soc. Perkin Trans. II*, 1984, 753.

[274] J. C. J. Bart, I. W. Bassi, M. Calcaterra, *Acta Crystallogr., Sec. B: Struct. Crystallogr. Cryst. Chem.*, 1982, **38**, 1932.

[275] H. Vogt, D. Wulff-Molder, F. Ritschl, M. Mucke, U. Skrabei, M Meisel, *Z. Anorg. Allg. Chem.*, 1999, **625**, 1025.

[276] J. Nolte, P. Neubauer, H. Vogt, M. Meisel, *Z. Naturforsch., B:Chem. Sci.*, 1999, **54**, 113.

[277] H. Vogt, V. Quaschnig, B. Ziemer, M. Meisel, *Z. Naturforsch., B:Chem. Sci.*, 1997, **52**, 1175.

[278] H. Thonnessen, T. Siedentop, P. G. Jones, R. Schmutzler, *Z. Anorg. Allg. Chem.*, 2001, **627**, 731.

[279] J. F. Bickley, M. C. Copsey, J. C. Jeffery, A. P. Leedham, C. A. Russell, D. Stalke, A. Steiner, T. Stey, S. Zacchini, *Dalton Trans.*, 2004, 989.

[280] R. Schwesinger, R. Link, P. Wenzl, S. Kossek, M. Keller, *Chem.-Eur. J.*, 2006, **12**, 429.

[281] H.-P. Schrödel, G. Jochem, A. Schmidpeter, H. Nöth, *Angew. Chem.* 1995, 107, 2006; *Angew. Chem., Int. Ed.*, 1995, **34**, 1853.

[282] G. Jochem, A. Schmidpeter, *Angew. Chem.* 1994, **106**, 708; *Angew. Chem., Int. Ed.*, 1994, **33**, 663.

[283] P. V. R. Schleyer, A. J. Kos, *Tetrahedron*, 1983, **39**, 1141

[284] a) A. J. Kirby, *Reactivity and Structure Concepts in Organic Chemistry*, **Vol. 15**: The Anomeric Effect and Related Stereoelectronic Effects at Oxygen, 1. Aufl., Springer-Verlag, Berlin., 1983, page.**71**.

b) A. J. Kirby, *Pure Appl. Chem.*, 1987, **59**, 1605.

[285] H. Hopf, C. Werner, *Nachr. Chemie, Technik, Labor.*, 1996, **44**, 17.

[286] R. C. Fuson, *Chem. Rev.*, 1935, **16**, 1.

[287] B. D. Chernokal′skii, A. S. Gel′fond, Gil′m Kamai, *J. Gen. Chem. USSR.*, 1967, **37**, 1324; *Zh. Obshch. Khim*, 1967, **37**, 1396.

[288] M. Wada, S. Natsume, S. Suzuki, A. Uo, M. Nakamura, S. Hayase, T. Erabi, *J. Organomet. Chem.*, 1997, **548**, 223.

[289] A. Michaelis, J. Rabinerson, *Justus Liebigs Ann. Chem.*, 1892, **270**, 139.

[290] K. A. Francesconi, D. Kuehnelt, *Analyst.*, 2004, **129**, 373.

[291] A. Watson, G. Svehla, *Analyst.,* 1975, **100**, 573.

[292] a) G. O. Doak, H. Eagle, H. G. Steinman, *J. Am. Chem. Soc.*, 1940, **62**, 3010

b) G. O. Doak, *J. Am. Chem. Soc.*, 1940, **62**, 167.

[293] C. F. Hamilton, J. F. Morgan, *Org. React.*, 1944, **2**, 415.

[294] G. Tomaschewski, *J. Prakt. Chem.*, 1966, **33**, 168.

[295] A. von Baeyer, *Justus Liebigs Ann. Chem.*, 1858, **107**, 257.

[296] W. S. Sheldrick, I. M. Müller, *Coord. Chem. Rev.*, 1999, **182**, 125.

[297] W. Steinkopf, S. Schmidt, *Chem. Ber.*, 1928, **61**, 675.

[298] F. F. Blicke, F. D. Smith, *J. Am. Chem. Soc.*, 1930, **52**, 2946.

[299] a) W. S. Sheldrick, T. Häusler, *Z. Naturforsch. Teil B.*, 1993, **48**, 1069.

b) M. Durand, J-P, Laurent, *J. Organomet. Chem.*, 1974, **77**, 225.

c) H. C. Marsmann, J. R. Van Wazer, *J. Am. Chem. Soc.*, 1970, **92**, 3969.

[300] A. M. Arif, A. H. Cowley, M. Pakulski, *J. Chem. Soc. Chem. Commun.*, 1987, 165.

[301] A.-J. DiMaio, A. L. Rheingold, *Organometallics.*, 1991, **10**, 3764.

[302] A. L. Rheingold, P. Choudhury, *J. Organomet. Chem.*, 1977, **128**, 155.

[303] I. M. Müller, J. Mühle, *Z. Anorg. Allg. Chem.*, 1999, **625**, 336.

[304] H. Sun, B. O. Patrick, W. R. Cullen, *Appl. Organomet. Chem.*, 2005, **19**, 129.

[305] G-Q. Chen, L. Zhou, M. Styblo, F. Walton, Y. Jing, R. Weinberg, Z. Chen, S. Waxman, *Cancer Res.*, 2003; **63**, 1853.

[306] W. R. Cullen, B. C. McBride, H. Manji, A. W. Pickett, J. Reglinski, *Appl. Organomet. Chem.*, 1989; **3**, 71.

[307] Z. Drobna, I. Jaspers, M. Styblo, In *Arsenic Exposure and Health Effects V, Proceedings of the International Conference on Arsenic Exposure and Health Effects*, W. R. Chappell, C. O. Abernathy, R. L. Calderon, D. J. Thomas, Eds. Elsevier, 2003; 267.

[308] M. Styblo, L. M. Del Razo, E. L. LeCluyse, G. A. Hamilton, C. Wang, W. R. Cullen, D. J. Thomas, *Chem. Res. Toxicol.,* 1999; **12**, 560.

[309] R. Gerhard, H. John, K. Aktories, I. Just, *Mol. Pharmacol.*, 2003; **63**, 1349.

[310] M. V. Linetska, L. G. Storchak, N. H. Himmelreich, *Neurochem. Int.*, 2003; **42**, 583.

[311] F. Challenger, *Chem. Rev.*, 1945, **36**, 315.

[312] J. Ellerman, L. Brehm, E. Lindner, W. Hiller, R. Fawzi, F. L. Dickert, M. Waidhas, *J. Chem. Soc. Dalton Trans*., 1986, 997.

[313] A. Tzschach, W. Lange, *Chem. Ber*., 1962, **95**, 1360.

[314] R. M. Bozorth, *J. Am. Chem. Soc*., 1923, **45**, 1621.

[315] L. R. Maxwell, S. B. Hendricks, L. S. Deming, *J. Chem. Phys*., 1937, **5**, 626.

[316] B. J. Mckerley, K. Reinhardt, J. L. Mills, G. M. Reisner, J. D. Korp, I. Bernal., *Inorg. Chim. Acta*., 1978, **31**, L411.

[317] J. Ellermann, H. Schössner, *Angew. Chem*., 1974, **86**, 646; *Angew. Chem. Int. Ed. Eng*., 1974, **13**, 601.

[318] G. Thiele, G. Zoubek, H. A. Lindner, J. Ellermann, *Angew. Chem*., 1978, 90, 133; *Angew. Chem. Int. Ed. Eng*., 1978, **17**, 135.

[319] J. Kopf, K. Von Denten, G. Klar, *Inorg. Chim. Acta*., 1980, **38**, 67.

[320] F. Popp, *Chem. Ber*., 1949, **82**, 152.

[321] A. I. Titiv, B. B. Levin, *Sbornik Statei Obshkei Khim*., 1953, **2**, 1469; C. A., 1955, **49**, 4503i.

[322] K. Sommer, *Z. Anorg. Allg. Chem*., 1970, **377**, 120.

[323] J. Ellermann, A. Veit, E. Lindner, S. Hoehne, *J. Organomet. Chem.*, 1983, **252**,153.

[324] J. Ellermann, A. Veit, E. Lindner, S. Hoehne, *J. Chem. Soc., Chem. Commun.*, 1982, 382.

[325] L. Sacconi, R. Morassi, *Inorg. Synth.,* 1976, **Vol. XVI**, 174.

[326] I. M. Müller, *Ph.d. Dissertation*, Ruhr-Universität Bochum, 1997; *or*; I. M. Müller, *Das Koordinationsverhalten von ambidentatem Methylcycloarsoxan, Bildung von supramolekularen Strukturen durch Selbstorganisation*, Utz-Verlag München, Bochum 1998.

[327] I. M. Müller, W. S. Sheldrick, *Eur. J. Inorg. Chem.*, 1998, 1999.

[328] G. M. Bodner, C. Gagnon, D. N. Whittern, *J. Organomet. Chem.*, 1983, **243**, 305.

[329] P. Velusamy, K. Pitchumani, C. Srinivasan, *Tetrahedron*, 1996, **52**, 3487.

[330] P. Kisliuk, C. H. Townes, *J. Chem. Phys.*, 1950, **18**, 1109.

[331] S. Konaka, *Bull. Chem. Soc. Jpn.*, 1970, **43**, 3107

[332] D. R. LIDE, JR, *Spectrochimica Acta.*, 1959, **15**, 473

[333] H. D. Springall, L. O. Brockway, *J. Am. Chem. Soc.*, 1938, **60**, 996

[334] Mazhar-Ul-Haque, H. A. Tayim, J. Ahmed, W. Horne, *J. Crystallogr. Spectrosc. Res.* 1985, **15**, 561.

[335] A. N. Sobolev, V. K. Belsky, N. Yu. Chernikova, F. Yu. Akhmadulina, *J. Organomet. Chem.*, 1983, **244**, 129.

[336] J. Trotter, *Can. J. Chem.*, 1962, **40**, 1590.

[337] N. M. Zaripov, R. G. Khusnutdinov, V. A. Naumov, R. R. Shagidullin, G. I. Kokarev, *J. Struc. Chem.*, 1988, 29, 547; *Zh. Strukt. Khim.*, 1988, **29**, 64.

[338] E. V. Avtomonov, K. Megges, S. Wocadlo, J. Lorberth, *J. Organomet. Chem.*, 1996, **524**, 253.

[339] Y. Ehleiter, G. Wolmershauser, H. Sitzmann, R. Boese, *Z. Anorg. Allg. Chem.*, 1996, **622**, 923.

[340] F. Breitsameter, A. Schmidpeter, H. Noth, *Chem.-Eur. J.*, 2000, **6**, 3531.

[341] C. J. Carmalt, A. H. Cowley, R. D. Culp, R. A. Jones, S. Kamepalli, N. C. Norman, *Inorg. Chem.*, 1997, **36**, 2770.

[342] B. Twamley, C. D. Sofield, M. M. Olmstead, P. P. Power, *J. Am. Chem. Soc.*, 1999, **121**, 3357.

[343] N. Burford, C. L. B. Macdonald, D. J. LeBlanc, T. S. Cameron., *Organometallics*, 2000, **19**, 152.

[344] A. S. Batsanov, S. M. Cornet, K. B. Dillon, A. E. Goeta, P. Hazendonk, A. L. Thompson, *J. Chem. Soc., Dalton. Trans.*, 2002, **24**, 4622.

[345] L. D. Pronicheva, B. I. Kuchkaev, B. A. Knyazev, *J. Struc. Chem.*, 1992, **33**, 673; *Zh. Strukt. Khim.*, 1992, **33**, 63

[346] R. J. Baker, M. Brym, C. Jones, M. Waugh, *J. Organomet. Chem.*, 2004, **689**, 781

[347] S. L. Hinchley, C. A. Morrison, D. W. H.Rankin, C. L. B. Macdonald, R. J. Wiacek, A. Voigt, A. H. Cowley, M. F. Lappert, G. Gundersen, J. A. C. Clyburne, P. P. Power, *J. Am. Chem. Soc.*, 2001, **123**, 9045

[348] R. J. Wiacek, J. N. Jones, C. L. B. Macdonald, A. H. Cowley, *Can. J. Chem.*, 2002, **80**, 1518.

[349] J. Trotter, *Can. J. Chem.*, 1963, **41**, 14.

[350] A. N. Sobolev, V. K. Belsky, *J. organomet. Chem.*, 1981, **214**, 41.

[351] A. N. Sobolev, L. P. Romm, N. Yu. Chernikova, V. K. Belsky, E. N. Guryanova, *J. Organomet. Chem.*, 1981, **219**, 35.

[352] S. Kamepalli, C. J. Carmalt, R. D. Clup, A. H. Cowley, R. A. Jones, N. C. Norman, *Inorg. Chem.*, 1996, **35**, 6179.

[353] A. L. Rheingold, D. L. Staley, M. E. Fountain, *J. Organomet. Chem.*, 1989, **365**, 123.

[354] H. MahalakshmiI, V. K. Jain , E. R. T. Tiekink, *Z. Kristallogr.-New. Cryst. Struct.*, 2003, **218**, 67

[355] J. Trotter, *Acta. Cryst.*, 1963, **16**, 1187.

[356] S. Sasaki, K. Sutoh, F. Murakami, M. Yoshifuji, *J. Am. Chem. Soc.*, 2002, **124**, 14830.

[357] P. D. C. Dietzel, M. Jansen; *Z. Naturforsch., B:Chem. Sci.*, 2004, **59b**, 345.

[358] S. Sasaki, F. Murakami, M. Yoshifuji, *Organometallics* , 2006, **25**, 140.

[359] K. Kitadai, M. Takahashi, M. Takeda, S. K. Bhargava, S. H. Priver, M. A. Bennett, *Dalton Trans.*, 2006, 2560.

[360] L. V. Vilkov, T. P. Timasheva, *Proc. Acad. Sci. USSR(Engl. Transl.)*, 1965, **161**, 261. Translated from *Dokl. Akad. Nauk SSSR.*, 1965, **161**, 351.

[361] V. P. Novikov, S. Samdal, L. V. Vilkov, *Russian Journal of General Chemistry*, 2004, **74**, 1247; Translated from *Zhurnal Obshchei Khimii*, 2004, **74**, 1348.

[362] T. Dahl, *Acta Crystallogr., Sect. C: Cryst. Struct. Commun.*, 1985, **41**, 931.

[363] T. Dahl, *Acta Crystallogr., Sect. C: Cryst. Struct. Commun.*, 2000, **56**, 708.

[364] H. Bock, K. Ziemer, C. Nather, H. Schodel, M. Kleine, M. Sievert, *Z. Naturforsch., B: Chem. Sci.*, 1996, **51**, 1538.

[365] T. Dahl, *Acta Crystallogr., Sect. B: Struct. Crystallogr. Cryst. Chem.*, 1981, **37**, 98.

[366] T. Dahl, *Acta Chem. Scand. A.*, 1981, **35**, 701.

[367] C. Courseille, A. Meresse, P. Dournel, L. H. Duparc, J. -J. Villenave, *Acta Crystallogr., Sect. C: Cryst. Struct. Commun.*, 1991, **47**, 100.

[368] R. S. Cahn, C. Ingold, V. Prelog, *Angew. Chem.*, 1966, **78**, 413; *Angew. Chem. Int. Ed. Eng.*, 1966, **5**, 385.

[369] G. P. Moss, *Pure & Appl. Chem.*, 1996, **68**, 2193.

[370] Inserting covalent radii [124] of 121, 77 and 74 pm for the elements Arsine, Carbon and Nitrogen, and pertinent *Alred-Rochow* electronegativities [60] of 2.20, 2.50 and 3.07 into the *Pauling´s* Modification of the *Schomaker-Stevenson* rule lead actually to the values 146 and 196 pm and then corrected to 144 and 194 pm by minus 2 pm for sp^2 hybridization

[371] A. D. Becke, *J. Chem. Phys.*, 1993, **98**, 5648.

[372] a) K. Raghavachari, J. A. Pople, E. S. Replogle, M. Head-Gordon, *J. Phys. Chem.*, 1990, 94, 5579; b) M. J. S. Dewar and C. H. Reynolds, *J. Computational. Chem.*, 1986, **7**, 140; c) A.

D. McLean, G. S. Chandler, *J. Chem. Phys.*, 1980, **72**, 5639; d) R. Krishnan, J. S. Binkley, R. Seeger, J. A. Pople, *J. Chem. Phys.* 1980, **72**, 650; e) A. J. H. Wachters, *J. Chem. Phys.*, 1970, 52, 1033; f) P. J. Hay, *J. Chem. Phys.*, 1977, **66**, 4377; g) K. Raghavachari, G. W. Trucks, *J. Chem. Phys.*, 1989, **91**, 1062; h) R. C. Binning Jr., L. A. Curtiss, *J. Computational. Chem.*, 1990, **11**, 1206; i) L. A. Curtiss, M. P. McGrath, J.-P. Blaudeau, N. E. Davis, R. C. Binning Jr., L. Radom, *J. Chem. Phys.*, 1995, **103**, 6104.

[373] C. Hansch, A. Leo, R. W. Taft, *Chem. Rev.*, 1991, **91**, 165

[374] A. Domenicano, P. Mazzeo, A. Vaciago, *Tetrahedron Letters*, 1976, **17**, 1029.

[375] A. Domenicano, A. Vaciago, C. A. Coulson, *Acta Cryst.*, 1975, **B31**, 221.

[376] A. Domenicano, A. Vaciago, C. A. Coulson, *Acta Cryst.*, 1975, **B31**, 1630.

[377] M. Schütze, *Angew. Cheme.*, 1958, **70**, 697.

[378] D. D. Perrin, W. L. F. Armarego, *Purification of Laboratory Chemicals*, 3rd Ed., Pergamon Press, Oxford., 1988.

[379] T. Kottke and D. Stalke, *J. Appl. Crystallogr.*, 1993, **26**, 615.

[380] W. Walter, W. Francke, *Lehrbuch der Organischen Chemie*, 20.Ed, Hirzel Verlag, Stuttgart. 1984, Page 17.

[381] W. Kuchen, W. Grünewald, *Angew. Chem.*, 1963, **75**, 576; *Angew. Chem. Int. Ed. Eng.*, 1963*,* **2**, 399.

[382] J. S. Han, W. Wolfsberger, *Z. Naturforsch. B.*, 1989, **44b**, 502.

[383] a) C. Mcbrearty, JR., k. Irgolic, R. A. Zingaro, *J. Organomet. Chem.*, 1968, **12**, 377; b) G. A. Olah, A. A. Oswald, *Can. J. Chem.*, 1960, **38**, 1428; c) G. Kamai, Z. L. Khisatova, *J. Gen. Chem.*, 1956, **26**, 125.

[384] D. T. Cromer, J. B. Mann, *Acta Cryst. A.*, 1968, **24**, 321.

[385] R. F. Stewart, E.R. Davidson, W.T. Simpson, *J. Chem. Phys.*, 1965, **42**, 3175.

[386] a) R. X. Fischer, E. Tilimanns, *Acta Cryst. C.*, 1988, **44**, 775.

b) G. M. Sheldrick, *Program system SHELXTL PLUS*, Rel. 4.0, 1989 (*Siemens Analytical X-ray Instruments, Inc., Madison, WI, USA*). Cited in: J. Grobe, D. Le Van, B. Broschk, M. Hegemann, B. Lüth, G. Becker, M. Böhringer, E-U. Würthwein, *J. Organomet. Chem.*, 1997, **529**, 177.

Danksagung

Die vorliegende Dissertation entstand unter Anleitung von Herrn Professor Dr. *Gerd Becker* am Institut für Anorganische Chemie der Universität Stuttgart. Ich danke für die Erlaubnis zur Benutzung der Insitutseinrichtungen, wodurch die Anfertigung dieser Arbeit erst ermöglicht wurde.
Mein besonderer Dank gilt für die Themenstellung und die stete Diskussionsbereitschaft.

Dem inzwischen verstorbenen Professor Dr. *J. Weidlein* danke ich für die Aufnahme der Raman-Spektren und für die engagierte Zusammenarbeit bei der Auswertung der Schwingungsspektren.

Herrn Dr. W. Schwarz und Herrn Dr. *M. Niemeyer* danke ich für die Sammlung der Diffraktometerdatensätze.

Herrn Dr. *M. Niemeyer* und Herrn Dr. *R. Ruf* bin ich für die große Hilfe bei den quantenchemischen Berechnungen zu erheblichem Dank verpflichtet.

Insbesondere möchte ich mich bei Herrn Dr. *S. Horner* für das Korrekturlesen und Herrn Dr. *R. Ruf* für die Durchsicht des deutschsprachigen Teils der Arbeit bedanken.

Mein Dank gilt ferner:

Frau *K. Török* und Herrn *P. Bergk* für die Aufnahme der NMR-Spektren,

Herrn Dr. *J. Opitz* und Herrn *F. Bender* für die Aufnahme der Massenspektren,

Frau *B. Förtsch* für die Durchführung der Elementaranalysen

sowie allen Mitgliedern des Arbeitskreises für die freundliche Aufnahme, die bereitwillige Unterstützung und anregende Diskussionen,
außerdem allen nicht namentlich genannten Mitarbeitern des Institutes.

Abschließend möchte ich noch meinen Eltern und meiner Frau für ihr Verständnis und ihre Rücksicht während meines Studiums danken.

Lebenslauf

Name	Mutasem Zaki Yousef Bani Fwaz (alternative Schreibweise Bani Fawaz)
Geburtstag/-ort	11. Nov. 1968 in Anjara, Ajlun/Jordanien
Eltern	Zaki Yousef Hasn Bani Fawaz Rawhieh Hussein Khaleel Zghool
Familienstand	seit 27. Okt. 1995 verheiratet mit Frau Feda Alfrihat vier Kinder: Munes, Lubna, Buthaina und Muhammad
Staatsanghörigkeit	Jordanisch
Adresse	Pfaffenwaldring 37 B, 70569 Stuttgart
E-Mail	banifawaz@yahoo.com
Schulbildung	
1975-1984	Grundschule “Anjara Elementry und Preparatory School”/Jordanien
1984-1986	“Anjara Secondary School”/Jordanien
1986-1987	“King Abdullah bin Al Hussein Secondary School”/Ajlun
Juli. 1987	Abschluß: Abitur “Ministry of education”/Jordanien
Hochschulbildung	
Sep. 1987-Jan. 1991	B. Sc. Studium an der Yarmouk Universität in Irbid/Jordanien
20. 01. 1991	Titel eines B. Sc.
Sep. 1991-Aug. 1995	M. Sc. Studium an der Yarmouk Universität in Irbid/Jordanien
Juni. 1994	“Comprehensive Exam”
Aug. 1995	M. Sc. Examen mit dem Thema “Kinetics and mechanism of the photolytic CO-substitution reactions of cyclopentadienyl iron thiocarboxylate complexes” bei Prof. Dr. K. Tawarah und Prof. Dr. I. Jibril am Institut für Chemie der Yarmouk Universität in Irbid/Jordanien
16. 08. 1995	Titel eines M. Sc.
Apr. 2000-März 2002	Gaststudium am Institut für Anorganische Chemie der Universität Stuttgart
seit Apr. 2002	Promotion am Institut für Anorganische Chemie der Universität Stuttgart Dissertation unter Anleitung von Herrn Prof. Dr. Gerd. Becker am Institut für Anorganische Chemie mit dem Thema “Unusual Phosphorus Oligocycles from $1\lambda^3$-Phosphaalkynes and Various Halides of Group 13 and 15 Elements”
09.01.2006	Mündliche Prüfung in Organischer Chemie der Universität Stuttgart bei Prof. Dr. S. Hashmi
12.10.2007	Mündliche Prüfung in Anorganischer Chemie der Universität Stuttgart bei Prof. Dr. G. Becker
21.12.2007	Tag der Mündlichen Prüfung bei Prof. Dr. G. Becker, Priv.-Doz. Dr. M. Niemeyer, Prof. Dr. S. Hashmi und Prof. Dr. T. Schleid
Beschäftigung	
Jan. 1992-Aug. 1995	Wissenschaftliche Hilfskraft “Teaching Assistant” an der Yarmouk Universität in Irbid/Jordanien
Sep. 1993-Feb. 1996	Lehrer bei “Ministry of education” Al Mafraq/Jordanien
Sep. 1995-März 2000	Wissenschaftlicher Angstellter (Full-time Lecturer and Teaching Assistant) an der “Jordan University of Science and Technology” Irbid- Jordanien
Apr. 2000-März 2002	Wissenschaftliche Hilfskraft am Institut für Anorganische Chemie der Universität Stuttgart
Apr. 2002-März 2003	Wissenschaftlicher Angestellter nach BAT IIa/2
Apr. 2003-Juli. 2003	Wissenschaftliche Hilfskraft
von Aug. 2003- bis Okt. 2006	Wissenschaftlicher Angestellter nach BAT IIa/2
seit Nov. 2006	Wissenschaftlicher Angestellter nach 13Ü TV-L
seit Apr. 2000	Praktikumsassistent im Anorganisch-Chemischen Grundpraktikum

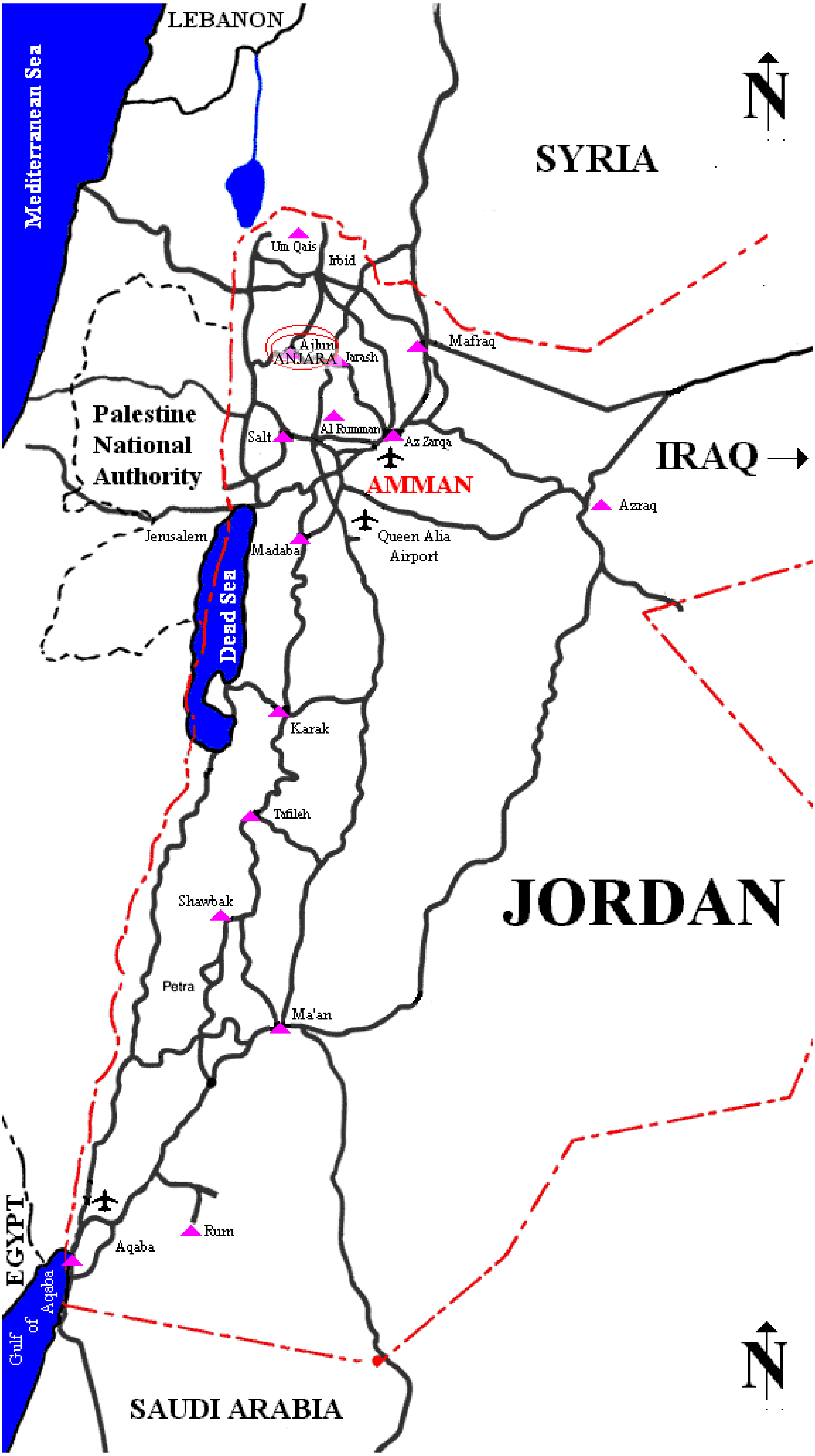
LEBANON
Mediterranean Sea
SYRIA
N
Um Qais
Irbid
Mafraq
Ajlun
ANJARA
Jarash
Palestine
National
Authority
Salt
Al Rumman
Az Zarqa
IRAQ →
AMMAN
Azraq
Jerusalem
Madaba
Queen Alia
Airport
Dead Sea
Karak
Tafileh
JORDAN
Shawbak
Petra
Ma'an
EGYPT
Rum
Aqaba
Gulf of Aqaba
N
SAUDI ARABIA

Formula Tables of Structures Prepared or Calculated in this Work

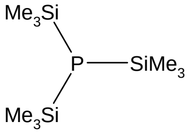

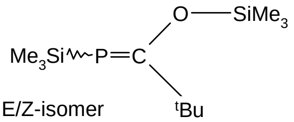

E/Z-isomer

$^{t}Bu{-}C{\equiv}P$

$(thf)_2Li{-}P(SiMe_3)_2$

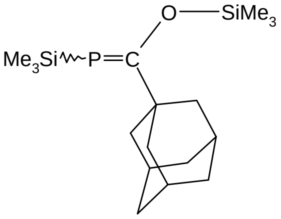

E/Z-isomer

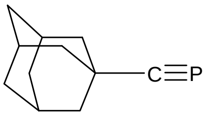

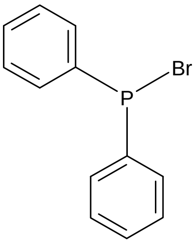

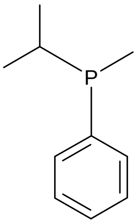

$(R`R``N)_nAsCl_{3-n}$

R` = methyl, R`` = methyl;
R` = ethyl, R`` = ethyl;
R` = *iso*-propyl, R`` = methyl;
R` = methyl, R`` = ethyl

n = 1, 2

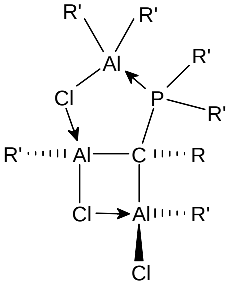

1a : R = *tert*-butyl, R` = methyl;
1b : R = *tert*-butyl, R` = ethyl;
1c : R = 1-adamantyl, R ` = methyl;
1d : R = 1-adamantyl, R` = ethyl

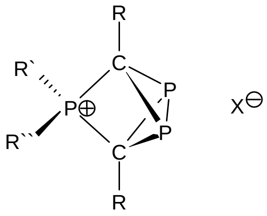

2a : R = *tert*-butyl, R` = R`` = methyl, X = Cl;
2b : R = *tert*-butyl, R´ = R`` = ethyl, X = Cl;
2c : R = *tert*-butyl, R` = isopropyl, R`` = phenyl, X = Cl;
2d.1 : R = *tert*-butyl, R` = R`` = phenyl, X = Cl;
2d.2 : R = *tert*-butyl, R` = R`` = phenyl, X = Br
2e : R = *tert*-butyl, R` = R`` = isopropyl, X = Cl

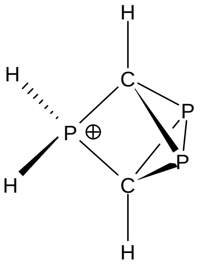

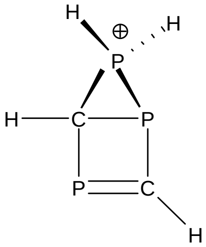

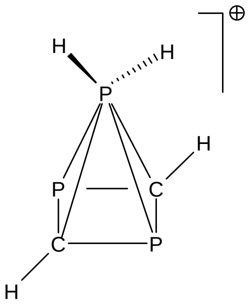

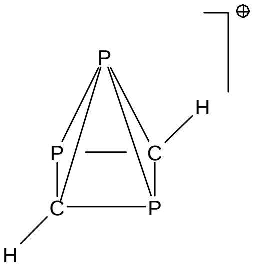

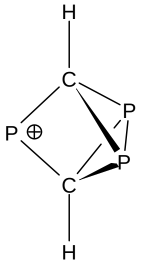

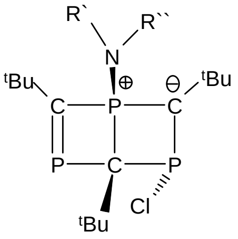

$(Me_2N)_{3\text{-}x}Me_xP$
(x = 0, 1, 2, 3)

$(H_2N)_{3\text{-}x}Me_xP{=}CH_2$
(x = 0, 1, 2, 3)

$R_3P{=}CH_2$
R = H_3Si, Cl, H

3a : R` = methyl, R`` = methyl;
3b : R` = ethyl, R`` = ethyl;
3c : R` = *iso*-propyl, R`` = methyl;
3d : R` = methyl, R`` = ethyl

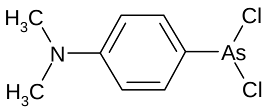

4

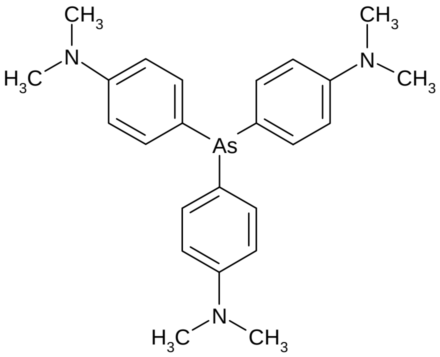

5

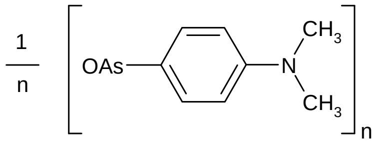

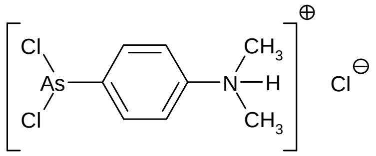

$(H_3C)_{3\text{-}n}AsCl_n$
(n = 0, 1, 2, 3)

$(H_5C_6)_{3\text{-}n}AsCl_n$
(n = 0, 1, 2, 3)

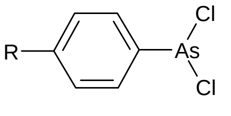

R = NMe_2, NH(OH), NO_2, $\overset{\oplus}{N_2}$

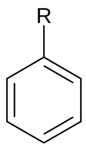

R = NH_2, NMe_2, NO_2, H

trans-Cl-CH=CHAsCl$_2$

ISBN 978-3-86186-549-0